U.S. DEPARTMENT OF THE INTERIOR
U.S. GEOLOGICAL SURVEY

EARTHQUAKE GROUND MOTIONS IN EXTENSIONAL TECTONIC REGIMES

By

P. Spudich, J. B. Fletcher, M. Hellweg, J. Boatwright, C. Sullivan, W. B. Joyner, T. C. Hanks, D. M. Boore, A. McGarr, L. M. Baker, and A. G. Lindh[1]

Open File Report 96–292

July 10, 1996

Prepared in cooperation with the
Nevada Operations Office
U.S. Department of Energy
(Interagency Agreement DE–AI08–78ET44802)

[1]Mail Stop 977, 345 Middlefield Road, Menlo Park, CA 94025

INTRODUCTION

As part of the investigation of the suitablility of the region around Yucca Mountain, Nevada, for a nuclear waste repository, the U.S. Department of Energy has prepared a document, the "Site Characterization Plan" (U.S. Dept. of Energy, 1988), which describes the investigations to be carried out. Chapter 8, "Preclosure Tectonics," section 8.3.1.17 calls for characterization of potential ground motions at the site. Under an interagency agreement (#DE–AI08–78ET44802) between the U.S. Geological Survey and the U.S. Department of Energy, the USGS conducted several studies prescribed by the Site Characterization Plan. Among them was Activity 8.3.1.17.3.3.1, Select or Develop Empirical Models for Earthquake Ground Motions. A report that compiled a global study of extensional regime earthquake ground motions (Spudich and others, 1996) was prepared for that Activity, in satisfaction of Milestone 3GSA200M. That report will be used as input by the Ground Motion Facilitation Team and its expert panel, and by the Seismic Design Basis Team. Both teams are part of the Yucca Mountain Seismic Hazards Evaluation Project of the U.S. Geological Survey, under John Whitney, Water Resources Division, USGS, Denver, CO.

Because the Spudich and others (1996) report was produced in a form not widely available to the public (it is an "Administrative Report," in USGS parlance, or a "Letter Report" in DOE parlance), we have chosen to reproduce it in the form of this Open File Report. This Open File Report is essentially identical to Spudich and others (1996). The only differences between this Open File Report and Spudich and others (1996) are that the first three paragraphs of the latter are replaced by these two introductory paragraphs, and additional references cited in these two introductory paragraphs are inserted into the reference list.

This report describes the results of two studies. The first, referred to as the 'Weak Motion Study' below, is an analysis of the aftershocks of the June 29, 1992, Little Skull Mountain, Nevada, earthquake. This earthquake occurred only 20 km from the proposed repository site, so we study its aftershocks to determine the anelastic attenuation Q and the geometric spreading exponent that best describe the variations of aftershock S wave amplitudes with distance and frequency. The second study, referred to as the 'Strong

Motion Study' below, assembles a global collection of strong motion seismograms relevant to Yucca Mountain and compares the amplitudes of the observed strong motions (peak acceleration, peak velocity, or response spectrum) to the predictions of empirically derived equations for predicting strong ground motions given event magnitude, distance, source mechanism, and site conditions. These equations are called 'predictive relations' or simply 'relations' below. Our goal is to derive corrections for both the mean and the standard errors of each existing prediction relation to make them more appropriate for application to earthquakes in extensional environments. In addition, we have developed new predictive equations from this data set.

In the case of Yucca Mountain, we have restricted the strong motion data set to "extensional-regime" earthquakes because this is the regional tectonic setting in which Yucca Mountain finds itself, a matter we discuss in greater detail later in this report in association with the earthquakes actually used in this study. We moreover restrict the data set to moment magnitude $\mathrm{M} \geq 5$ and distances $R \lesssim 100$ km, the magnitude-distance space for which one anticipates potentially damaging ground motion given the firm to hard site conditions at and near Yucca Mountain.

WEAK MOTION STUDY

The problem of separating source excitation from site response in recorded seismograms also lies at the heart of most analyses for near-field and regional attenuation characteristics. A number of recent papers, notably Boatwright *et al.* (1991), Fletcher and Boatwright (1991), Boatwright (1994), Humphreys and Anderson (1995), and Benz *et al.*(1996) have performed inversions of multiply recorded sets of earthquakes that effect this separation while solving for attenuation parameters. In general, these inversions require a distribution of earthquake locations that provides a sufficient range of epicentral distances for a subset of the stations.

This constraint on the earthquake-station geometry is necessitated by the lack of constraint on the site response in these inversions. If the earthquakes occur in a single cluster, the estimated site response for each station can trade off with the estimated attenuation. If there are enough recording sites, however, another method of constraint can be used, that is, the technique of grouping stations into site-groups that have roughly similar site response. This technique makes use of the intuitive fact that site response is a generally bounded function of frequency, and for those stations that do not exhibit strong resonances, can be reasonably similar between stations.

We apply this technique to an inversion of S-wave spectra of small aftershocks of the 1992 Little Skull Mountain earthquake obtained from the Southern Great Basin Seismic Network. The network is relatively dense: some 50 SGBSN stations recorded this aftershock sequence. The results obtained from grouping stations into similar site-groups compare well with other attenuation studies in the area, notably Rogers *et al.* (1987a) and Benz *et al.* (1996), as well as the observed attenuation of the response spectra from the Little Skull Mountain main shock.

The Southern Great Basin Seismic Network and the 1992 Little Skull Mountain Earthquake Sequence.

The Southern Great Basin Seismic Network, in its operating configuration during June and July, 1992, extended to epicentral distances of 170 km to the north, east, and northwest, and 120 km to the south and west of the Little Skull Mountain earthquake. The locations of the SGBSN stations are shown in Figure 1, along with the locations of the Little Skull Mountain earthquakes. This geometry makes the digital recordings of the aftershock sequence an invaluable data set for discerning the attenuation of weak motion in the southern Great Basin, near the proposed Yucca Mountain Repository. The data set of SGBSN recordings of this aftershock sequence, compiled by Meremonte *et al.* (1995), comprises recordings of some 230 aftershocks, ranging from $M = 1.7$ to $M = 4.5$, approximately.

The SGBSN is run as a high-gain, mostly vertical-seismometer, telemetered network, whose primary purpose is the reliable detection and location of $M > 1.5$ earthquakes throughout the southern Great Basin, with particular emphasis on the western areas of the Nevada Test Site, specifically, Yucca Mountain, Jackass Flats, and Little Skull Mountain. Thirteen stations of the SGBSN lie within 30 km of the Little Skull Mountain main shock: six are deployed around the proposed site of the Yucca Mountain Repository. The stations predominately consist of vertical seismometers, although there are six sites (JON, EPM, PRN, PAN, GMR, and GMN) with both vertical and horizontal seismometers, and two sites (LSM and YMT4) with 3 component seismometers.

The high-gain character of the SGBSN ensures that moderate-size earthquakes occurring within the network will yield clipped recordings at most of the stations. For the Little Skull Mountain aftershock sequence, $M > 3$ earthquakes clipped all of the stations. Fortunately, however, $M \leq 2$ earthquakes could be recorded without clipping at almost all stations, even those within 30 km epicentral distance. Because of the gain settings for the vertical seismometers at stations LSM and YMT1, YMT2, YMT3, YMT4, YMT5, and YMT6, these recordings were almost always clipped and unusable for spectral analysis. In contrast, the two horizontal seismometers at LSM were recorded at a particularly low-gain: unclipped recordings were obtained from these horizontal components for most Little Skull aftershocks $M < 2$. This recording configuration greatly improves the resolution of the weak-motion attenuation characteristics.

Method of Analysis.

The initial spectral analysis of these recordings follows the approach of Boatwright *et al.* (1991) and Fletcher and Boatwright (1991). Relatively long (15 s) samples of the S-waves were tapered, detrended, and Fourier transformed. Shorter (5 s) samples of the P-wave codas were used as estimates of the noise in the S-waves. The factor $\sqrt{l_s/l_n}$ was used to correct for the difference in sample length, where l_s is the sample length of the signal and l_n is the sample length of the noise (this factor assumes that the noise is both stationary and incoherent). Both the signal and noise spectra were corrected for the instrument type (Rogers *et al.* 1987b) and recording response, using a subroutine provided by Harmsen (written communication, 1995).

The signal to noise characteristics of the logarithms of the spectra are constrained following Andrews (1986) as

$$\sigma(f) \propto n(f)/r(f) \geq 1/2 \tag{1}$$

who assumed that the ratio of the signal spectrum $r(f)$ to the noise spectrum $n(f)$ was less than or equal to two throughout the frequency band analyzed.

In the inversion, we fit spectral amplitudes from 1 Hz to 30 Hz: a few stations had sufficiently low noise to allow frequencies up to 30 Hz to be used. From a visual inspection of the instrument-corrected spectra and the expectation of a distinct high-frequency falloff resulting from both the regional attenuation characteristics and the source spectra, we assigned a high frequency limit to each station that ranged from 7 Hz to 30 Hz. These estimates were made without reference to epicentral distance. The records from eight of the stations (AMR, EMN, LCH, CPY, NOP, JON, WCT, and SDH) were discarded entirely, as high-frequency limits could not be reliably determined. The corrected spectra from these stations showed no apparent attenuation or high-frequency falloff, although these stations range from 20 to 150 km in epicentral distance. Unfortunately, four of these stations are located to the south-southeast of the Little Skull Mountain sequence, yielding an azimuthal gap in the network coverage in this direction.

After this initial inspection of the record spectra, the data set was reduced to the spectra of 585 recordings of 42 earthquakes on 43 components. The inversion for source, site, and attenuation parameters was then carried out using the logarithms of the corrected velocity spectra, as detailed by Boatwright *et al.* (1991). In general, this class of inversions minimizes the least-squares error

$$\chi^2 = \sum_{k,n} \left(\ln r_k(f_n) - \ln s_i(f_n) - \ln \varepsilon_j(f_n) + \ln g(f_n, \tau_k)\right)^2 df_n/\sigma^2(f_n) \qquad (2)$$

where f_n are the frequencies and $df_n = f_{n+1} - f_n$ the frequency interval and $r_k(f)$ is the spectrum of the kth recording. χ^2 is minimized as a function of the site response spectrum of the ith station $s_i(f)$, the velocity source spectrum of the jth earthquake,

$$\varepsilon_j(f) = 2\pi f \Omega_j / \left(1 + (f/f_{cj})^4\right)^{1/2}$$

which depends on the low-frequency level Ω_j and the corner frequency f_{cj}, and the parameters in the general attenuation function $g(f, T_k)$, which depends on the travel time T_k, hypocentral distance R_k, and frequency f as

$$\ln g(f, T_k) = \gamma \ln R_k + \pi f \kappa + \pi f T_k/Q$$

The κ term contains the average near-site attenuation first described by Anderson and Hough (1984) while the exponent γ controls the geometrical attenuation. The Q term contains the average distance-dependent attenuation: in this analysis, we consider attenuation functions in which Q is constant with frequency as well as $Q \propto f^{\alpha}$.

Grouping Stations by Site Response.

Inversions of this generality require that the earthquake locations be distributed areally: for earthquakes in a single cluster, estimates of the site response can trade off arbitrarily with the attenuation function. Since we are analyzing only Little Skull Mountain aftershocks, we cannot simultaneously invert for site response and attenuation characteristics without further constraints.

To resolve the attenuation, then, we assume that the vertical recordings at most of the SGBSN sites share similar site responses. The data set is composed almost entirely of vertical component data: the only horizontal components that were used were the recordings obtained from LSM and YMT4. The geologic characteristics of the recording sites range from hard to relatively soft rock, as indicated in Table 1 (Harmsen, written communication, 1995). Their near-surface velocity structure is unknown. Thus, we cannot make this assumption blindly: we first test the stations for similarity among their site response. Constraining $\gamma = 1$ and starting the iterated inversion with $Q = 800$, as indicated by the results of Rogers *et al.* (1987a), allows us to test the site response of the stations.

When we make this preliminary inversion, we obtain $Q = 802$ and find the assumption of similar site response among the SGBSN stations to be reasonable. 24 of the 39 vertical component SGBSN stations have site response functions that are sufficiently similar to be grouped together, as plotted in Figure 2a. Three stations (BLT, GLR, and GMR) have anomalously low site amplifications. Stations TCN and GVN have site amplifications that increase with frequency, while stations SSP and TMBR have site amplifications that decrease sharply above 6 Hz. These three station-groups are also spatially clustered, so that their similar "site response" functions may represent an anomalous propagation or attenuation characteristic.

In contrast, the six stations (NPN, QCS, BMTN, PRN, MGM, and SGV) plotted together in Figure 2d have site responses that are peaked around 4 Hz. These six stations are areally scattered at epicentral distances of 60 to 160 km from the Little Skull Mountain earthquakes, so that these similar site responses cannot represent an anomalous propagation characteristic. Two other stations, EPR and SRG, have apparently unique site response functions.

The site response of the two stations with two horizontal components, LSM and YMP4, are shown in Figure 2f. The site response on the two horizontals at each station is similar, but there is a substantial difference between the two stations. Although we expect the horizontal components of the S-waves to be more strongly amplified than the vertical components (by perhaps 50%), the marked amplification of the YMP4 horizontals is surprising.

We invert the spectral data using a number of different groupings of stations into site-groups. The first grouping (G1) is the simplest: we group the 39 vertical components into a single site-group and the four horizontal components at LSM and YMP4 into two different site-groups. Inverting the resulting data set reduces the variance to 0.725% of the initial variance and yields the attenuation parameters $\gamma = 0.526$, $Q = 623$, and $\kappa = -0.002$ s. The (unphysical) negative estimate of κ may be derived from an unconstrained trade-off between the average κ and the site response as a function of frequency. These attenuation parameters are compiled in Table 2, along with the median corner frequency from the set of aftershocks. The corner frequencies of the 42 aftershocks range from 8 to 21 Hz.

In the second grouping (G2), we reduce the pool of similar vertical-component SGBSN stations to 34, extracting the 5 most anomalous stations: EPR, SSP, TCN, TMBR, and SRG. Inverting the spectra with this grouping of stations into site-groups reduces the variance to 0.508% and yields the attenuation parameters $\gamma = 0.611$, $Q = 644$, and $\kappa = -0.007$ s. Note that this estimate of κ is more negative than that obtained in the (G1) inversion. The corner frequencies of the events range from 7 to 19 Hz.

In the third grouping (G3), we form a specific site-group out of the six stations NPN, BMTN, QCS, PRN, MGM, and SGV whose site response spectra are slightly peaked between 3 and 4 Hz. The station SRG is added back to the pool of SGBSN stations. The variance of the least-squares fit decreased to 0.494% of the initial variance and the attenuation parameters are slightly changed to $\gamma = 0.684$, $Q = 707$, and $\kappa = -0.007$ s. This grouping indicates that the resolution of the attenuation parameters is partially controlled by a trade-off between the geometric and anelastic attenuation, where Q and γ increase or decrease together.

In the fourth grouping (G4), we form the site-groups suggested by the similarities among the site response spectra plotted in Figure 2. We group GVN together with TCN, SSP with TMBR, and BLT, GLR, and GMR together. SRG is added to the group of six stations whose site responses are peaked at 4 Hz. The resulting inversion reduces the variance to 0.394% of the initial variance and yields the attenuation parameters $\gamma = 0.776$, $Q = 662$, and $\kappa = 0.003$ s. The geometric attenuation is increased while the anelastic attenuation stayed about the same. The corner frequencies of the events are also increased, ranging from 7 to 22 Hz.

Figure 3 shows the site response spectra obtained from this inversion for the eight site-groups. The site response for the 24 vertical-component SGBSN stations is approximately flat, while the other five vertical-component site-groups vary as shown in Figure 2. The site response for the two horizontal component stations are largest at low frequency and decrease as the frequency increases above 2 Hz. The ($\pm\sigma$) uncertainties are shown as vertical lines, plotted at every third frequency.

Figure 4 plots "corrected" spectral amplitudes as a function of distance for four different frequencies (1.5, 6, 12, and 24 Hz). These spectral amplitudes are corrected by subtracting the logarithms of the site response spectra $s_i(f)$ and the fitted velocity source spectra $\varepsilon_j(f)$, from the recorded spectra, as in equation (2). In addition, we subtract the residual source spectra (that is, the residuals to equation (2) regressed onto the 42 earthquakes) from the spectral amplitudes. This additional correction accommodates any variations of the source spectra from the omega-square spectral model. The corrected spectral amplitudes scatter around the fitted attenuation curves by about a factor of 60%. The spectral amplitudes plotted for $f = 24$ Hz show all the spectral estimates in the data-set at this frequency: the stations further than 100 km from the Little Skull Mountain sequence had high frequency limits less than 24 Hz.

Incorporating Frequency Dependent Q's.

Some recent analyses of regional data have incorporated frequency-dependent Q's of the form $Q = Q_0 f^{\alpha}$. To consider this possible behavior, we adopt this form for Q, evaluating the variance reduction for a suite of α's. We invert the G4 grouping of stations into site-groups, with $\alpha = 0.1$, 0.3, 0.5, and 0.7; the resulting attenuation parameters are compiled in Table 2. The estimates of γ and Q_0 generally decrease as α increases.

The largest variance reduction for the G4 grouping is obtained for $\alpha = 0.35$ and the parameters $\gamma = 0.601$, $Q_o = 238$, and $\kappa = 0.002$ s. We denote this inversion as G4F and retain these parameters as our preferred attenuation model, as this inversion obtained the greatest variance reduction of the set of inversions compiled in Table 2. We note that the 2% reduction in variance beyond the G4 inversion with a frequency independent Q (0.394% to 0.385%) is relatively small, however, and indicates that the frequency dependence of the attenuation is not well resolved.

To consider whether this result is biased by the choice of site-groups for the G4 grouping (which are predicated on the assumption of $\gamma = 1$), we also searched for the α that maximizes the variance reduction for the grouping G1, the grouping in which all the vertical component stations were included in a single site-group. For this inversion, denoted as G1F, the derived frequency dependence of Q is relatively small: $\alpha = 0.15$ and $Q_0 = 401$. The geometric attenuation exponent, $\gamma = 0.450$, is less than that expected for surface waves ($\gamma = 1/2$), however.

Figure 5 compares the falloff, as a function of distance and frequency, for six of the attenuation functions compiled in Table 2. The variation among the attenuation functions plotted in Figure 5 is relatively small, although the various curves are clearly separated at 1.5 and 6 Hz. If we use the range of attenuation parameters compiled in Table 2 to estimate the uncertainty of these parameters, we obtain $\gamma = 0.601 \pm 0.096$, $Q_0 = 238 \pm 11$ for $\alpha = 0.35$, and $\kappa = 0.002 \pm 0.005$ s. These uncertainties are larger than the formal uncertainties returned by the inversions. We also plot Benz *et al.*'s (1996) estimate of the attenuation of Lg waves recorded at regional broadband stations within the Great Basin: fixing $\gamma = 1/2$, he obtained $Q = 232 f^{0.57}$ for the frequencies from 0.8 to 7 Hz. His attenuation model fits within the range of our curves for 1.5 and 6 Hz, but underestimates the SGBSN attenuation at 12 and 24 Hz. Note that the *Lg* waves in his data-set span a larger area than the SGBSN.

Although we have slightly improved the fit to the SGBSN data using a frequency-dependent Q, we have not significantly reduced the variance. Nor has incorporating this frequency-dependent Q identified a specific functional form for the regional attenuation of *S*-waves and *Lg*-waves in the southern Great Basin. While the rough correspondence with Benz *et al.*'s (1996) result is gratifying, we cannot claim to have entirely described the regional attenuation in the Great Basin.

Main Shock Response Spectra.

The general incentive for analyzing weak motion is the prediction of strong ground motion. The $M = 5.7$ Little Skull Mountain main shock was recorded by eight strong motion instruments within 100 km of the epicenter (Lum and Honda, undated). These instruments were sited on a range of rock-type, from deep soil to hard rock. The instrument locations and rock-types are compiled in Table 3.

Figure 6 compares the attenuation of the pseudo-velocity response spectral ordinates at frequencies of 1.0, 3.3, and 10 Hz to the attenuation curves obtained from our inversions of the aftershock spectra. The two points plotted at each hypocentral distance represent the response spectra ordinates for each horizontal component. Although the response spectra at 1.0 and 3.3 Hz are strongly variable, as a function of distance, the spectra at 10 Hz are well fit by the attenuation curve derived from the aftershocks, assuming that the deep soil sites slightly attenuate the ground motions. In contrast, the deep soil types appear to amplify the ground motion at the lower frequencies.

In plotting these attenuation curves against the strong motion data, we have shifted the curves to obtain the best fit to the stations sited on rock. The zero crossings for the attenuation curves are 10.6, 45.6, and 23.6 cm/s^2, for the 1.0, 3.3, and 10 Hz fits, respectively. Although the peak at 3.3 Hz cannot be fit by an omega-square model for the acceleration spectrum, the relatively low value at 1.0 Hz indicates that the corner frequency may be 1.5 to 2 Hz.

Conclusions.

We have spectrally analyzed 585 recordings of 42 aftershocks of the 1992 Little Skull Mountain earthquake, modifying the inversion technique of Boatwright *et al.* (1991) to invert these data, by grouping the site response of the 50 SGBSN stations into 8 site-groups, depending on the component of ground motion recorded and on the site response obtained from a preliminary inversion of the aftershock spectra. Twenty-four of the vertical-component stations are included in the largest group, while seven stations with a distinctive peak near 4 Hz comprise the second largest group. We have obtained stable estimates of the S-wave attenuation in the southern Great Basin. Our preferred attenuation model has a geometric attenuation of $R^{-0.6}$ and a frequency-dependent Q of $238f^{0.35}$. This slight frequency dependence is not strongly constrained. Our attenuation model roughly agrees with the attenuation of Lg-waves in the Great Basin at distances of 50 to 200 km of $Q = 232f^{0.57}$ discerned by Benz *et al.* (1996) who assume the geometric attenuation to be $R^{-0.5}$.

STRONG-MOTION STUDY

Predictive Relations Considered.

We compared our world-wide extensional-regime data set with predictive relations for peak acceleration, peak velocity, and response spectrum by Boore *et al.* (1993, 1994), Campbell (1989, 1990, 1993), Campbell and Bozorgnia (1994), Idriss (1993), Joyner and Boore (1982, 1988), Sabetta and Pugliese (1996), and Sadigh *et al.* (1993), summarized in Appendix A, and with a new predictive relation we have derived (Appendix B) referred to as 'Sea96' below. We chose these relations because, in our judgment, they constituted a representative sample of recently-derived, widely-used relations which, if not published, at least had been subject to some scrutiny by the engineering seismology and geotechnical engineering community. Use of an exhaustive list of relations would be impractical and not particularly useful.

In some cases the predictor variables were given different definitions for the different relations. Boore *et al.* (1993, 1994), Campbell and Bozorgnia (1994), Joyner and Boore (1988), and Sadigh *et al.* (1993) used moment magnitude M as the measure of earthquake size, while Campbell (1989, 1990, 1993) and Idriss (1993) used local magnitude (M_L) for magnitudes (type unspecified) less than 6.0 and surface-wave magnitude (M_S) for magnitudes greater than or equal to 6.0. Sabetta and Pugliese (1996) used M_S if both M_S and M_L were greater than or equal to 5.5, otherwise they used M_L. In this project we used moment magnitude as the magnitude variable in all the relations and substituted it for M_L or M_S as appropriate when using the relations of Campbell, Idriss, and Sabetta and Pugliese. The values for moment magnitude are approximately the same as the other definitions, as was noted by Campbell (1989, 1990, 1993) and Idriss (1993), and using moment magnitude in all the relations avoided the problem that, for a world-wide data set, local magnitudes are not always defined in a way that ensures equivalence from region to region.

The distance measure used by Joyner and Boore (1988), Boore *et al.* (1993, 1994), Sabetta and Pugliese (1996), and our new relation is closest distance to the vertical projection of the ruptured area onto the surface of the earth, which we denote r_b here and in Appendix A. Idriss (1993) and Sadigh *et al.* (1993) used closest distance to the rupture surface, r_i. Campbell (1989, 1990, 1993) and Campbell and Bozorgnia (1994) used r_c, closest distance to the seismogenic rupture, on the presumption that fault rupture within a few km of the earth's surface does not contribute significantly to ground motion. In this project we used with each relation the distance definition given by the authors of the relation. We assumed that the slip surface for each earthquake could be represented by a dipping planar surface or set of dipping planar surfaces. Each planar surface was described by its strike and dip and the latitude, longitude, and depth of a reference point on the surface. The boundary of the slipped zone was represented by a rectangle enclosing the region of significant slip. The location of the rectangle was defined in terms of the specified reference point. The conventions of Aki and Richards (1980, p. 106) were used in defining the coordinate system for describing the slipped surface and the boundary of the slipped zone, as illustrated in Figure 7. This representation of the slipped surface was used to compute the recording-site distance as defined for each of the relations. The boundary of the slipped zone was determined from seismological or geodetic inversions if available; otherwise the distribution of early aftershocks was used if known. In cases where neither inversions or aftershock distributions were available but fault strike was known, a rectangle was constructed enclosing the hypocenter, using the Wells and Coppersmith (1994) relation between area and moment magnitude to determine the area of the rectangle. The rectangle was placed such that the hypocenter was located at the middle of the bottom edge of the rectangle, since earthquakes tend to nucleate deep and propagate to a more shallow depth. If fault strike was unknown, then it was impossible to determine where the slipped rectangle should be, so we approximated the source as a point at the hypocenter for the distance calculation. The distances we obtained are listed in Table 4.

The authors of the different relations used different classifications for geologic site conditions. In this project we grouped sites of our world-wide extensional-regime data set into the six categories given in the heading of Table 5. These categories were chosen so as to fit the classifications of the different relations as well as possible given the limited information available for the sites in our data set. The classifications "soil of unknown thickness" and "rock of unknown hardness" were necessitated by the lack in many cases of the information for more specific classification. In general, since most soil sites are "deep soil" sites, "soil of unknown thickness" was treated as "deep soil," and, since most rock sites are "soft rock" sites, "rock of unknown hardness" was treated as "soft rock." Table 5 shows how our six site categories map into the categories used with each of the relations. For comparisons with the relations of Boore *et al.* (1993, 1994) we used the shear-wave velocities of 620 m/s for our rock categories and 310 m/s for our soil categories, which represent the averages we determined for his data set of downhole measurements. In addition, the relations of Campbell (1989, 1990, 1993) use a parameter 'depth to basement' for each site. Campbell defines basement as either the top of unweathered crystalline igneous or metamorphic rock, or the depth at which P velocities of 5.0 km/s or S velocities of 3.0 km/s are reached and velocity gradients are low (personal communication, 1995). Campbell (1989) has already estimated depth to basement for many of the stations we study, and for those stations we use his estimates. For other stations we estimated depth to basement when necessary geologic information was available. When it was not, we listed depth to basement as unknown. In general, we could still use the relations of Campbell (1989, 1990, 1993) in a limited period band even when depth to basement was unknown because these three relations are independent of depth to basement for periods less than or equal to 1.0 s, 0.75 s, and 0.3 s, respectively. Table 6 lists the site codes and geologies of all stations we used.

Some of the relations gave different values for strike-slip and reverse-slip faulting. In all cases we compared our data set with the strike-slip relation except for the relationships of Boore *et al.* (1993, 1994), Sabetta and Pugliese (1996), and our new relation, which are independent of mechanism. Note that Campbell (1993) gives a relation for normal faulting which we chose not to use because it was unconstrained by data and because it leads to ground motions which are greater than those for equivalent strike-slip events, which seemed unlikely.

Different authors had different ways of representing the horizontal components of ground motion and we used each as the author intended. We used the larger horizontal component of ground motion in comparing our world-wide extensional-regime data set with the relations of Sabetta and Pugliese (1996); we used the arithmetic mean of the two horizontal components in comparing with the response spectral relations of Campbell (1989, 1990, 1993); and we used the geometric mean of the two horizontal components in comparing with the relations of Joyner and Boore (1988), Boore *et al.* (1993, 1994), Idriss (1993), Sadigh *et al.* (1993), and Campbell and Bozorgnia (1994), and our new relation.

At Campbell's suggestion (written communication, 1995) we divided the *horizontal* response spectral values by the peak horizontal acceleration for Campbell (1989, 1990, 1993) and then multiplied by the peak acceleration from Campbell and Bozorgnia (1994). The vertical response values from Campbell (1989, 1990, 1993) were not changed.

In summary, we compared our world-wide extensional-regime data set with the relations detailed in Table 5 and Appendices A and B. See those appendices for definitions of the abbreviations used to denote each relation.

Correction factors.

Our objectives in this study are to derive correction factors for the predicted ground motions and their standard errors for each relationship. By 'correction factors' we mean the following. Each author's relation is of the form

$$\log(y) = f(M, R, G_i, C_j, D, F, T_k)\ , \tag{1}$$

(natural or common log, depending on the author) and the predicted standard error of $\log(y)$ is of the form

$$\sigma = g(M, pga, C_j, T_k) \tag{2}$$

where y is the predicted ground motion parameter (*e.g.,* peak acceleration, peak velocity, pseudo-velocity response, pseudo-absolute acceleration), M is magnitude, R is distance, D is depth to basement, F is a source mechanism term, pga is peak ground acceleration, G_i is a site geology term (with i = 1, ..., 6, being the 6 defined site conditions), and C_j is a component orientation (with j = horizontal or vertical), and T_k is period where k = 1, 2, ..., m. The term σ is commonly called the 'dispersion' of the relationship. Note that not all authors give relations for all possible combinations of site geology G_i, component of motion C_j, and period T_k. In fact, we have only 23 possible distinct combinations of these factors, *i.e.,* 23 predictive relations (Appendix A, B).

We determine two sets of correction factors for each relation. One is a set of biases b_{ijk} (defined for each site category i, direction of motion j, and period k) to be added to the right side of equation (1) for each relation. It is simply a constant offset in the $\log(y)$ curve needed to bring the curve into agreement with our data set. The actual calculation of the corrections b_{ijk} is straightforward. If y_o is an observed value of ground motion parameter y, and y_{ijk} is its predicted value from equation (1), then we define the observed residual to be

$$r = \log_{10}(y_o) - \log_{10}(y_{ijk})\ . \tag{3}$$

The bias term b_{ijk} is simply the mean value of the observed residuals for the particular relation under consideration, with the mean taken over the population of all observations in the ground motion data set appropriate to the i-th site class, the j-th direction of motion, and the k-th period.

The second type of correction factor is a set of scalars e_{ijk} (defined for each relation, site class, direction of motion, and period) to be multiplied with the right side of equation (2) in order to make the authors' predicted dispersions consistent with our observed residuals. These correction factors for the dispersion σ are easily derived. If we have a particular observed residual r, we form the demeaned residual $r' = r - b_{ijk}$. Corresponding to this demeaned residual is some predicted dispersion σ from (2). The observed population standard deviation σ_p of the residuals is given by

$$\sigma_p = \left[N_{ijk}^{-1}\,\Sigma\,(r')^2\right]^{1/2} \tag{4}$$

and σ_b, the standard deviation of the bias, is given by $\sigma_b = N_{ijk}^{-1/2}\,\sigma_p$, where the sum is taken over the population of appropriate earthquake-station pairs for the i-th site condition, the j-th component of motion, and the k-th period, and where N_{ijk} is the number of those data. Let v_{ijk} be the variance of the random variable r'/σ, taken over the same population. The dispersion correction factor is $e_{ijk} = \sqrt{(v_{ijk})}$. In other words, the random variable $r'/(e_{ijk}\sigma)$ will have unit variance. The variance v_{ijk} is calculated using

$$v_{ijk} = N_{ijk}^{-1}\Sigma(r'/\sigma)^2$$

where the sum is taken over all data for the ijk combination of site, component, and period.

We estimate the significance of the dispersion corrections e_{ijk} in two ways. The standard deviation of e_{ijk} is given by

$$\sigma_{e_{ijk}} = \left(\frac{N_{ijk} - M}{2}\right)^{1/2} \frac{e_{ijk}}{N_{ijk}}$$

where M is the number of degrees of freedom, taken to be 1 because we have removed the mean from our residuals r'. We additionally use a χ^2 test to determine whether for each author and for each combination of i, j, and k the theoretical dispersions (2) are consistent with the observed scatter of residuals. χ_0^2 is the sum over N_{ijk} earthquake-station pairs of $(r'/\sigma)^2$. We calculate the probability $Q(\chi_0^2|\nu) = 1 - P(\nu/2, \chi_0^2/2)$, where $P(a, x)$ is the incomplete gamma function (Press *et al.*, 1986, pp. 160–165). ν is the number of degrees of freedom (usually taken to be $N_{ijk} - M$, where M is the number of model parameters). In our case $\nu = N_{ijk} - 1$ because our single model parameter is the mean residual b_{ijk} which is removed from r'. The interpretation of Q requires some care. $Q(\chi_0^2|\nu)$ is the probability of obtaining from the null hypothesis (*i.e.*, from a set of residuals drawn from a population having the predicted σ) a χ^2 that is greater than the observed χ_0^2. Loosely speaking, if Q is very nearly 1, then it is highly likely that the observed scatter in the residuals is less than the predicted dispersion, and if Q is very nearly zero, then that situation is very unlikely. Strictly speaking, however, for many realizations of the null hypothesis, the set of Qs from these realizations is uniformly distributed between 0 and 1. Thus, there is a 5% chance of obtaining a Q value greater than 0.975 or less than 0.025 from the null hypothesis. Consequently, we regard Q values above 0.975 or below 0.025 as indicating a 95% probability that the observed residuals are significantly different from the predicted residuals.

The correction factors we derive for the previously existing predictive relations may be used to alter those relations to make their predictions more consistent with the extensional regime data set we have assembled. Note that we calculate the same 'correction factors' for our newly developed relations, Sea96, but the 'correction factors' for Sea96 are to be used only for the purpose of comparing Sea96 to the other relations. They should not be used to correct Sea96.

It is important to note that all of the correction factors discussed above are calculated assuming that the observed residuals (3) are statistically independent, which is not the case. Some authors, such as Joyner and Boore (1988) consider the residuals to be a sum of an earthquake source term and a station term, which implies correlations between the residuals. Consequently, our correction factors should be used cautiously.

Magnitude and Distance Dependence.

Part of any assessment of the adequacy of the predictive relations is the determination of whether the magnitude- and distance-dependences in the functional forms are correct for our data set. If these dependences are correct for a particular relation, then the residuals with respect to that relation should show no dependence on magnitude and distance. For each relationship, component of motion, and predicted value (*i.e.*, peak acceleration, peak velocity, and response spectrum), we fit least-squares straight lines through the residuals as functions of magnitude or $\log_{10}$ X, where distance $X = \sqrt{r_b^2 + 5^2}$ for relations using r_b, and $X = r_c$ or r_i for relations using those distances (Appendix A). The pseudo-depth $h = 5$ was used to avoid the case of $r_b = 0$, and it corresponds almost exactly to the average value of h in Boore, Joyner, and Fumal (1993, Table 7b). We determined parameters s_r and σ_r, the slope of the distance dependence and its standard deviation, and s_m and σ_m, the slope of the magnitude dependence and its standard deviation. We used a χ^2 test to estimate goodness-of-fit parameters Q_r and Q_m, using Press *et al.* (1986, eqn. 14.2.12, pp. 504–506). These parameters should not be confused with the probability Q associated with the dispersion correction factors, discussed earlier. In calculating Q_r and Q_m, the theoretical dispersions (2) were used in the calculation of χ^2 (Press *et al.*, 1986, eqn. 14.2.2), so Q_r and Q_m assess whether the residuals from the fitted straight lines are consistent with the theoretical dispersions.

These slope parameters are intended simply to facilitate comparison of the predictive relations; they are not meant to be used to further correct the relations. Consequently, we have ignored any biases that would be introduced into them by correlations between magnitudes and distances of recordings. Since in Appendix B we derive new predictive relations that handle such correlations properly, there was no need to apply such rigor here, too.

Data Processing.

Because of advances in the art of strong-motion record processing, the original processing of data does not always meet current quality standards. In order to ensure high quality and uniformity we had all the records of our world-wide extensional-regime data set reprocessed by Walter Silva of Pacific Engineering and Analysis (PEA), with the exception of the Little Skull Mountain data as discussed below. PEA had already reprocessed about half of the data set (first batch) before the initiation of this study. During the course of this study we sent an additional $\sim$ 130 records to PEA for processing (second batch). An important desirable aspect of the PEA processing was their choice of low-pass and high-pass filters that constricted the passband of the data as little as possible.

The PEA correction procedure used involved a series of eight steps: 1) interpolation of uncorrected unevenly sampled records to 400 samples/sec, 2) frequency domain low-pass filtering using a causal 5-pole Butterworth filter with corner frequencies selected for each record based on visual examination of the Fourier amplitude spectrum, 3) decimating to 100 or 200 samples/s depending upon the low pass corner frequencies, 4) removing the instrument response, 5) examining the Fourier amplitude spectrum to choose high pass filters and assess the adequacy of the low pass anti-alias filters, 6) high pass filtering of the accelerations, 7) frequency domain integration to velocity and displacement to evaluate low frequency noise levels (baseline drifts) in the time domain, and 8) either baseline correct or refilter if the low frequency noise is minor or severe, respectively. The baseline correction procedure fits a polynomial (typically of degree 5) to the displacement time history and subtracts it from the acceleration record. The high pass filters (corner and order number) are based on a visual examination of the Fourier amplitude spectra as well as integrations to velocity and displacement time histories.

As an additional check on the selected high pass filter corners, for the first batch of data PEA examined the records' phase spectra. The phase spectrum controls the timing and shape of the waveform. Seismic ground motions are expected to have smoothly varying phase at long periods whereas noise will have random phase. PEA examined the derivative of the phase with respect to frequency using a phase unwrapping algorithm by Tribolet (1977). Long period energy having a random phase structure was considered to be noise, and the high pass filters that had been chosen based upon visual examination of the Fourier amplitude spectrum and the integrated records resulted in good phase stability out the filter corner frequencies.

We reviewed the acceleration, velocity, and displacement time series of the records processed by Pacific Engineering. In a few cases where we saw evidence of excessive long-period noise on the displacement time series we sent the record back for reprocessing. In all cases we were satisfied with the reprocessing. Along with the processed data Pacific Engineering gave us the list of filter corner frequencies they used. For each record we used only the part of the passband between 1.25 f_h and 0.75 f_l, where f_h is the high-pass corner frequency and f_l is the low-pass corner, to ensure that the data we used were not affected by filter roll-off near the corner frequencies. When we reviewed the time series we excluded from the data set all records where it appeared that the instrument had been triggered by the S-wave. In the case of such records there is generally no way of knowing whether or not the largest amplitudes of motion were missed. For records triggered before the S-wave the largest amplitude of horizontal motion is probably recorded. Since most of the instruments that recorded our data set lacked pre-event memory, there is no way to exclude from analysis records in which significant initial vertical P motion may have been lost by the trigger. In addition to excluding records triggered by the S wave we also excluded from the data set all records from building three stories or higher or from stations in deeply embedded basements.

In the case of the Little Skull Mountain mainshock data, we have only the data files supplied by URS/Blume (Lum and Honda, undated). At this time we do not know what instrument constants were used when those records were processed and we cannot have them reprocessed by PEA until the instrument constants are obtained. We have had PEA calculate response spectra from the existing URS/Blume processed records. Because of uncertainties about the low and high frequency characteristics of the processed data, we have used the horizontal data only for peak acceleration and response spectra in the 0.05 to 0.5 s band, and we have used the vertical data for peak acceleration and response spectra in the 0.05 to 1.0 s band. We have used the peak velocities from the URS/Blume processed records. In a few cases, for vertical motions at larger distances, these peak velocities may be biased slightly high owing to excessive long period noise in the processed velocities. However, it was not clear from inspection that the long periods were in fact noise rather than signal, so we chose to keep them.

SELECTION OF DATA

Table 7 is a list of 'candidate' earthquakes, *i.e.,* a list of earthquakes we considered for any reason. Once an earthquake was deemed to be a candidate for study, we did further investigations to determine whether it satisfied the following criteria: 1) located in an extensional regime, 2) moment magnitude 5.0 or greater, and 3) had usable digitized ground motion recordings made within 105 km of the earthquake source ('usable' data meaning that the S waves were not truncated by late triggering of the instrument, and the instrument was in a building of 2 stories above ground or less). We had initially used a 100 km maximum distance, but we raised it when we found a few events that were well recorded at that distance.

Extensional Regime Criterion.

There are several issues associated with the first criterion that merit discussion because this is the least orthodox aspect of this study. Situated in the southern Basin and Range Province, Yucca Mountain is in an extensional region, for which the lithosphere is expanding areally. This areal expansion is the result of applied forces that yield a state of stress for which $S_v > S_{H_{\max}} > S_{H_{\min}}$, where S_v, $S_{H_{\max}}$, and $S_{H_{\min}}$ represent principal stresses that are oriented approximately vertically and in two orthogonal horizontal directions. These terms are defined in McGarr and Gay (1978). For the Basin and Range, $S_{H_{\min}}$ is oriented WNW–ESE, the direction of lithospheric extension.

Specifically, for this study the ideal ground motion data set would involve recordings of earthquakes of M > 5 within about 100 km of Yucca Mountain. Unfortunately this data set is thoroughly inadequate for purposes of determining, or even testing, ground motion prediction relations as this set includes no events of M > 6 and very few of M > 5. Even broadening the area of interest to the entire Basin and Range helps little to augment the ground motion data set. Accordingly, we were forced to consider ground motion from earthquakes within active extensional tectonic regimes world wide to ensure an adequate data set for the purpose of this study.

There are two reasons for restricting our attention to ground motion data from earthquakes in extensional provinces. First, there is observational evidence that the state of stress, extensional or compressional, affects the amplitude of the ground motion from an earthquake after other factors, such as magnitude and hypocentral distance have been taken into account (*e.g.,* McGarr, 1984; Abrahamson, 1993, Boore *et al.*, 1994; Campbell and Bozorgnia, 1994). The observational data clearly suggest that ground motions from reverse faults exceed that from strike slip faults for similar magnitude earthquakes. This is a source effect. It has been suggested (McGarr, 1984) that normal faulting events have lower motions than strike slip events. However, none of the strong ground motion relations, except Sabetta and Pugliese (1996), has been developed based on data sets including much data from normal faults, or from extensional regimes in general, so it is important to study these classes of events more thoroughly than has been done in the past.

A second way in which the stress state might affect the recorded ground motion involves possible differences in wave propagation characteristics between extensional and compressional tectonic regimes. Intuitively, it seems plausible that dissipation should be higher in extensional regimes because of lower crack-closure stresses as well as the attendant higher heat flow. Studies investigating such effects, however, have yet to be done. In addition, extensional regimes have some degree of similarity in crustal structure worldwide. Christensen and Mooney (1995) report that extended crust and rifts have thinner crust and higher average crustal velocity gradients with depth than other continental crust. These factors might affect the geometric spreading of S waves (probably driving amplitudes upward), and they may affect the distances at which Moho reflections are observed. There may also be systematic differences between the thickness of the Moho transition in extensional regions and in other regions. Such differences would also affect the strength and location of a Moho reflection. Catchings and Mooney (1991) report that a strong Moho bounce is observed in P wave refraction profiles in northwestern Nevada, and they show that it has a strong effect on the observed amplitude-distance curves. Mooney and Meissner (1992) state that in regions where the latest tectonic event was extensional, such as much of western Europe, the Basin and Range, and many passive margins, the lower crust tends to be highly reflective and the Moho tends to be nearly horizontal, generating readily observable Moho reflections.

Magnitude, Distance, and Usability Criteria.

The magnitude criterion was chosen, somewhat arbitrarily, to be well below the threshold of damage to a well designed repository facility at a hard-rock site. The third criterion, involving the distance limit was chosen so as to take into account the Death Valley–Furnace Creek fault system, which is deemed capable of producing earthquakes of $7\frac{1}{2} \leq \mathbf{M} \leq 8$;

faults at greater ranges, it turns out, probably cannot increase the seismic hazard estimate of Yucca Mountain. As employed here, the phrase "usable ground motion" connotates seismograms that include at least all of the S wave, recorded at free-field sites for which site conditions could readily be taken into account. Needless to say, earthquakes yielding such ground motion data at multiple sites were assigned higher priority than those with records at only one location. Larger earthquakes were assigned higher priority also, not only for their increase damage potential, but also because they tended to have more recordings.

Candidacy and Relevance.

With specific regard to the events listed in Table 7, the following criteria, in addition to those already mentioned, were used to decide whether an earthquake was a candidate for this study:

1.) All earthquakes listed in Table 1 of Westaway and Smith (1989) were accepted as having occurred in extensional tectonic regimes on the basis of the focal mechanism criteria applied to these events. Many of these events, however, did not satisfy some of the criteria applied here such as magnitude threshold or useful ground motion data within 100 km of the fault.

2.) The earthquakes in Italy and Greece, not studied by Westaway and Smith (1989) are included here if either the focal mechanism or the neotectonic stress indicators warrant the extensional tectonic classification; many of these events occur in areas of back-arc spreading. Similar remarks apply to events in Central America.

3.) In Turkey, the right-lateral strike-slip Anatolian fault system plays the primary tectonic role, but, localized extensional regions occur where the Anatolian fault segments are offset rightward; an example of this is the 1992 Erzincan earthquake.

4.) In the western United States active tectonic extension is associated with the Basin and Range, the Yellowstone Hot Spot, the Salton trough, the Long Valley (Mammoth Lakes) volcanism and numerous other geothermally-active areas. The earthquakes in Table 7 associated with these features include Imperial Valley events (Salton trough), Mammoth Lakes (Long Valley), Victoria, Mexico (Salton trough), Borah Peak, ID (Basin and Range), Round Valley (Long Valley), Superstition Hills and Elmore Ranch

(Salton Trough), Little Skull Mountain and Double Spring Flat (Basin and Range) and finally Klammath Falls, OR which also is within the Basin and Range. Although at least several of the Mammoth Lakes events may have non-double-couple focal mechanisms (*e.g.,* Julian and Sipkin, 1985) the classification of these events as extensional is, nonetheless, appropriate inasmuch as normal faulting comprises a significant part of the mechanism.

Having so broadened the potential data set, the next question that arises involves the criteria needed to confirm that a particular earthquake did, indeed, occur in an extensional regime. In most cases an earthquake is deemed to have occurred in an extensional regime on the basis of its focal mechanism involving a measureable component of dip-slip in the normal-faulting sense; similarly, if the focal mechanism includes a component of reverse slip then the earthquake is clearly not in the extensional category. Strike-slip earthquakes occur in extensional regimes, but for strike-slip earthquakes with no significant dip-slip component, other information is required to decide its tectonic category. Geodetic measurements of crustal deformation, for instance, may indicate ongoing areal expansion in the region that includes the epicenter. The recent stress indicators in the area, as well as the tectonic framework, may provide guidance as well. Examples of stress-indicators include slip vectors observed on exposed fault planes, aligned volcanic features (cinder cones or dikes) and, of course, various types of *in situ* stress measurements. Observations indicative of extensional tectonics include recent volcanism, lithospheric thinning, and high heat flow. An example, used in this study, of a tectonic feature that gives rise to at least a localized extensional regime is a right-stepping offset of a right-lateral, strike-slip fault; within the offset region the crustal area tends to increase.

If the three data selection criteria were met the event was called 'relevant,' and we attempted to acquire the digital data and to assemble the necessary source information (*e.g.,* source extent, etc.) and geologic site information. Of course, in the process of acquiring source and site information it was occasionally discovered that an event initially thought to be relevant was not actually so, and it was then declared irrelevant.

Table 7 shows our assessment of relevance and the subset of relevant events whose ground motion data have actually been analyzed in this report (see 'used here' column of

Table 7). For relevant events in Table 7 not analyzed in this report, we at present lack either the necessary processed digital data or geologic source or site condition information.

Figure 8 shows the distribution of magnitudes of events studied in this report, and Figure 9 shows the distribution in magnitude-distance space of records studied. Unfortunately, the range of magnitudes in Figure 9 is not wide enough to enable development of a predictive relation solely from this data set (see Appendix B for more details).

We have neither identified nor excluded from analysis those records recorded at distances greater than the distance of the first non-triggered station (the so-called 'cutoff' distance). Some authors do not use data recorded beyond the cutoff distance since these data may be a biased sample of the ground motions, owing to the lack of recordings of low (untriggered) motions. Rather, we have included all available records for two reasons. First, for many events outside the U.S. it is difficult to determine from the available literature which stations did not trigger in various earthquakes. Second, owing to the paucity of relevant ground motion data, we were hesitant to discard data that would help define the variability of ground motions at large distances, even though such data might have a biased mean. Figure 9 suggests that our data set is probably not severely biased by inclusion of data beyond the cutoff distance. The dashed line in Figure 9 shows an empirically determined cutoff distance derived from other ground motion data sets (N. Abrahamson, written communication, 1995). Very little of our data comes from distances beyond this empirical curve, at which the non-triggering might be a problem. Note that we used all data in Figure 9, including that beyond the cutoff distance. Figure 10 shows raw peak acceleration, peak velocity, and response spectral data (pseudo-absolute acceleration) as a function of distance, separated by magnitude, period, and component of motion for records used in this report (Table 4). Table 8 gives a list of records excluded because they were S-triggers, poorly digitized, or in large structures.

Geometric complexity of faults caused us to give special handling to two earthquakes. The 1979 Imperial Valley earthquake ruptured both the Imperial Fault and the Brawley Fault nearly simultaneously, with the Brawley Fault generating observable ground motions (Archuleta, 1984). For this earthquake, distances were calculated for each station to both of the faults, and the shorter distance was assigned to each station. The other earthquake was the 1980 Irpinia, Italy, earthquake. This event has been analyzed as consisting of slip on three rupture planes (Cocco and Pacor, 1993). Two of the planes were contiguous and ruptured in quick succession (the main shock). The third plane was about 15 km from the others, and ruptured about 40 s after the initiation of slip on the first plane (the so-called '40 s subevent'). Consequently, most of the ground motion recordings have what appears to be a main shock with a large aftershock (the 40 s subevent) in the main shock coda. Since the main shock and the 40 s subevent occurred on separate faults and have fairly well separated bursts of energy on the records, we treated these as two separate events. The records were broken into two just before the 40 s subevent, and each section was processed separately. (In one case, Torre del Greco, this was not done as this station was far from the third plane and the 40 s subevent did not cause motions larger than the main shock coda.) We assigned moment magnitudes separately for the main shock and the 40 s subevent, and we calculated distances separately. We used peak accelerations, velocity, and response spectra from the main shock, but we used only peak accelerations and velocity from the 40 s subevent because we felt that the 40 s subevent response spectra may have been contaminated by substantial long period coda from the main event.

RESULTS

Calculation of Correction Factors and Slope Parameters.

Correction factors b_{ijk}, σ_b, σ_p, e_{ijk}, σ_e, and Q, and slope parameters s_r, σ_r, Q_r, s_m, σ_m, and Q_m were calculated for each predictive relation for peak velocity and for periods including $T = 0$ (peak acceleration), 0.05, 0.1, 0.15, 0.2, 0.3, 0.4, 0.5, 0.75, 1.0, 1.5, and 2.0 s. We first calculated these correction factors using data from all distances. Before discussing the significance of all these factors, we will present them in a variety of plotted formats.

Figure 11 and Figure 12 specifically illustrate the various correction factors and slopes. Figure 11a shows the residuals as a function of distance for *pga* ($T = 0$ s) and for various response spectral periods. These residuals in Figure 11a are calculated with respect to the relation BJF94h for soil conditions $G = 0$, 1, and 2. The bias is the mean value of the residuals, and the distance dependence of the residuals is shown by the best fitting straight line (dashed). Its slope is s_r. Figure 12 shows *pga* and response spectral residuals as a function of magnitude. Peak velocity residuals are shown as functions of distance and magnitude in Figure 13 and Figure 14, respectively.

These correction factors and slopes are summarized for all the relations in Figure 15, Figure 16, and Figure 17. They are tabulated in Table 9, Table 10, and Table 11. Figure 15 shows correction factors and measures of their significance for *pga* and response spectra. Figure 16 shows the correction factors and slopes plotted compactly for easier comparison of the *pga* and response spectral relationships. Figure 17 shows the correction factors and slopes for the peak velocity relations. To facilitate assessment of the significance of the b, e, s_r, and s_m, we have used a χ^2 test to calculate a significance Q_s for each predictive relation, plotted to the right of each relation in Figure 16. Considering for example the distance dependences at 11 periods for BJF94h $G = 0$, 1, 2 in Figure 16e, we form χ_0^2 by summing $(s_r/\sigma_r)^2$ over the 11 values and we calculate Q_s, the probability of obtaining a χ^2 greater than χ_0^2 if BJF94h had no distance dependences in the residuals. The plot tells us that $1 - Q_s \simeq 0.99$, so $Q_s \simeq 0.01$ and we would be very unlikely to get a χ^2 larger than χ_0^2 if the distance dependence were zero, *i.e.,* BJF94h $G = 0, 1, 2$ has a significant distance dependence. Note that in calculation Q_s we assumed that the number of degrees of freedom was equal to the number of periods (*i.e.,* we assumed the number of model parameters was zero) for all predictive relations. This is true for all relations except Sea96, which was derived from our extensional data set.

We repeated the determination of correction factors for a subset of the data having distances less than or equal to 20 km. We chose the 20 km boundary because hazard at Yucca Mountain may be strongly influenced by nearby events, so that correction factors determined from short-distance records may be important. We initially tried a 15 km boundary between the two subsets, but we had too few records at distances less than 15 km to enable a good comparison. Correction factors for distances less than or equal to 20 km are given in Table 12 and plotted in Figures 18, 19, and 20.

Comparison of Relations.

Before comparing the results for various relations, we caution the reader that the results for Campbell's relations should be compared with the results for all other relations very cautiously, because the data sets are somewhat different. Campbell's relations require a depth to basement parameter be used for predictions at long periods. We do not have depth to basement for all our stations, so apparent differences between Campbell's and others' correction factors may be caused by systematic differences in the data sets. Since in many cases we are using depths to basement assigned by Campbell for stations used by him to derive his relationships, our data set is not a truly independent test of his relationships. In addition, we do not have depth to basement for stations recording the the 1980 Irpinia, 1983 Borah Peak, and the 1992 Little Skull Mountain earthquakes. Borah Peak and Little Skull Mountain contribute heavily to the data at large distances, and Borah Peak and Irpinia contribute significantly to the high magnitude data. Consequently, the omission of these data when considering Campbell's relations may affect the estimation of his relations' magnitude and distance dependences for longer periods, where the depth to basement has an effect.

Examination of the residuals for individual earthquakes (Figure 21 and Figure 22) shows that for distances less than about 50 km the various predictive relations differ among themselves very little, and most of the scatter in the residuals comes from scatter in the observations. This is seen most clearly in the 1981 Westmorland earthquake residuals (Figure 21i–j), in which the BJF94 (1), C89 (2), SP96 (6), and Sea96 (c) residuals plot nearly on top of each other, while the scatter among stations is much larger. This is also seen for the 1979 Imperial Valley main shock (Figures 21a–b), the 1980 Irpinia event (Figures 21e–h), and the 1986 Chalfant Valley main shock (Figures 21u–x). On the other hand, for distances greater than about 50 km, substantial differences are seen among the relations, particularly at the longest periods. Examples are the 1992 Roermond earthquake (Figures 21y–ab), and the 1992 Little Skull Mountain earthquake (Figures 21ac–af, Figures 22n, 23). (The Little Skull Mountain event will be discussed in more detail later.) An event having intermediate behavior between these extremes is the 1983/10/29 2329 Borah Peak aftershock (Figures 21o–p). An interesting intermediate case is the 1983 Borah Peak main shock (Figures 21m–n), in which there is moderate disagreement between the relations at long period. However, this event shows the largest residuals of all events considered.

A comparison of biases for all relations is shown in Figures 16a, 16b, and 17a. Not surprisingly, our new relation, Sea96 (Appendix B), has in general the lowest biases of all the relations, both for horizontal pga and response spectra.

The dispersion correction factor e_{ijk} has been tabulated in Tables 9 and 12 for all periods and relations, and it has been plotted in Figures 16c and 16d, and in the bottom panels of Figures 15 and 18, for all distances and for distance less than or equal to 20 km, respectively. As mentioned earlier, these dispersion corrections are calculated assuming all the residuals are statistically independent, which is not the case. Consequently, they may be useful to compare one relation to another, but their absolute values may be biased.

While our extensional regime data set appears to have a larger dispersion than that predicted by some authors and a smaller dispersion than that predicted by others, taken as a whole our extensional regime data set does not appear to have a radically different dispersion from other ground motion data sets. Interestingly, we note that the dispersion correction for Sea96 (Figure 16c) is systematically less than unity, which appears to be saying that the Sea96 dispersions are too big for the extensional regime data set. However, the Sea96 dispersions were derived from the extensional regime data set, and must therefore be consistent. This discrepancy is probably caused by ignoring the correlations in the residual when calculating the dispersion corrections.

We note in passing that the Q statistic is more reliable than the σ_e statistic for assessing the significance of the dispersion corrections, owing to the better behavior of Q for small number of data points. For example, consider in Figure 18e the e value and σ_e for the longest period for C90/94h when data having $r < 20$ km are used. While it appears from the miniscule σ_e that the e value is significantly less than 1, the associated probability Q is less than 0.95 (actually 0.869), meaning that this low value of e is not significantly different from unity. Inspection of the residuals for $T = 2$ s in Figure 11j shows that for this period there are only 2 residuals at distances less than 20 km, and these two residuals happen to be fairly similar, leading to the low value of σ_e. When the distance range being considered is expanded to include the third data point at distance slightly greater than 20 km, the σ_e becomes much larger (Figure 15e), and the dispersion correction e is no longer significant. Clearly, for small numbers of data points reliance on σ_e is problematic, whereas the Q value is more reliable.

There are several reasons why our observed dispersions may differ from the dispersions predicted by other authors. First, most of the predictive relations are developed from data sets drawn from geographic regions, *e.g.,* California or Italy, that are more restricted than our global data set. Second, it must be remembered that the predicted dispersions have been minimized by each author in the process of determining the coefficients and functional forms of the predictive relations. Although the authors try to compensate for this minimization by considering the number of degrees of freedom when determining the predicted dispersion, perhaps this correction is imperfect in some cases. A third related possibility is that in developing the predictive relationships, it is usually assumed that the independent variables, such as magnitude, are known perfectly. If they are not known perfectly, then the predicted dispersions may underestimate the true dispersion. For example, some of the predictive relations have been developed based on data sets dominated by a small number of very well recorded events. In such a situation, the fitting procedure will tend to produce coefficients that compensate for systematic errors in source-related parameters, such as earthquake magnitude. We use a very heterogeneous set of earthquake sources in our study, and our errors of magnitude assessment for each earthquake will map into increased dispersions. Finally, it must be recalled that we have used each of the relationships in distance and magnitude ranges implicitly or explicitly forbidden by their authors. For example, according to their authors, CB94 is valid only out to 60 km, as is I93, C90 is appropriate only out to 30 km for $\mathbf{M} < 6.25$ and out to 50 km for $\mathbf{M} > 6.25$. Similarly, BJF94 only uses two events having $\mathbf{M} < 6.0$.

For a predictive relation to be 'correctable,' its residuals must have small magnitude and distance dependences. It is interesting to compare the distance dependences of the relations (Figures 16e,f), since some of the relations have very similar functional forms. BJF94, SP96, and Sea96 all use the same functional form, and in each of them the coefficient of the R term is zero for all periods, so variations of the distance dependence between these relations are caused by the period dependences of h and the $\log(R)$ coefficient. BJF94 has a systematic negative s_r for all periods, causing it to overpredict the data at large distances. We speculate that BJF94h tends to overpredict for large distances because this relationship was developed from data sets dominated by the 1989 Loma Prieta and 1992 Landers earthquakes. The former data set has amplified motions at large distances because of a Moho-reflected S wave (Somerville and Yoshimura, 1990; McGarr *et al.*, 1991), and the latter may have Moho reflection amplification in some azimuths (J. Mori, personal communication, 1995). The BJF94 tendency to overpredict at large distance is largely ameliorated in Sea96, owing to its more negative b_5 term. In general, Sea96 has little bias except at periods of 1 s or more for large distances (Figures 11aa–ad). In SP96 the $\log(R)$ coefficient is the most negative of the three relations, being -1 for all periods, leading to an overall distance dependence comparably good to Sea96 and with a tendency to underpredict at long periods and large distances. I93, S93h, and S93z have similar functional forms, and all have similar distance dependences, with $s_r > 0$ for most periods. C89/94h for $G = 5$, 6 has an excellent distance independence, but the remaining Campbell relations seem also to have substantially positive distance slopes, although in some cases the standard deviations of the slope are large.

The shared heritages of many of the relations are manifested in their similar magnitude dependences (Figures 16g–h, Figure 17b). Sea96 was forced to have the same magnitude dependence as BJF94, and both of these relations have fairly significant magnitude dependence in their residuals. SP96, which uses a similar functional form, has similar dependences of residuals on magnitude and period. I93 and S93h and z have generally low magnitude slopes, whose period dependences resemble each other.

Little Skull Mountain Earthquake.

Because of its proximity to Yucca Mountain, the Little Skull Mountain earthquake data warrant special attention. The residuals shown in Figure 21ac–af are plotted in expanded scale in Figures 22m–n and Figure 23. There are two main phenomena visible in these figures for the horizontal components. First, qualitative examination of the plots shows that many of the predictive relationships have residuals that grow progressively more negative with distance. This is clearly seen in BJF94h (1 on the plots) and SP96h(6), and it is also seen to some extent in C89h(2). Relations I93h(5) and S93h(7) show less distance dependence. The second phenomenon is that the average level of all residuals seems to decrease with period. For example, in Figure 23a almost all the residuals at distances less than 60 km are positive, whereas in Figure 23e almost all are negative in the same distance range. Vertical component residuals do not show such clear behaviors.

The distance dependent residuals of BJF94h have already been explained above. The observed period dependent behavior of all the residuals for Little Skull Mountain could occur if the near surface attenuation factor κ (Anderson and Hough, 1984) were smaller (less attenuation) than that characterizing the data sets from which the predictive relations were derived.

Comparison of Ground Motions from Strike-Slip and Normal Faulting Events.

Because our extensional data set contains both normal faulting and strike-slip events, we are able to compare the ground motions to determine whether the two mechanisms produce systematically different ground motions. Our data suggest that normal faulting events may have slightly lower motions than strike-slip events.

We compared ground motions from the two mechanisms by comparing the mean *pga* and *psv* residuals for the two mechanisms. Residuals were calculated with respect to the reference relation Sea96h for *pga* and *psv* for our standard set of periods and for horizontal motions. These residuals were partitioned into groups for normal faulting events (having rakes between $-135°$ and $-45°$) and strike-slip events (all other events for which we know the rake), yielding 837 strike-slip residuals and 354 normal faulting residuals. The strike-slip residual distribution was reasonably Gaussian, but the normal faulting residuals had an asymmetric tail with several outliers around -1.4. All of the normal faulting residuals having values less than -0.75 were from station TAN that recorded the 1983 Borah Peak earthquake (see the residuals around -1.4 at 85 km in Figure 21n). We arbitrarily deleted all TAN residuals from the data set. Deleting TAN's residuals leaves 343 residuals in the normal faulting group, and the distribution is as in Figure 24. We calculated the mean and standard deviation of each group of residuals (without TAN), and we also calculated Student's t statistic and the associated probablity (Press *et al.*, 1986, p. 465). These values are listed below:

0.03015 – mean residual, strike-slip

0.2316 – std. dev, strike slip residual

−0.01254 – mean residual, normal faulting

0.2606 – std. dev, normal residual

−2.77 – Student's t statistic

0.9943 – probability that the two means are different

When TAN is deleted from the data set, the probability that the two means are different is 99.4%, and the difference itself is about 0.043 $\log_{10}$ unit, with strike slip faults having 10% larger motions than normal faults. For comparison, to account for thrust faults most authors add a correction term having a value of about 0.25 ln units (or about 0.11 $\log_{10}$ units), causing predicted thrust motions to be about 28% higher than strike-slip motions.

Consequently, we interpret these observations to suggest that strike-slip faults may produce horizontal ground motions slightly larger than those of normal faults. We caution that this conclusion depends on the assumption of a reference ground motion prediction curve, which we have chosen to be Sea96. Because Sea96 has magnitude dependent residuals and other possible undesired correlations, it is possible that this dependence might interact with a systematic correlation (if one exists) between magnitude and mechanism in our sparse data set, causing an apparent difference between normal and strike-slip residuals. Our observation should be checked against larger data sets before accepting as established fact that normal events have lower horizontal motions than strike-slip events.

Comparison of Weak Motion Attenuation Results with Strong Motion Predictive Relations.

The ground motion amplitudes predicted by the preferred attenuation model G4F agree reasonably well with those predicted by the strong motion relations, but because the frequency dependence of G4F is not well constrained, it is impossible to make a particularly detailed comparison. Figure 25 shows the weak motion amplitude predicted by G4F as a function of epicentral distance, for a point source buried at 6 km depth, for periods of 0.1, 0.3, and 1 s. The 6 km source depth corresponds roughly to the mean depth of the aftershocks used in the weak motion analysis, and it also corresponds to the depth to the top of the Little Skull Mountain fault surface. Predicted peak velocities derived from strong motion relations are also shown in Figure 25. Although plotted against epicentral distance, these amplitudes have been calculated using epicentral or hypocentral distance, as appropriate to each relation. All curves have been normalized to unit amplitude at 10 km.

Although the frequency dependence of the weak motion model is not strongly constrained, it causes a factor of 3 difference in amplitude at 100 km distance. This factor of 3 is more than twice the difference between the amplitudes of the strong motion relations for peak velocity at 100 km, also shown in Figure 25. To some extent, the significant aspect of this comparison is not the absolute level of the curves but rather the slopes of the curves at large distance. All the strong motion velocity relations have slopes roughly within the range of slopes spanned by the G4F curves.

Predicted strong motion response spectra generally tend to decay with distance faster than the G4F weak motion predictions in the 10–50 km distance range, although their distance decays match the weak motion decays better for distances greater than 50 km (Figure 26). For 0.1 s period (Figure 26a) the G4F predictions match I93 and S93 best. At large distances BJF94h, SP96, and Sea96 decay too slowly, and the others decay at about the right rate. For 0.3 s and 1.0 s period all the relations except BJF94h, SP96h, and Sea96 decay more quickly than G4F.

Finally, it is interesting to compare the strong motion relations' frequency dependences with that of G4F. This can be done by examining the predicted amplitudes at 100 km for the different frequencies. The G4F predicted amplitude at 100 km drops with increasing frequency, as do the predictions of C93h, S93h, and Sea96h. BJF94h, C89h, C90h, and I93h are largely frequency independent at 100 km, and SP96h amplitude rise with frequency, contrary to the weak motion predictions.

CONCLUSIONS

It is impossible for us to say which predictive relation is best to use for evaluating ground motions at Yucca Mountain, because the choice of 'best' is dictated by the user's requirements. For example, if the user is most concerned about ground motions from distant earthquakes, then the relationships showing little distance dependence may be preferable. On the other hand, perhaps the user will consider the 'best' relationship to be that which has the lowest biases, or perhaps the relationship having the lowest corrected dispersion, or the relation requiring the least correction to its dispersion, or the relationship that best fits the Little Skull Mountain strong motion data. All of these choices depend on the use of our information, which we cannot predict. Consequently, we have simply tabluated the desired numbers and pointed out a few relevant observations, leaving the evaluation to the users.

ACKNOWLEDGMENTS

We are grateful to legions of people who have contributed to this work. Seismic data and site information were contributed by N. Ambraseys, E. Carro, M. Çelebi, R. Darraugh, D. Rinaldis, J. Gomberg, M. Henger, S. Jackson, V. Margaris, G. McVerry, R. Pelzing, A. Shapiro, R. B. Smith, L. Valensise, and R. Westaway. Reviews were provided by N. Abrahamson, J. Gomberg, C. Mueller, and A. Rogers. S. Pezzopane provided much help and solace regarding the management of this project. Much thanks to all.

REFERENCES

Abrahamson, N. A., 1993, Estimation of hanging wall and foot wall effects on strong ground motions (to appear in *Proc. International Workshop on Strong Ground Motion*, Menlo Park, CA, December 13–17, 1993).

Aki, K. and P. G. Richards, 1980, *Quantitative Seismology*, W. H. Freeman, San Francisco.

Anderson, J. G. and S. E. Hough, 1984, A model for the shape of the Fourier amplitude spectrum of acceleration at high frequencies, *Bull. Seismol. Soc. Am. 74*, 1969–1993.

Andrews, D. J., 1986, Objective determination of source parameters and similarity of earthquakes of different size, in *Earthquake Source Mechanics*, S. Das, J. Boatwright, and C.H. Scholz (editors), *American Geophysical Union*, Washington D.C., 259–268.

Archuleta, R. J., 1984, A faulting model for the 1979 Imperial Valley earthquake, *J. Geophys. Res. 89*, 4559–4585.

Benz, H., A. Frankel, and D. M. Boore, 1996, Regional *Lg* attenuation for the continental United States using broadband data, submitted to *Bull. Seismol. Soc. Am.*

Boatwright, J., 1994, Regional propagation characteristics and source parameters of earthquakes in northeastern North America, *Bull. Seismol. Soc. Am. 84*, 1–15.

Boatwright, J., J. B. Fletcher, and T. E. Fumal, 1991, A general inversion scheme for source, site, and propagation characteristics using multiply recorded sets of moderate-sized earthquakes, *Bull. Seismol. Soc. Am. 81*, 1754–1782.

Boore, D. M., W. B. Joyner, and T. E. Fumal, 1993, Estimation of response spectra and peak accelerations from western North American earthquakes: An interim report, *U.S. Geol. Surv. Open-File Rep. 93-509*, 72 pp.

Boore, D. M., W. B. Joyner, and T. E. Fumal, 1994, Estimation of response spectra and peak accelerations from western North American earthquakes: An interim report, Part 2, *U.S. Geol. Surv. Open-File Rep. 94-127*, 40 pp.

Campbell, K. W., 1989, Empirical prediction of near-source ground motion for the Diablo Canyon power plant site, San Luis Obispo County, California, *U.S. Geol. Surv. Open-File Rep. 89-484*, 115 pp.

Campbell, K. W., 1990, Empirical prediction of near-source soil and soft-rock ground motion for the Diablo Canyon Power Plant Site, San Luis Obispo County, CA, LLNL, 33 pp.

Campbell, K. W., 1993, Empirical prediction of near-source ground motion from large earthquakes, *Int. Workshop on Eq. Hazard and Large Dams in the Himalaya*, New Delhi, India, Jan. 15–16, 17 pp.

Campbell, K. W. and Y. Bozorgnia, 1994, Near-source attenuation of peak horizontal acceleration from Worldwide Accelerograms recorded from 1957 to 1993, *Fifth U.S. Nat'l Conf. on Eq. Eng.*, Chicago, IL, July 10–14, 1994.

Catchings, R. D. and W. D. Mooney, 1991, Basin and Range crustal and upper mantle structure, northwest to central Nevada, *J. Geophys. Res. 96*, 6247–6267.

Christensen, N. and W. D. Mooney, 1995, Seismic velocity structure and composition of the continental crust: A global view, *J. Geophys. Res. 100*, 9761–9788.

Cocco, M. and F. Pacor, 1993, The rupture process of the 1980 Irpinia, Italy, earthquake from the inversion of strong motion waveforms, *Tectonophysics*, *218*, 157–177.

Fletcher, J. B. and J. Boatwright, 1991, Source parameters of Loma Prieta aftershocks and wave propagation characteristics along the San Francisco peninsula from a joint inversion of digital seismograms, *Bull. Seismol. Soc. Am. 81*, 1783–1812.

Humphrey, J. R., and J. G. Anderson, 1995, Seismic source parameters from the Guerrero subduction zone, *Bull. Seismol. Soc. Am. 84*, 1754–1769.

Idriss, I. M., 1993, Procedures for selecting earthquake ground motions at rock sites, National Inst. of Standards and Tech., Gaithersburg, MD, revised 1993.

Joyner, W. B., and D. M. Boore, 1982, Prediction of earthquake response spectra, *U.S. Geol. Surv. Open-File Rep. 82-977*, 16 pp.

Joyner, W. B., and D. M. Boore, 1988, Measurement, characterization, and prediction of strong ground motion, *Proc. Earthq. Eng. Soil Dynamics II,* GT Div/ASCE, Park City, UT, June 27–30, 1988.

Joyner, W. B., and D. M. Boore, 1993, Methods for regression analysis of strong motion data, *Bull. Seismol. Soc. Am. 83*, 469–487.

Joyner, W. B., and D. M. Boore, 1994, Errata—Methods for regression analysis of strong motion data, *Bull. Seismol. Soc. Am. 84*, 955–956.

Julian, B. R. and S. A. Sipkin, 1985, Earthquake processes in the Long Valley Caldera area, California, *J. Geophys. Res. 90*, 11,155–11,169.

McGarr, A. and N. C. Gay, 1978, State of stress in the earth's crust, *Ann. Rev. Earth and Plan. Sci.*, *6*, 405–436.

McGarr, A., 1984, Scaling of ground motion parameters, state of stress, and focal depth, *J. Geophys. Res. 89*, 6969–6979.

McGarr, A., M. Celebi, E. Sembera, T. Noce, and C. Mueller, 1991, Ground motion at the San Francisco International Airport from the Loma Prieta earthquake sequence, 1989, *Bull. Seismol. Soc. Am. 81*, 1923–1944.

Meremonte, M., J. Gomberg, and E. Cranswick, 1995, Constraints on the June 29, 1992, Little Skull Mountain, Nevada, earthquake sequence provided by robust hypocenter estimates, *Bull. Seismol. Soc. Am. 85*, 1039–1049.

Mooney, W. D. and R. Meissner, 1992, Multi-genetic origin of crustal reflectivity: a review of seismic reflection profiling of the continental lower crust and Moho, in *The Lower Continental Crust*, eds. D. M.Fountain, R. Arculus, and R. W. Kay, Elsevier, Amsterdam, pp. 45–79.

Press, W. H., B. P. Flannery, S. A. Teukolsky, and W. T. Vetterling, 1986, *Numerical Recipes*, Cambridge University Press, Cambridge.

Pugliese, A. and F. Sabetta, 1989, Stima di spettri di risposta da registrazioni di forti terremoti italiani, *Ingegneria Sismica, 6*, 3–14.

Rogers, A. M., S. C. Harmsen, R. B. Herrmann, and M. E. Meremonte, 1987a, A study of ground motion attenuation in the southern Great Basin, Nevada–California, using several techniques of estimates of Q, $\log A_o$, and coda Q, *J. Geophys. Res. 92*, 3527–3540.

Rogers, A. M., S. C. Harmsen, and M. E. Meremonte, 1987b, Evaluation of the seismicity of the southern Great Basin and its relationship to the tectonic framework of the region, *U.S. Geol. Surv. Open-File Rep. 87-408*, Denver, CO.

Sabetta, F. and A. Pugliese, 1987, Attenuation of peak horizontal acceleration and velocity from Italian strong-motion records, *Bull. Seismol. Soc. Am. 77*, 1491–1513.

Sabetta, F., and A. Pugliese, 1996, Estimation of response spectra and simulation of non-stationary earthquake ground motions, *Bull. Seismol. Soc. Am. 86*, 337–352.

Sadigh, K., C.–Y. Chang, N. A. Abrahamson, S. J. Chiou, and M. S. Power, 1993, Specification of long-period ground motions: Updated attenuation relationships for rock site conditions and adjustment factors for near-fault effects, *Proc. ATC-17-1 Seminar on Seismic Isolation, Passive Energy Dissipation, and Active Control*, San Francisco, CA, March 11–12.

Somerville, P. and J. Yoshimura, 1990, The influence of critical Moho reflections on strong ground motions recorded in San Francisco and Oakland during the 1989 Loma Prieta earthquake, *Geophys. Res. Lett. 17*, 1203–1206.

Spudich, P., Fletcher, J., Hellweg, M., Boatwright, J., Sullivan, C., Joyner, W., Hanks, T., Boore, D., McGarr, A., Baker, L., and Lindh, A., 1996, Earthquake ground motions in extensional tectonic regimes, U.S. Geological Survey Administrative Report, dated May 30, 1996, 351 pp.

Tribolet, J., 1977, A new phase unwrapping algorithm, *IEEE Trans. Acoustics, Speach, and Signal Proc.*, *ASSP-25*, 170–177.

U.S. Department of Energy, 1988, Site Characterization Plan, vol. 5, part B, report DOE/RW–0199.

Westaway, R. and R. B. Smith, 1989, Strong ground motion in normal-faulting earthquakes, *Geophysical Journal*, *96*, 529–559.

Wells, D. L. and K. J. Coppersmith, 1994, New empirical relationships among magnitude, rupture length, rupture width, rupture area, and surface displacement, *Bull. Seismol. Soc. Am. 84*, 974–1002.

APPENDIX A. Summary of previous ground-motion prediction relations.

This appendix summarizes the ground-motion prediction relations used in the report. Note that the relations used here may vary slightly from those given by the developers of the relations, having been adapted to the needs of this project. While the numerical coefficients we use here are identical to those given by the developers, in some cases we have substituted moment magnitude where the original source used some other magnitude, or we have defined site classes differently, or we have chosen particular definitions of standard errors, or we have ignored magnitude and distance restrictions specified by the developers. User beware!

Definitions of commonly used terms below:

ln	-	natural logarithm
log	-	base–10 logarithm
M	-	moment magnitude
r_b	-	Boore, Joyner, and Fumal (1993) distance to fault, km
r_c	-	Campbell (1989) distance to fault
r_i	-	Idriss (1993) distance to fault
F_c	=	0 for strike-slip and normal events
	=	1 for reverse, reverse-oblique, and thrust events (not used in this report)
T	-	period, s. $T = 0$ for peak acceleration.
D	-	Campbell (1989, 1990, 1993) depth to basement, km

CB94

From Campbell and Bozorgnia (1994),

$$\begin{aligned}\ln A_{CB94} = & -3.512 + 0.904\ M - 1.328\ \ln\left(r_c^2 + [0.149\ \exp(0.647\ M)]\right)^{1/2} \\ & + [1.125 - 0.112\ \ln r_c - 0.0957\ M]\,F_c \\ & + [0.440 - 0.171\ \ln\ r_c]\,S_{sr} + [0.405 - 0.222\ \ln r_c]\,S_{hr}\end{aligned} \tag{A1}$$

where

A_{CB94} = geometric mean of two horizontal peak accelerations, in g

$$[S_{sr}\,,\,S_{hr}] = \begin{cases} [0\ ,0] & \text{for site classes } G = 5, 6, \text{or } 7 \\ [1\ ,0] & \text{for site classes } G = 0 \text{ or } 2 \\ [0\ ,1] & \text{for site classes } G = 1 \end{cases}$$

$$\sigma_{\ln A_{CB94}} = \begin{cases} 0.55 & \text{if } A_{CB94} < 0.068 \\ 0.173 - 0.140 \ln A_{CB94} & \text{if } 0.068 \leq A_{CB94} \leq 0.21 \\ 0.39 & \text{if } A_{CB94} > 0.21 \end{cases} \tag{A2}$$

BJF94

From Boore, Joyner, and Fumal (1993, 1994),

$$\begin{aligned} \log Y = {} & b_1 + b_2(M-6) + b_3(M-6)^2 + b_4\, R + b_5 \log R \\ & + b_v(\log v_s - \log v_a) \end{aligned} \tag{A3}$$

where

Y = peak horizontal acceleration in g for randomly oriented horizontal or 5%-damped pseudo-velocity response spectra in cm/s for randomly oriented horizontal ($\equiv$ geometric mean horizontal)

R = $(r_b^2 + h^2)^{1/2}$

$b_1, b_2, b_3, b_4, b_5, h$ - coefficients taken from Boore *et al.* (1993) Table 7b for response spectra, or Boore *et al.* (1993) Table 9 for random component of peak accleration

b_v, v_a - coefficients taken from Boore *et al.* (1994) Table 2 for random component of 5%-damped response spectrum, or from Boore *et al.* (1994) Table 3 for random component of peak accleration

v_s - average S-wave velocity to 30 m depth, in m/s

= 620 m/s for site classes G = 0, 1, or 2

= 310 m/s for site classes G = 5, 6, 7

Note that (A3) is derived from Boore *et al.* (1993) equation (1) and Boore *et al.* (1994) equation (3).

$$\sigma_{\log Y} = \left(S1^2 + SE^2\right)^{1/2} \tag{A4}$$

is the standard deviation of the *geometric* mean horizontal, where

$S1$, SE - terms from Boore *et al.* (1993) Table 7b for response spectra and from their Table 9 for the random component of peak acceleration

Note that (A4) is not explicitly given in Boore *et al.* (1993) or Boore et al (1994).

C89/94h, C89z, C90/94h, C90z

Campbell (1989) and Campbell (1990) with Campbell and Borzorgnia (1994) scaling,

$$\ln Y_{C*/94} = \ln Y_{C*} + k\,[\ln A_{CB94} - \ln Y_{C*}(T=0)] \tag{A5}$$

where

$$C* = \begin{cases} \text{C89} & \text{for Campbell (1989)} \\ \text{C90} & \text{for Campbell (1990)} \end{cases}$$

for vertical motion:

$Y_{C*/94}$ = peak ground acceleration in g or 5% damped pseudo-velocity response spectra in cm/s

k = 0 ($\Longrightarrow Y_{C*/94} = Y_{C*}$)

for horizontal motion:

$Y_{C*/94}$ = arithmetic mean of two horizontal peak accelerations in g or 5% damped pseudo-velocity response spectra in cm/s

k = 1

for both components of motion:

A_{CB94} = geometric mean of peak horizontal accelerations in g from Campbell and Bozorgnia (1994)

$$\ln Y_{C*} = a + bM + d \ln [r_c + c_1 \exp (c_2 M)] + e\, F_c$$
$$+ f_1 \tanh\ [f_2(M + f_3)] + g_1 \tanh\ (g_2\, D) \tag{A6}$$

$a, b, c_1, c_2, d, e, f_1, f_2, g_1, g_2$ - coefficients from Campbell (1989) or Campbell (1990) Table 1 (horizontal) or Table 2 (vertical)

$$\sigma_{\ln Y_{C*/94}} = \begin{cases} \sigma_{\ln Y_{C*}} & \text{for vertical peak acceleration and response} \\ & \text{spectra, and for horizontal response spectra} \\ \sigma_{\ln A_{CB94}} & \text{for horizontal p.g.a.} \end{cases} \tag{A7}$$

$\sigma_{\ln Y_{C89}}$ - from Table 1 (horizontal motions) and from Table 2 (vertical motions) of Campbell (1989)

$\sigma_{\ln Y_{C90}}$ - from σ_t of Table 4, Campbell (1990), taken from the M 4.7–6.1 column if $M \leq 6.15$, or the M 6.2–7.8 column if $M > 6.15$.

C89Vh, C89Vz

Expressions for peak velocity, from Campbell (1989), where

Y_{C89V} = same as (A6)

For (horizontal; vertical)

Y_{C89V} = (arithmetic mean of peak horizontal velocities; peak vertical velocity) in cm/s

$a, b, c_1, c_2, d, e, f_1, f_2, g_1, g_2$ - coefficients taken from Campbell (1989) (Table 1; Table 2)

$\sigma_{\ln Y_{CB89V}}$ - from Campbell (1989) (Table 1; Table 2)

C90Vh, C90Vz

Expressions for peak velocity, from Campbell (1990), where

Y_{C90V} = same as (A6)

For (horizontal; vertical) motions

Y_{C90V} = (arithmetic mean of peak horizontal velocities; peak vertical velocity) in cm/s

$a, b, c_1, c_2, d, e, f_1, f_2, g_1, g_2$ - coefficients from Campbell (1990) (Table 1; Table 2)

For $M \leq 6.15$

$$\sigma_{\ln Y_{C90V}} = \sigma_t \text{ from Campbell (1990) (Table 4; Table 5) magnitude range 4.7–6.1}$$

For $M > 6.15$

$$\sigma_{\ln Y_{C90V}} = \sigma_t \text{ from Campbell (1990) (Table 4; Table 5) magnitude range 6.2–7.8}$$

C93/94h

From Campbell (1993) with Campbell and Bozorgnia (1994) scaling,

$$\ln Y_{C93/94} = \ln Y'_{C93} + \ln A_{CB94} - \ln Y'_{C93}(T=0) \tag{A8}$$

where

$Y_{C93/94}$ = arithmetic mean of two horizontal peak accelerations in g or 5% damped pseudo-acceleration response spectra in g

$Y'_{C93}(T)$ = max $[Y_{C93}(T=0)\ ,\ Y_{C93}(T)]$, $T > 0$, *i.e.*, the pseudo-acceleration response is constrained to equal or exceed the predicted peak acceleration

A_{CB94} = geometric mean of peak horizontal accelerations in g from Campbell and Bozorgnia (1994)

$$\begin{aligned}\ln Y_{C93} = \beta_0 &+ 0.683M + \beta_1 \tanh\ [0.647(M-4.7)] \\ &- \ln\rho - \alpha r_c + 0.27\ F_c + (\beta_2 - 0.105\ \ln r_c)S \\ &+ \beta_3 \tanh\ (0.62D)\end{aligned} \tag{A9}$$

$$\rho = \left(r_c^2 + [0.0586\ \exp(0.683M)]^2\right)^{1/2}$$

$$\alpha = \beta_4 + \beta_5 M$$

$$S = \begin{cases} 0 & \text{for soil (not used in this report)} \\ 1 & \text{for site condition } G = 1\text{, hard rock} \end{cases}$$

β_0, β_1, β_2, β_3, β_4, β_5 from Campbell (1993) Table 1.

$$\sigma_{\ln Y_{C93/94}} = \begin{cases} \sigma_{\ln Y_{C93}} & \text{for horizontal response spectra} \\ \sigma_{\ln A_{CB94}} & \text{for horizontal peak acceleration} \end{cases} \tag{A10}$$

$\sigma_{\ln Y_{C93}}$ from Table 1, Campbell (1993). Note that Campbell (1993) says that $F_c = 0.5$ for normal faults, but we do not use $F_c = 0.5$ in any case.

I93h

From Idriss (1993),

$$\ln Y_{I93} = \alpha_0 + \exp(\alpha_1 + \alpha_2 M) + [\beta_0 - \exp(\beta_1 + \beta_2 M)] \ln(r_i + 20) + 0.2\ F \tag{A11}$$

where

Y_{I93} = geometric mean of two horizontal components of peak acceleration in g or pseudo-absolute spectral acceleration in g

$$F = \begin{cases} 0 & \text{for strike slip fault} \\ 0.5 & \text{for oblique slip (not used in this study)} \\ 1 & \text{for reverse fault (not used in this study)} \end{cases}$$

$\alpha_0, \alpha_1, \alpha_2, \beta_0, \beta_1, \beta_2$ - from Idriss (1993) Table A–4 Part 1 for $M \leq 6$,

- from Idriss (1993) Table A–4 Part 2 for $M > 6$

$\sigma_{\ln Y_{I93}}$ - from Idriss (1993) Table A–4 Parts 1 or 2, as appropriate, depending on M

JB88Vh, JB88Vz

From Joyner and Boore (1982, 1988)

$$\log Y = a + b\,(M - 6) + c\,(M - 6)^2 + d \log R + kR + s\Gamma \tag{A12}$$

where

Y = peak horizontal velocity in cm/s for a randomly oriented horizontal ($\equiv$ geometric mean)

R = $(r_b^2 + h^2)^{1/2}$

a, b, c, d, k, s, h - coefficients from Joyner and Boore (1988) Table 2

Γ = 0 for rock (site classes $G = 0, 1, 2$)

= 1 for soil (site classes $G = 5, 6, 7$)

(Note: factor s in Joyner and Boore, 1988, equation 5, implicitly included Γ)

Joyner and Boore (1988) give $\sigma'_{\log Y}$ for the randomly oriented horizontal, which differs from the standard deviation of the geometric mean horizontals. We use an approximate expression for the standard deviation of the geometric mean horizontal.

$$\sigma_{\log Y} = \left[\left(\sigma'_{\log Y}\right)^2 - SC^2\right]^{1/2} \tag{A13}$$

where

$\sigma_{\log Y}$ = standard deviation of the geometric mean horizontal peak velocity

$\sigma'_{\log Y}$ = standard deviation of the randomly oriented horizontal peak velocity, from Joyner and Boore (1988) Table 2

= 0.33

SC = component-to-component standard deviation for 5%-damped smoothed response spectra at 1.0 s period, from Boore *et al.* (1993) Table 7b

= 0.141

SP96h, SP96Vh

From Sabetta and Pugliese (1996),

$$\log Y_{SP} = a + bM - \log\left[\left(r_b^2 + h^2\right)^{1/2}\right] + e_1 S_1 + e_2 S_2 \tag{A14}$$

where

Y_{SP} = larger horizontal peak acceleration in g, or 5% damped pseudo-velocity response spectrum in cm/s, or larger horizontal peak velocity in cm/s

$$[S_1, S_2] = \begin{cases} [0,0] & \text{for rock, } G = 0,\ 1, \text{ or } 2 \\ [0,1] & \text{for deep soil, } G = 5 \text{ or } 6 \\ [1,0] & \text{for shallow soil, } G = 7 \end{cases}$$

a, b, e_1, e_2, h - from "smooth" coefficients from Sabetta and Pugliese (1996) Table 1.

$\sigma_{\log Y_{PS}}$ - from "smooth" coefficients, Table 1.

Note that all coefficients in Sabetta and Pugliese (1996) Table 1 are identical to those in Pugliese and Sabetta (1989), except for those for peak ground velocity. The peak ground velocity coefficients of Sabetta and Pugliese (1996) agree with those of Sabetta and Pugliese (1987, Table 5).

S93h, S93z

From Sadigh *et al.* (1993),

$$\begin{aligned} \ln Y_{S93} = c_1 + c_2 M + c_3 (8.5 - M)^{2.5} + c_4 \ln\left[r_i + \exp\left(c_5 + c_6 M\right)\right] \\ + c_7 \ln(r_i + 2) + c_8 \end{aligned} \tag{A15}$$

where

for vertical motion

Y_{S93} = peak ground acceleration in g, or response spectral acceleration in g

c_1, c_2, c_3, c_4, c_5, c_6 from Sadigh *et al.* (1989) Table 3.

$c_7 \equiv 0$.

$$c_8 \begin{cases} = 0 & \text{for strike-slip faulting} \\ = \ln(1.048) & \text{for oblique faulting (not used in this report)} \\ = \ln(1.1) & \text{for reverse faulting (not used in this report)} \end{cases}$$

for horizontal motion

Y_{S93} = geometric mean of two horizontal components of peak accelerations in g or response spectral acceleration in g

c_1, c_2, c_3, c_4, c_5, c_6, c_7 from Sadigh *et al.* (1989) Table 1.

$$c_8 \begin{cases} = 0 & \text{for strike-slip faulting} \\ = \ln(1.09) & \text{for oblique faulting (not used in this report)} \\ = \ln(1.2) & \text{for reverse faulting (not used in this report)} \end{cases}$$

for all components.

$\sigma_{\ln Y_{S93}}$ - from their p. 62, for vertical motion

- from their Table 2 for horizontal motion

APPENDIX B. A new ground motion prediction relationship developed from extensional regime data.

We have developed new ground-motion prediction equations for geometric mean peak horizontal acceleration and 5% damped response for the extensional region strong-motion data set. We initially attempted to derive a new regression relation solely from our extensional regime data set, using the computer programs used by Boore *et al.* (1993), based on algorithms for the two-stage regression method described by Joyner and Boore (1993, 1994). For periods of 0.1 s and greater, the resulting relationship was satisfactory within the magnitude range covered by the extensional regime data set, but it could not validly be extrapolated to magnitudes 7.0 and larger. The main problem is that our extensional regime data set does not span a magnitude range that is wide enough to determine the coefficients of magnitude dependent terms accurately. In the two-stage method, the magnitude dependence is determined in the second stage of the regression. A linear or quadratic dependence can be chosen, as in equation (3) of Joyner and Boore (1988). In the analysis of the extensional regime data set, we chose a linear dependence for all periods (*i.e.,* we set the quadratic coefficient $c = 0$ in equation (3) of Joyner and Boore, 1988), even though the quadratic coefficient was statistically significant for some short period response values. We chose the linear dependence because the quadratic magnitude dependence caused predicted short period response values for a magnitude 7.5 event to be less than those for a magnitude 6.5 event. This behavior does not occur in other strong-motion data sets and was considered inappropriate, so we rejected the quadratic dependence. Examination of the scatter plots of the output from the first stage regression confirmed that the data do not support a quadratic magnitude dependence. Because of the linear magnitude dependence, extrapolation of the initial relation to higher magnitudes beyond the range of the data was particularly inappropriate, since some data sets (Joyner and Boore, 1981, 1982; Boore *et al.*, 1993) clearly show that the response values do not increase linearly with magnitude at larger magnitudes. Consequently, we were forced to discard our initial relationship.

In order to develop a relationship that would be valid for magnitude 7 and larger we retained the magnitude dependence determined from a larger data set by Boore *et al.* (1993, 1994) and used our extensional regime data set to constrain the distance and site dependent terms. This approach made maximum use of the extensional regime data set consistent with the desire for a relation valid above magnitude 7. It is unfortunate that we are forced to adopt the magnitude dependence developed from a different tectonic regime, since it would have been interesting to investigate whether the magnitude dependence of extensional regime events differs from that of other regimes. However, our data set does not span a range of magnitudes wide enough to answer that question in any case. To develop a relation for the extensional regime data set, at each period we formed the following residuals:

$$r_j = y_j - b_2(M-6) - b_3(M-6)^2$$

where y_j are common logarithms of the the extensional regime data set ground-motion values, b_2 and b_3 are the Boore *et al.* (1994) coefficients, and M is moment magnitude. We then used the two-stage regression method (Joyner and Boore, 1993, 1994) to fit the residuals by an equation of the form

$$b_1 + b_5 \log_{10}(R) + b_6 \Gamma \ ,$$

where $R = \sqrt{(r_b^2 + h^2)}$, r_b is the Boore–Joyner distance, h is from Boore *et al.* (1994), Γ is zero for rock sites and 1 for soil sites, and b_1, b_5, and b_6 are adjusted to fit the data. The resulting set of coefficients for 5% damped horizontal response were smoothed by fitting cubics or quadratics. Curves for *psv* predicted from unsmoothed and smoothed coefficients for a variety of magnitudes, distances, and site classes are given in Figures B1 through B8.

The equations for the predictive relations follow. σ_1 and σ_2 are the standard deviations of ϵ_r and ϵ_e (Boore *et al.*, 1993, equation 1), which are respectively the record to record variation and the earthquake to earthquake variation in the residuals. Note that Table B1 contains a column for σ_3, which is the component standard deviation (*i.e.*, it is σ_c in Boore *et al.*, 1993, equation 3). σ_3 is not used to define the standard deviation of the geometric mean, but it is used to form the standard deviation of the randomly oriented horizontal, which is $\sqrt{(\sigma_1^2 + \sigma_2^2 + \sigma_3^2)}$. This relation may be used in the 5.0–7.7 magnitude range and the 0–100 km distance range.

Sea96h

$$\log Y = b_1 + b_2(M-6) + b_3(M-6)^2 + b_4 R + b_5 \log R + b_6 \Gamma \qquad \text{(B1)}$$

$$\sigma_{\log Y} = (\sigma_1^2 + \sigma_2^2)^{1/2}$$

where

$$R = (r_b^2 + h^2)^{1/2}$$

Γ = 0 for rock (site classes $G = 0, 1, 2$)

= 1 for soil (site classes $G = 5, 6, 7$)

$\sigma_{\log Y}$ = the standard deviation of $\log Y$

Y = peak horizontal acceleration (g) or pseudovelocity response (cm/s) at 5% damping for the geometric mean horizontal component of motion

$b_1, b_2, b_3, b_4, b_5, b_6, h, \sigma_1, \sigma_2$ - from Table B1.

LIST OF TABLES

LIST OF FIGURES

a frequency-independent Q, and the inversions of the G1 and G4 groupings with the frequency-dependent $Q = Q_0 f^{\alpha}$ where $\alpha = 0.15$ and 0.35, respectively. The attenuation of Lg-waves in the Great Basin, determined by Benz *et al.* (1996) is also plotted.

Figure 6. Weak motion attenuation curves plotted against the pseudo-velocity response spectral ordinates for 1.0, 3.3, and 10 Hz. The two points plotted at each hypocentral distance are the two horizontal components of each station. The attenuation curves have been shifted to fit the spectral ordinates for the rock stations.

Figure 7. Definition of fault geometry and the rectangular region taken to be the source area.

Figure 8. Histogram of moment magnitudes of earthquakes analyzed in this report.

Figure 9. Magnitude/distance sampling for the data set used in this report. Circle shows closest distance to the rupture surface, used by relations I93 and S93 (dIS in Table 1). + shows distance to the surface projection of the rupture surface, used by relations BJF94, SP96, and our new relationship Sea96. (dBJ in Table 1). The dashed line is an empirical curve indicating the distance at which non-triggered stations tend to occur. a) rock sites (G = 0, 1, 2). b.) soil sites (G = 5, 6, 7).

Figure 10. Summary of ground motion data used in this report. Site geology symbols are: o - G = 0, 2, soft rock or rock of unknown hardness; . - G = 1, hard rock; + - G = 5, 6, deep soil or soil of unknown thickness; $\times$ - G = 7, shallow soil. Period and magnitude range shown at the top of each panel, with T = 0 s corresponding to peak acceleration. Upper panel in each plot shows values for each horizontal component. Lower panel shows values for vertical component. a–av) peak acceleration and pseudo-absolute acceleration. aw–az) peak velocity.

Figure 11. Residuals for each predictive relation for *pga* as a function of distance for each period, using data at all distances. Annotation at the top of each panel indicates the relation used, the direction of motion (h = horizontal, z = vertical), the site geology code G (see Table 5), a code identifying the computer run ('may1696b'), and T, the period of motion. The *pga* residuals are labelled as $T = 0$ s, and plots for other periods are response spectral residuals (*psv* or *paa*, as appropriate to the relation). Plotted symbols depend on magnitude: dot - $5.0 \leq \mathbf{M} < 5.5$; o - $5.5 \leq \mathbf{M} < 6.0$; $\times$ - $6.0 \leq \mathbf{M} < 6.5$; + - $6.5 \leq \mathbf{M} < 7.0$; * - $7.0 \leq \mathbf{M}$. On the plots, in the labels 'bias $= a + / - b$', a and b correspond to the terms b_{ijk} and σ_b, respectively, and '$sigma - p$' is the term σ_p. Vertical line at -5 km distance is the mean b_{ijk} plus/minus one standard deviation of the mean σ_b. Vertical line at -7.5 km distance is the mean b_{ijk} plus/minus one population standard deviation σ_p. s_r is the slope of the dashed line.

Figure 12. Residuals for each predictive relation for *pga* and response spectrum as a function of magnitude. Annotation is identical to that of Figure 11, with s_m being the slope of the best fitting line. Plotted symbols depend on distance: dot - $0 \leq r < 20$ km; o - $20 \leq r < 40$ km; $\times$ - $40 \leq r < 60$ km; + - $60 \leq r < 80$ km; $*$ - $r \geq 80$ km. Note that each panel of this figure contains exactly the same data points as the corresponding panel of Figure 11, so the biases are identical between this figure and Figure 11.

Figure 13. Residuals for each predictive relation for peak velocity as a function of distance. Annotation is identical to that of Figure 11, with s_r being the slope of the best fitting line.

Figure 14. Residuals for each predictive relation for peak velocity as a function of magnitude. Annotation is identical to that of Figure 12, with s_m being the slope of the best fitting line. Note that each panel of this figure contains exactly the same data points as the corresponding panel of Figure 13, so the biases are identical between this figure and Figure 13.

Figure 15. *pga* and response spectral correction factors for data at all distances. Upper panel of each figure shows the bias b, the standard deviation of the bias, σ_b (inner error bars) and the population standard deviation σ_p (outer error bars) taken from Figure 11 and Table 9. Middle panel shows probability Q (plotted as +'s) (or $1 - Q$, plotted as $\times$'s) for each attenuation relation. Q values below 0.05 are plotted as $\times$'s at ordinate values of $1 - Q$ (*i.e.*, $Q = 0.01$ is plotted as an $\times$ at 0.99); Q values above 0.95 are plotted as +'s, and Q values between 0.05 and 0.95 are plotted as o's along the bottom axis. Values for *pga* are plotted at period = 0.02 s ($\log 10(0.02) = -1.7$). Lower panel: Dispersion correction factor e_{ijk} and its standard deviation σ_e. σ_e and Q are two different measures of the significance of the dispersion correction factor.

Figure 16. Comparison of all relations' peak acceleration and response spectral correction factors and slope parameters as functions of period. Q_s statistic plotted to the right of each author's results. See Figure 15 caption for explanation of o, $\times$, and + symbols.

a) Bias b_{ijk} for all relations, horizontal motions. Error bars are σ_b.

b) Bias b_{ijk} for all relations, vertical motions. Error bars are σ_b.

c) Dispersion correction e_{ijk} for all relations, horizontal motions. Error bars are σ_e.

d) Dispersion correction e_{ijk} for all relations, vertical motions. Error bars are σ_e.

e) Slope s_r of the dependence of residuals on distance for all relations, horizontal motions. Error bars are σ_r.

f) Slope s_r of the dependence of residuals on distance for all relations, vertical motions. Error bars are σ_r.

g) Slope s_m of the dependence of residuals on magnitude for all relations, horizontal motions. Error bars are σ_m.

h) Slope s_m of the dependence of residuals on magnitude for all relations, vertical motions. Error bars are σ_m.

Figure 17. Peak velocity correction factors and slope parameters for all prediction relations. In all plots there is one data point per prediction relation (horizontal axis in all plots corresponds to an arbitrary prediction relation number). a) Same format as Figure 15. Middle panel has labels identifying each prediction relation explicitly. b) Dependences of residuals on distance and magnitude. Upper (first) panel shows s_r with error bars σ_r. Second panel shows χ^2 statistic Q_r associated with straight line fit. Third panel shows s_m with error bars σ_m. Fourth panel shows χ^2 statistic Q_m associated with straight line fit.

Figure 18. Correction factors for *pga* and response spectra for data at distances less than or equal to 20 km, taken from Table 12. See Figure 15 caption for details.

Figure 19. Comparison of all relations' *pga* and response spectra correction factors and slope parameters for data at distances less than or equal to 20 km. Distance dependences not shown owing to restricted distance interval. See Figure 16 caption for details.

Figure 20. Comparison of all peak velocity relations' correction factors for data at distances less than or equal to 20 km. See Figure 17 for details.

Figure 21. *pga* and response spectral residuals as a function of distance and period for individual earthquakes and components. The *pga* residuals are labeled as $T =$ 0 s, and plots for other periods are response spectral residuals (*psv* or *paa*, as appropriate to the predictive relation). Relations are indicated by the following symbols: 1 = BJF94, 2 = C89/94 h or C89 z, 3 = C90/94 h or C90 z, 4 = C93/94 h, 5 = I93 h, 6 = SP96 h, 7 = S93 h or S93 z, and d = Sea96 h. Annotations at the top of each plot give the event, period, and direction of motion (h = horizontal, z = vertical). Events are a,b,c,d) 1979 Imperial Valley main shock $\mathbf{M} = 6.5$; e,f,g,h) 1980 Irpinia main shock $\mathbf{M} = 6.9$; i,j,k,l) 1981 Westmorland, California, earthquake $\mathbf{M} = 5.8$; m,n) 1983 Borah Peak, Idaho, main shock (horizontals only) $\mathbf{M} = 6.9$; o,p) 1983 Borah Peak aftershock, $\mathbf{M} =$ 5.1; q,r,s,t) 1986 Chalfant Valley, California, foreshock $\mathbf{M} = 5.8$; u,v,w,x) 1986 Chalfant Valley, California, main shock $\mathbf{M} = 6.3$; y,z,aa,ab) 1992 Roermond,

The Netherlands, main shock **M** = 5.31; ac, ad, ae, af) 1992 Little Skull Mountain, Nevada, main shock **M** = 5.7.

Figure 22. Peak velocity residuals for selected earthquakes and components as a function of distance. Relations are indicated by the following symbols: 8 = C89V h or z, 9 = C90V h or z, 10 = JB88V h or z, 11 = SP96V h. Events are a,b) 1979 Imperial Valley main shock **M** = 6.5; c,d) 1980 Irpinia main shock **M** = 6.9; e,f) 1981 Westmorland, California, earthquake **M** = 5.8; g) 1983 Borah Peak, Idaho, main shock (horizontals only) **M** = 6.9; h) 1983 Borah Peak aftershock, **M** = 5.1; i,j) 1986 Chalfant Valley, California, foreshock **M** = 5.8; k,l) 1986 Chalfant Valley, California, main shock **M** = 6.3; m) 1992 Roermond, The Netherlands, main shock **M** = 5.31; n,o) 1992 Little Skull Mountain, Nevada, main shock **M** = 5.7.

Figure 23. *pga* and response spectral residuals as a function of distance and component for Little Skull Mountain earthquake of 1992/6/29 1014 with expanded residual scale.

Figure 24. Comparison of *pga* and *psv* residuals at all periods and for both horizontal and vertical motions, for normal faulting and strike-slip events. Upper left panel shows number of ground motion records associated with event rakes ('reflected rake' is true rake reflected around a vertical axis). Lower left panel shows distribution of residuals for strike-slip events. Lower right panel shows distribution of residuals for normal faulting events.

Figure 25. Comparison of strong motion relations' predicted peak velocities with weak motion predictions at 3 different periods. Assumed point source is at 6 km depth, and the appropriate distance (epicentral or hypocentral) is used for each predictive relation.

Figure 26. Comparison of strong motion relations' predicted response spectra with weak motion predictions at 3 different periods. Assumed point source is at 6 km depth, and the appropriate distance (epicentral or hypocentral) is used for each predictive relation. a) 0.1 s period. b) 0.3 s period. c) 1.0 s period.

FIGURE CAPTIONS

Figure B1. Predicted *psv* from unsmoothed coefficients (thin lines) and from smoothed coefficients used in Sea96 (thick lines). Rock site at distance $r_b = 0$ km, for magnitudes 5.5, 6.5, and 7.5.

Figure B2. Predicted *psv* from unsmoothed coefficients (thin lines) and from smoothed coefficients used in Sea96 (thick lines). Soil site at distance $r_b = 0$ km, for magnitudes 5.5, 6.5, and 7.5.

Figure B3. Predicted *psv* from unsmoothed coefficients (thin lines) and from smoothed coefficients used in Sea96 (thick lines). Magnitude 5.5 at a rock site, distances $r_b = 0$, 10, 20, 40, and 80 km.

Figure B4. Predicted *psv* from unsmoothed coefficients (thin lines) and from smoothed coefficients used in Sea96 (thick lines). Magnitude 5.5 at a soil site, distances $r_b = 0$, 10, 20, 40, and 80 km.

Figure B5. Predicted *psv* from unsmoothed coefficients (thin lines) and from smoothed coefficients used in Sea96 (thick lines). Magnitude 6.5 at a rock site, distances $r_b = 0$, 10, 20, 40, and 80 km.

Figure B6. Predicted *psv* from unsmoothed coefficients (thin lines) and from smoothed coefficients used in Sea96 (thick lines). Magnitude 6.5 at a soil site, distances $r_b = 0$, 10, 20, 40, and 80 km.

Figure B7. Predicted *psv* from unsmoothed coefficients (thin lines) and from smoothed coefficients used in Sea96 (thick lines). Magnitude 7.5 at a rock site, distances $r_b = 0$, 10, 20, 40, and 80 km.

Figure B8. Predicted *psv* from unsmoothed coefficients (thin lines) and from smoothed coefficients used in Sea96 (thick lines). Magnitude 7.5 at a soil site, distances $r_b = 0$, 10, 20, 40, and 80 km.

TABLE 1. SGBSN Stations

Station	Latitude	Longitude	EQs	Δ (km)	f_{max} (Hz)	Geology
AMR	36° 23.85'	-116° 28.56'	0	-	-	conglomerate
APKW	36° 19.19'	-115° 35.25'	19	79	30	limestone, dolomite
BGB	37° 2.24'	-116° 13.75'	11	35	7	bedded tuff
BLT	37° 28.98'	-116° 7.41'	14	87	10	ash-flow tuff
BMTN	37° 17.50'	-116° 38.41'	13	71	18	trachyte lava
CDH1	36° 51.82'	-116° 18.97'	9	16	10	argillite
CPY	36° 55.73'	-116° 3.53'	0	-	-	limestone
CTS	37° 39.37'	-116° 43.59'	7	110	20	intrusive mafic rock
DLM	37° 36.35'	-114° 44.27'	12	170	15	limestone, dolomite
EMN	35° 55.31'	-114° 45.33'	0	-	-	andesite and basalt
EPM	37° 13.57'	-116° 20.08'	10	56	30	ash-flow tuff
EPR	37° 10.12'	-115° 11.23'	18	110	20	volcanic rock
FMT	36° 38.27'	-116° 47.00'	11	47	20	metamorphic rock
GLR	37° 11.94'	-116° 1.01'	6	60	20	limestone, dolomite
GMN	37° 18.04'	-117° 15.44'	18	109	17	granite
GMR	37° 20.02'	-115° 46.36'	15	82	20	limestone, dolomite
GVN	36° 59.94'	-117° 20.78'	21	100	20	fanglomerate
GWY	36° 11.15'	-116° 40.21'	12	70	8	volcanic rock
HCR	38° 14.01'	-116° 26.20'	14	169	12	ash-flow tuff
JON	36° 26.39'	-116° 6.28'	0	-	-	quartzite
KRNA	37° 44.53'	-116° 22.89'	17	114	20	ash-flow tuff
LOP	36° 51.27'	-116° 10.11'	6	21	30	lava
LCH	37° 13.95'	-117° 38.78'	0	-	-	limestone, dolomite
LSME	36° 44.55'	-116° 16.33'	32	10	30	basalt
MCA	36° 38.77'	-117° 16.69'	14	90	20	limestone, dolomite
MCY	36° 39.64'	-115° 57.67'	7	33	20	limestone, dolomite
MGM	37° 26.44'	-117° 29.93'	20	135	10	quartzite
MTI	37° 40.68'	-115° 16.72'	6	138	15	carbonates
NOP	36° 7.63'	-116° 9.26'	0	-	-	limestone
NPN	37° 39.12'	-114° 56.21'	19	158	17	ash-flow tuff
PAN	36° 23.59'	-117° 6.05'	18	83	20	limestone, dolomite
PPK	37° 25.51'	-117° 54.42'	13	165	15	granite
PRN	37° 24.40'	-115° 3.05'	10	133	15	ash-flow tuff
QCS	37° 45.39'	-115° 56.58'	19	118	15	basalt
QSM	35° 57.85'	-116° 52.05'	15	100	25	tuff
SDH	36° 38.72'	-116° 20.38'	0	-	-	quartzite
SGV	36° 58.92'	-117° 2.11'	11	74	15	rhyolite
SHRG	36° 30.33'	-115° 9.61'	12	103	10	limestone, dolomite
SPRG	36° 41.64'	-115° 48.63'	17	45	7	tuffaceous sediment

Table1 p1/2

SRG	37° 52.93'	-115° 4.15'	9	168	16	volcanic rock
SSP	36° 55.53'	-116° 13.26'	6	23	20	ash-flow tuff
SVP	37° 42.89'	-117° 48.20'	4	174	15	andesite and breccia
TCN	37° 8.80'	-116° 43.52'	10	61	30	ash-flow tuff
TMBR	37° 2.11'	-116° 23.21'	6	37	30	granitic ring-dikes
TMO	36° 48.29'	-117° 24.30'	13	100	15	limestone, dolomite
TPU	37° 36.27'	-115° 39.06'	18	113	20	shale and sandstone
WCT	36° 47.79'	-116° 37.62'	0	-	-	alluvium
WRN	37° 58.89'	-115° 35.58'	16	153	15	limestone, dolomite
EYM4	36° 50.99'	-116° 27.18'	13	22	30	welded tuff
NYM4	36° 50.99'	-116° 27.18'	15	22	30	welded tuff

Table 2. Propagation Parameters

grouping	#g	variance	γ	Q_0	Q(16)	α	κ	median f_c
G1	3	0.725%	0.526	623	623	0.0	-0.002 s	13.48 Hz
G1F	3	0.722%	0.450	401	608	0.15	-0.001 s	12.87 Hz
G2	8	0.508%	0.609	643	643	0.0	-0.007 s	11.12 Hz
G3	8	0.494%	0.684	706	706	0.0	-0.007 s	10.55 Hz
G4	8	0.394%	0.776	662	662	0.0	+0.003 s	12.41 Hz
G41	8	0.390%	0.722	489	642	0.1	+0.003 s	12.57 Hz
G43	8	0.385%	0.625	274	629	0.3	+0.004 s	12.61 Hz
G4F	8	0.385%	0.601	238	628	0.35	+0.002 s	12.31 Hz
G45	8	0.387%	0.539	159	637	0.5	+0.005 s	11.90 Hz
G47	8	0.399%	0.514	100	696	0.7	+0.007 s	10.59 Hz

Table 2 p!

Table 3. Strong motion stations.

Station	Latitude	Longitude	Δ (km)	Geology
LTHP/LSM1	36°38.4′	−116°24.0′	16	deep soil
CPT1/LSM2	36°55.8′	−116°03.6′	25	"unknown" rock
BTYA/LSM3	36°54.6′	−116°45.6′	46	"unknown" rock
PAH2/LSM4	36°13.8′	−116° 7.4′	60	deep soil
PAHA/LSM5	36°12.6′	−115°58.8′	65	deep soil
CALB/LSM6	36° 9.0′	−115°24.6′	100	hard rock
ANNR/LSM7	36°15.6′	−115°18.6′	100	deep soil
SCT2/LSM8	37° 1.8′	−117°20.4′	98	"unknown" rock

Table 3 p 1/1

Table 4. List of studied earthquakes and records, with their associated parameters (ymay1696a.rpt).

QCod, Scod - arbitrary numbers assigned to each earthquake and station. See Table 6 for station names
M - moment magnitude assigned in this report
Rake - slip angle assigned in this report (= -999 when not known)
G - site geology code assigned in this report
dBJ dCA dIS - distances, according to the BJF94, Campbell(1989), and Idriss(1993) definitions
pah1 pah2 pav - peak accelerations on horizontal and vertical channels of the PEA-processed data (blank when record missing)
D_2_B - depth to basement, km, according to Campbell(1989) definition (= -99 when not known)
Direc FileNH1 FileNH2 FileNV - directory and file names of the response spectral files (blank when response spectrum not used)

QCod	Date____	HrMn	M___	Rake	SCod	G	dBJ__	dCA__	dIS__	pah1_	pah2_	pa_v_	pvh1_	pvh2_	pv_v_	Direc____	FileN_H1	FileN_H2	FileN_V	D_2_B
8	40.05.19	536	6.87	180	14	6	6.3	7.6	6.3	.313	.215	.205	29.8	30.2	10.7	impvall	i-elc180	i-elc270	i-elcvrt	5.0
79	72.12.23	629	6.20	-99	1139	6	3.5	4.8	4.1	.421	.337	.377	21.4	26.1	12.5	Managua	a-man090	a-man180	a-mandwn	-99.0
364	79.09.19	2135	5.90	-999	1353	0	4.3	7.4	7.4	.200	.161	.146	8.5	11.6	4.2	italy	f-cas-ew	f-cas-ns	f-cas-vt	-99.0
364	79.09.19	2135	5.90	-999	1357	6	36.0	36.5	36.5	.040	.023	.025	2.1	1.1	.9	italy	f-bev-ns	f-bev-ew	f-bev-vt	-99.0
147	79.10.15	2316	6.50	180	89	2	24.5	25.0	24.5	.195	.109	.077	5.2	8.8	2.3	impvall	h-sup135	h-sup045	h-sup-up	-99.0
147	79.10.15	2316	6.50	180	104	6	8.6	9.7	8.6	.224	.171	.105	47.5	41.0	8.8	impvall	h-e10320	h-e10050	h-e10-up	4.9
147	79.10.15	2316	6.50	180	159	6	35.4	36.7	36.7	.109	.069	.034	11.9	8.3	3.8	impvall	h-nil090	h-nil360	h-nil-up	2.2
147	79.10.15	2316	6.50	180	222	6	1.0	3.2	1.0	.519	.379	.537	46.9	90.5	38.5	impvall	h-e05140	h-e05230	h-e05-up	5.7
147	79.10.15	2316	6.50	180	224	6	4.2	5.2	4.2	.485	.360	.248	37.4	76.6	16.0	impvall	h-e04140	h-e04230	h-e04-up	5.6
147	79.10.15	2316	6.50	180	798	6	.6	3.4	.6	.463	.338	.544	47.6	109.3	26.4	impvall	h-e07230	h-e07140	h-e07-up	5.4
147	79.10.15	2316	6.50	180	821	6	12.5	13.3	12.5	.204	.111	.159	17.8	16.1	6.8	impvall	h-pts315	h-pts225	h-pts-up	4.8
147	79.10.15	2316	6.50	180	823	6	10.4	11.4	10.4	.275	.202	.187	21.2	16.0	6.7	impvall	h-cxo225	h-cxo315	h-cxo-up	5.0
147	79.10.15	2316	6.50	180	824	6	.4	3.8	2.7	.775	.588	.425	45.2	45.9	12.2	impvall	h-bcr230	h-bcr140	h-bcr-up	4.8
147	79.10.15	2316	6.50	180	825	6	5.5	7.8	7.6	.253	.221	.230	48.8	49.8	9.9	impvall	h-hvp225	h-hvp315	h-hvp-up	5.3
147	79.10.15	2316	6.50	180	826	6	15.9	16.2	15.9	.139	.134	.056	16.0	10.7	3.8	impvall	h-e01140	h-e01230	h-e01-up	3.5
147	79.10.15	2316	6.50	180	827	6	9.1	9.6	9.1	.266	.221	.127	46.8	39.9	8.7	impvall	h-e03140	h-e03230	h-e03-up	5.7
147	79.10.15	2316	6.50	180	828	6	12.5	13.4	12.5	.380	.364	.140	34.5	42.1	11.1	impvall	h-e11230	h-e11140	h-e11-up	5.0
147	79.10.15	2316	6.50	180	829	6	22.0	22.8	22.0	.139	.117	.046	14.7	13.0	3.2	impvall	h-e13230	h-e13140	h-e13-up	3.3
147	79.10.15	2316	6.50	180	830	6	8.4	10.3	9.9	.220	.160	.146	35.9	38.9	8.4	impvall	h-bra315	h-bra225	h-bra-up	5.2
147	79.10.15	2316	6.50	180	831	6	23.3	24.7	24.7	.128	.078	.055	15.4	13.3	3.9	impvall	h-cal225	h-cal315	h-cal-up	5.1
147	79.10.15	2316	6.50	180	836	6	48.8	49.8	49.8	.128	.115	.038	12.5	15.6	3.6	impvall	h-cc4135	h-cc4045	h-cc4-up	-99.0
147	79.10.15	2316	6.50	180	874	6	10.4	10.9	10.4	.315		.110	31.5		7.6	impvall	h-e02140		h-e02-up	5.5
147	79.10.15	2316	6.50	180	912	6	7.4	8.5	7.4	.235	.213	.246	37.5	68.8	18.1	impvall	h-elc092	h-elc002	h-elc-up	4.8
147	79.10.15	2316	6.50	180	913	6	0.0	3.2	.1	.314	.296	.248	71.7	90.5	28.9	impvall	h-emo000	h-emo270	h-emo-up	4.5
147	79.10.15	2316	6.50	180	917	6	0.0	3.1	.9	.439	.410	1.655	64.9	109.8	57.5	impvall	h-e06230	h-e06140	h-e06-up	5.6
147	79.10.15	2316	6.50	180	918	6	3.9	5.5	3.9	.602	.454	.439	54.3	49.1	22.3	impvall	h-e08140	h-e08230	h-e08-up	5.1
147	79.10.15	2316	6.50	180	924	6	5.2	6.5	5.2	.480	.352	.707	71.2	40.8	20.7	impvall	h-eda360	h-eda270	h-eda-up	5.0
147	79.10.15	2316	6.50	180	928	6	14.6	15.3	15.1	.110	.074		21.2	21.9		impvall	h-wsm180	h-wsm090		5.2
147	79.10.15	2316	6.50	180	1141	6	18.0	18.8	18.0	.143	.116	.066	17.6	21.8	6.7	impvall	h-e12140	h-e12230	h-e12-up	4.4
147	79.10.15	2316	6.50	180	1215	6	0.0	3.2	.4	.327	.260	.142	42.8	24.9	5.6	impvall	h-aep045	h-aep315	h-aep-up	4.8
147	79.10.15	2316	6.50	180	1216	6	0.0	3.2	.7	.370	.221		35.6	42.4		impvall	h-ag003	h-ag273		5.0
147	79.10.15	2316	6.50	180	1217	2	15.2	16.0	15.2	.169	.157	.212	11.6	18.6	6.8	impvall	h-cp147	h-cp237	h-cpdwn	-99.0
147	79.10.15	2316	6.50	180	1218	6	7.2	8.2	7.2	.270	.254	.218	24.9	30.1	5.1	impvall	h-ch012	h-ch282	h-chdwn	6.0
147	79.10.15	2316	6.50	180	1219	6	13.5	15.3	15.3	.186	.147	.075	13.9	9.5	2.9	impvall	h-cmp015	h-cmp285	h-cmpdwn	4.5
147	79.10.15	2316	6.50	180	1220	6	1.0	3.3	1.1	.309		.140	36.3		3.1	impvall	h-qkp085		h-qkp-up	6.0
147	79.10.15	2316	6.50	180	1221	6	21.9	22.4	21.9	.351	.238	.145	26.0	33.0	14.8	impvall	h-dta352	h-dta262	h-dtadwn	7.5
147	79.10.15	2316	6.50	180	1223	6	31.8	32.1	31.8	.167	.122	.059	6.4	8.3	1.6	impvall	h-vct345	h-vct075	h-vct-up	7.0
157	80.05.25	1633	6.20	-35	431	6	1.1	6.6	6.6	.442	.416	.388	23.3	23.1	20.5	mammoth	i-cvk180	i-cvk090	i-cvk-up	-99.0
157	80.05.25	1633	6.20	-35	559	6	4.5	6.6	4.7	.321	.239	.253	11.2	15.7	13.9	mammoth	i-mls270	i-mls360	i-mls-up	-99.0

Table 4 p 1/3

159	80.05.25	1649	5.80	0	431	6	2.9	9.5	9.5	.178	.160	.129	11.3	12.2	9.0	mammoth	j-cvk180	j-cvk090	j-cvk-up	-99.0
159	80.05.25	1649	5.80	0	559	6	3.5	9.7	9.7	.441	.390	.264	22.5	23.9	9.0	mammoth	j-mls000	j-mls270	j-mls-up	-99.0
160	80.05.25	1944	5.80	-11	431	6	1.7	10.6	10.6	.219	.208	.195	18.5	16.1	8.5	mammoth	a-cvk090	a-cvk180	a-cvk-up	-99.0
160	80.05.25	1944	5.80	-11	1330	1	10.1	18.0	18.0	.107	.070	.078	5.9	5.5	4.4	mammoth	a-lvd090	a-lvd000	a-lvd-up	.1
162	80.05.25	2035	5.70	-999	431	6	2.8	5.7	5.7	.432	.380	.345	13.3	21.0	6.2	mammoth	b-cvk180	b-cvk090	b-cvk-up	-99.0
162	80.05.25	2035	5.70	-999	1330	1	14.2	15.1	15.1	.089	.046	.058	5.0	2.3	2.1	mammoth	b-lvd000	b-lvd090	b-lvd-up	.1
167	80.05.27	1450	6.00	-28	250	5	41.0	43.3	43.3	.114	.091	.084	5.5	5.3	3.0	mammoth	l-bpl160	l-bpl070	l-bpl-up	1.2
167	80.05.27	1450	6.00	-28	431	6	5.9	9.3	9.3	.316	.266	.188	19.1	16.2	9.6	mammoth	l-cvk180	l-cvk090	l-cvk-up	-99.0
167	80.05.27	1450	6.00	-28	432	5	41.8	44.1	44.1	.175	.109	.064	7.0	11.2	3.1	mammoth	l-ben360	l-ben270	l-ben-up	1.2
167	80.05.27	1450	6.00	-28	1354	5	6.0	9.3	9.3	.400	.395	.179	14.4	14.8	10.4	mammoth	l-fis090	l-fis000	l-fis-up	-99.0
171	80.06.09	328	6.32	0	1220	6	25.1	25.4	25.4	.092		.067	13.1		10.9	vict	cup085		cup-up	6.0
171	80.06.09	328	6.32	0	1222	6	38.6	38.8	38.8	.101	.068	.047	7.8	9.0	2.4	vict	shp010	shp280	shp-up	5.5
360	80.11.23	1834	6.90	-90	1321	2	24.9	28.1	28.1	.100	.083	.067	23.6	12.5	14.2	italy	a-bis000	a-bis270	a-bisvrt	-99.0
360	80.11.23	1834	6.90	-90	1322	6	43.1	45.0	45.0	.053	.038	.023	2.5	2.8	1.6	italy	a-bov270	a-bov000	a-bovvrt	-99.0
360	80.11.23	1834	6.90	-90	1324	2	11.2	16.3	16.3	.176	.132	.146	16.7	18.7	9.1	italy	a-cal270	a-cal000	a-calvrt	-99.0
360	80.11.23	1834	6.90	-90	1325	6	36.3	38.3	36.4	.145	.089	.054	8.9	10.7	2.5	italy	a-mer270	a-mer000	a-mervrt	.1
360	80.11.23	1834	6.90	-90	1326	2	25.9	29.0	29.0	.106	.104	.067	6.3	6.1	4.2	italy	a-rio000	a-rio270	a-riovrt	-99.0
360	80.11.23	1834	6.90	-90	1327	2	16.2	17.6	17.6	.358	.251	.260	37.0	52.7	26.0	italy	a-stu270	a-stu000	a-stuvrt	-99.0
360	80.11.23	1834	6.90	-90	1328	1	67.7	69.4	67.7	.063	.040	.033	6.8	9.4	6.8	italy	a-tor000	a-tor270	a-torvrt	-99.0
360	80.11.23	1834	6.90	-90	1355	0	63.0	64.1	63.0	.041	.031	.019	2.9	2.4	2.4	italy	a-ari270	a-ari000	a-arivrt	-99.0
360	80.11.23	1834	6.90	-90	1356	0	10.9	13.3	10.9	.202	.139	.108	22.1	32.0	14.2	italy	a-bag270	a-bag000	a-bagvrt	-99.0
367	80.11.23	1835	6.20	-90	1320	2	28.9	30.0	30.0	.023	.019	.016	2.4	2.3	2.6					-99.0
367	80.11.23	1835	6.20	-90	1321	2	22.1	23.7	22.1	.076	.072	.050	10.5	14.4	7.0					-99.0
367	80.11.23	1835	6.20	-90	1322	6	43.0	44.5	43.0	.026	.022	.017	2.4	2.1	1.2					-99.0
367	80.11.23	1835	6.20	-90	1323	6	41.9	42.8	42.8	.043	.040	.024	3.7	3.5	1.7					-99.0
367	80.11.23	1835	6.20	-90	1324	2	8.4	10.3	8.4	.177	.165	.147	23.6	26.1	22.6					-99.0
367	80.11.23	1835	6.20	-90	1325	6	43.9	44.8	44.8	.043	.042	.017	3.1	3.2	1.1					.1
367	80.11.23	1835	6.20	-90	1326	2	22.3	23.8	22.3	.099	.096	.067	12.7	8.5	5.9					-99.0
367	80.11.23	1835	6.20	-90	1327	2	20.3	20.8	20.3	.077	.071	.037	3.5	4.5	2.4					-99.0
367	80.11.23	1835	6.20	-90	1329	6	64.4	64.8	64.4	.026	.021	.014	2.9	2.6	1.0					-99.0
367	80.11.23	1835	6.20	-90	1356	0	18.2	19.9	19.9	.058	.049	.032	4.5	3.5	2.9					-99.0
178	81.04.26	1209	5.90	0	89	2	19.1	19.3	19.2	.116	.071	.045	3.6	5.0	1.3	westmorl	sup135	sup045	sup-up	-99.0
178	81.04.26	1209	5.90	0	159	6	15.1	15.4	15.3	.176	.105	.126	5.6	6.6	2.9	westmorl	nil090	nil000	nil-up	2.2
178	81.04.26	1209	5.90	0	821	6	16.5	16.7	16.6	.242	.155	.157	39.2	26.6	11.2	westmorl	pts225	pts315	pts-up	4.8
178	81.04.26	1209	5.90	0	830	6	15.3	15.6	15.4	.171	.169	.101	12.7	5.8	2.2	westmorl	bra315	bra225	bra-up	5.2
178	81.04.26	1209	5.90	0	832	6	8.0	8.5	8.2	.199	.176	.214	16.4	12.3	4.8	westmorl	wlf225	wlf315	wlf-up	4.7
178	81.04.26	1209	5.90	0	928	6	6.2	6.8	6.5	.496	.368	.838	48.7	34.4	10.4	westmorl	wsm180	wsm090	wsm-up	5.2
369	83.08.06	1543	6.74	-179	1358	5	81.0	81.4	81.4	.026	.026	.024	1.4	1.4	.4	greek	a-ier-ns	a-ier-we	a-ier-up	-99.0
216	83.10.28	1406	6.90	-70	1381	7	83.1	84.2	83.1	.086	.067		2.5	2.6		borahpk	cppbsou	cppbeas		-99.0
216	83.10.28	1406	6.90	-70	1384	7	84.9	86.9	84.9	.052	.040		2.8	2.8		borahpk	tan260	tan350		-99.0
217	83.10.29	2329	5.10	-65	1394	5	16.9	19.4	19.4	.073	.055		5.9	8.1		borahpk	bor090	bor000		-99.0
217	83.10.29	2329	5.10	-65	1395	2	22.0	23.9	23.9	.025	.019		2.1	1.7		borahpk	cem000	cem090		-99.0
217	83.10.29	2329	5.10	-65	1396	1	49.3	50.2	50.2	.033	.029		.6	.5		borahpk	hau090	hau000		-99.0
373	84.05.07	1749	5.80	-96	1397	0	19.2	19.6	19.6	.113	.093	.076	3.4	4.1	2.1	abruzzo	ati-we	ati-ns	ati-up	-99.0
373	84.05.07	1749	5.80	-96	1398	6	41.0	41.2	41.2	.079	.068	.034	3.4	2.1	2.1	abruzzo	ise-ns	ise-we	ise-up	-99.0
373	84.05.07	1749	5.80	-96	1399	6	49.7	50.6	50.6	.074	.058	.016	5.8	7.0	1.0	abruzzo	gar-we	gar-ns	gar-up	-99.0
373	84.05.07	1749	5.80	-96	1400	6	30.2	31.8	31.8	.072	.071	.021	5.1	3.1	1.3	abruzzo	pon-ns	pon-we	pon-up	-99.0
373	84.05.07	1749	5.80	-96	1401	6	45.6	46.7	46.7	.047	.030	.032	2.9	4.6	2.5	abruzzo	roc-we	roc-ns	roc-up	-99.0
276	86.07.20	1429	5.80	20	250	5	17.5	18.2	17.5	.129	.094	.049	8.5	8.6	3.3	chalfant	b-lad180	b-lad270	b-lad-up	1.2
276	86.07.20	1429	5.80	20	432	5	25.0	26.0	26.0	.061	.052	.030	3.0	2.4	1.3	chalfant	b-ben270	b-ben360	b-ben-up	1.2
276	86.07.20	1429	5.80	20	659	2	14.0	15.3	15.3	.095	.046	.067	1.7	6.3	2.9	chalfant	b-par160	b-par070	b-par-up	.3

Table 4 p2/3

276	86.07.20	1429	5.80	20	663	5	7.4	8.4	8.1	.285	.207	.205	17.3	22.3	5.4	chalfant	b-zak270	b-zak360	b-zak-up	1.0
276	86.07.20	1429	5.80	20	768	5	25.2	26.5	26.5	.051	.031	.029	2.2	1.8	.9	chalfant	b-she009	b-she099	b-she-up	.1
277	86.07.21	1442	6.30	-160	250	5	19.4	21.3	21.3	.248	.175	.140	19.2	19.4	6.7	chalfant	a-lad180	a-lad270	a-lad-up	1.2
277	86.07.21	1442	6.30	-160	431	6	31.8	33.3	33.3	.071	.060	.036	4.0	3.9	3.1	chalfant	a-cvc090	a-cvc000	a-cvc-up	-99.0
277	86.07.21	1442	6.30	-160	432	5	20.3	20.7	20.7	.209	.177	.127	13.6	15.7	6.8	chalfant	a-ben270	a-ben360	a-ben-up	1.2
277	86.07.21	1442	6.30	-160	659	2	17.9	20.4	20.4	.165	.161	.127	4.9	12.4	5.9	chalfant	a-par070	a-par160	a-par-up	.3
277	86.07.21	1442	6.30	-160	663	5	4.4	6.0	6.0	.447	.400	.321	36.9	44.5	12.5	chalfant	a-zak270	a-zak360	a-zak-up	1.0
277	86.07.21	1442	6.30	-160	727	6	28.7	30.4	30.4	.083	.078	.069	2.3	2.4	1.4	chalfant	a-mcg360	a-mcg270	a-mcg-up	0.0
277	86.07.21	1442	6.30	-160	768	5	24.7	26.6	26.6	.163	.091	.085	7.0	5.5	3.2	chalfant	a-she009	a-she099	a-she-up	.1
277	86.07.21	1442	6.30	-160	775	1	37.2	38.5	38.5	.048	.042	.026	2.2	2.8	1.6	chalfant	a-mam290	a-mam020	a-mam-up	-99.0
277	86.07.21	1442	6.30	-160	1330	1	21.0	23.2	23.2	.095	.056	.047	4.8	6.4	3.4	chalfant	a-lvd000	a-lvd090	a-lvd-up	.1
277	86.07.21	1442	6.30	-160	1332	1	56.8	57.6	57.6	.037	.037	.023	3.6	6.3	1.7	chalfant	a-tin000	a-tin090	a-tin-up	-99.0
278	86.07.21	1451	5.60	-999	250	5	24.9	25.4	25.4	.106	.070	.057	4.9	6.5	2.2	chalfant	c-lad270	c-lad360	c-lad-up	1.2
278	86.07.21	1451	5.60	-999	659	2	11.9	12.9	12.9	.061	.037	.053	1.9	2.1	1.1	chalfant	c-par160	c-par070	c-par-up	.3
278	86.07.21	1451	5.60	-999	663	5	15.2	16.0	16.0	.143	.108	.079	7.4	5.1	2.1	chalfant	c-zak270	c-zak360	c-zak-up	1.0
279	86.07.31	722	5.80	160	250	5	22.1	22.3	22.2	.176	.120	.067	10.4	12.2	2.8	chalfant	d-lad160	d-lad070	d-lad-up	1.2
279	86.07.31	722	5.80	160	663	5	8.7	9.3	9.0	.064	.060	.046	4.1	4.3	1.6	chalfant	d-zak270	d-zak360	d-zak-up	1.0
280	86.10.10	1749	5.76	0	1345	6	3.7	7.0	7.0	.612	.406	.480	60.5	65.7	12.9	SANSALV	ngi270	ngi180	ngi-up	-99.0
280	86.10.10	1749	5.76	0	1346	6	2.1	6.3	6.3	.875	.475	.392	59.3	48.4	12.1	Sansalv	gic090	gic180	gic-up	-99.0
371	87.03.02	142	6.60	-110	1385	7	18.9	20.1	19.1	.344	.256	.150	21.8	21.7	10.0	newzeal	a-mat353	a-mat083	a-mat-up	-99.0
371	87.03.02	142	6.60	-110	1390	7	70.1	70.6	70.2	.040	.030	.018	2.0	1.9	.9	newzeal	a-mar040	a-mar130	a-mar-up	-99.0
372	87.03.02	150	5.80	-999	1385	7	33.6	38.1	38.1	.055	.053	.026	3.7	5.1	2.7	newzeal	b-mat353	b-mat083	b-mat-up	-99.0
295	87.11.24	154	6.20	180	968	6	19.8	20.0	19.8	.134	.132	.186	12.7	13.4	4.6	superst	a-ivw360	a-ivw090	a-ivw-up	4.7
297	87.11.24	1315	6.60	178	912	6	18.2	18.7	18.7	.358	.258	.128	46.4	40.9	8.4	superst	b-icc000	b-icc090	b-icc-up	4.8
297	87.11.24	1315	6.60	178	928	6	13.1	13.7	13.7	.211	.172	.249	23.5	31.0	8.7	superst	b-wsm180	b-wsm090	b-wsm-up	5.2
368	92.03.13	1718	6.70	-163	1360	6	1.8	3.8	1.8	.515	.496	.248	83.9	64.3	18.3	Erzikan	erzins	erziew	erziup	.5
370	92.04.13	120	5.31	-94	1391	1	55.8	58.1	58.1	.012	.012		.6	.7		roermond	gsh-ew	gsh-ns		0.0
370	92.04.13	120	5.31	-94	1392	1	80.7	82.6	82.6	.006	.006	.004	.4	.3	.5	roermond	olf-ew	olf-ns	olf-up	0.0
370	92.04.13	120	5.31	-94	1393	1	102.1	103.2	103.2	.009	.005	.006	.3	.5	.4	roermond	wbs-ew	wbs-ns	wbs-up	0.0
366	92.06.29	1014	5.70	-70	1362	6	14.1	16.1	16.1	.204	.133	.084	4.1	11.5	2.4	lsm	lsm1-w	lsm1-n	lsm1-v	-99.0
366	92.06.29	1014	5.70	-70	1364	0	23.8	24.6	24.6	.118	.089	.066	5.1	4.6	2.6	lsm	lsm2-n	lsm2-w	lsm2-v	-99.0
366	92.06.29	1014	5.70	-70	1366	0	45.2	45.6	45.6	.061	.036	.033	1.1	2.1	.67	lsm	lsm3-w	lsm3-n	lsm3-v	-99.0
366	92.06.29	1014	5.70	-70	1367	6	58.6	59.8	59.8	.021	.019	.015	1.1	1.3	.56	lsm	lsm4-w	lsm4-n	lsm4-v	-99.0
366	92.06.29	1014	5.70	-70	1368	6	63.7	64.8	64.8	.016	.015	.011	.83	.74	.42	lsm	lsm5-n	lsm5-w	lsm5-v	-99.0
366	92.06.29	1014	5.70	-70	1369	1	99.4	100.1	100.1	.008	.008	.006	.31	.27	.22	lsm	lsm6-w	lsm6-n	lsm6-v	-99.0
366	92.06.29	1014	5.70	-70	1370	6	98.9	99.6	99.6	.007	.005	.005	.52	.36	.33	lsm	lsm7-n	lsm7-w	lsm7-v	-99.0
366	92.06.29	1014	5.70	-70	1371	0	98.2	98.4	98.4	.013	.012	.009	.52	.43	.31	lsm	lsm8-w	lsm8-n	lsm8-v	-99.0
365	94.09.12	1223	5.90	-25	646	6	12.5	12.9	12.9	.086	.060	.123	7.7	8.3	4.4	Doubsprg	woo090	woo000	woo-up	-99.0

Table 4 p 3/

Table 5: Correspondence between various authors' site classifications and the classifications used in this work.
• *indicates the combinations of Campbell's relations and site classes actually used in this report*

Authors	Predicted parameters (7) (*italic*=used in this study)	horizontal used	Our soil classes(4): rock of unknown hardness (3,6) (G=0)	hard rock (6) (G=1)	soft rock (6) (G=2)	soil of unknown thickness (G=5)	deep soil (h > 20m) (G=6)	shallow soil (5m < h < 20m) (G=7)
BJF 94	*pha, psvh*	geom. mean (5)	Vs = 620 m/s	Vs = 620 m/s	Vs = 620 m/s	Vs = 310 m/s	Vs = 310 m/s	Vs = 310 m/s
C 89 (2)	pha, *phv, psvh pza, pzv, psvz*	arith. mean	"soil/soft rock" (3)	n/a	"soil/soft rock"	•"soil/soft rock"	•"soil/soft rock"	•"soil/soft rock"
C 90	pha, *phv, psvh pza, pzv, psvz*	arith. mean	•'>10m soil or soft rock'	n/a	•'>10m soil or soft rock'	'>10m soil or soft rock'	'>10m soil or soft rock'	n/a
C 93 (1)	pha, *psah*	arith. mean	'rock'(1)	•'rock' (1)	'rock' (1)	'soil' (1)	'soil' (1)	'soil' (1)
CB 94	*pha*	geom. mean	•'soft rock'	•'hard rock'	•'soft rock'	•'alluvium'	•'alluvium'	•'alluvium'
JB 88	psvh, pha, *phv*	geom. mean (5)	'rock'	'rock'	'rock'	'soil'	'soil'	'soil'
Idriss 93	*pha, psah*	geom. mean	'rock'	'rock'	'rock'	n/a	n/a	n/a
SP 96	*pha, phv, psvh*	larger	'stiff <5m soil'	'stiff <5m soil'	'stiff <5m soil'	'deep soil, >20m soil'	'deep soil, >20m soil'	'shallow, 5-20m soil'
S 93	*pha, psah, pza, psaz*	geom. mean	'rock'	'rock'	'rock'	n/a	n/a	n/a

(1) C93 has two site catagories: "Quaternary deposits (soil)" and "Tertiary or older sedimentary, metamorphic, and igneous deposits (rock)". Campbell (written communication, 1995) says we should use this relation for psa on *hard* rock only.
(2) C89 was developed using soil data only, but stated to be appropriate for soft rock also. Campbell (written communication, 1995) says we should use this relation for psvh, pza, psvz and psaz on soil.
(3) rock of unknown hardness is assumed to be a soft rock, as true hard rock sites are relatively rare, particularly in the Western US.
(4) G is an arbitrary site code number. Numbers 3 and 4 are not used.
(5) Coefficients for the random horizontal were used, which is identical to the geometric mean. See Appendix A for $\sigma^2_{\log y}$ calculation.
(6) Sites having 5m of soil or less are considered rock sites
(7) Abbreviations: h=horizontal, z=vertical, a=acceleration, v=velocity, pza=peak vertical acceleration, psah=horizontal pseudospectral acceleration, etc ...

Table 5 p 1/1

Table 6. Site geologies for each station

SCod - our internally assigned station code (see Table 1)
G - site geology code (=0 rock of unknown hardness, =1 hard rock, =2 soft rock, =5 soil of unknown thickness, =6 deep soil, =7 shallow soil)
D_2_B - depth to basement as defined by Campbell (1989), in km. = -99 when unknown

SCod	Station Name	G	D_2_B
14	El Centro Array Sta 9	6	5.0
89	Superstition Mtn	2	-99.0
104	El Centro Array Sta 10	6	4.9
159	Niland	6	2.2
222	El Centro Array Sta 5	6	5.7
224	El Centro Array Sta 4	6	5.6
250	Bishop	5	1.2
431	Convict Creek	6	-99.0
432	Benton	5	1.2
559	Mammoth Lakes H.S.	6	-99.0
613	Oroville Airport	5	-99.0
646	Woodfords	6	-99.0
659	Bishop	2	.3
663	Chalfant	5	1.0
727	McGee Creek	6	0.0
768	Crowley Lake	5	.1
775	Mammoth Lakes	1	-99.0
798	El Centro Array Sta 7	6	5.4
821	Parachute Test Site	6	4.8
822	Plaster City	6	.8
823	Calexico	6	5.0
824	Bonds Corner	6	4.8
825	Holtville	6	5.3
826	El Centro Array Sta 1	6	3.5
827	El Centro Array Sta 3	6	5.7
828	El Centro Array Sta 11	6	5.0
829	El Centro Array Sta 13	6	3.3
830	Brawley	6	5.2
831	Calipatria	6	5.1
832	Salton Sea Wildlife Refuge	6	4.7
836	Coachella Canal Sta 4	6	-99.0
874	El Centro Array Sta 2	6	5.5
912	El Centro: Imp. Cnty Cntr FF	6	4.8
913	El Centro: Meloland Overpass	6	4.5
917	El Centro Arry Sta 6	6	5.6
918	El Centro Arry Sta 8	6	5.1
924	El Centro: Differential Array	6	5.0
928	Westmorland	6	5.2
968	Imperial Wildlife	6	4.7
1139	Managua: ESSO Refinery	6	-99.0
1141	El Centro Array Station 12	6	4.4
1215	Aeropuerto	6	4.8
1216	Agrarias	6	5.0
1217	Cerro Prieto	2	-99.0
1218	Chihuahua	6	6.0
1219	Compuertas	6	4.5
1220	Cucapah	6	6.0
1221	Delta	6	7.5
1222	Mexicali SAHOP	6	5.5
1223	Victoria	6	7.0
1320	Auletta	2	-99.0
1321	Bisaccia	2	-99.0
1322	Bovino	6	-99.0
1323	Brienza	6	-99.0
1324	Calitri	2	-99.0

1325	Mercato San Severino	6	.1
1326	Rionero in Vulture	2	-99.0
1327	Sturno	2	-99.0
1328	Torre del Greco	1	-99.0
1329	Tricarico	6	-99.0
1330	Long Valley Dam	1	.1
1332	Tinemaha Reservoir -- FF	1	-99.0
1345	IGN, San Salvador	6	-99.0
1346	CIG, San Salvador	6	-99.0
1353	Cascia	0	-99.0
1354	Fish and Game	5	-99.0
1355	Arienzo	0	-99.0
1356	Bagnoli Irpinio	0	-99.0
1357	Bevagna	6	-99.0
1358	Ierissos	5	-99.0
1362	Lathrop-A	6	-99.0
1364	NTS C.P.1 A	0	-99.0
1366	Beatty	0	-99.0
1367	Pahrump 2	6	-99.0
1368	Pahrump 1	6	-99.0
1369	Calico Basin	1	-99.0
1370	Ann Road	6	-99.0
1371	Scottie's Castle	0	-99.0
1381	CPP-610	7	-99.0
1384	TAN-719	7	-99.0
1385	Matahina Dam	7	-99.0
1385	Matahina Dam	7	-99.0
1390	Maraenui ES	7	-99.0
1391	GSH	1	0.0
1392	OLF	1	0.0
1393	WBS	1	0.0
1394	BOR	5	-99.0
1395	CEM	2	-99.0
1396	HAU	1	-99.0
1397	Atina	0	-99.0
1398	Isernia-Satn'agapito	6	-99.0
1399	Garigliano-Centrale Nucleare	6	-99.0
1400	Pontecorvo	6	-99.0
1401	Roccamonfina	6	-99.0

Table 7. List of candidate, relevant, and used earthquakes

An earthquake is a "candidate" if it has been suggested for any reason to be possibly relevant to this project.

An earthquake is "relevant" if it is in an extensional regime, has moment magnitude >=5.0, and has usable strong motion d

GRAY signifies irrelevant event

Explanation of columns:

Year ... hr:mn	Approximate earthquake origin time
Approx MAG	Approx MAG is ML, Ms, Mw, or other estimates, w/o references; italic is moment magnitude
Rlvnt?	Rlvnt is our current opinion of whether this event is relevant for further study
W&S	This event was studied by Westaway and Smith (1989)
used\tot stns	number of usable stations\total number of stations we know about

Year	Month	day	hr:mn	NAME or LOCATION	Approx MAG	Rlvnt?	why	W&S	used\tot recs	used here?
1935	10	31	18:38	Helena, Mt	6.2	n	1 rec in 5 story bldg	*		
1935	10	31	1918	Helena, Mt		n	1 rec in 4 story bldg			
1935	11	21	20:58	Helena, Mt	5.8	n	1 rec in 4 story bldg			
1935	11	28	7:42	Helena, Mt	5.8	n	1 rec in 4 story bldg	*		
1938	6	6	2:42	Imperial Valley, CA	5	n	extens (16); only rec is Strig		0\1	
1940	5	19	4:37	Imperial Valley, CA	*6.87*	Y	IV extens (16)		1\1	y
1949	4	13	19:55	Western Washington	7.1, 6.7	n	too deep (10)	*		
1951	1	24	7:17	Imperial Valley, CA	5.6	n	extens (16); only rec is Strig		0\1	
1953	6	14	4:17	Imperial Valley, CA	5.5	Y	IV extens (16)		1\1	
1955	12	17	6:07	Imperial Valley, CA	5.4	n	extens (16); only rec is Strig		0\1	
1959	8	18	6:37	Hebgen Lake, Mt	7	Y	/S89; stns > 100km, no dig	*	1\2	
1962	8	30	13:35	Cache Valley, UT	ML5.7,Ms5.7(W&S)	n	1 rec in 3 story bldg	*		
1972	12	23	6:29	Managua	*6.2*	Y	extensional (26)		1\1	y
1972	12	23	7:17	Managua	5	n	extensional (26) bad data			
1972	12	23	7:19	Managua	5.2	Y	extensional (26)		1\1	
1972	2	6	21:44	Ancona, Italy	3.5, 4.4	n	too small(1)	*		
1972	2	8	12:19	Ancona, Italy	3.9, 4.6	n	too small(1)	*		
1972	6	14	18:55	Ancona, Italy	4.6, 4.7	n	too small(1)	*		
1972	6	14	21:01	Ancona, Italy	3.3, 4.7	n	too small(1)	*		
1972	6	21	15:06	Ancona, Italy	2.7, 4.0	n	too small(1)	*		
1974	1	29	15:12	Patras, Greece	3.5, 4.4	n	too small(1)	*		
1975	4	4	5:16	Patras, Greece	4.6, 5.1	n	in WS89; too deep (26)	*	1\1	
1975	5	13	0:22	Xylokastron, Greece	3.9, 4.6	n	too small(1)	*		
1975	10	12	8:23	Corinth, Greece	4.5, 4.6	n	too small(1)	*		
1975	8	1	20:02	Oroville, CA	5.7	n	only digital rec is S trig	*	0\5	

Table 7 p 1/7

Year	Month	day	hr:mn	NAME or LOCATION	Approx MAG	Rlvnt?	why	W&S	used\tot recs	used here?
1975	8	2	20:22	Oroville, CA	*5*	Y	in WS89	*	1\2	
1975	8	2	20:59	Oroville, CA	4.4, 5.2	n	in WS89; too small	*	3\3	
1975	8	3	1:03	Oroville, CA	4.5,4.8	n	too small(1)	*		
1975	8	3	2:47	Oroville, CA	3.7, 4.3	n	too small(1)	*		
1975	8	6	3:05	Oroville, CA	4.0, 4.7	n	too small(1)	*		
1975	8	8	7:00	Oroville, CA	4.5, 4.6	n	too small(1)	*		
1975	8	11	6:11	Oroville, CA	4.3, 4.4	n	too small(1)	*		
1975	8	16	5:48	Oroville, CA	3.3, 4.1	n	too small(1)	*		
1975	9	26	2:31	Oroville, CA	2.9, 4.2	n	too small(1)	*		
1975	9	27	22:34	Oroville, CA	Mw 4.67 (21)	n	too small	*		
1976	8	19	1:12	Denizli, Turkey	4.9	n	too small(1)			
1977	12	9	15:33	Izmir, Turkey	4.3, 4.9	n	too small(1)	*		
1977	12	16	7:37	Izmir, Turkey	4.9, 5.3	Y	in WS89	*	1\1	
1978	6	20	20:03	Thessaloniki, Greece	Ms 6.5	n	‹tensional (25), 1 rec lrg bl‹	*		
1978	7	4		Thessaloniki, Greece	Ms 5.1	n	‹tensional (25), 1 rec lrg bldg			
1979	7	18	13:12	Dursunbey, Turkey	4.9, 5.2	Y	in WS89	*	1\1	
1979	9	19	21:35	Valnerina, Italy	*5.9*	Y	in WS89	*	3\7	y
1979	10	15	23:16	Imperial Valley, CA	*6.5*	Y	IV extens (16)		33\35	y
1979	10	15	23:19	Imperial Valley, CA	*4.8*	n	IV extens (16)		16\16	
1979	10	16	6:58	Imperial Valley, CA	5.5	Y	IV extens (16)		1\1	
1980	5	25	16:34	Mammoth Lakes, CA	*6.2*	Y	extensional (17)	3	2\3	y
1980	5	25	16:36	Mammoth Lakes, CA	ML 5.0	n	‹ borderline, only 1 rec - tch		?\1	
1980	5	25	16:49	Mammoth Lakes, CA	*5.8*	Y	extensional (17)	*	2\3	y
1980	5	25	19:44	Mammoth Lakes, CA	*5.8*	Y	extensional (17)	*	2\4	y
1980	5	25	20:35	Mammoth Lakes, CA	*5.7*	Y	extensional (17)		2\4	y
1980	5	25	20:59	Mammoth Lakes, CA	Mb4.2 ML5.5(20)	Y	extensional (17)		?	
1980	5	26	1:19	Mammoth Lakes, CA	Mb4.4 ML4.7(20)	Y	extensional (17)		?	
1980	5	26	12:24	Mammoth Lakes, CA	Mb4.7 ML5.6(20)	Y	extensional (17)		?	
1980	5	26	18:57	Mammoth Lakes, CA	5.8, 6.1	Y	extensional (17)		1\2	
1980	5	27	14:50	Mammoth Lakes, CA	*6*	Y	extensional (17)	*	4\6	y
1980	5	27	19:01	Mammoth Lakes, CA	Mm=4.6, TCH 6/23	n	extensional (17), too small	*	6\6	
1980	5	28	4:03	Mammoth Lakes, CA	2.6, 4.0	n	too small(1)	*		
1980	5	28	5:16	Mammoth Lakes, CA	3.7, 4.9	n	too small(1)	*		
1980	5	31	0:58	Mammoth Lakes, CA	2.7, 4.4	n	too small(1)	*		
1980	5	31	10:11	Mammoth Lakes, CA	3.0, 4.2	n	too small(1)	*		
1980	5	31	15:16	Mammoth Lakes, CA	, 4.9,ML4.9 Mb4.1(	n	too small(1)	*		
1980	5	31	15:02	Mammoth Lakes, CA	2.9, 4.0	n	too small(1)	*		

72

Table 7 p2/7

Year	Month	day	hr:mn	NAME or LOCATION	Approx MAG	Rlvnt?	why	W&S	used\tot recs	used here?
1980	6	5	19:41	Mammoth Lakes, CA	2.4, 4.3	n	too small(1)	*		
1980	6	9	3:28	Victoria, Mexico	*6.32*	Y	IV extens (16)		2\7	y
1980	6	9	3:30	Victoria, Mexico	not in PDE	n	bogus event			
1980	6	9	10:00	Mexicali VAlley	Mb4.4, ML4.5 (15)	n	too small			
1980	6	9	23:33	Mexicali Valley	ML4.2(pas)	n	too small			
1980	6	11	4:41	Mammoth Lakes, CA	Mm=4.0 TCH 6/23	n	extensional (17), too small		7\9	
1980	7	16		Volos, Greece	Ms 4.9	n	extensional (25), too small			
1980	8	11		Volos, Greece	Ms5.2, ML4.7		extensional (25)		1\1	
1980	9	26		Volos, Greece	Ms 4.8	n	extensional (25), too small			
1980	11	23	18:34	Campania (Irpinia), Italy	*6.9*	Y	in WS89	*	9\19	y
1980	11	23	18:35	Campania (Irpinia), Italy	*6.2*	Y	in WS89	*	10\10	y
1980	11	24	0:23	Campania (Irpinia), Italy	4.7	n	too small(1)	*		
1980	12	1	19:04	Campania (Irpinia), Italy	4.6	n	too small(1)	*		
1981	1	16	0:37	Campania (Irpinia), Italy	4.7	n	too small(1)	*		
1981	2	24	20:53	Corinth, Greece	6.7	Y	in WS89	*	1\1	
1981	2	25	2:35	Corinth, Greece	6.4	Y	in WS89	*	1\1	
1981	3	4	21:58	Corinth, Greece	Ms6.4(12)	Y	normal (12)		1\1	
1981	4	26	12:09	Westmorland, CA (11)	*5.8*	Y	IV extens (16)		6\6	y
1981	9	30	11:53	Mammoth Lakes, CA	b5.6 Ms5.8 ML5.8(2	Y	extensional (17)		?	
1981	9	30	13:06	Mammoth Lakes, CA	Mb4.7 ML4.6(20)	Y	extensional (17)		?	
1983	1	7	1:38	Mammoth Lakes, CA	Ms5.0 (15) ML5.0	Y	extensional (17)		1\1	
1983	1	7	3:24	Mammoth Lakes, CA	Ms5.0 (15) ML5.4	Y	extensional (17)		1\1	
1983	1	17		Argostoli, Greece (mainsh	Ms 7.0	n	not extensional (25)			
1983	1	17		Argostoli, Greece (aftersh	Ms 5.3	n	not extensional (25)			
1983	1	19		Argostoli, Greece (aftersh	Ms 5.7	n	not extensional (25)			
1983	1	31		Argostoli, Greece (aftersh	Ms 5.3	n	not extensional (25)			
1983	2	2		Zakynthos, Greece	Ms 5.4	n	not extensional (25)			
1983	3	16		Lefkada, Greece (mainsh)	Ms 5.2	n	not extensional (25)			
1983	3	23		Lefkada, Greece (aftersh)	Ms 5.2	n	not extensional (25)			
1983	3	23		Argostoli, Greece (aftersh	Ms 6.2	n	not extensional (25)			
1983	3	24		Argostoli, Greece (aftersh	Ms 5.5	n	not extensional (25)			
1983	7	5	12:01	Biga, Turkey	5.8, 6.1	Y	in WS89	*	≤1\5	
1983	8	6	15:43	North Aegean, Greece	*6.74*	Y	extensional (25)		1\1	y
1983	8	26		Ouranopolis, Greece	Ms4.9	n	too small			
1983	10	28	14:06	Borah Peak, ID	*6.9*	Y	in WS89	*	2\8	y
1983	10	29	23:29	Borah Peak, ID	*5.1*	Y	in WS89	*	3\5	y
1983	10	29	23:39	Borah Peak, ID	Mm=4.8 (23)	n	in WS89	*		

Table 7 p 3/7

Year	Month	day	hr:mn	NAME or LOCATION	Approx MAG	Rlvnt?	why	W&S	used\tot recs	used here?
1983	10	30	1:24	Borah Peak, ID	3.5, 4.8	n	too small(1)	*		
1983	10	30	1:59	Borah Peak, ID	3.1, 4.7	n	too small(1)	*		
1983	11	2	23:43	Borah Peak, ID	3.5, 4.2	n	too small(1)	*		
1983	11	6	21:04	Borah Peak, ID	3.3, 4.6	n	too small(1)	*		
1983	11	8		Liege, Belgium	5.1	n?	no d<100 km?		?	
1984	2	19		Poligiros, Greece	Ms 4.9	n	ensional (25), too small, S trig			
1984	3	5	2:07	South Taupo, NZ	5.5	?		*	1\1	
1984	4	29	5:02	Umbria, Italy	5.0, 5.6	Y	in WS89	*	?\6	
1984	5	7	17:49	Lazio-Abruzzo, Italy	*5.8*	Y	in WS89	*	5\16	y
1984	5	11	10:41	Lazio-Abruzzo, Italy	5.2, 5.5	Y	in WS89	*	?\10	
1984	5	11	10:05	Lazio-Abruzzo, Italy	4.2	n	too small(1)	*		
1984	5	11	11:26	Lazio-Abruzzo, Italy	4.2	n	too small(1)	*		
1984	5	11	13:14	Lazio-Abruzzo, Italy	4.3	n	too small(1)	*		
1984	5	11	13:39	Lazio-Abruzzo, Italy	4.1	n	too small(1)	*		
1984	5	11	16:39	Lazio-Abruzzo, Italy	4.3	n	too small(1)	*		
1984	5	11	23:35	Lazio-Abruzzo, Italy	4.1	n	too small(1)	*		
1984	6	24		Granada, Spain	5	?			1\6	
1984	7	9		Edessa, Greece	Ms5.3, ML4.8	n	nsional (25), 2 recs in big bldgs		1\1	
1984	10	4		Zakynthos, Greece	Ms 5.0	n	not extensional (25)			
1984	10	10		Pelekanada, Greece	Ms5.0, ML4.5	Y	extensional (25)		≥1\2	
1984	11	23	18:08	Round Valley, CA	)5.6 Ms5.7 ML6.2(2	Y	extensional (17)		?	
1984	11	23	19:12	Bishop, (Round Valley), CA	)4.8 Ms4.7 ML5.4(2	Y	extensional (17)		1\1	
1985	3	3		Amfilochia (main shock)	Ms4.5	n	not extensional (25)			
1985	3	3		Amfilochia (aftersh)	Ms4.5	n	not extensional (25)			
1985	8	31		Lefkada, Greece	Ms 5.2	n	not extensional (25)			
1985	11	9		Drama, Greece	Ms5.5, ML5.0	Y	extensional (25)		2\2	
1986	2	18		Edessa, Greece	Ms 5.0	Y	extensional (25)		?	
1986	7	20	14:29	Chalfant Valley, CA	*5.8*	Y	extensional(18)		5\5	y
1986	7	21	14:42	Chalfant Valley, CA	*6.3*	Y	extensional(18)		10\11	y
1986	7	21	14:51	Chalfant Valley, CA	*5.6*	Y	extensional(18)		3\3	y
1986	7	31	7:22	Chalfant Valley, CA	*5.8*	Y	extensional(18)		2\2	y
1986	9	13	17:24	Kalamata, Greece (mainsh	Ms6.2	n	in WS89; 1 rec in big bldg	*	1\1	
1986	9	15	11:41	Kalamata, Greece (aftersh	Ms5.4	n	in WS89; too small	*	3\3	
1986	10	10	17:49	San Salvador, El Salvador	*5.76*				2\9	y
1987	2	7	3:45	Cerro Prieta, Mexico	Ml=5.4	Y	IV extens (16)		1\1	
1987	3	2	1:35	Edgecomb, New Zeleand	5.2	Y	in WS89	*	?\1	
1987	3	2	1:42	Edgecomb, New Zeleand	*6.6*	Y	in WS89	*	2\3	y

Table 7 p 4/7

									used\tot	used
Year	Month	day	hr:mn	NAME or LOCATION	Approx MAG	Rlvnt?	why	W&S	recs	here?
1987	3	2	1:51	Edgecomb, New Zeleand	*5.8*	Y	in WS89	*	1\2	y
1987	11	24	1:54	Elmore Ranch, CA	*6.2*	Y	IV extens (16)		1\1	y
1987	11	24	13:15	Superstition Hills, CA	*6.6*	Y	IV extens (16)		2\3	y
1988	8	14	20:03	San Rafael Swell, UT	5.21(27)		West US probably extensional		?	
1988	10	16		Kyllini, Greece (mainsh)	Ms 5.9	n	not extensional (25)			
1988	10	17		Kyllini, Greece (aftersh)	Ms 4.4	n	not extensional (25)			
1988	10	20		Kyllini, Greece (aftersh)	Ms 4.1	n	not extensional (25)			
1988	10	22		Kyllini, Greece (aftersh)	Ms 4.5	n	not extensional (25)			
1988	10	23		Kyllini, Greece (aftersh)	Ms 4.3	n	not extensional (25)			
1988	10	23		Kyllini, Greece (aftersh)	Ms 4.5	n	not extensional (25)			
1988	10	23		Kyllini, Greece (aftersh)	Ms ?	n	not extensional (25)			
1988	10	28		Kyllini, Greece (aftersh)	Ms 4.4	n	not extensional (25)			
1988	10	31		Kyllini, Greece (aftersh)	Ms 4.3	n	not extensional (25)			
1988	10	17		Kyllini, Greece (aftersh)	Ms 4.4	n	not extensional (25)			
1988	11	11		Kyllini, Greece (aftersh)	Ms 4.3	n	not extensional (25)			
1989	1	30	4:06	So Wasatch Plateau, UT	5.12 (27)		West US probably extensional		?	
1990	10	24	6:15	Lee Vining, CA	5.29 (27)		West US probably extensional		?	
1990	12	21		Griva, Greece	Ms5.9	Y	extensional (25)		2\2	
1991	2	24		Korinth, Greece	Ms 6.7	n	not extensional (25)			
1991	12	3	17:54	Mexicali, Mexico	5.18 (27)		IV/Baja probably extensional		?	
1992	3	13	17:19	Erzincan, Turkey	*6.7*	Y	extensional(6)		1\2	y
1992	4	12	1:02	Roermond, Holland	*5.31*				3\19	y
1992	6	22	17:43	Matata, NZ	5.7	?			1\2	
1992	6	28	11:58	Landers, CA		n	not extens(19)			
1992	6	28		Big Bear, CA	Mw=5.3 (7)	n	not extens(19)			
1992	6	29	10:14	Little Skull Mtn, NV	*5.7*	Y	normal (7)		8\24	y
1992	9	2	10:26	St. George, UT	Mw=5.5 (7)	n	no good records			
1992	10	11	13:09	Dahshur, Egypt	Ml=5.9	n	no records			
1993	3	26		Pyrgos, Greece (aftersh)	Ms 5.0	n	not extensional (25)			
1993	3	26		Pyrgos, Greece (aftersh)	Ms 5.1	n	not extensional (25)			
1993	3	26		Pyrgos, Greece (mainsh)	Ms 5.2	n	not extensional (25)			
1993	3	26		Pyrgos, Greece (aftersh)	Ms 4.9	n	›o small, not extensional (25)			
1993	3	26		Pyrgos, Greece (aftersh)	Ms 4.7	n	›o small, not extensional (25)			
1993	4	29		Pyrgos, Greece (aftersh)	Ms 4.8	n	o small, not extensional (25)			
1993	4	29	8:21	Cataract Creek, AZ	5.27 (27)		West US probably extensional		?	
1993	5	17		Eureka Valley, CA	Mw=6.0 (7)	n	3 analog, no digital recs			
1993	7	14		Patras, Greece	Ms 5.4	n	›xtensional (25), poor digitiz			

Table 7 p 5/7

Year	Month	day	hr:mn	NAME or LOCATION	Approx MAG	Rlvnt?	why	W&S	used\tot recs	used here?
1993	9	21	3:28	Klammath Falls, OR	Mw=6.0 (7)	Y	normal (7)		?	
1993	9	21	5:45	Klammath Falls, OR	Mw=6.0 (7)	Y	normal (7)		?	
1993	12	4	22:15	Klammath Falls, OR	Mw=5.5 (9)	Y	normal (9)		?	
1994	2	3	9:05	Drainey Peak, ID	Mw=5.7 (7)	Y?	normal (7)		?	
1994	6	7	13:30	Near Borah Peak, ID	5.01-5.12 (28)		West US probably extensional		?	
1994	9	12	12:23	Double Springs Flat	*5.9*	Y			1\5	y
1994	9	12	23:57	Double Springs Flat	-(brk)5.0, Md-reno	n	no digital records, too small			
1995	4	14	0:32	Western Texas	5.62 (27)		West US probably extensional		?	
1995	5	4		Thesaloniki(?), Greece	Ms 5.8	n	data withheld till mid?1996		?	
1995	5	13	8:47	Kozani, Greece	Ms=6.6 (30)	Y	normal (30)		1\1	
1995	5	15	4:13	Kozani, Greece af A	Ms=5.5 (30)	Y	aftershock, prob extensional		1\1	
1995	5	17	4:14	Kozani, Greece af B	Ms=5.4 (30)	Y	aftershock, prob extensional		1\1	
1995	5	19	6:48	Kozani, Greece af C	M=5.1 (31)	Y	aftershock, prob extensional		1\1	
1995	6	11	18:51	Kozani, Greece af D	M=4.8 (31)	Y	aftershock, prob extensional		2\2	
1995	6	15		Greece	Ms=6.0? (31)	?	few small recs r>40km (31)			
1995	8	17		Ridgecrest, CA	ML=5.4 (32)	Y	normal mech (32)		?\5?	
1995	9	20		Ridgecrest, CA	ML=5.8 (32)	Y	str-slip, extensional (32)		?\5?	
1995	11	22	0416?	Gulf of Aqaba	Mw=7.1(33)	?	Probably extensional(29)		2\7	
1995	11	23	18:08	Gulf of Aqaba aft A	ML=5.4(33)	?	Probably extensional(29)		1\1	
1995	12	26	6:19	Gulf of Aqaba aft B	ML=5.0(33)	?	Probably extensional(29)		1\1	

Footnotes:

(1) too small: none of the magnitudes in Table 1 of WS89 equals or exceeds 5.0
(6) Erzincan is strike-slip but is in extensional zone.
(7) from Ritsema and Lay JGR, 1995
(8) Ritsema and Lay (1995) report rake = -14 for this event
(9) from Braunmiller et al (1995)
(10) 70 km deep, Nuttli (BSSA, 1952)
(11) see Maley and Etheredge (1981), also "Seismological Notes",. BSSA, v72,1982, also McJunkin and Kaliakin (1981)
(12) see Abercrombie et al (1995)
(13) CDMG OSMS 86-07 , 1986
(14) CDMG 0SMS 87-04, 1988
(15)NEIS
(16) this Imperial Valley event determined in extensional region
(17) Long Valley and nearby events are extensional
(18) Associated with range-front normal faults in extensional zone
(19) No extensional strains seen in geodetics or in stress indicators

Table 7 p6/7

Year	Month	day	hr:mn	NAME or LOCATION	Approx MAG	Rlvnt?	why	W&S	used\tot recs	used here?
(20) PDE, ML from PAS										
(21) Mw from Mo from Fletcher et al, BSSA, 1984										
(22) CDMG Bulletin SR 150										
(23) Jackson and Boatwright, BSSA, 1987										
(24) Calif Strong Motion Instrumentation Program (1994) CSMIP strong motion data from the South Lake Tahoe area										
	earthquake of September 12, 1994, CSMIP Report OSMS 94-19, 9 pp.									
(25) D Boore and V Margaris went through Greek catalog of strong motion records and partitioned into extensional										
	and not extensional regimes									
(26) Patras 4/4/75, depth = 53 km, Brady OFR 78-1022. Depth probably from NEIC										
(27) Mw estimated from coda, Mayeda and Walter (1995)										
(28) Mw est from Berkeley network, M. Pasayanos and D. Dreger, pers commun, reported in Mayeda and Walter (1995)										
(29) Dead Sea rift system										
(30) Papazachoset al, 1996.										
(31) magnitude from readme file sent by Margaris with data										
(32) Hauksson et al, 1995										
References:										
WS89: Westaway and Smith, 1989, Geophysical Journal, v96, pp 529-559										
Ritsema, J. and T. Lay, 1995, J. Geophys. Res., v100, 9853-9864.										
Braunmiller, J., J. Nabelek, and B. Leitner, Geophys. Res. Let., v22, pp105-108, 1995.										
Maley, R.P., and E. Etheredge, 1981, USGS OFR 81-1149, 18pp.										
McJunkin, R.D. and N.A. Kaliakin, 1981, CDMG, 41pp.										
Abercrombie, R., I. Main, A. Douglas, and P. Burton, 1995, GJI, v120, pp393-405.										
Nuttli, O., BSSA, 1952										
Jackson, S., and J. Boatwright, 1987, BSSA, v77, 724-738.										
Mayeda, K., and W. Walter, 1995, JGR, submitted.										
Hauksson et al, 1995,				Seismol. Res. Let., v66, pp 54-60.						
Papazachos, B.C., DG Panagiotopoulos, EM Scordilis, GF Karakaisis, Ch.A. Papaioannou, BG Karacostas,										
	EE Papadimitriou, AA Kiratzi, PM Hatzidimitriou, GN Leventakis, Ph.S. Voidomatis, KI Peftitselis, and TM Tsapanos,									
	Focal properties of the 13 May 1995 Large (Ms=6.6) earthquake int he Kozani area (north Greece), GRL, submitted									
	1996;									

77

Table 7 p 7/7

TABLE 8; RECORDS OMITTED BECAUSE OF STRUCTURE, S TRIGGER, OR POOR DATA QUALITY

GRAY signifies irrelevant event

Earthquake Name	Date	Station No	Station Name	bad blgd?	S trig/ bad data?	Notes
Helena, Montana	1935 1031 1838	??	Helena Fed Bldg	y		bsmt, 4 story bldg
Helena, Montana	1935 1031 1918	2229	Helena Fed Bldg	y		bsmt, 4 story bldg
Helena, Montana	1935 1121 2028		Helena Fed Bldg	y		bsmt, 4 story bldg
Helena, Montana	1935 1128 0742		Helena Fed Bldg	y		bsmt, 4 story bldg
Imperial Valley	1938 0606 0242	USGS 117	El Centro Array #9		y	**S trigger**
Imperial Valley	1951 0124 0717	USGS 117	El Centro Array #9		y	**S trigger**
Imperial Valley	1955 1217 0607	USGS 117	El Centro Array #9		y	**S trigger**
Hebgen Lake, MT	1959 0818 0637	USGS	BOZ - Bozeman, MT	y		3 story bldg
Cache Valley, UT	1962 0830 1335	USGS	LOG - Logan, UT	y		3 story bldg
Oroville	1975 0801 2020	CDWR 1051	Oroville Dam Seismograph Station		y	**S trigger**
Oroville	1975 0802 2022	CDMG 1546	OR1 - Up & Down Cafe		y	**S trigger**
Thessaloniki, GR	1978 0620 2003		Thessaloniki, City Hotel	y		7 story bldg-Hotel
Thessaloniki, GR	1978 0407 0000		Thessaloniki, City Hotel	y		7 story bldg-Hotel
Valnerina (Norcia) Italy	1979 0919 2135	ENEA	NOU - Nocera Umbra		y	**S trigger**
Valnerina (Norcia) Italy	1979 0919 2135	ENEA	ADT - Arquata del Tronto		y	**S trigger**
Valnerina (Norcia) Italy	1979 0919 2135	ENEA	MAS - Mascioni		y	**S trigger**
Valnerina (Norcia) Italy	1979 0919 2135	ENEA	- San Vittorino		y	**S trigger**
Imperial Valley	1979 1015 2316	USGS 5052	Plaster City		y	bad data
Imperial Valley	1979 1015 2316	UNAM 6618	Agrarias		y	z comp bad, other ok
Imperial Valley	1979 1015 2316	UNAM 6619	SAHOP Casa Flores		y	bad data
Imperial Valley	1979 1015 2316	CDMG 5169	Westmorland Fire Sta		y	z comp bad, other ok
Mammoth Lakes	1980 0525 1634	CDMG 54214	Long Valley Dam (Upr L Abut)	y		upper left abutment records contaminated
Mammoth Lakes	1980 0525 1649	CDMG 54214	Long Valley Dam (Upr L Abut)	y		upper left abutment records contaminated
Mammoth Lakes	1980 0525 1944	CDMG 54214	Long Valley Dam (Upr L Abut)	y		upper left abutment records contaminated
Mammoth Lakes	1980 0525 2035	CDMG 54214	Long Valley Dam (Upr L Abut)	y		upper left abutment records contaminated
Mammoth Lakes	1980 0526 1858	CDMG 54214	Long Valley Dam (Upr L Abut)	y		upper left abutment records contaminated
Mammoth Lakes	1980 0527 1451	CDMG 54214	Long Valley Dam (Upr L Abut)	y		upper left abutment records contaminated
Mammoth Lakes	1980 0531 1516	USC 35	Long Valley Fire Sta		y	**S trigger**
Victoria, Mexico	**1980 0609 0328**	UNAM 6604	Cerro Prieto			bad data
Victoria, Mexico	1980 0609 0328		Mexicali Hosp Sot.		y	**S trigger**
Victoria, Mexico	1980 0609 0328		Victoria		y	glitchy digital data
Victoria, Mexico	1980 0609 0328	UNAM 6624	Victoria Hospital Sotano		y	**S trigger**
Mammoth Lakes	1980 0611 0441	USGS 45	MGE - McGee Creek		y	**S trigger**
Mammoth Lakes	1980 0611 0441	USC 40	USC Convict Lakes		y	**S trigger**
Campania (Irpinia)	**1980 1123 1834**	ENEA	AU3 - Auletta		y	**S trigger**
Campania (Irpinia)	1980 1123 1834	ENEA	BZ4 - Brienza		y	**S trigger**
Campania (Irpinia)	1980 1123 1834	ENEA	GA4 - Garigliano		y	**S trigger**
Campania (Irpinia)	1980 1123 1834	ENEA	SS4 - San Severo		y	**S trigger**
Campania (Irpinia)	1980 1123 1834	ENEA	VI4 - Vieste		y	**S trigger**

Table 8 p 1/2

Earthquake Name	Date	Station No	Station Name	bad blgd?	S trig/ bad data?	Notes
Campania (Irpinia)	1980 1123 1834	ENEA	TC4 - Tricarico		y	**S trigger**
Biga, Turkey	1983 0705 12:01	ERI	GON - Goenen		y	poor digitization
Biga, Turkey	1983 0705 1201	ERI	EDK - Edincik		y	poor digitization
Biga, Turkey	1983 0705 1201	ERI	BSR - Balikesir		y	poor digitization
Biga, Turkey	1983 0705 1201	ERI	EDR - Edremit		y	poor digitization
Borah Peak, ID	1983 1028 1406	INEL	ANL 767	y		basement, 6-story bldg
Borah Peak, ID	1983 1028 1406	INEL	ANL 768	y		basement, 4 story bldg
Borah Peak, ID	1983 1028 1406	INEL	CPP-601 basement	y		10 m deep embedment in soil
Borah Peak, ID	1983 1028 1406	INEL	PBF-620	y		second basement, reactor building
Borah Peak, ID	1983 1028 1406	INEL	TRA-642	y		basement, 4-story bldg
Borah Peak, ID	1983 1028 1406	INEL	TRA-670	y		4 story building
Lazio-Abruzzo, Italy	1984 0507 1749	ENEA	Bussi		y	**S trigger**
Lazio-Abruzzo, Italy	1984 0507 1749	ENEA	LDP - Lama dei Peligni		y	**S trigger**
Lazio-Abruzzo, Italy	1984 0507 1749	ENEA	MAN - Manoppello		y	**S trigger**
Lazio-Abruzzo, Italy	1984 0507 1749	ENEA	ORT - Ortucchio		y	**S trigger**
Granada, Spain	1984 0624	IGN	Beznar		y	Dam abutment, S trigger
Granada, Spain	1984 0624	IGN	Alhama		y	bad data
Granada, Spain	1984 0624	NARS	NE14		y	bad data
Edessa, Greece	1984 0709		Edessa	y		5-story bldg, basement
Edessa, Greece	1984 0709		Veroia	y		3-story bldg, basement
Drama, Greece	1985 1109		Drama	y		4-story, basement
Chalfant Valley	1986 0721 1442	CDMG 54424	Bishop - Paradise Lodge		y	**S trigger**
Chalfant Valley	1986 0721 1442	CDMG 54214	Long Valley Dam (L Abut)	y		left abutment not used; downstream available
Kalamata, Greece	1986 0913 1724		Kalamata	y		7, 4-story, basement
Kalamata, Greece	1986 0915 1141		Kalamata	y		7, 4-story, basement
Kalamata, Greece	1986 0915 1141		Kalamata-2	y		7, 4-story, basement
San Salvador	1986 1010 1749		HCR Hotel El Camino Real	y		10-story, 2nd floor
San Salvador	1986 1010 1749		HSH Hotel Sheraton	y		10-story, 1st floor
San Salvador	1986 1010 1749		IVU Inst. Urban Construction	y		6-story, 1st floor
San Salvador	1986 1010 1749		UCA Centro Americana Un.	y		6-story, 1st floor
San Salvador	1986 1010 1749		MDE Minist de Educacion	y		4-story, 1st floor
Edgecomb, NZ	1987 0302 0151		Maraenui Primary School		y	**S trigger**
Superstitn Hills (A)	**1987 1124 0154**	USGS 5210	Wildlife Liquef. Array		y	**local liquefaction affected record**
Griva, Greece	1990 1221		Edessa	y		5-story, basement
Matata, New Zealand	1992 0622 1743	GNS	Kawerau Police St.		y	**S trigger**
Double Springs Flat	1994 0912 1223	CDMG 65430	Indian Creek Dam	y		earth dam crest

Table 8 p2/2

Table 9. Correction factors for each predictive relation, determined from data at all distances.

BJF94 h G=0,1,2 may2196b

T(s)	bijk	sigma-b	sigma-p	eijk	sigma-e	Q	N
0.00	-0.180	0.034	0.202	0.973	0.115	5.11e-01	35
0.05	-	-	-	-	-	-	0
0.10	-0.128	0.043	0.231	1.210	0.156	3.91e-02	29
0.15	-0.204	0.042	0.226	1.215	0.157	3.63e-02	29
0.20	-0.213	0.045	0.242	1.301	0.168	8.16e-03	29
0.30	-0.211	0.045	0.245	1.275	0.164	1.33e-02	29
0.40	-0.190	0.042	0.228	1.139	0.147	1.06e-01	29
0.50	-0.157	0.040	0.214	1.031	0.133	3.25e-01	29
0.75	-0.160	0.046	0.246	1.117	0.144	1.38e-01	29
1.00	-0.164	0.049	0.265	1.150	0.148	9.20e-02	29
1.50	-0.116	0.061	0.291	1.201	0.173	5.92e-02	23
2.00	-0.219	0.074	0.338	1.363	0.205	6.64e-03	21

BJF94 h G=5,6,7 may2196b

T(s)	bijk	sigma-b	sigma-p	eijk	sigma-e	Q	N
0.00	-0.083	0.021	0.204	0.981	0.072	5.55e-01	93
0.05	-	-	-	-	-	-	0
0.10	-0.040	0.024	0.225	1.179	0.088	7.34e-03	89
0.15	-0.065	0.025	0.238	1.284	0.096	8.89e-05	89
0.20	-0.087	0.026	0.247	1.330	0.099	7.97e-06	89
0.30	-0.118	0.024	0.229	1.193	0.089	4.42e-03	89
0.40	-0.139	0.026	0.245	1.224	0.091	1.28e-03	89
0.50	-0.099	0.027	0.256	1.235	0.092	8.14e-04	89
0.75	-0.110	0.034	0.318	1.443	0.108	6.46e-09	89
1.00	-0.122	0.034	0.323	1.397	0.104	1.39e-07	89
1.50	-0.084	0.035	0.322	1.329	0.102	1.39e-05	84
2.00	-0.084	0.038	0.333	1.346	0.107	1.12e-05	78

C89/94 h G=5,6,7 may2196b

T(s)	bijk	sigma-b	sigma-p	eijk	sigma-e	Q	N
0.00	-0.012	0.019	0.188	0.973	0.071	5.96e-01	93
0.05	0.090	0.022	0.195	1.021	0.081	3.45e-01	78
0.10	0.064	0.024	0.222	1.064	0.079	1.67e-01	89
0.15	0.022	0.025	0.240	1.107	0.082	6.39e-02	89
0.20	0.003	0.026	0.249	1.148	0.086	2.00e-02	89
0.30	-0.027	0.023	0.221	1.017	0.076	3.60e-01	89
0.40	-0.030	0.025	0.238	1.097	0.082	8.11e-02	89
0.50	-0.003	0.026	0.242	1.116	0.083	5.05e-02	89
0.75	-0.042	0.033	0.310	1.427	0.106	1.97e-08	89
1.00	-0.064	0.033	0.309	1.423	0.106	2.66e-08	89
1.50	-0.043	0.032	0.243	1.117	0.103	8.26e-02	58
2.00	-0.017	0.032	0.242	1.116	0.105	8.66e-02	56

C89 z G=5,6,7 may2196b

T(s)	bijk	sigma-b	sigma-p	eijk	sigma-e	Q	N
0.00	-0.008	0.024	0.223	0.904	0.068	8.78e-01	88
0.05	0.179	0.031	0.280	1.040	0.082	2.66e-01	79
0.10	0.103	0.036	0.327	1.215	0.093	2.38e-03	84
0.15	0.023	0.028	0.257	0.956	0.073	6.71e-01	84
0.20	0.078	0.030	0.272	1.012	0.078	3.89e-01	84
0.30	0.197	0.031	0.281	1.044	0.080	2.44e-01	84
0.40	0.070	0.035	0.321	1.190	0.091	5.87e-03	84
0.50	-0.010	0.035	0.317	1.179	0.090	8.62e-03	84
0.75	-0.100	0.039	0.346	1.285	0.102	1.87e-04	79
1.00	-0.078	0.041	0.357	1.325	0.107	4.33e-05	75
1.50	-0.152	0.053	0.378	1.405	0.138	2.86e-05	51
2.00	-0.161	0.051	0.351	1.303	0.133	1.45e-03	47

C89V h G=5,6,7 may1696c

T(s)	bijk	sigma-b	sigma-p	eijk	sigma-e	Q	N
pk vel	0.026	0.026	0.200	1.168	0.107	2.67e-02	59

C89V z G=5,6,7 may1696c

T(s)	bijk	sigma-b	sigma-p	eijk	sigma-e	Q	N
pk vel	0.029	0.027	0.255	1.129	0.085	3.57e-02	88

C90/94 h G=0,2 may2196b

T(s)	bijk	sigma-b	sigma-p	eijk	sigma-e	Q	N
0.00	-0.121	0.042	0.205	0.966	0.136	4.97e-01	24
0.05	0.094	0.057	0.219	0.901	0.159	5.91e-01	15
0.10	0.033	0.062	0.261	1.067	0.173	2.50e-01	18
0.15	-0.044	0.064	0.271	1.110	0.180	1.78e-01	18
0.20	-0.058	0.065	0.276	1.081	0.175	2.24e-01	18
0.30	-0.149	0.076	0.321	1.398	0.227	5.86e-03	18
0.40	-0.177	0.058	0.247	1.077	0.174	2.32e-01	18
0.50	-0.161	0.053	0.224	1.011	0.164	3.64e-01	18
0.75	-0.238	0.048	0.206	0.865	0.140	7.05e-01	18
1.00	-0.426	0.102	0.177	0.548	0.183	6.38e-01	3
1.50	-0.225	0.136	0.235	0.987	0.329	2.32e-01	3
2.00	-0.206	0.137	0.238	1.048	0.349	1.92e-01	3

C90 z G=0,2 may2196b

T(s)	bijk	sigma-b	sigma-p	eijk	sigma-e	Q	N
0.00	-0.071	0.043	0.206	0.916	0.132	6.28e-01	23
0.05	0.168	0.062	0.233	0.867	0.158	6.51e-01	14
0.10	0.000	0.054	0.222	0.756	0.126	8.81e-01	17
0.15	-0.017	0.051	0.209	0.725	0.121	9.16e-01	17
0.20	-0.059	0.062	0.256	0.899	0.150	6.19e-01	17
0.30	-0.052	0.058	0.240	0.826	0.137	7.72e-01	17
0.40	-0.049	0.054	0.224	0.761	0.127	8.75e-01	17
0.50	-0.032	0.053	0.217	0.824	0.137	7.76e-01	17
0.75	-0.071	0.066	0.247	0.992	0.181	3.90e-01	14
1.00	-0.105	0.049	0.084	0.319	0.106	8.58e-01	3
1.50	0.190	0.107	0.186	0.567	0.189	6.18e-01	3
2.00	0.223	0.168	0.291	0.914	0.305	2.86e-01	3

C90V h G=0,2 may1696c

T(s)	bijk	sigma-b	sigma-p	eijk	sigma-e	Q	N
pk vel	-0.264	0.127	0.220	1.082	0.361	1.72e-01	3

C90V z G=0,2 may1696c

T(s)	bijk	sigma-b	sigma-p	eijk	sigma-e	Q	N
pk vel	-0.115	0.139	0.240	0.951	0.317	2.58e-01	3

C93/94 h G=1 may2196b

T(s)	bijk	sigma-b	sigma-p	eijk	sigma-e	Q	N
0.00	0.087	0.053	0.176	0.770	0.157	7.70e-01	11
0.05	0.157	0.115	0.344	1.391	0.309	2.62e-02	9
0.10	0.086	0.059	0.195	0.772	0.157	7.66e-01	11
0.15	0.102	0.052	0.172	0.662	0.135	9.03e-01	11
0.20	0.122	0.050	0.165	0.594	0.121	9.53e-01	11
0.30	0.233	0.053	0.175	0.662	0.135	9.02e-01	11
0.40	0.304	0.089	0.218	0.774	0.204	6.10e-01	6
0.50	0.309	0.112	0.275	0.944	0.249	3.74e-01	6
0.75	0.274	0.085	0.209	0.696	0.183	7.15e-01	6
1.00	0.274	0.075	0.184	0.590	0.155	8.37e-01	6
1.50	0.172	0.076	0.169	0.709	0.200	6.43e-01	5
2.00	0.126	0.093	0.207	0.916	0.259	3.80e-01	5

I93 h G=0,1,2 may2196b

T(s)	bijk	sigma-b	sigma-p	eijk	sigma-e	Q	N
0.00	-0.142	0.033	0.193	0.801	0.094	9.35e-01	35
0.05	-0.097	0.051	0.249	0.954	0.135	5.30e-01	24
0.10	-0.145	0.042	0.225	0.914	0.118	6.71e-01	29
0.15	-0.168	0.042	0.226	0.933	0.120	6.15e-01	29
0.20	-0.172	0.040	0.218	0.872	0.113	7.78e-01	29
0.30	-0.158	0.048	0.259	0.991	0.128	4.40e-01	29
0.40	-0.143	0.044	0.237	0.903	0.117	6.99e-01	29
0.50	-0.098	0.041	0.220	0.795	0.103	9.18e-01	29
0.75	-0.084	0.044	0.235	0.872	0.113	7.79e-01	29
1.00	-0.055	0.043	0.231	0.858	0.111	8.10e-01	29
1.50	0.042	0.047	0.225	0.871	0.126	7.37e-01	23
2.00	0.042	0.056	0.255	0.928	0.140	5.81e-01	21

JB88V h G=0,1,2 may1696c

T(s)	bijk	sigma-b	sigma-p	eijk	sigma-e	Q	N
pk vel	-0.036	0.035	0.208	0.696	0.082	9.94e-01	35

JB88V h G=5,6,7 may1696c

T(s)	bijk	sigma-b	sigma-p	eijk	sigma-e	Q	N

pk vel	-0.032	0.025	0.237	0.793	0.058	9.97e-01	93

SP96 h G=0,1,2 may2196b

T(s)	bijk	sigma-b	sigma-p	eijk	sigma-e	Q	N
0.00	-0.060	0.031	0.184	1.064	0.125	2.34e-01	35
0.05	0.023	0.055	0.270	1.486	0.210	3.66e-04	24
0.10	-0.037	0.050	0.271	1.426	0.184	5.49e-04	29
0.15	-0.098	0.047	0.251	1.255	0.162	1.88e-02	29
0.20	-0.110	0.050	0.269	1.250	0.161	2.05e-02	29
0.30	-0.105	0.048	0.259	1.059	0.137	2.55e-01	29
0.40	-0.077	0.039	0.211	0.800	0.103	9.11e-01	29
0.50	-0.071	0.037	0.198	0.731	0.094	9.73e-01	29
0.75	-0.109	0.042	0.227	0.804	0.104	9.06e-01	29
1.00	-0.100	0.041	0.219	0.757	0.098	9.56e-01	29
1.50	-0.049	0.048	0.229	0.775	0.112	9.08e-01	23
2.00	-0.011	0.057	0.259	0.873	0.132	7.15e-01	21

SP96 h G=5,6 may2196b

T(s)	bijk	sigma-b	sigma-p	eijk	sigma-e	Q	N
0.00	0.089	0.021	0.201	1.164	0.087	1.24e-02	88
0.05	0.128	0.023	0.200	1.100	0.089	9.00e-02	75
0.10	0.146	0.023	0.214	1.129	0.087	3.91e-02	84
0.15	0.099	0.025	0.230	1.148	0.088	2.31e-02	84
0.20	0.074	0.027	0.244	1.136	0.087	3.20e-02	84
0.30	0.019	0.024	0.218	0.890	0.068	9.08e-01	84
0.40	-0.039	0.025	0.230	0.871	0.067	9.42e-01	84
0.50	-0.028	0.027	0.246	0.907	0.070	8.62e-01	84
0.75	-0.119	0.032	0.296	1.048	0.080	2.29e-01	84
1.00	-0.158	0.033	0.299	1.032	0.079	2.93e-01	84
1.50	-0.058	0.033	0.298	1.009	0.080	4.05e-01	79
2.00	0.054	0.033	0.286	0.963	0.079	6.22e-01	73

SP96 h G=7 may2196b

T(s)	bijk	sigma-b	sigma-p	eijk	sigma-e	Q	N
0.00	-0.003	0.066	0.148	0.856	0.242	4.54e-01	5
0.05	-0.024	0.112	0.194	1.068	0.356	1.80e-01	3
0.10	-0.192	0.189	0.423	2.225	0.629	5.62e-05	5
0.15	-0.118	0.196	0.438	2.188	0.619	8.20e-05	5
0.20	-0.167	0.216	0.483	2.247	0.635	4.51e-05	5
0.30	-0.234	0.196	0.437	1.785	0.505	3.11e-03	5
0.40	-0.260	0.246	0.551	2.088	0.591	2.20e-04	5
0.50	-0.253	0.215	0.481	1.773	0.502	3.41e-03	5
0.75	-0.441	0.239	0.535	1.893	0.535	1.28e-03	5
1.00	-0.315	0.251	0.561	1.933	0.547	9.06e-04	5
1.50	-0.288	0.274	0.613	2.077	0.587	2.45e-04	5
2.00	-0.200	0.287	0.641	2.158	0.610	1.11e-04	5

SP96V h G=0,1,2 may1696c

T(s)	bijk	sigma-b	sigma-p	eijk	sigma-e	Q	N
pk vel	0.020	0.039	0.232	1.081	0.127	1.94e-01	35

SP96V h G=5,6,7 may1696c

T(s)	bijk	sigma-b	sigma-p	eijk	sigma-e	Q	N
pk vel	0.062	0.026	0.254	1.180	0.086	6.21e-03	93

S93 h G=0,1,2 may2196b

T(s)	bijk	sigma-b	sigma-p	eijk	sigma-e	Q	N
0.00	-0.104	0.034	0.199	0.828	0.098	8.99e-01	35
0.05	0.016	0.056	0.275	1.081	0.153	2.14e-01	24
0.10	-0.070	0.044	0.236	0.946	0.122	5.77e-01	29
0.15	-0.117	0.043	0.234	0.949	0.122	5.67e-01	29
0.20	-0.108	0.043	0.231	0.908	0.117	6.85e-01	29
0.30	-0.093	0.049	0.265	0.991	0.128	4.38e-01	29
0.40	-0.073	0.045	0.244	0.876	0.113	7.70e-01	29
0.50	-0.031	0.042	0.227	0.780	0.101	9.35e-01	29
0.75	-0.071	0.044	0.235	0.823	0.106	8.77e-01	29
1.00	-0.106	0.042	0.228	0.789	0.102	9.25e-01	29
1.50	-0.058	0.047	0.223	0.799	0.115	8.76e-01	23
2.00	-0.087	0.056	0.258	0.928	0.140	5.82e-01	21

S93 z G=0,1,2 may2196b

T(s)	bijk	sigma-b	sigma-p	eijk	sigma-e	Q	N
0.00	-0.065	0.040	0.228	0.873	0.107	7.95e-01	32

0.05	0.096	0.053	0.245	0.855	0.129	7.56e-01	21
0.10	0.019	0.049	0.248	0.812	0.110	8.76e-01	26
0.15	0.046	0.045	0.229	0.765	0.104	9.36e-01	26
0.20	0.065	0.050	0.257	0.855	0.116	7.97e-01	26
0.30	0.105	0.053	0.271	0.902	0.123	6.84e-01	26
0.40	0.092	0.053	0.269	0.877	0.119	7.47e-01	26
0.50	0.051	0.043	0.220	0.741	0.101	9.57e-01	26
0.75	0.025	0.054	0.255	0.889	0.131	6.88e-01	22
1.00	0.061	0.059	0.268	0.930	0.140	5.77e-01	21
1.50	0.101	0.049	0.214	0.771	0.122	8.81e-01	19
2.00	0.158	0.055	0.220	0.802	0.137	8.01e-01	16

Sea96 h G=0,1,2 may2196b

T(s)	bijk	sigma-b	sigma-p	eijk	sigma-e	Q	N
0.00	-0.071	0.032	0.188	0.870	0.103	8.16e-01	35
0.05	-	-	-	-	-	-	0
0.10	-0.022	0.042	0.225	0.840	0.108	8.46e-01	29
0.15	-0.059	0.041	0.222	0.803	0.104	9.07e-01	29
0.20	-0.043	0.044	0.239	0.834	0.108	8.58e-01	29
0.30	-0.020	0.045	0.244	0.812	0.105	8.95e-01	29
0.40	-0.001	0.042	0.228	0.727	0.094	9.75e-01	29
0.50	0.022	0.040	0.214	0.660	0.085	9.94e-01	29
0.75	-0.019	0.045	0.245	0.710	0.092	9.82e-01	29
1.00	-0.046	0.048	0.260	0.719	0.093	9.78e-01	29
1.50	-0.003	0.060	0.286	0.738	0.106	9.46e-01	23
2.00	-0.074	0.072	0.330	0.809	0.122	8.43e-01	21

Sea96 h G=5,6,7 may2196b

T(s)	bijk	sigma-b	sigma-p	eijk	sigma-e	Q	N
0.00	0.027	0.020	0.191	0.883	0.064	9.34e-01	93
0.05	-	-	-	-	-	-	0
0.10	0.023	0.023	0.221	0.825	0.062	9.89e-01	89
0.15	0.008	0.025	0.235	0.849	0.063	9.74e-01	89
0.20	0.007	0.026	0.245	0.857	0.064	9.67e-01	89
0.30	0.006	0.024	0.228	0.756	0.056	9.99e-01	89
0.40	-0.005	0.026	0.244	0.780	0.058	9.98e-01	89
0.50	0.038	0.027	0.255	0.789	0.059	9.97e-01	89
0.75	0.007	0.034	0.317	0.920	0.069	8.30e-01	89
1.00	-0.020	0.034	0.320	0.886	0.066	9.22e-01	89
1.50	0.011	0.035	0.317	0.819	0.063	9.89e-01	84
2.00	0.034	0.036	0.321	0.787	0.063	9.96e-01	78

Table 10. Distance dependences for each predictive relation, determined from data at all distances.

BJF94 h G=0,1,2 may2196b Distance dependence

T(s)	ar	sigma-ar	sr	sigma-sr	cas	ras	Qr	N
0.00	1.93e-01	1.68e-01	-2.62e-01	1.15e-01	-1.89e-02	-0.978	7.18e-01	35
0.05	-	-	-	-	-	-	-	0
0.10	1.20e-01	1.64e-01	-1.71e-01	1.10e-01	-1.76e-02	-0.976	5.03e-02	29
0.15	-2.12e-02	1.59e-01	-1.26e-01	1.07e-01	-1.67e-02	-0.976	3.75e-02	29
0.20	2.47e-02	1.59e-01	-1.64e-01	1.07e-01	-1.67e-02	-0.976	1.05e-02	29
0.30	-1.80e-01	1.65e-01	-2.10e-02	1.11e-01	-1.78e-02	-0.976	9.67e-03	29
0.40	-1.61e-01	1.72e-01	-2.00e-02	1.15e-01	-1.93e-02	-0.976	8.47e-02	29
0.50	-1.44e-01	1.78e-01	-8.72e-03	1.20e-01	-2.07e-02	-0.976	2.79e-01	29
0.75	8.75e-02	1.89e-01	-1.70e-01	1.27e-01	-2.35e-02	-0.976	1.55e-01	29
1.00	3.62e-01	1.98e-01	-3.63e-01	1.33e-01	-2.58e-02	-0.976	2.74e-01	29
1.50	2.30e-01	2.41e-01	-2.50e-01	1.70e-01	-4.01e-02	-0.978	7.30e-02	23
2.00	1.80e-01	2.54e-01	-2.94e-01	1.83e-01	-4.54e-02	-0.977	9.36e-03	21

BJF94 h G=5,6,7 may2196b Distance dependence

T(s)	ar	sigma-ar	sr	sigma-sr	cas	ras	Qr	N
0.00	1.60e-01	7.48e-02	-2.01e-01	5.90e-02	-4.23e-03	-0.958	8.35e-01	93
0.05	-	-	-	-	-	-	-	0
0.10	9.30e-02	7.02e-02	-1.11e-01	5.63e-02	-3.79e-03	-0.958	1.15e-02	89
0.15	6.22e-02	6.82e-02	-1.07e-01	5.47e-02	-3.57e-03	-0.958	1.53e-04	89
0.20	1.63e-02	6.83e-02	-8.61e-02	5.47e-02	-3.58e-03	-0.958	1.04e-05	89
0.30	2.06e-02	7.05e-02	-1.16e-01	5.66e-02	-3.82e-03	-0.958	7.38e-03	89
0.40	-2.23e-02	7.35e-02	-9.78e-02	5.89e-02	-4.15e-03	-0.958	1.71e-03	89
0.50	3.16e-02	7.61e-02	-1.09e-01	6.10e-02	-4.45e-03	-0.958	1.19e-03	89
0.75	7.86e-02	8.10e-02	-1.58e-01	6.50e-02	-5.04e-03	-0.958	2.18e-08	89
1.00	8.32e-02	8.48e-02	-1.71e-01	6.80e-02	-5.53e-03	-0.958	4.95e-07	89
1.50	1.51e-01	9.47e-02	-2.02e-01	7.83e-02	-7.12e-03	-0.960	4.78e-05	84
2.00	3.36e-01	1.01e-01	-3.65e-01	8.43e-02	-8.18e-03	-0.961	5.78e-04	78

C89/94 h G=5,6,7 may2196b Distance dependence

T(s)	ar	sigma-ar	sr	sigma-sr	cas	ras	Qr	N
0.00	-8.65e-02	6.20e-02	5.85e-02	5.29e-02	-3.11e-03	-0.948	6.11e-01	93
0.05	4.58e-02	7.04e-02	3.90e-02	5.85e-02	-3.92e-03	-0.952	3.28e-01	78
0.10	3.31e-02	7.11e-02	2.59e-02	5.71e-02	-3.86e-03	-0.951	1.52e-01	89
0.15	-8.40e-02	7.41e-02	8.93e-02	5.94e-02	-4.19e-03	-0.951	7.38e-02	89
0.20	-1.23e-01	7.41e-02	1.07e-01	5.94e-02	-4.19e-03	-0.951	2.72e-02	89
0.30	-7.74e-02	7.41e-02	4.27e-02	5.94e-02	-4.19e-03	-0.951	3.46e-01	89
0.40	-6.15e-02	7.41e-02	2.63e-02	5.94e-02	-4.19e-03	-0.951	7.24e-02	89
0.50	-3.76e-03	7.41e-02	8.96e-04	5.94e-02	-4.19e-03	-0.951	4.34e-02	89
0.75	6.59e-02	7.41e-02	-9.15e-02	5.94e-02	-4.19e-03	-0.951	2.55e-08	89
1.00	4.38e-02	7.41e-02	-9.07e-02	5.94e-02	-4.19e-03	-0.951	3.41e-08	89
1.50	-4.34e-02	9.75e-02	6.45e-04	8.56e-02	-7.97e-03	-0.956	6.96e-02	58
2.00	-7.75e-03	9.94e-02	-8.92e-03	8.86e-02	-8.43e-03	-0.956	7.31e-02	56

C89 z G=5,6,7 may2196b Distance dependence

T(s)	ar	sigma-ar	sr	sigma-sr	cas	ras	Qr	N
0.00	-1.12e-01	8.69e-02	8.70e-02	6.92e-02	-5.73e-03	-0.953	8.89e-01	88
0.05	2.61e-01	1.00e-01	-7.01e-02	8.20e-02	-7.84e-03	-0.953	2.58e-01	79
0.10	-5.69e-01	9.68e-02	3.97e-01	7.86e-02	-7.25e-03	-0.953	1.04e-01	84
0.15	-1.86e-01	9.68e-02	1.78e-01	7.86e-02	-7.25e-03	-0.953	7.87e-01	84
0.20	-2.97e-01	9.68e-02	3.19e-01	7.86e-02	-7.25e-03	-0.953	8.36e-01	84
0.30	-2.47e-01	9.68e-02	3.78e-01	7.86e-02	-7.25e-03	-0.953	8.59e-01	84
0.40	-4.32e-01	9.68e-02	4.27e-01	7.86e-02	-7.25e-03	-0.953	2.70e-01	84
0.50	-5.24e-01	9.68e-02	4.39e-01	7.86e-02	-7.25e-03	-0.953	3.71e-01	84
0.75	-7.52e-01	1.03e-01	5.73e-01	8.67e-02	-8.55e-03	-0.956	2.11e-01	79
1.00	-6.60e-01	1.06e-01	5.18e-01	9.02e-02	-9.15e-03	-0.956	2.44e-02	75
1.50	-7.38e-01	1.29e-01	5.43e-01	1.14e-01	-1.41e-02	-0.956	5.12e-03	51
2.00	-6.72e-01	1.35e-01	4.89e-01	1.24e-01	-1.60e-02	-0.957	3.13e-02	47

C89V h G=5,6,7 may1696c Distance dependence

T(s)	ar	sigma-ar	sr	sigma-sr	cas	ras	Qr	N
pk vl	-8.05e-02	7.59e-02	9.65e-02	6.60e-02	-4.79e-03	-0.956	3.15e-02	59

C89V z G=5,6,7 may1696c Distance dependence

T(s)	ar	sigma-ar	sr	sigma-sr	cas	ras	Qr	N
pk vl	-3.78e-02	7.94e-02	5.58e-02	6.32e-02	-4.78e-03	-0.953	3.39e-02	88

C90/94 h G=0,2 may2196b Distance dependence

T(s)	ar	sigma-ar	sr	sigma-sr	cas	ras	Qr	N
0.00	-6.30e-01	2.40e-01	3.81e-01	1.82e-01	-4.31e-02	-0.986	7.12e-01	24
0.05	-6.31e-01	4.15e-01	5.35e-01	3.08e-01	-1.26e-01	-0.989	7.63e-01	15
0.10	-2.25e-01	3.17e-01	1.72e-01	2.31e-01	-7.23e-02	-0.986	2.34e-01	18
0.15	-5.09e-01	3.33e-01	3.44e-01	2.42e-01	-7.97e-02	-0.986	2.12e-01	18
0.20	-7.19e-01	3.19e-01	4.98e-01	2.32e-01	-7.30e-02	-0.986	4.27e-01	18
0.30	-8.29e-01	2.77e-01	5.11e-01	2.01e-01	-5.50e-02	-0.986	2.62e-02	18
0.40	-5.39e-01	2.74e-01	2.82e-01	2.00e-01	-5.40e-02	-0.987	2.86e-01	18
0.50	-6.24e-01	2.75e-01	3.61e-01	2.00e-01	-5.45e-02	-0.987	5.41e-01	18
0.75	-1.80e-01	3.29e-01	-2.34e-02	2.39e-01	-7.76e-02	-0.987	6.58e-01	18
1.00	-1.28e+00	2.19e+00	6.97e-01	1.75e+00	-3.82e+00	-0.998	3.91e-01	3
1.50	-3.62e+00	2.14e+00	2.82e+00	1.74e+00	-3.72e+00	-0.998	8.96e-01	3
2.00	-3.62e+00	2.00e+00	2.85e+00	1.64e+00	-3.26e+00	-0.998	6.59e-01	3

C90 z G=0,2 may2196b Distance dependence

T(s)	ar	sigma-ar	sr	sigma-sr	cas	ras	Qr	N
0.00	-1.22e-01	2.97e-01	2.40e-02	2.19e-01	-6.41e-02	-0.987	5.77e-01	23
0.05	2.08e-01	5.96e-01	-3.74e-02	4.42e-01	-2.61e-01	-0.991	5.73e-01	14
0.10	6.42e-03	3.71e-01	-1.48e-02	2.70e-01	-9.89e-02	-0.987	8.41e-01	17
0.15	-2.84e-01	3.82e-01	1.90e-01	2.78e-01	-1.05e-01	-0.986	9.04e-01	17
0.20	-2.03e-01	3.57e-01	1.15e-01	2.60e-01	-9.13e-02	-0.985	5.64e-01	17
0.30	-2.83e-01	3.50e-01	1.76e-01	2.55e-01	-8.78e-02	-0.985	7.46e-01	17
0.40	-4.10e-01	3.71e-01	2.96e-01	2.70e-01	-9.86e-02	-0.985	9.12e-01	17
0.50	-4.04e-01	3.55e-01	3.02e-01	2.58e-01	-9.04e-02	-0.986	8.35e-01	17
0.75	-5.95e-01	4.33e-01	4.21e-01	3.24e-01	-1.39e-01	-0.988	4.58e-01	14
1.00	-1.32e+00	2.54e+00	1.01e+00	2.05e+00	-5.20e+00	-0.998	8.95e-01	3
1.50	-2.39e+00	2.90e+00	2.15e+00	2.35e+00	-6.79e+00	-0.998	8.64e-01	3
2.00	-3.41e+00	2.63e+00	3.02e+00	2.16e+00	-5.66e+00	-0.998	4.64e-01	3

C90V h G=0,2 may1696c Distance dependence

T(s)	ar	sigma-ar	sr	sigma-sr	cas	ras	Qr	N
pk vl	-3.36e+00	1.78e+00	2.57e+00	1.45e+00	-2.58e+00	-0.998	7.61e-01	3

C90V z G=0,2 may1696c Distance dependence

T(s)	ar	sigma-ar	sr	sigma-sr	cas	ras	Qr	N
pk vl	-3.32e+00	2.11e+00	2.66e+00	1.73e+00	-3.64e+00	-0.998	5.93e-01	3

C93/94 h G=1 may2196b Distance dependence

T(s)	ar	sigma-ar	sr	sigma-sr	cas	ras	Qr	N
0.00	-5.88e-01	4.10e-01	4.02e-01	2.45e-01	-9.90e-02	-0.985	9.24e-01	11
0.05	-6.34e-01	4.64e-01	4.76e-01	2.75e-01	-1.25e-01	-0.984	4.45e-02	9
0.10	-6.77e-01	4.63e-01	4.57e-01	2.73e-01	-1.25e-01	-0.986	9.25e-01	11
0.15	-6.87e-01	4.79e-01	4.73e-01	2.83e-01	-1.34e-01	-0.986	9.91e-01	11
0.20	-3.37e-01	5.11e-01	2.75e-01	3.02e-01	-1.52e-01	-0.986	9.62e-01	11
0.30	-2.35e-01	4.87e-01	2.80e-01	2.88e-01	-1.38e-01	-0.986	9.19e-01	11
0.40	-5.43e-01	5.67e-01	5.35e-01	3.51e-01	-1.95e-01	-0.979	8.68e-01	6
0.50	-9.31e-01	5.84e-01	7.84e-01	3.62e-01	-2.07e-01	-0.979	9.57e-01	6
0.75	-5.69e-01	6.02e-01	5.33e-01	3.72e-01	-2.19e-01	-0.979	9.31e-01	6
1.00	-4.36e-01	6.28e-01	4.49e-01	3.89e-01	-2.39e-01	-0.979	9.45e-01	6
1.50	1.18e-01	5.16e-01	3.57e-02	3.33e-01	-1.68e-01	-0.978	4.75e-01	5
2.00	1.43e-01	4.88e-01	-1.10e-02	3.15e-01	-1.51e-01	-0.978	2.41e-01	5

I93 h G=0,1,2 may2196b Distance dependence

T(s)	ar	sigma-ar	sr	sigma-sr	cas	ras	Qr	N
0.00	-4.52e-01	1.94e-01	2.14e-01	1.33e-01	-2.53e-02	-0.980	9.65e-01	35
0.05	-3.97e-01	2.42e-01	2.09e-01	1.67e-01	-3.97e-02	-0.980	5.66e-01	24
0.10	-1.67e-01	2.17e-01	1.21e-02	1.47e-01	-3.13e-02	-0.980	6.20e-01	29
0.15	-3.46e-01	2.22e-01	1.17e-01	1.50e-01	-3.24e-02	-0.980	5.98e-01	29
0.20	-3.89e-01	2.22e-01	1.54e-01	1.50e-01	-3.24e-02	-0.980	7.87e-01	29
0.30	-6.06e-01	2.30e-01	3.02e-01	1.55e-01	-3.48e-02	-0.980	5.96e-01	29
0.40	-6.22e-01	2.30e-01	3.27e-01	1.55e-01	-3.48e-02	-0.980	8.63e-01	29
0.50	-5.98e-01	2.38e-01	3.44e-01	1.60e-01	-3.73e-02	-0.980	9.84e-01	29
0.75	-3.50e-01	2.46e-01	1.86e-01	1.66e-01	-3.99e-02	-0.979	7.97e-01	29
1.00	-3.31e-02	2.46e-01	-7.92e-03	1.66e-01	-3.99e-02	-0.979	7.72e-01	29
1.50	5.15e-02	2.81e-01	1.16e-02	1.96e-01	-5.42e-02	-0.981	6.97e-01	23
2.00	2.68e-02	3.10e-01	3.46e-02	2.21e-01	-6.72e-02	-0.981	5.36e-01	21

JB88V h G=0,1,2 may1696c Distance dependence

T(s)	ar	sigma-ar	sr	sigma-sr	cas	ras	Qr	N
pk vl	-2.29e-01	2.41e-01	1.36e-01	1.65e-01	-3.90e-02	-0.978	9.94e-01	35

JB88V h G=5,6,7 may1696c Distance dependence

T(s)	ar	sigma-ar	sr	sigma-sr	cas	ras	Qr	N

pk vl	-1.12e-01	1.07e-01	6.58e-02	8.46e-02	-8.70e-03	-0.958	9.97e-01	93

SP96 h G=0,1,2 may2196b Distance dependence

T(s)	ar	sigma-ar	sr	sigma-sr	cas	ras	Qr	N
0.00	7.01e-03	1.40e-01	-4.74e-02	9.59e-02	-1.31e-02	-0.978	2.06e-01	35
0.05	2.00e-01	1.77e-01	-1.22e-01	1.20e-01	-2.07e-02	-0.978	3.17e-04	24
0.10	3.02e-01	1.63e-01	-2.33e-01	1.10e-01	-1.75e-02	-0.976	1.34e-03	29
0.15	8.61e-02	1.72e-01	-1.27e-01	1.15e-01	-1.93e-02	-0.976	1.85e-02	29
0.20	1.15e-01	1.84e-01	-1.55e-01	1.24e-01	-2.24e-02	-0.976	2.19e-02	29
0.30	-1.37e-01	2.10e-01	2.18e-02	1.41e-01	-2.90e-02	-0.976	2.15e-01	29
0.40	-1.36e-01	2.26e-01	4.09e-02	1.52e-01	-3.37e-02	-0.976	8.88e-01	29
0.50	-2.39e-01	2.32e-01	1.16e-01	1.56e-01	-3.55e-02	-0.976	9.70e-01	29
0.75	-1.19e-01	2.43e-01	7.07e-03	1.63e-01	-3.87e-02	-0.976	8.79e-01	29
1.00	1.88e-01	2.49e-01	-1.99e-01	1.67e-01	-4.07e-02	-0.976	9.67e-01	29
1.50	8.98e-02	2.94e-01	-1.00e-01	2.07e-01	-5.95e-02	-0.978	8.87e-01	23
2.00	1.22e-01	3.05e-01	-9.79e-02	2.19e-01	-6.53e-02	-0.977	6.69e-01	21

SP96 h G=5,6 may2196b Distance dependence

T(s)	ar	sigma-ar	sr	sigma-sr	cas	ras	Qr	N
0.00	8.81e-02	6.50e-02	1.12e-03	5.25e-02	-3.27e-03	-0.959	1.02e-02	88
0.05	1.42e-01	7.46e-02	-1.17e-02	6.28e-02	-4.50e-03	-0.959	7.81e-02	75
0.10	2.48e-01	7.36e-02	-8.73e-02	6.06e-02	-4.28e-03	-0.959	4.46e-02	84
0.15	1.04e-01	7.74e-02	-4.02e-03	6.38e-02	-4.74e-03	-0.959	1.93e-02	84
0.20	-7.85e-03	8.32e-02	7.02e-02	6.86e-02	-5.48e-03	-0.959	3.15e-02	84
0.30	-4.55e-02	9.48e-02	5.57e-02	7.82e-02	-7.11e-03	-0.959	9.02e-01	84
0.40	-1.30e-01	1.02e-01	7.88e-02	8.43e-02	-8.26e-03	-0.959	9.42e-01	84
0.50	-1.43e-01	1.05e-01	9.86e-02	8.65e-02	-8.71e-03	-0.959	8.70e-01	84
0.75	-2.18e-01	1.10e-01	8.54e-02	9.03e-02	-9.49e-03	-0.959	2.26e-01	84
1.00	-3.01e-01	1.12e-01	1.23e-01	9.26e-02	-9.97e-03	-0.959	3.12e-01	84
1.50	-3.21e-01	1.25e-01	2.34e-01	1.06e-01	-1.28e-02	-0.964	5.26e-01	79
2.00	-2.29e-01	1.33e-01	2.55e-01	1.15e-01	-1.47e-02	-0.965	7.46e-01	73

SP96 h G=7 may2196b Distance dependence

T(s)	ar	sigma-ar	sr	sigma-sr	cas	ras	Qr	N
0.00	4.16e-01	5.28e-01	-2.46e-01	3.07e-01	-1.60e-01	-0.989	3.89e-01	5
0.05	1.17e+00	7.26e-01	-7.69e-01	4.62e-01	-3.32e-01	-0.989	4.19e-01	3
0.10	1.19e+00	5.80e-01	-8.10e-01	3.37e-01	-1.93e-01	-0.989	2.77e-04	5
0.15	1.34e+00	6.10e-01	-8.54e-01	3.54e-01	-2.14e-01	-0.989	4.11e-04	5
0.20	9.40e-01	6.56e-01	-6.50e-01	3.81e-01	-2.47e-01	-0.989	5.58e-05	5
0.30	1.44e+00	7.47e-01	-9.83e-01	4.34e-01	-3.21e-01	-0.989	1.28e-02	5
0.40	2.39e+00	8.06e-01	-1.55e+00	4.68e-01	-3.73e-01	-0.989	1.31e-02	5
0.50	2.33e+00	8.27e-01	-1.51e+00	4.80e-01	-3.93e-01	-0.989	1.23e-01	5
0.75	2.34e+00	8.63e-01	-1.63e+00	5.01e-01	-4.28e-01	-0.989	6.36e-02	5
1.00	2.24e+00	8.85e-01	-1.50e+00	5.14e-01	-4.50e-01	-0.989	1.71e-02	5
1.50	3.15e+00	9.00e-01	-2.02e+00	5.23e-01	-4.66e-01	-0.989	8.27e-02	5
2.00	2.99e+00	9.06e-01	-1.87e+00	5.26e-01	-4.72e-01	-0.989	1.39e-02	5

SP96V h G=0,1,2 may1696c Distance dependence

T(s)	ar	sigma-ar	sr	sigma-sr	cas	ras	Qr	N
pk vl	1.7[illegible]e-01	1.74e-01	-1.05e-01	1.19e-01	-2.02e-02	-0.978	1.85e-01	35

SP96V h G=5,6,7 may1696c Distance dependence

T(s)	ar	sigma-ar	sr	sigma-sr	cas	ras	Qr	N
pk vl	1.36e-01	7.74e-02	-6.05e-02	6.10e-02	-4.52e-03	-0.958	6.01e-03	93

S93 h G=0,1,2 may2196b Distance dependence

T(s)	ar	sigma-ar	sr	sigma-sr	cas	ras	Qr	N
0.00	-5.63e-01	1.94e-01	3.17e-01	1.33e-01	-2.53e-02	-0.980	9.82e-01	35
0.05	-6.67e-01	2.42e-01	4.66e-01	1.67e-01	-3.97e-02	-0.980	5.78e-01	24
0.10	-4.10e-01	2.17e-01	2.28e-01	1.47e-01	-3.13e-02	-0.980	6.59e-01	29
0.15	-5.19e-01	2.22e-01	2.72e-01	1.50e-01	-3.24e-02	-0.980	6.97e-01	29
0.20	-4.98e-01	2.26e-01	2.76e-01	1.52e-01	-3.36e-02	-0.980	8.05e-01	29
0.30	-6.72e-01	2.34e-01	3.95e-01	1.58e-01	-3.61e-02	-0.980	7.27e-01	29
0.40	-6.70e-01	2.46e-01	4.11e-01	1.66e-01	-3.99e-02	-0.979	9.51e-01	29
0.50	-6.32e-01	2.54e-01	4.13e-01	1.71e-01	-4.25e-02	-0.979	9.95e-01	29
0.75	-3.75e-01	2.62e-01	2.12e-01	1.76e-01	-4.52e-02	-0.979	8.98e-01	29
1.00	-6.63e-02	2.66e-01	-1.91e-02	1.79e-01	-4.66e-02	-0.979	9.04e-01	29
1.50	-2.40e-02	3.05e-01	-4.60e-03	2.13e-01	-6.36e-02	-0.981	8.49e-01	23
2.00	-3.28e-02	3.15e-01	-1.22e-02	2.24e-01	-6.94e-02	-0.981	5.41e-01	21

S93 z G=0,1,2 may2196b Distance dependence

T(s)	ar	sigma-ar	sr	sigma-sr	cas	ras	Qr	N
0.00	-6.11e-01	2.22e-01	3.80e-01	1.54e-01	-3.35e-02	-0.980	9.55e-01	32

0.05	-3.67e-01	3.21e-01	3.13e-01	2.20e-01	-6.94e-02	-0.980	8.25e-01	21
0.10	-4.77e-01	2.72e-01	3.37e-01	1.84e-01	-4.92e-02	-0.979	9.51e-01	26
0.15	-5.53e-01	2.72e-01	4.03e-01	1.84e-01	-4.92e-02	-0.979	9.93e-01	26
0.20	-5.33e-01	2.72e-01	4.08e-01	1.84e-01	-4.92e-02	-0.979	9.45e-01	26
0.30	-5.53e-01	2.72e-01	4.41e-01	1.84e-01	-4.92e-02	-0.979	9.12e-01	26
0.40	-5.54e-01	2.72e-01	4.36e-01	1.84e-01	-4.92e-02	-0.979	9.39e-01	26
0.50	-4.76e-01	2.72e-01	3.56e-01	1.84e-01	-4.92e-02	-0.979	9.92e-01	26
0.75	-4.51e-01	3.00e-01	3.23e-01	2.10e-01	-6.18e-02	-0.980	7.84e-01	22
1.00	-3.99e-01	3.05e-01	3.18e-01	2.12e-01	-6.35e-02	-0.980	6.66e-01	21
1.50	1.48e-01	3.34e-01	-3.66e-02	2.29e-01	-7.50e-02	-0.982	8.42e-01	19
2.00	1.00e-01	3.48e-01	4.22e-02	2.41e-01	-8.22e-02	-0.981	7.43e-01	16

Sea96 h G=0,1,2 may2196b Distance dependence

T(s)	ar	sigma-ar	sr	sigma-sr	cas	ras	Qr	N
0.00	6.73e-02	1.74e-01	-9.75e-02	1.20e-01	-2.04e-02	-0.978	8.07e-01	35
0.05	-	-	-	-	-	-	-	0
0.10	6.00e-02	2.30e-01	-5.68e-02	1.55e-01	-3.47e-02	-0.976	8.16e-01	29
0.15	2.46e-02	2.38e-01	-5.79e-02	1.60e-01	-3.71e-02	-0.976	8.85e-01	29
0.20	1.29e-01	2.46e-01	-1.18e-01	1.65e-01	-3.96e-02	-0.976	8.45e-01	29
0.30	-2.03e-02	2.58e-01	5.61e-04	1.74e-01	-4.39e-02	-0.976	8.66e-01	29
0.40	1.01e-02	2.69e-01	-7.96e-03	1.81e-01	-4.75e-02	-0.976	9.65e-01	29
0.50	1.86e-02	2.77e-01	2.48e-03	1.87e-01	-5.06e-02	-0.976	9.91e-01	29
0.75	1.98e-01	2.96e-01	-1.50e-01	1.99e-01	-5.74e-02	-0.976	9.81e-01	29
1.00	4.21e-01	3.10e-01	-3.22e-01	2.09e-01	-6.32e-02	-0.976	9.91e-01	29
1.50	2.24e-01	3.85e-01	-1.65e-01	2.72e-01	-1.03e-01	-0.978	9.36e-01	23
2.00	1.56e-01	4.18e-01	-1.69e-01	3.01e-01	-1.23e-01	-0.977	8.16e-01	21

Sea96 h G=5,6,7 may2196b Distance dependence

T(s)	ar	sigma-ar	sr	sigma-sr	cas	ras	Qr	N
0.00	7.50e-02	7.77e-02	-3.98e-02	6.13e-02	-4.56e-03	-0.958	9.29e-01	93
0.05	-	-	-	-	-	-	-	0
0.10	2.71e-02	9.85e-02	-3.57e-03	7.90e-02	-7.45e-03	-0.958	9.86e-01	89
0.15	6.12e-02	1.02e-01	-4.45e-02	8.16e-02	-7.96e-03	-0.958	9.70e-01	89
0.20	5.94e-02	1.05e-01	-4.40e-02	8.44e-02	-8.50e-03	-0.958	9.62e-01	89
0.30	1.19e-01	1.11e-01	-9.53e-02	8.88e-02	-9.41e-03	-0.958	1.00e+00	89
0.40	9.76e-02	1.15e-01	-8.57e-02	9.23e-02	-1.02e-02	-0.958	9.98e-01	89
0.50	1.54e-01	1.19e-01	-9.76e-02	9.53e-02	-1.09e-02	-0.958	9.98e-01	89
0.75	1.68e-01	1.27e-01	-1.35e-01	1.02e-01	-1.23e-02	-0.958	8.48e-01	89
1.00	1.30e-01	1.33e-01	-1.26e-01	1.07e-01	-1.36e-02	-0.958	9.28e-01	89
1.50	1.41e-01	1.52e-01	-1.12e-01	1.25e-01	-1.82e-02	-0.960	9.89e-01	84
2.00	3.16e-01	1.66e-01	-2.45e-01	1.39e-01	-2.21e-02	-0.961	9.98e-01	78

Table 11. Magnitude dependences for each predictive relation, determined from data at all distances.

BJF94 h G=0,1,2 may2196b Magnitude dependence

T(s)	am	sigma-am	sm	sigma-sm	cas	ras	Qm	N
0.00	-1.03e+00	3.96e-01	1.40e-01	6.48e-02	-2.56e-02	-0.996	6.92e-01	35
0.05	-	-	-	-	-	-	-	0
0.10	-4.10e-01	3.65e-01	4.66e-02	5.98e-02	-2.17e-02	-0.995	3.39e-02	29
0.15	-7.84e-01	3.54e-01	9.55e-02	5.81e-02	-2.05e-02	-0.995	5.00e-02	29
0.20	-1.46e+00	3.54e-01	2.06e-01	5.81e-02	-2.05e-02	-0.995	1.05e-01	29
0.30	-1.05e+00	3.66e-01	1.38e-01	6.01e-02	-2.19e-02	-0.995	3.38e-02	29
0.40	-1.19e+00	3.82e-01	1.65e-01	6.26e-02	-2.38e-02	-0.995	2.87e-01	29
0.50	-1.19e+00	3.95e-01	1.70e-01	6.49e-02	-2.55e-02	-0.995	6.32e-01	29
0.75	-1.38e+00	4.21e-01	2.01e-01	6.90e-02	-2.89e-02	-0.995	4.27e-01	29
1.00	-1.63e+00	4.40e-01	2.42e-01	7.23e-02	-3.17e-02	-0.995	4.58e-01	29
1.50	-2.23e+00	5.06e-01	3.43e-01	8.16e-02	-4.10e-02	-0.995	7.95e-01	23
2.00	-2.70e+00	5.18e-01	4.03e-01	8.36e-02	-4.30e-02	-0.995	6.71e-01	21

BJF94 h G=5,6,7 may2196b Magnitude dependence

T(s)	am	sigma-am	sm	sigma-sm	cas	ras	Qm	N
0.00	-1.01e-01	3.59e-01	2.75e-03	5.76e-02	-2.07e-02	-0.998	5.26e-01	93
0.05	-	-	-	-	-	-	-	0
0.10	8.27e-01	3.30e-01	-1.39e-01	5.29e-02	-1.74e-02	-0.998	1.84e-02	89
0.15	8.17e-01	3.21e-01	-1.42e-01	5.14e-02	-1.65e-02	-0.998	3.35e-04	89
0.20	4.37e-01	3.21e-01	-8.42e-02	5.15e-02	-1.65e-02	-0.998	1.09e-05	89
0.30	4.79e-01	3.32e-01	-9.58e-02	5.32e-02	-1.76e-02	-0.998	6.29e-03	89
0.40	5.07e-01	3.46e-01	-1.04e-01	5.54e-02	-1.91e-02	-0.998	1.97e-03	89
0.50	9.97e-01	3.58e-01	-1.76e-01	5.74e-02	-2.05e-02	-0.998	3.73e-03	89
0.75	1.13e+00	3.81e-01	-1.99e-01	6.11e-02	-2.32e-02	-0.998	7.59e-08	89
1.00	8.56e-01	3.99e-01	-1.57e-01	6.40e-02	-2.55e-02	-0.998	4.55e-07	89
1.50	9.31e-01	4.44e-01	-1.63e-01	7.10e-02	-3.15e-02	-0.998	3.45e-05	84
2.00	-1.98e-01	4.71e-01	1.81e-02	7.53e-02	-3.54e-02	-0.998	8.19e-06	78

C89/94 h G=5,6,7 may2196b Magnitude dependence

T(s)	am	sigma-am	sm	sigma-sm	cas	ras	Qm	N
0.00	7.05e-01	3.47e-01	-1.16e-01	5.53e-02	-1.91e-02	-0.998	7.01e-01	93
0.05	9.03e-01	3.73e-01	-1.31e-01	5.98e-02	-2.23e-02	-0.998	4.59e-01	78
0.10	1.14e+00	3.60e-01	-1.73e-01	5.78e-02	-2.08e-02	-0.998	3.43e-01	89
0.15	1.28e+00	3.75e-01	-2.02e-01	6.02e-02	-2.25e-02	-0.998	2.01e-01	89
0.20	8.56e-01	3.75e-01	-1.37e-01	6.02e-02	-2.25e-02	-0.998	3.61e-02	89
0.30	6.76e-01	3.75e-01	-1.13e-01	6.02e-02	-2.25e-02	-0.998	4.32e-01	89
0.40	8.56e-01	3.75e-01	-1.42e-01	6.02e-02	-2.25e-02	-0.998	1.37e-01	89
0.50	1.36e+00	3.75e-01	-2.19e-01	6.02e-02	-2.25e-02	-0.998	2.05e-01	89
0.75	1.59e+00	3.75e-01	-2.62e-01	6.02e-02	-2.25e-02	-0.998	1.79e-06	89
1.00	1.51e+00	3.75e-01	-2.53e-01	6.02e-02	-2.25e-02	-0.998	1.73e-06	89
1.50	6.57e-01	5.77e-01	-1.11e-01	9.12e-02	-5.25e-02	-0.999	8.69e-02	58
2.00	3.01e-01	5.83e-01	-5.03e-02	9.20e-02	-5.35e-02	-0.999	7.64e-02	56

C89 z G=5,6,7 may2196b Magnitude dependence

T(s)	am	sigma-am	sm	sigma-sm	cas	ras	Qm	N
0.00	1.64e+00	4.71e-01	-2.65e-01	7.56e-02	-3.55e-02	-0.998	9.87e-01	88
0.05	2.02e+00	5.43e-01	-2.97e-01	8.73e-02	-4.73e-02	-0.998	5.83e-01	79
0.10	2.38e+00	5.13e-01	-3.99e-01	8.24e-02	-4.22e-02	-0.998	8.01e-02	84
0.15	1.89e+00	5.13e-01	-3.01e-01	8.24e-02	-4.22e-02	-0.998	9.36e-01	84
0.20	1.76e+00	5.13e-01	-2.71e-01	8.24e-02	-4.22e-02	-0.998	6.90e-01	84
0.30	1.99e+00	5.13e-01	-2.89e-01	8.24e-02	-4.22e-02	-0.998	5.66e-01	84
0.40	2.13e+00	5.13e-01	-3.32e-01	8.24e-02	-4.22e-02	-0.998	6.03e-02	84
0.50	2.36e+00	5.13e-01	-3.82e-01	8.24e-02	-4.22e-02	-0.998	1.50e-01	84
0.75	2.24e+00	5.51e-01	-3.76e-01	8.82e-02	-4.85e-02	-0.998	5.45e-03	79
1.00	2.58e+00	5.72e-01	-4.25e-01	9.13e-02	-5.22e-02	-0.999	3.40e-03	75
1.50	3.16e+00	8.18e-01	-5.22e-01	1.29e-01	-1.05e-01	-0.999	1.28e-03	51
2.00	2.49e+00	8.31e-01	-4.17e-01	1.31e-01	-1.08e-01	-0.999	1.06e-02	47

C89V h G=5,6,7 may1696c Magnitude dependence

T(s)	am	sigma-am	sm	sigma-sm	cas	ras	Qm	N
pk vl	3.38e-01	4.55e-01	-4.94e-02	7.19e-02	-3.27e-02	-0.999	2.36e-02	59

C89V z G=5,6,7 may1696c Magnitude dependence

T(s)	am	sigma-am	sm	sigma-sm	cas	ras	Qm	N
pk vl	1.47e+00	4.30e-01	-2.32e-01	6.91e-02	-2.97e-02	-0.998	1.30e-01	88

C90/94 h G=0,2 may2196b Magnitude dependence

T(s)	am	sigma-am	sm	sigma-sm	cas	ras	Qm	N
0.00	-2.03e-01	5.24e-01	1.09e-02	8.33e-02	-4.35e-02	-0.997	4.44e-01	24
0.05	7.72e-01	6.96e-01	-1.10e-01	1.10e-01	-7.65e-02	-0.996	5.97e-01	15
0.10	8.89e-01	6.58e-01	-1.36e-01	1.02e-01	-6.66e-02	-0.997	2.99e-01	18
0.15	4.97e-01	6.97e-01	-8.35e-02	1.07e-01	-7.46e-02	-0.997	1.57e-01	18
0.20	-2.47e-01	6.68e-01	3.13e-02	1.03e-01	-6.84e-02	-0.997	1.83e-01	18
0.30	-5.50e-01	5.67e-01	6.43e-02	8.78e-02	-4.97e-02	-0.997	4.53e-03	18
0.40	-5.85e-01	5.97e-01	6.57e-02	9.12e-02	-5.43e-02	-0.997	2.14e-01	18
0.50	-9.99e-01	6.23e-01	1.32e-01	9.46e-02	-5.88e-02	-0.998	4.47e-01	18
0.75	-1.03e+00	7.02e-01	1.26e-01	1.08e-01	-7.54e-02	-0.997	7.55e-01	18
1.00	-1.39e+00	2.93e+00	1.60e-01	4.82e-01	-1.41e+00	-0.999	3.76e-01	3
1.50	-4.78e+00	2.89e+00	7.71e-01	4.80e-01	-1.39e+00	-0.999	7.94e-01	3
2.00	-4.95e+00	2.71e+00	8.04e-01	4.54e-01	-1.23e+00	-0.999	7.74e-01	3

C90 z G=0,2 may2196b Magnitude dependence

T(s)	am	sigma-am	sm	sigma-sm	cas	ras	Qm	N
0.00	2.59e-01	7.11e-01	-5.47e-02	1.12e-01	-7.92e-02	-0.998	5.92e-01	23
0.05	1.41e+00	1.12e+00	-1.94e-01	1.73e-01	-1.93e-01	-0.997	6.83e-01	14
0.10	5.40e-01	9.08e-01	-8.44e-02	1.38e-01	-1.25e-01	-0.998	8.62e-01	17
0.15	7.90e-01	9.06e-01	-1.25e-01	1.39e-01	-1.25e-01	-0.998	9.19e-01	17
0.20	-2.05e-01	8.26e-01	2.44e-02	1.27e-01	-1.05e-01	-0.997	5.52e-01	17
0.30	-4.15e-01	8.09e-01	5.72e-02	1.25e-01	-1.01e-01	-0.997	7.27e-01	17
0.40	-9.89e-01	8.58e-01	1.51e-01	1.32e-01	-1.13e-01	-0.997	9.17e-01	17
0.50	-1.30e+00	8.51e-01	2.00e-01	1.30e-01	-1.10e-01	-0.998	8.91e-01	17
0.75	-2.30e+00	1.04e+00	3.44e-01	1.58e-01	-1.64e-01	-0.998	7.21e-01	14
1.00	-1.78e+00	3.41e+00	2.85e-01	5.66e-01	-1.93e+00	-0.999	9.26e-01	3
1.50	-3.25e+00	3.90e+00	5.82e-01	6.48e-01	-2.52e+00	-0.999	8.07e-01	3
2.00	-4.47e+00	3.57e+00	7.95e-01	6.00e-01	-2.14e+00	-0.999	3.93e-01	3

C90V h G=0,2 may1696c Magnitude dependence

T(s)	am	sigma-am	sm	sigma-sm	cas	ras	Qm	N
pk vl	-4.39e+00	2.41e+00	6.98e-01	4.00e-01	-9.62e-01	-0.999	6.55e-01	3

C90V z G=0,2 may1696c Magnitude dependence

T(s)	am	sigma-am	sm	sigma-sm	cas	ras	Qm	N
pk vl	-4.32e+00	2.86e+00	7.12e-01	4.79e-01	-1.37e+00	-0.999	5.05e-01	3

C93/94 h G=1 may2196b Magnitude dependence

T(s)	am	sigma-am	sm	sigma-sm	cas	ras	Qm	N
0.00	5.05e-01	7.77e-01	-7.37e-02	1.33e-01	-1.03e-01	-0.996	7.21e-01	11
0.05	2.14e+00	1.14e+00	-3.51e-01	2.01e-01	-2.27e-01	-0.997	4.53e-02	9
0.10	4.97e-01	8.25e-01	-7.05e-02	1.41e-01	-1.16e-01	-0.996	7.08e-01	11
0.15	5.18e-01	8.53e-01	-7.15e-02	1.46e-01	-1.24e-01	-0.996	8.69e-01	11
0.20	-6.66e-01	9.10e-01	1.35e-01	1.56e-01	-1.41e-01	-0.996	9.59e-01	11
0.30	-4.85e-01	8.68e-01	1.23e-01	1.48e-01	-1.28e-01	-0.996	9.02e-01	11
0.40	2.48e+00	1.79e+00	-3.86e-01	3.18e-01	-5.67e-01	-0.998	7.15e-01	6
0.50	3.49e+00	1.84e+00	-5.66e-01	3.27e-01	-6.03e-01	-0.998	6.68e-01	6
0.75	3.14e+00	1.90e+00	-5.09e-01	3.37e-01	-6.39e-01	-0.998	9.60e-01	6
1.00	1.95e+00	1.98e+00	-2.98e-01	3.52e-01	-6.96e-01	-0.998	8.49e-01	6
1.50	-1.35e+00	1.66e+00	2.68e-01	2.91e-01	-4.82e-01	-0.998	6.45e-01	5
2.00	-1.55e+00	1.57e+00	2.95e-01	2.75e-01	-4.31e-01	-0.998	3.84e-01	5

I93 h G=0,1,2 may2196b Magnitude dependence

T(s)	am	sigma-am	sm	sigma-sm	cas	ras	Qm	N
0.00	6.96e-02	4.46e-01	-3.48e-02	7.11e-02	-3.16e-02	-0.996	9.23e-01	35
0.05	5.42e-02	5.00e-01	-2.53e-02	8.10e-02	-4.03e-02	-0.995	4.76e-01	24
0.10	5.06e-02	4.64e-01	-3.20e-02	7.39e-02	-3.42e-02	-0.996	6.30e-01	29
0.15	1.51e-01	4.72e-01	-5.23e-02	7.53e-02	-3.54e-02	-0.996	5.90e-01	29
0.20	-3.63e-01	4.72e-01	3.15e-02	7.53e-02	-3.54e-02	-0.996	7.44e-01	29
0.30	1.74e-01	4.89e-01	-5.48e-02	7.81e-02	-3.80e-02	-0.996	4.14e-01	29
0.40	-3.17e-02	4.89e-01	-1.84e-02	7.81e-02	-3.80e-02	-0.996	6.52e-01	29
0.50	-1.43e-01	5.06e-01	7.37e-03	8.08e-02	-4.07e-02	-0.996	8.94e-01	29
0.75	-3.12e-01	5.23e-01	3.73e-02	8.35e-02	-4.35e-02	-0.996	7.45e-01	29
1.00	-5.16e-01	5.23e-01	7.57e-02	8.35e-02	-4.35e-02	-0.996	8.10e-01	29
1.50	-9.50e-01	5.88e-01	1.61e-01	9.25e-02	-5.42e-02	-0.996	8.60e-01	23
2.00	-1.17e+00	6.26e-01	1.96e-01	9.84e-02	-6.13e-02	-0.995	7.92e-01	21

JB88V h G=0,1,2 may1696c Magnitude dependence

T(s)	am	sigma-am	sm	sigma-sm	cas	ras	Qm	N
pk vl	-5.74e-01	5.69e-01	8.83e-02	9.30e-02	-5.27e-02	-0.996	9.94e-01	35

JB88V h G=5,6,7 may1696c Magnitude dependence

T(s)	am	sigma-am	sm	sigma-sm	cas	ras	Qm	N

pk vl	3.94e-01	5.15e-01	-6.85e-02	8.27e-02	-4.26e-02	-0.998	9.97e-01	93

SP96 h G=0,1,2 may2196b Magnitude dependence

T(s)	am	sigma-am	sm	sigma-sm	cas	ras	Qm	N
0.00	-2.35e-01	3.30e-01	2.87e-02	5.39e-02	-1.77e-02	-0.996	2.08e-01	35
0.05	-2.73e-01	3.91e-01	4.98e-02	6.53e-02	-2.54e-02	-0.995	2.74e-04	24
0.10	-5.37e-01	3.63e-01	8.24e-02	5.95e-02	-2.15e-02	-0.995	6.32e-04	29
0.15	-8.21e-01	3.82e-01	1.19e-01	6.26e-02	-2.38e-02	-0.995	3.25e-02	29
0.20	-1.31e+00	4.10e-01	1.97e-01	6.73e-02	-2.75e-02	-0.995	1.01e-01	29
0.30	-9.84e-01	4.67e-01	1.45e-01	7.67e-02	-3.57e-02	-0.995	3.64e-01	29
0.40	-6.60e-01	5.04e-01	9.61e-02	8.27e-02	-4.15e-02	-0.995	9.26e-01	29
0.50	-5.80e-01	5.17e-01	8.39e-02	8.49e-02	-4.37e-02	-0.995	9.76e-01	29
0.75	-3.11e-01	5.40e-01	3.34e-02	8.86e-02	-4.76e-02	-0.995	8.84e-01	29
1.00	-6.48e-01	5.53e-01	9.02e-02	9.08e-02	-5.00e-02	-0.995	9.60e-01	29
1.50	-1.07e+00	6.16e-01	1.66e-01	9.94e-02	-6.09e-02	-0.995	9.62e-01	23
2.00	-1.40e+00	6.21e-01	2.26e-01	1.00e-01	-6.19e-02	-0.995	9.26e-01	21

SP96 h G=5,6 may2196b Magnitude dependence

T(s)	am	sigma-am	sm	sigma-sm	cas	ras	Qm	N
0.00	7.95e-01	3.16e-01	-1.14e-01	5.08e-02	-1.60e-02	-0.998	2.24e-02	88
0.05	4.79e-01	3.63e-01	-5.64e-02	5.83e-02	-2.11e-02	-0.998	8.79e-02	75
0.10	5.40e-01	3.47e-01	-6.35e-02	5.58e-02	-1.93e-02	-0.998	4.00e-02	84
0.15	8.55e-01	3.65e-01	-1.22e-01	5.87e-02	-2.14e-02	-0.998	3.68e-02	84
0.20	4.91e-01	3.92e-01	-6.72e-02	6.31e-02	-2.47e-02	-0.998	3.19e-02	84
0.30	4.25e-01	4.47e-01	-6.54e-02	7.19e-02	-3.21e-02	-0.998	9.07e-01	84
0.40	8.01e-01	4.82e-01	-1.35e-01	7.75e-02	-3.73e-02	-0.998	9.62e-01	84
0.50	1.49e+00	4.94e-01	-2.45e-01	7.95e-02	-3.93e-02	-0.998	9.70e-01	84
0.75	1.32e+00	5.16e-01	-2.33e-01	8.30e-02	-4.28e-02	-0.998	4.07e-01	84
1.00	1.18e+00	5.29e-01	-2.16e-01	8.51e-02	-4.50e-02	-0.998	4.47e-01	84
1.50	1.14e+00	5.74e-01	-1.93e-01	9.20e-02	-5.27e-02	-0.998	5.12e-01	79
2.00	3.62e-01	6.02e-01	-4.95e-02	9.65e-02	-5.79e-02	-0.998	5.98e-01	73

SP96 h G=7 may2196b Magnitude dependence

T(s)	am	sigma-am	sm	sigma-sm	cas	ras	Qm	N
0.00	-8.57e-01	1.26e+00	1.30e-01	1.92e-01	-2.42e-01	-0.998	3.61e-01	5
0.05	-1.22e+00	1.77e+00	1.88e-01	2.79e-01	-4.92e-01	-0.998	8.49e-02	3
0.10	8.86e-01	1.39e+00	-1.64e-01	2.11e-01	-2.92e-01	-0.998	2.32e-05	5
0.15	1.57e+00	1.46e+00	-2.58e-01	2.22e-01	-3.23e-01	-0.998	4.90e-05	5
0.20	8.01e-01	1.57e+00	-1.48e-01	2.39e-01	-3.73e-01	-0.998	1.66e-05	5
0.30	3.12e+00	1.79e+00	-5.11e-01	2.72e-01	-4.85e-01	-0.998	6.14e-03	5
0.40	4.36e+00	1.93e+00	-7.05e-01	2.93e-01	-5.63e-01	-0.998	1.13e-03	5
0.50	4.32e+00	1.98e+00	-6.97e-01	3.01e-01	-5.93e-01	-0.998	1.58e-02	5
0.75	5.65e+00	2.06e+00	-9.29e-01	3.14e-01	-6.47e-01	-0.998	2.72e-02	5
1.00	5.22e+00	2.12e+00	-8.43e-01	3.22e-01	-6.79e-01	-0.998	8.03e-03	5
1.50	6.79e+00	2.15e+00	-1.08e+00	3.27e-01	-7.03e-01	-0.998	1.34e-02	5
2.00	7.18e+00	2.17e+00	-1.12e+00	3.30e-01	-7.13e-01	-0.998	8.75e-03	5

SP96V h G=0,1,2 may1696c Magnitude dependence

T(s)	am	sigma-am	sm	sigma-sm	cas	ras	Qm	N
pk vl	-9.82e-01	4.10e-01	1.64e-01	6.70e-02	-2.74e-02	-0.996	3.80e-01	35

SP96V h G=5,6,7 may1696c Magnitude dependence

T(s)	am	sigma-am	sm	sigma-sm	cas	ras	Qm	N
pk vl	4.61e-01	3.71e-01	-6.42e-02	5.96e-02	-2.21e-02	-0.998	6.19e-03	93

S93 h G=0,1,2 may2196b Magnitude dependence

T(s)	am	sigma-am	sm	sigma-sm	cas	ras	Qm	N
0.00	1.66e-01	4.46e-01	-4.45e-02	7.11e-02	-3.16e-02	-0.996	8.87e-01	35
0.05	8.17e-01	5.00e-01	-1.34e-01	8.10e-02	-4.03e-02	-0.995	2.94e-01	24
0.10	3.07e-01	4.64e-01	-6.19e-02	7.39e-02	-3.42e-02	-0.996	5.64e-01	29
0.15	1.36e-01	4.72e-01	-4.16e-02	7.53e-02	-3.54e-02	-0.996	5.31e-01	29
0.20	-4.38e-01	4.81e-01	5.45e-02	7.67e-02	-3.67e-02	-0.996	6.65e-01	29
0.30	7.82e-02	4.98e-01	-2.82e-02	7.94e-02	-3.93e-02	-0.996	3.92e-01	29
0.40	-6.64e-02	5.23e-01	-1.15e-03	8.35e-02	-4.35e-02	-0.996	7.25e-01	29
0.50	-3.95e-02	5.39e-01	1.21e-03	8.63e-02	-4.63e-02	-0.995	9.14e-01	29
0.75	-2.95e-01	5.56e-01	3.68e-02	8.90e-02	-4.93e-02	-0.995	8.52e-01	29
1.00	-6.52e-01	5.64e-01	8.98e-02	9.04e-02	-5.08e-02	-0.995	9.31e-01	29
1.50	-1.17e+00	6.34e-01	1.80e-01	9.98e-02	-6.30e-02	-0.996	9.58e-01	23
2.00	-1.49e+00	6.35e-01	2.28e-01	9.99e-02	-6.31e-02	-0.995	8.63e-01	21

S93 z G=0,1,2 may2196b Magnitude dependence

T(s)	am	sigma-am	sm	sigma-sm	cas	ras	Qm	N
0.00	4.95e-01	5.74e-01	-8.99e-02	9.07e-02	-5.19e-02	-0.997	8.00e-01	32

0.05	9.39e-01	7.39e-01	-1.39e-01	1.19e-01	-8.75e-02	-0.996	7.88e-01	21
0.10	5.13e-01	6.57e-01	-7.98e-02	1.04e-01	-6.80e-02	-0.996	8.68e-01	26
0.15	9.96e-01	6.57e-01	-1.54e-01	1.04e-01	-6.80e-02	-0.996	9.67e-01	26
0.20	6.14e-01	6.57e-01	-8.84e-02	1.04e-01	-6.80e-02	-0.996	7.91e-01	26
0.30	1.16e+00	6.57e-01	-1.71e-01	1.04e-01	-6.80e-02	-0.996	7.89e-01	26
0.40	1.06e+00	6.57e-01	-1.56e-01	1.04e-01	-6.80e-02	-0.996	8.20e-01	26
0.50	6.74e-01	6.57e-01	-1.01e-01	1.04e-01	-6.80e-02	-0.996	9.61e-01	26
0.75	8.70e-01	7.28e-01	-1.36e-01	1.14e-01	-8.26e-02	-0.997	7.29e-01	22
1.00	6.20e-01	7.53e-01	-8.92e-02	1.17e-01	-8.80e-02	-0.997	5.53e-01	21
1.50	1.34e-01	7.86e-01	-5.88e-03	1.22e-01	-9.53e-02	-0.997	8.41e-01	19
2.00	-9.73e-02	8.21e-01	3.96e-02	1.26e-01	-1.03e-01	-0.997	7.48e-01	16

Sea96 h G=0,1,2 may2196b Magnitude dependence

T(s)	am	sigma-am	sm	sigma-sm	cas	ras	Qm	N
0.00	-7.81e-01	4.12e-01	1.17e-01	6.73e-02	-2.76e-02	-0.996	8.88e-01	35
0.05	-	-	-	-	-	-	-	0
0.10	-2.14e-01	5.11e-01	3.16e-02	8.39e-02	-4.27e-02	-0.995	8.16e-01	29
0.15	-5.83e-01	5.29e-01	8.64e-02	8.67e-02	-4.56e-02	-0.995	9.12e-01	29
0.20	-1.26e+00	5.46e-01	2.00e-01	8.96e-02	-4.87e-02	-0.995	9.67e-01	29
0.30	-8.38e-01	5.75e-01	1.35e-01	9.43e-02	-5.40e-02	-0.995	9.30e-01	29
0.40	-9.96e-01	5.98e-01	1.64e-01	9.81e-02	-5.84e-02	-0.995	9.92e-01	29
0.50	-9.99e-01	6.17e-01	1.68e-01	1.01e-01	-6.22e-02	-0.995	9.99e-01	29
0.75	-1.22e+00	6.58e-01	1.98e-01	1.08e-01	-7.06e-02	-0.995	9.97e-01	29
1.00	-1.49e+00	6.90e-01	2.37e-01	1.13e-01	-7.77e-02	-0.995	9.98e-01	29
1.50	-2.10e+00	8.09e-01	3.39e-01	1.30e-01	-1.05e-01	-0.995	1.00e+00	23
2.00	-2.51e+00	8.52e-01	3.96e-01	1.38e-01	-1.16e-01	-0.995	9.99e-01	21

Sea96 h G=5,6,7 may2196b Magnitude dependence

T(s)	am	sigma-am	sm	sigma-sm	cas	ras	Qm	N
0.00	4.72e-02	3.73e-01	-3.32e-03	5.99e-02	-2.23e-02	-0.998	9.24e-01	93
0.05	-	-	-	-	-	-	-	0
0.10	9.11e-01	4.63e-01	-1.43e-01	7.43e-02	-3.43e-02	-0.998	9.95e-01	89
0.15	9.02e-01	4.79e-01	-1.44e-01	7.68e-02	-3.67e-02	-0.998	9.86e-01	89
0.20	5.38e-01	4.95e-01	-8.54e-02	7.93e-02	-3.92e-02	-0.998	9.69e-01	89
0.30	6.06e-01	5.21e-01	-9.65e-02	8.35e-02	-4.34e-02	-0.998	1.00e+00	89
0.40	6.44e-01	5.41e-01	-1.04e-01	8.68e-02	-4.69e-02	-0.998	9.99e-01	89
0.50	1.14e+00	5.59e-01	-1.77e-01	8.96e-02	-5.00e-02	-0.998	9.99e-01	89
0.75	1.25e+00	5.96e-01	-2.00e-01	9.55e-02	-5.68e-02	-0.998	8.95e-01	89
1.00	9.71e-01	6.25e-01	-1.59e-01	1.00e-01	-6.25e-02	-0.998	9.41e-01	89
1.50	1.02e+00	7.10e-01	-1.62e-01	1.14e-01	-8.06e-02	-0.998	9.92e-01	84
2.00	-8.17e-02	7.75e-01	1.84e-02	1.24e-01	-9.59e-02	-0.998	9.95e-01	78

Table 12. Correction factors for each predictive relation and period, determined from data at distance less than or equal to 20 km.

BJF94 h G=0,1,2 may2196c<=20

T(s)	bijk	sigma-b	sigma-p	eijk	sigma-e	Q	N
0.00	-0.115	0.044	0.165	0.793	0.144	7.87e-01	14
0.05	-	-	-	-	-	-	0
0.10	-0.059	0.054	0.188	0.984	0.192	3.92e-01	12
0.15	-0.166	0.064	0.223	1.200	0.235	9.95e-02	12
0.20	-0.171	0.072	0.248	1.334	0.261	2.99e-02	12
0.30	-0.229	0.084	0.292	1.519	0.297	3.59e-03	12
0.40	-0.195	0.080	0.278	1.391	0.272	1.64e-02	12
0.50	-0.168	0.069	0.239	1.154	0.226	1.42e-01	12
0.75	-0.095	0.068	0.237	1.075	0.210	2.41e-01	12
1.00	-0.050	0.064	0.221	0.959	0.187	4.41e-01	12
1.50	-0.056	0.085	0.281	1.159	0.236	1.40e-01	11
2.00	-0.175	0.100	0.331	1.338	0.272	3.24e-02	11

BJF94 h G=5,6,7 may2196c<=20

T(s)	bijk	sigma-b	sigma-p	eijk	sigma-e	Q	N
0.00	-0.035	0.023	0.169	0.811	0.076	9.72e-01	56
0.05	-	-	-	-	-	-	0
0.10	-0.020	0.025	0.188	0.982	0.092	5.12e-01	56
0.15	-0.043	0.029	0.217	1.169	0.109	2.90e-02	56
0.20	-0.080	0.027	0.204	1.100	0.103	1.17e-01	56
0.30	-0.100	0.025	0.190	0.989	0.093	4.83e-01	56
0.40	-0.112	0.027	0.206	1.029	0.096	3.23e-01	56
0.50	-0.060	0.029	0.214	1.033	0.097	3.05e-01	56
0.75	-0.072	0.034	0.252	1.143	0.107	5.17e-02	56
1.00	-0.079	0.034	0.251	1.087	0.102	1.43e-01	56
1.50	-0.034	0.034	0.255	1.052	0.099	2.43e-01	55
2.00	-0.015	0.036	0.264	1.065	0.102	2.05e-01	53

C89/94 h G=5,6,7 may2196c<=20

T(s)	bijk	sigma-b	sigma-p	eijk	sigma-e	Q	N
0.00	-0.042	0.024	0.174	1.010	0.096	3.95e-01	54
0.05	0.066	0.026	0.187	0.980	0.096	5.16e-01	51
0.10	0.044	0.026	0.190	0.911	0.087	7.80e-01	54
0.15	-0.010	0.031	0.224	1.033	0.098	3.09e-01	54
0.20	-0.045	0.028	0.209	0.964	0.092	5.84e-01	54
0.30	-0.059	0.025	0.187	0.862	0.082	9.04e-01	54
0.40	-0.053	0.026	0.195	0.896	0.085	8.26e-01	54
0.50	-0.008	0.027	0.200	0.923	0.088	7.40e-01	54
0.75	-0.034	0.035	0.256	1.181	0.113	2.38e-02	54
1.00	-0.060	0.034	0.248	1.142	0.109	5.47e-02	54
1.50	-0.053	0.036	0.228	1.050	0.116	2.65e-01	40
2.00	-0.025	0.037	0.234	1.079	0.119	1.90e-01	40

C89 z G=5,6,7 may2196c<=20

T(s)	bijk	sigma-b	sigma-p	eijk	sigma-e	Q	N
0.00	-0.026	0.034	0.245	0.992	0.097	4.66e-01	51
0.05	0.200	0.040	0.282	1.047	0.105	2.63e-01	49
0.10	-0.185	0.049	0.352	1.306	0.128	9.35e-04	51
0.15	-0.021	0.039	0.276	1.027	0.101	3.33e-01	51
0.20	-0.017	0.037	0.264	0.981	0.096	5.12e-01	51
0.30	0.090	0.039	0.279	1.038	0.102	2.93e-01	51
0.40	-0.054	0.043	0.309	1.147	0.112	5.38e-02	51
0.50	-0.126	0.041	0.296	1.098	0.108	1.27e-01	51
0.75	-0.237	0.040	0.285	1.057	0.105	2.32e-01	50
1.00	-0.206	0.041	0.287	1.064	0.106	2.13e-01	49
1.50	-0.261	0.057	0.343	1.273	0.148	7.99e-03	36
2.00	-0.239	0.052	0.309	1.148	0.133	7.84e-02	36

C89V h G=5,6,7 may1696e<=20

T(s)	bijk	sigma-b	sigma-p	eijk	sigma-e	Q	N
pk vl	0.006	0.030	0.187	1.091	0.120	1.62e-01	40

C89V z G=5,6,7 may1696e<=20

T(s)	bijk	sigma-b	sigma-p	eijk	sigma-e	Q	N
pk vl	0.002	0.034	0.243	1.076	0.106	1.77e-01	51

C90/94 h G=0,2 may2196c<=20

T(s)	bijk	sigma-b	sigma-p	eijk	sigma-e	Q	N
0.00	-0.196	0.049	0.164	0.865	0.176	6.06e-01	11
0.05	-0.009	0.043	0.123	0.548	0.128	9.34e-01	8
0.10	-0.024	0.061	0.184	0.808	0.180	6.61e-01	9
0.15	-0.160	0.077	0.230	0.933	0.207	4.49e-01	9
0.20	-0.172	0.095	0.285	1.167	0.259	1.40e-01	9
0.30	-0.264	0.117	0.350	1.699	0.378	1.05e-03	9
0.40	-0.245	0.105	0.315	1.487	0.331	1.07e-02	9
0.50	-0.225	0.087	0.261	1.161	0.258	1.46e-01	9
0.75	-0.231	0.079	0.237	0.945	0.210	4.30e-01	9
1.00	-0.440	0.152	0.216	0.661	0.234	3.50e-01	2
1.50	-0.374	0.092	0.131	0.438	0.155	5.36e-01	2
2.00	-0.374	0.021	0.030	0.117	0.041	8.69e-01	2

C90 z G=0,2 may2196c<=20

T(s)	bijk	sigma-b	sigma-p	eijk	sigma-e	Q	N
0.00	-0.087	0.056	0.186	0.862	0.175	6.12e-01	11
0.05	0.136	0.072	0.191	0.755	0.187	6.78e-01	7
0.10	-0.026	0.083	0.250	0.889	0.198	5.25e-01	9
0.15	-0.127	0.052	0.156	0.632	0.141	8.91e-01	9
0.20	-0.103	0.101	0.302	1.092	0.243	2.18e-01	9
0.30	-0.122	0.080	0.239	0.898	0.200	5.10e-01	9
0.40	-0.176	0.064	0.193	0.711	0.158	8.04e-01	9
0.50	-0.127	0.067	0.200	0.804	0.179	6.67e-01	9
0.75	-0.096	0.075	0.225	0.793	0.176	6.85e-01	9
1.00	-0.164	0.004	0.005	0.015	0.005	9.83e-01	2
1.50	0.081	0.090	0.127	0.311	0.110	6.60e-01	2
2.00	0.091	0.193	0.273	0.823	0.291	2.44e-01	2

C90V h G=0,2 may1696e<=20

T(s)	bijk	sigma-b	sigma-p	eijk	sigma-e	Q	N
pk vl	-0.395	0.103	0.146	0.591	0.209	4.03e-01	2

C90V z G=0,2 may1696e<=20

T(s)	bijk	sigma-b	sigma-p	eijk	sigma-e	Q	N
pk vl	-0.241	0.139	0.197	0.716	0.253	3.11e-01	2

C93/94 h G=1 may2196c<=20

T(s)	bijk	sigma-b	sigma-p	eijk	sigma-e	Q	N
0.00	-0.112	0.072	0.101	0.466	0.165	5.10e-01	2
0.05	-0.134	0.076	0.107	0.432	0.153	5.42e-01	2
0.10	-0.071	0.020	0.028	0.110	0.039	8.76e-01	2
0.15	-0.049	0.025	0.035	0.133	0.047	8.51e-01	2
0.20	0.048	0.036	0.051	0.183	0.065	7.96e-01	2
0.30	0.087	0.108	0.153	0.577	0.204	4.15e-01	2
0.40	0.137	0.141	0.200	0.707	0.250	3.17e-01	2
0.50	0.028	0.107	0.152	0.521	0.184	4.61e-01	2
0.75	0.148	0.075	0.106	0.353	0.125	6.18e-01	2
1.00	0.153	0.055	0.077	0.247	0.087	7.27e-01	2
1.50	0.102	0.101	0.142	0.596	0.211	3.99e-01	2
2.00	0.089	0.172	0.244	1.079	0.381	1.27e-01	2

I93 h G=0,1,2 may2196c<=20

T(s)	bijk	sigma-b	sigma-p	eijk	sigma-e	Q	N
0.00	-0.204	0.044	0.157	0.720	0.136	8.74e-01	13
0.05	-0.188	0.041	0.129	0.607	0.129	9.31e-01	10
0.10	-0.152	0.053	0.175	0.757	0.154	7.89e-01	11
0.15	-0.227	0.063	0.208	0.885	0.180	5.70e-01	11
0.20	-0.218	0.076	0.252	1.053	0.214	2.72e-01	11
0.30	-0.252	0.090	0.300	1.214	0.247	9.35e-02	11
0.40	-0.224	0.085	0.282	1.108	0.225	1.97e-01	11
0.50	-0.182	0.068	0.225	0.858	0.174	6.20e-01	11
0.75	-0.096	0.065	0.217	0.797	0.162	7.27e-01	11
1.00	-0.020	0.062	0.205	0.795	0.162	7.31e-01	11
1.50	0.023	0.080	0.253	1.017	0.216	3.23e-01	10
2.00	-0.002	0.093	0.294	1.095	0.232	2.14e-01	10

JB88V h G=0,1,2 may1696e<=20

T(s)	bijk	sigma-b	sigma-p	eijk	sigma-e	Q	N
pk vl	-0.098	0.055	0.207	0.694	0.126	9.14e-01	14

JB88V h G=5,6,7 may1696e<=20

T(s)	bijk	sigma-b	sigma-p	eijk	sigma-e	Q	N

pk vl	-0.036	0.030	0.223	0.748	0.070	9.96e-01	56

SP96 h G=0,1,2 may2196c<=20

T(s)	bijk	sigma-b	sigma-p	eijk	sigma-e	Q	N
0.00	-0.045	0.040	0.152	0.876	0.159	6.33e-01	14
0.05	0.045	0.056	0.187	1.029	0.209	3.10e-01	11
0.10	0.066	0.054	0.188	0.988	0.193	3.86e-01	12
0.15	-0.054	0.066	0.229	1.144	0.224	1.52e-01	12
0.20	-0.063	0.072	0.250	1.164	0.227	1.32e-01	12
0.30	-0.133	0.083	0.289	1.179	0.230	1.18e-01	12
0.40	-0.079	0.073	0.251	0.952	0.186	4.54e-01	12
0.50	-0.105	0.065	0.227	0.837	0.164	6.76e-01	12
0.75	-0.086	0.065	0.226	0.799	0.156	7.44e-01	12
1.00	-0.026	0.050	0.175	0.603	0.118	9.58e-01	12
1.50	-0.019	0.063	0.209	0.708	0.144	8.54e-01	11
2.00	-0.012	0.077	0.256	0.863	0.175	6.10e-01	11

SP96 h G=5,6 may2196c<=20

T(s)	bijk	sigma-b	sigma-p	eijk	sigma-e	Q	N
0.00	[illegible]3	0.025	0.183	1.059	0.100	2.19e-01	55
0.05	[illegible]22	0.026	0.184	1.012	0.098	3.87e-01	52
0.10	[illegible].155	0.026	0.195	1.028	0.097	3.26e-01	55
0.15	0.096	0.031	0.230	1.151	0.109	4.45e-02	55
0.20	0.047	0.030	0.224	1.043	0.099	2.71e-01	55
0.30	-0.001	0.027	0.203	0.828	0.078	9.55e-01	55
0.40	-0.053	0.029	0.217	0.823	0.078	9.60e-01	55
0.50	-0.036	0.030	0.224	0.825	0.078	9.58e-01	55
0.75	-0.123	0.037	0.272	0.962	0.091	5.95e-01	55
1.00	-0.176	0.036	0.264	0.912	0.086	7.81e-01	55
1.50	-0.079	0.039	0.284	0.963	0.092	5.89e-01	54
2.00	0.034	0.039	0.284	0.956	0.093	6.11e-01	52

SP96 h G=7 may2196c<=20

T(s)	bijk	sigma-b	sigma-p	eijk	sigma-e	Q	N
0.00	0.206	0.000	0.000	-	-	-	1
0.05	0.247	0.000	0.000	-	-	-	1
0.10	0.190	0.000	0.000	-	-	-	1
0.15	0.242	0.000	0.000	-	-	-	1
0.20	0.143	0.000	0.000	-	-	-	1
0.30	0.072	0.000	0.000	-	-	-	1
0.40	0.287	0.000	0.000	-	-	-	1
0.50	0.275	0.000	0.000	-	-	-	1
0.75	0.029	0.000	0.000	-	-	-	1
1.00	0.132	0.000	0.000	-	-	-	1
1.50	0.320	0.000	0.000	-	-	-	1
2.00	0.290	0.000	0.000	-	-	-	1

SP96V h G=0,1,2 may1696e<=20

T(s)	bijk	sigma-b	sigma-p	eijk	sigma-e	Q	N
pk vl	0.024	0.060	0.223	1.036	0.189	3.06e-01	14

SP96V h G=5,6,7 may1696e<=20

T(s)	bijk	sigma-b	sigma-p	eijk	sigma-e	Q	N
pk vl	0.091	0.031	0.231	1.075	0.101	1.73e-01	56

S93 h G=0,1,2 may2196c<=20

T(s)	bijk	sigma-b	sigma-p	eijk	sigma-e	Q	N
0.00	-0.197	0.042	0.152	0.698	0.132	8.98e-01	13
0.05	-0.135	0.042	0.133	0.635	0.135	9.09e-01	10
0.10	-0.134	0.052	0.172	0.748	0.152	8.02e-01	11
0.15	-0.[illegible]7	0.064	0.211	0.902	0.183	5.37e-01	11
0.20	-0.1[illegible]	0.077	0.256	1.052	0.214	2.73e-01	11
0.30	-0.21[illegible]	0.092	0.304	1.209	0.246	9.71e-02	11
0.40	-0.174	0.085	0.283	1.039	0.211	2.94e-01	11
0.50	-0.131	0.066	0.219	0.778	0.158	7.57e-01	11
0.75	-0.087	0.062	0.206	0.707	0.144	8.55e-01	11
1.00	-0.064	0.059	0.196	0.698	0.142	8.65e-01	11
1.50	-0.067	0.078	0.245	0.907	0.192	5.11e-01	10
2.00	-0.116	0.092	0.290	1.064	0.226	2.54e-01	10

S93 z G=0,1,2 may2196c<=20

T(s)	bijk	sigma-b	sigma-p	eijk	sigma-e	Q	N
0.00	-0.141	0.051	0.182	0.788	0.149	7.79e-01	13

Table 12 p 3/4

0.05	0.021	0.061	0.183	0.724	0.161	7.87e-01	9
0.10	-0.059	0.072	0.240	0.831	0.169	6.69e-01	11
0.15	-0.084	0.053	0.175	0.627	0.127	9.31e-01	11
0.20	-0.026	0.083	0.274	0.915	0.186	5.13e-01	11
0.30	0.003	0.073	0.243	0.799	0.162	7.24e-01	11
0.40	-0.042	0.067	0.221	0.701	0.143	8.62e-01	11
0.50	-0.048	0.043	0.143	0.471	0.096	9.92e-01	11
0.75	0.022	0.052	0.171	0.570	0.116	9.65e-01	11
1.00	0.047	0.047	0.150	0.479	0.102	9.86e-01	10
1.50	0.156	0.047	0.132	0.491	0.115	9.64e-01	8
2.00	0.150	0.080	0.211	0.770	0.191	6.56e-01	7

Sea96 h G=0,1,2 may2196c<=20

T(s)	bijk	sigma-b	sigma-p	eijk	sigma-e	Q	N
0.00	-0.051	0.046	0.171	0.792	0.144	7.89e-01	14
0.05	-	-	-	-	-	-	0
0.10	0.012	0.056	0.194	0.726	0.142	8.51e-01	12
0.15	-0.042	0.065	0.227	0.818	0.160	7.10e-01	12
0.20	-0.015	0.072	0.249	0.871	0.170	6.12e-01	12
0.30	-0.045	0.084	0.292	0.971	0.190	4.18e-01	12
0.40	-0.010	0.080	0.279	0.890	0.174	5.76e-01	12
0.50	0.007	0.069	0.240	0.741	0.145	8.32e-01	12
0.75	0.039	0.069	0.237	0.689	0.135	8.93e-01	12
1.00	0.054	0.064	0.222	0.615	0.120	9.52e-01	12
1.50	0.035	0.086	0.285	0.735	0.149	8.20e-01	11
2.00	-0.057	0.101	0.335	0.821	0.167	6.86e-01	11

Sea96 h G=5,6,7 may2196c<=20

T(s)	bijk	sigma-b	sigma-p	eijk	sigma-e	Q	N
0.00	0.035	0.023	0.170	0.789	0.074	9.85e-01	56
0.05	-	-	-	-	-	-	0
0.10	0.018	0.025	0.190	0.710	0.067	9.99e-01	56
0.15	0.016	0.029	0.218	0.788	0.074	9.85e-01	56
0.20	0.004	0.027	0.205	0.715	0.067	9.99e-01	56
0.30	0.019	0.025	0.190	0.631	0.059	1.00e+00	56
0.40	0.019	0.028	0.206	0.658	0.062	1.00e+00	56
0.50	0.074	0.029	0.215	0.665	0.062	1.00e+00	56
0.75	0.039	0.034	0.253	0.734	0.069	9.97e-01	56
1.00	0.012	0.034	0.254	0.703	0.066	9.99e-01	56
1.50	0.043	0.035	0.259	0.670	0.063	1.00e+00	55
2.00	0.081	0.036	0.264	0.648	0.062	1.00e+00	53

Table B1. Smoothed coefficients for regression relation Sea96, for geometric mean horizontal *pga* and 5% damped *psv*.

$T(s)$	NR	NQ	b_1	b_2	b_3	b_4	b_5	b_6	h (km)	σ_1	σ_2	σ_3
pga	128	30	0.156	0.229	0.000	0.0	−0.945	0.077	5.57	0.216	0.000	0.094
0.100	118	29	1.772	0.327	−0.098	0.0	−1.051	0.079	6.27	0.268	0.000	0.111
0.110	118	29	1.830	0.318	−0.100	0.0	−1.043	0.092	6.65	0.270	0.000	0.112
0.120	118	29	1.876	0.313	−0.101	0.0	−1.035	0.102	6.91	0.272	0.000	0.114
0.130	118	29	1.912	0.309	−0.101	0.0	−1.026	0.112	7.08	0.274	0.000	0.115
0.140	118	29	1.941	0.307	−0.100	0.0	−1.018	0.120	7.18	0.276	0.000	0.116
0.150	118	29	1.964	0.305	−0.099	0.0	−1.009	0.127	7.23	0.277	0.001	0.117
0.160	118	29	1.982	0.305	−0.098	0.0	−1.001	0.134	7.24	0.279	0.003	0.118
0.170	118	29	1.996	0.305	−0.096	0.0	−0.994	0.139	7.21	0.281	0.005	0.119
0.180	118	29	2.008	0.306	−0.094	0.0	−0.986	0.145	7.16	0.283	0.008	0.120
0.190	118	29	2.016	0.308	−0.092	0.0	−0.979	0.150	7.10	0.284	0.010	0.120
0.200	118	29	2.023	0.309	−0.090	0.0	−0.972	0.154	7.02	0.286	0.012	0.121
0.220	118	29	2.032	0.313	−0.086	0.0	−0.958	0.162	6.83	0.289	0.015	0.122
0.240	118	29	2.035	0.318	−0.082	0.0	−0.946	0.168	6.62	0.292	0.019	0.124
0.260	118	29	2.036	0.323	−0.078	0.0	−0.935	0.174	6.39	0.295	0.022	0.125
0.280	118	29	2.034	0.329	−0.073	0.0	−0.925	0.179	6.17	0.297	0.024	0.126
0.300	118	29	2.030	0.334	−0.070	0.0	−0.915	0.183	5.94	0.300	0.027	0.126
0.320	118	29	2.025	0.340	−0.066	0.0	−0.907	0.187	5.72	0.302	0.030	0.127
0.340	118	29	2.020	0.345	−0.062	0.0	−0.899	0.190	5.50	0.304	0.032	0.128
0.360	118	29	2.014	0.350	−0.059	0.0	−0.892	0.193	5.30	0.307	0.034	0.128
0.380	118	29	2.008	0.356	−0.055	0.0	−0.885	0.196	5.10	0.309	0.036	0.129
0.400	118	29	2.001	0.361	−0.052	0.0	−0.879	0.198	4.91	0.311	0.038	0.129
0.420	118	29	1.995	0.365	−0.049	0.0	−0.874	0.200	4.74	0.313	0.040	0.130
0.440	118	29	1.989	0.370	−0.047	0.0	−0.869	0.202	4.57	0.315	0.042	0.130
0.460	118	29	1.983	0.375	−0.044	0.0	−0.864	0.203	4.41	0.317	0.043	0.131
0.480	118	29	1.977	0.379	−0.042	0.0	−0.860	0.205	4.26	0.319	0.045	0.131
0.500	118	29	1.971	0.384	−0.039	0.0	−0.857	0.206	4.13	0.320	0.047	0.132
0.550	118	29	1.958	0.394	−0.034	0.0	−0.849	0.209	3.82	0.325	0.050	0.132
0.600	118	29	1.946	0.403	−0.030	0.0	−0.843	0.211	3.57	0.329	0.054	0.133
0.650	118	29	1.937	0.411	−0.026	0.0	−0.838	0.212	3.36	0.332	0.057	0.134
0.700	118	29	1.929	0.418	−0.023	0.0	−0.835	0.213	3.20	0.336	0.059	0.134
0.750	118	29	1.922	0.425	−0.020	0.0	−0.833	0.214	3.07	0.339	0.062	0.135
0.800	118	29	1.917	0.431	−0.018	0.0	−0.833	0.214	2.98	0.343	0.065	0.135

(Continued)

Table B1 p1 of 2

Table B1. (Continued)

$T(s)$	NR	NQ	b_1	b_2	b_3	b_4	b_5	b_6	h (km)	σ_1	σ_2	σ_3
0.850	118	29	1.914	0.437	−0.016	0.0	−0.833	0.215	2.92	0.346	0.067	0.136
0.900	118	29	1.912	0.442	−0.015	0.0	−0.833	0.215	2.89	0.349	0.069	0.136
0.950	118	29	1.911	0.446	−0.014	0.0	−0.835	0.215	2.88	0.352	0.071	0.136
1.000	118	29	1.912	0.450	−0.014	0.0	−0.837	0.214	2.90	0.354	0.073	0.137
1.100	109	27	1.916	0.457	−0.013	0.0	−0.842	0.214	2.99	0.359	0.077	0.137
1.200	108	27	1.923	0.462	−0.014	0.0	−0.850	0.213	3.14	0.364	0.080	0.138
1.300	108	27	1.934	0.466	−0.015	0.0	−0.858	0.212	3.36	0.369	0.083	0.138
1.400	107	27	1.948	0.469	−0.017	0.0	−0.868	0.210	3.62	0.373	0.086	0.138
1.500	107	27	1.964	0.471	−0.019	0.0	−0.879	0.209	3.92	0.377	0.089	0.139
1.600	107	27	1.981	0.472	−0.022	0.0	−0.890	0.207	4.26	0.381	0.091	0.139
1.700	99	27	2.001	0.473	−0.025	0.0	−0.902	0.205	4.62	0.385	0.093	0.139
1.800	99	27	2.022	0.472	−0.029	0.0	−0.914	0.204	5.01	0.388	0.096	0.139
1.900	99	27	2.045	0.472	−0.032	0.0	−0.927	0.202	5.42	0.392	0.098	0.139
2.000	99	27	2.068	0.471	−0.037	0.0	−0.940	0.200	5.85	0.395	0.100	0.140

NR is the number of records that were used for each period.
NQ is the number of earthquakes that were used for each period.

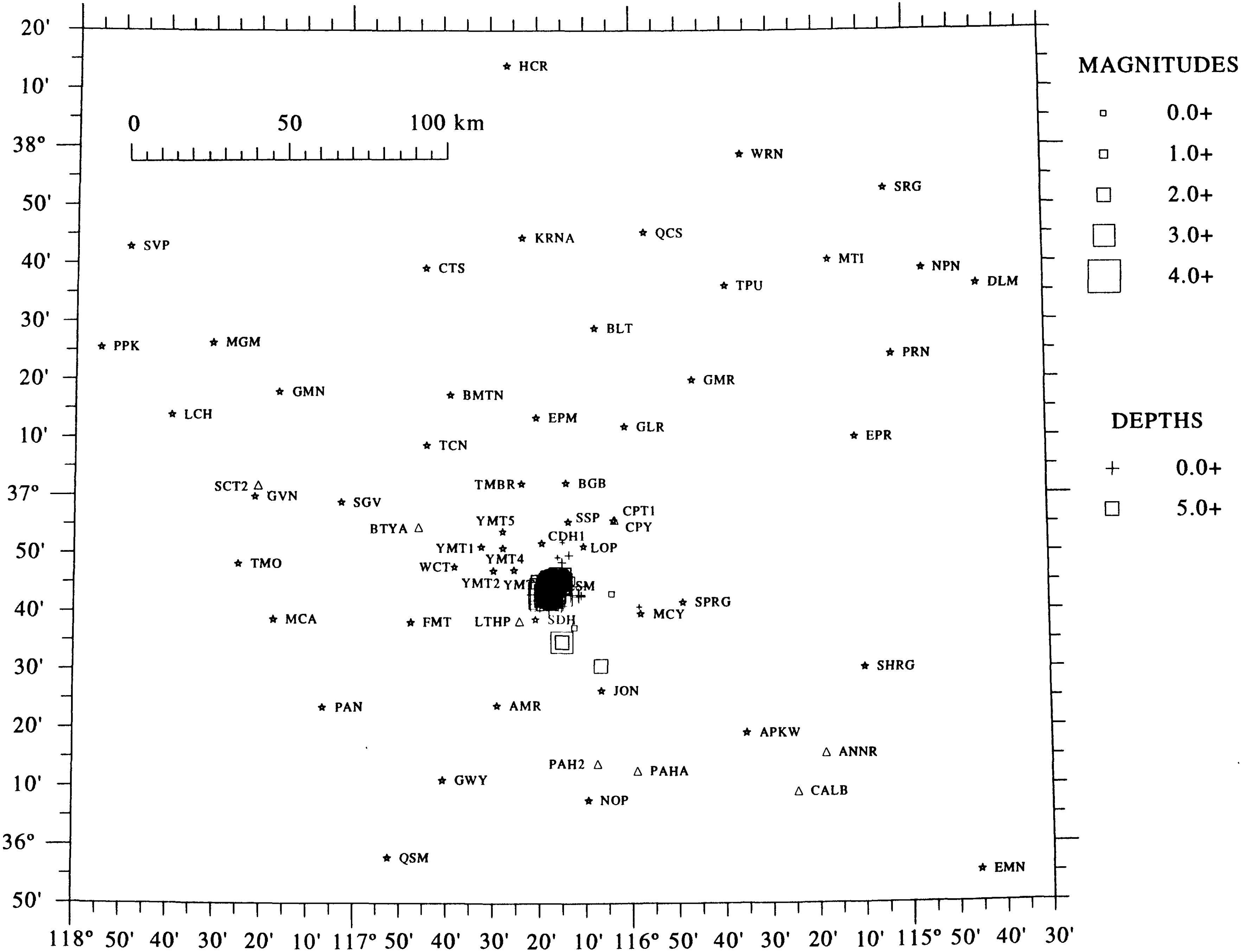
MAGNITUDES
0.0+
1.0+
2.0+
3.0+
4.0+
DEPTHS
0.0+
5.0+
0
50
100 km
HCR
WRN
SRG
SVP
KRNA
QCS
CTS
MTI
NPN
DLM
TPU
PPK
MGM
BLT
PRN
GMN
BMTN
GMR
LCH
EPM
GLR
EPR
TCN
SCT2
GVN
TMBR
BGB
SGV
SSP
CPT1
CPY
BTYA
YMT5
CDH1
YMT1
LOP
YMT4
TMO
WCT
YMT2
SM
SPRG
MCA
FMT
LTHP
SDH
MCY
SHRG
JON
PAN
AMR
APKW
ANNR
PAH2
PAHA
GWY
CALB
NOP
QSM
EMN
20'
10'
38°
50'
40'
30'
20'
10'
37°
50'
40'
30'
20'
10'
36°
50'
118°
50'
40'
30'
20'
10'
117°
50'
40'
30'
20'
10'
116°
50'
40'
30'
20'
10'
115°
50'
40'
30'

1

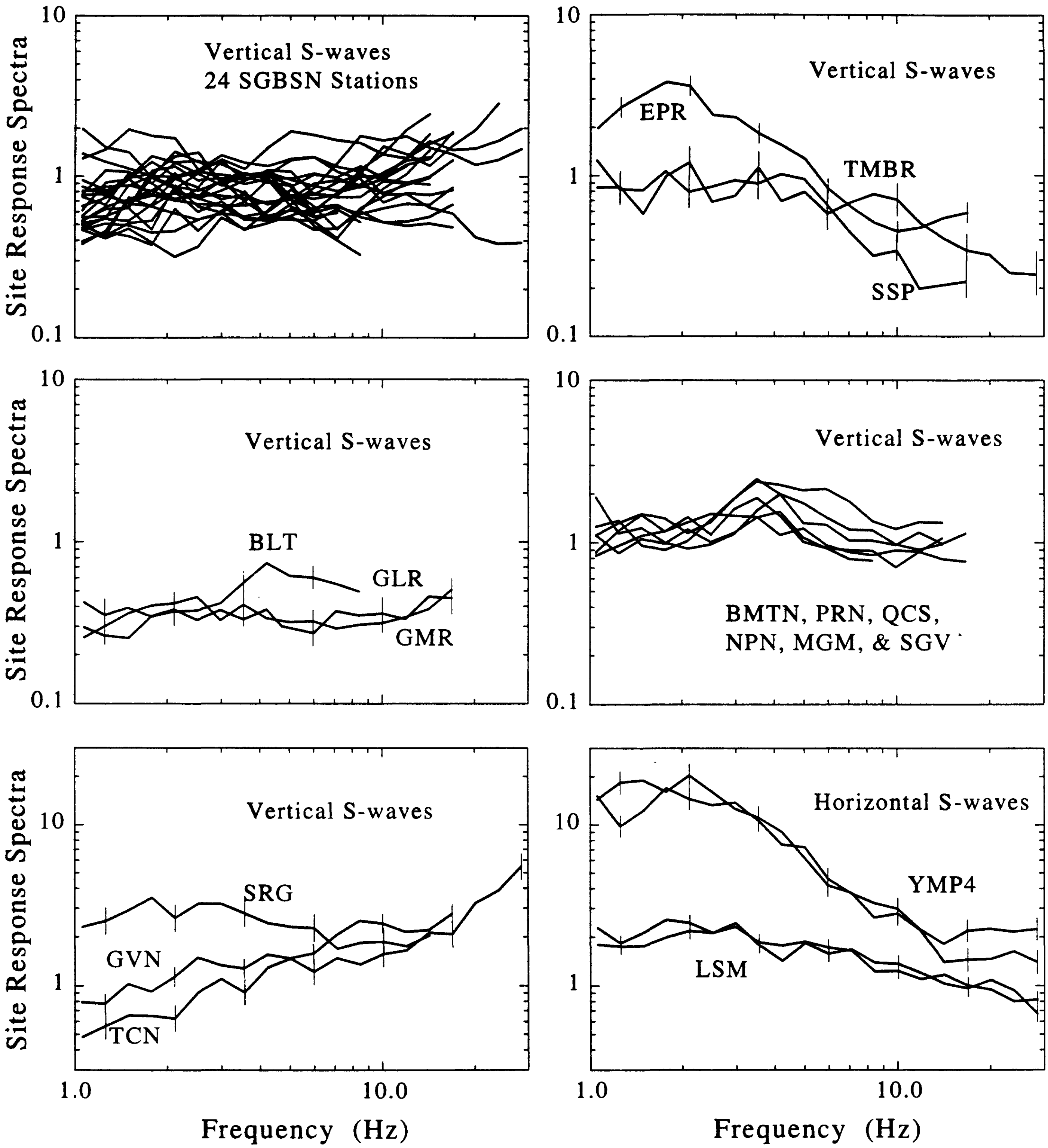
Vertical S-waves
24 SGBSN Stations
Vertical S-waves
EPR
TMBR
SSP
Vertical S-waves
BLT
GLR
GMR
Vertical S-waves
BMTN, PRN, QCS,
NPN, MGM, & SGV
Vertical S-waves
SRG
GVN
TCN
Horizontal S-waves
YMP4
LSM
Site Response Spectra
Frequency (Hz)
0.1
1
10
1.0
10.0

2

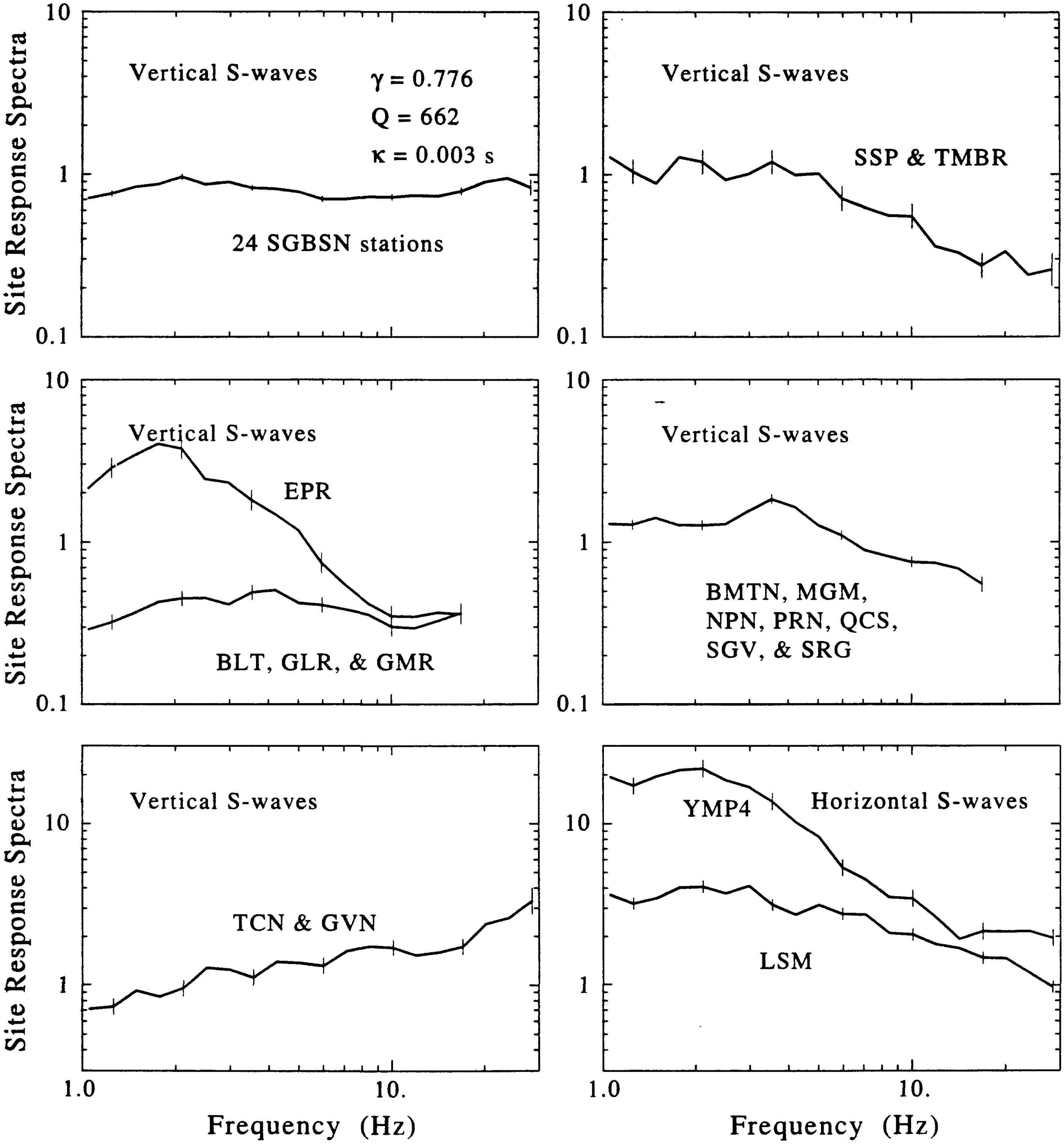

Vertical S-waves
γ = 0.776
Q = 662
κ = 0.003 s
24 SGBSN stations
Vertical S-waves
SSP & TMBR
Vertical S-waves
EPR
BLT, GLR, & GMR
Vertical S-waves
BMTN, MGM,
NPN, PRN, QCS,
SGV, & SRG
Vertical S-waves
TCN & GVN
YMP4
Horizontal S-waves
LSM
Site Response Spectra
Frequency (Hz)
10
1
0.1
1.0
10.

3

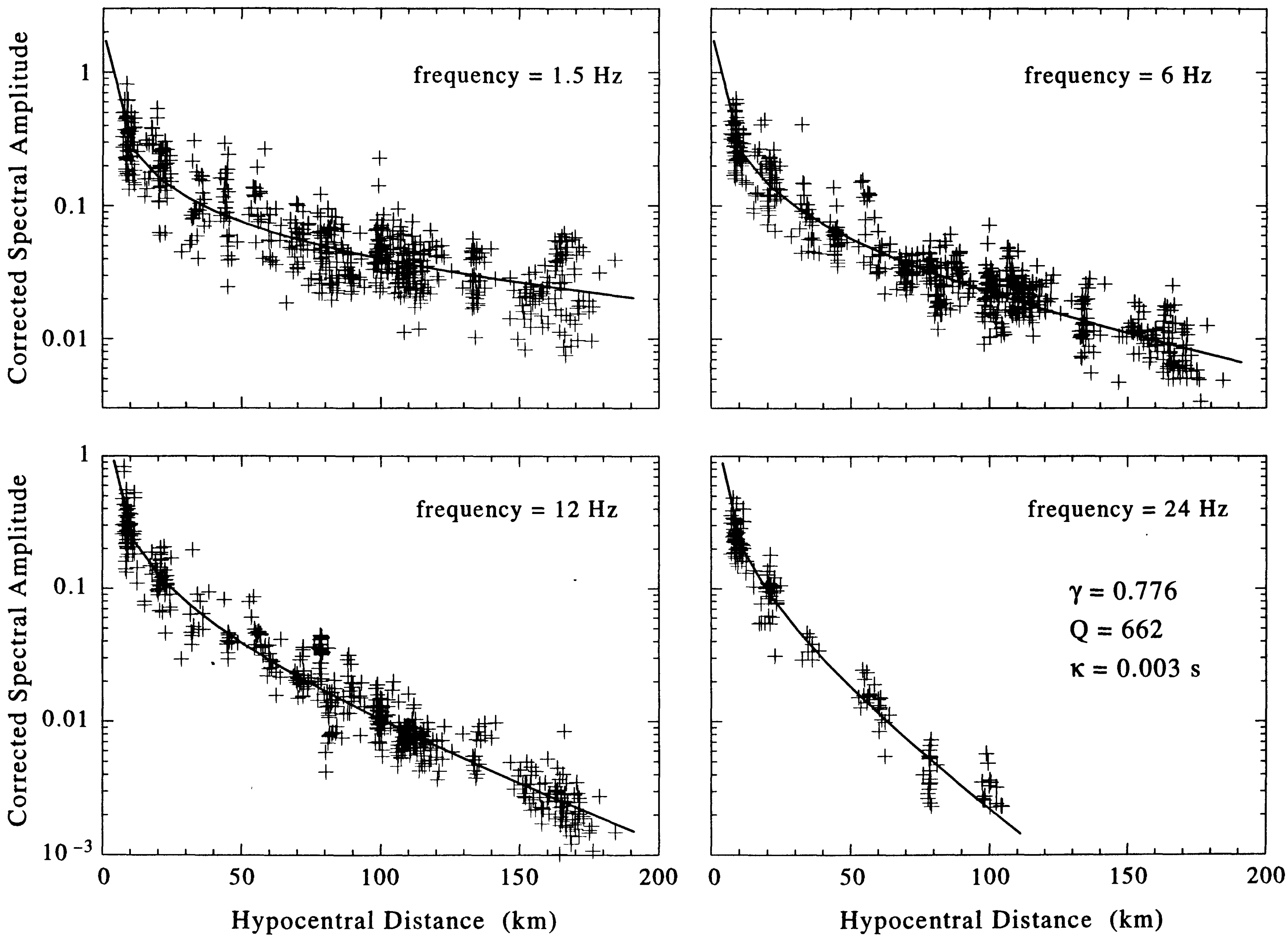

Corrected Spectral Amplitude
1
0.1
0.01
10 −3
frequency = 1.5 Hz
frequency = 6 Hz
frequency = 12 Hz
frequency = 24 Hz
γ = 0.776
Q = 662
κ = 0.003 s
0
50
100
150
200
Hypocentral Distance (km)

4

101

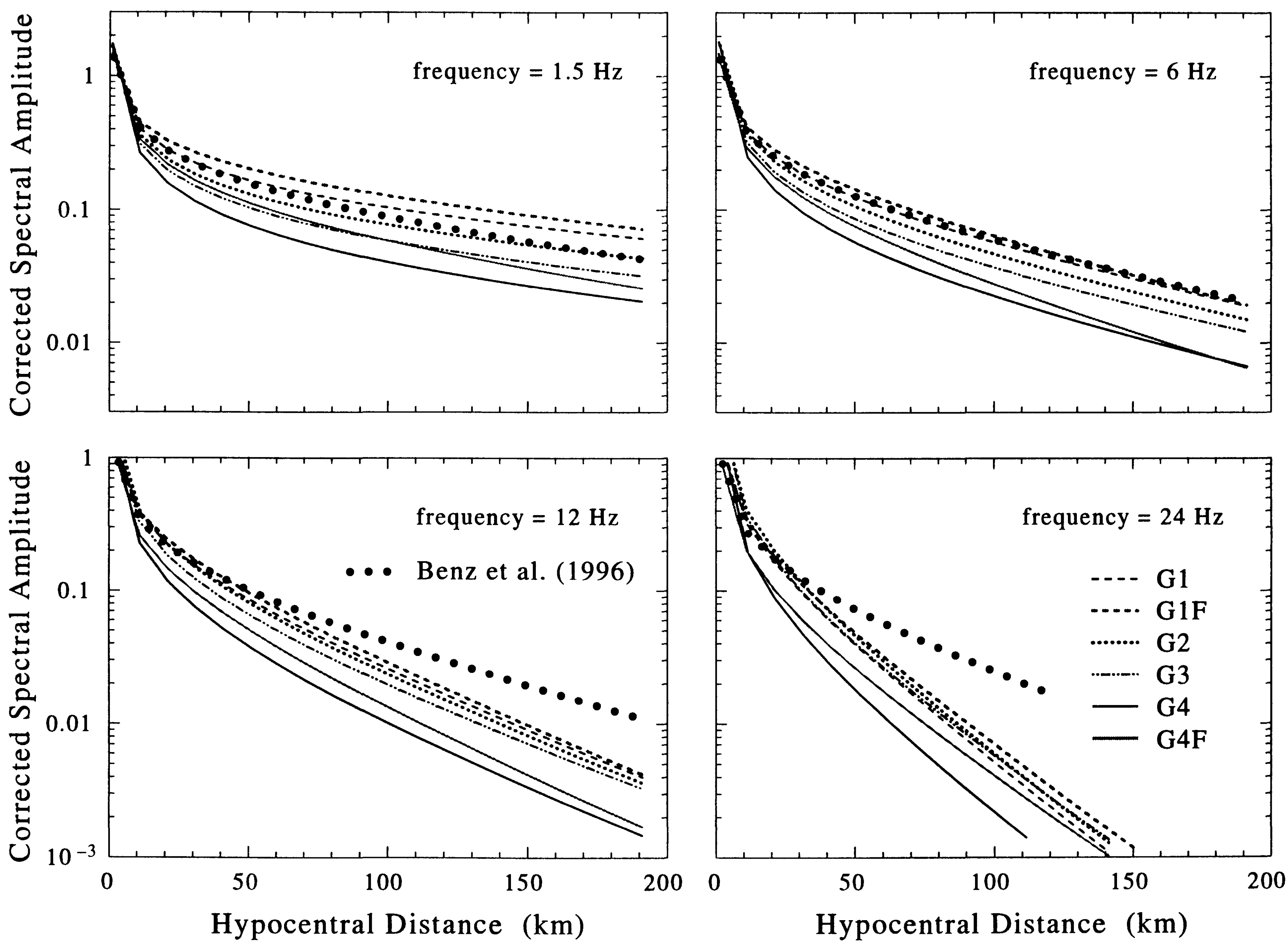

Corrected Spectral Amplitude
frequency = 1.5 Hz
frequency = 6 Hz
frequency = 12 Hz
frequency = 24 Hz
Benz et al. (1996)
G1
G1F
G2
G3
G4
G4F
1
0.1
0.01
10^{-3}
0
50
100
150
200
Hypocentral Distance (km)

5

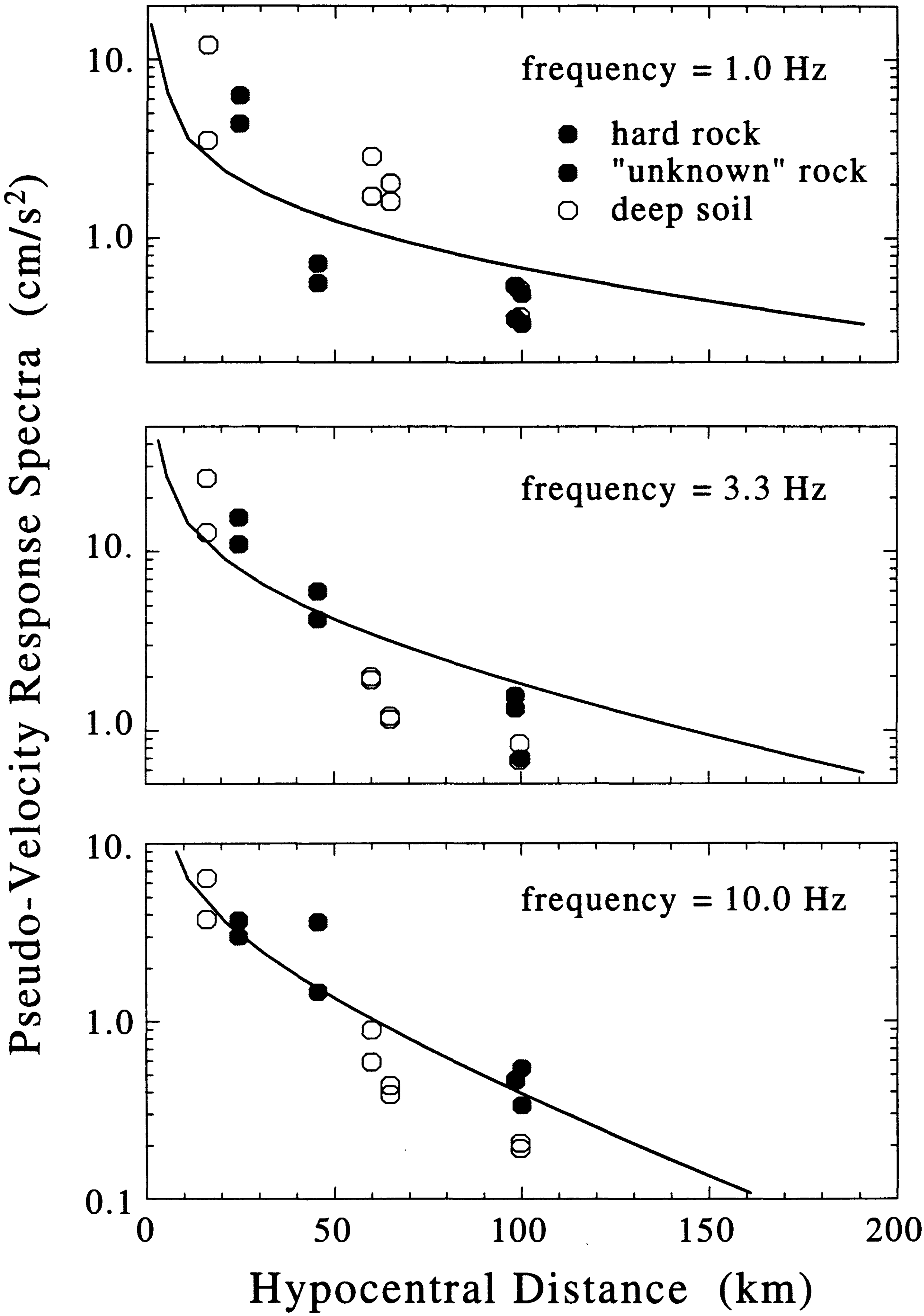
frequency = 1.0 Hz
hard rock
"unknown" rock
deep soil
frequency = 3.3 Hz
frequency = 10.0 Hz
10.
1.0
10.
1.0
10.
1.0
0.1
0
50
100
150
200
Pseudo-Velocity Response Spectra (cm/s2)
Hypocentral Distance (km)

6

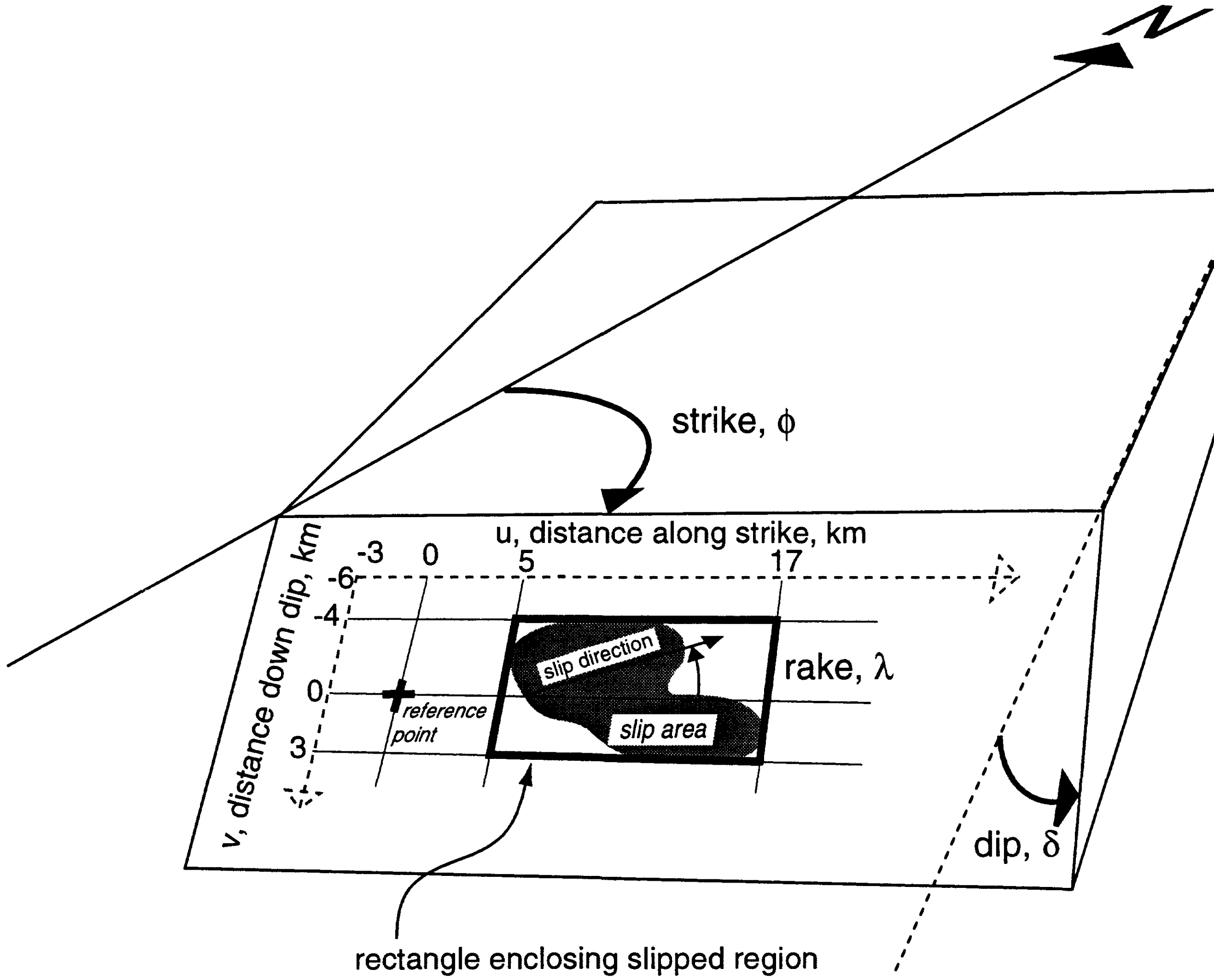
N
strike, φ
u, distance along strike, km
-3
0
5
17
-6
-4
0
3
v, distance down dip, km
slip direction
rake, λ
reference point
slip area
dip, δ
rectangle enclosing slipped region

7

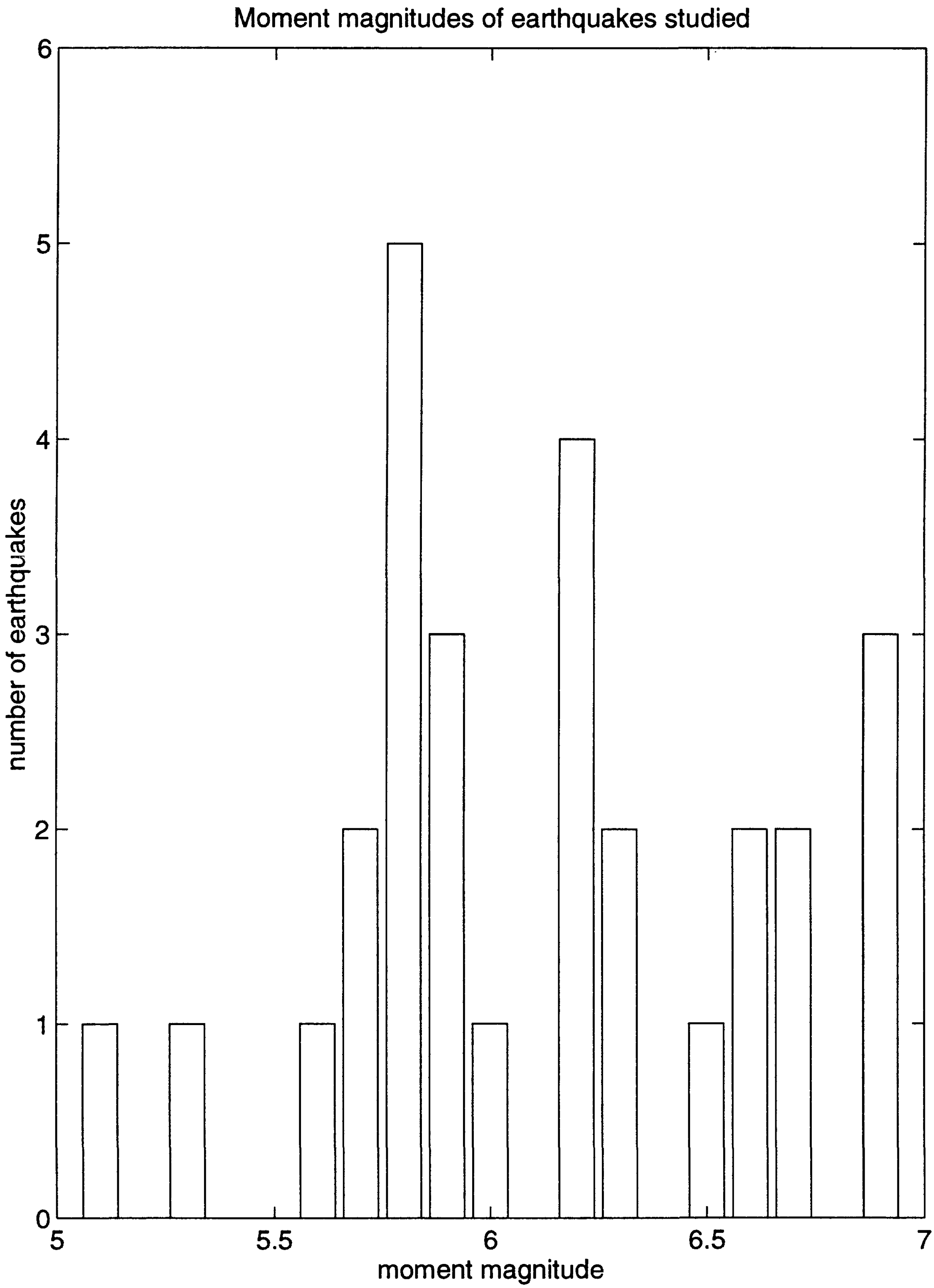

ymay1696a.rpt

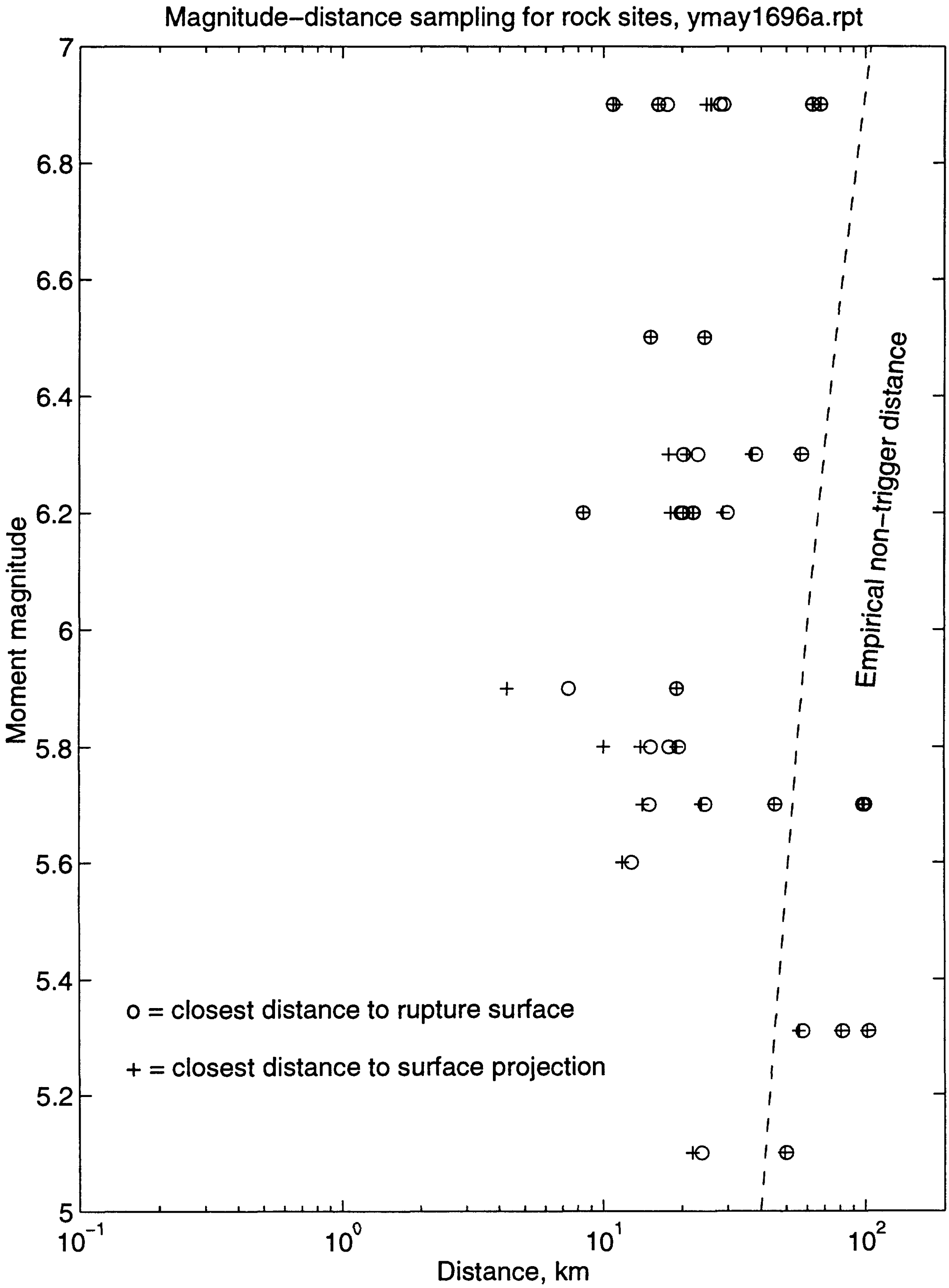

Magnitude–distance sampling for rock sites, ymay1696a.rpt
Moment magnitude
Distance, km
7
6.8
6.6
6.4
6.2
6
5.8
5.6
5.4
5.2
5
10^{-1}
10^{0}
10^{1}
10^{2}
Empirical non–trigger distance
o = closest distance to rupture surface
+ = closest distance to surface projection

9a

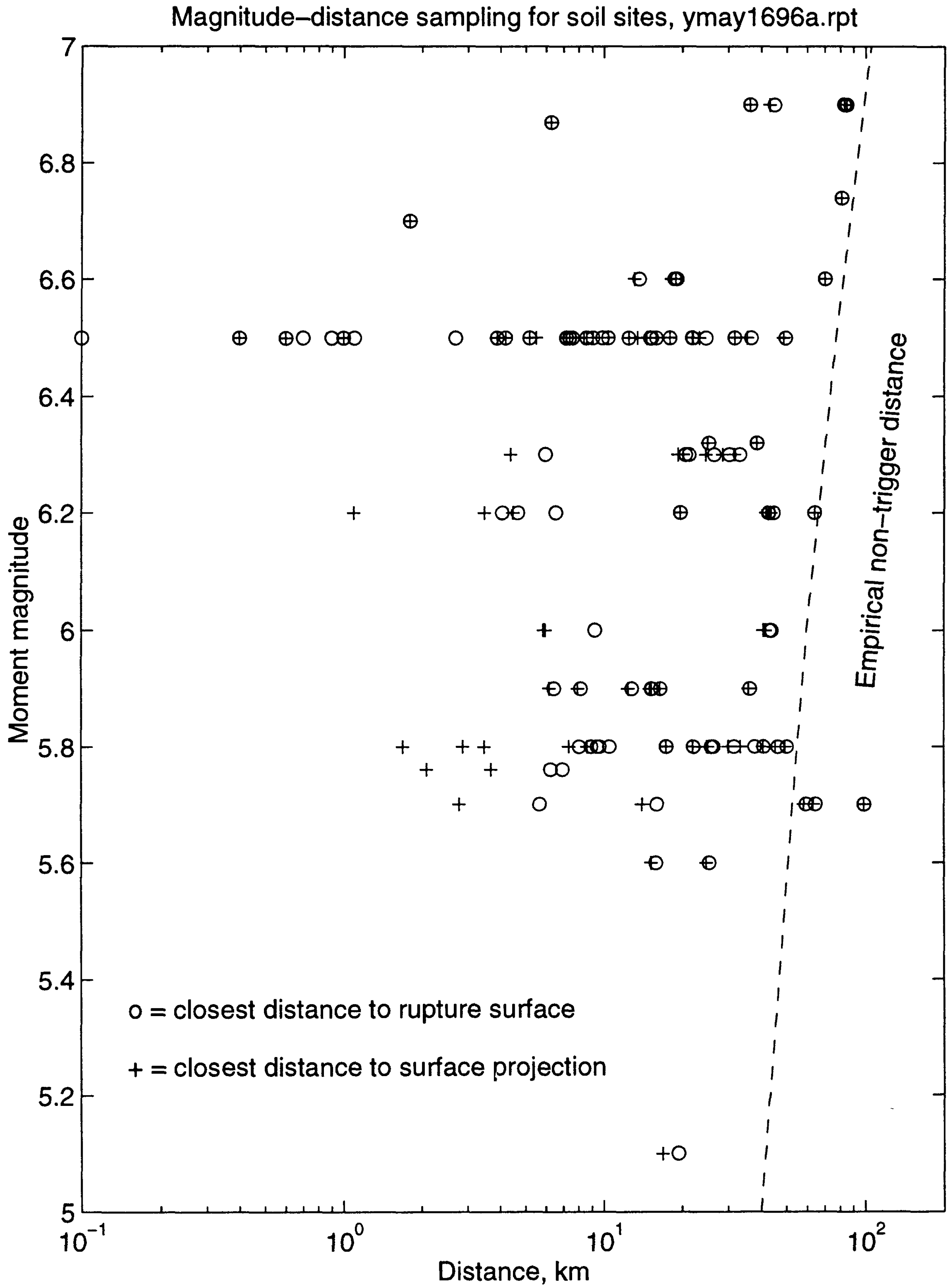
Magnitude–distance sampling for soil sites, ymay1696a.rpt
Moment magnitude
Distance, km
o = closest distance to rupture surface
+ = closest distance to surface projection
Empirical non–trigger distance
7
6.8
6.6
6.4
6.2
6
5.8
5.6
5.4
5.2
5
10^{-1}
10^{0}
10^{1}
10^{2}

96

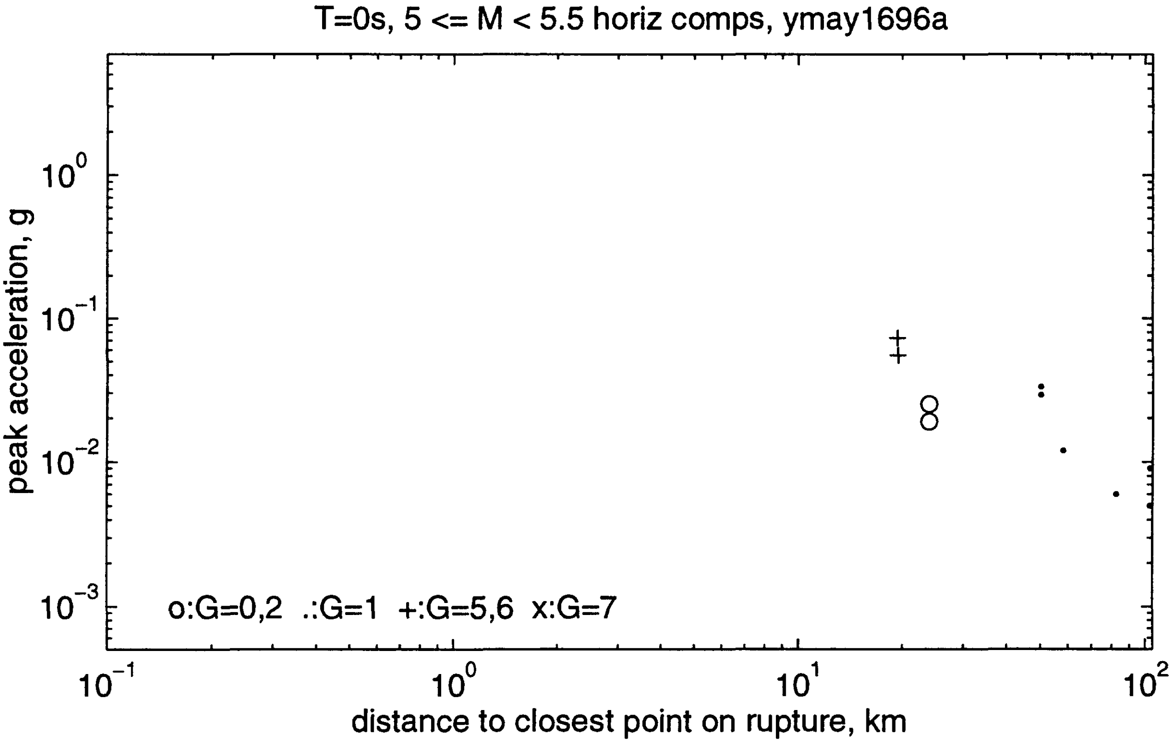
T=0s, 5 <= M < 5.5 horiz comps, ymay1696a
peak acceleration, g
10^{0}
10^{-1}
10^{-2}
10^{-3}
o:G=0,2 .:G=1 +:G=5,6 x:G=7
10^{-1}
10^{0}
10^{1}
10^{2}
distance to closest point on rupture, km

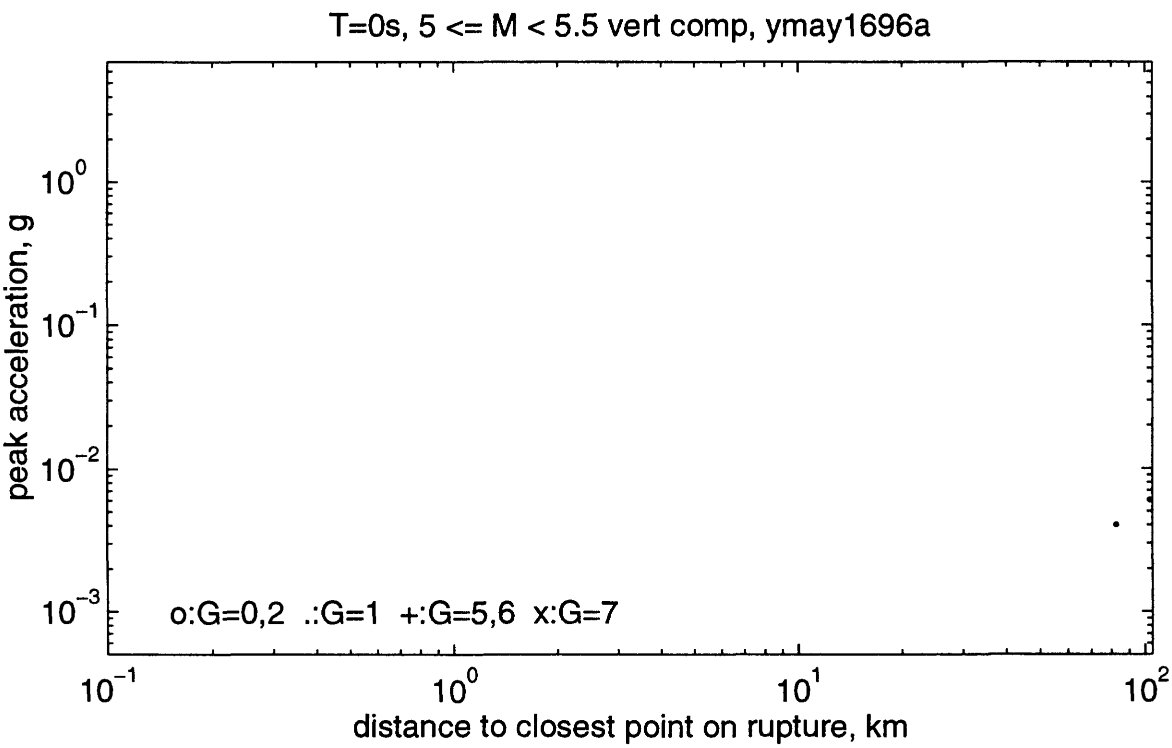
T=0s, 5 <= M < 5.5 vert comp, ymay1696a
peak acceleration, g
10^{0}
10^{-1}
10^{-2}
10^{-3}
o:G=0,2 .:G=1 +:G=5,6 x:G=7
10^{-1}
10^{0}
10^{1}
10^{2}
distance to closest point on rupture, km

10a

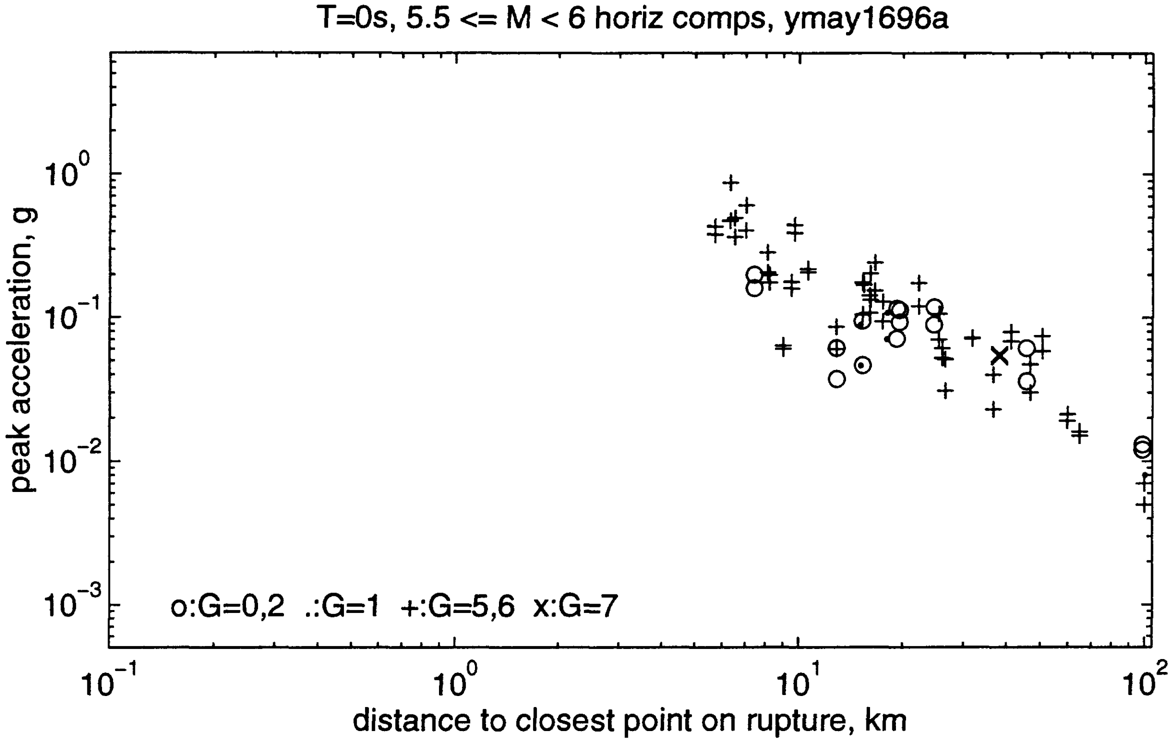
T=0s, 5.5 <= M < 6 horiz comps, ymay1696a
peak acceleration, g
distance to closest point on rupture, km
o:G=0,2 .:G=1 +:G=5,6 x:G=7
10^-1
10^0
10^1
10^2
10^-3
10^-2

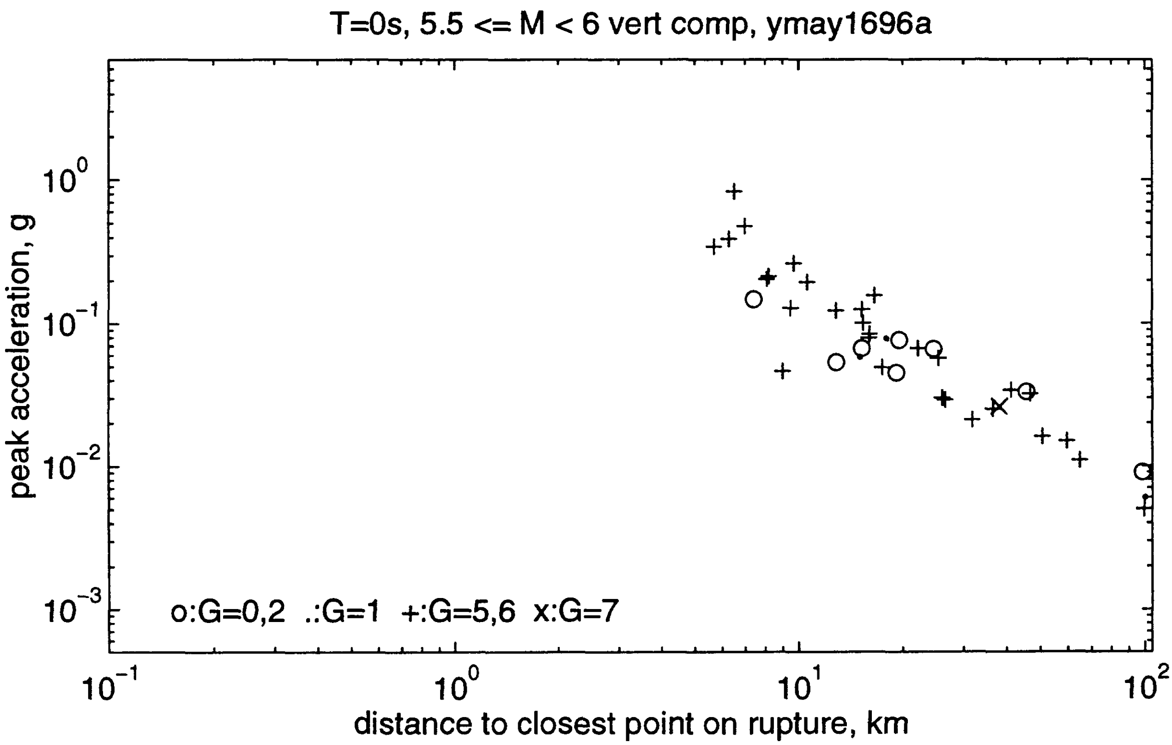
T=0s, 5.5 <= M < 6 vert comp, ymay1696a
peak acceleration, g
distance to closest point on rupture, km
o:G=0,2 .:G=1 +:G=5,6 x:G=7
10^-1
10^0
10^1
10^2
10^-3
10^-2

10 b

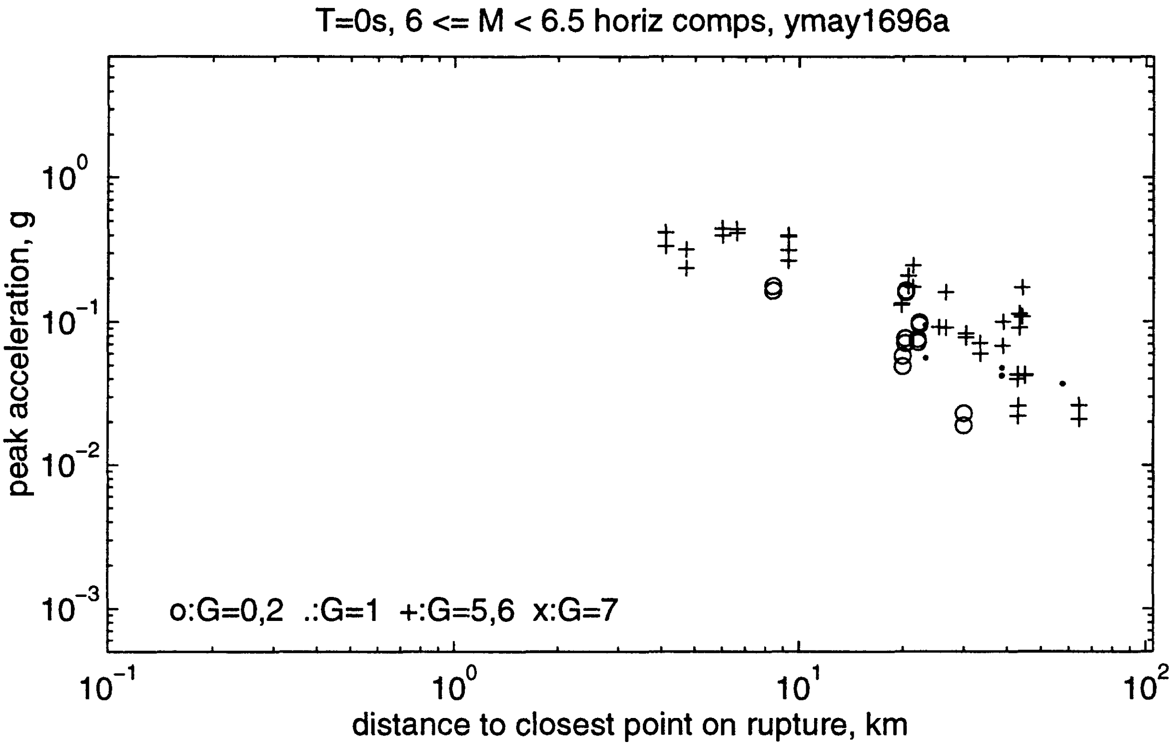
T=0s, 6 <= M < 6.5 horiz comps, ymay1696a
peak acceleration, g
distance to closest point on rupture, km
o:G=0,2 .:G=1 +:G=5,6 x:G=7
10^0
10^-1
10^-2
10^-3
10^-1
10^0
10^1
10^2

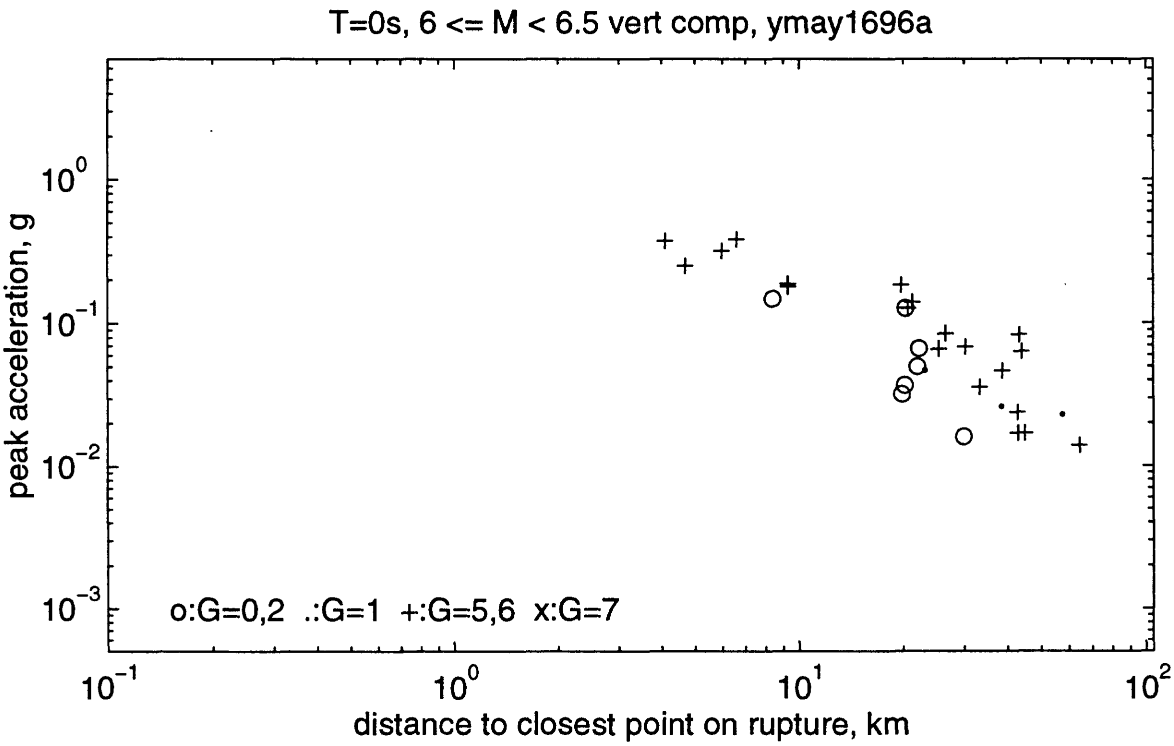
T=0s, 6 <= M < 6.5 vert comp, ymay1696a
peak acceleration, g
distance to closest point on rupture, km
o:G=0,2 .:G=1 +:G=5,6 x:G=7
10^0
10^-1
10^-2
10^-3
10^-1
10^0
10^1
10^2

10c

T=0s, 6.5 <= M < 7.5 horiz comps, ymay1696a

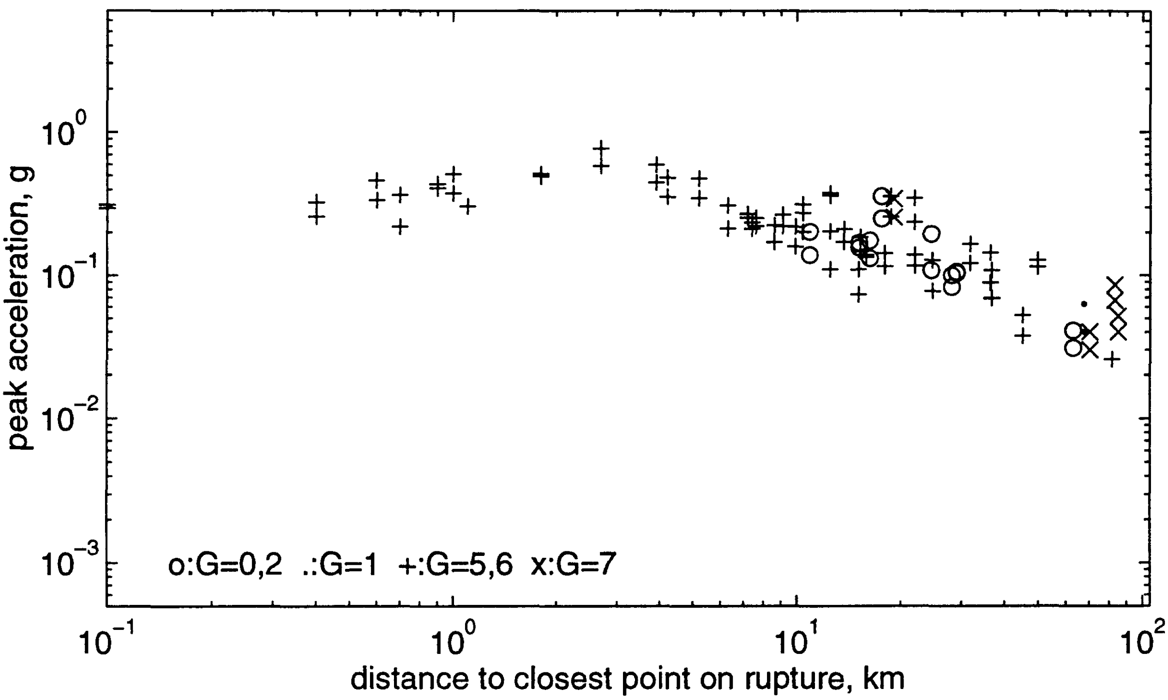

T=0s, 6.5 <= M < 7.5 vert comp, ymay1696a

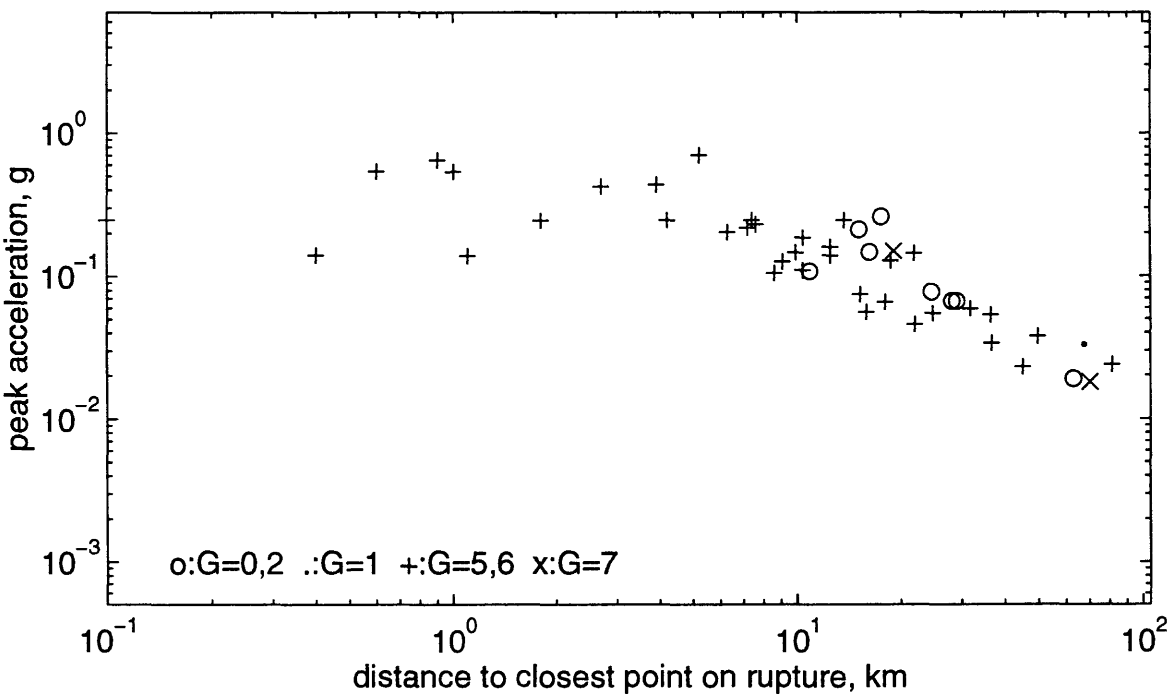

10d

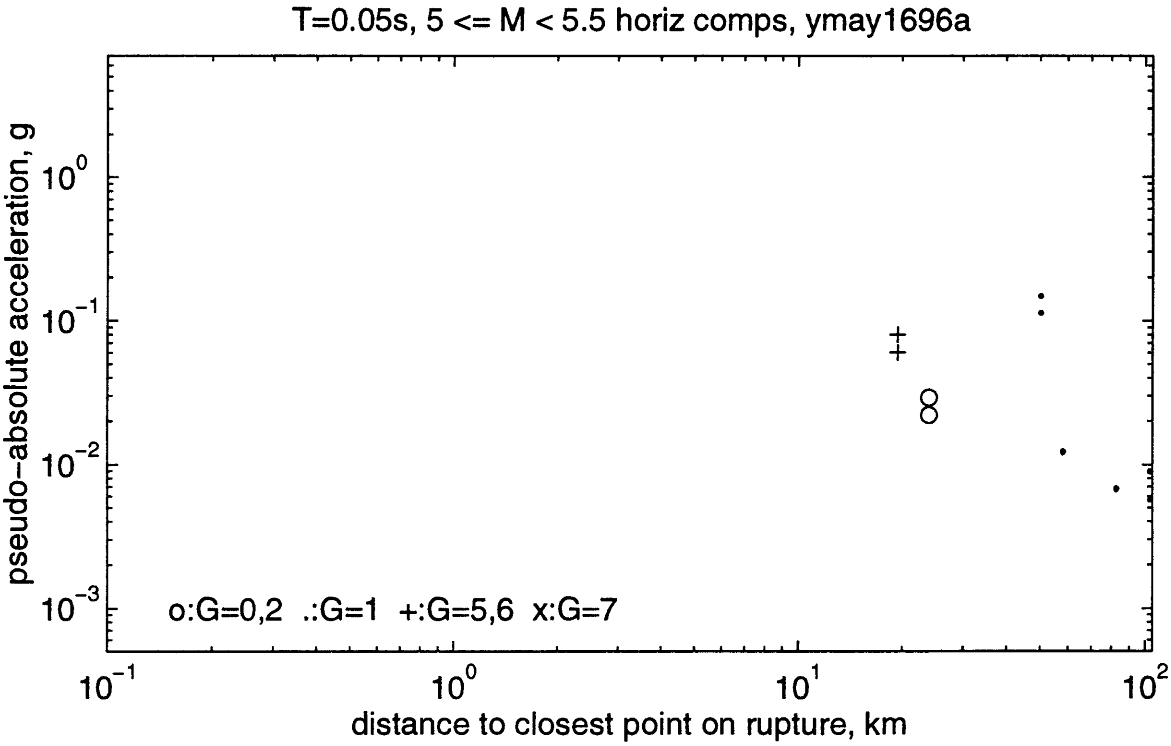
T=0.05s, 5 <= M < 5.5 horiz comps, ymay1696a
pseudo-absolute acceleration, g
distance to closest point on rupture, km
o:G=0,2 .:G=1 +:G=5,6 x:G=7

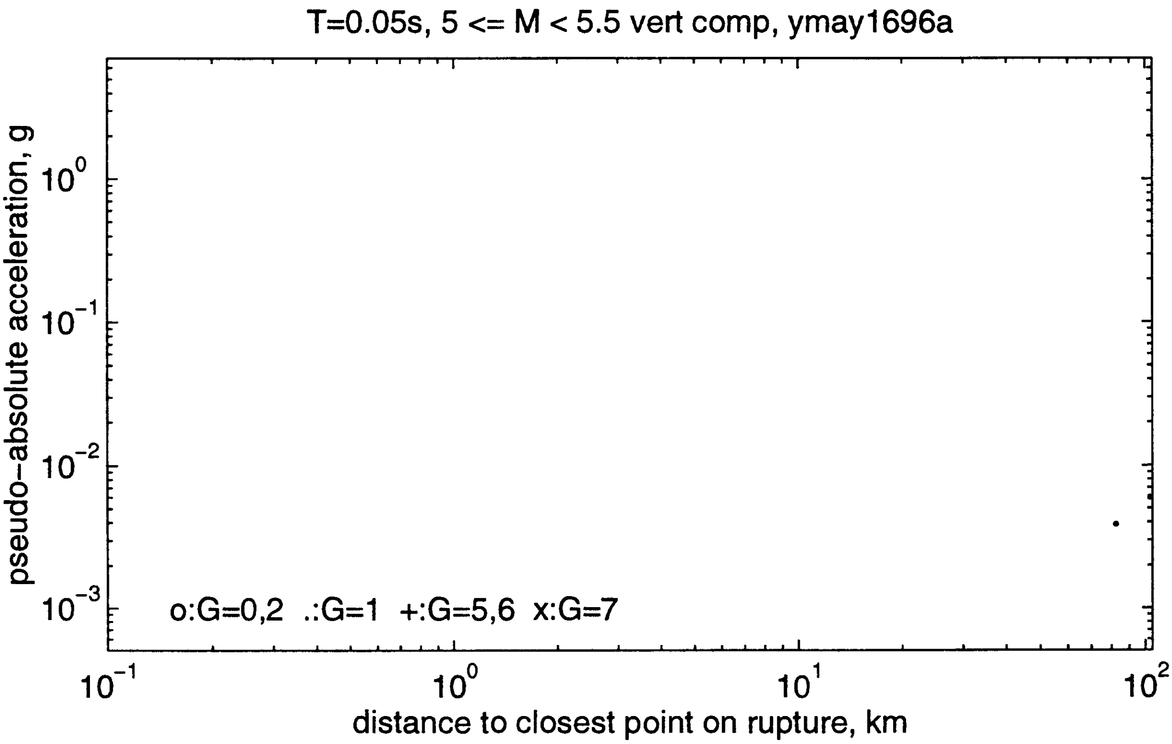
T=0.05s, 5 <= M < 5.5 vert comp, ymay1696a
pseudo-absolute acceleration, g
distance to closest point on rupture, km
o:G=0,2 .:G=1 +:G=5,6 x:G=7

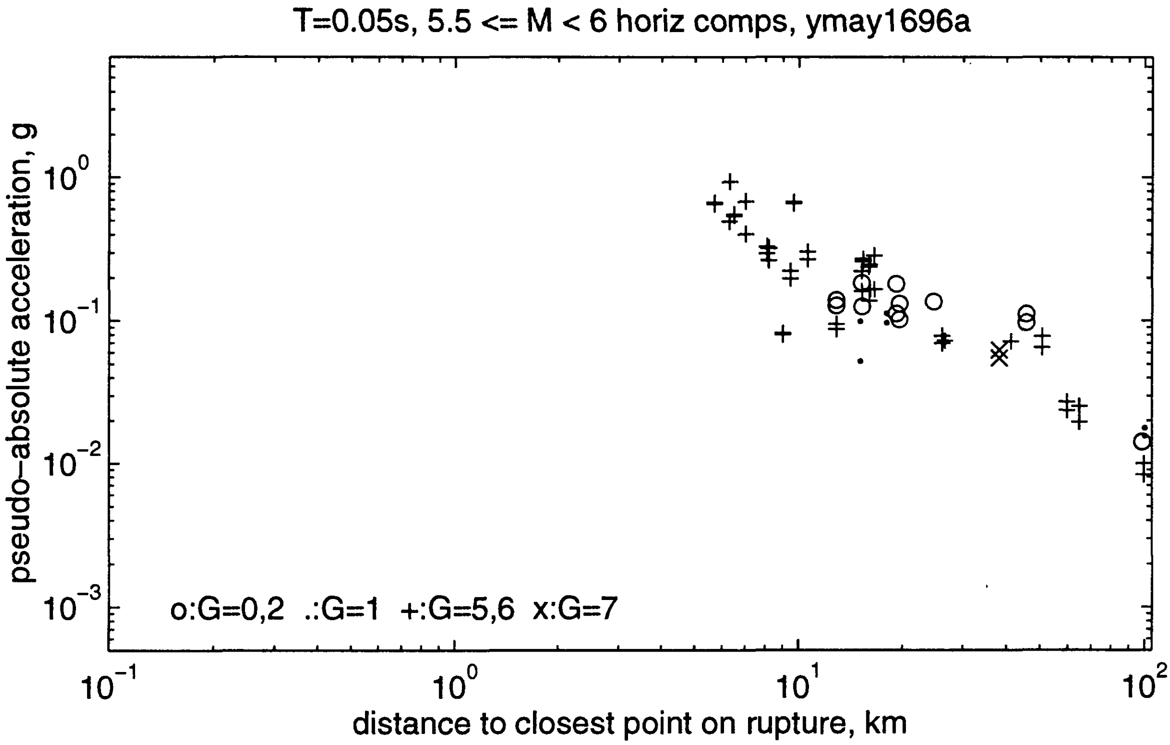
T=0.05s, 5.5 <= M < 6 horiz comps, ymay1696a
pseudo–absolute acceleration, g
distance to closest point on rupture, km
o:G=0,2 .:G=1 +:G=5,6 x:G=7
10^{0}
10^{-1}
10^{-2}
10^{-3}
10^{-1}
10^{0}
10^{1}
10^{2}

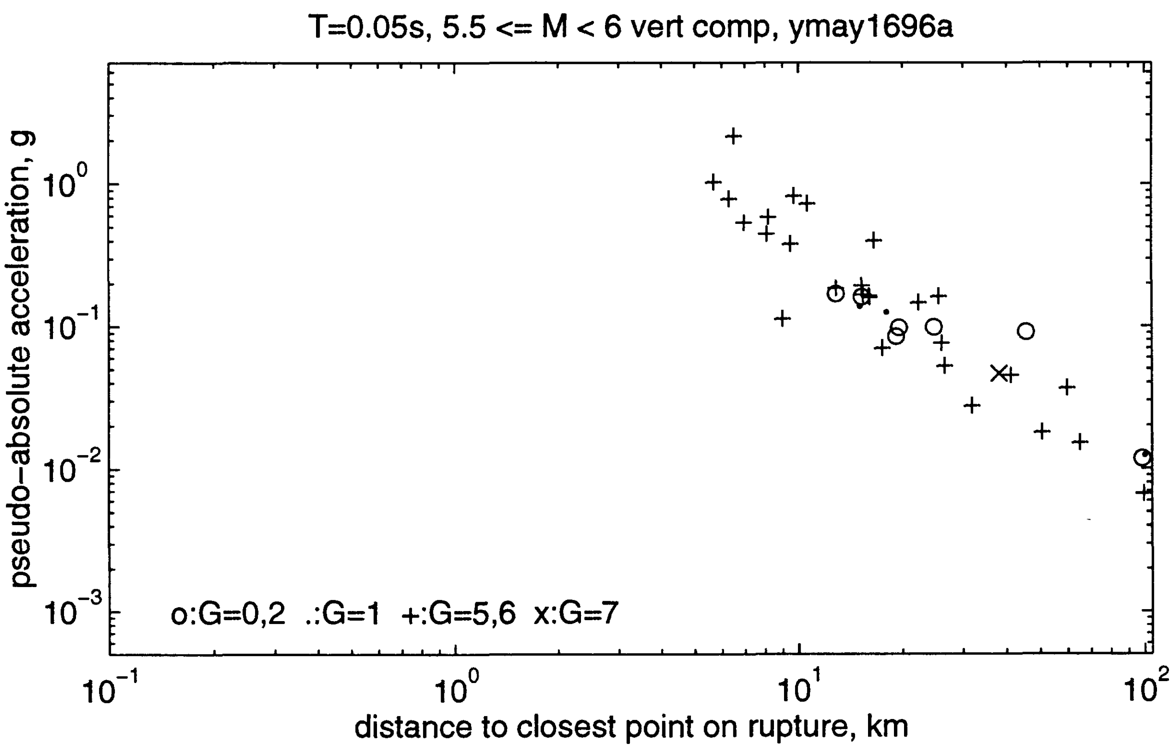
T=0.05s, 5.5 <= M < 6 vert comp, ymay1696a
pseudo–absolute acceleration, g
distance to closest point on rupture, km
o:G=0,2 .:G=1 +:G=5,6 x:G=7
10^{0}
10^{-1}
10^{-2}
10^{-3}
10^{-1}
10^{0}
10^{1}
10^{2}

10f

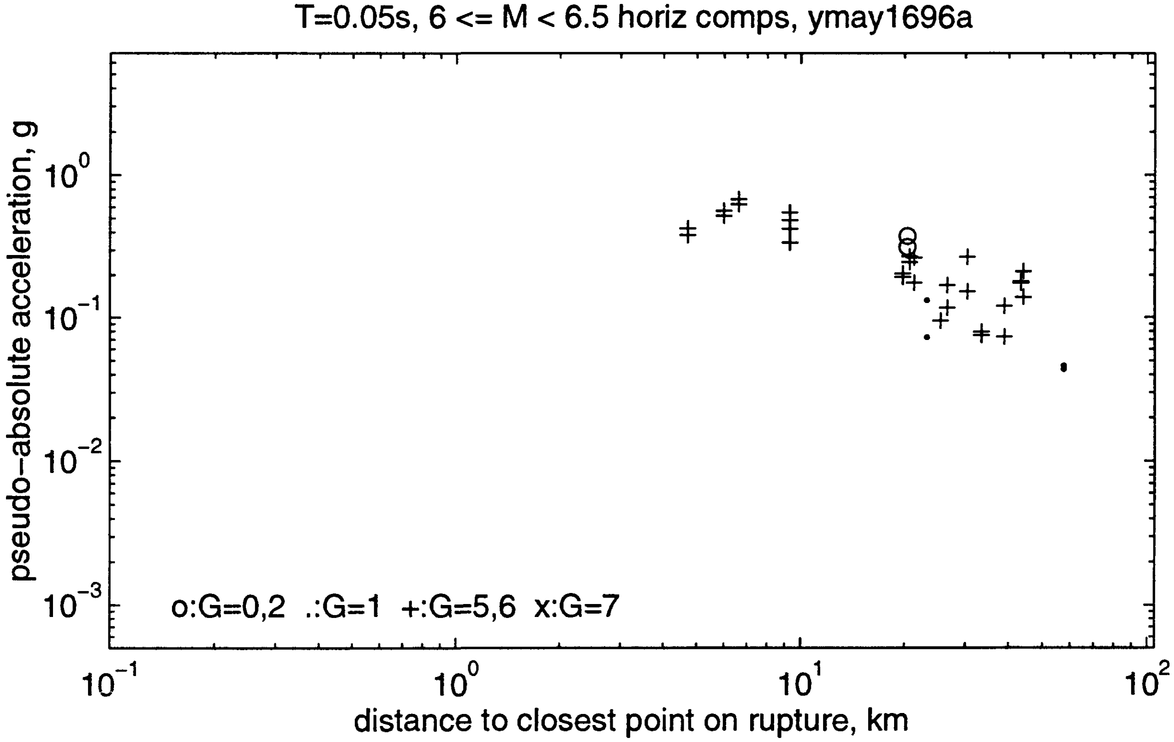
T=0.05s, 6 <= M < 6.5 horiz comps, ymay1696a
pseudo-absolute acceleration, g
10^0
10^-1
10^-2
10^-3
o:G=0,2 .:G=1 +:G=5,6 x:G=7
10^-1
10^0
10^1
10^2
distance to closest point on rupture, km

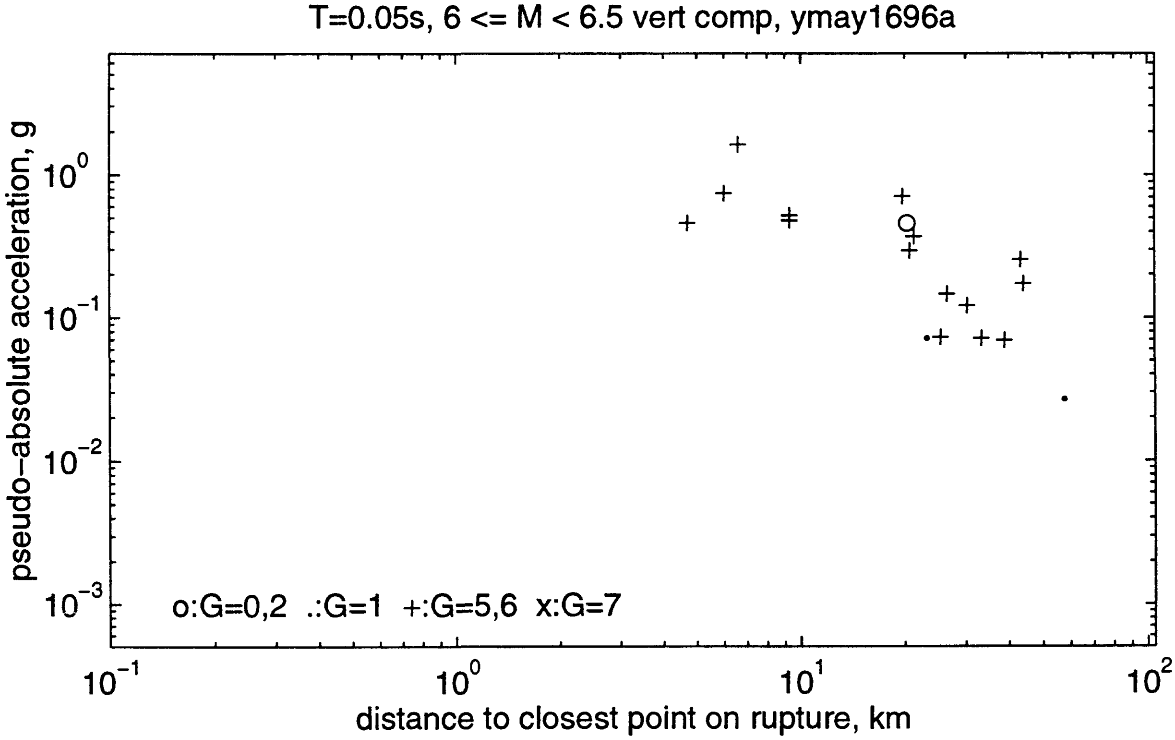
T=0.05s, 6 <= M < 6.5 vert comp, ymay1696a
pseudo-absolute acceleration, g
10^0
10^-1
10^-2
10^-3
o:G=0,2 .:G=1 +:G=5,6 x:G=7
10^-1
10^0
10^1
10^2
distance to closest point on rupture, km

10 g

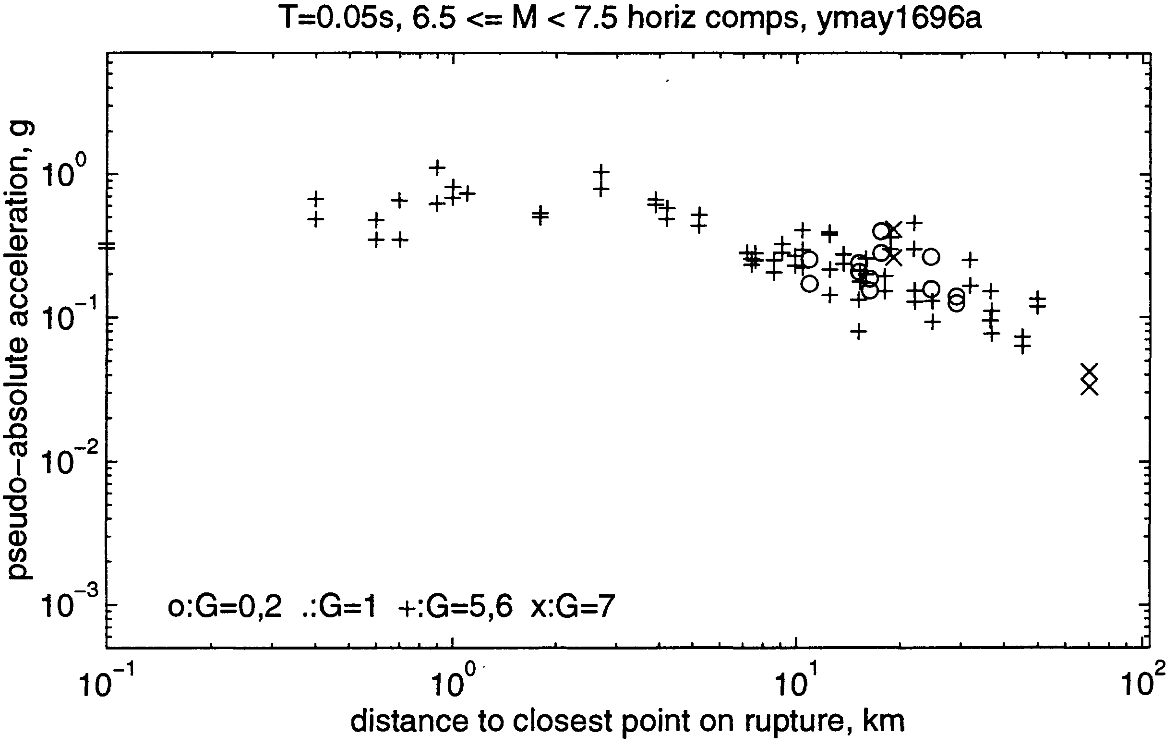
T=0.05s, 6.5 <= M < 7.5 horiz comps, ymay1696a
pseudo-absolute acceleration, g
distance to closest point on rupture, km
o:G=0,2 .:G=1 +:G=5,6 x:G=7

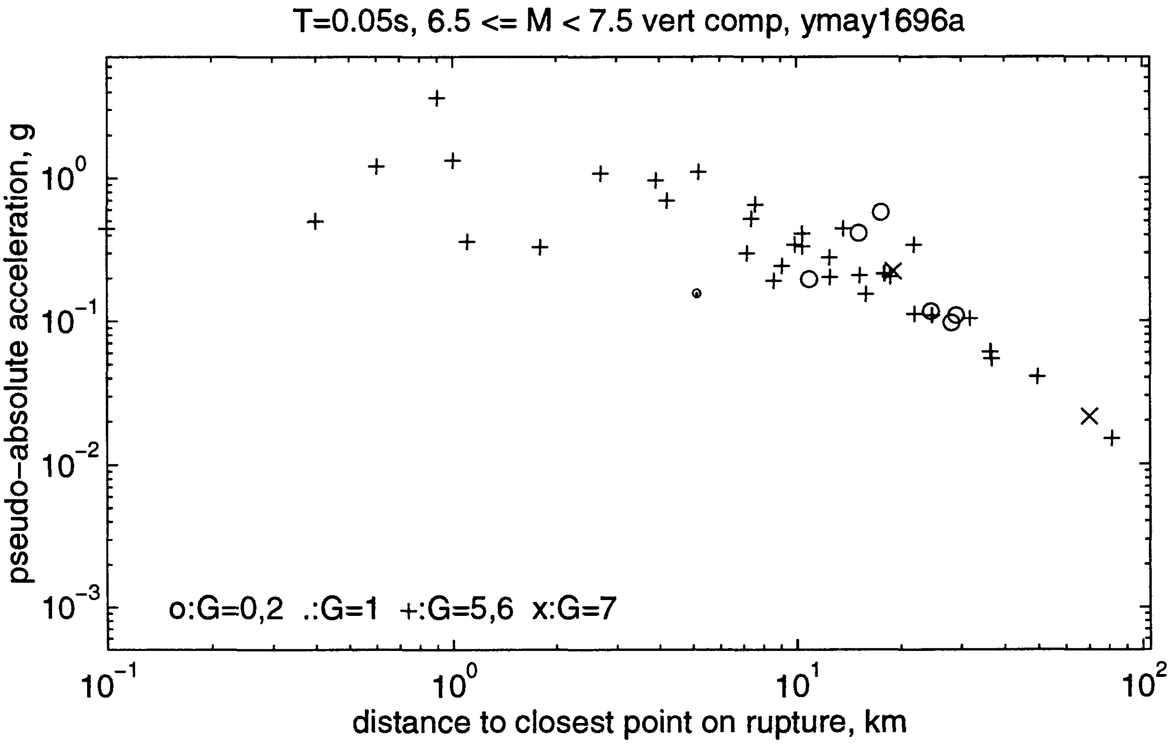
T=0.05s, 6.5 <= M < 7.5 vert comp, ymay1696a
pseudo-absolute acceleration, g
distance to closest point on rupture, km
o:G=0,2 .:G=1 +:G=5,6 x:G=7

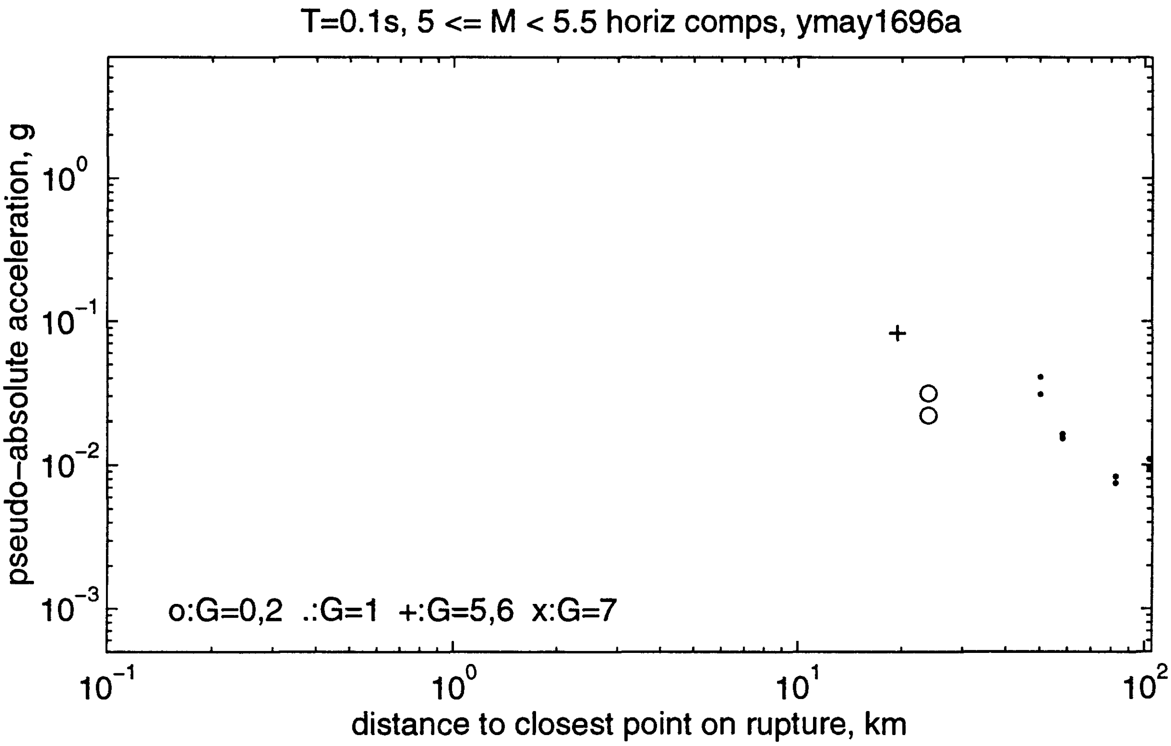

T=0.1s, 5 <= M < 5.5 horiz comps, ymay1696a
pseudo–absolute acceleration, g
distance to closest point on rupture, km
o:G=0,2 .:G=1 +:G=5,6 x:G=7

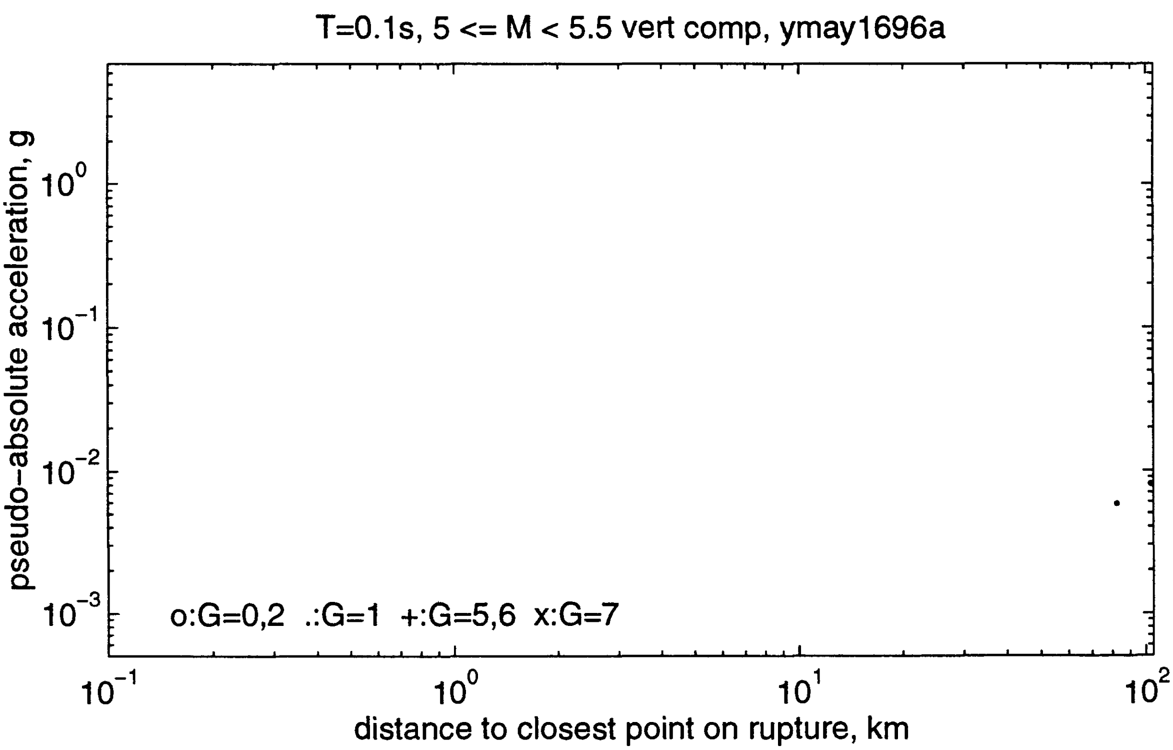

T=0.1s, 5 <= M < 5.5 vert comp, ymay1696a
pseudo–absolute acceleration, g
distance to closest point on rupture, km
o:G=0,2 .:G=1 +:G=5,6 x:G=7

10i

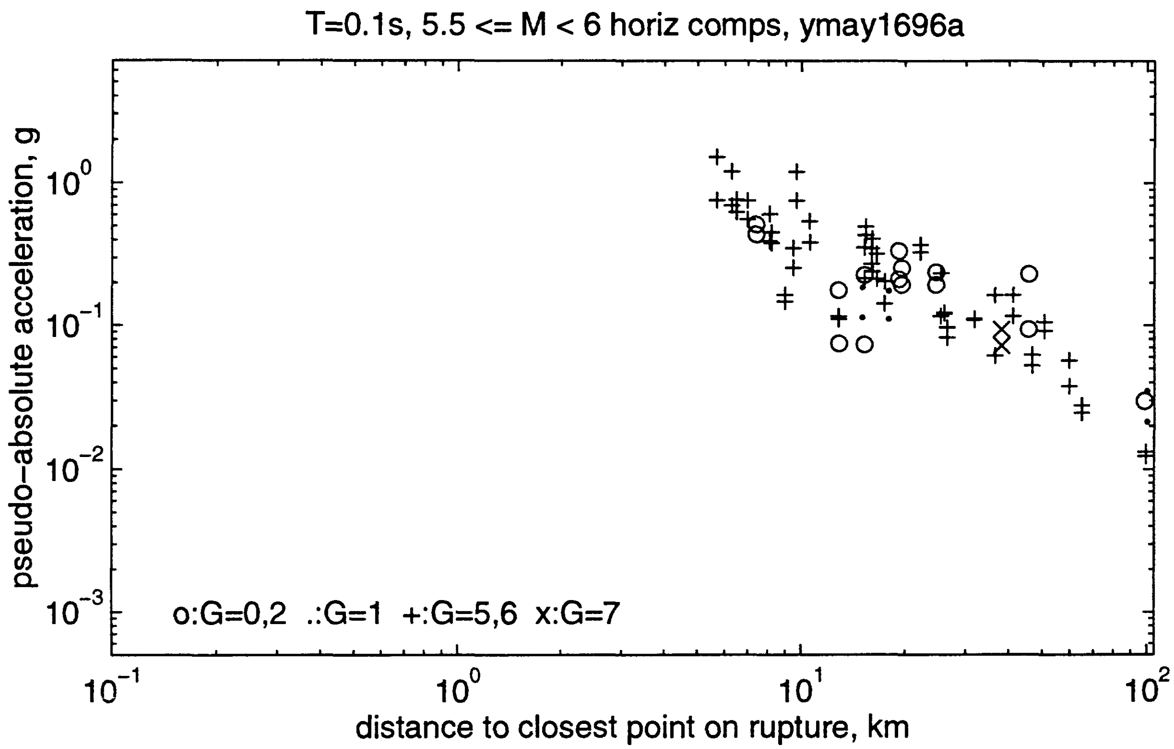
T=0.1s, 5.5 <= M < 6 horiz comps, ymay1696a
pseudo-absolute acceleration, g
distance to closest point on rupture, km
o:G=0,2 .:G=1 +:G=5,6 x:G=7

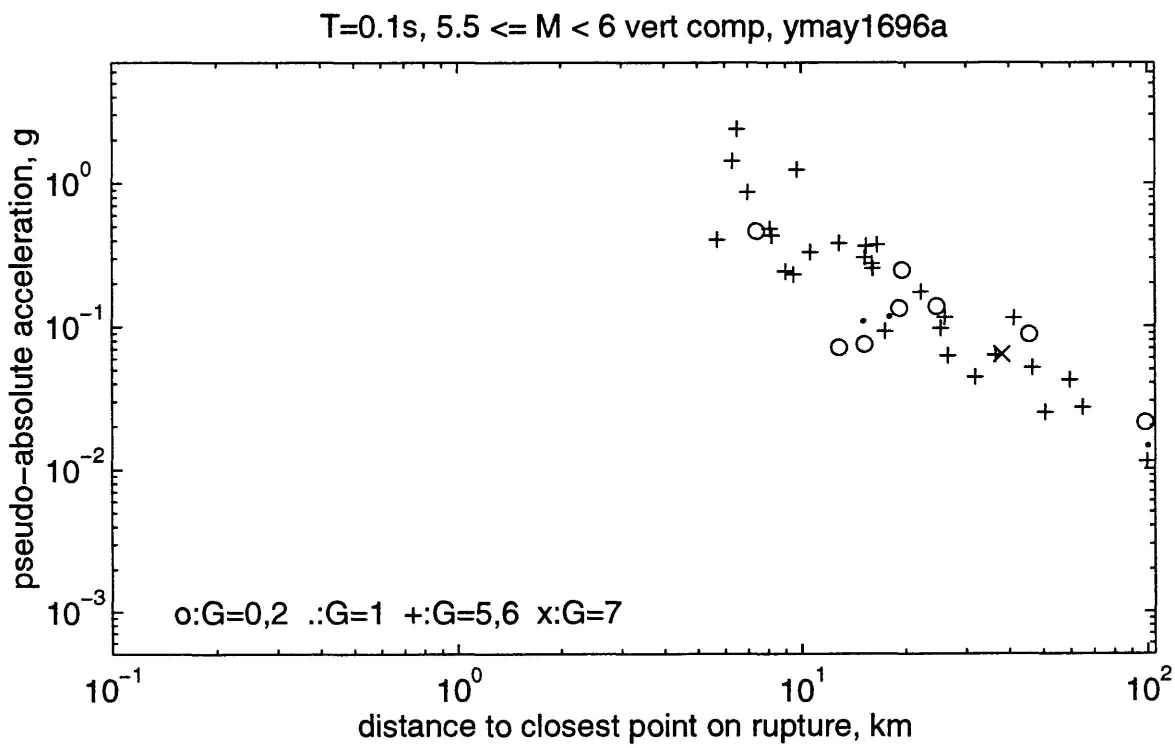
T=0.1s, 5.5 <= M < 6 vert comp, ymay1696a
pseudo-absolute acceleration, g
distance to closest point on rupture, km
o:G=0,2 .:G=1 +:G=5,6 x:G=7

T=0.1s, 6 <= M < 6.5 horiz comps, ymay1696a

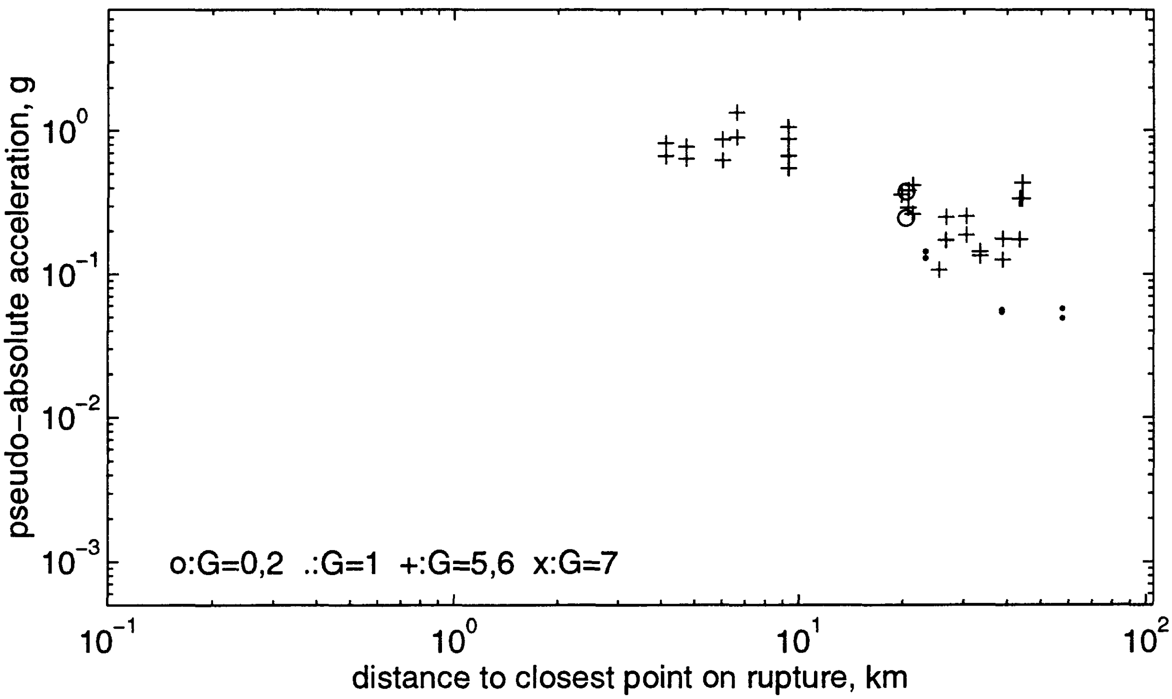

T=0.1s, 6 <= M < 6.5 vert comp, ymay1696a

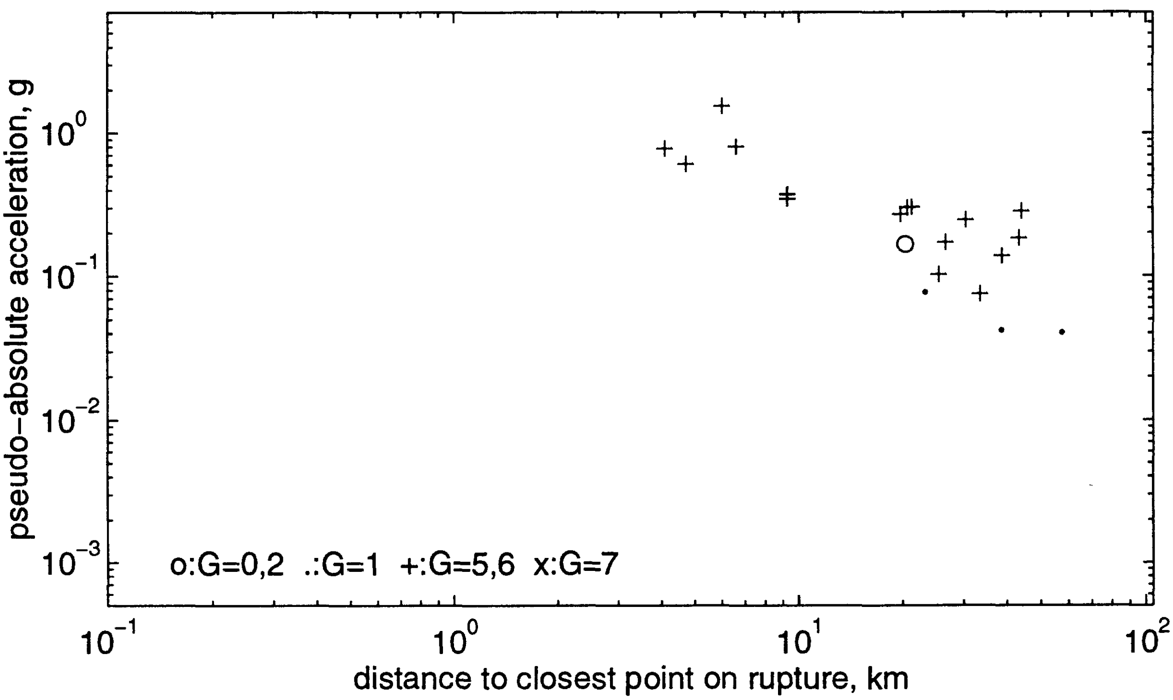

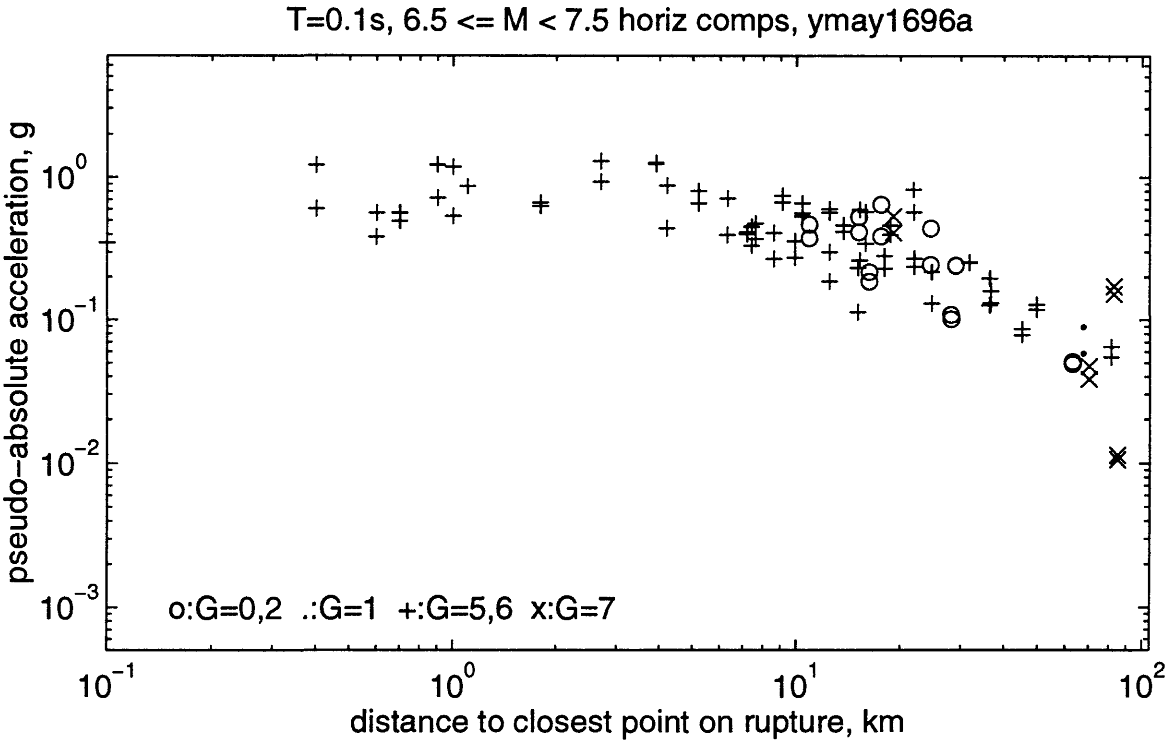
T=0.1s, 6.5 <= M < 7.5 horiz comps, ymay1696a
pseudo–absolute acceleration, g
10^{0}
10^{-1}
10^{-2}
10^{-3}
o:G=0,2 .:G=1 +:G=5,6 x:G=7
10^{-1}
10^{0}
10^{1}
10^{2}
distance to closest point on rupture, km

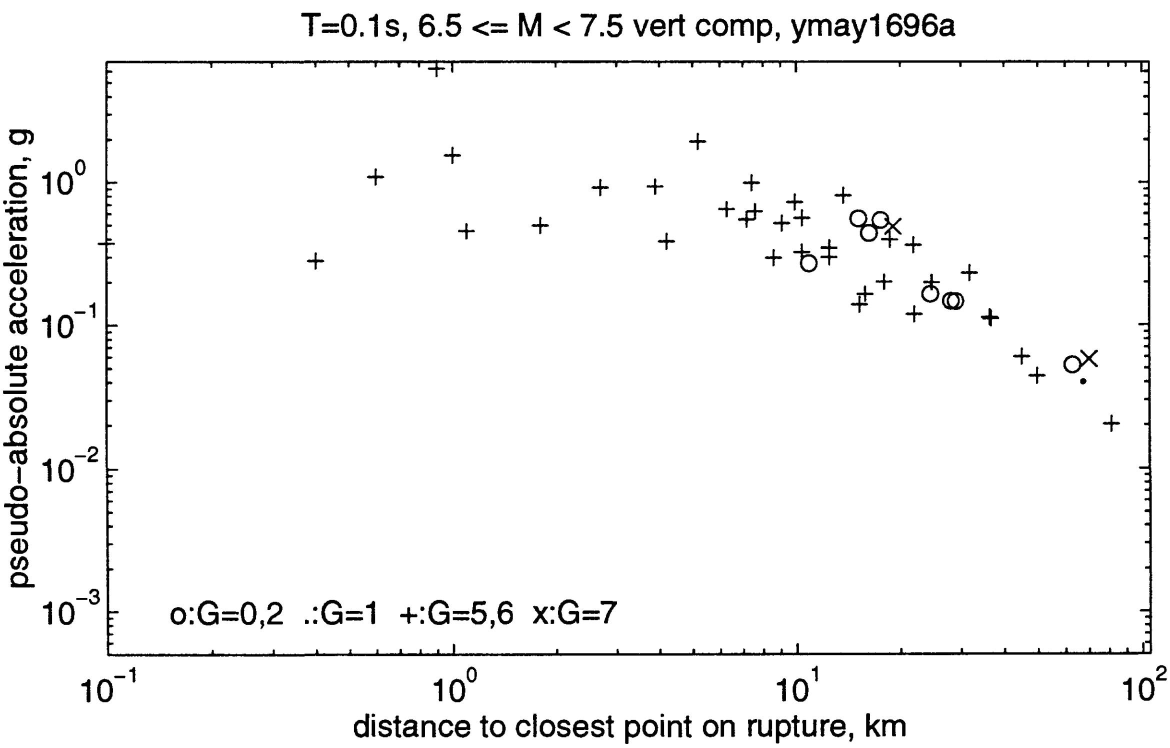
T=0.1s, 6.5 <= M < 7.5 vert comp, ymay1696a
pseudo–absolute acceleration, g
10^{0}
10^{-1}
10^{-2}
10^{-3}
o:G=0,2 .:G=1 +:G=5,6 x:G=7
10^{-1}
10^{0}
10^{1}
10^{2}
distance to closest point on rupture, km

T=0.15s, 5 <= M < 5.5 horiz comps, ymay1696a

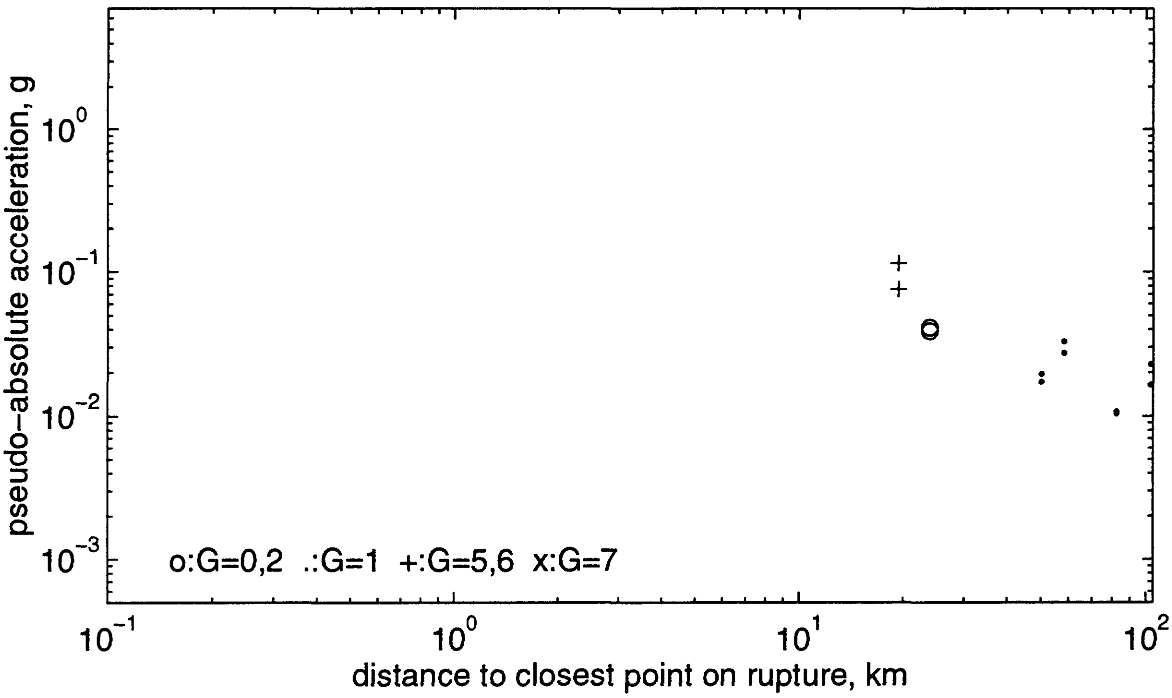

T=0.15s, 5 <= M < 5.5 vert comp, ymay1696a

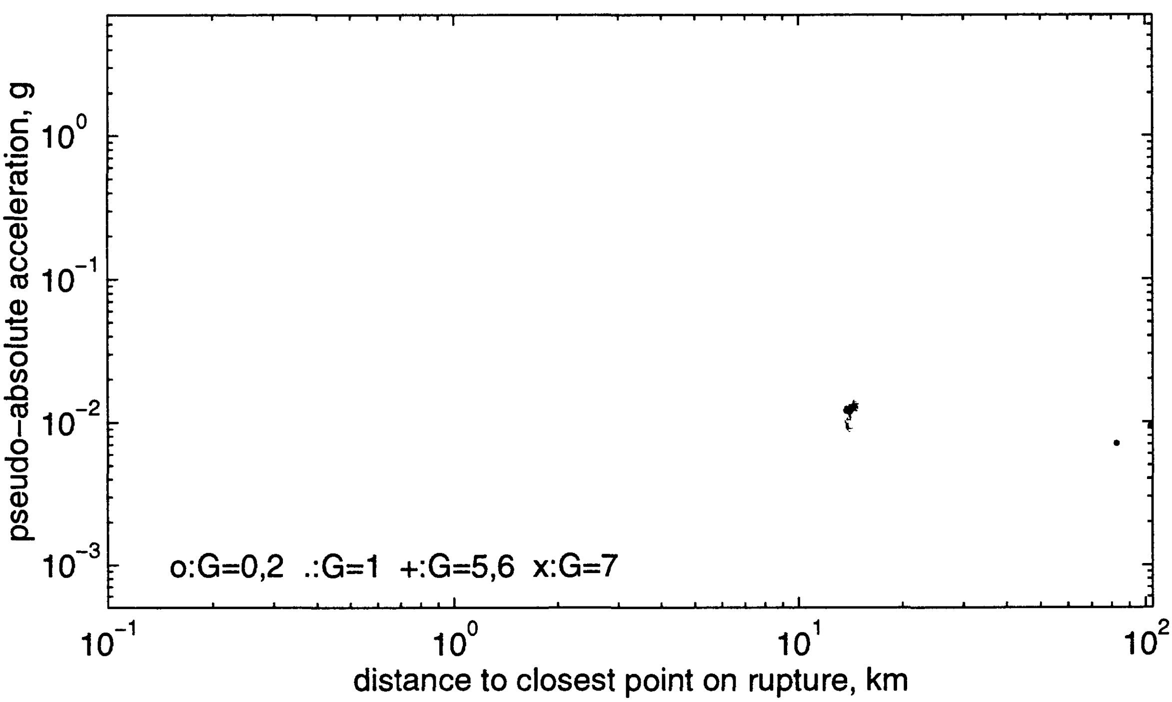

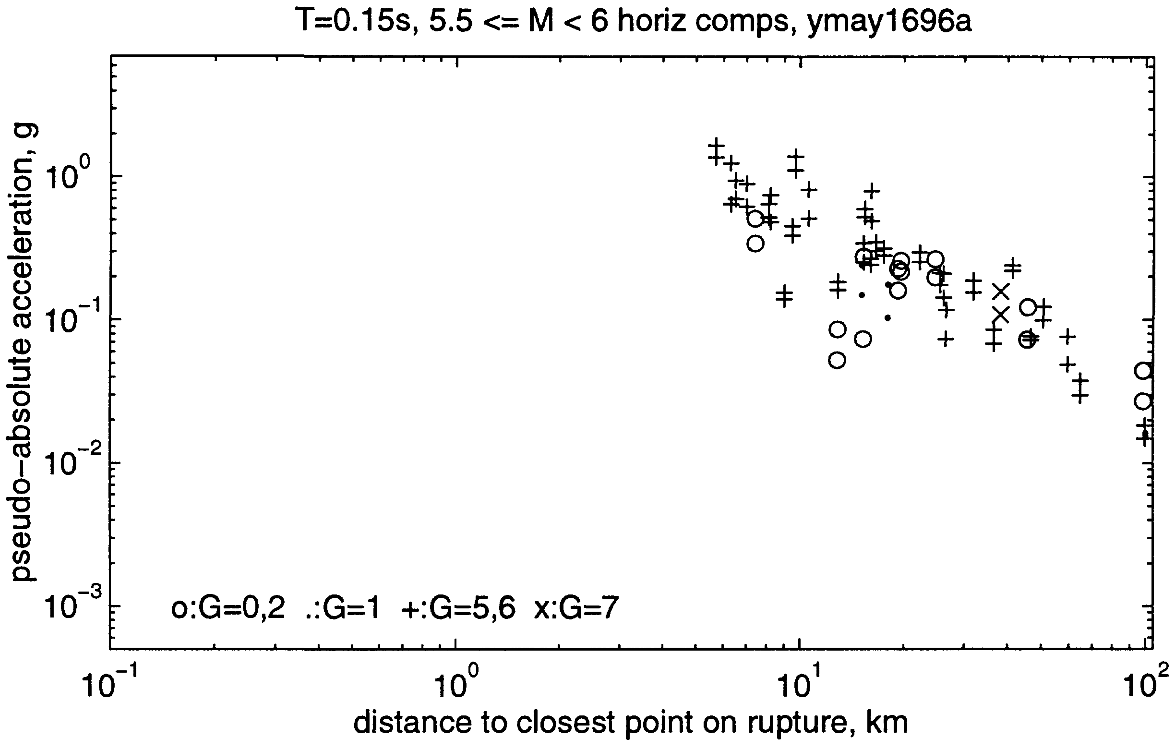
T=0.15s, 5.5 <= M < 6 horiz comps, ymay1696a
pseudo−absolute acceleration, g
10^0
10^{-1}
10^{-2}
10^{-3}
o:G=0,2 .:G=1 +:G=5,6 x:G=7
10^{-1}
10^0
10^1
10^2
distance to closest point on rupture, km

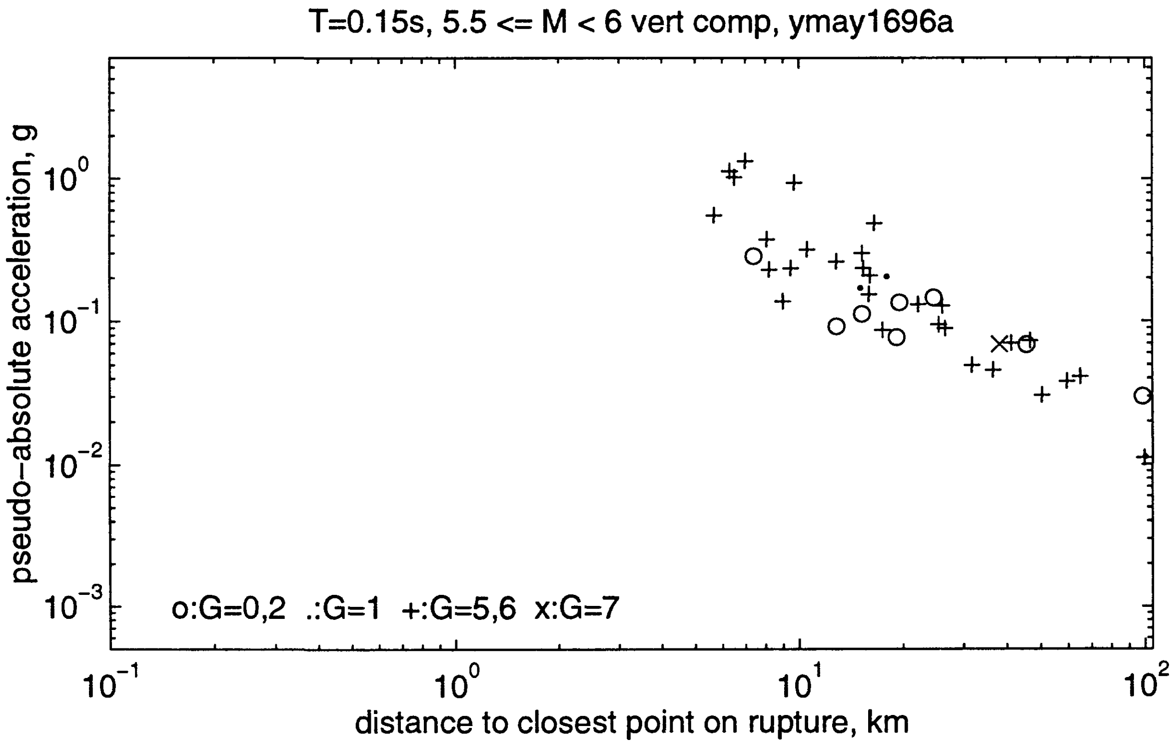
T=0.15s, 5.5 <= M < 6 vert comp, ymay1696a
pseudo−absolute acceleration, g
10^0
10^{-1}
10^{-2}
10^{-3}
o:G=0,2 .:G=1 +:G=5,6 x:G=7
10^{-1}
10^0
10^1
10^2
distance to closest point on rupture, km

10 n

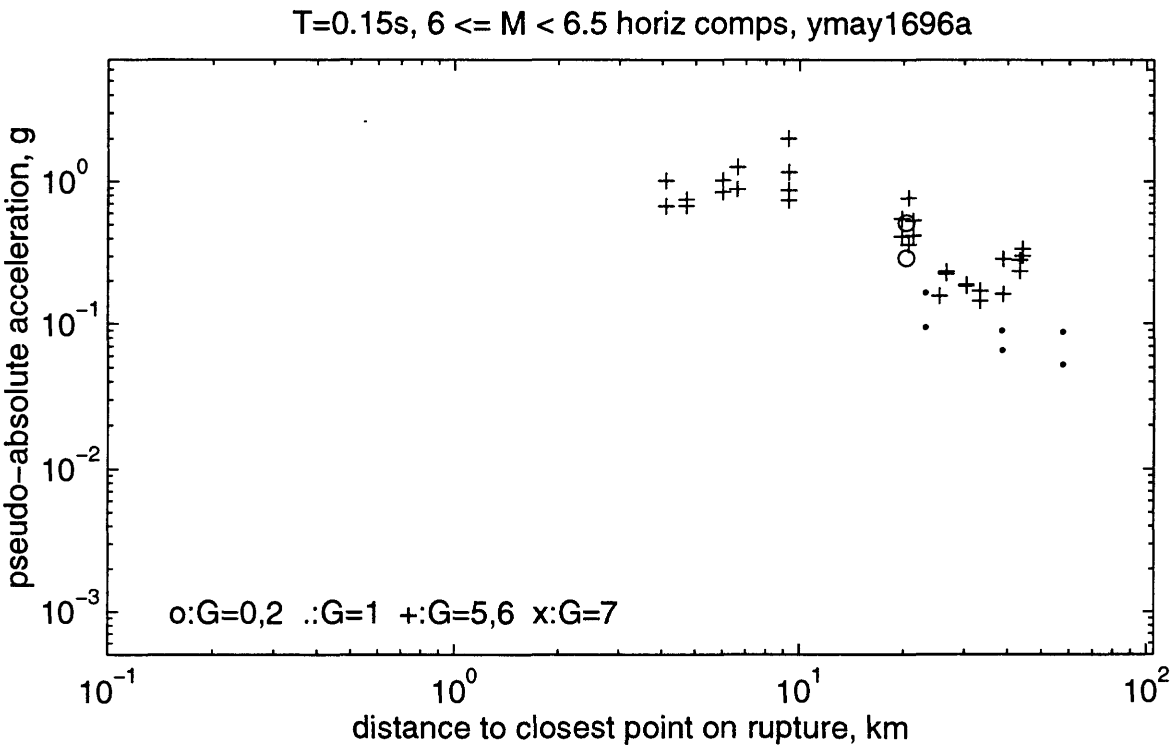
T=0.15s, 6 <= M < 6.5 horiz comps, ymay1696a
pseudo-absolute acceleration, g
distance to closest point on rupture, km
o:G=0,2 .:G=1 +:G=5,6 x:G=7

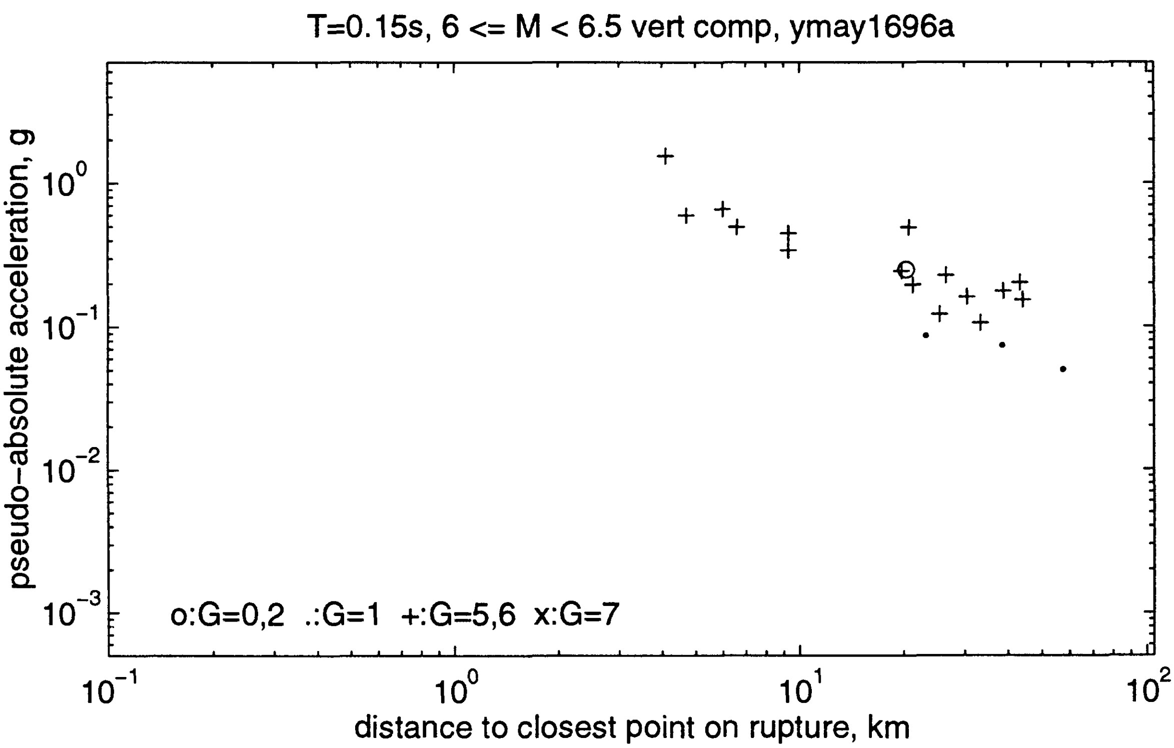
T=0.15s, 6 <= M < 6.5 vert comp, ymay1696a
pseudo-absolute acceleration, g
distance to closest point on rupture, km
o:G=0,2 .:G=1 +:G=5,6 x:G=7

100

T=0.15s, 6.5 <= M < 7.5 horiz comps, ymay1696a

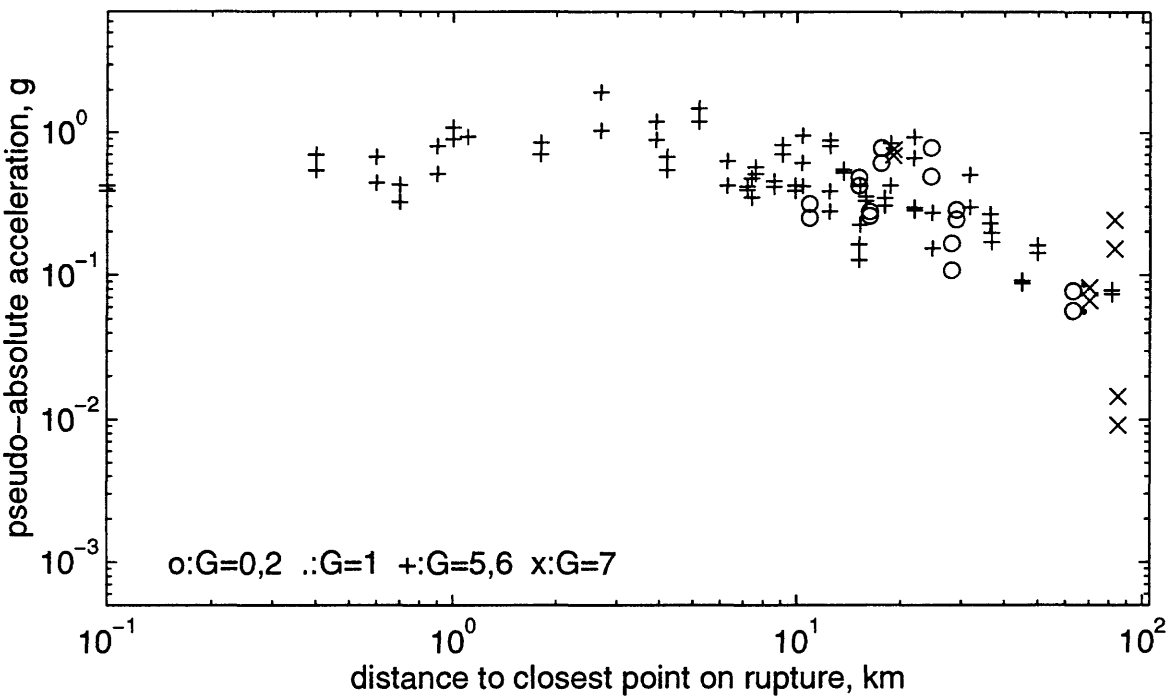

T=0.15s, 6.5 <= M < 7.5 vert comp, ymay1696a

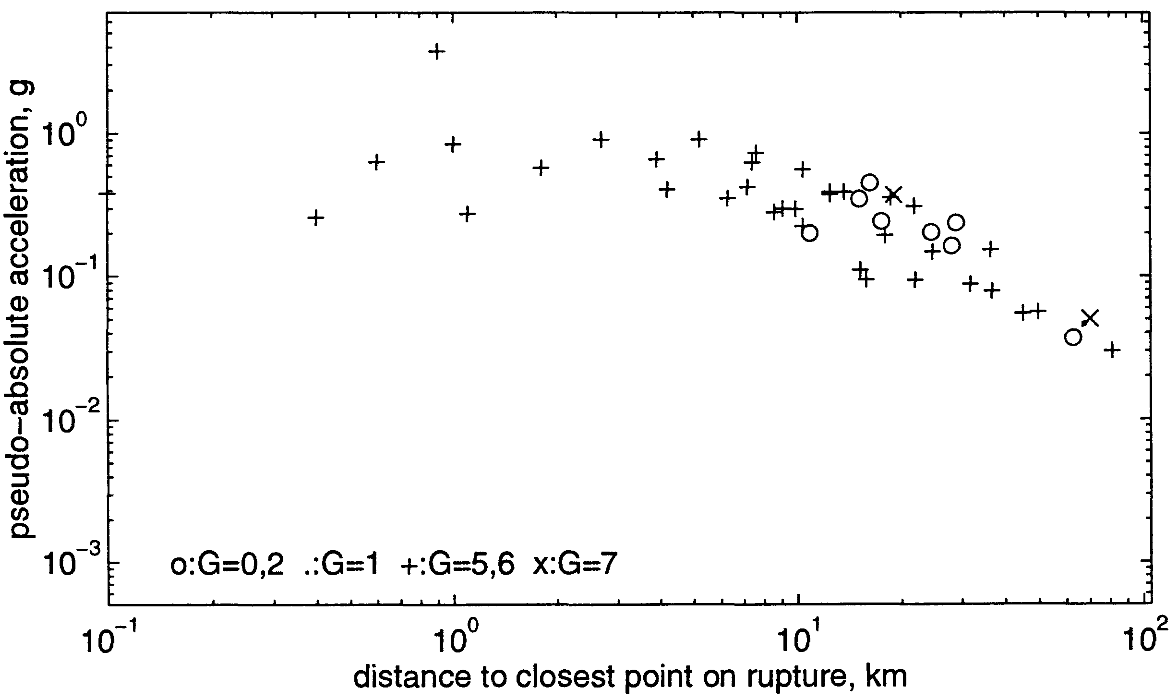

T=0.2s, 5 <= M < 5.5 horiz comps, ymay1696a

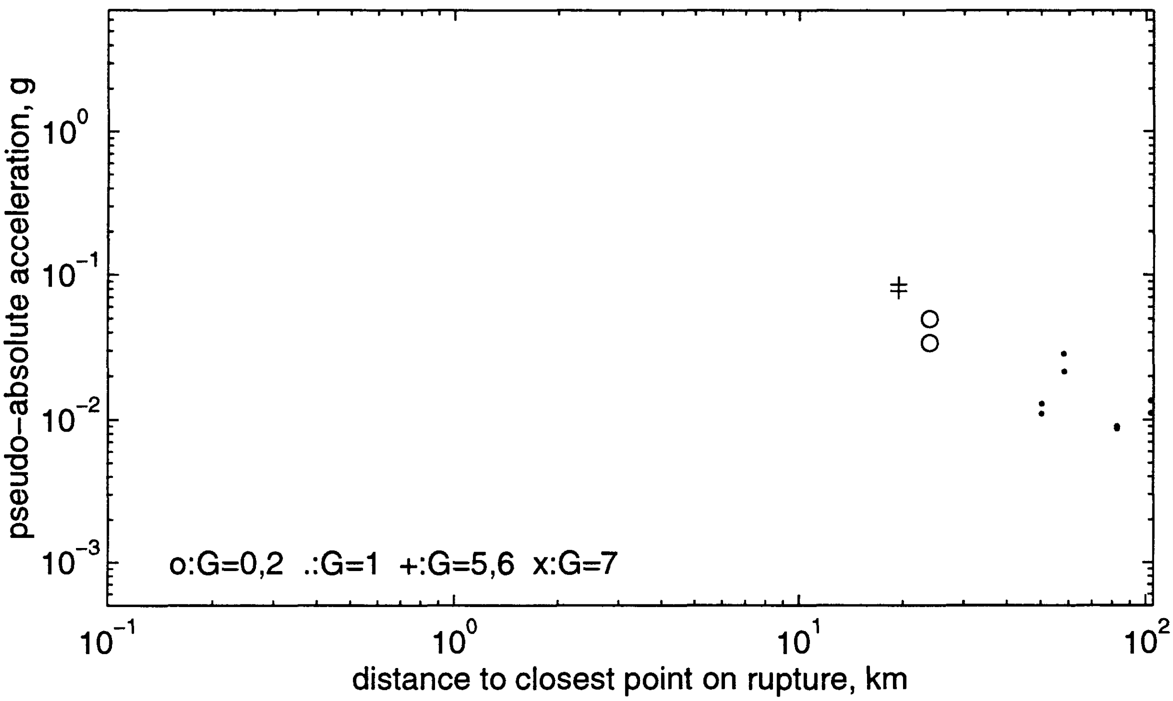

T=0.2s, 5 <= M < 5.5 vert comp, ymay1696a

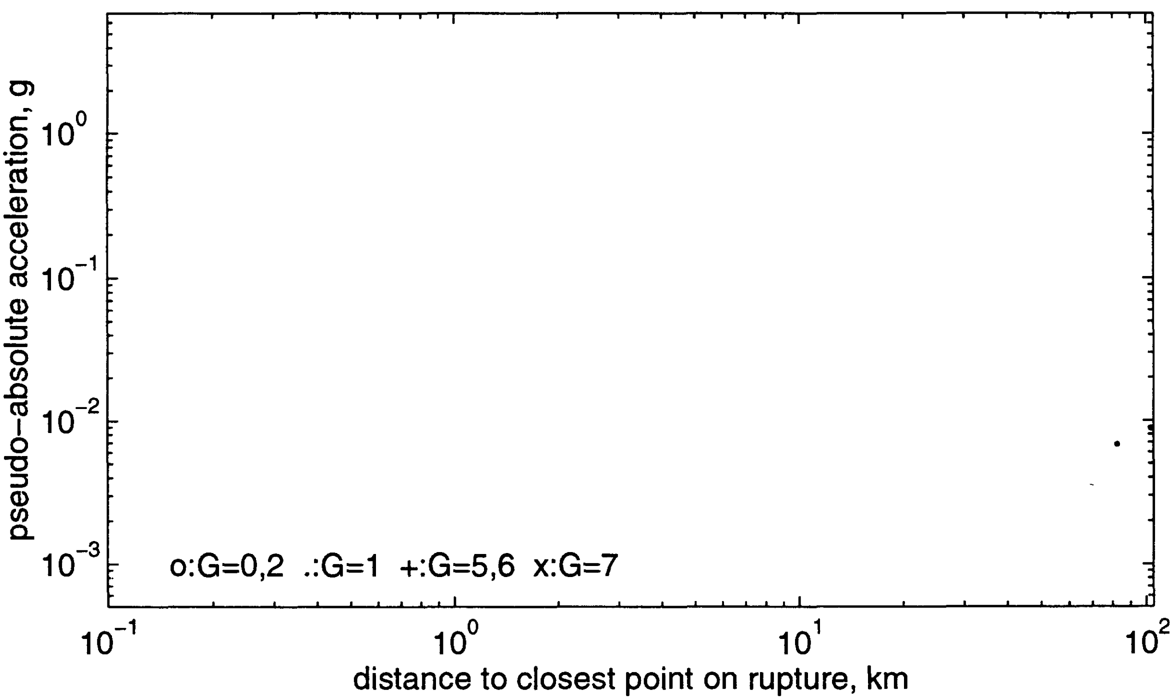

T=0.2s, 5.5 <= M < 6 horiz comps, ymay1696a

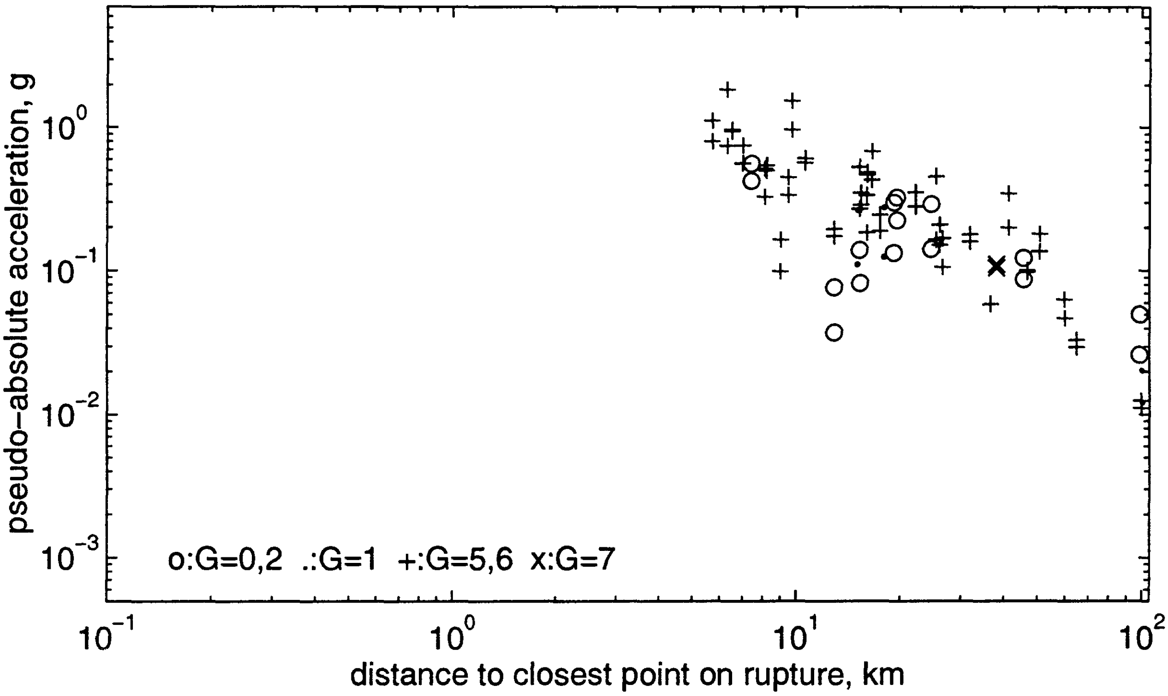

T=0.2s, 5.5 <= M < 6 vert comp, ymay1696a

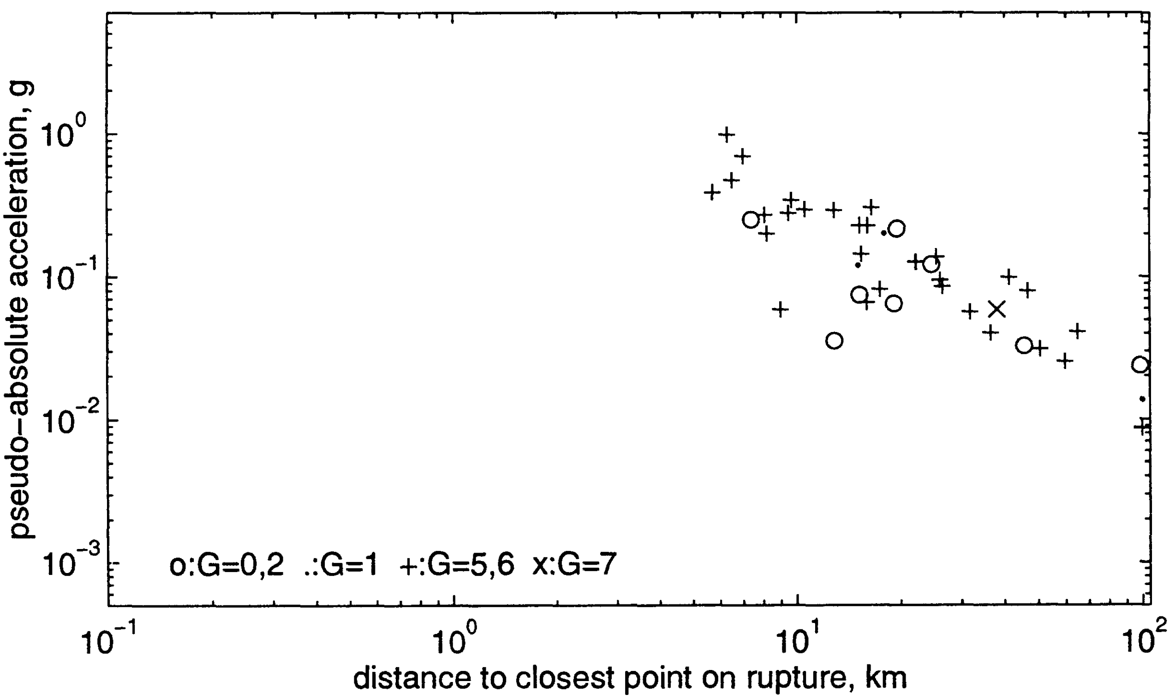

10r

T=0.2s, 6 <= M < 6.5 horiz comps, ymay1696a

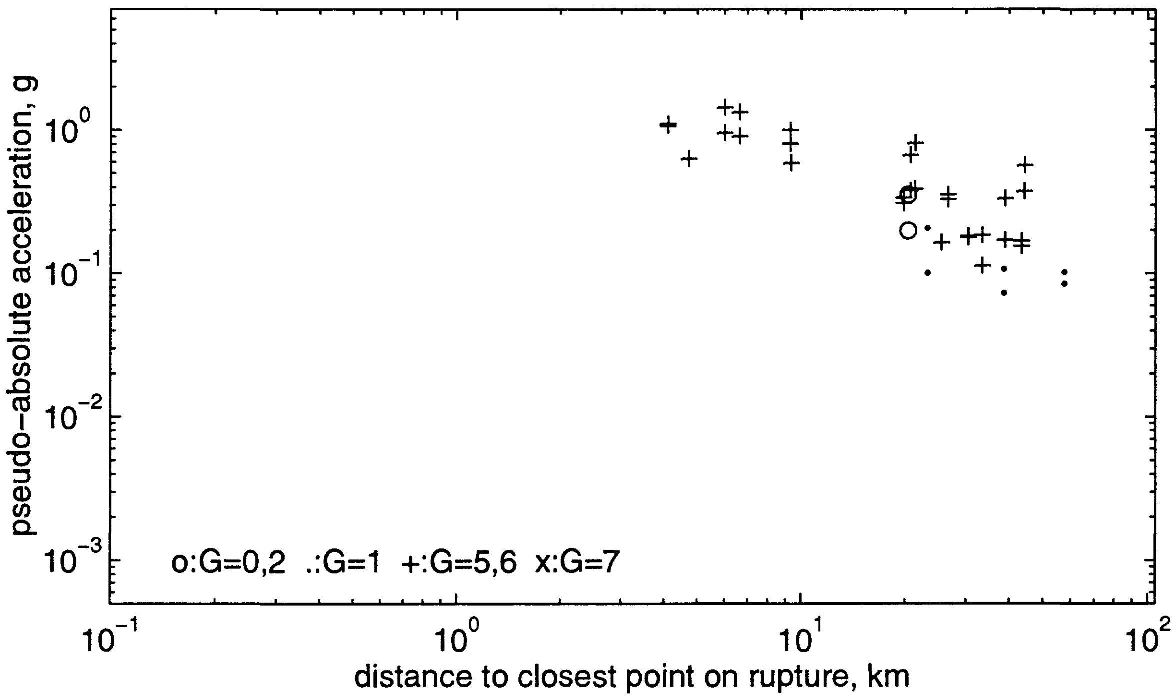

T=0.2s, 6 <= M < 6.5 vert comp, ymay1696a

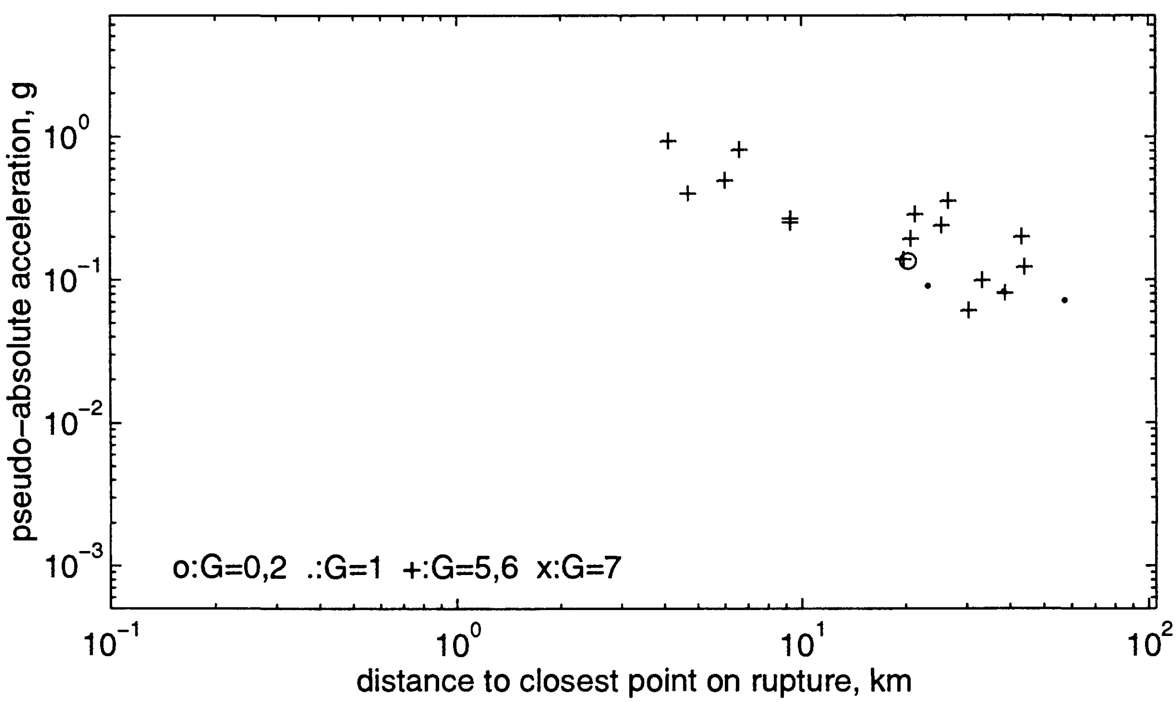

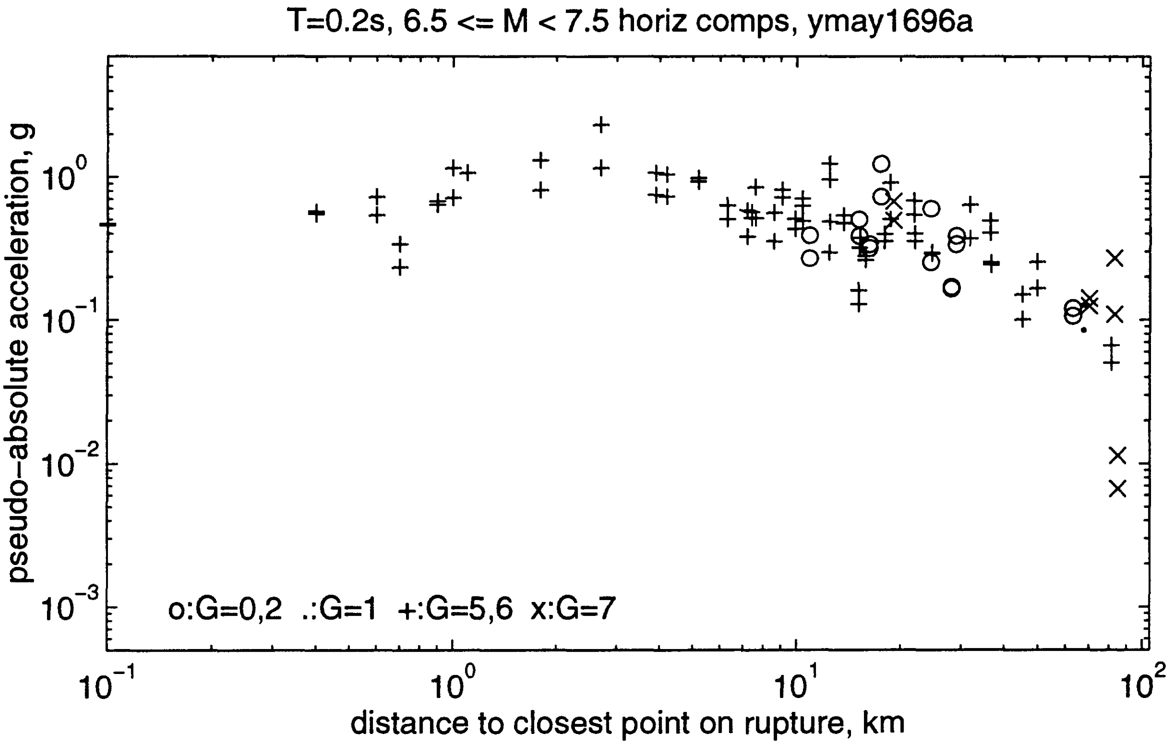
T=0.2s, 6.5 <= M < 7.5 horiz comps, ymay1696a
pseudo-absolute acceleration, g
10^0
10^{-1}
10^{-2}
10^{-3}
o:G=0,2 .:G=1 +:G=5,6 x:G=7
10^{-1}
10^0
10^1
10^2
distance to closest point on rupture, km

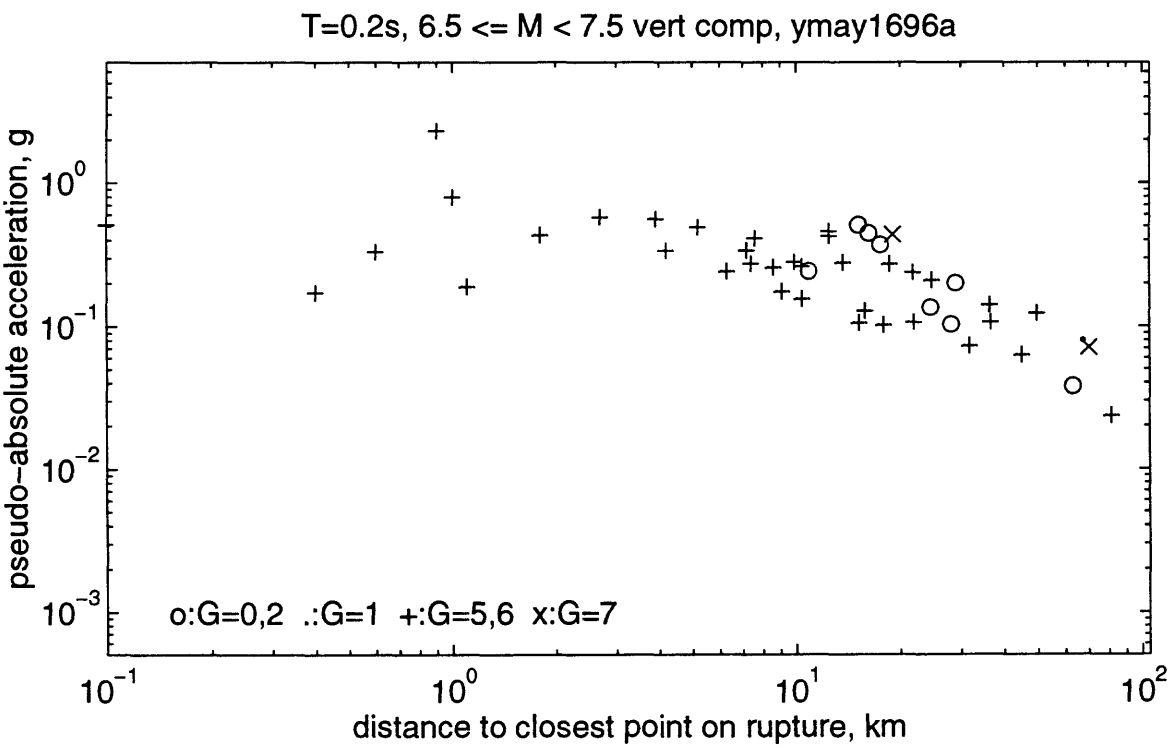
T=0.2s, 6.5 <= M < 7.5 vert comp, ymay1696a
pseudo-absolute acceleration, g
10^0
10^{-1}
10^{-2}
10^{-3}
o:G=0,2 .:G=1 +:G=5,6 x:G=7
10^{-1}
10^0
10^1
10^2
distance to closest point on rupture, km

10t

T=0.3s, 5 <= M < 5.5 horiz comps, ymay1696a

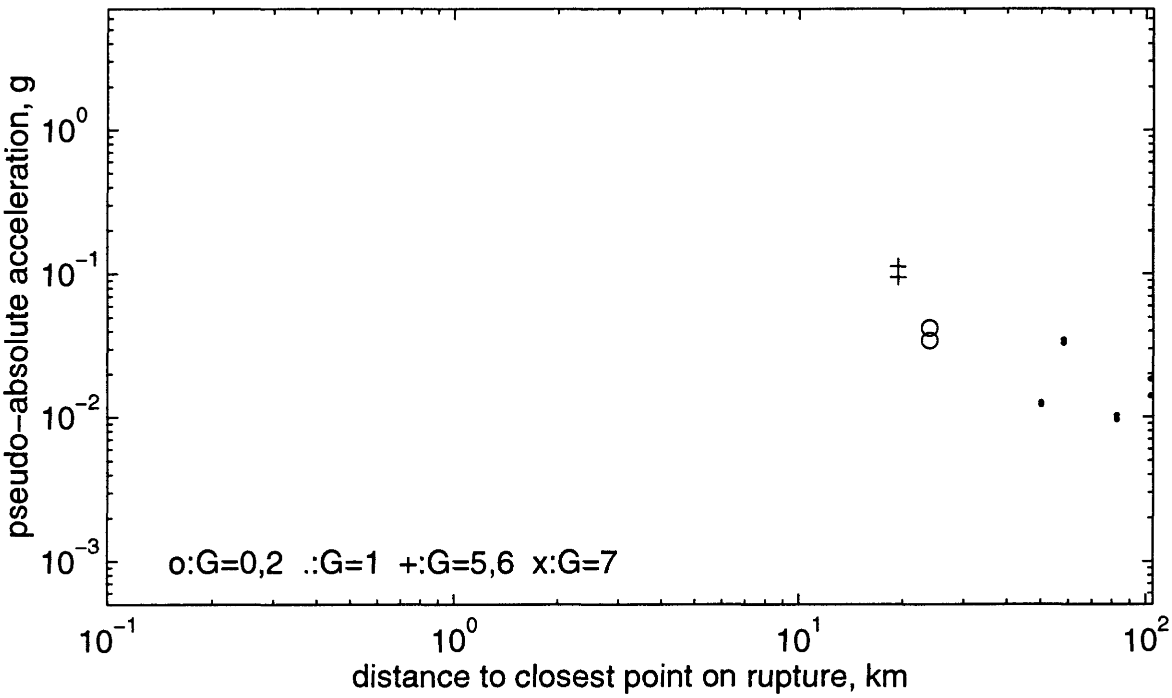

T=0.3s, 5 <= M < 5.5 vert comp, ymay1696a

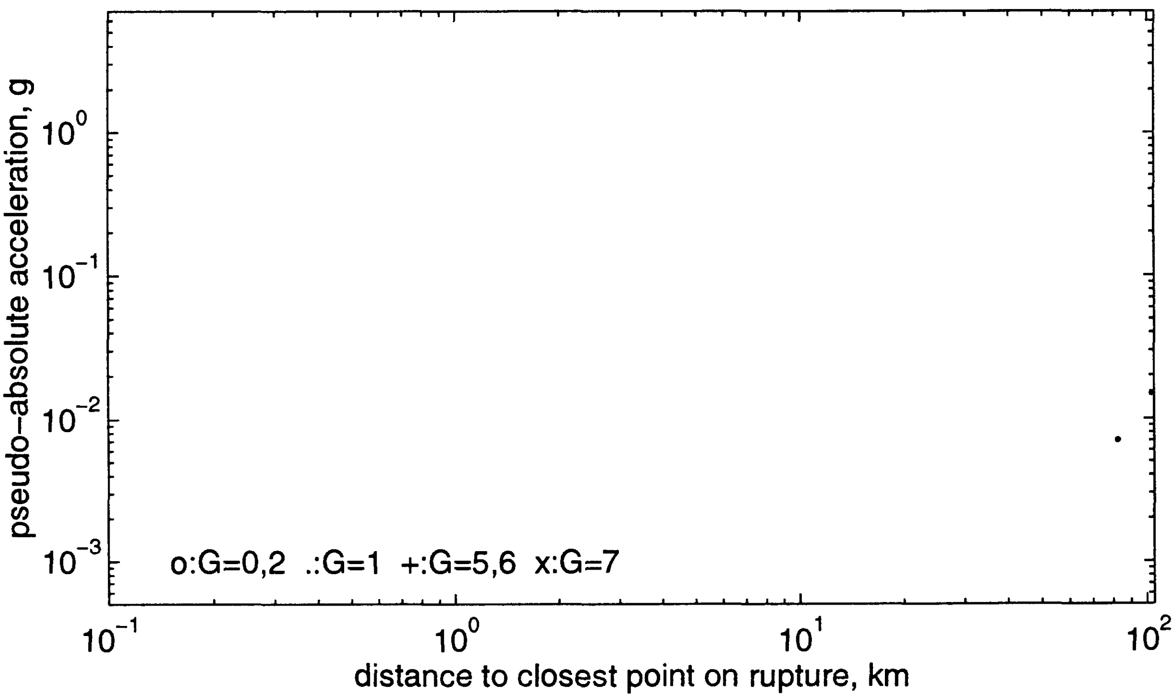

10u

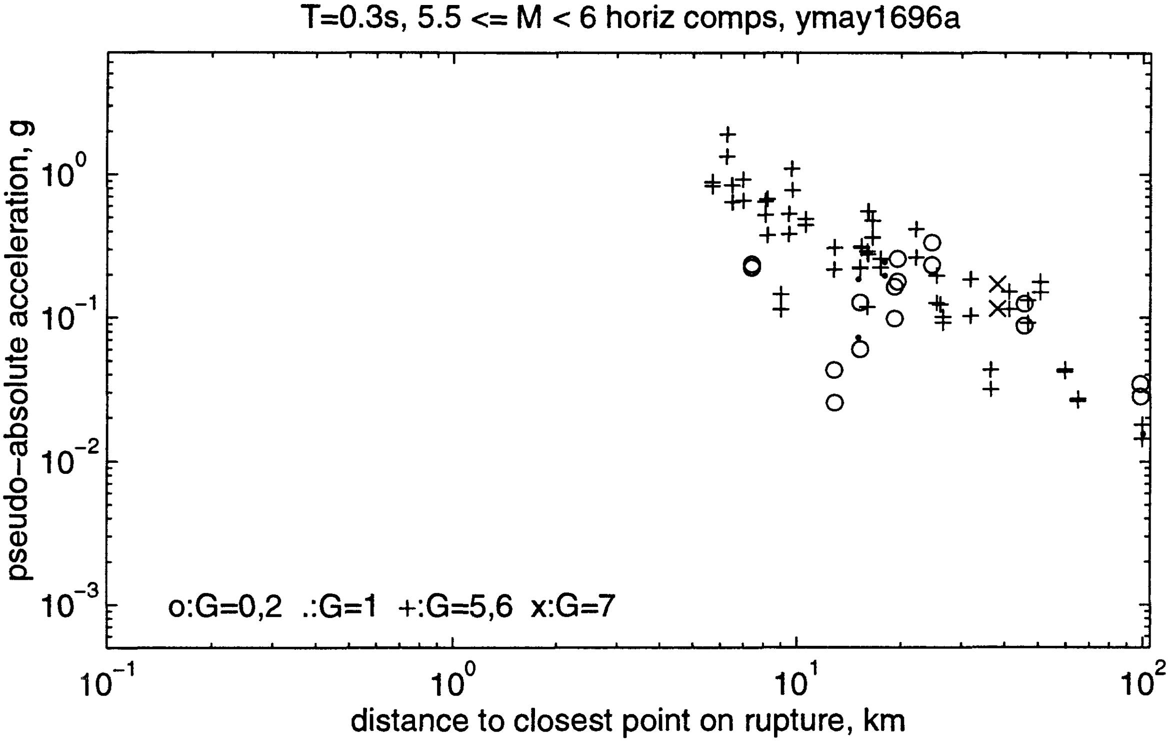
T=0.3s, 5.5 <= M < 6 horiz comps, ymay1696a
pseudo-absolute acceleration, g
distance to closest point on rupture, km
o:G=0,2 .:G=1 +:G=5,6 x:G=7

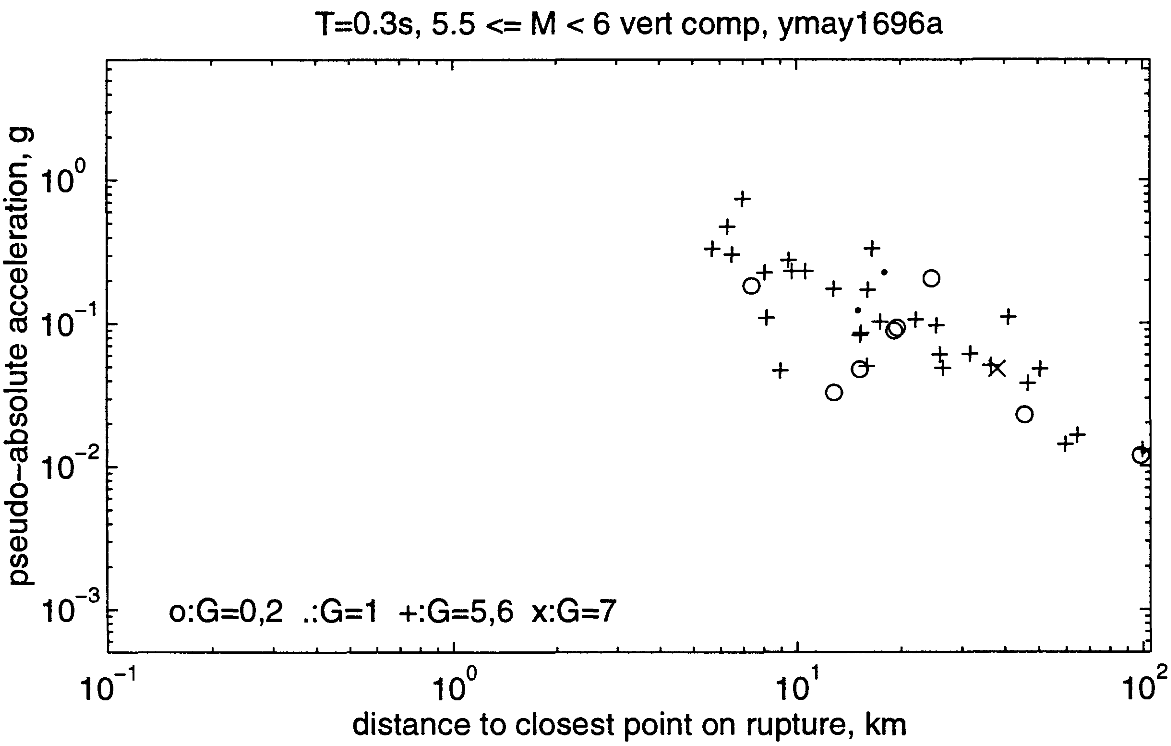
T=0.3s, 5.5 <= M < 6 vert comp, ymay1696a
pseudo-absolute acceleration, g
distance to closest point on rupture, km
o:G=0,2 .:G=1 +:G=5,6 x:G=7

10 v

T=0.3s, 6 <= M < 6.5 horiz comps, ymay1696a

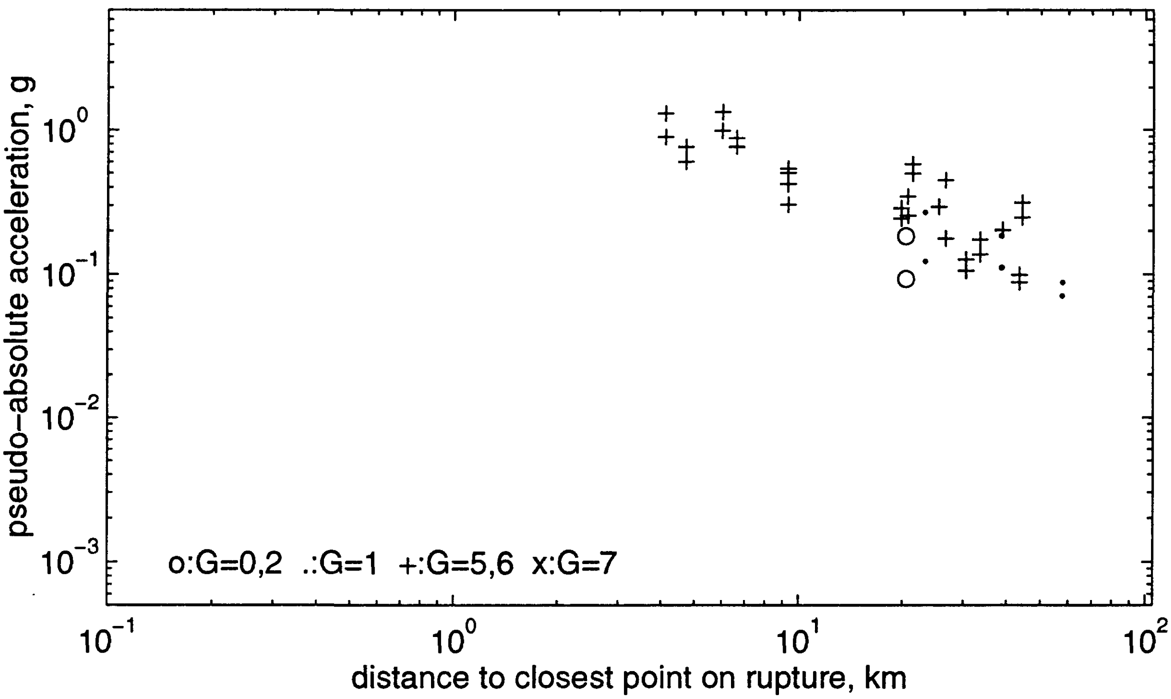

T=0.3s, 6 <= M < 6.5 vert comp, ymay1696a

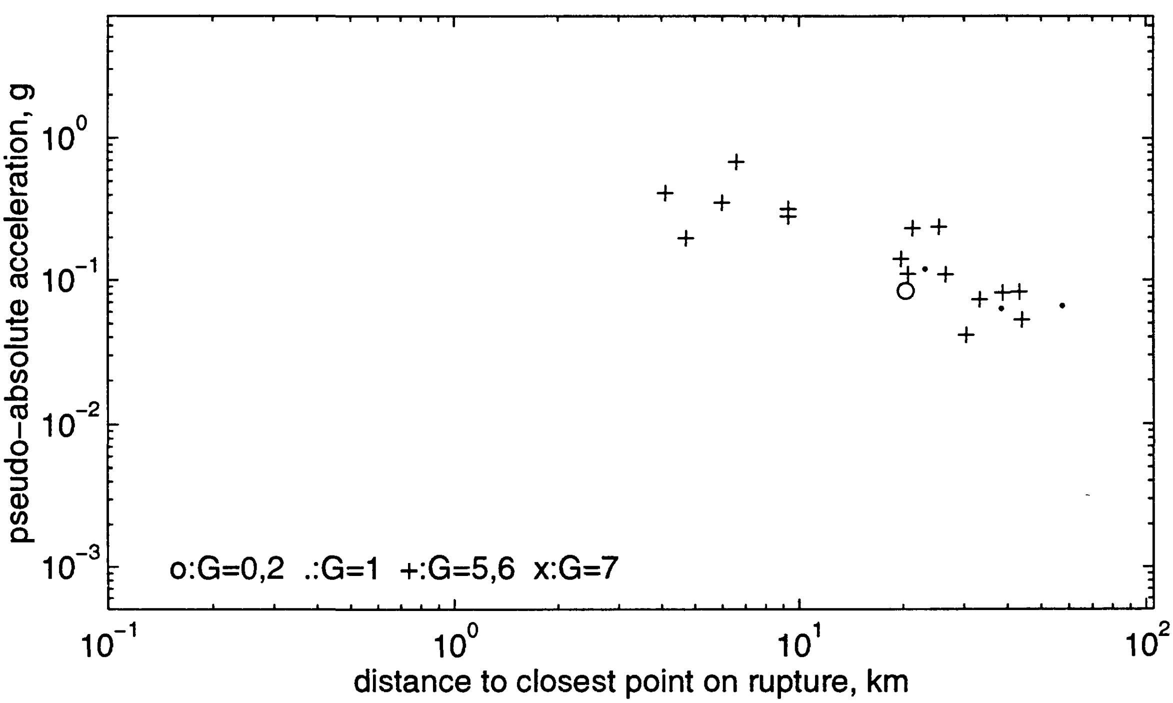

10 w

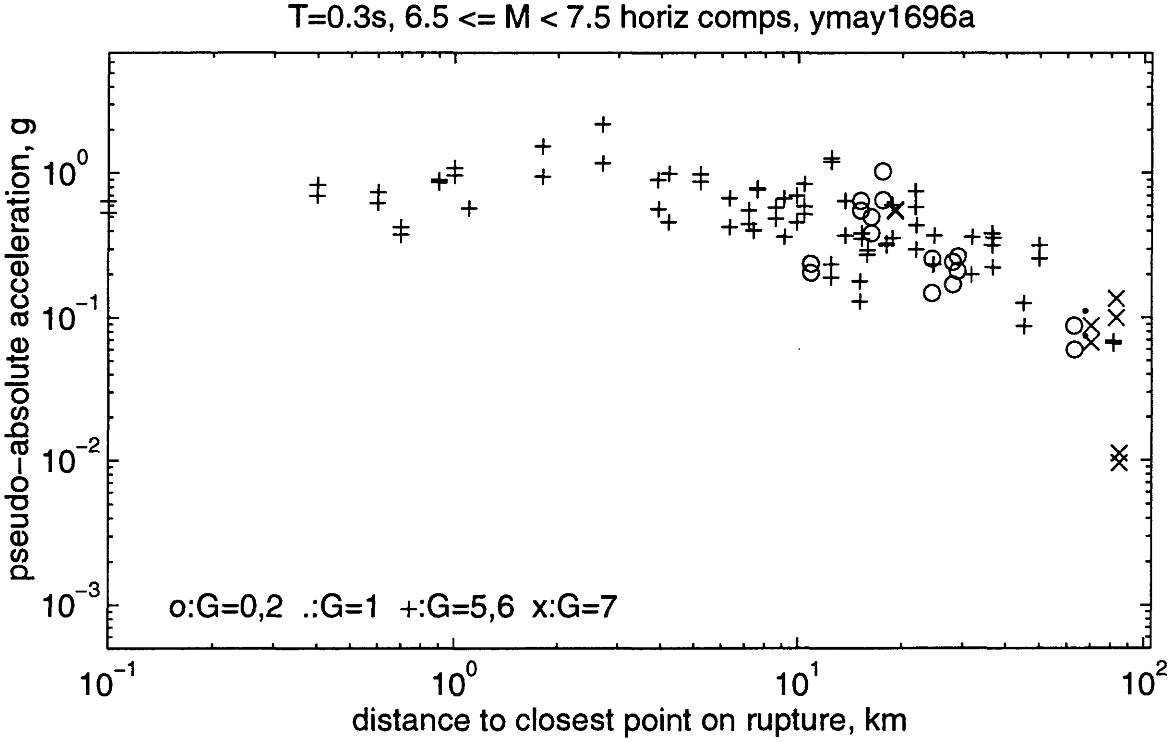
T=0.3s, 6.5 <= M < 7.5 horiz comps, ymay1696a
pseudo-absolute acceleration, g
o:G=0,2 .:G=1 +:G=5,6 x:G=7
distance to closest point on rupture, km

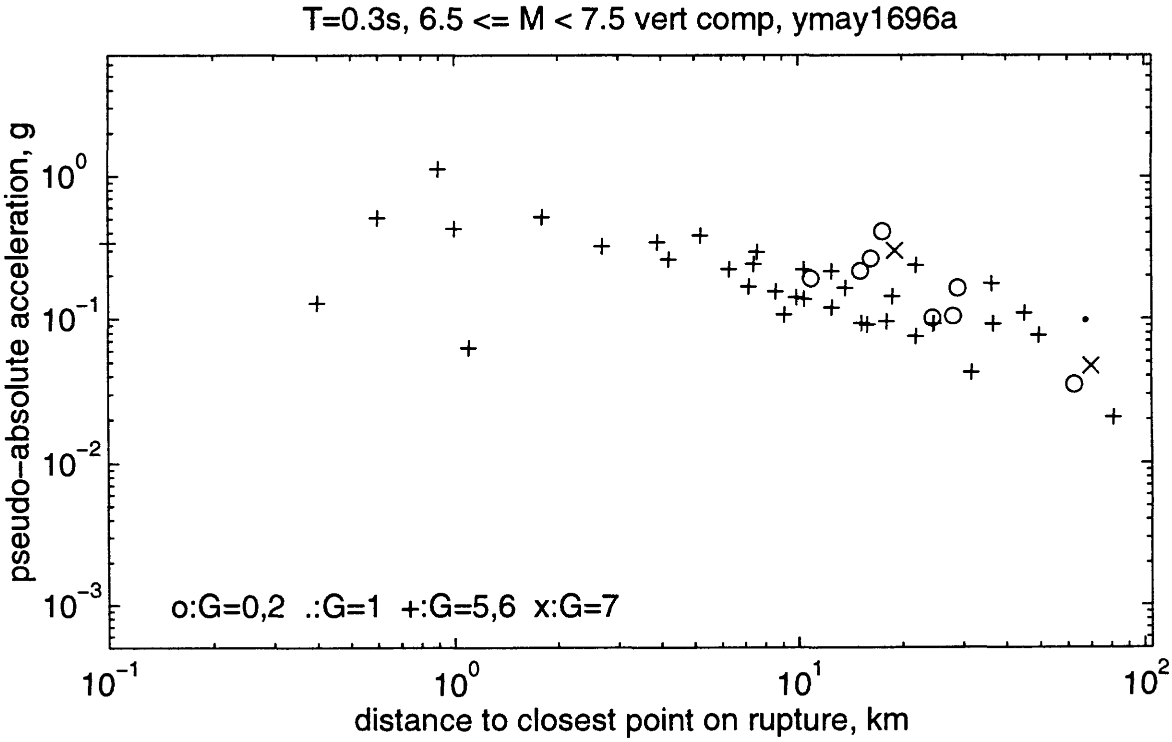
T=0.3s, 6.5 <= M < 7.5 vert comp, ymay1696a
pseudo-absolute acceleration, g
o:G=0,2 .:G=1 +:G=5,6 x:G=7
distance to closest point on rupture, km

10x

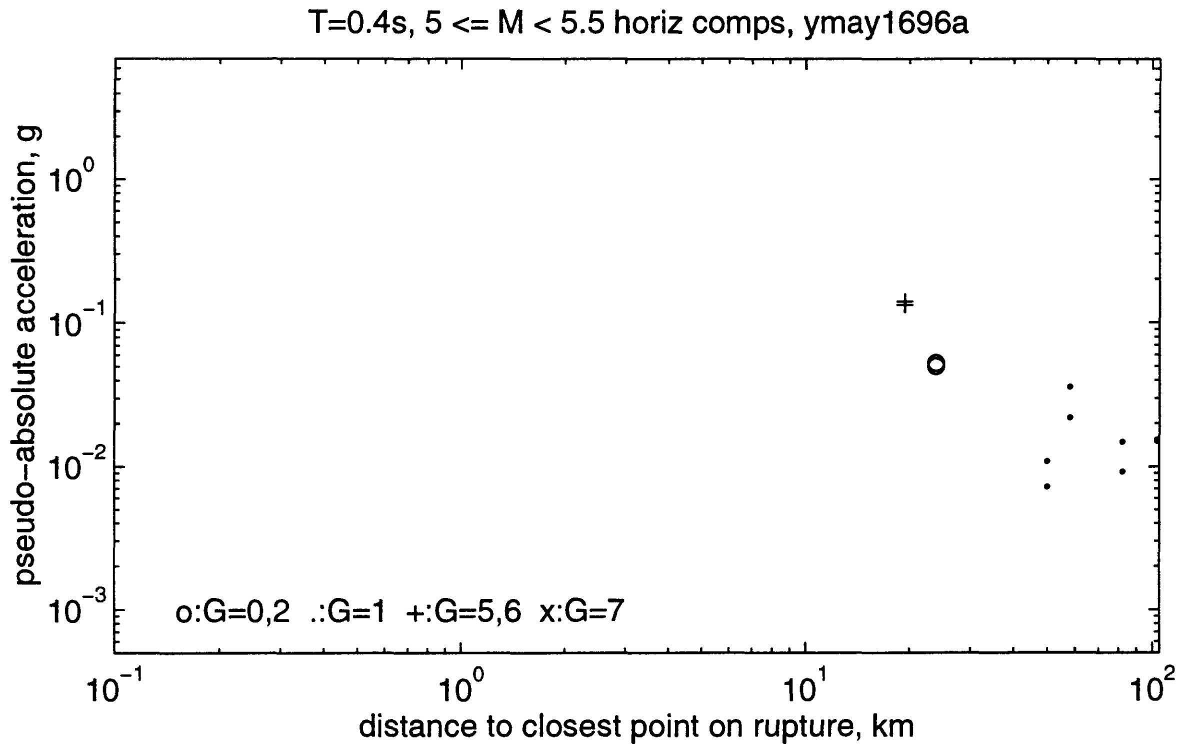
T=0.4s, 5 <= M < 5.5 horiz comps, ymay1696a
pseudo-absolute acceleration, g
distance to closest point on rupture, km
o:G=0,2 .:G=1 +:G=5,6 x:G=7

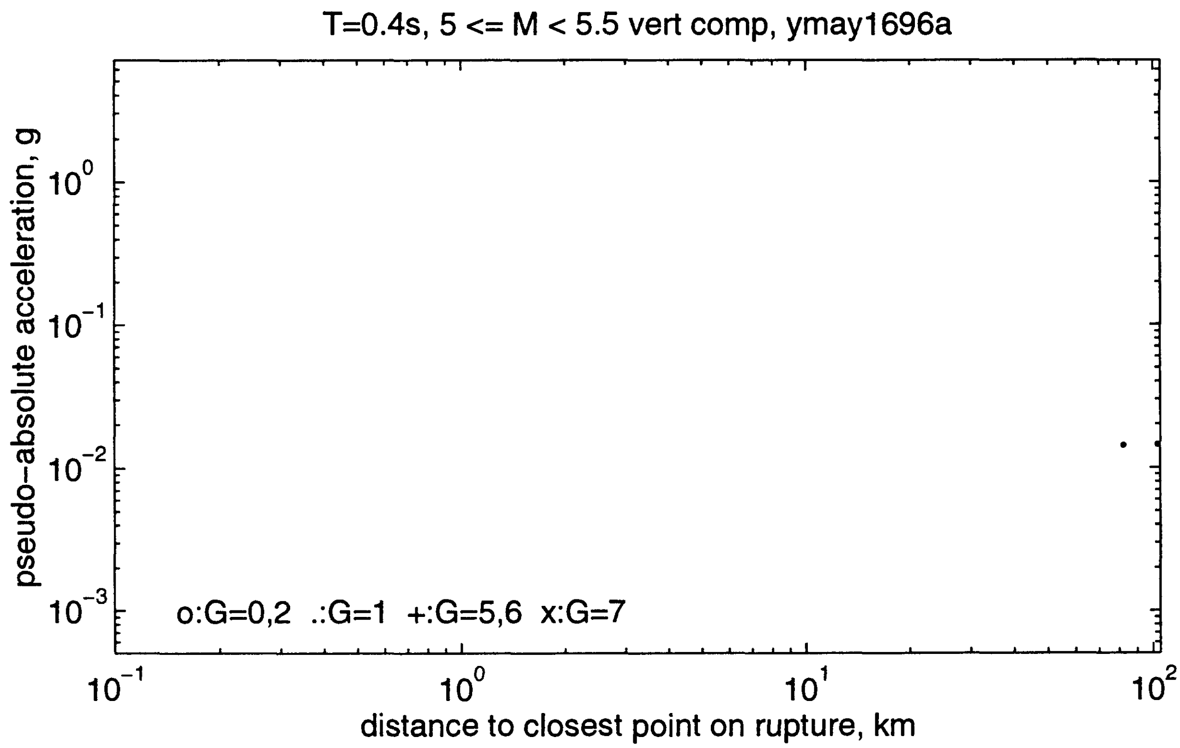
T=0.4s, 5 <= M < 5.5 vert comp, ymay1696a
pseudo-absolute acceleration, g
distance to closest point on rupture, km
o:G=0,2 .:G=1 +:G=5,6 x:G=7

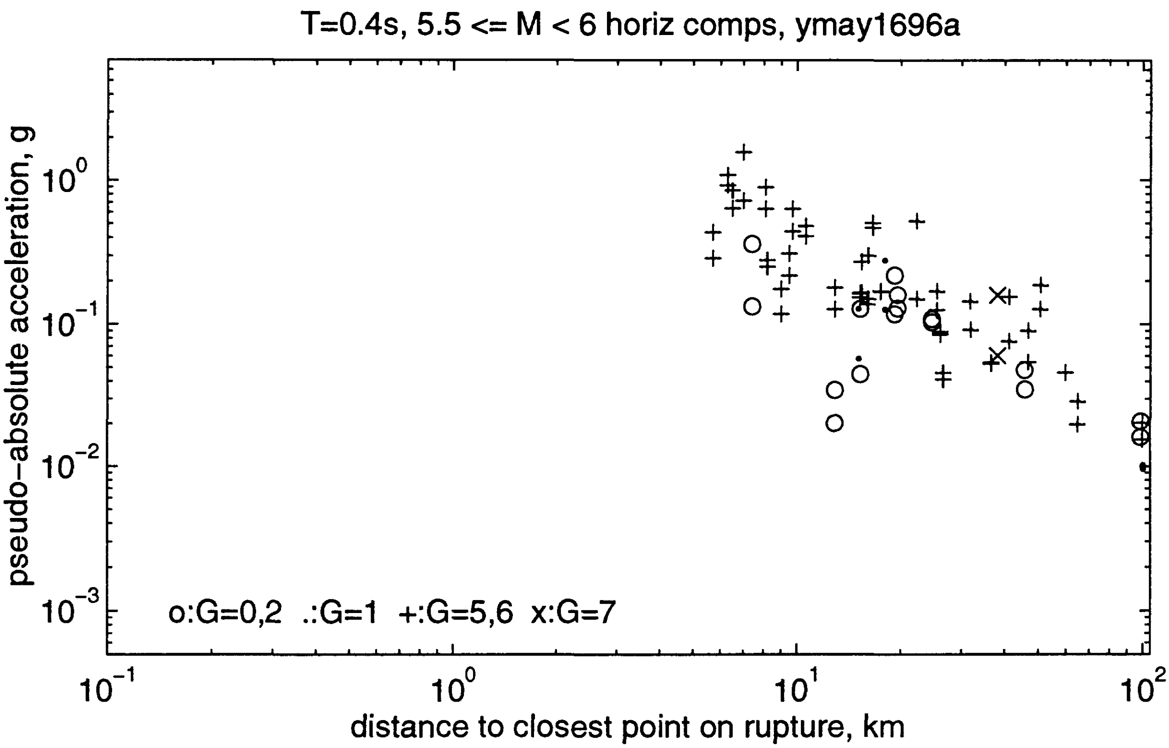

T=0.4s, 5.5 <= M < 6 horiz comps, ymay1696a
pseudo-absolute acceleration, g
distance to closest point on rupture, km
o:G=0,2 .:G=1 +:G=5,6 x:G=7

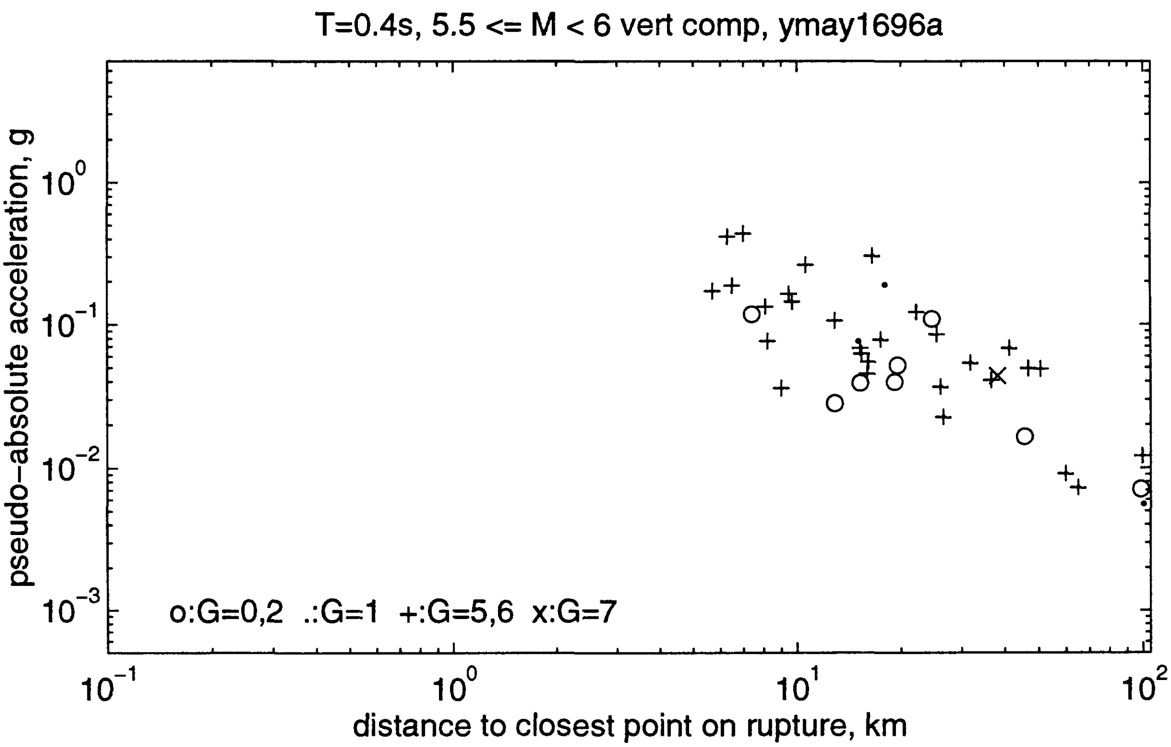

T=0.4s, 5.5 <= M < 6 vert comp, ymay1696a
pseudo-absolute acceleration, g
distance to closest point on rupture, km
o:G=0,2 .:G=1 +:G=5,6 x:G=7

102

T=0.4s, 6 <= M < 6.5 horiz comps, ymay1696a

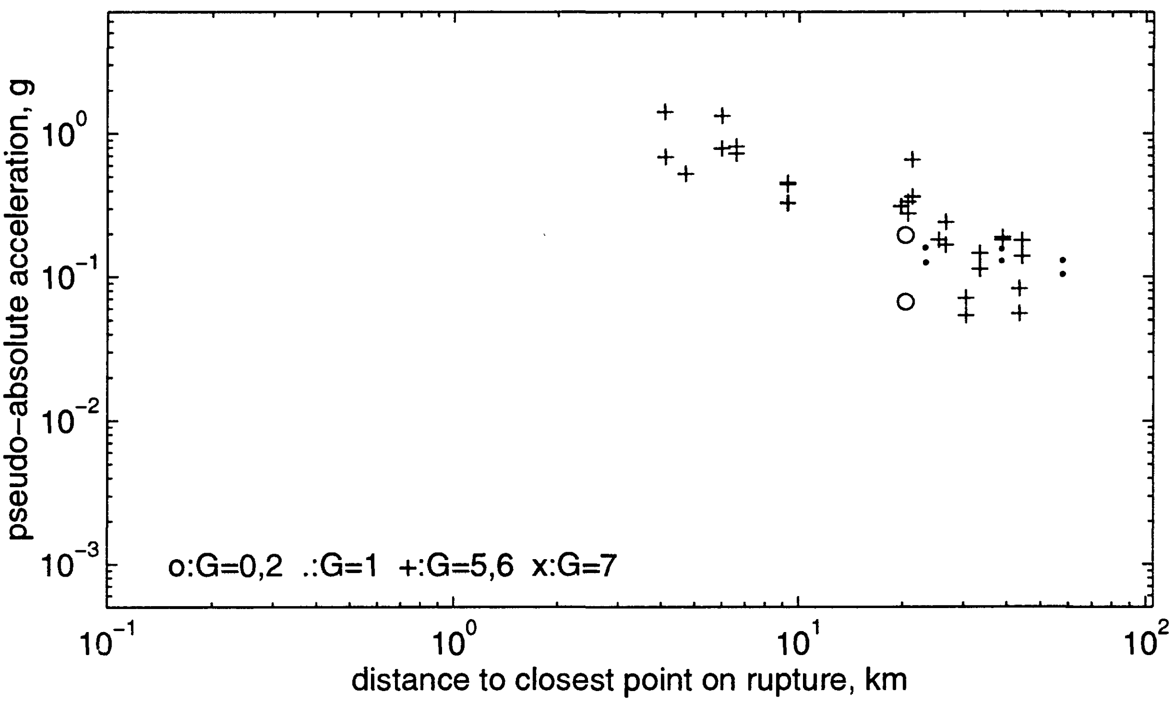

T=0.4s, 6 <= M < 6.5 vert comp, ymay1696a

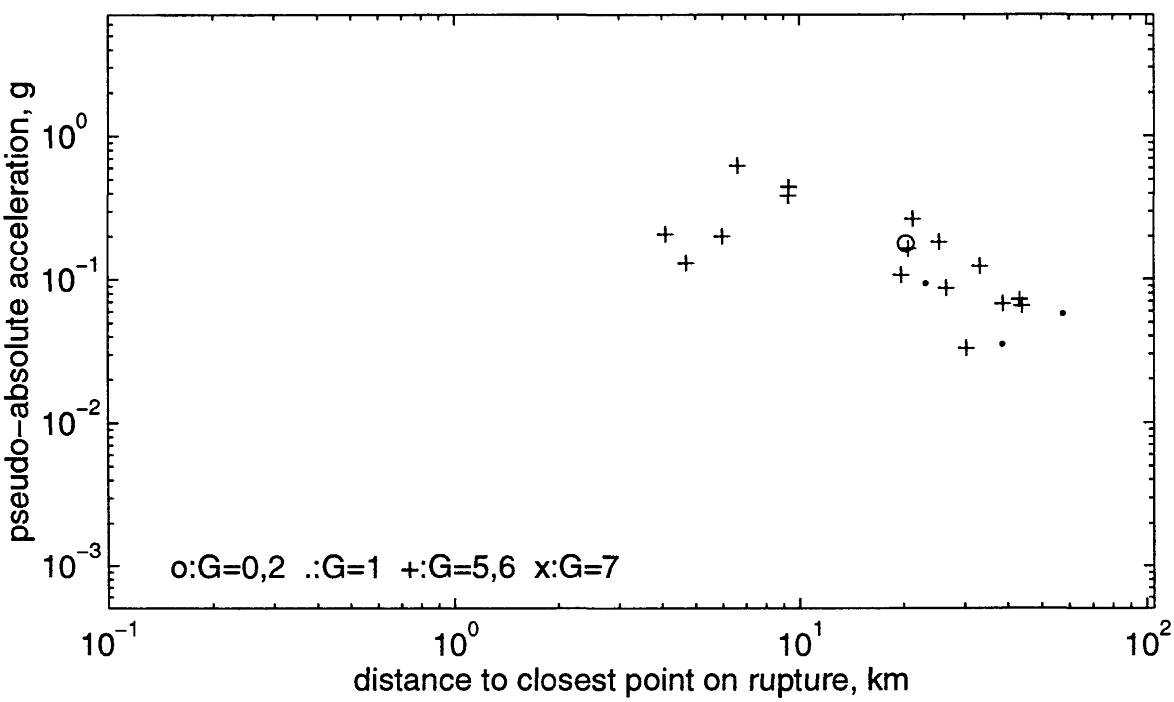

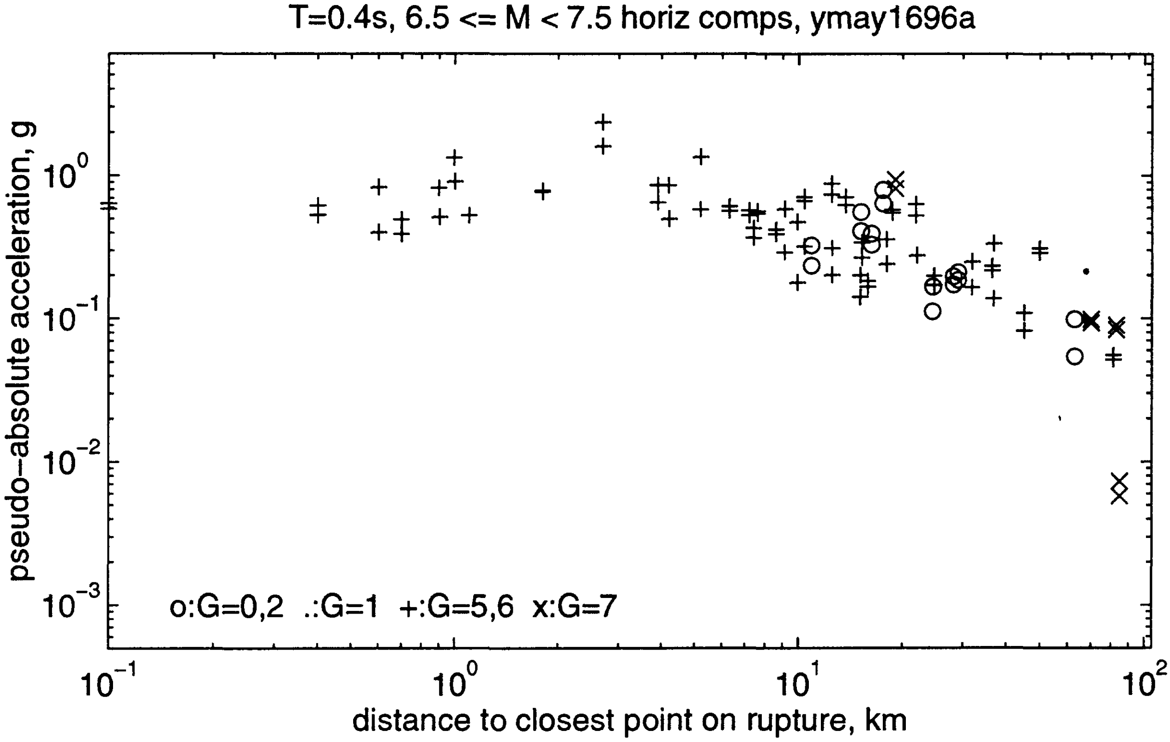
T=0.4s, 6.5 <= M < 7.5 horiz comps, ymay1696a
pseudo-absolute acceleration, g
10^0
10^{-1}
10^{-2}
10^{-3}
o:G=0,2 .:G=1 +:G=5,6 x:G=7
10^{-1}
10^0
10^1
10^2
distance to closest point on rupture, km

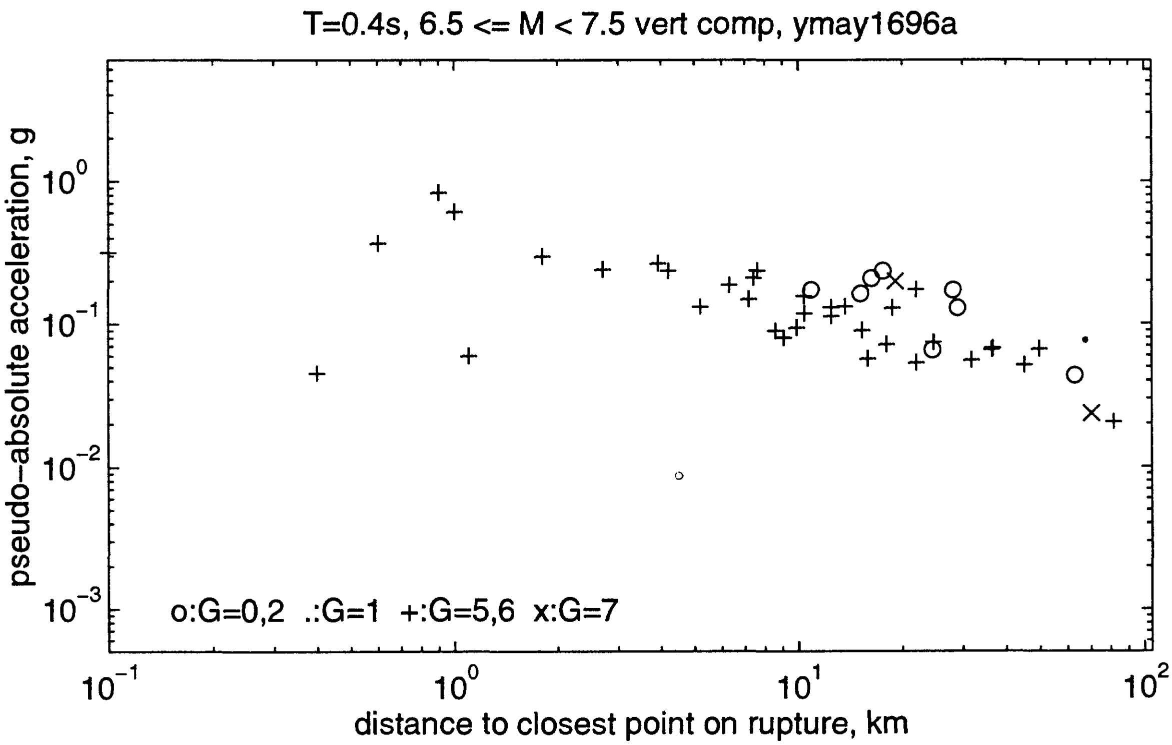
T=0.4s, 6.5 <= M < 7.5 vert comp, ymay1696a
pseudo-absolute acceleration, g
10^0
10^{-1}
10^{-2}
10^{-3}
o:G=0,2 .:G=1 +:G=5,6 x:G=7
10^{-1}
10^0
10^1
10^2
distance to closest point on rupture, km

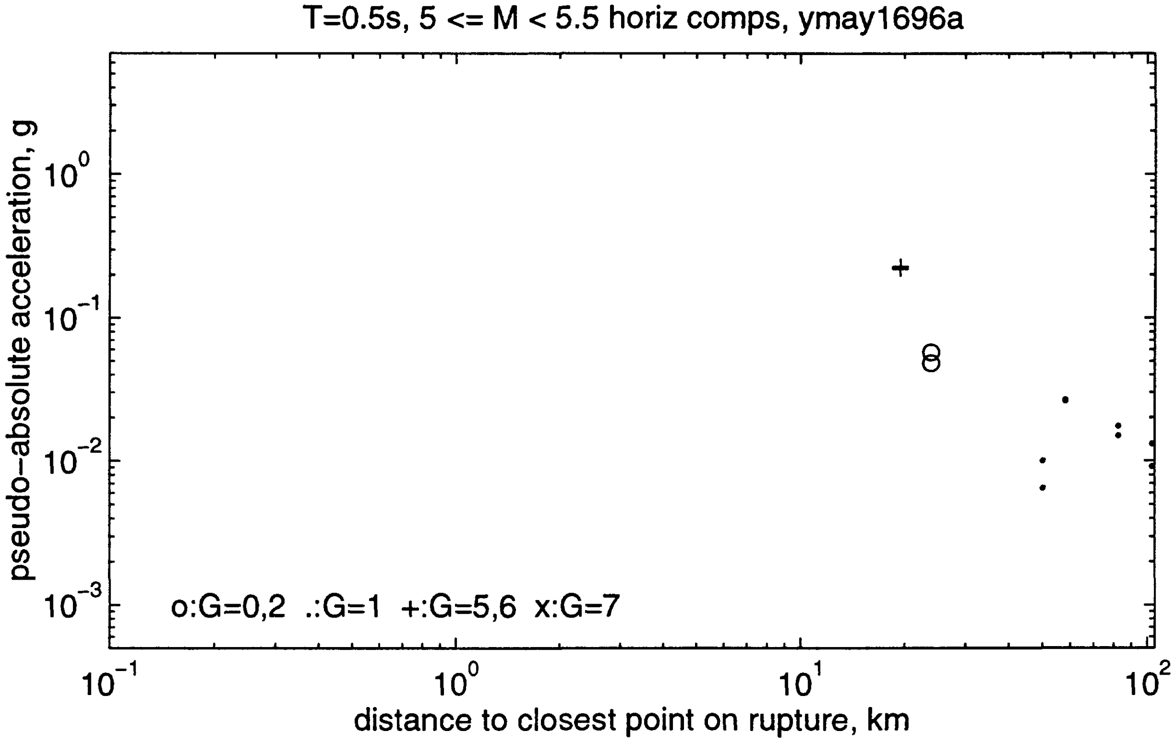

T=0.5s, 5 <= M < 5.5 horiz comps, ymay1696a
pseudo-absolute acceleration, g
o:G=0,2 .:G=1 +:G=5,6 x:G=7
distance to closest point on rupture, km

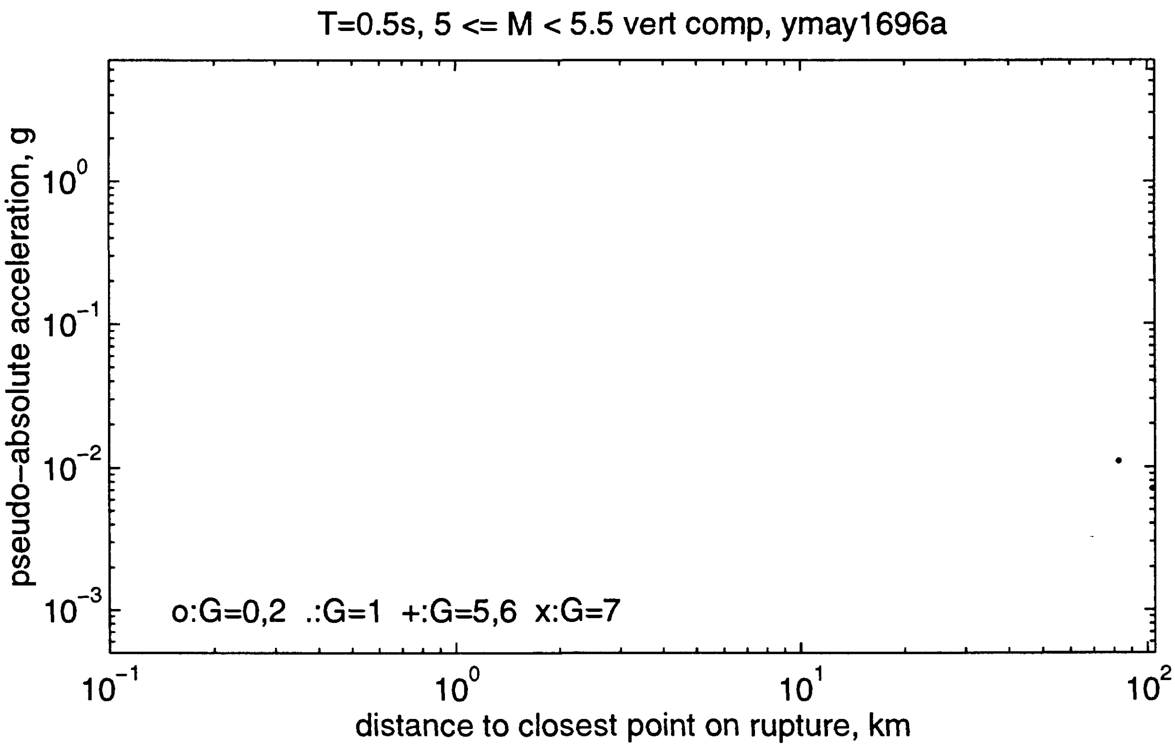

T=0.5s, 5 <= M < 5.5 vert comp, ymay1696a
pseudo-absolute acceleration, g
o:G=0,2 .:G=1 +:G=5,6 x:G=7
distance to closest point on rupture, km

10 oc

T=0.5s, 5.5 <= M < 6 horiz comps, ymay1696a

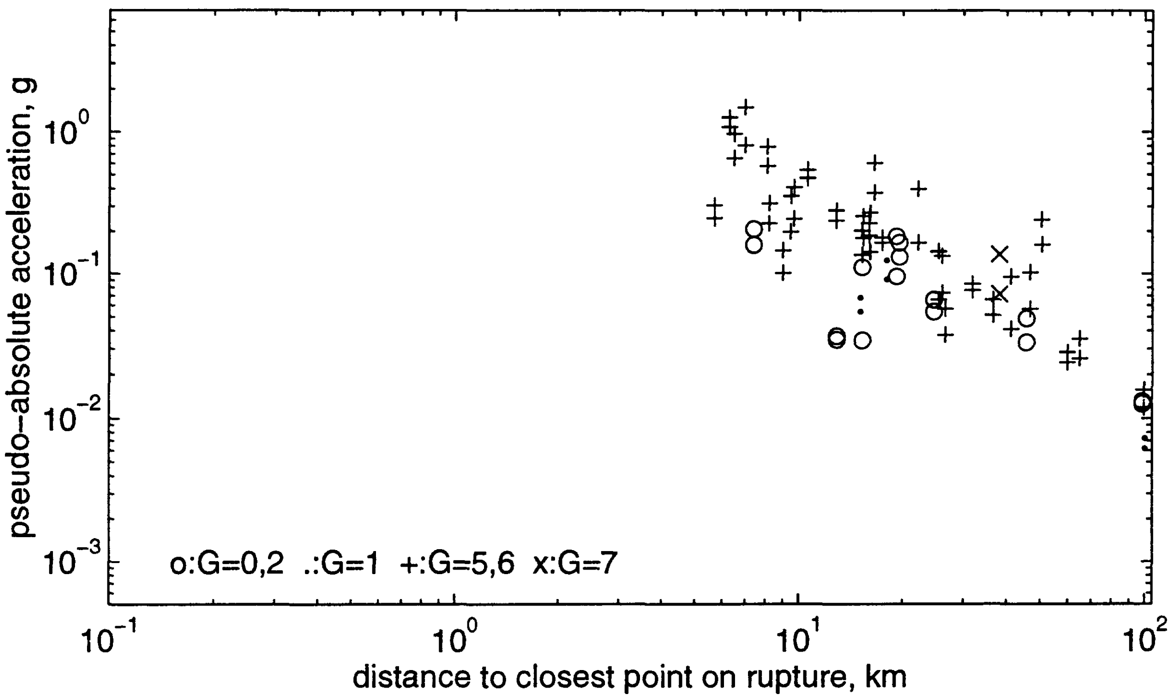

T=0.5s, 5.5 <= M < 6 vert comp, ymay1696a

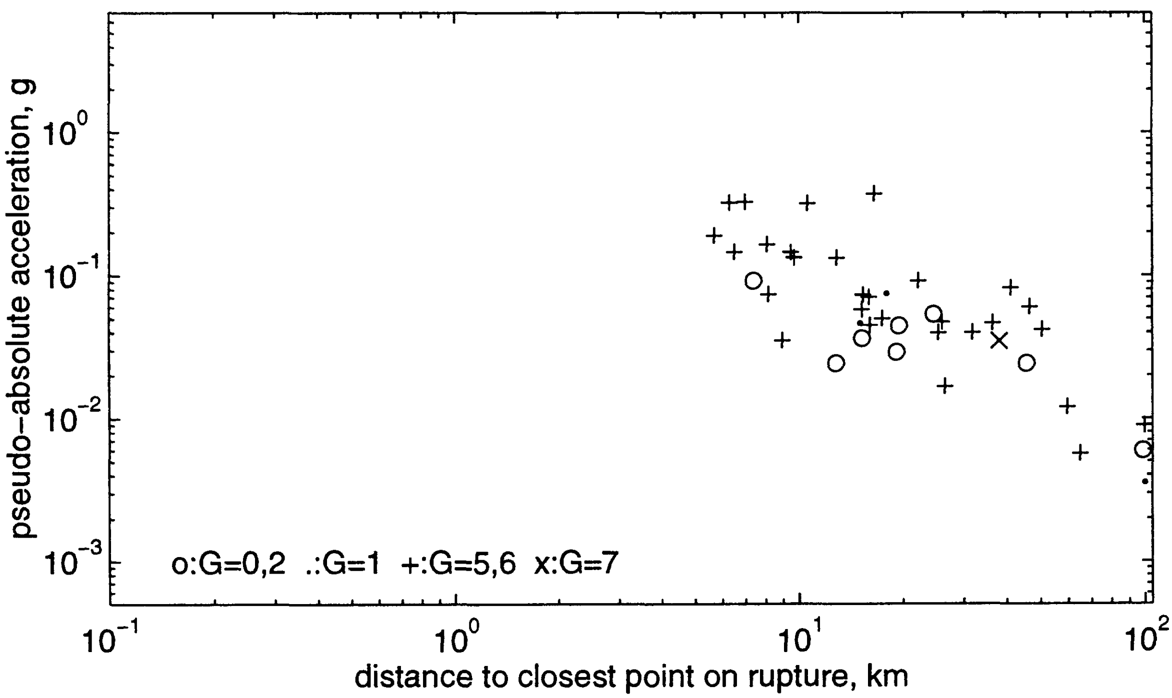

10 of

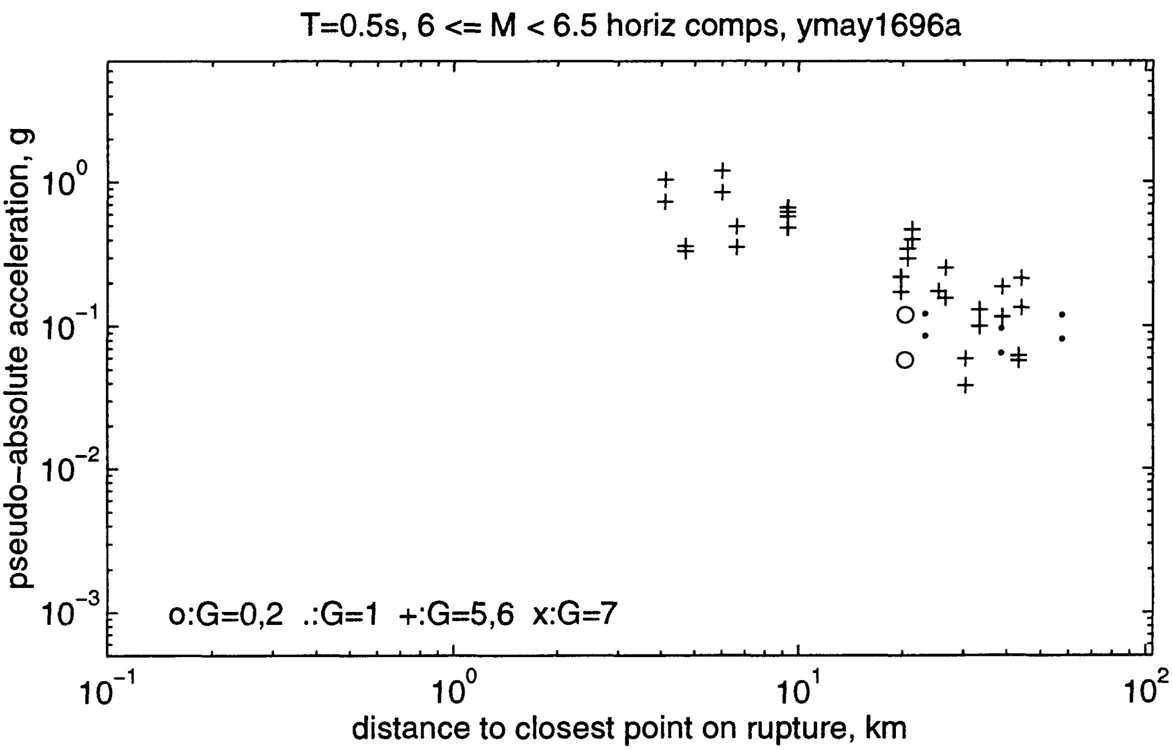
T=0.5s, 6 <= M < 6.5 horiz comps, ymay1696a
pseudo–absolute acceleration, g
10^0
10^{-1}
10^{-2}
10^{-3}
o:G=0,2 .:G=1 +:G=5,6 x:G=7
10^{-1}
10^0
10^1
10^2
distance to closest point on rupture, km

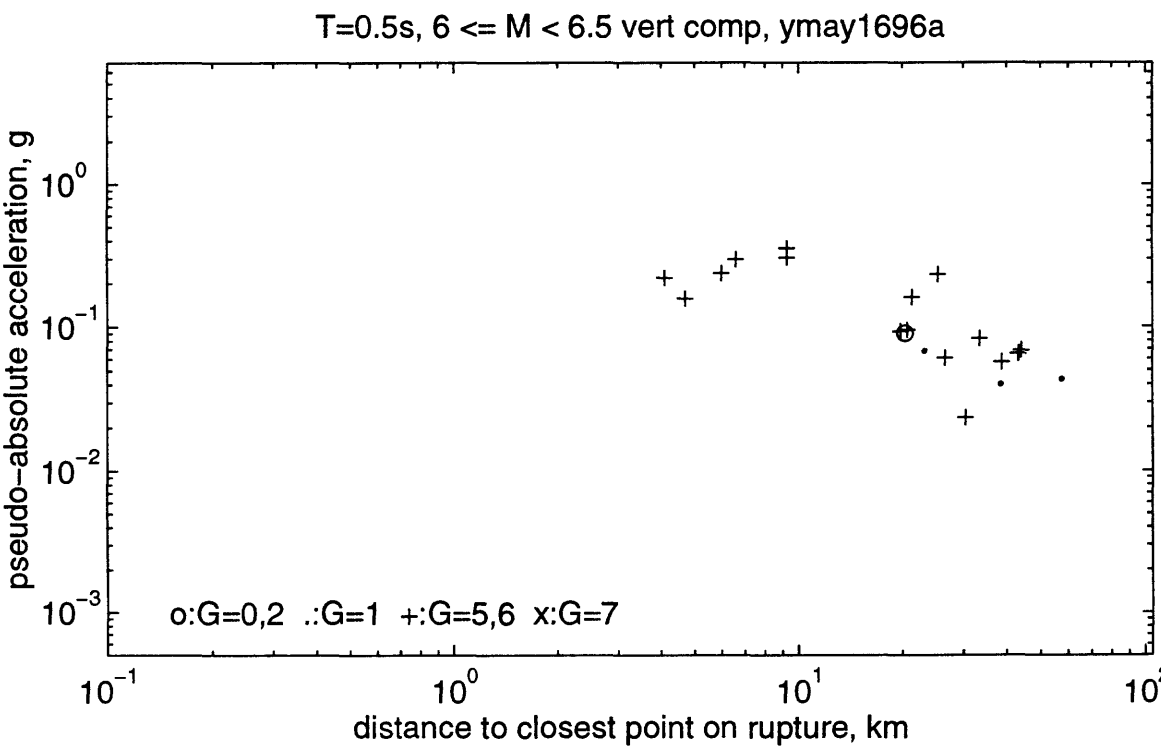
T=0.5s, 6 <= M < 6.5 vert comp, ymay1696a
pseudo–absolute acceleration, g
10^0
10^{-1}
10^{-2}
10^{-3}
o:G=0,2 .:G=1 +:G=5,6 x:G=7
10^{-1}
10^0
10^1
10^2
distance to closest point on rupture, km

10 ac

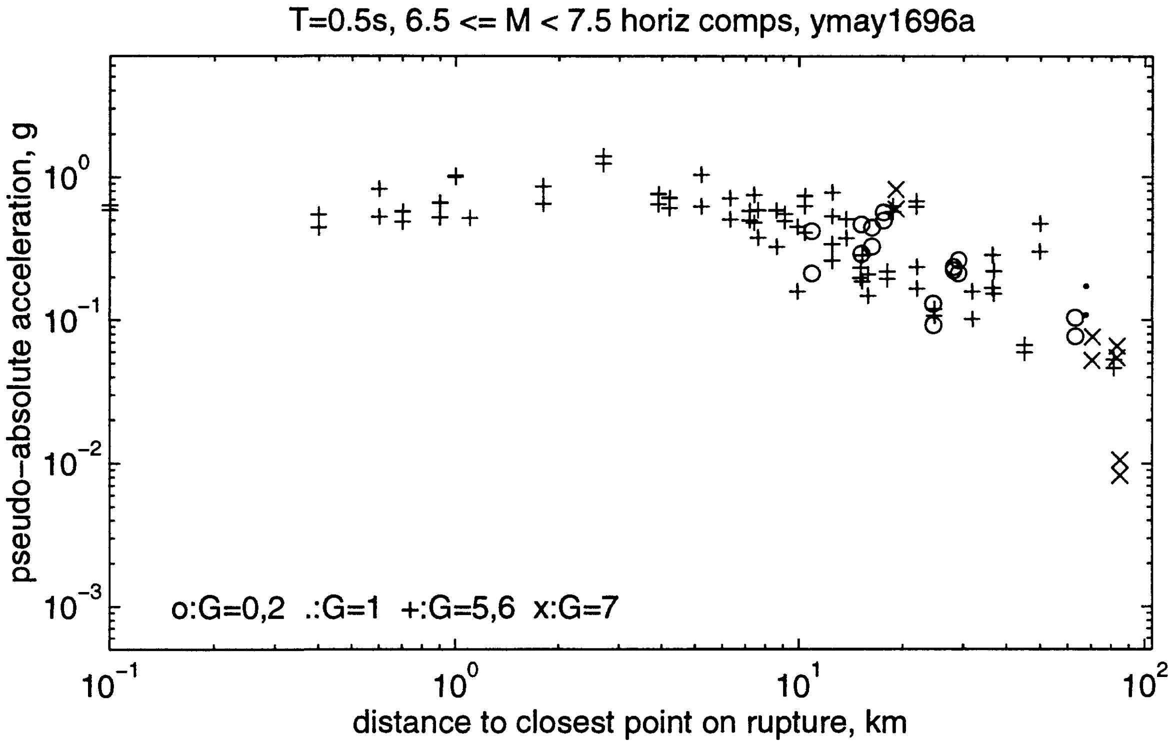
T=0.5s, 6.5 <= M < 7.5 horiz comps, ymay1696a
pseudo-absolute acceleration, g
10^0
10^{-1}
10^{-2}
10^{-3}
o:G=0,2 .:G=1 +:G=5,6 x:G=7
10^{-1}
10^0
10^1
10^2
distance to closest point on rupture, km

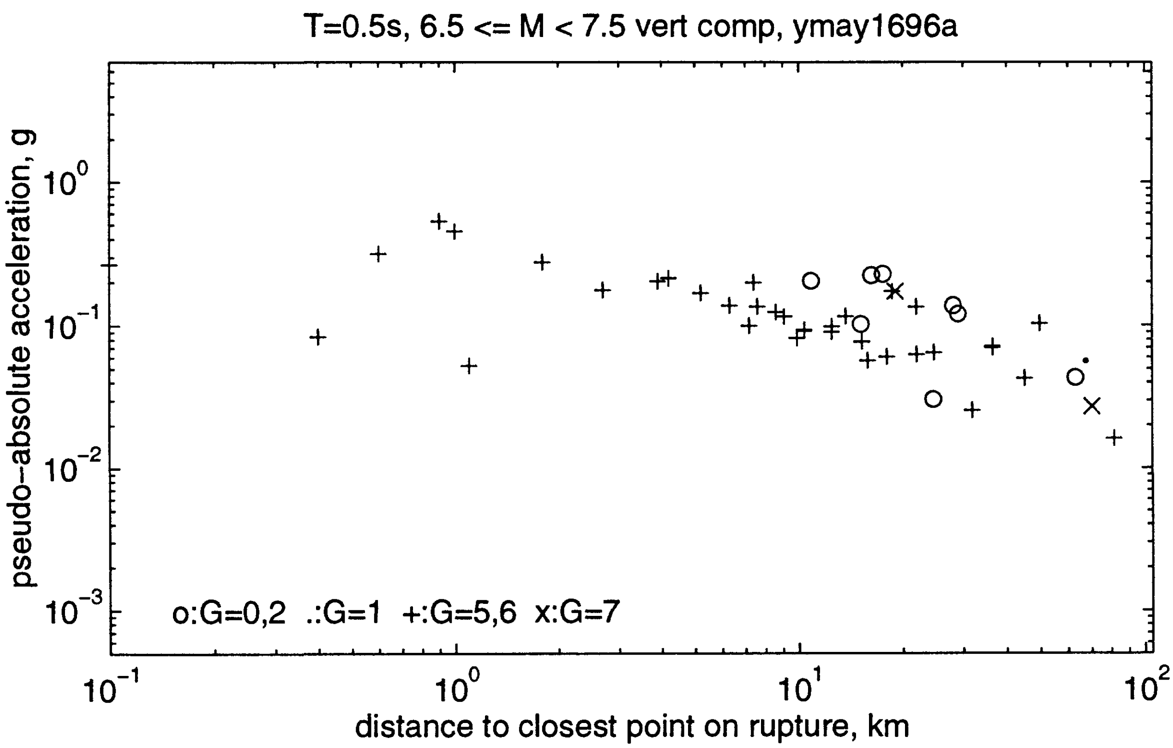
T=0.5s, 6.5 <= M < 7.5 vert comp, ymay1696a
pseudo-absolute acceleration, g
10^0
10^{-1}
10^{-2}
10^{-3}
o:G=0,2 .:G=1 +:G=5,6 x:G=7
10^{-1}
10^0
10^1
10^2
distance to closest point on rupture, km

10af

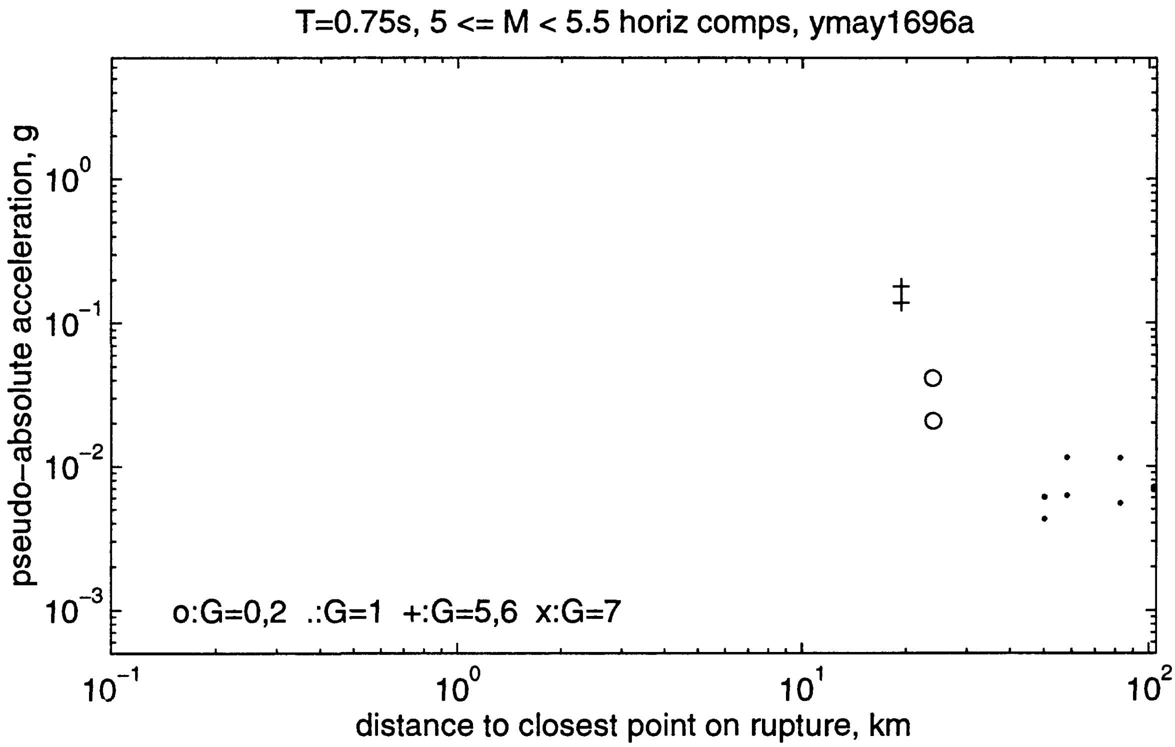
T=0.75s, 5 <= M < 5.5 horiz comps, ymay1696a
pseudo–absolute acceleration, g
distance to closest point on rupture, km
o:G=0,2 .:G=1 +:G=5,6 x:G=7

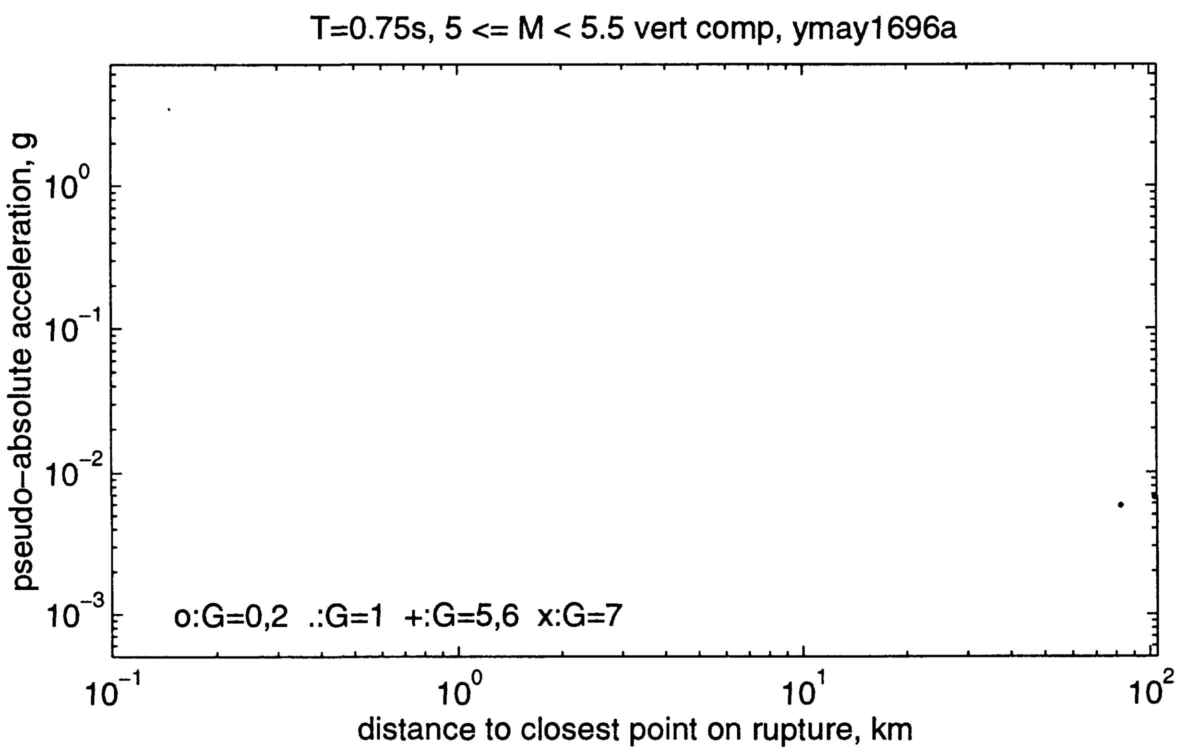
T=0.75s, 5 <= M < 5.5 vert comp, ymay1696a
pseudo–absolute acceleration, g
distance to closest point on rupture, km
o:G=0,2 .:G=1 +:G=5,6 x:G=7

10 ag

T=0.75s, 5.5 <= M < 6 horiz comps, ymay1696a

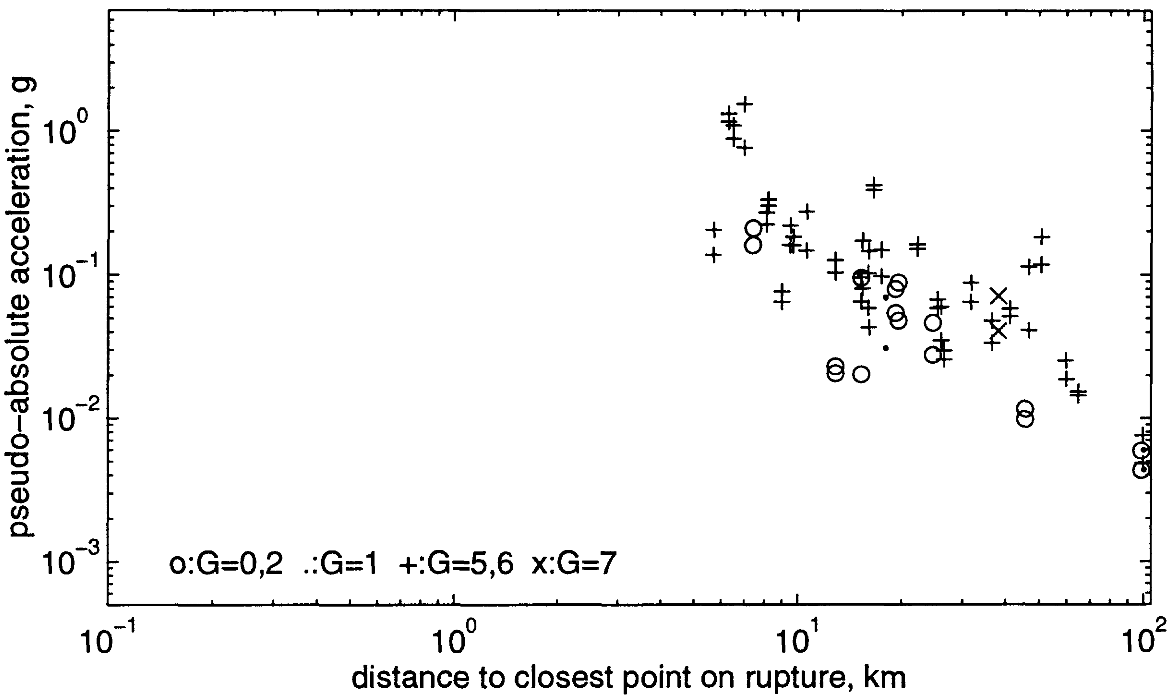

T=0.75s, 5.5 <= M < 6 vert comp, ymay1696a

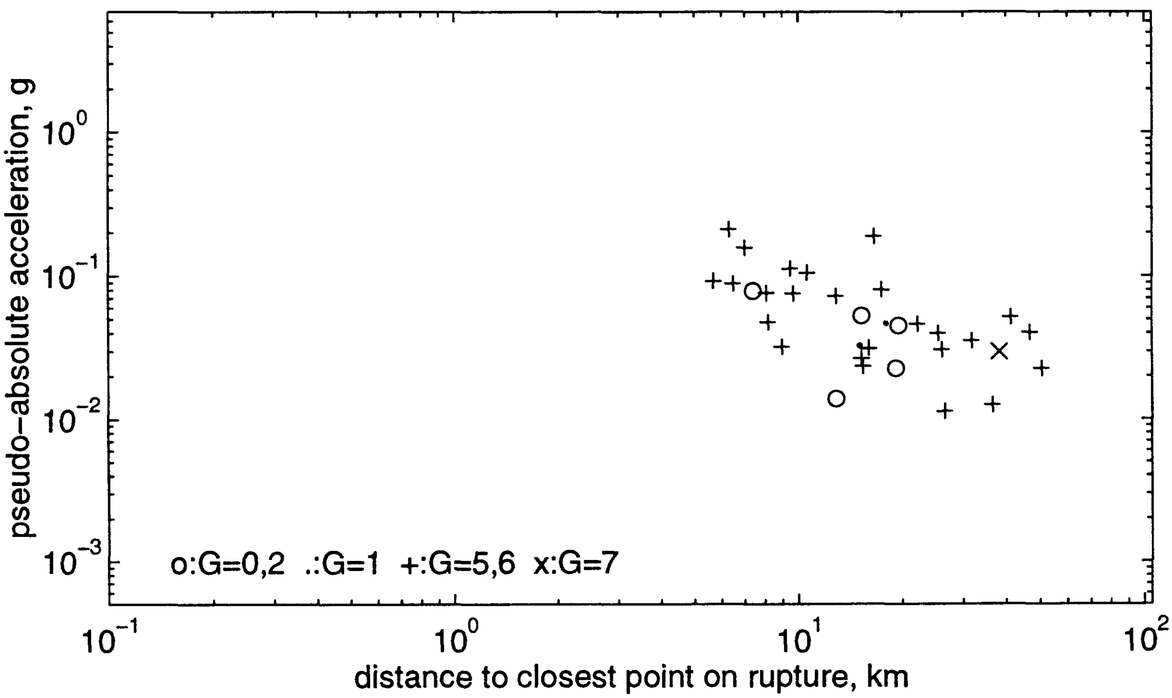

10 ah

T=0.75s, 6 <= M < 6.5 horiz comps, ymay1696a

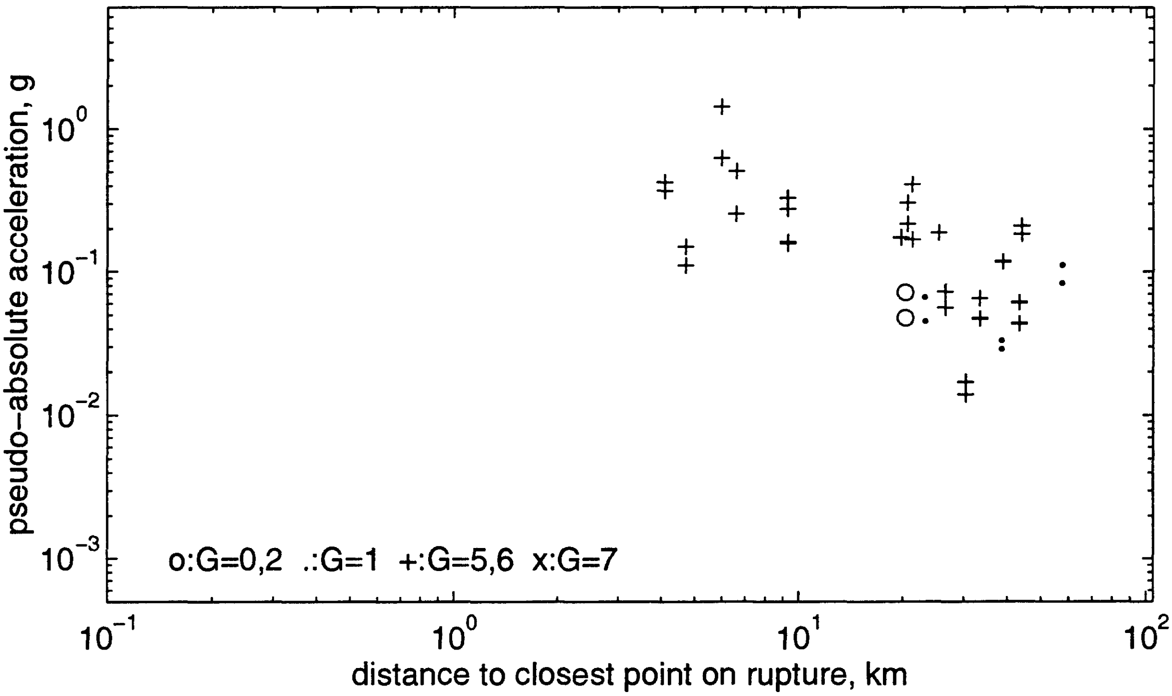

T=0.75s, 6 <= M < 6.5 vert comp, ymay1696a

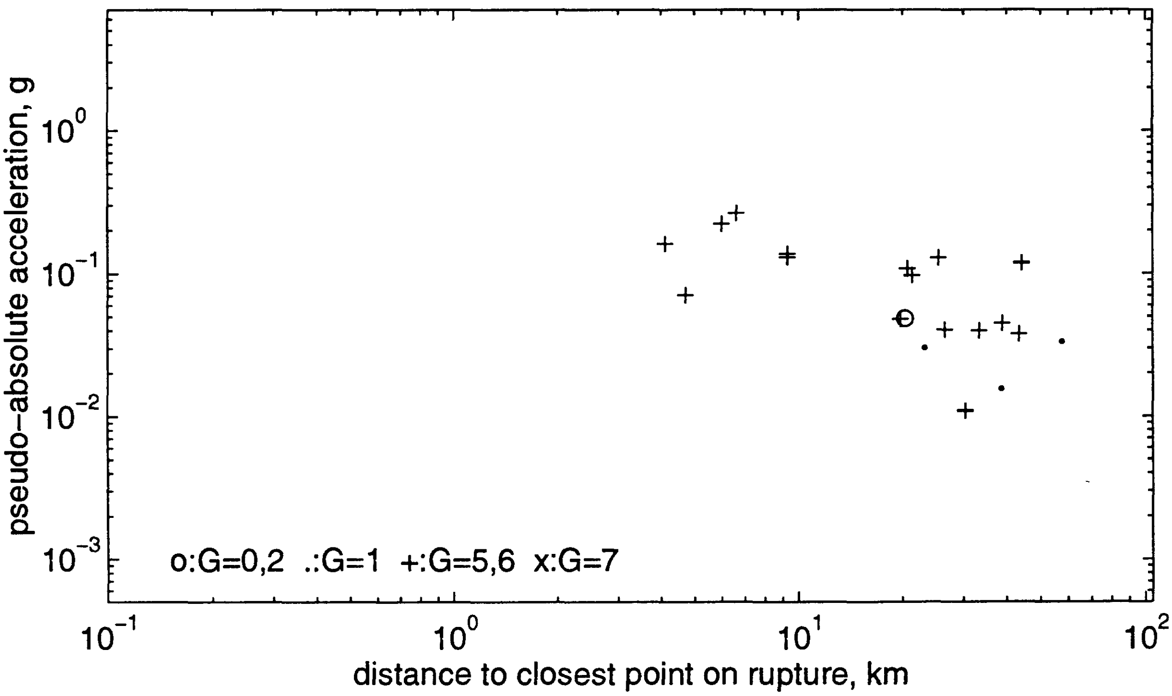

10ai

T=0.75s, 6.5 <= M < 7.5 horiz comps, ymay1696a

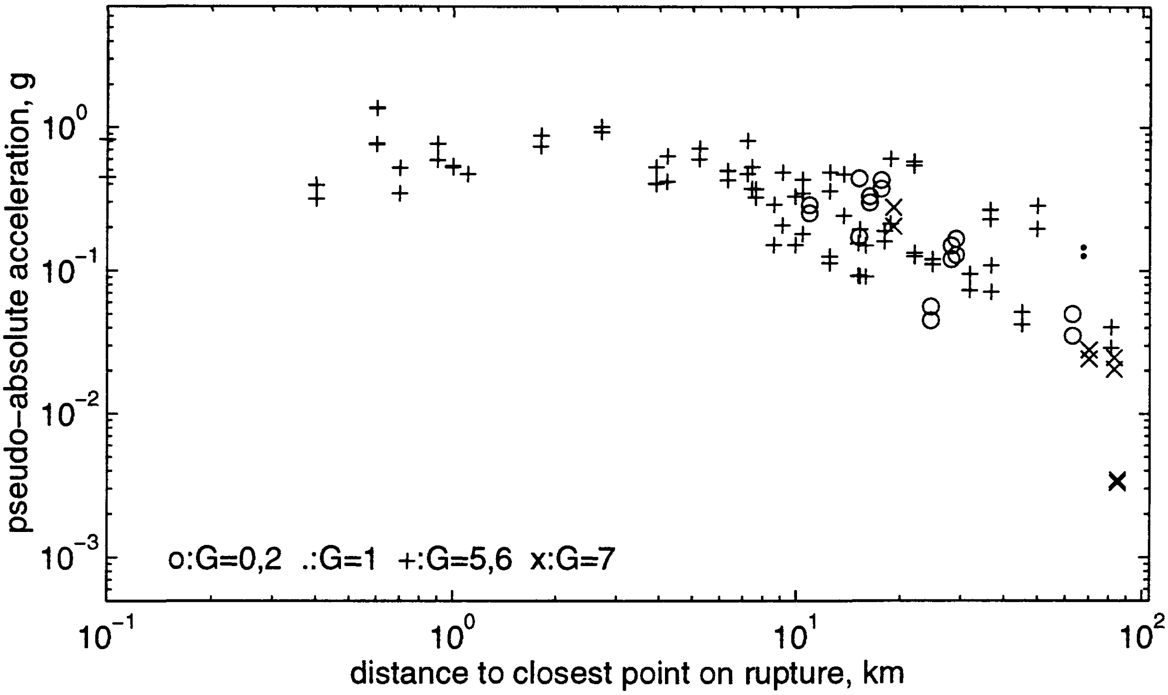

T=0.75s, 6.5 <= M < 7.5 vert comp, ymay1696a

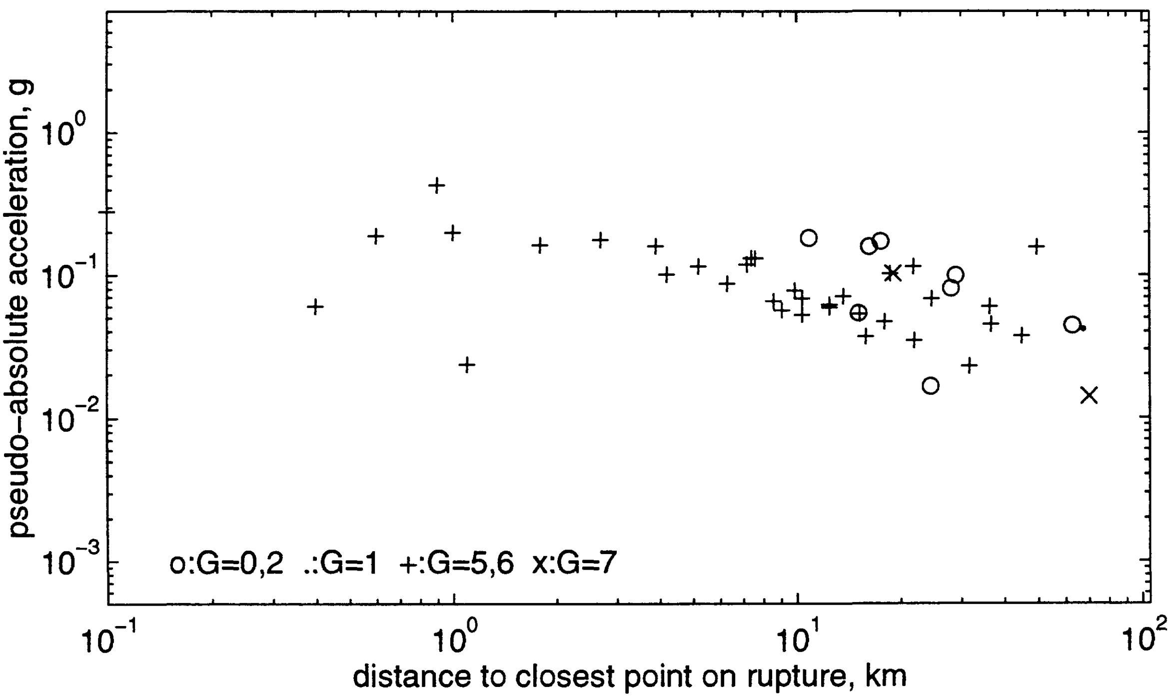

10 aj

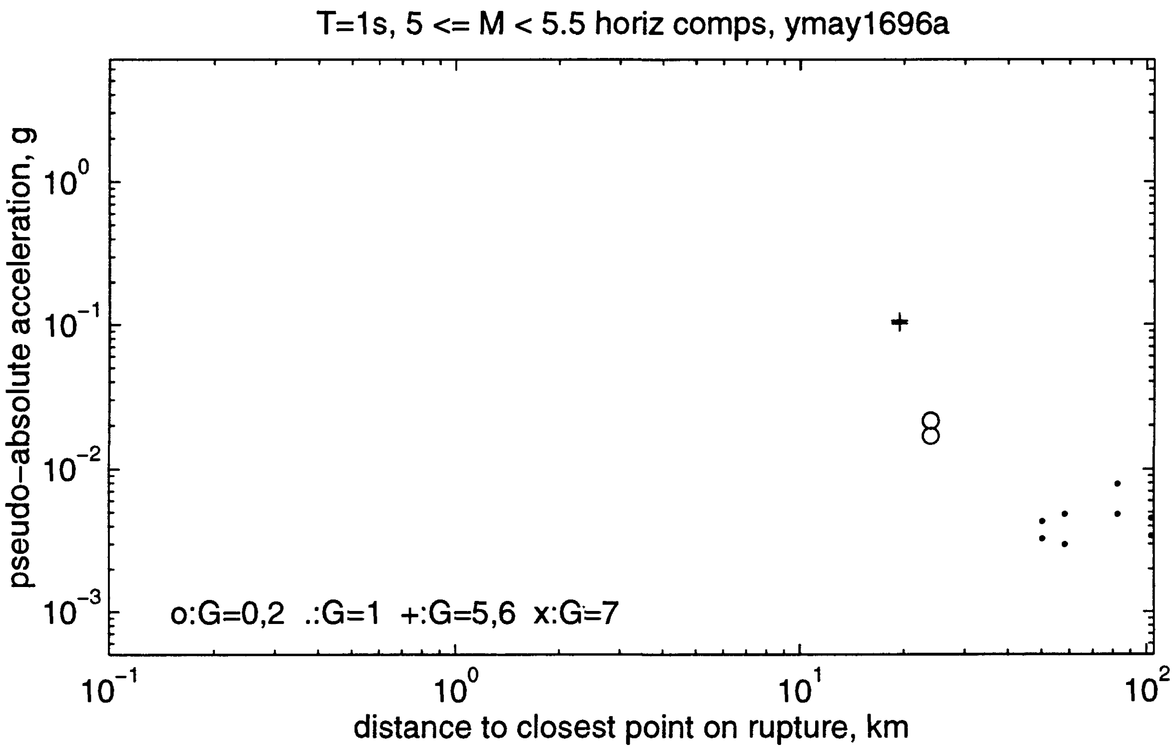
T=1s, 5 <= M < 5.5 horiz comps, ymay1696a
pseudo–absolute acceleration, g
10^0
10^-1
10^-2
10^-3
o:G=0,2 .:G=1 +:G=5,6 x:G=7
10^-1
10^0
10^1
10^2
distance to closest point on rupture, km

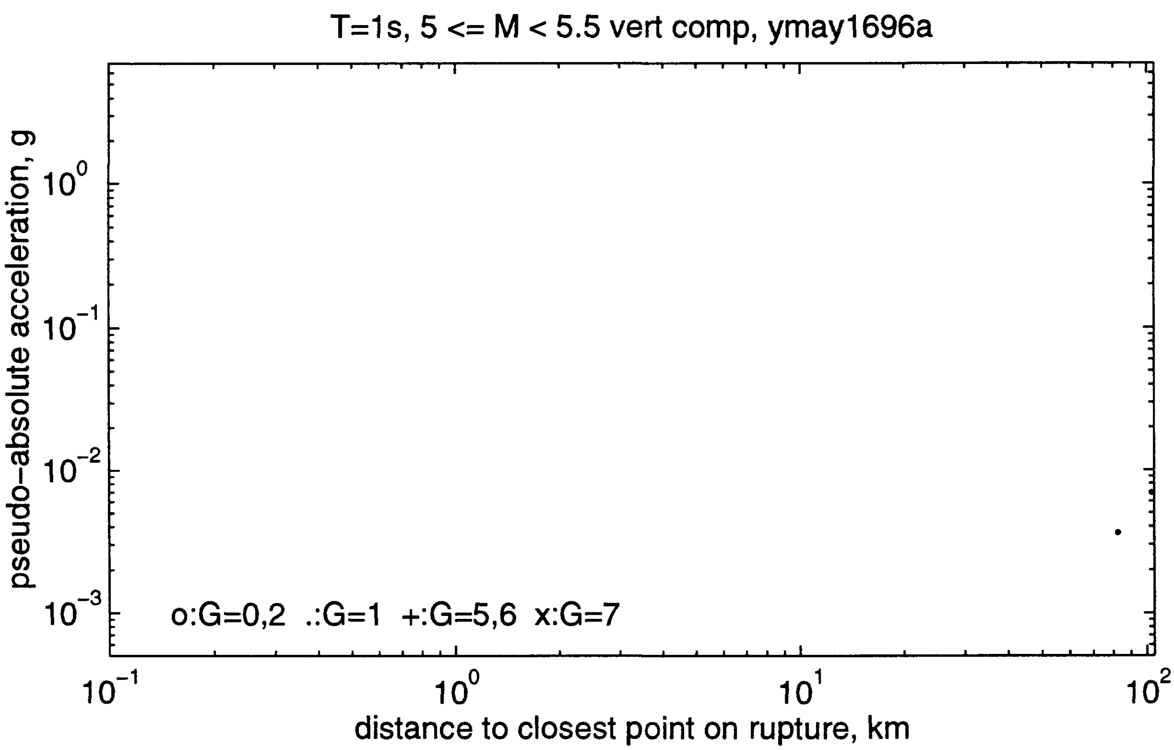
T=1s, 5 <= M < 5.5 vert comp, ymay1696a
pseudo–absolute acceleration, g
10^0
10^-1
10^-2
10^-3
o:G=0,2 .:G=1 +:G=5,6 x:G=7
10^-1
10^0
10^1
10^2
distance to closest point on rupture, km

10 ak

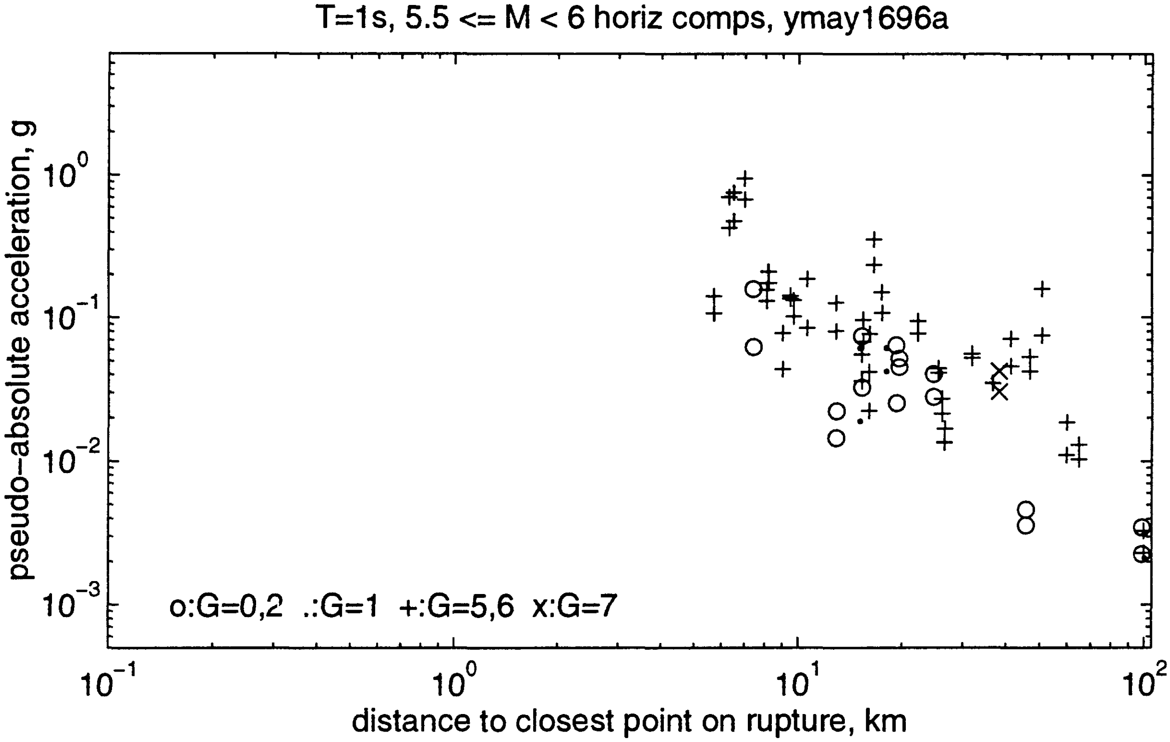
T=1s, 5.5 <= M < 6 horiz comps, ymay1696a
pseudo-absolute acceleration, g
distance to closest point on rupture, km
o:G=0,2 .:G=1 +:G=5,6 x:G=7

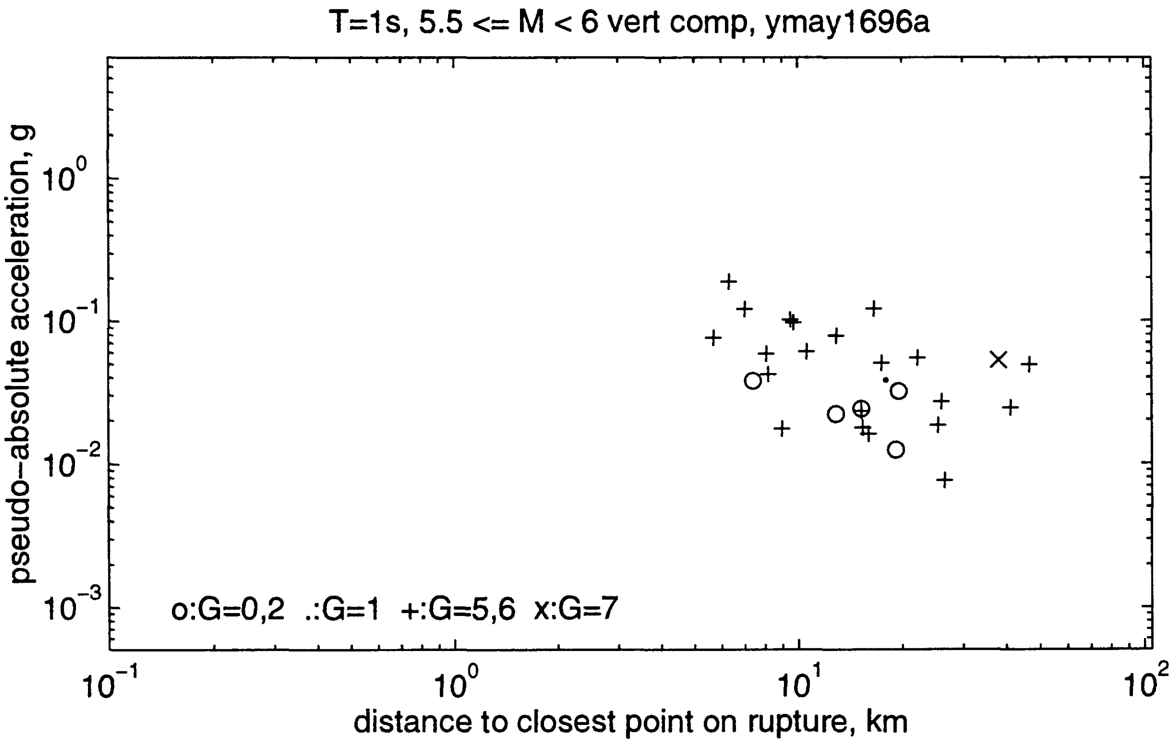
T=1s, 5.5 <= M < 6 vert comp, ymay1696a
pseudo-absolute acceleration, g
distance to closest point on rupture, km
o:G=0,2 .:G=1 +:G=5,6 x:G=7

10a1

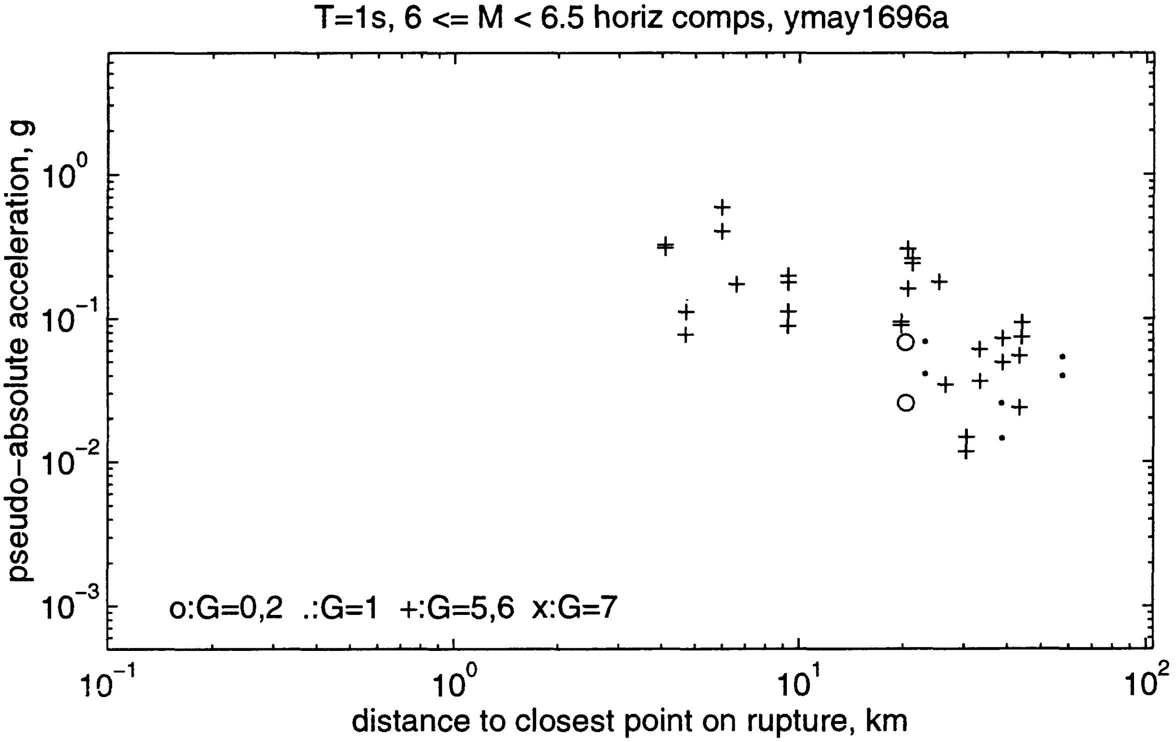
T=1s, 6 <= M < 6.5 horiz comps, ymay1696a
pseudo-absolute acceleration, g
distance to closest point on rupture, km
o:G=0,2 .:G=1 +:G=5,6 x:G=7

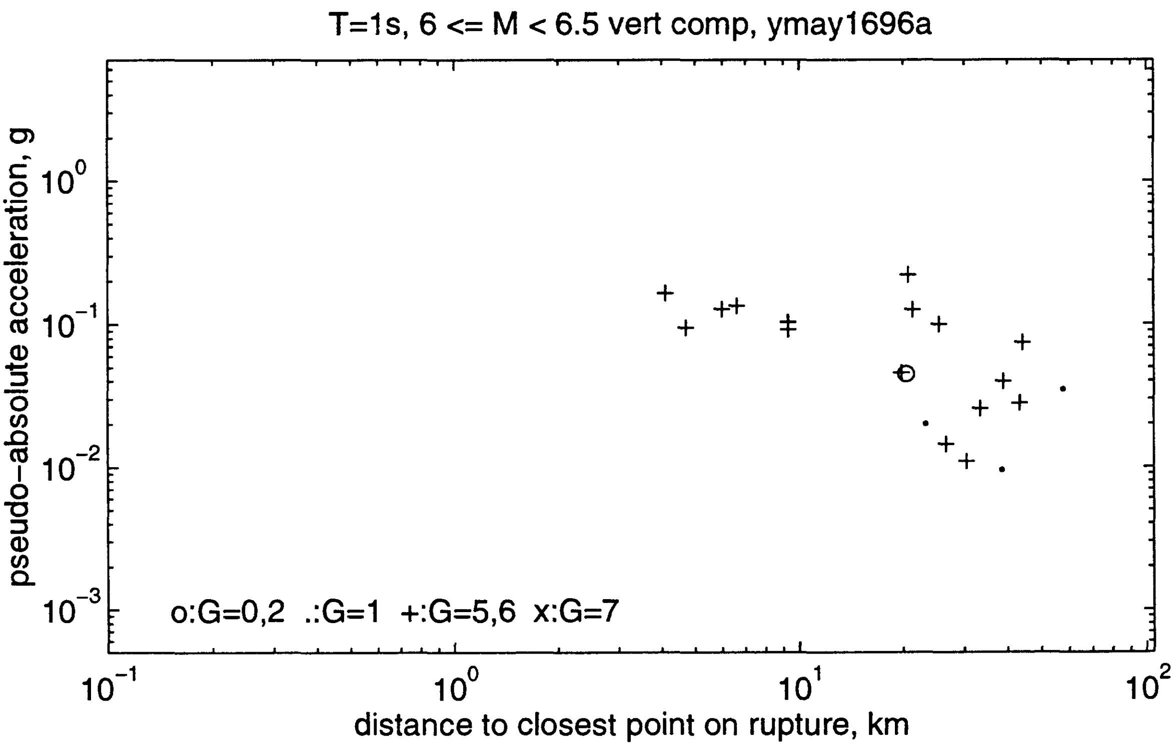
T=1s, 6 <= M < 6.5 vert comp, ymay1696a
pseudo-absolute acceleration, g
distance to closest point on rupture, km
o:G=0,2 .:G=1 +:G=5,6 x:G=7

10 om

T=1s, 6.5 <= M < 7.5 horiz comps, ymay1696a

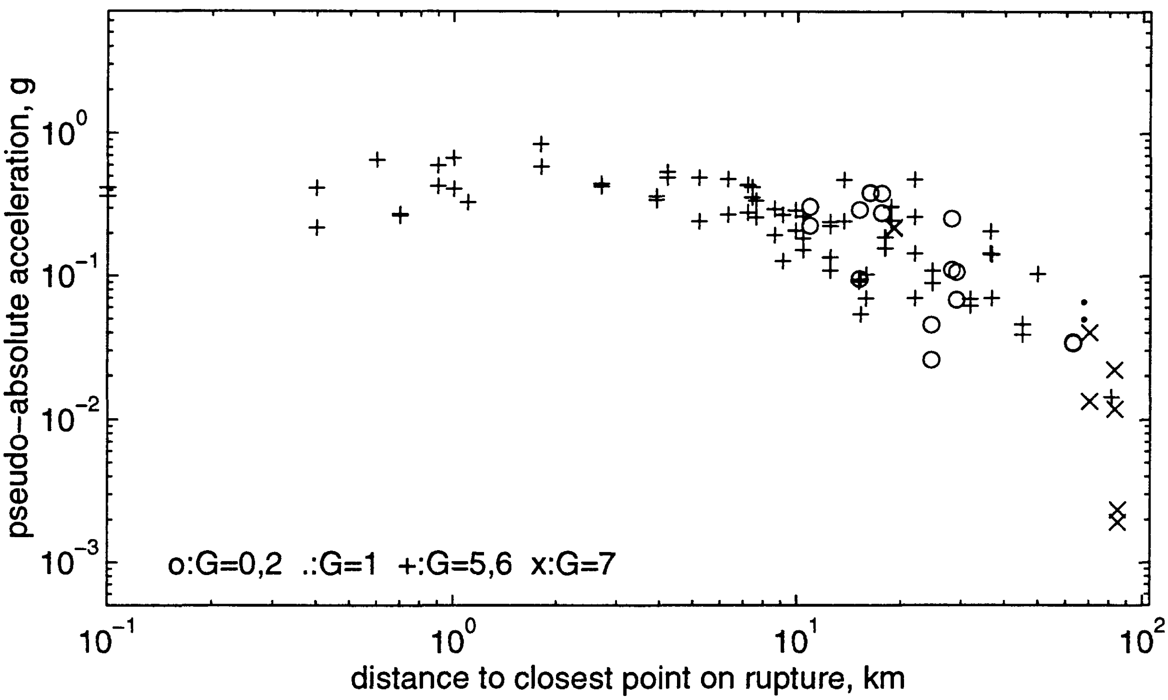

T=1s, 6.5 <= M < 7.5 vert comp, ymay1696a

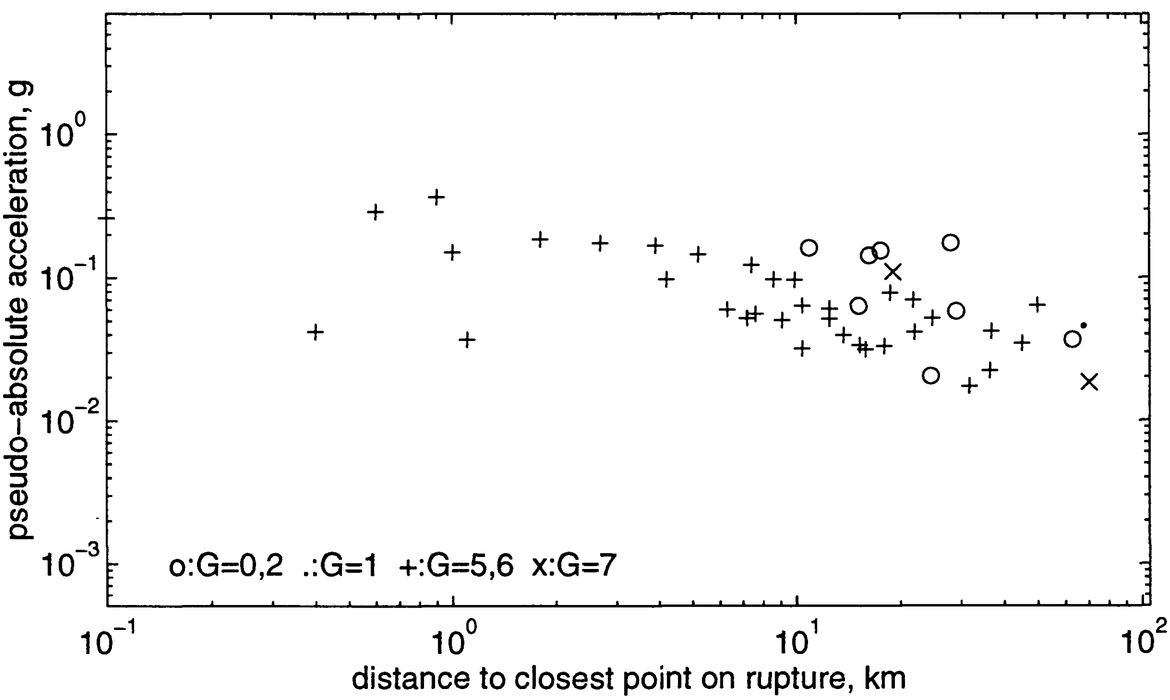

10 an

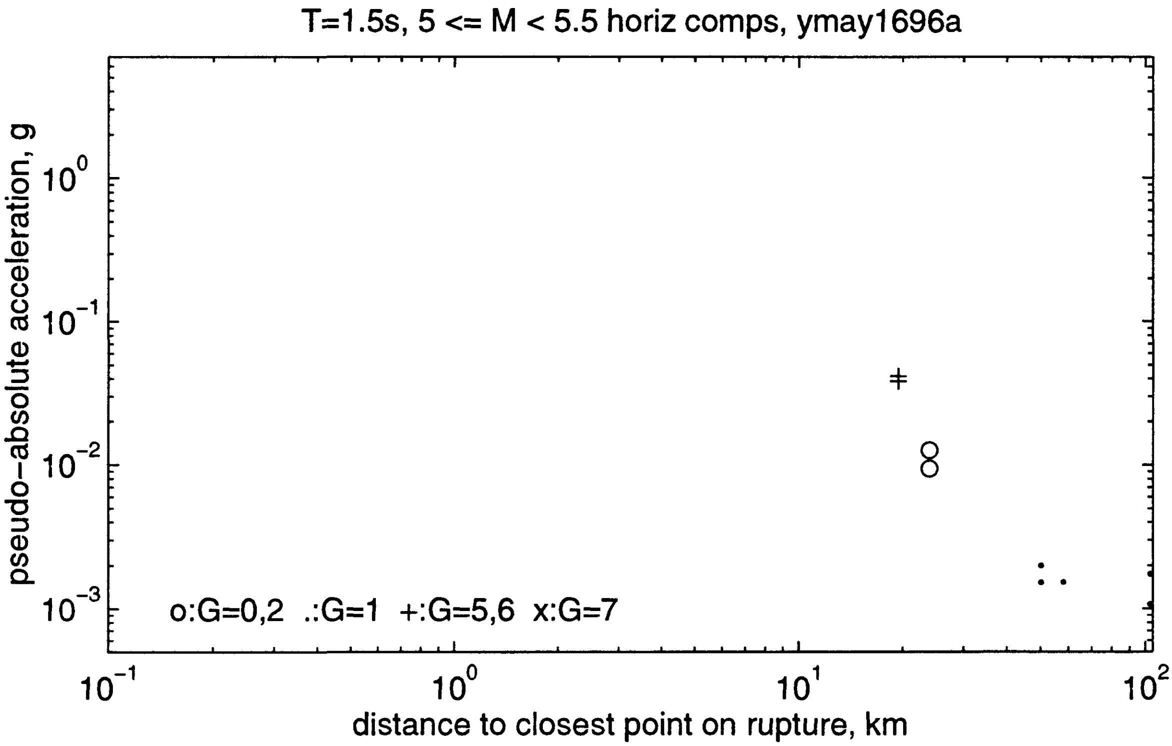

T=1.5s, 5 <= M < 5.5 horiz comps, ymay1696a
pseudo-absolute acceleration, g
10^0
10^{-1}
10^{-2}
10^{-3}
o:G=0,2 .:G=1 +:G=5,6 x:G=7
10^{-1}
10^0
10^1
10^2
distance to closest point on rupture, km

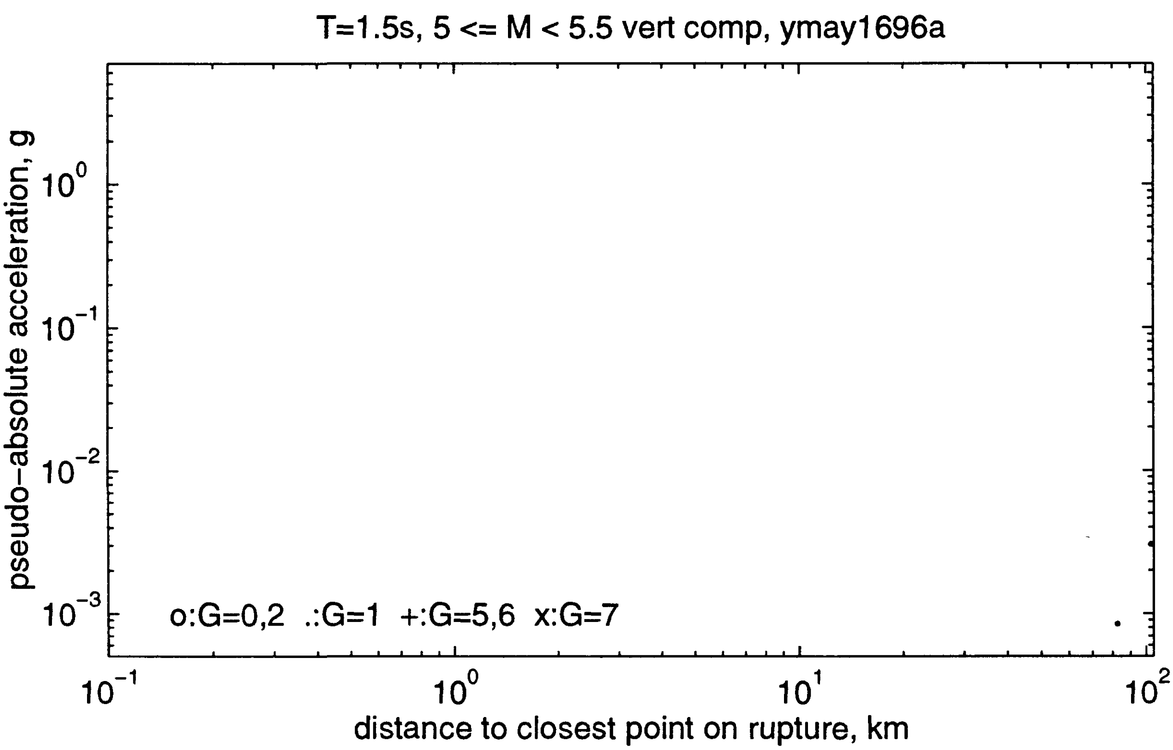

T=1.5s, 5 <= M < 5.5 vert comp, ymay1696a
pseudo-absolute acceleration, g
10^0
10^{-1}
10^{-2}
10^{-3}
o:G=0,2 .:G=1 +:G=5,6 x:G=7
10^{-1}
10^0
10^1
10^2
distance to closest point on rupture, km

10 a.2

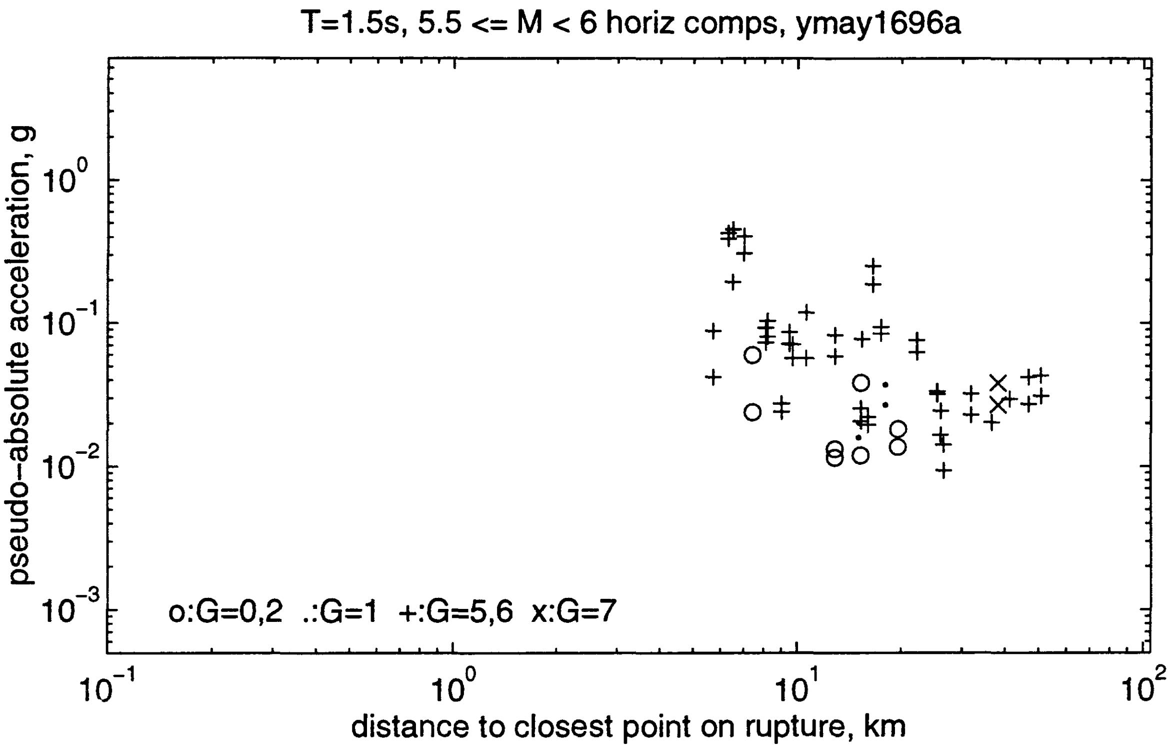
T=1.5s, 5.5 <= M < 6 horiz comps, ymay1696a
pseudo-absolute acceleration, g
10^0
10^{-1}
10^{-2}
10^{-3}
o:G=0,2 .:G=1 +:G=5,6 x:G=7
10^{-1}
10^0
10^1
10^2
distance to closest point on rupture, km

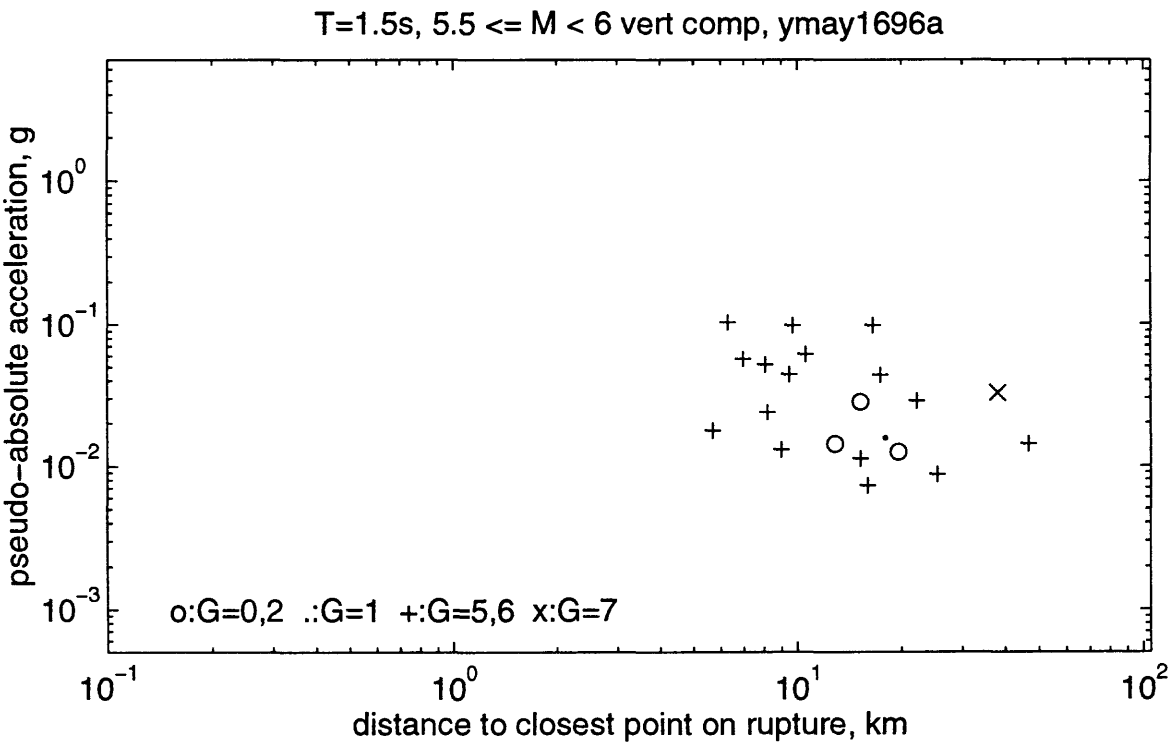
T=1.5s, 5.5 <= M < 6 vert comp, ymay1696a
pseudo-absolute acceleration, g
10^0
10^{-1}
10^{-2}
10^{-3}
o:G=0,2 .:G=1 +:G=5,6 x:G=7
10^{-1}
10^0
10^1
10^2
distance to closest point on rupture, km

10cf

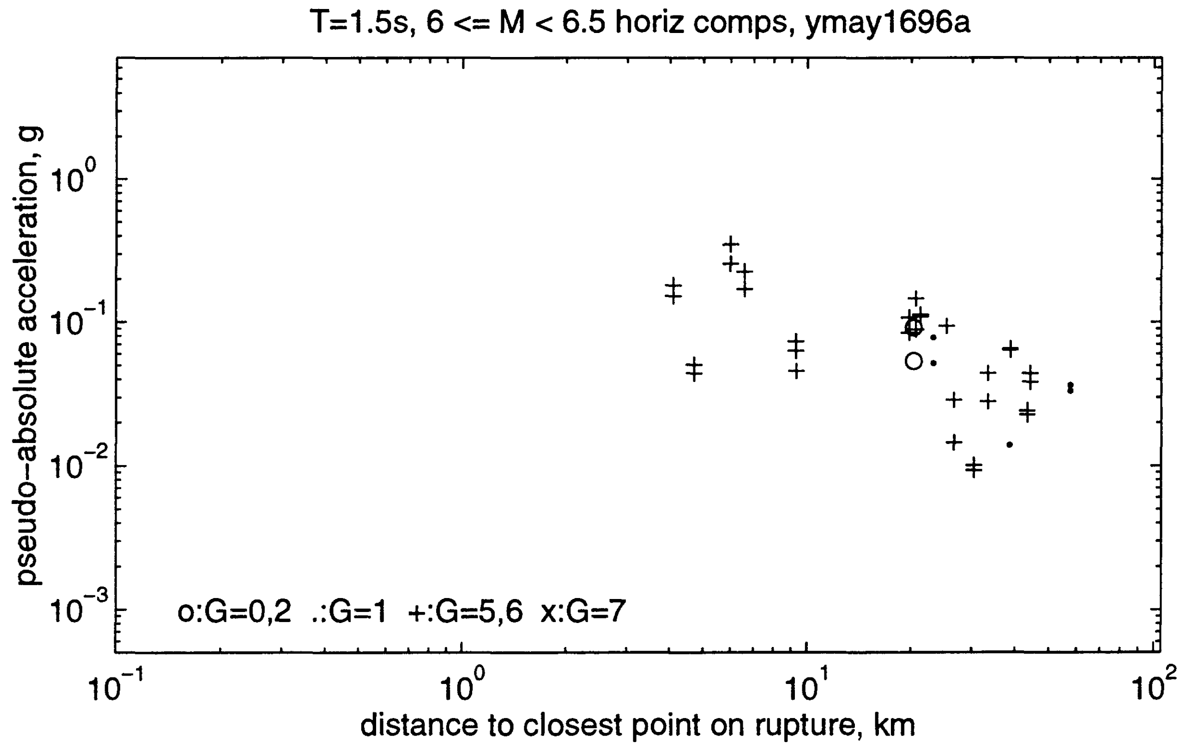
T=1.5s, 6 <= M < 6.5 horiz comps, ymay1696a
pseudo-absolute acceleration, g
distance to closest point on rupture, km
o:G=0,2 .:G=1 +:G=5,6 x:G=7

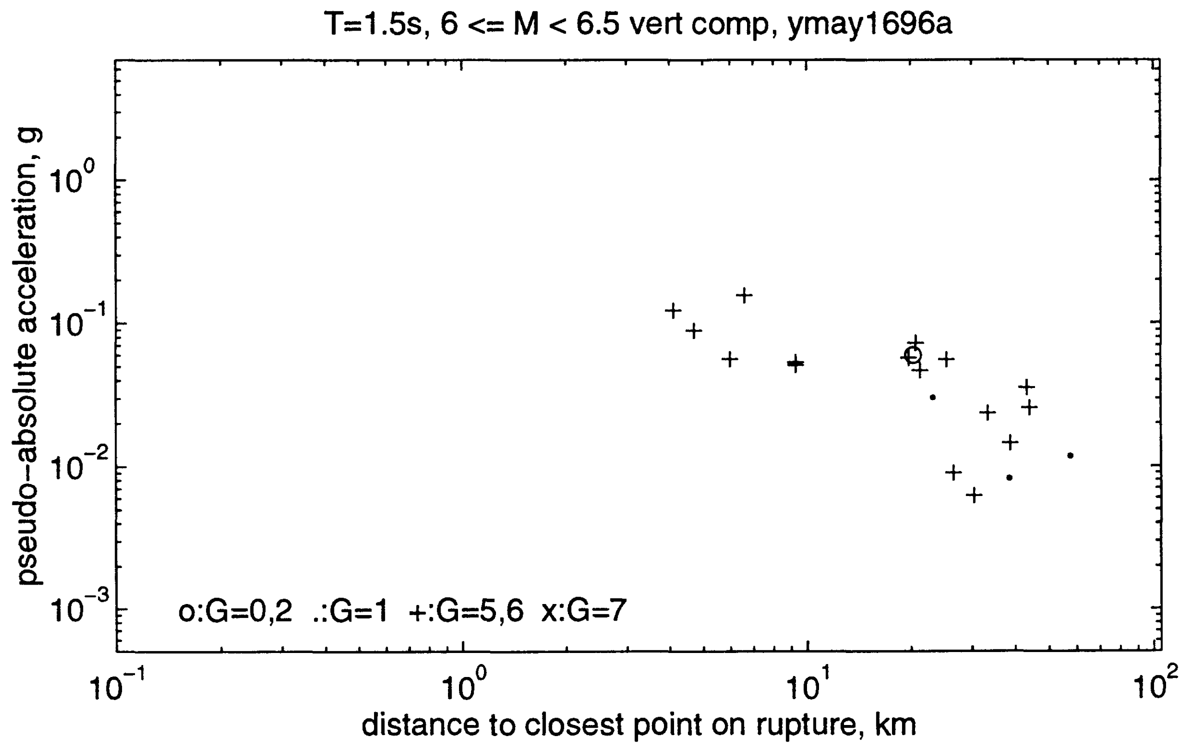
T=1.5s, 6 <= M < 6.5 vert comp, ymay1696a
pseudo-absolute acceleration, g
distance to closest point on rupture, km
o:G=0,2 .:G=1 +:G=5,6 x:G=7

T=1.5s, 6.5 <= M < 7.5 horiz comps, ymay1696a

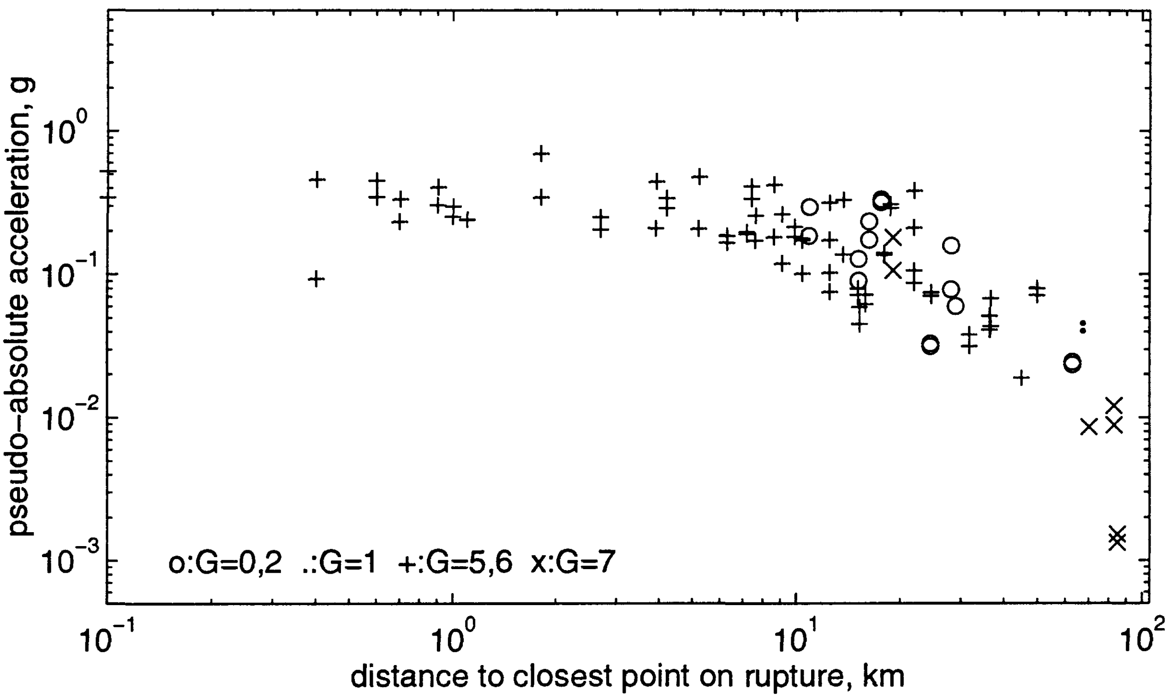

T=1.5s, 6.5 <= M < 7.5 vert comp, ymay1696a

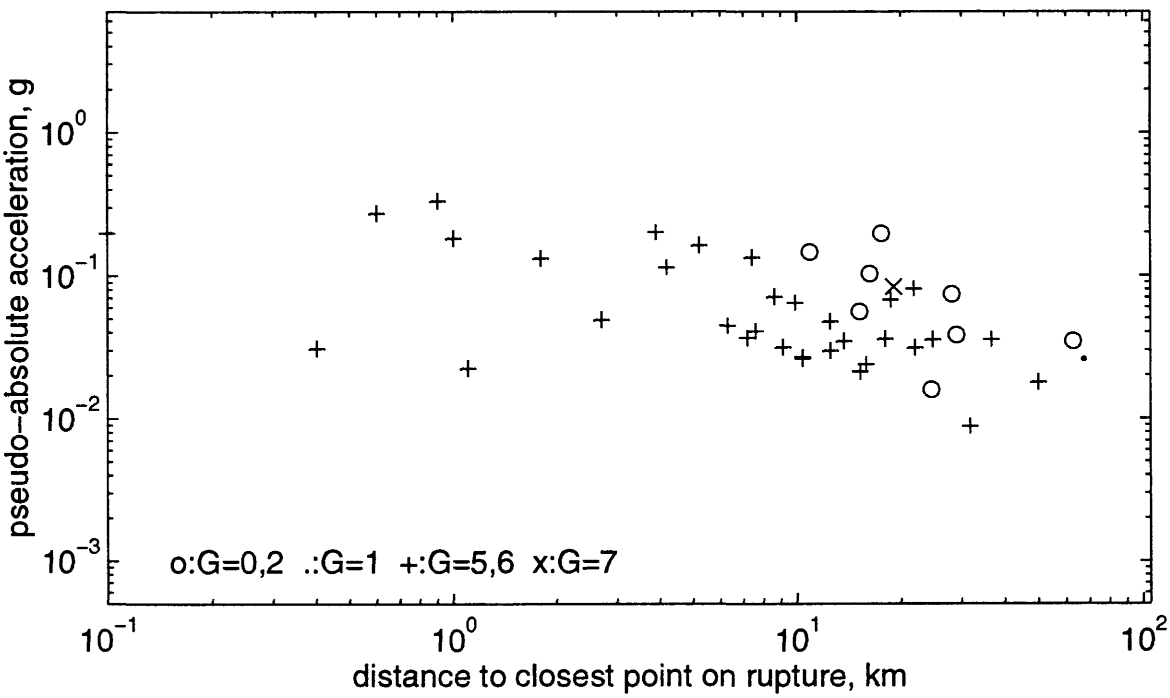

10ar

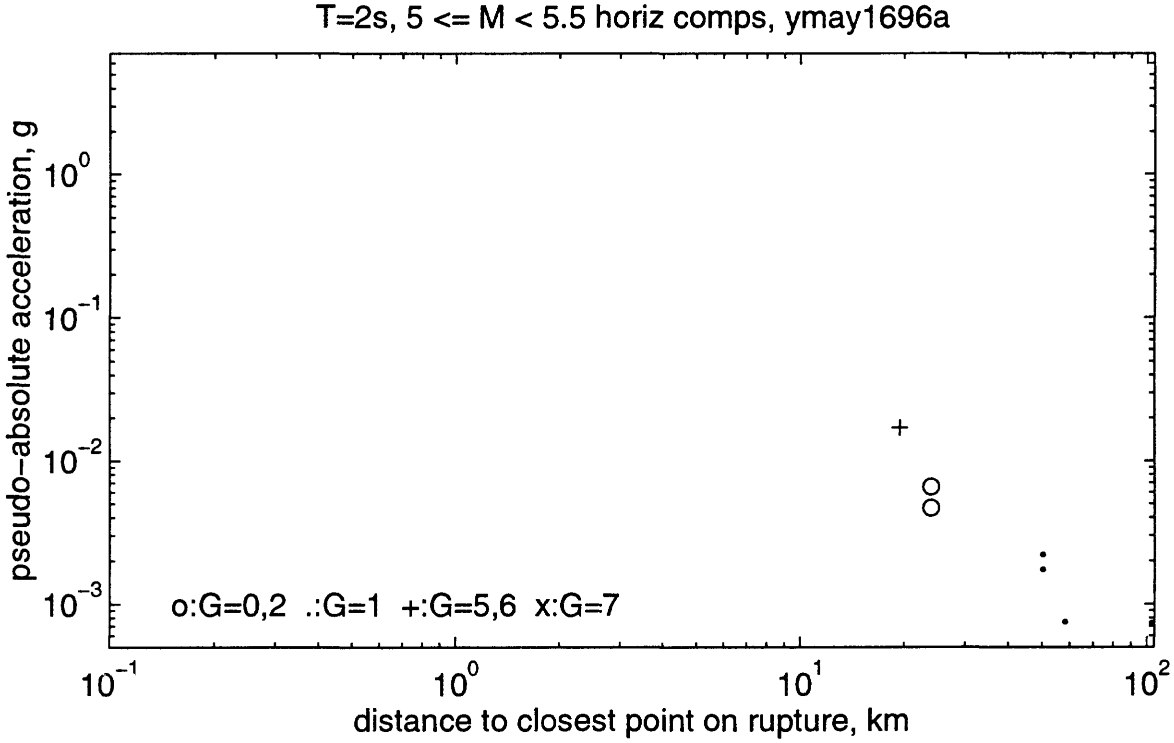

T=2s, 5 <= M < 5.5 horiz comps, ymay1696a
pseudo-absolute acceleration, g
10^0
10^-1
10^-2
10^-3
o:G=0,2 .:G=1 +:G=5,6 x:G=7
10^-1
10^0
10^1
10^2
distance to closest point on rupture, km

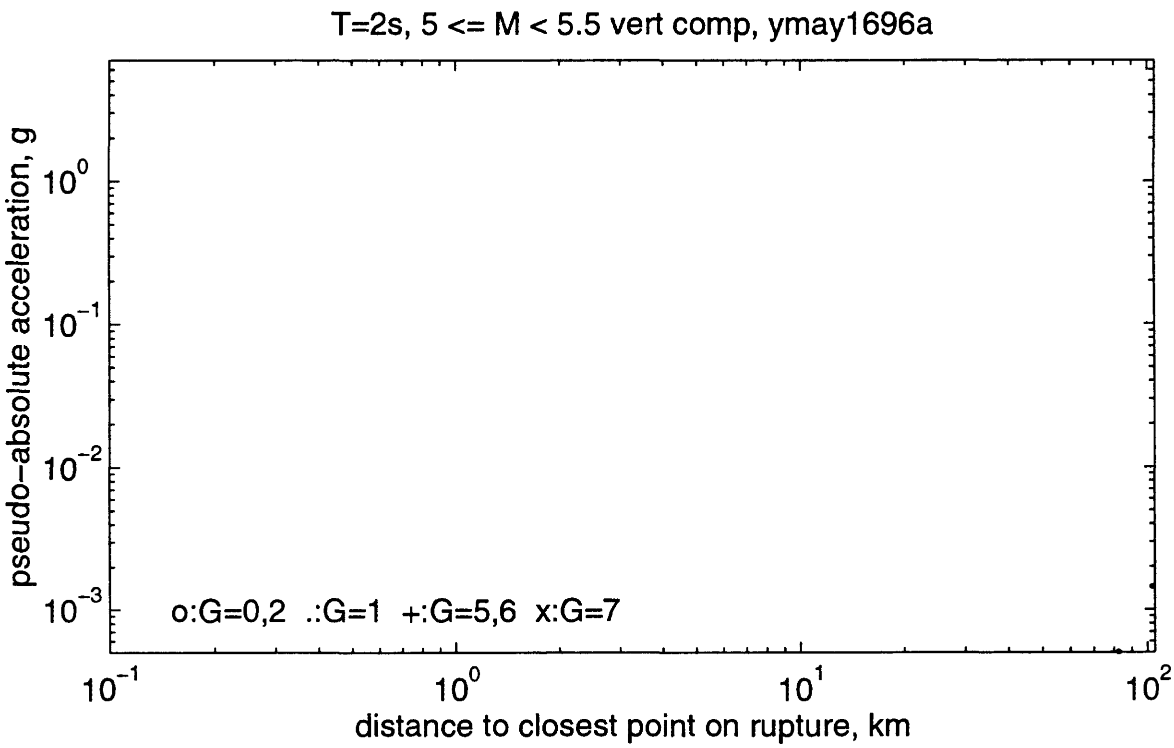

T=2s, 5 <= M < 5.5 vert comp, ymay1696a
pseudo-absolute acceleration, g
10^0
10^-1
10^-2
10^-3
o:G=0,2 .:G=1 +:G=5,6 x:G=7
10^-1
10^0
10^1
10^2
distance to closest point on rupture, km

10 as

T=2s, 5.5 <= M < 6 horiz comps, ymay1696a

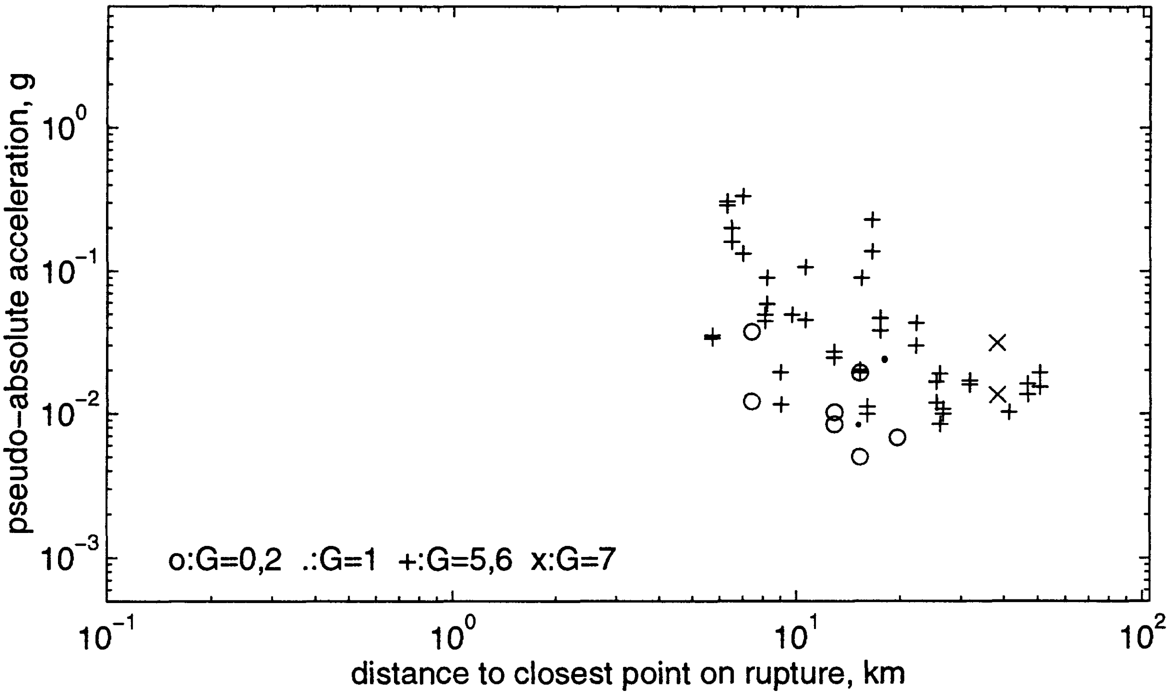

T=2s, 5.5 <= M < 6 vert comp, ymay1696a

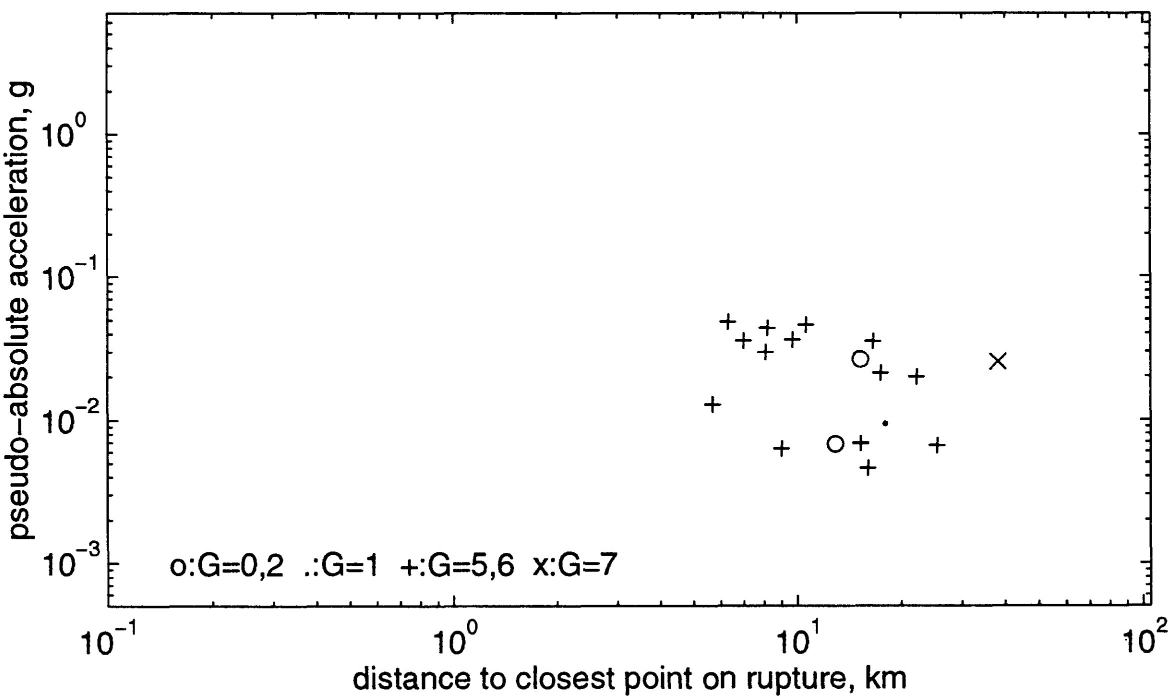

10 at

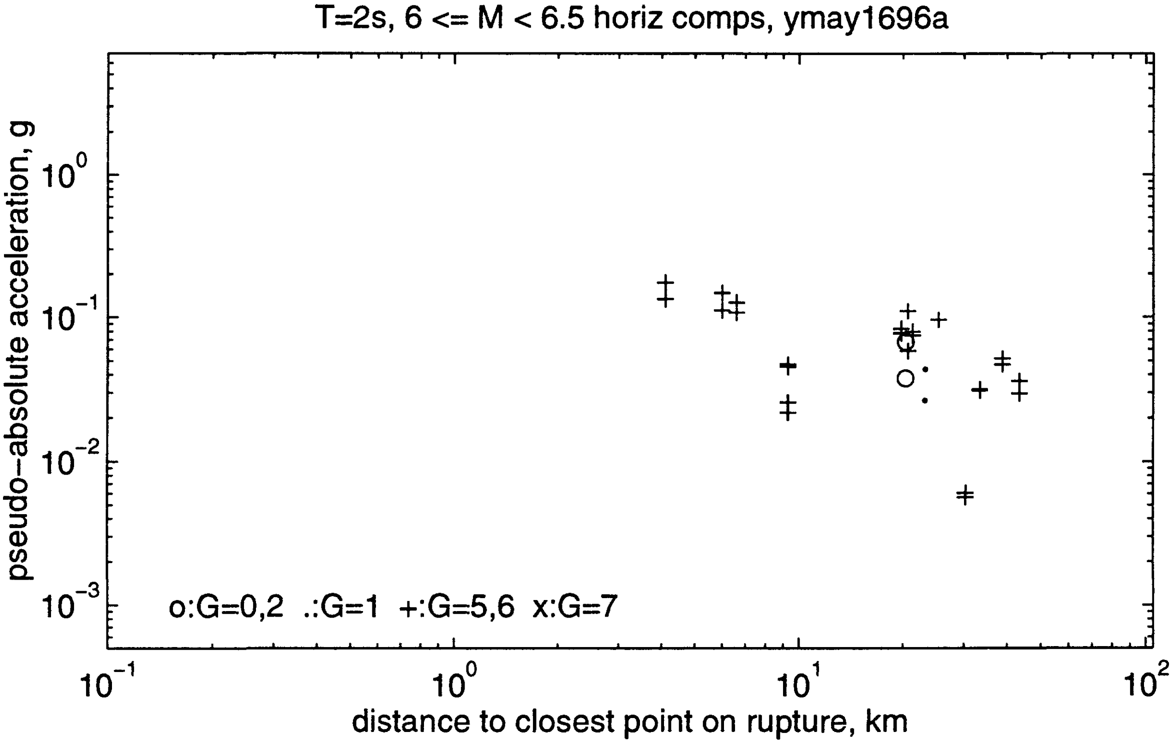
T=2s, 6 <= M < 6.5 horiz comps, ymay1696a
pseudo-absolute acceleration, g
distance to closest point on rupture, km
o:G=0,2 .:G=1 +:G=5,6 x:G=7

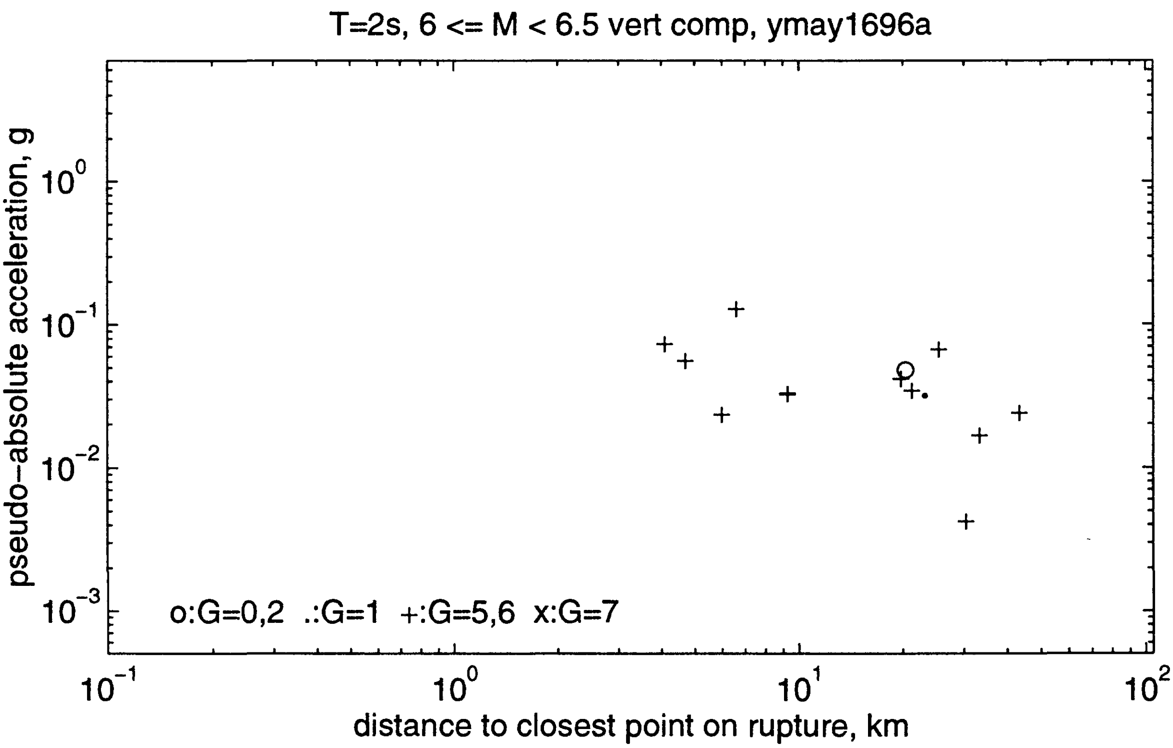
T=2s, 6 <= M < 6.5 vert comp, ymay1696a
pseudo-absolute acceleration, g
distance to closest point on rupture, km
o:G=0,2 .:G=1 +:G=5,6 x:G=7

10 aU

T=2s, 6.5 <= M < 7.5 horiz comps, ymay1696a

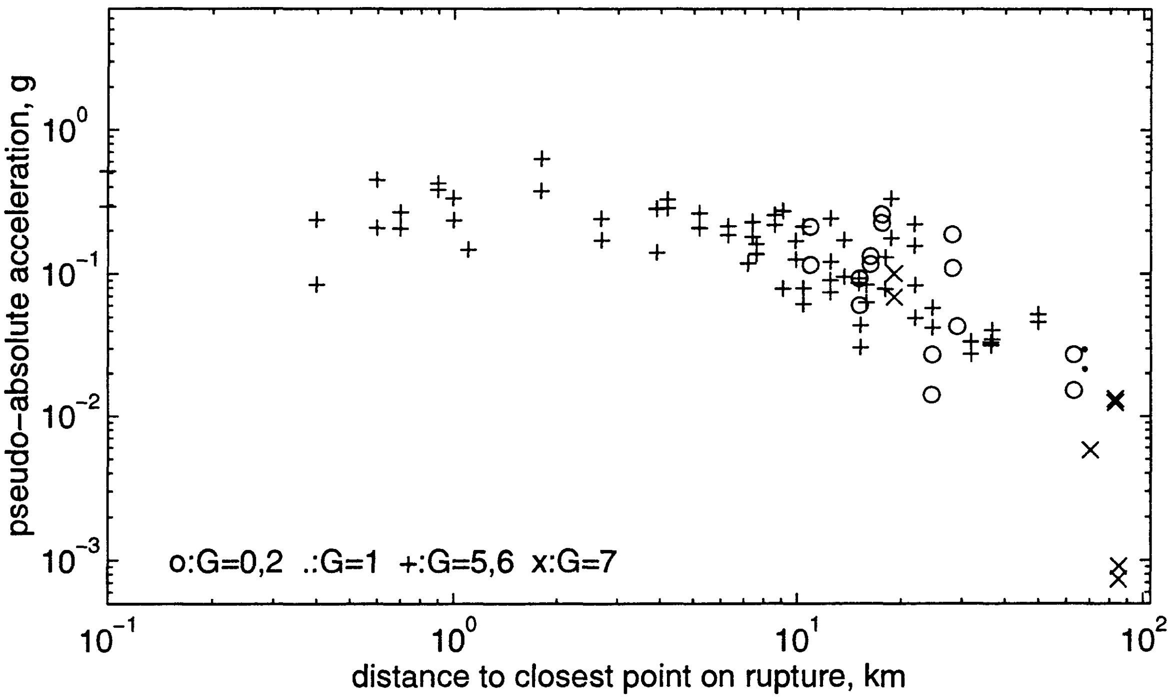

T=2s, 6.5 <= M < 7.5 vert comp, ymay1696a

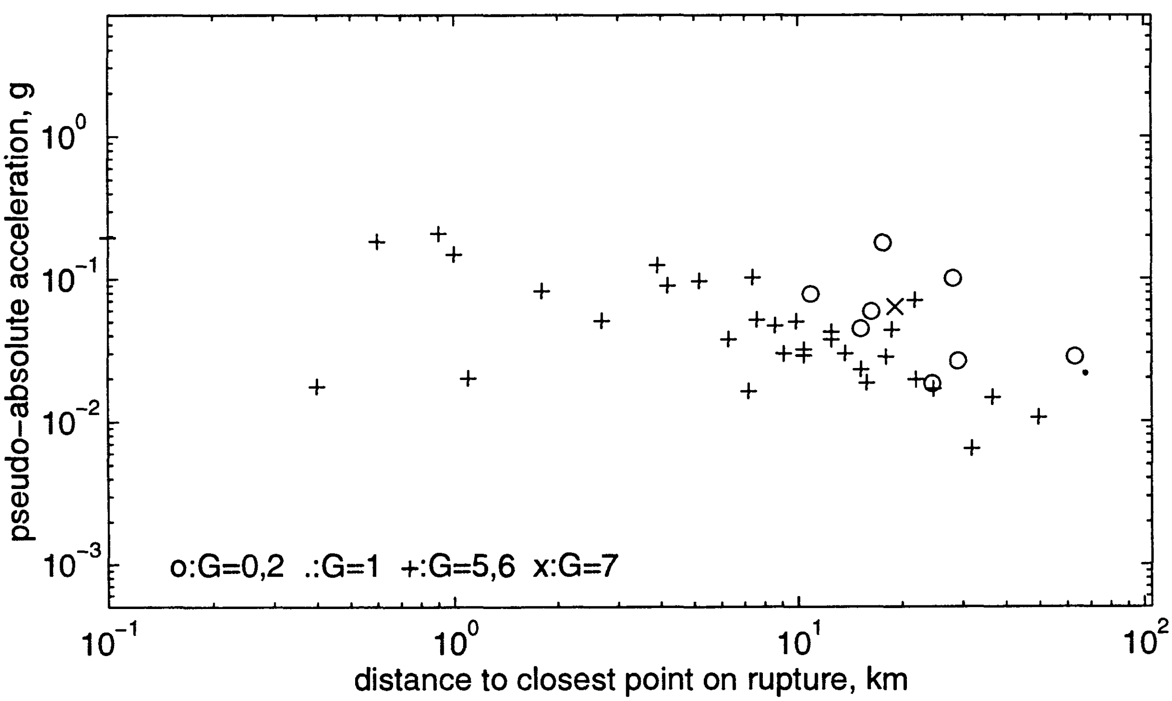

1000

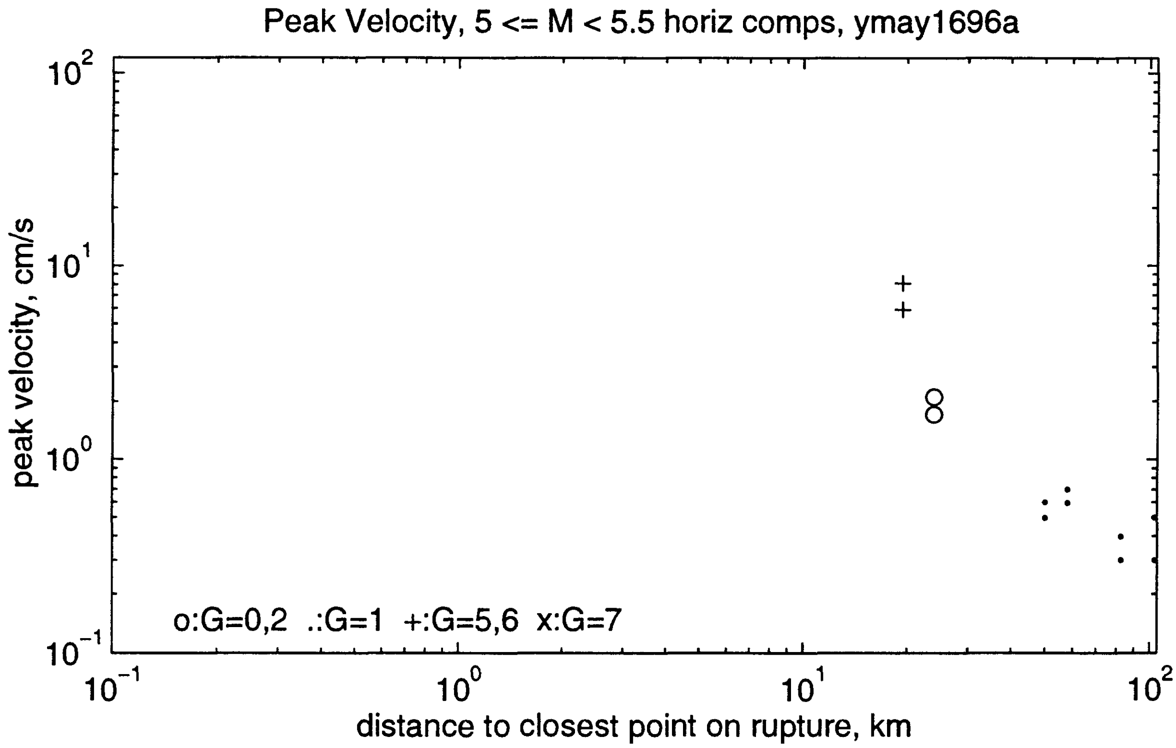
Peak Velocity, 5 <= M < 5.5 horiz comps, ymay1696a
peak velocity, cm/s
10^2
10^1
10^0
10^{-1}
o:G=0,2 .:G=1 +:G=5,6 x:G=7
10^{-1}
10^0
10^1
10^2
distance to closest point on rupture, km

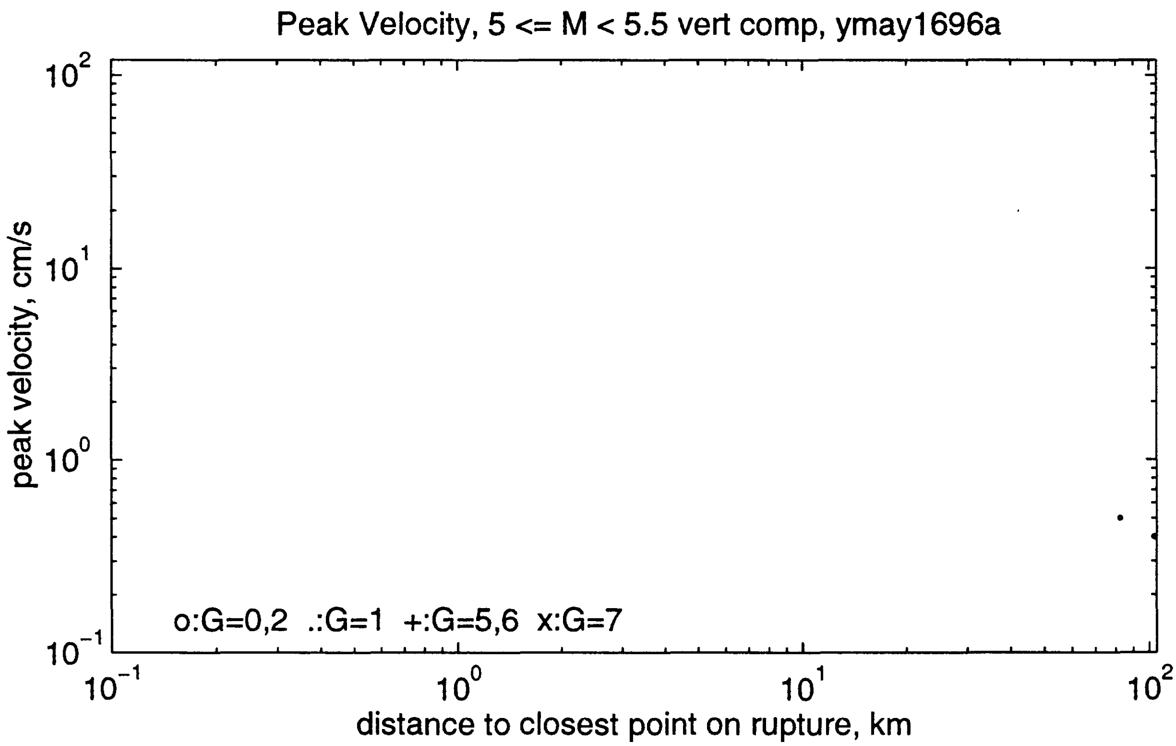
Peak Velocity, 5 <= M < 5.5 vert comp, ymay1696a
peak velocity, cm/s
10^2
10^1
10^0
10^{-1}
o:G=0,2 .:G=1 +:G=5,6 x:G=7
10^{-1}
10^0
10^1
10^2
distance to closest point on rupture, km

10 aw

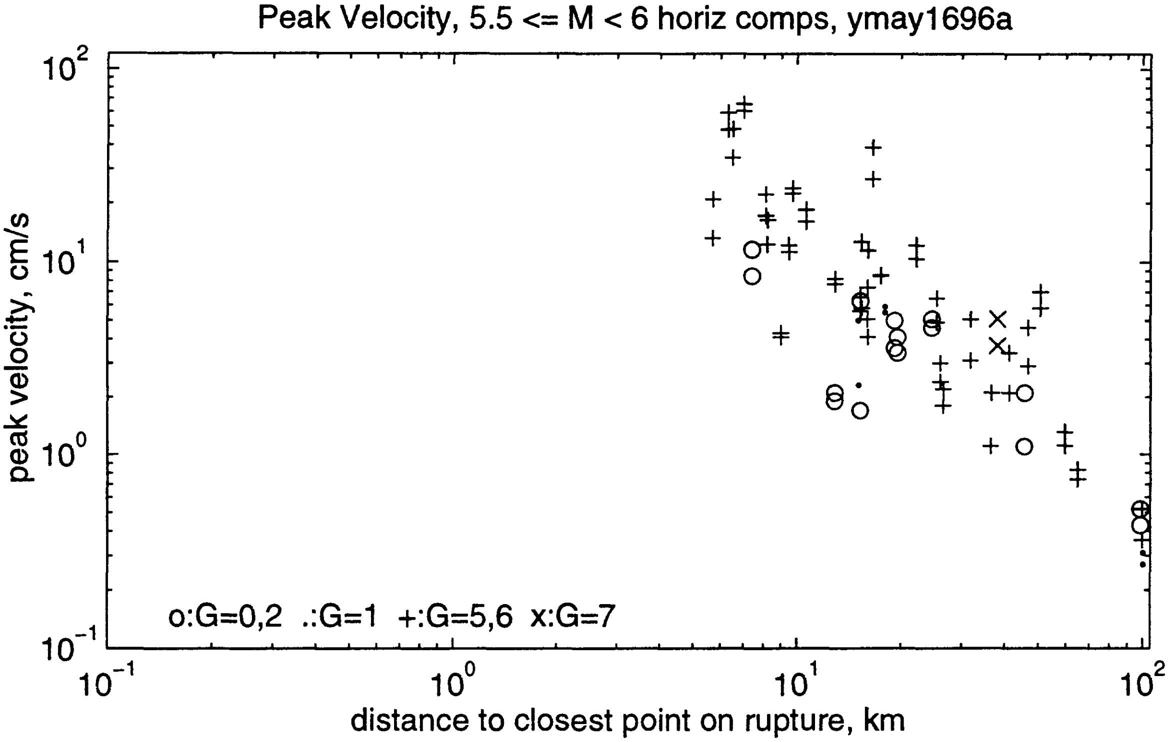
Peak Velocity, 5.5 <= M < 6 horiz comps, ymay1696a
peak velocity, cm/s
distance to closest point on rupture, km
o:G=0,2 .:G=1 +:G=5,6 x:G=7

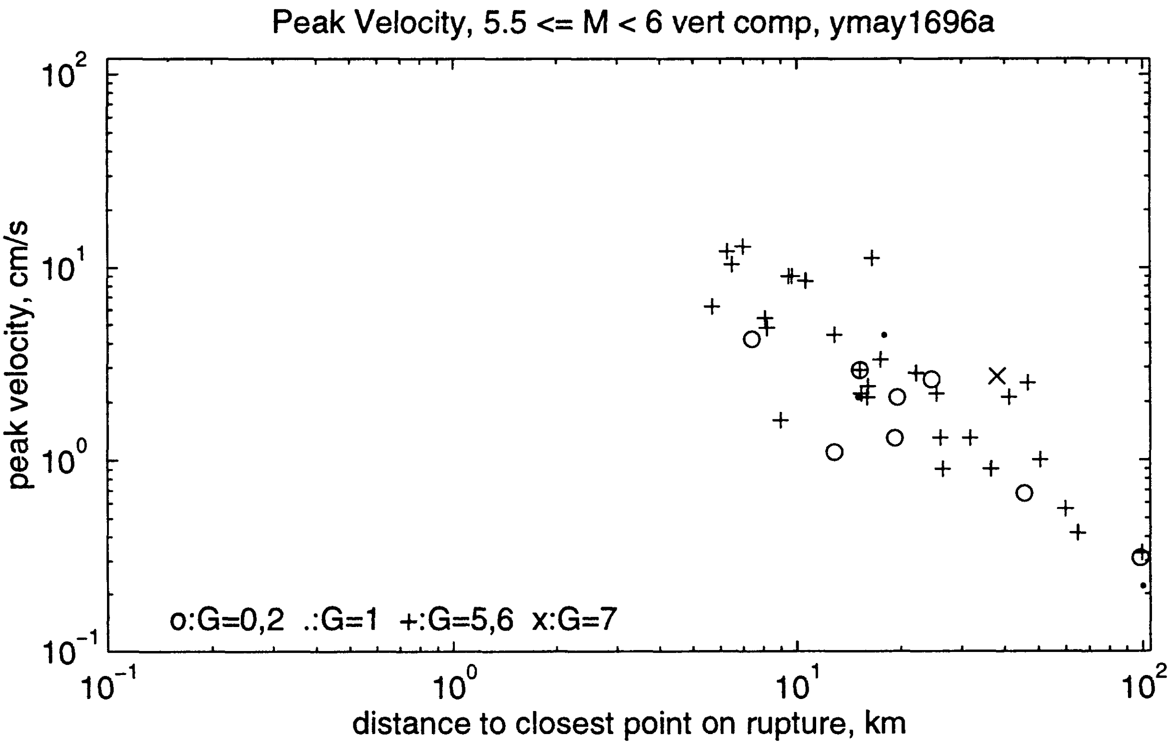
Peak Velocity, 5.5 <= M < 6 vert comp, ymay1696a
peak velocity, cm/s
distance to closest point on rupture, km
o:G=0,2 .:G=1 +:G=5,6 x:G=7

10 of

Peak Velocity, 6 <= M < 6.5 horiz comps, ymay1696a

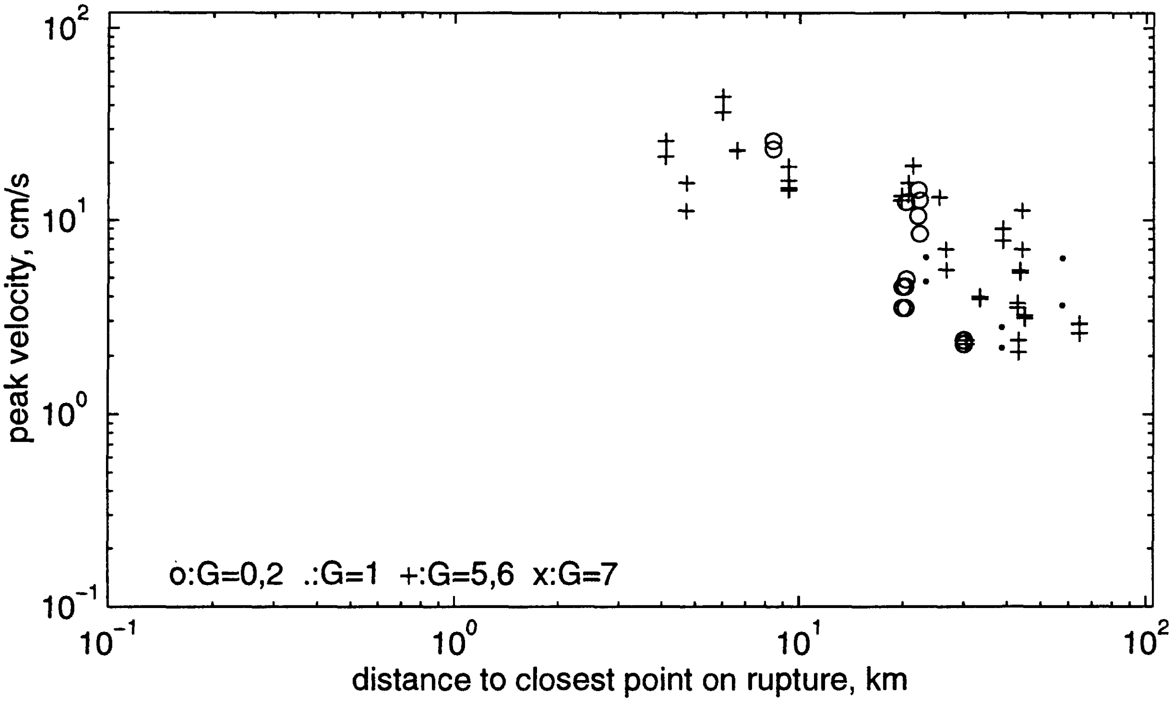

Peak Velocity, 6 <= M < 6.5 vert comp, ymay1696a

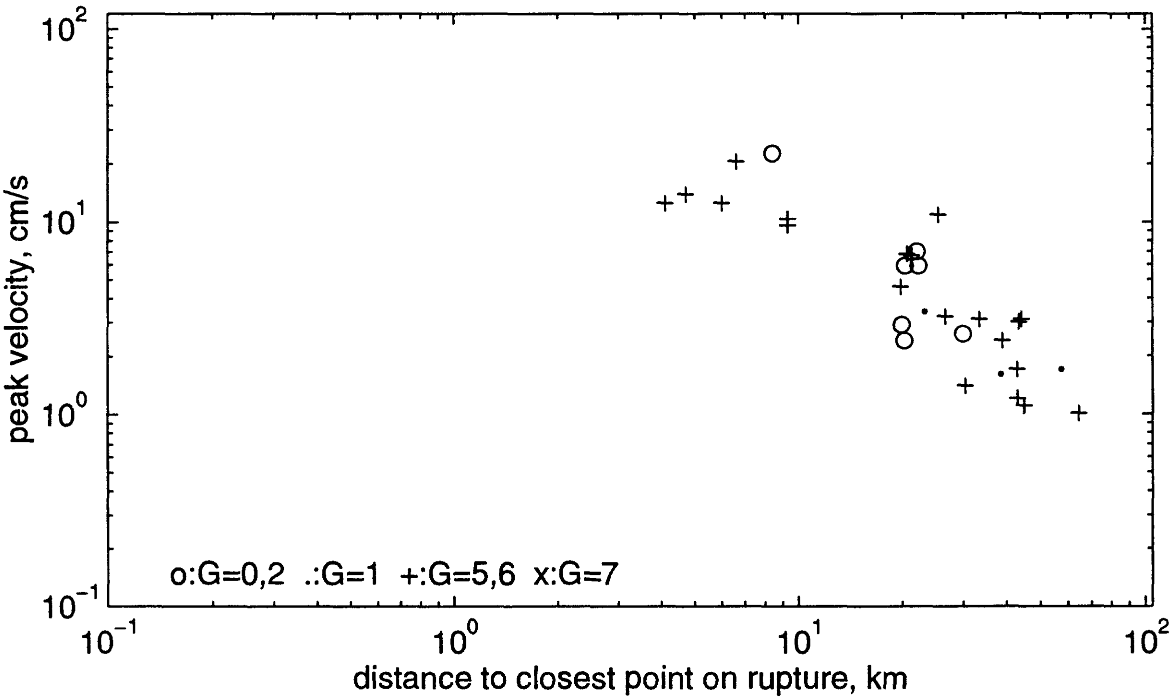

10ay

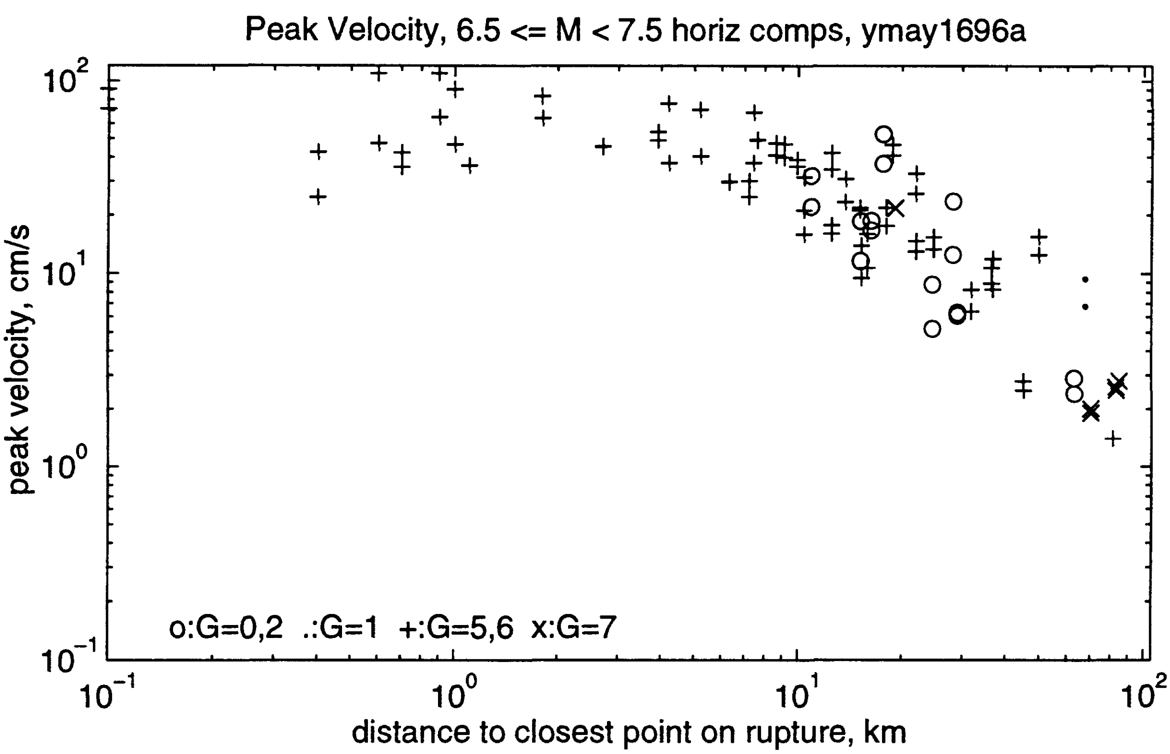

Peak Velocity, 6.5 <= M < 7.5 horiz comps, ymay1696a
peak velocity, cm/s
distance to closest point on rupture, km
o:G=0,2 .:G=1 +:G=5,6 x:G=7

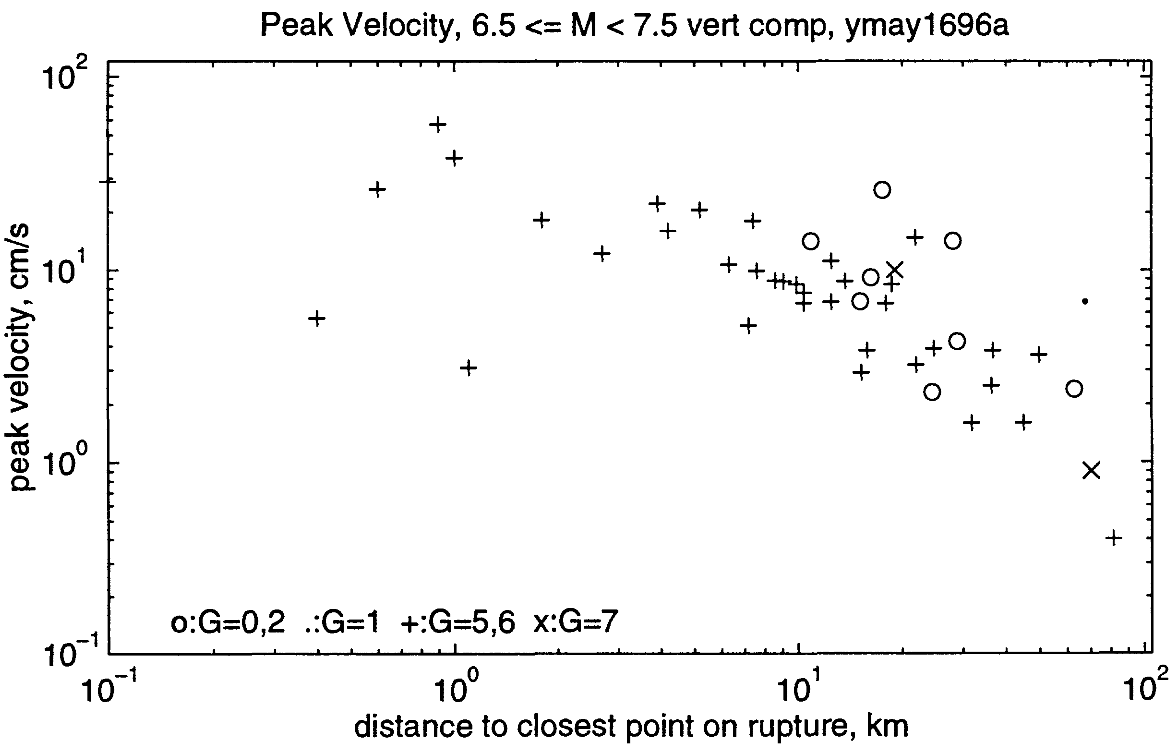

Peak Velocity, 6.5 <= M < 7.5 vert comp, ymay1696a
peak velocity, cm/s
distance to closest point on rupture, km
o:G=0,2 .:G=1 +:G=5,6 x:G=7

10 of

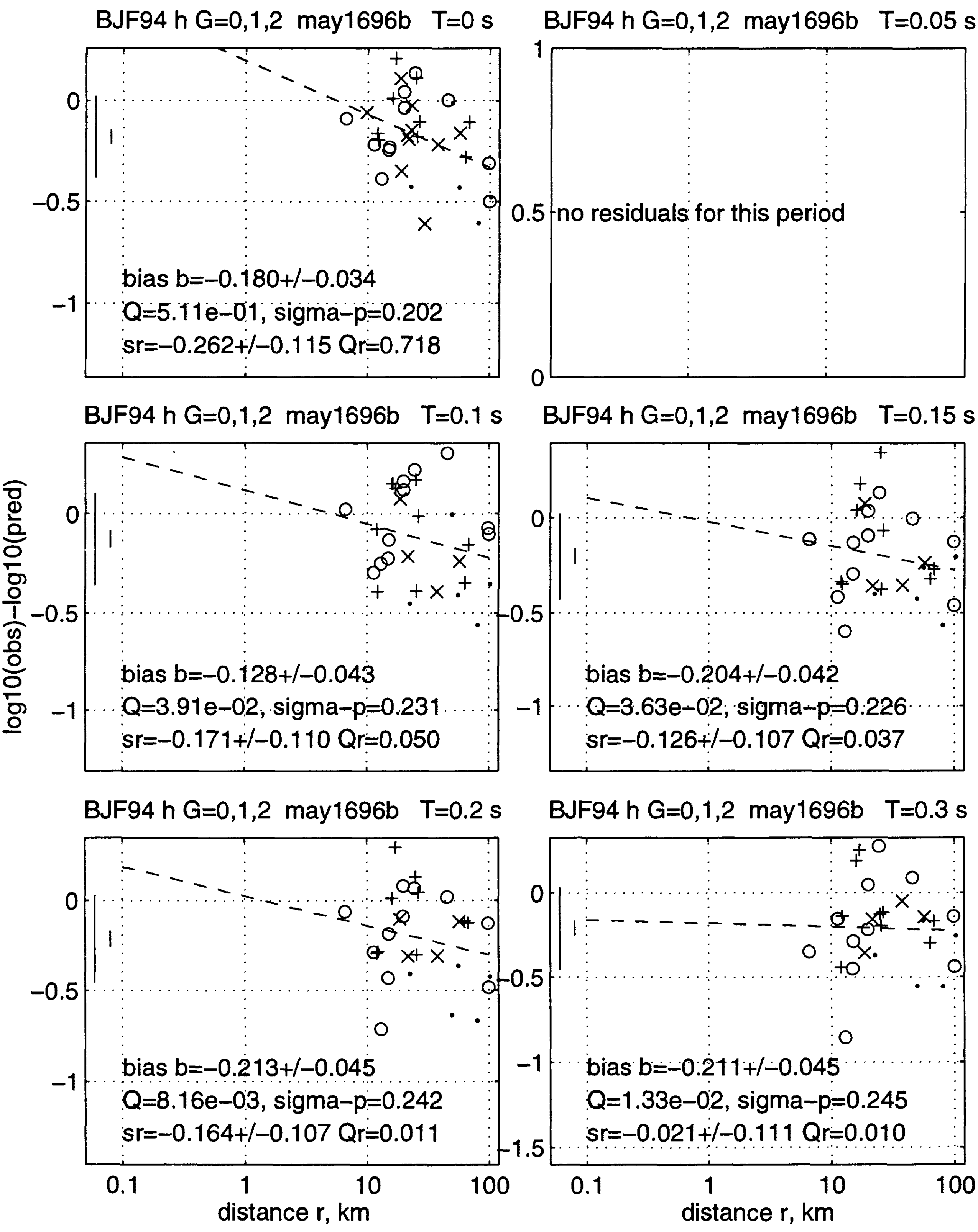

96/5/16 19:30 ymp1:[sp]may1696b1d1.eps

11a

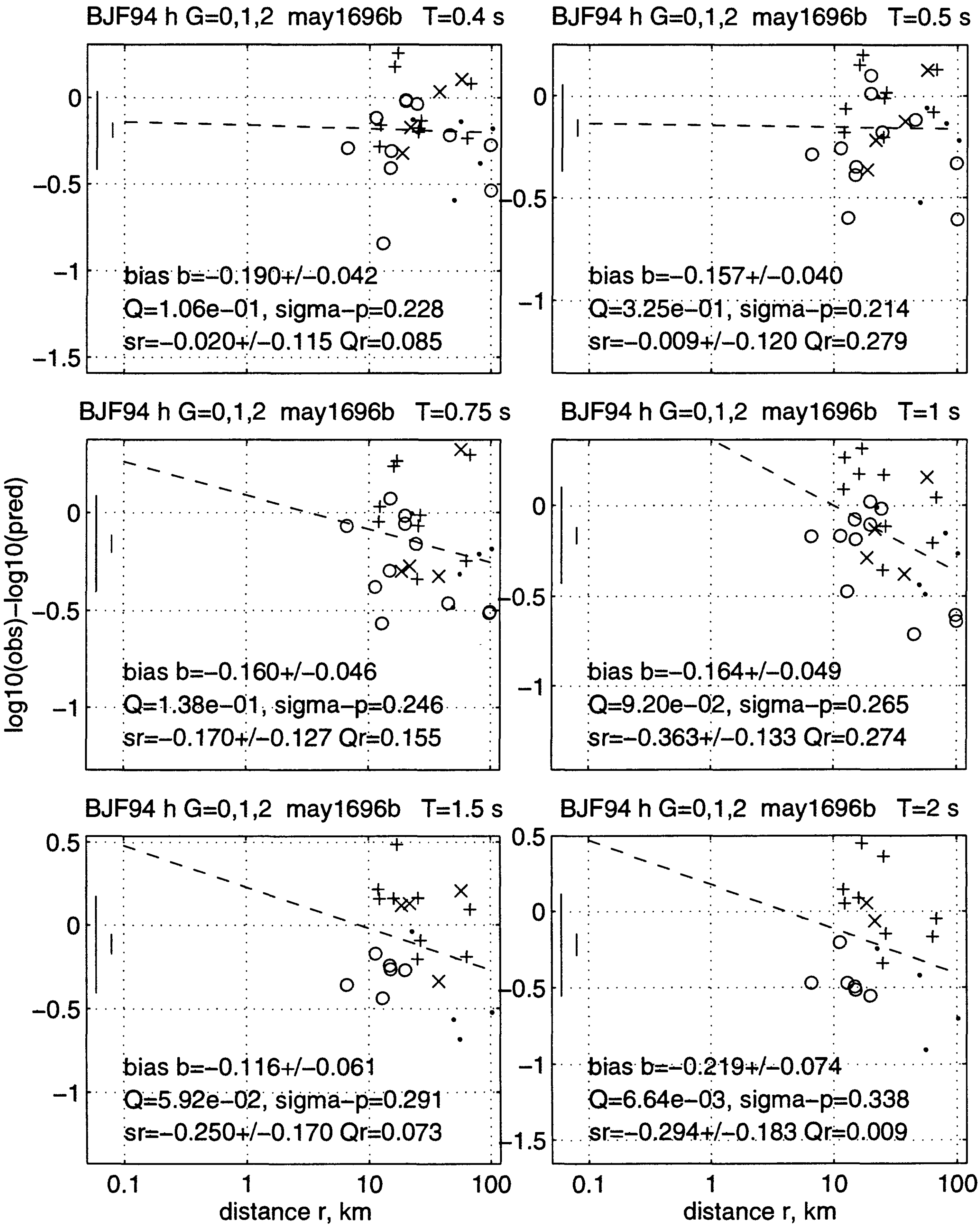

96/5/16 19:30 ymp1:[sp]may1696b1d2.eps

11 b

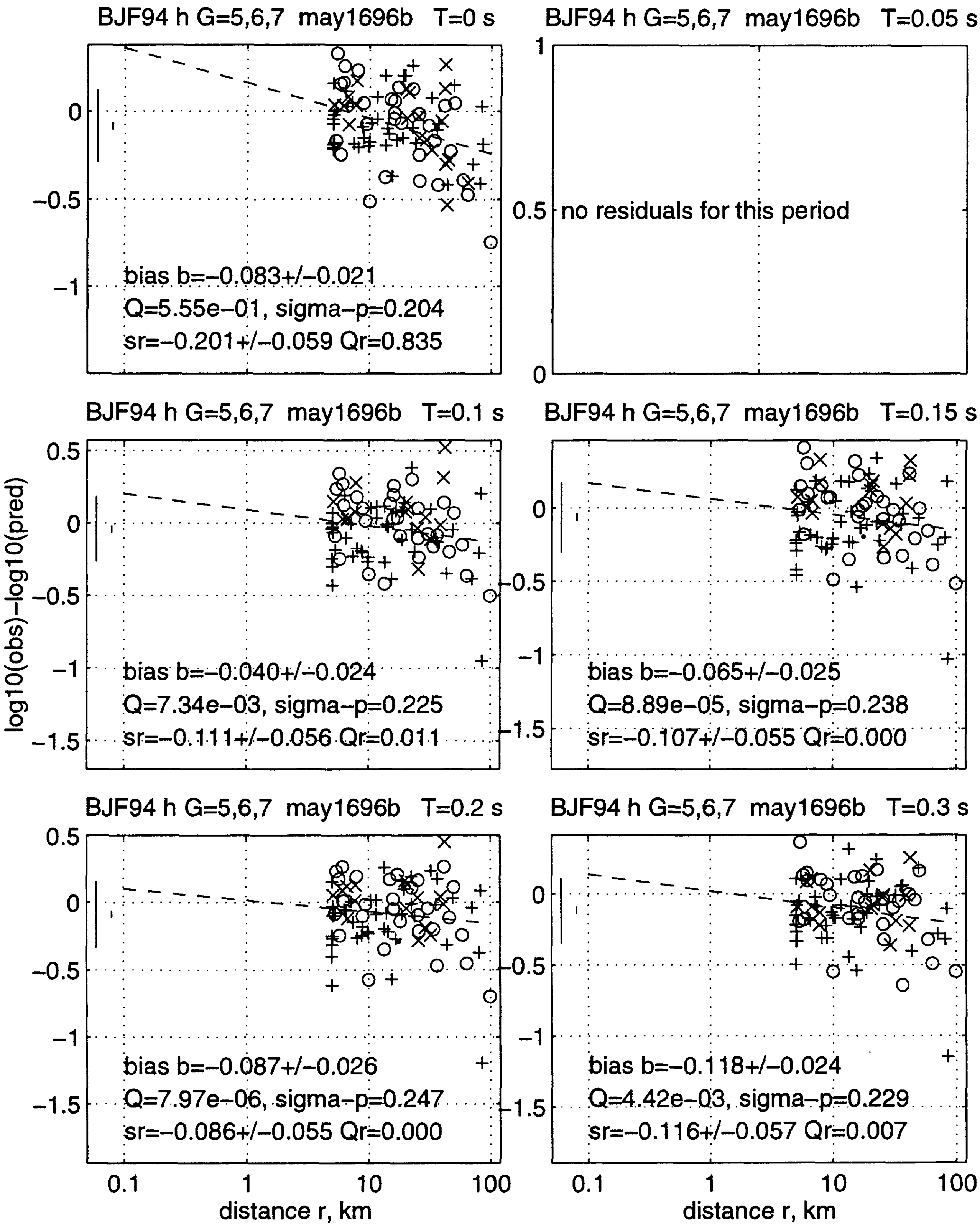

96/5/16 19:31 ymp1:[sp]may1696b2d1.eps

11c

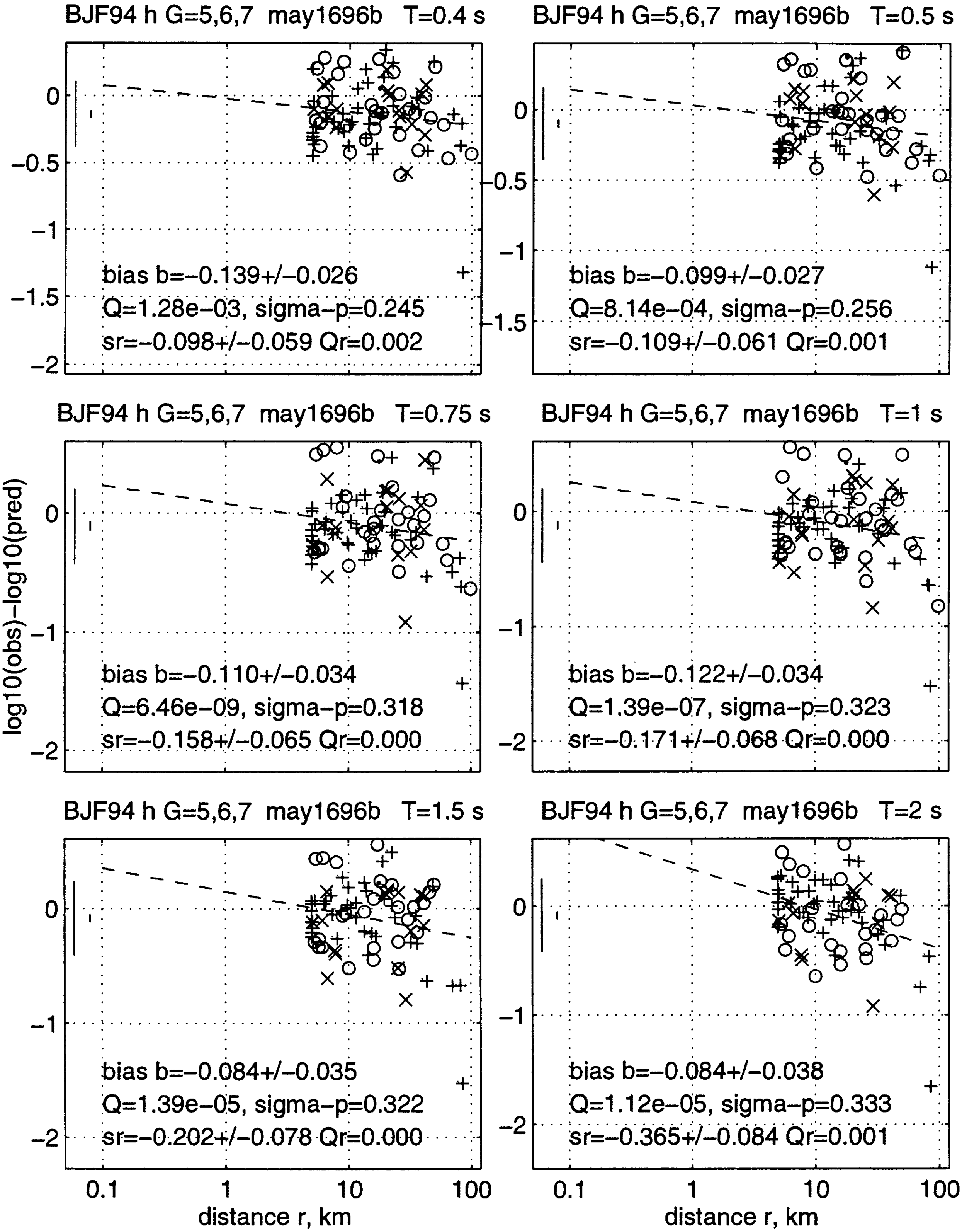

96/5/16 19:31 ymp1:[sp]may1696b2d2.eps

11d

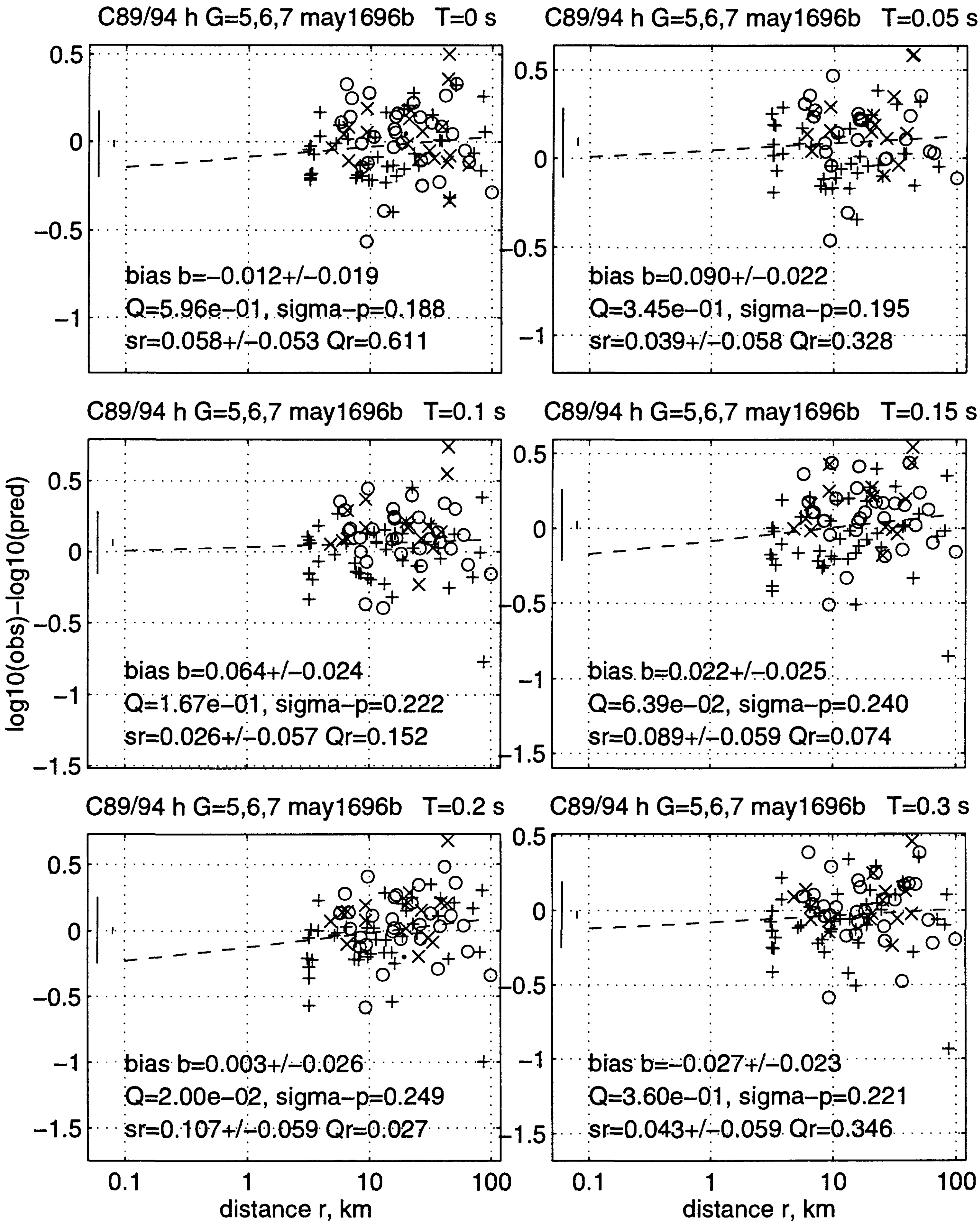

96/5/16 19:32 ymp1:[sp]may1696b3d1.eps

11e

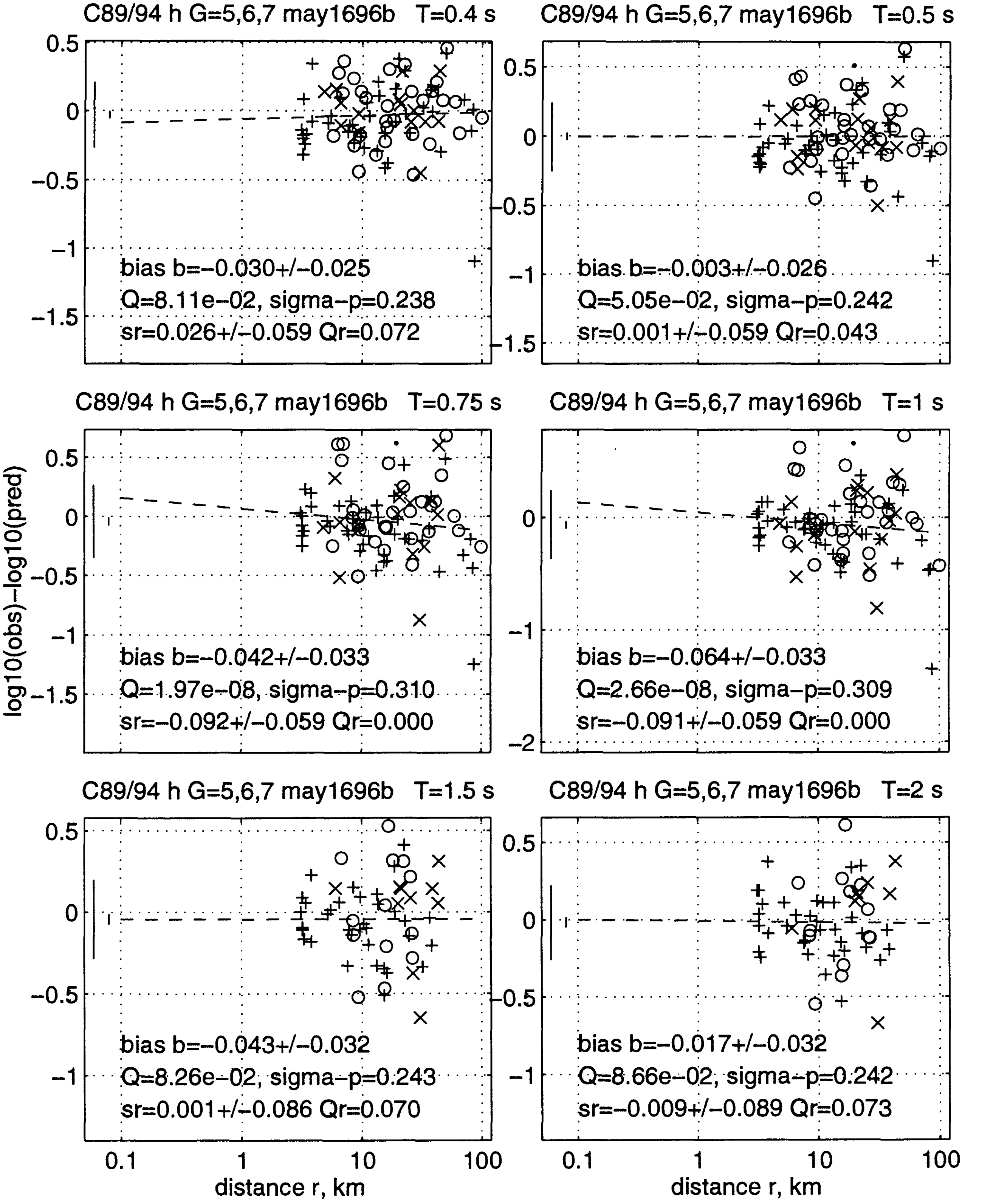

96/5/16 19:33 ymp1:[sp]may1696b3d2.eps

11f

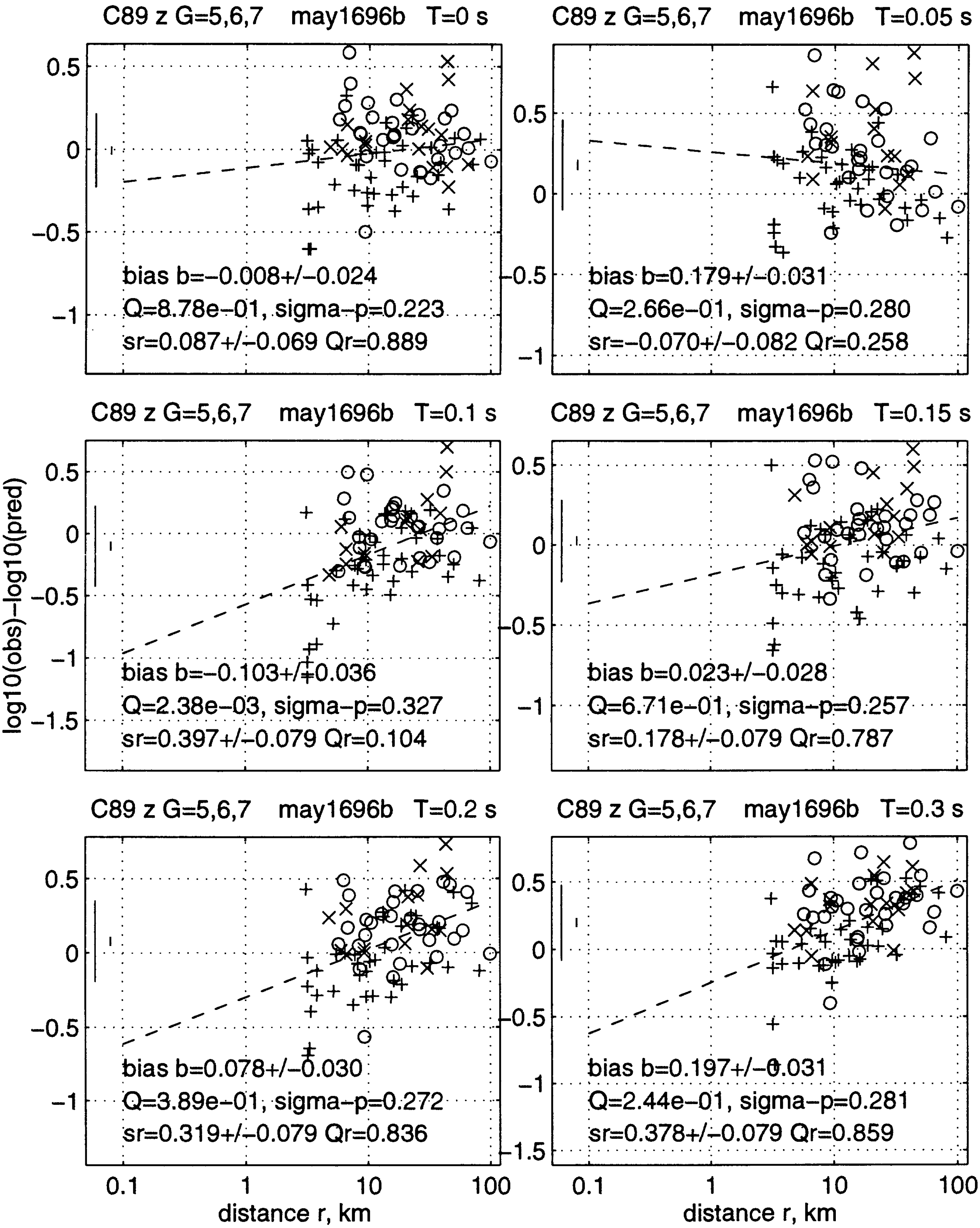

96/5/16 19:34 ymp1:[sp]may1696b4d1.eps

11g

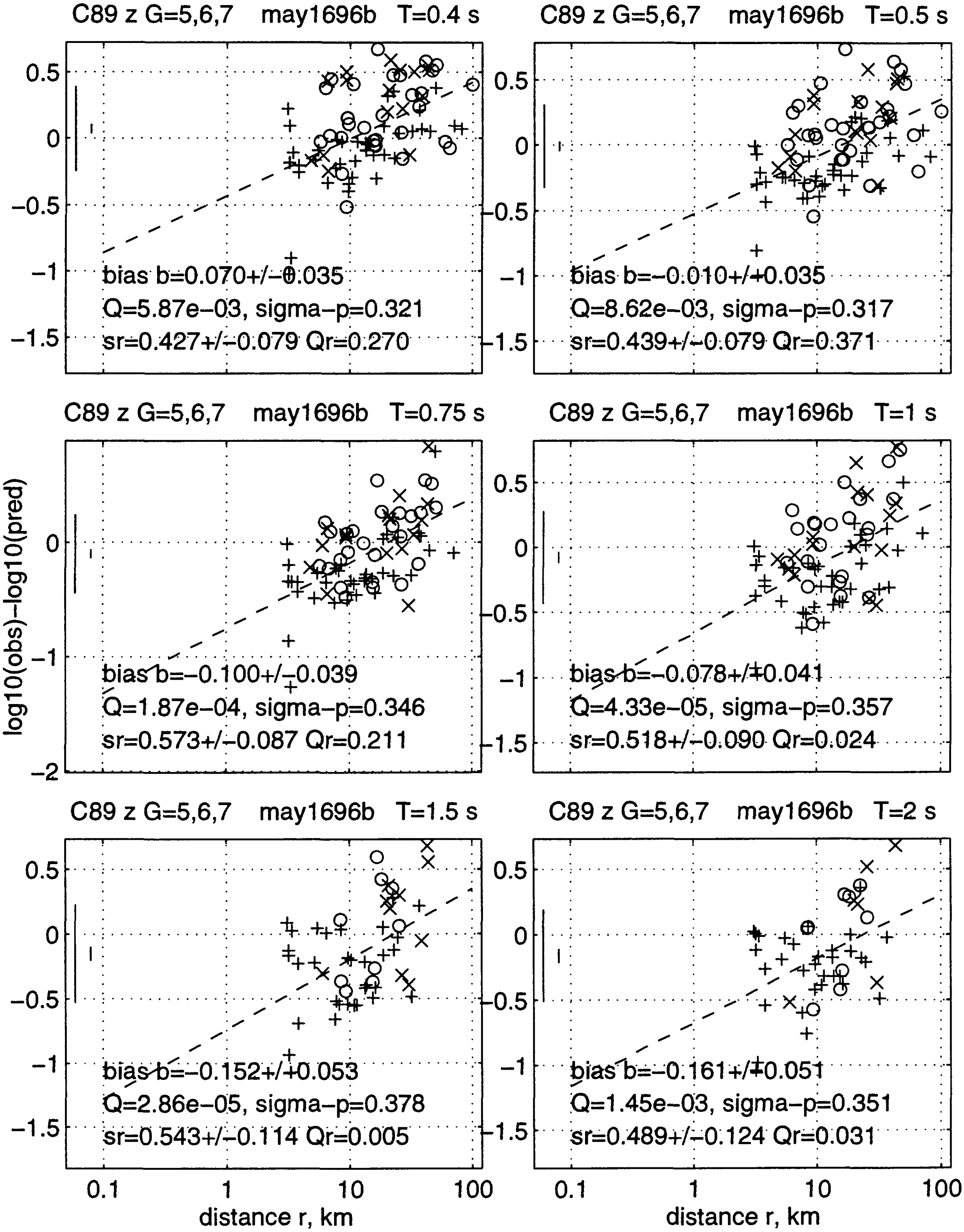

96/5/16 19:34 ymp1:[sp]may1696b4d2.eps

11h

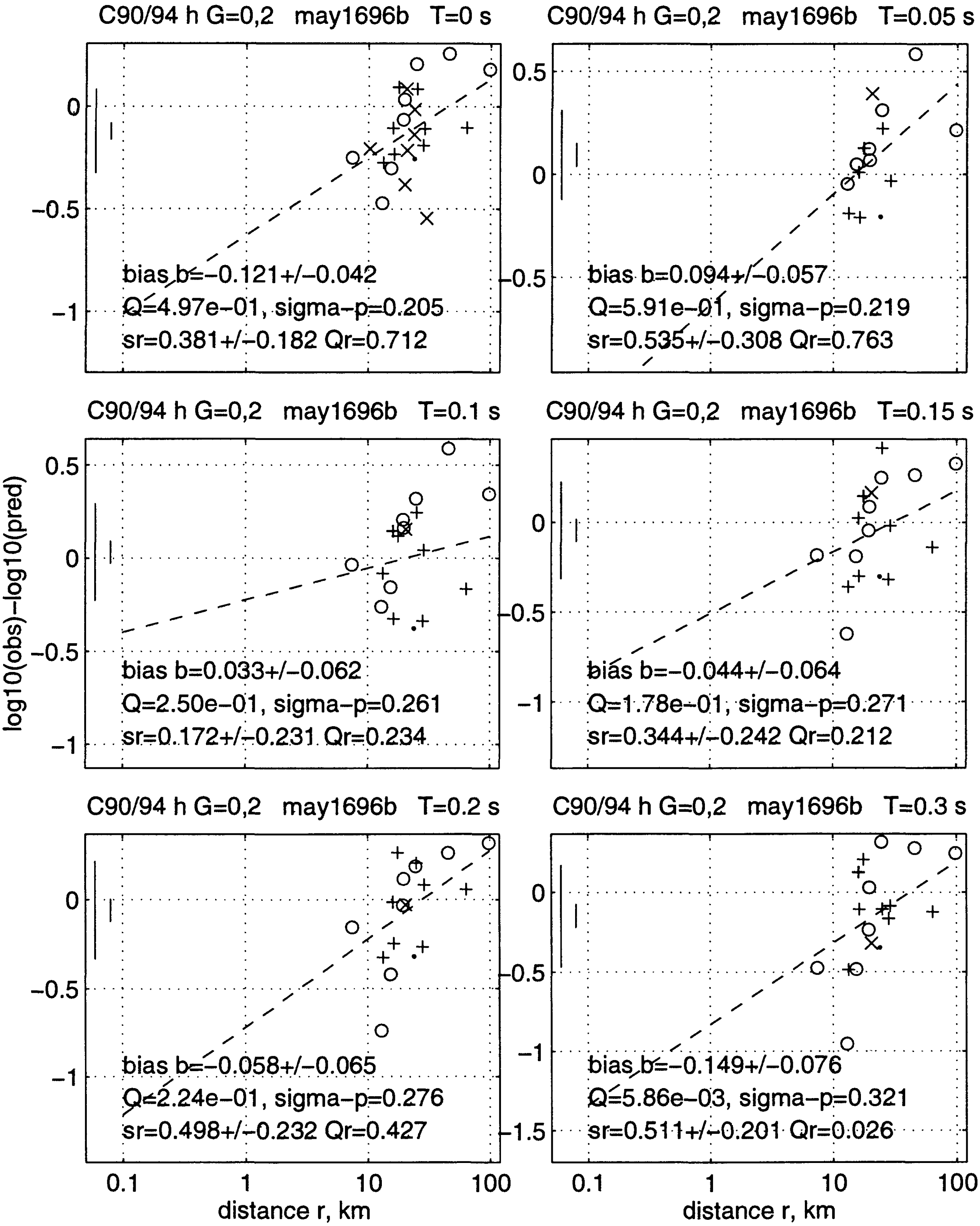

96/5/16 19:35 ymp1:[sp]may1696b5d1.eps

11i

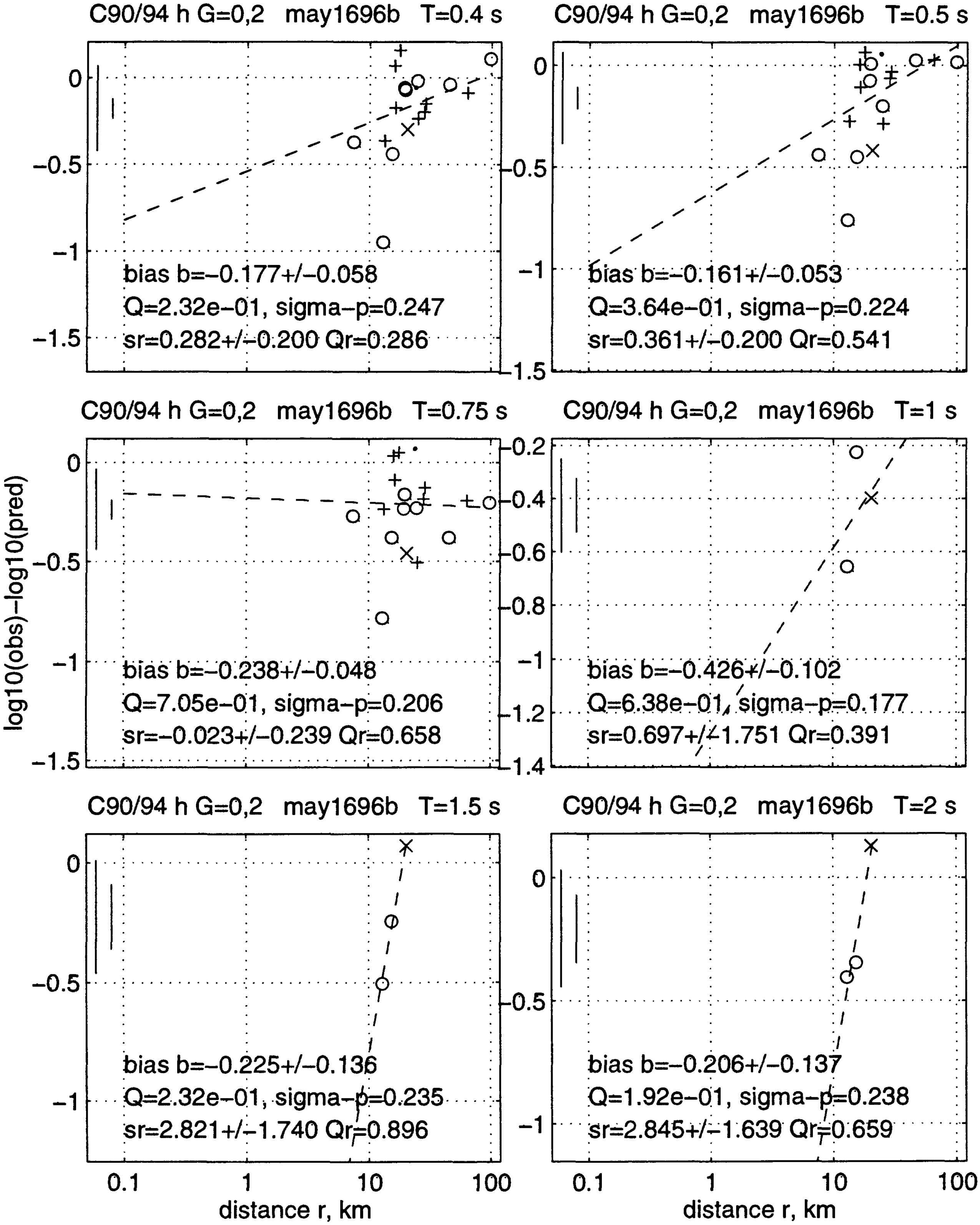

96/5/16 19:35 ymp1:[sp]may1696b5d2.eps

11j

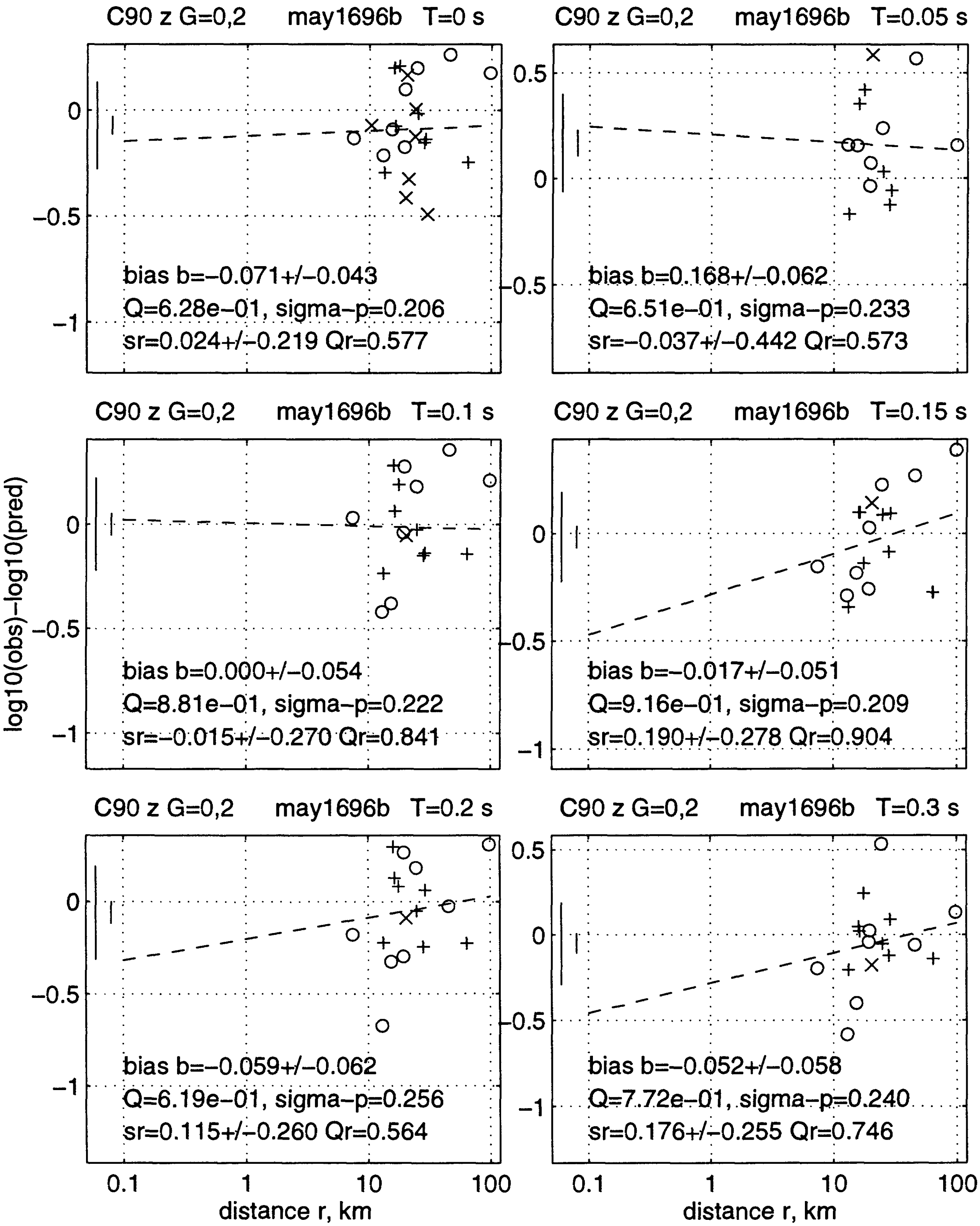

96/5/16 19:36 ymp1:[sp]may1696b6d1.eps

11k

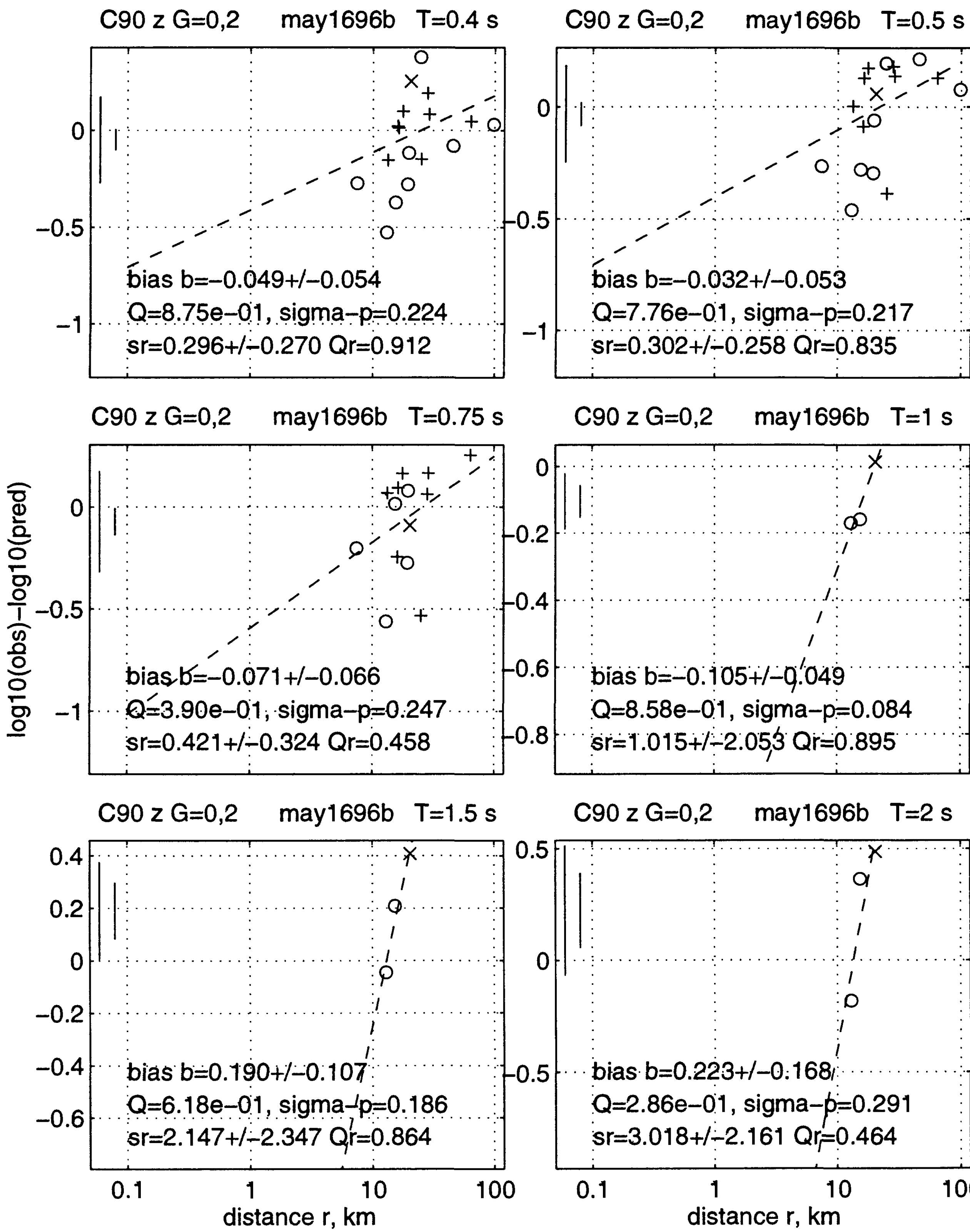

96/5/16 19:36 ymp1:[sp]may1696b6d2.eps

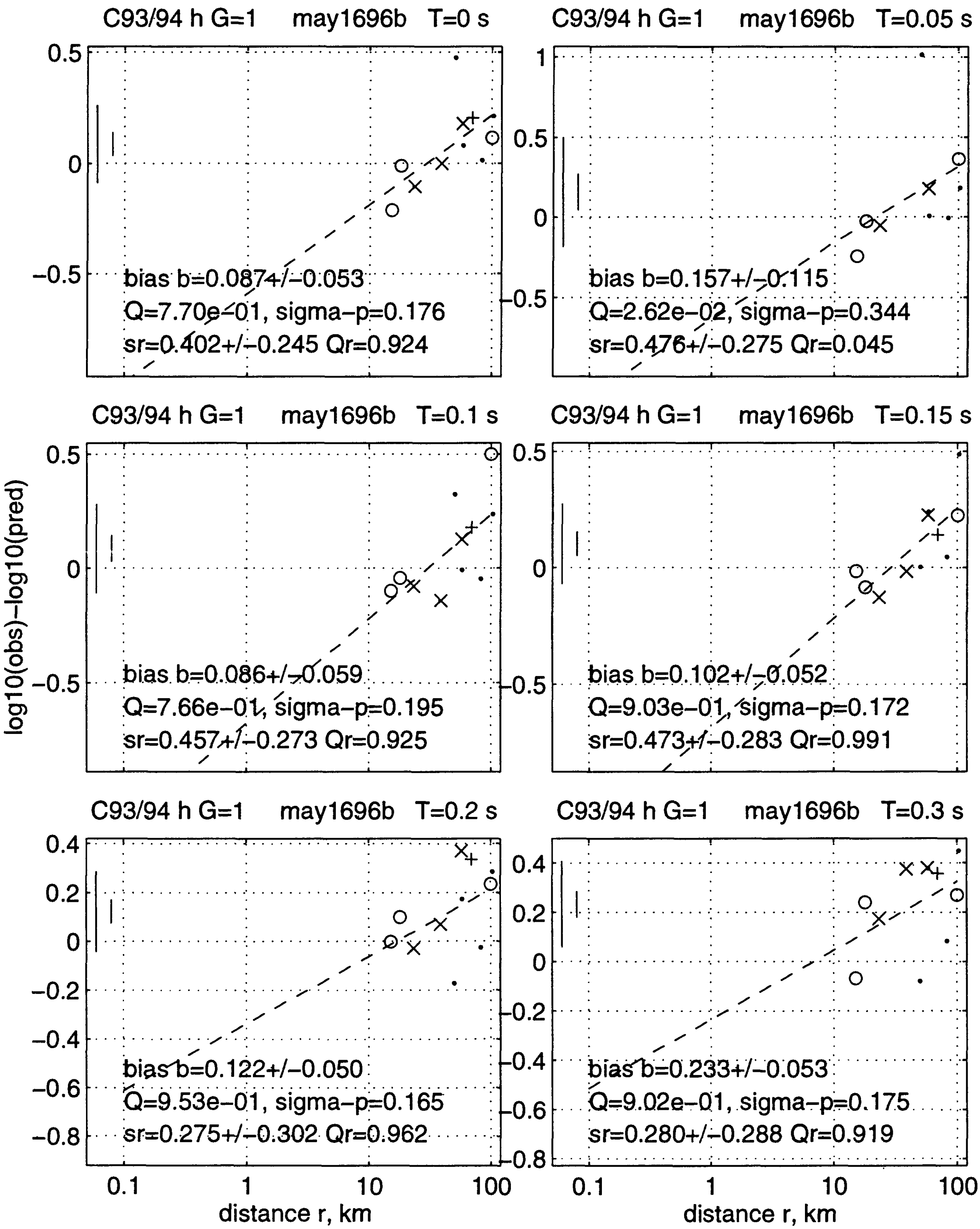

96/5/16 19:37 ymp1:[sp]may1696b7d1.eps

11m

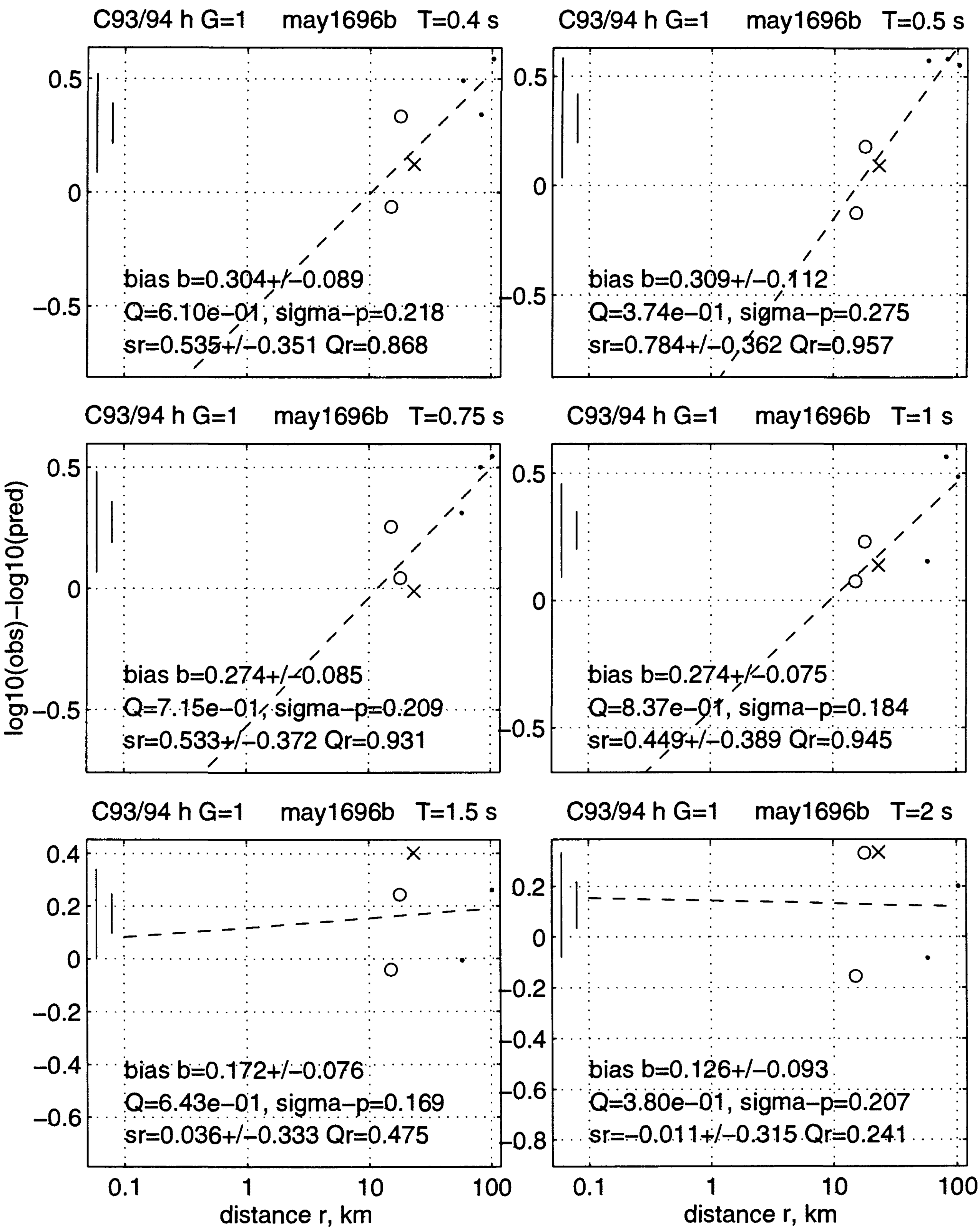

96/5/16 19:38 ymp1:[sp]may1696b7d2.eps

11n

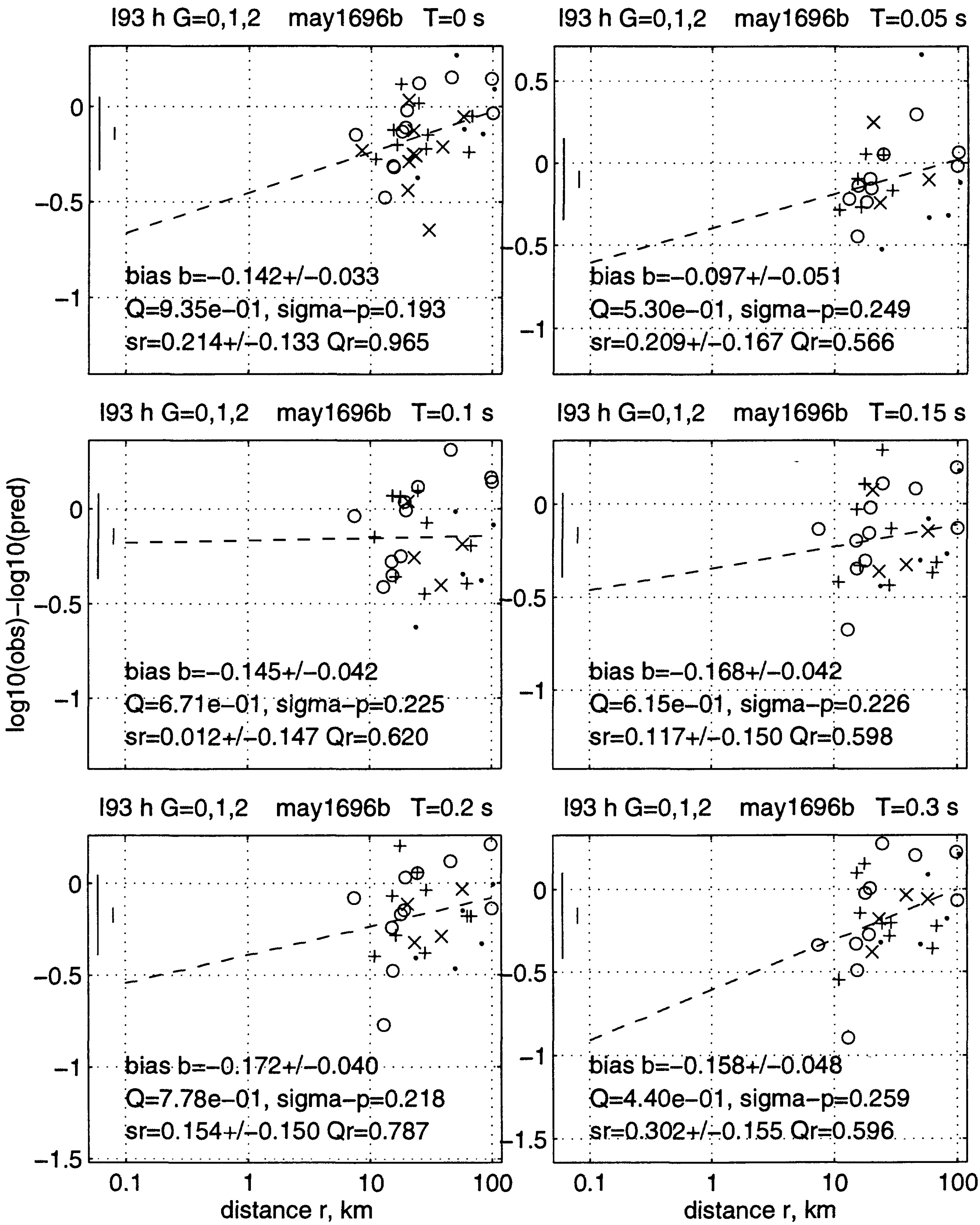

96/5/16 19:39 ymp1:[sp]may1696b8d1.eps

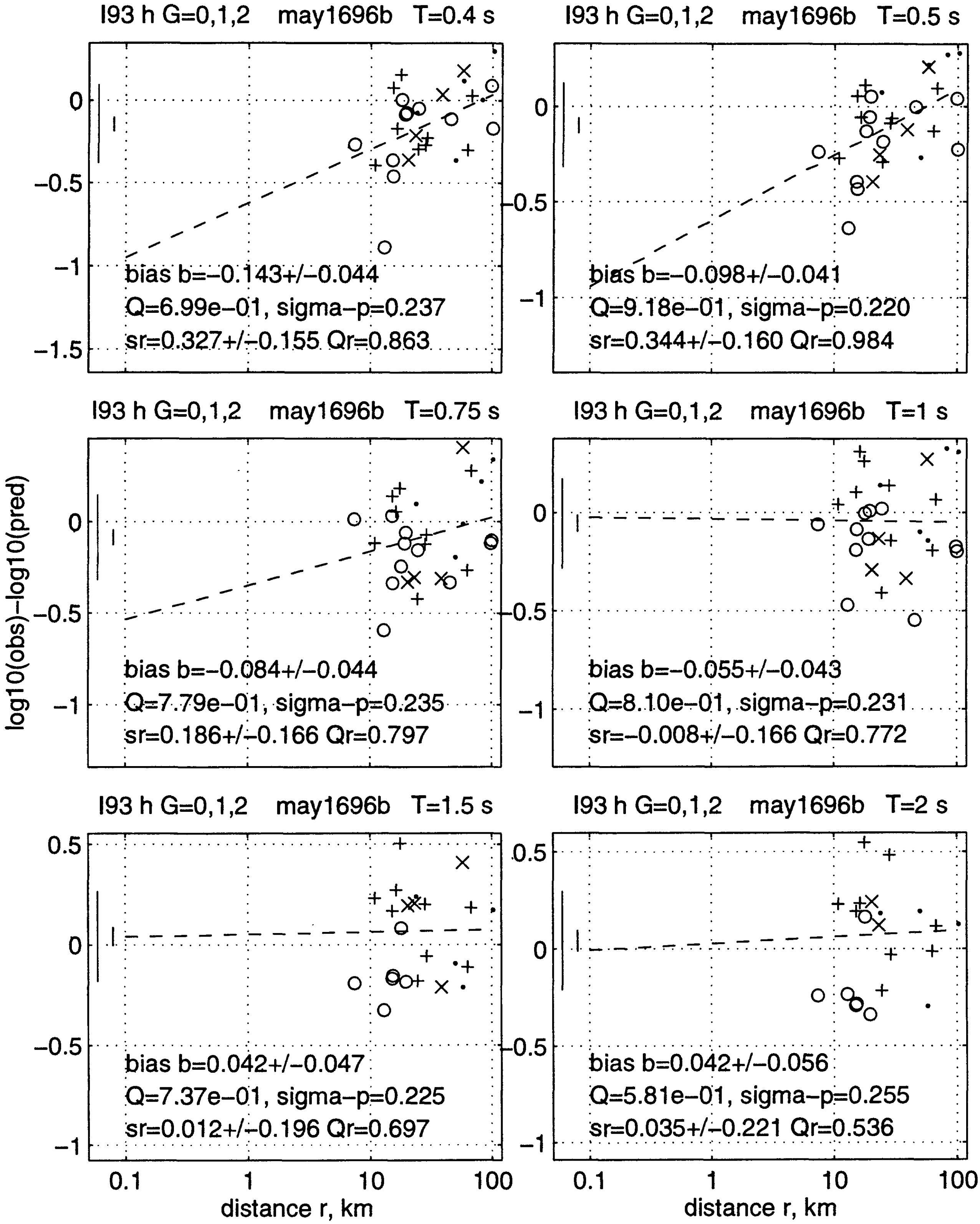

96/5/16 19:39 ymp1:[sp]may1696b8d2.eps

11p

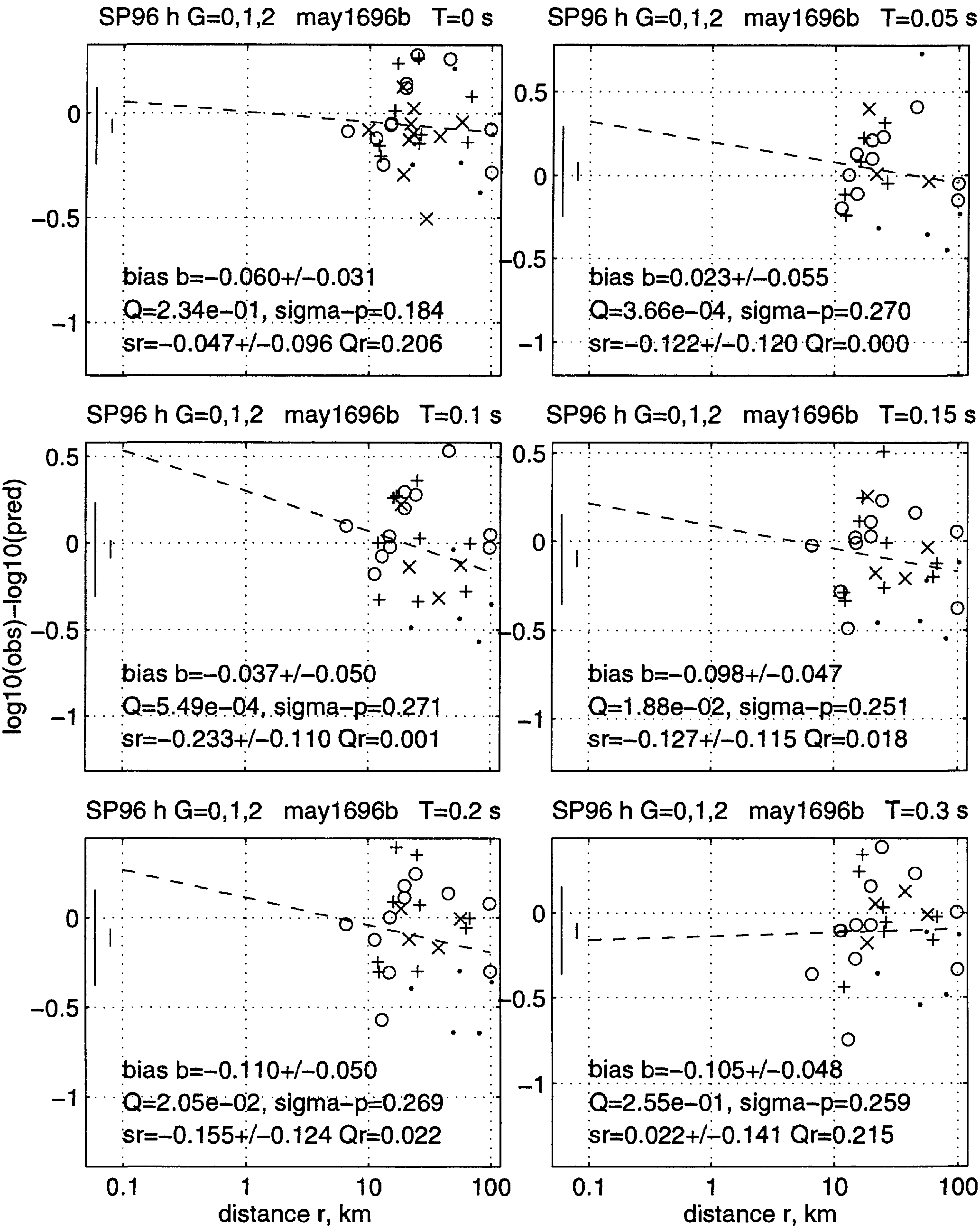

96/5/16 19:40 ymp1:[sp]may1696b9d1.eps

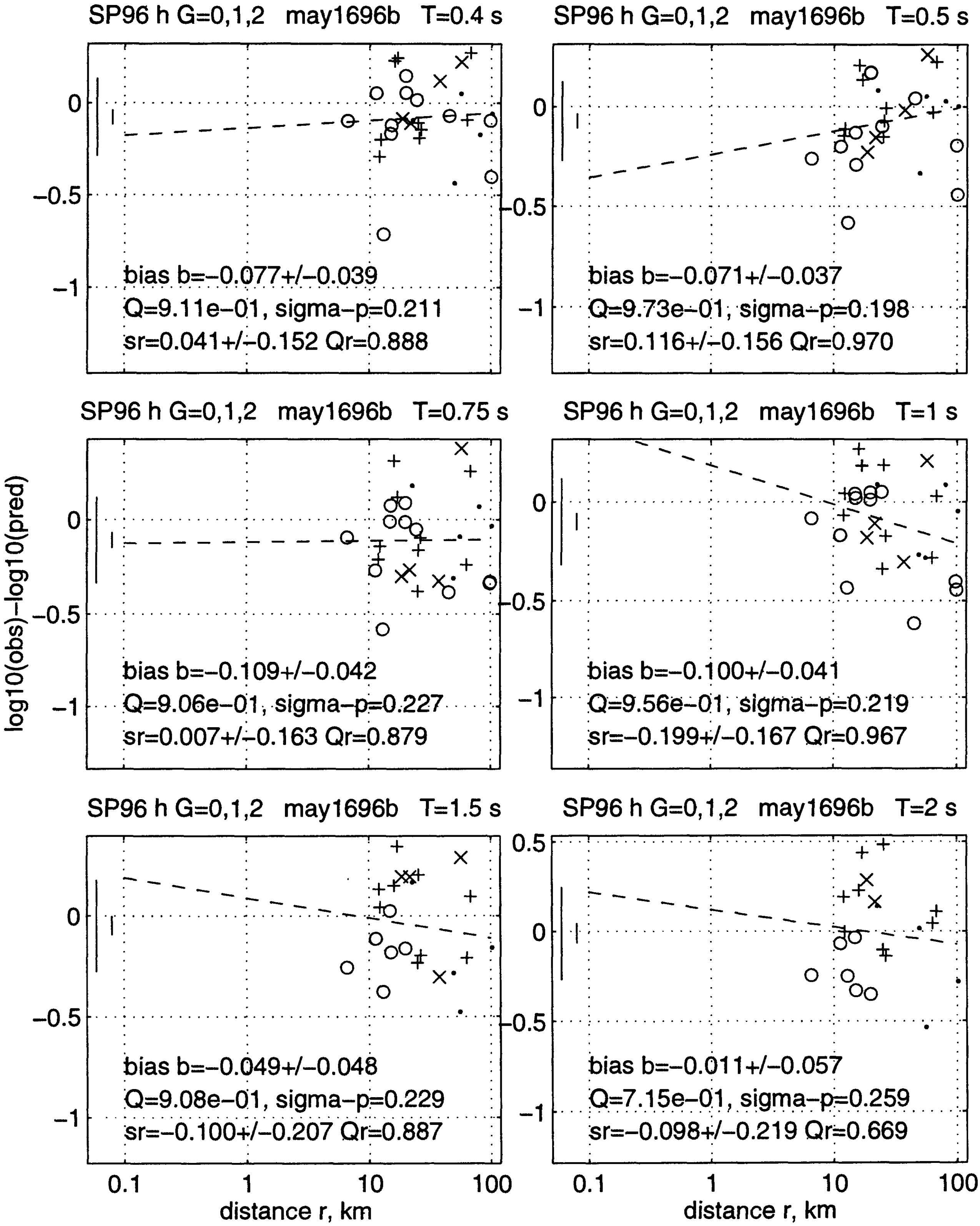

96/5/16 19:40 ymp1:[sp]may1696b9d2.eps

11r

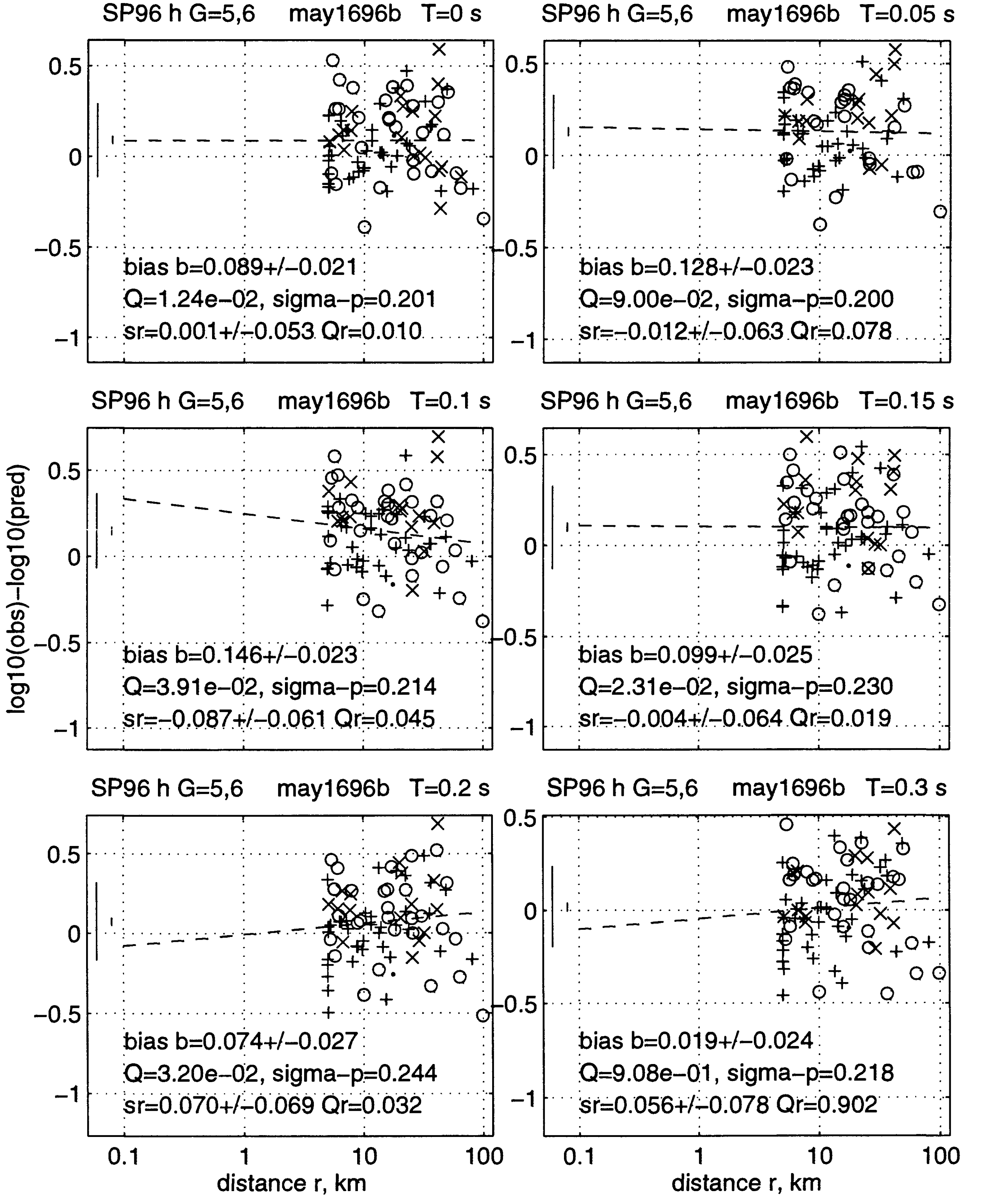

96/5/16 19:41 ymp1:[sp]may1696b10d1.eps

11s

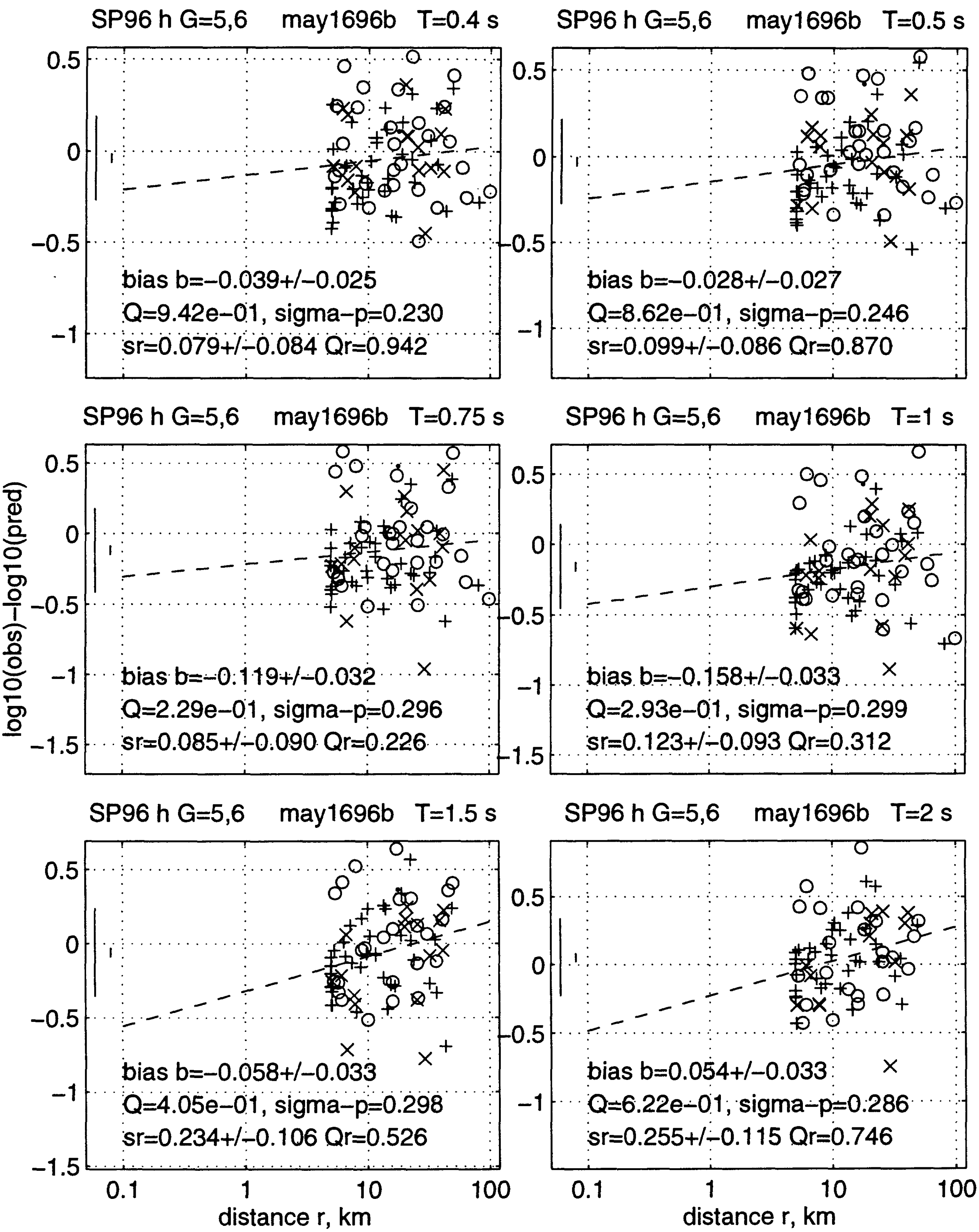

96/5/16 19:42 ymp1:[sp]may1696b10d2.eps

11t

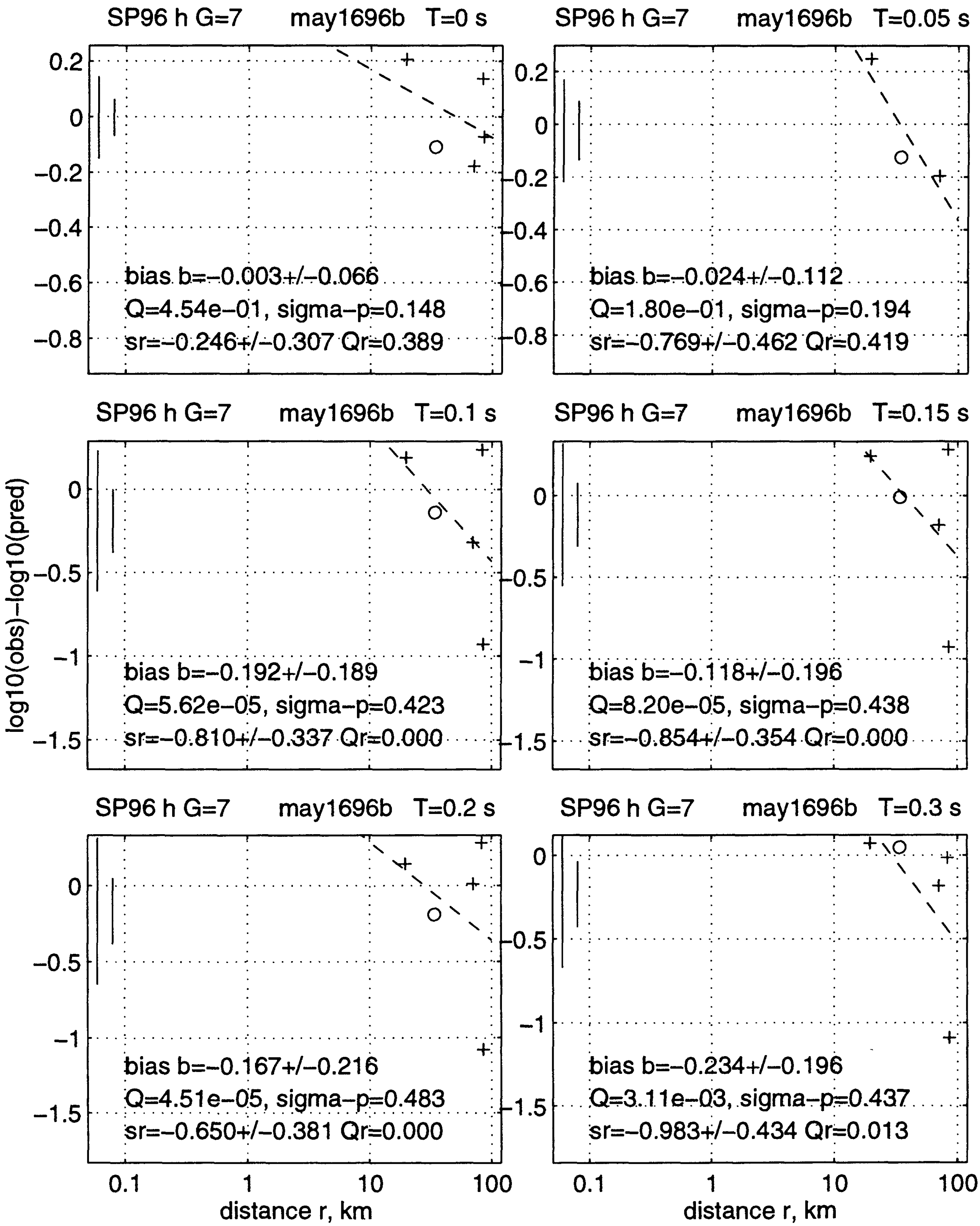

96/5/16 19:43 ymp1:[sp]may1696b11d1.eps

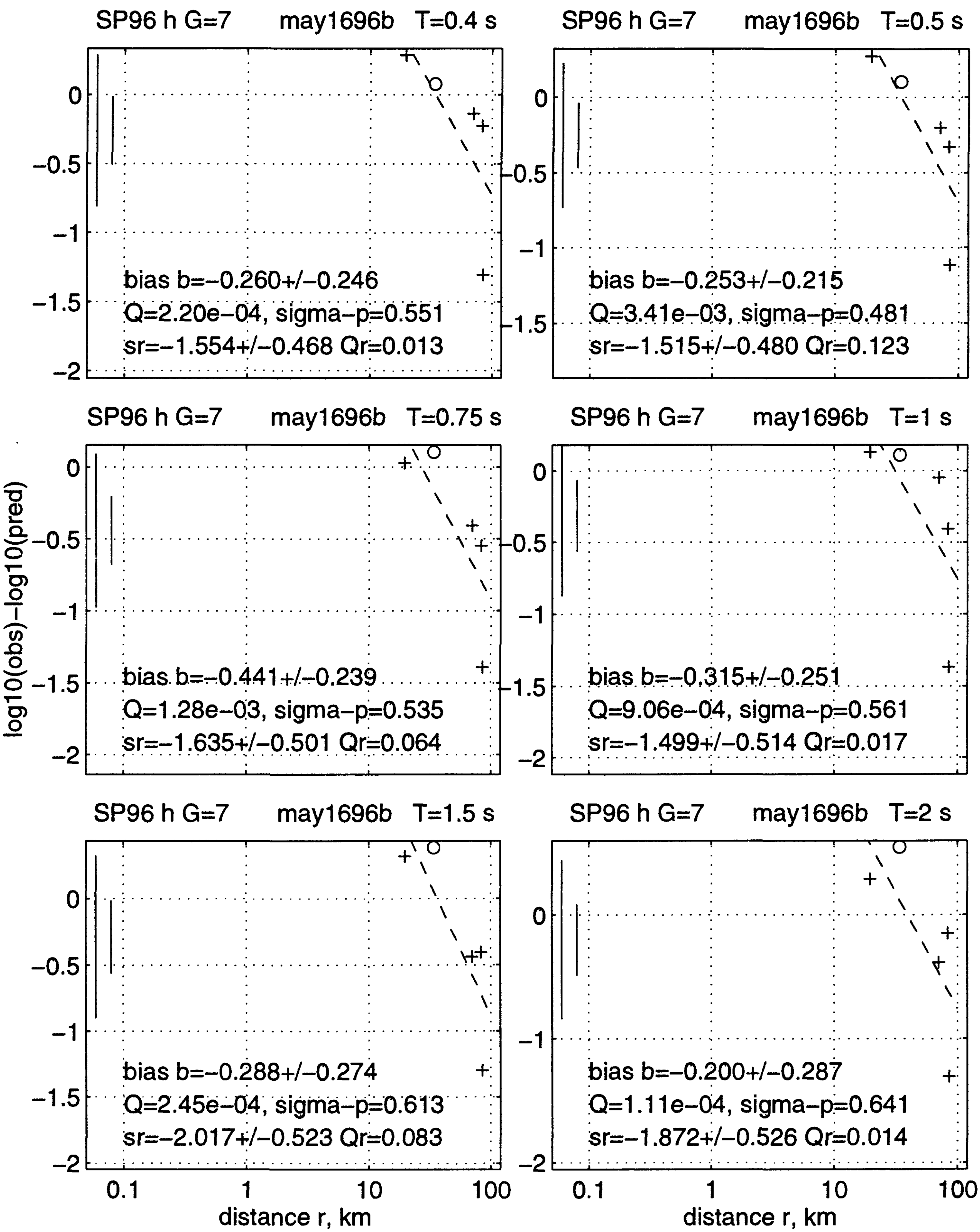

96/5/16 19:43 ymp1:[sp]may1696b11d2.eps

11 v

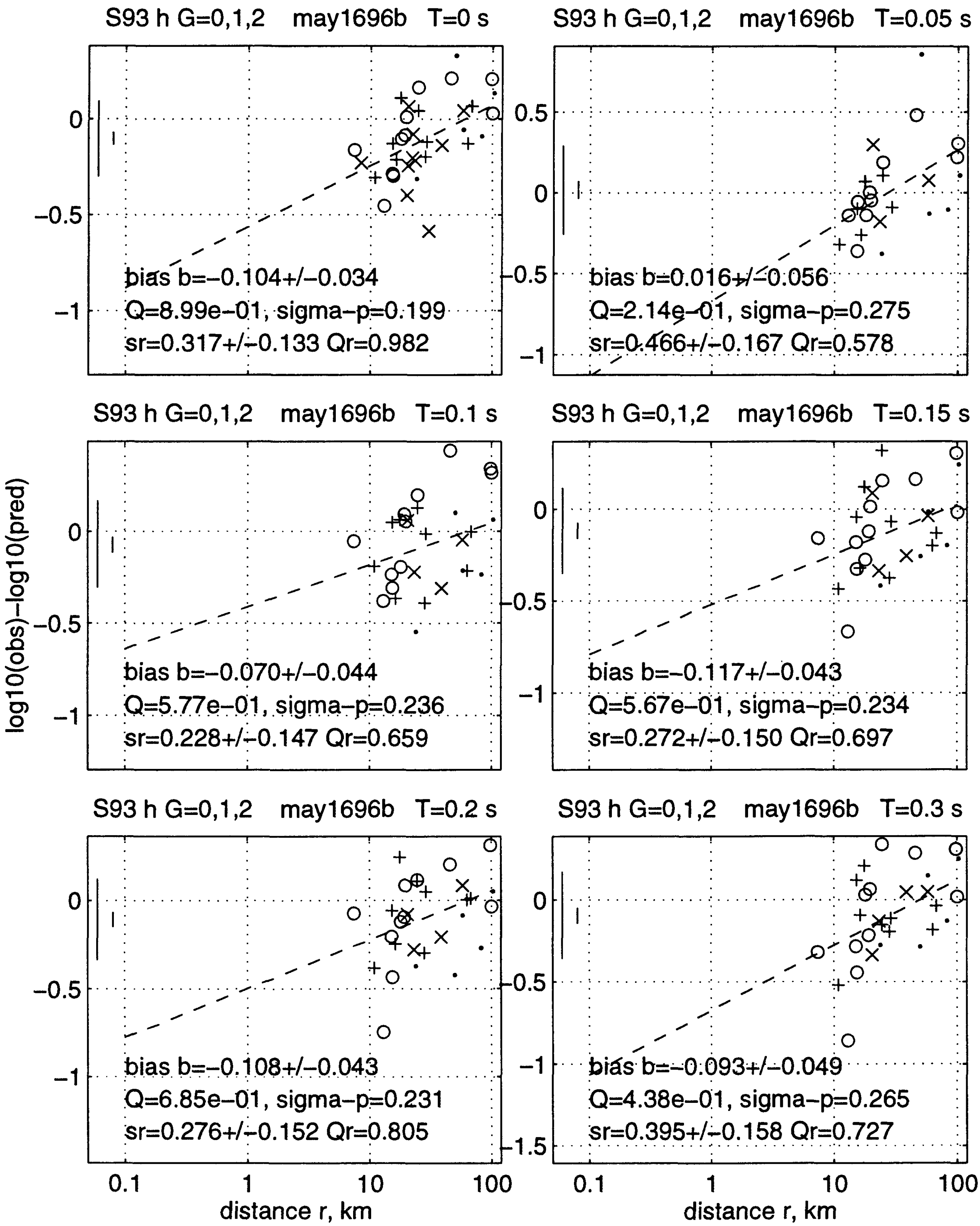

96/5/16 19:44 ymp1:[sp]may1696b12d1.eps

11w

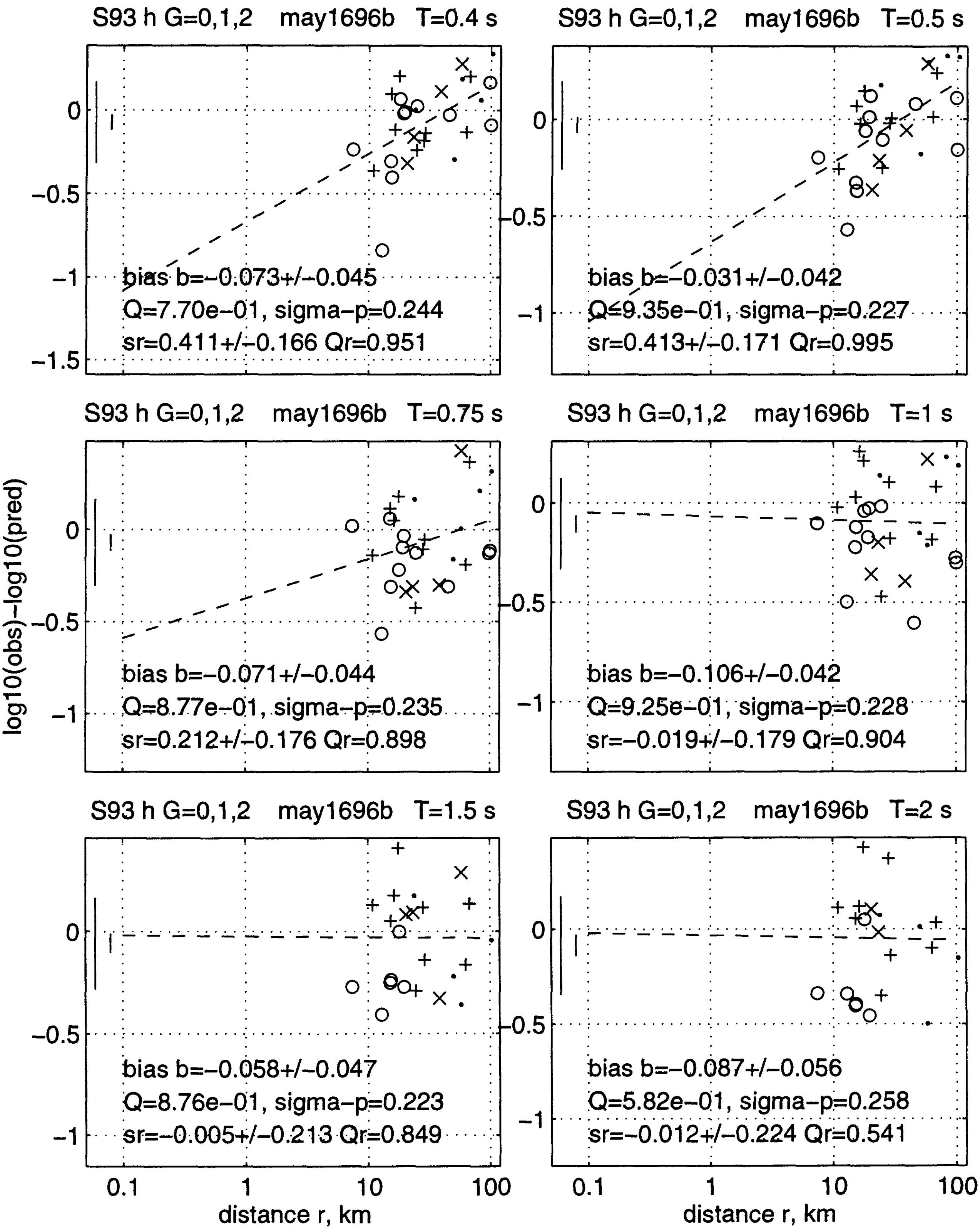

96/5/16 19:44 ymp1:[sp]may1696b12d2.eps

11X

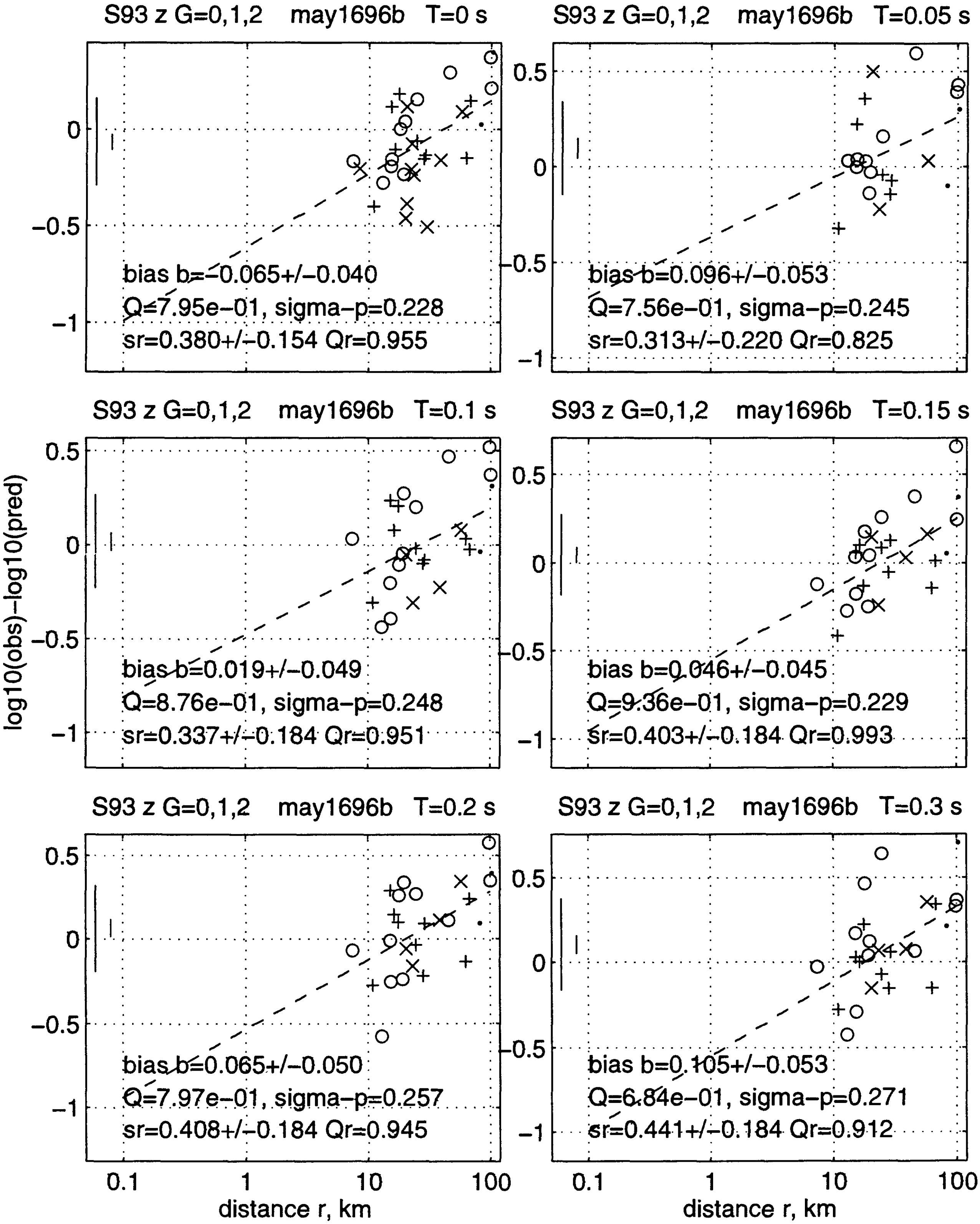

96/5/16 19:45 ymp1:[sp]may1696b13d1.eps

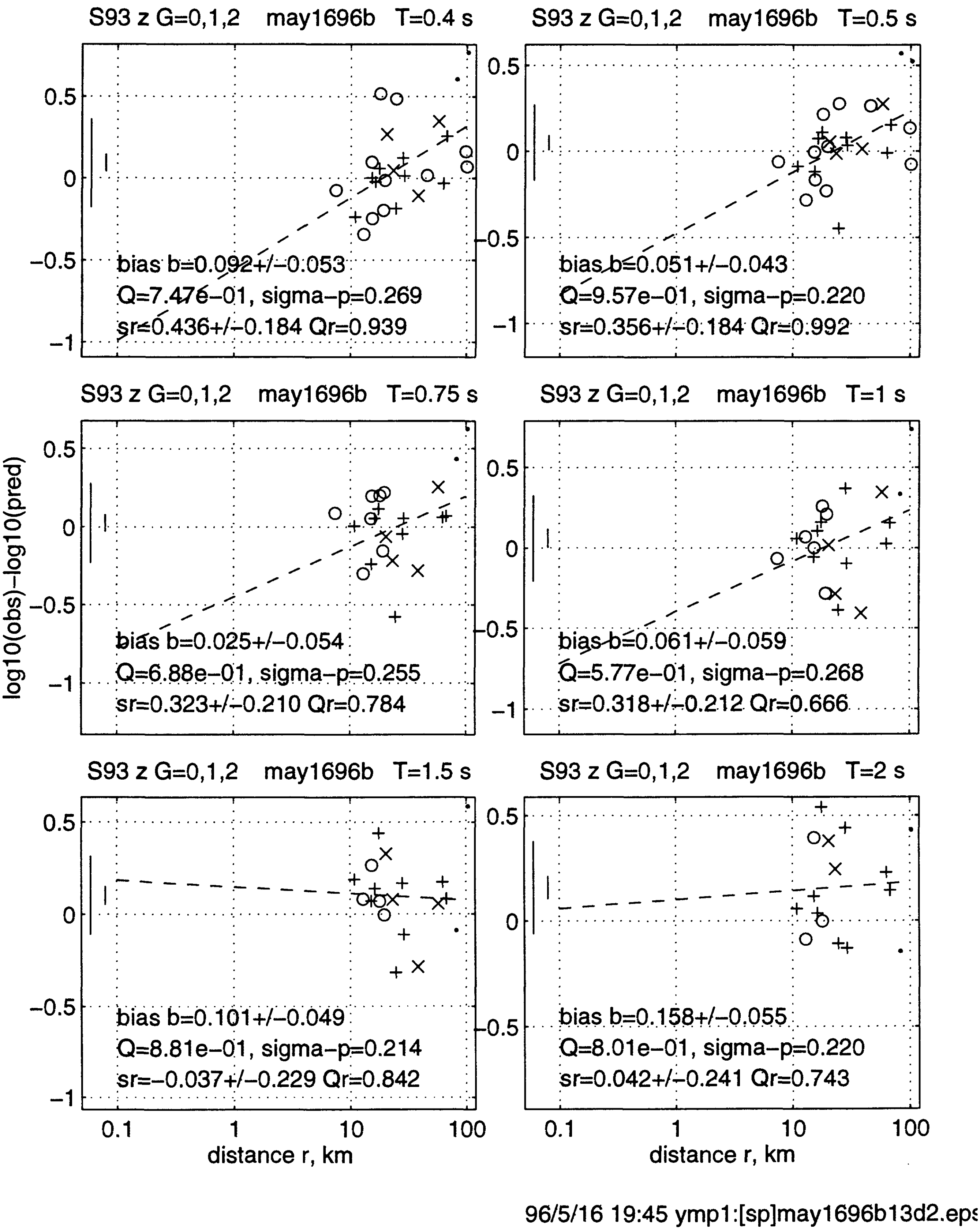
S93 z G=0,1,2 may1696b T=0.4 s
bias b=0.092+/-0.053
Q=7.47e-01, sigma-p=0.269
sr=0.436+/-0.184 Qr=0.939
S93 z G=0,1,2 may1696b T=0.5 s
bias b=0.051+/-0.043
Q=9.57e-01, sigma-p=0.220
sr=0.356+/-0.184 Qr=0.992
S93 z G=0,1,2 may1696b T=0.75 s
bias b=0.025+/-0.054
Q=6.88e-01, sigma-p=0.255
sr=0.323+/-0.210 Qr=0.784
S93 z G=0,1,2 may1696b T=1 s
bias b=0.061+/-0.059
Q=5.77e-01, sigma-p=0.268
sr=0.318+/-0.212 Qr=0.666
S93 z G=0,1,2 may1696b T=1.5 s
bias b=0.101+/-0.049
Q=8.81e-01, sigma-p=0.214
sr=-0.037+/-0.229 Qr=0.842
S93 z G=0,1,2 may1696b T=2 s
bias b=0.158+/-0.055
Q=8.01e-01, sigma-p=0.220
sr=0.042+/-0.241 Qr=0.743
log10(obs)-log10(pred)
distance r, km
0.1
1
10
100
96/5/16 19:45 ymp1:[sp]may1696b13d2.eps

117

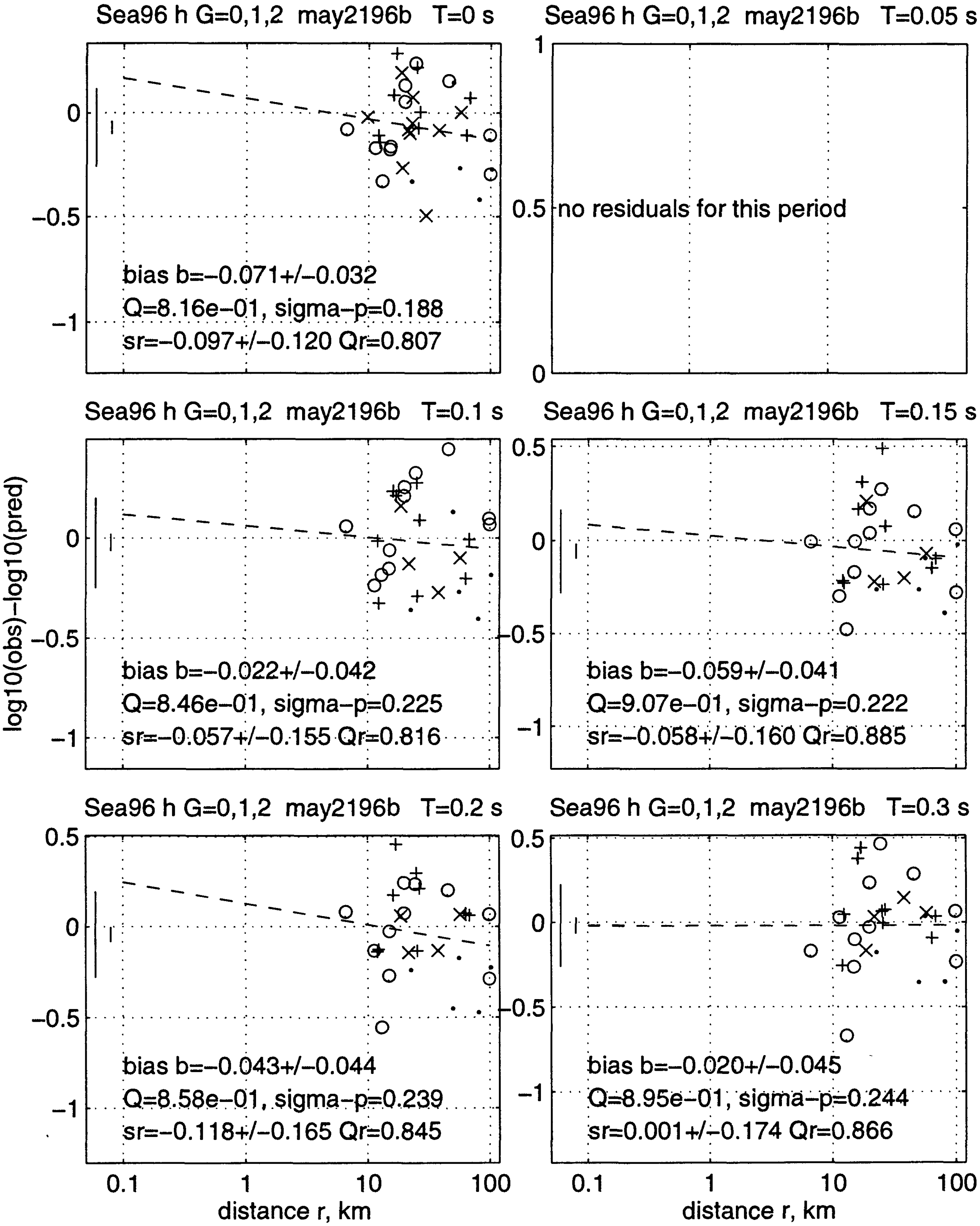

96/5/22 13:39 ymp1:[sp]may2196b22d1.eps

11aa

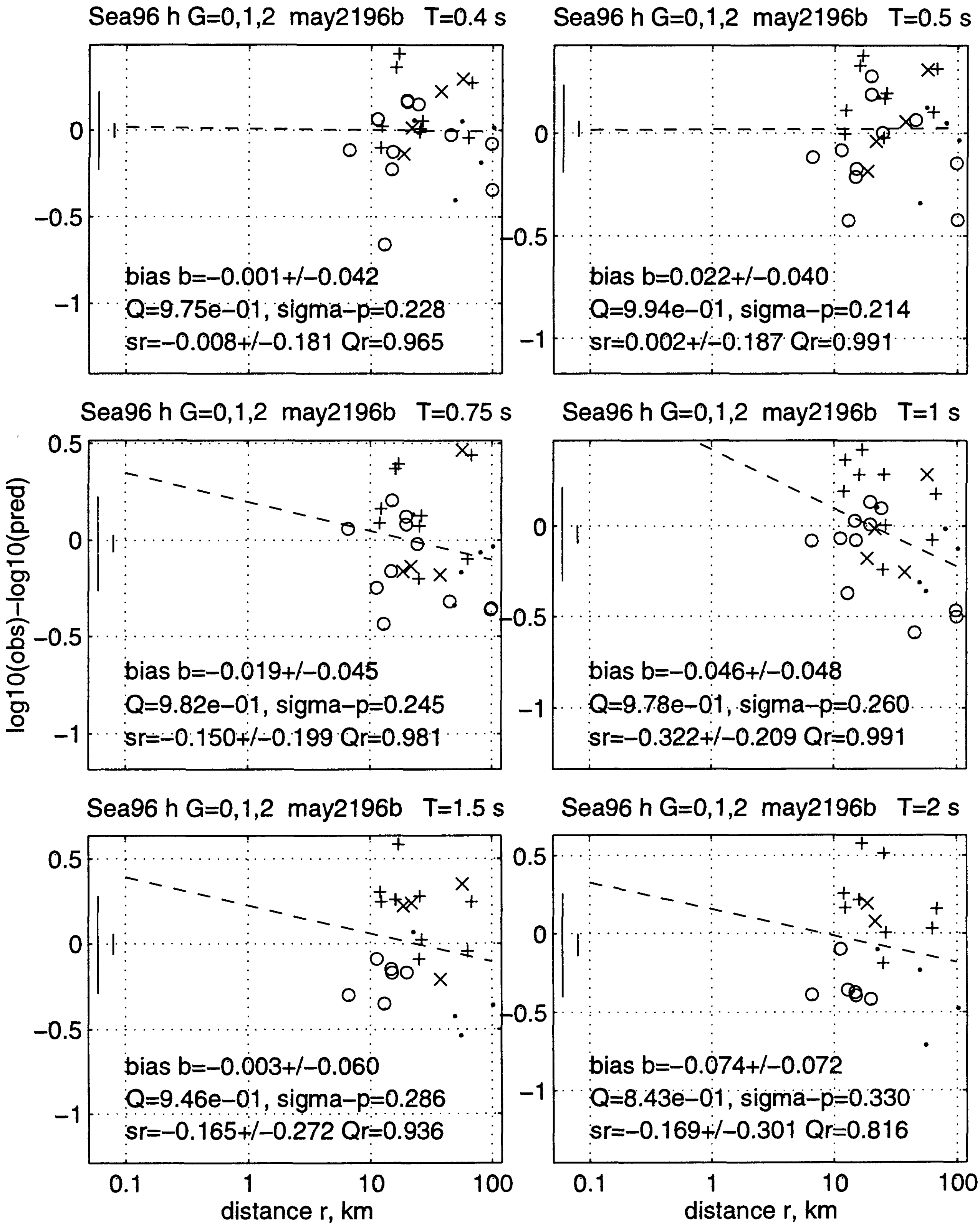

96/5/22 13:39 ymp1:[sp]may2196b22d2.eps

11ab

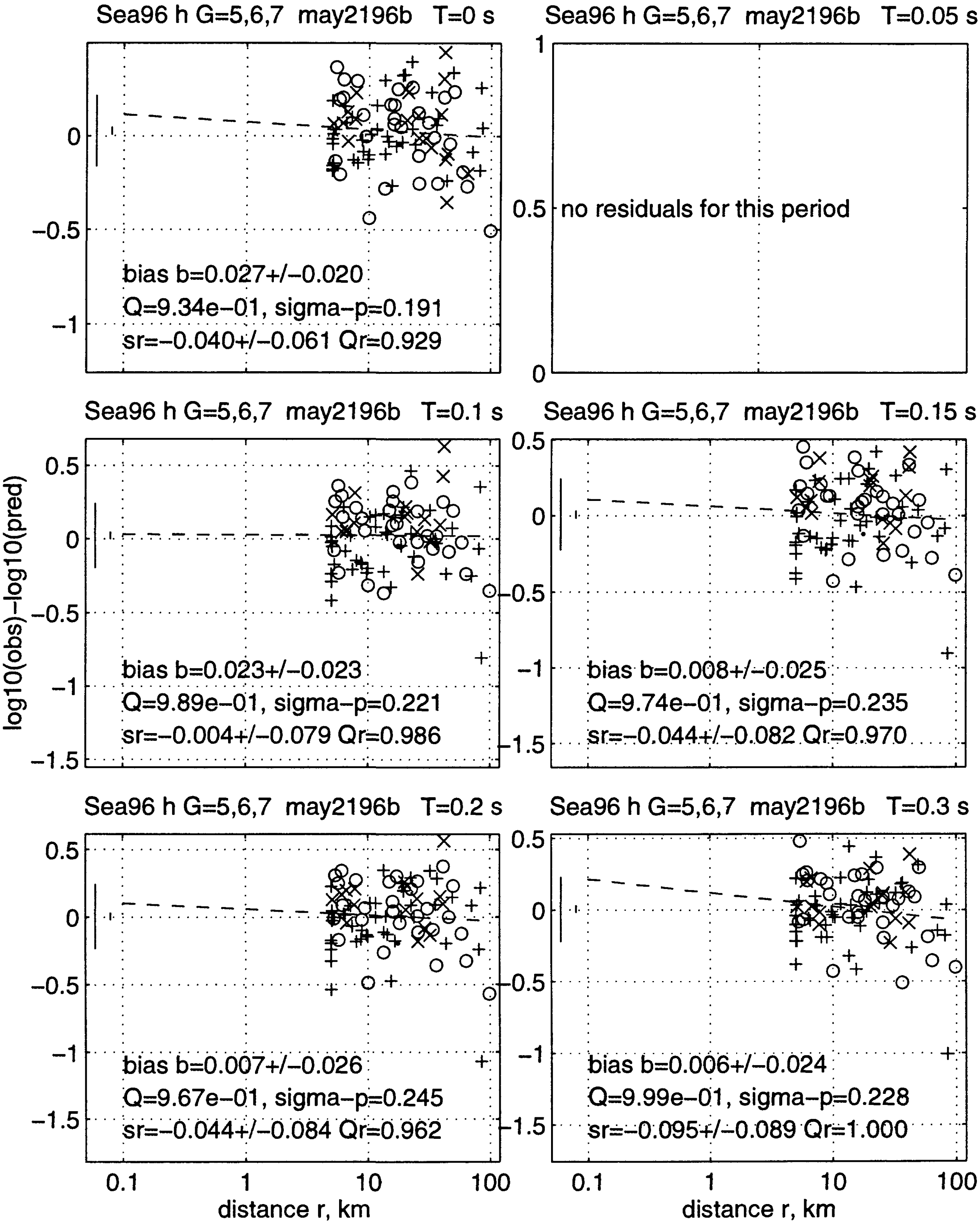

96/5/22 13:28 ymp1:[sp]may2196b23d1.eps

11ac

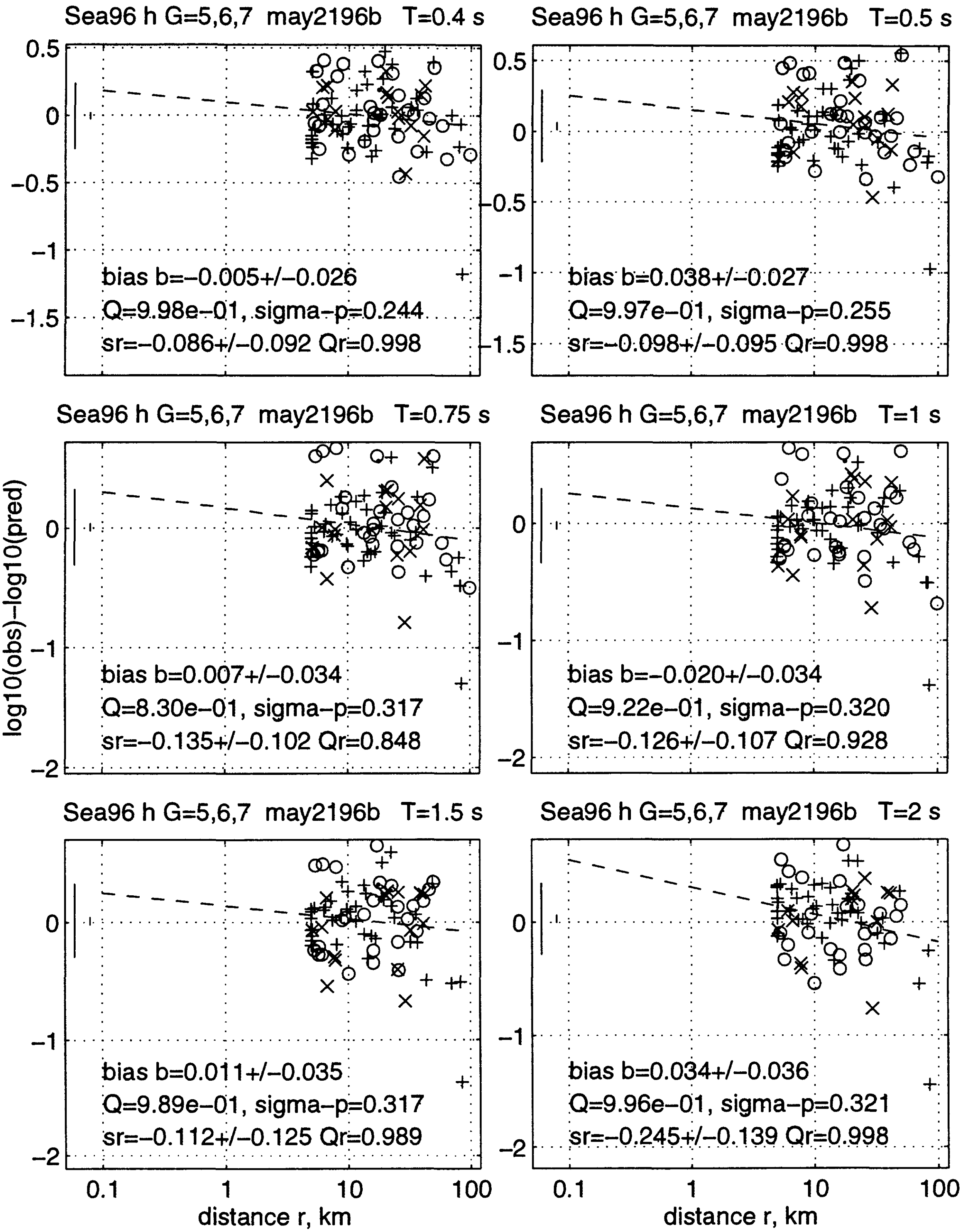

96/5/22 13:28 ymp1:[sp]may2196b23d2.eps

11ad

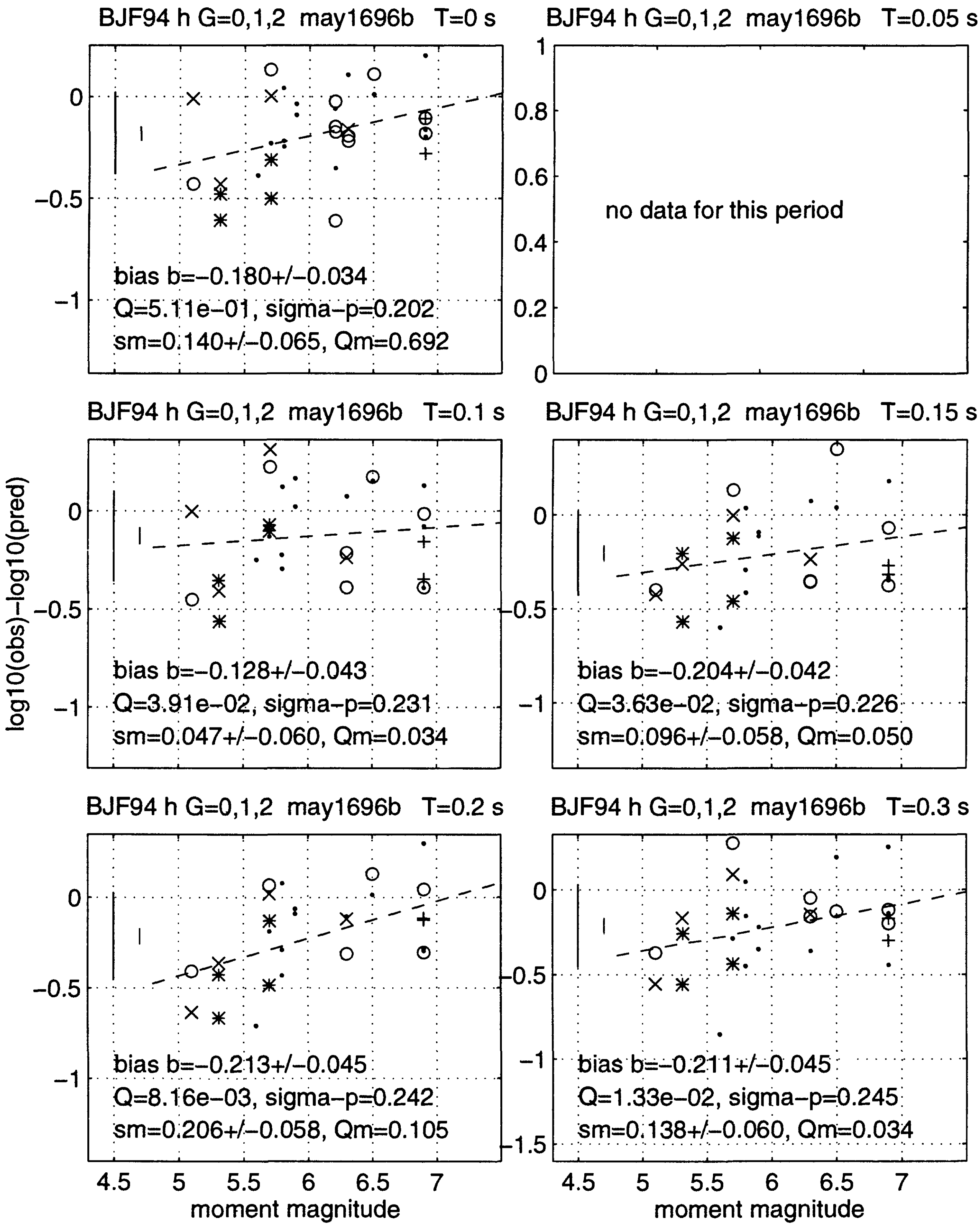

96/5/16 19:30 ymp1:[sp]may1696b1m1.eps

12a

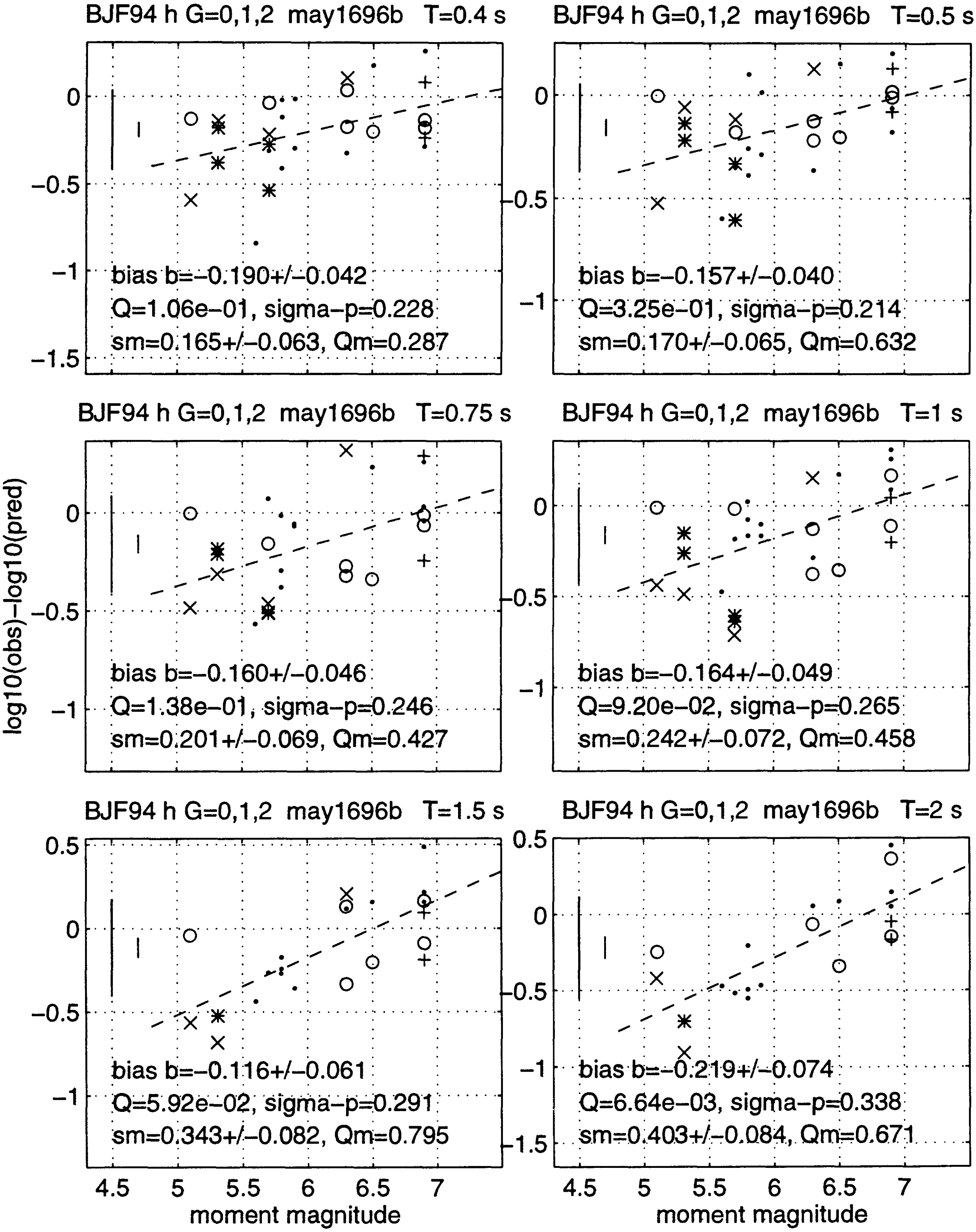

96/5/16 19:30 ymp1:[sp]may1696b1m2.eps

12b

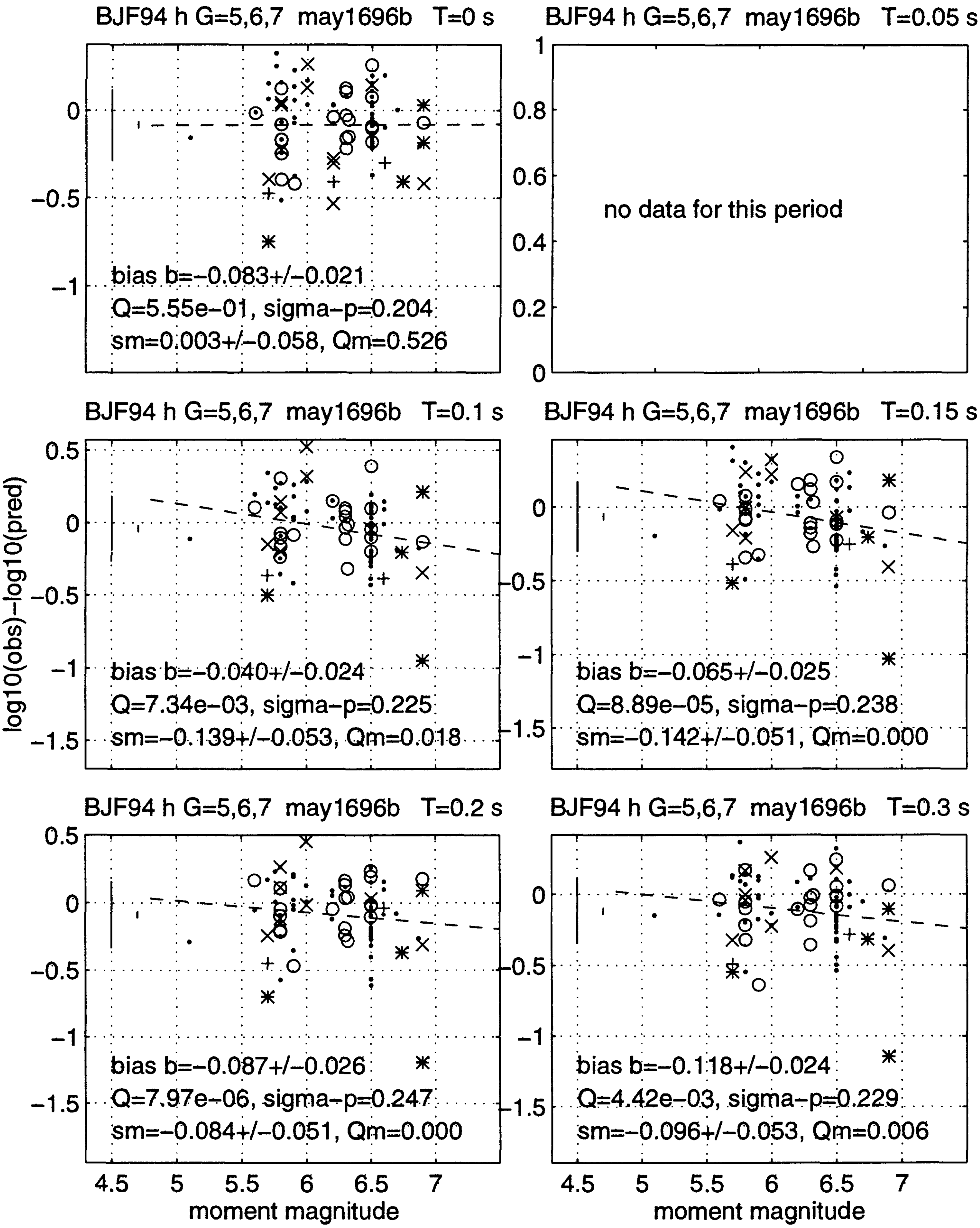

96/5/16 19:31 ymp1:[sp]may1696b2m1.eps

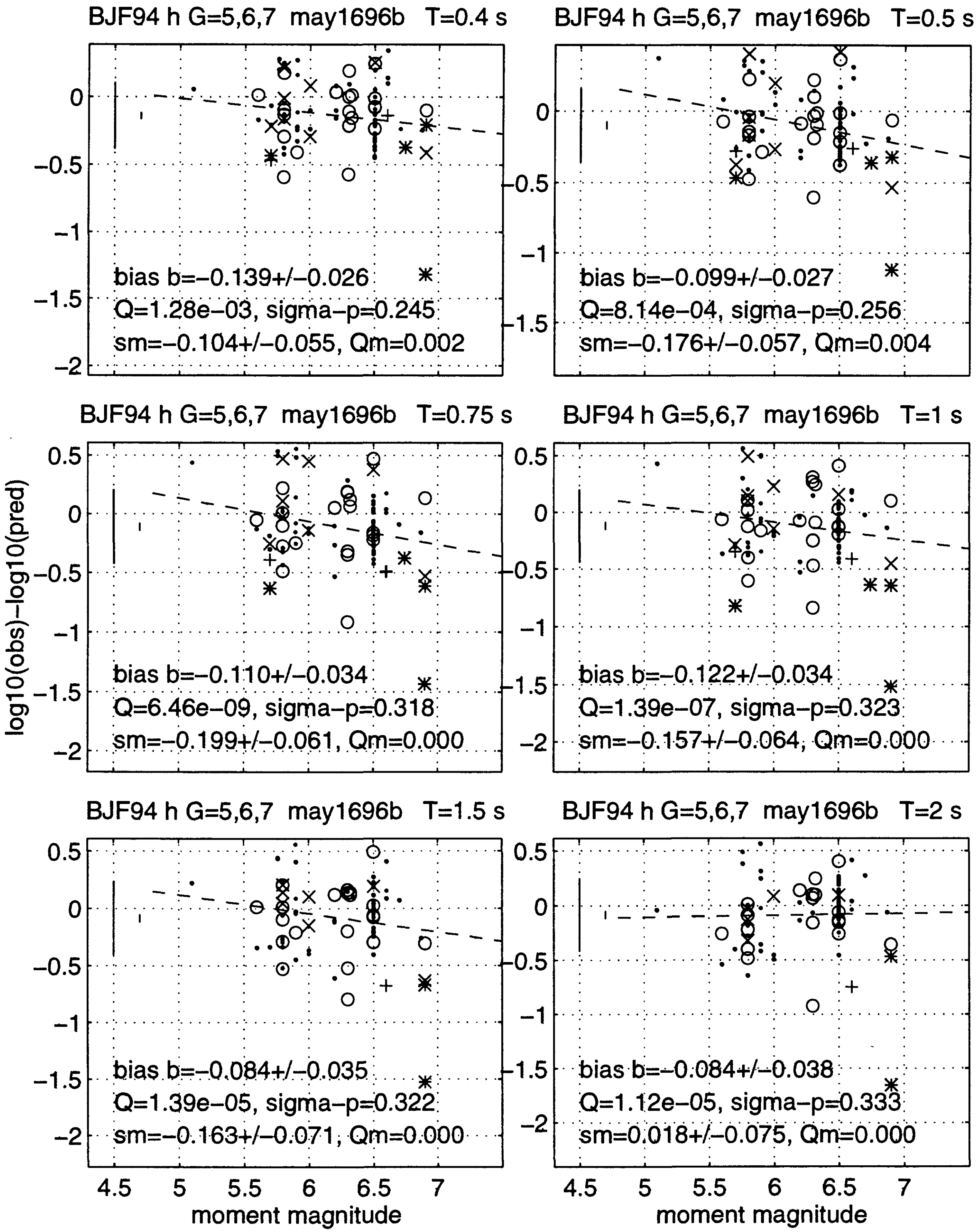

96/5/16 19:32 ymp1:[sp]may1696b2m2.eps

12d

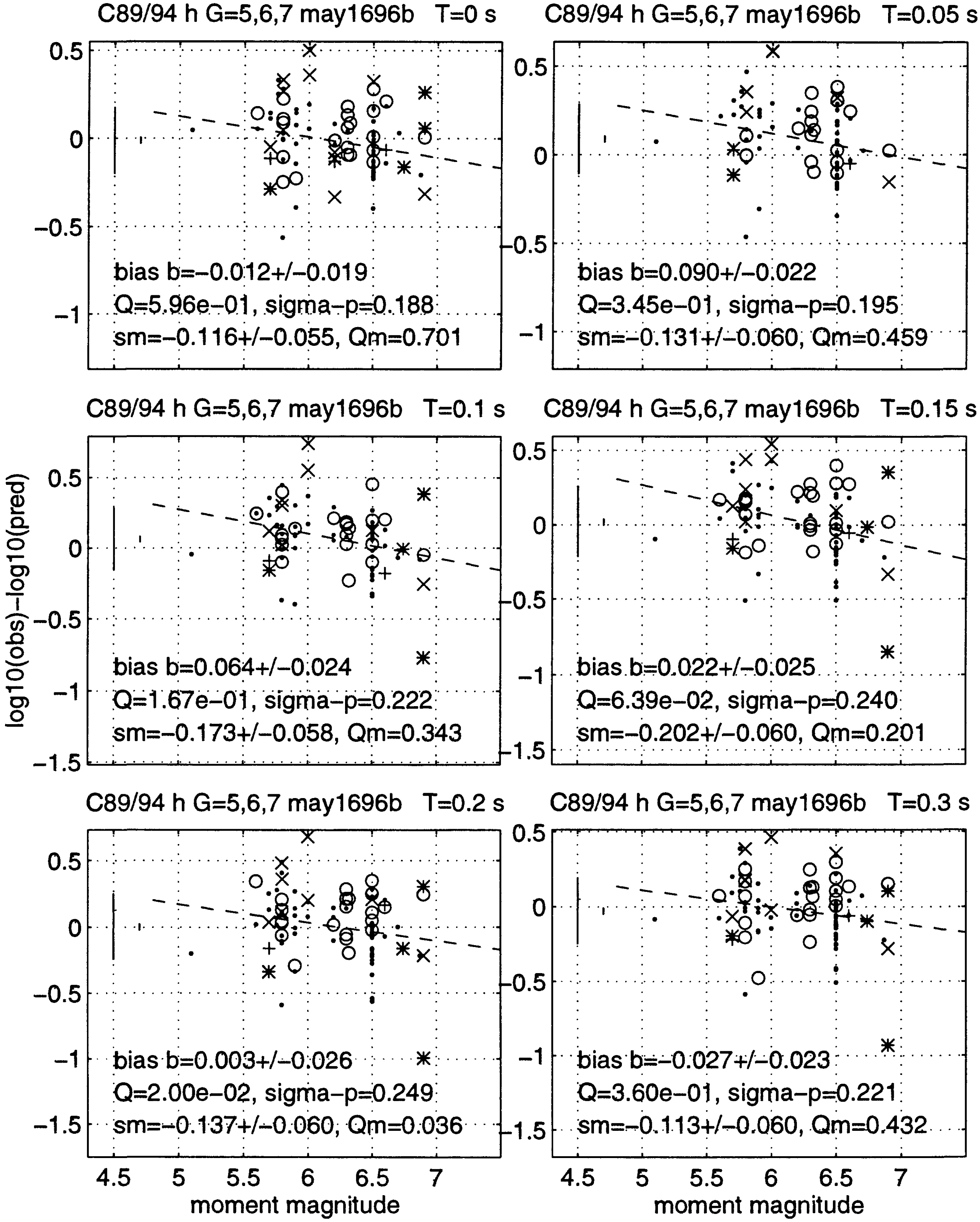

96/5/16 19:33 ymp1:[sp]may1696b3m1.eps

12e

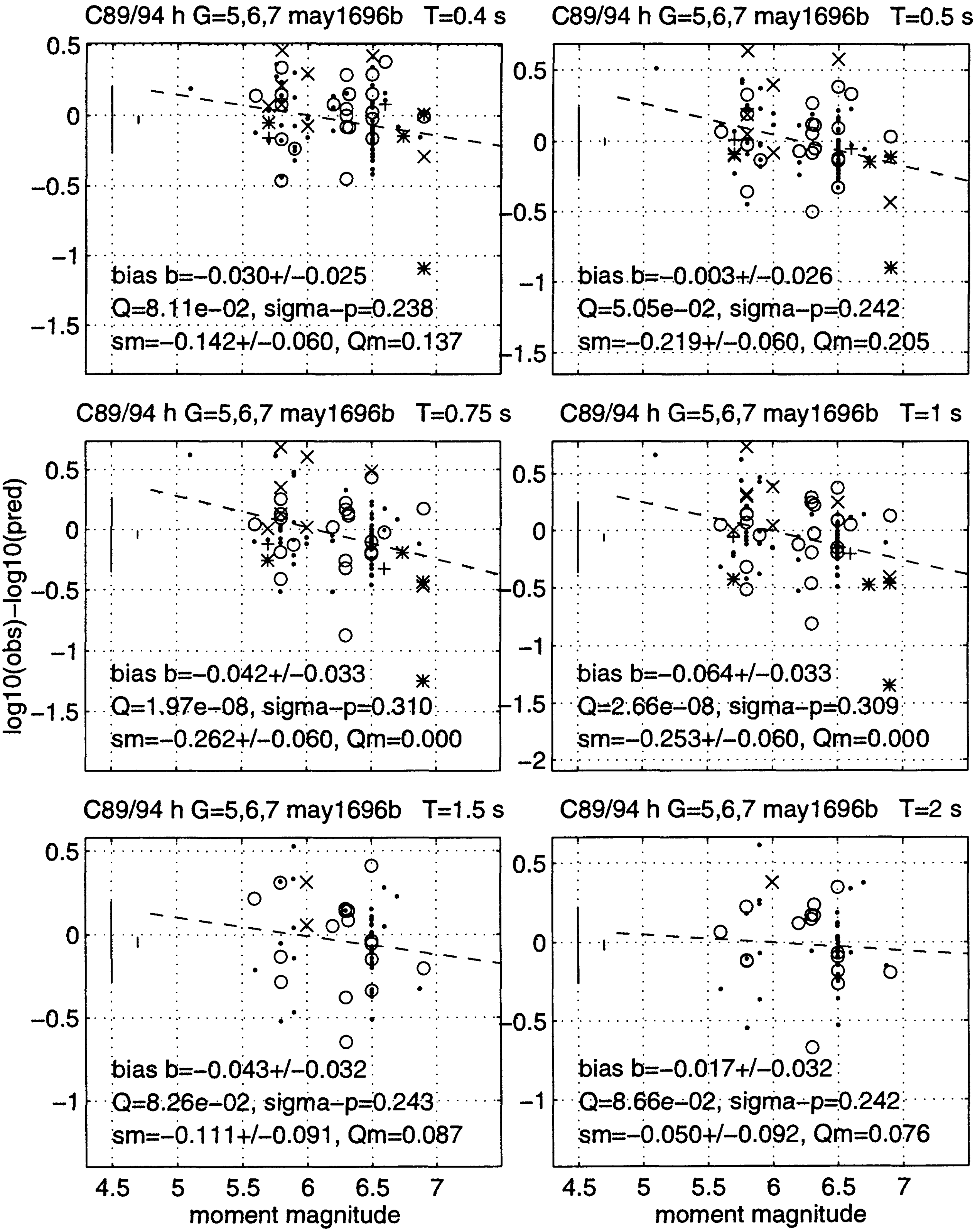

96/5/16 19:33 ymp1:[sp]may1696b3m2.eps

12f

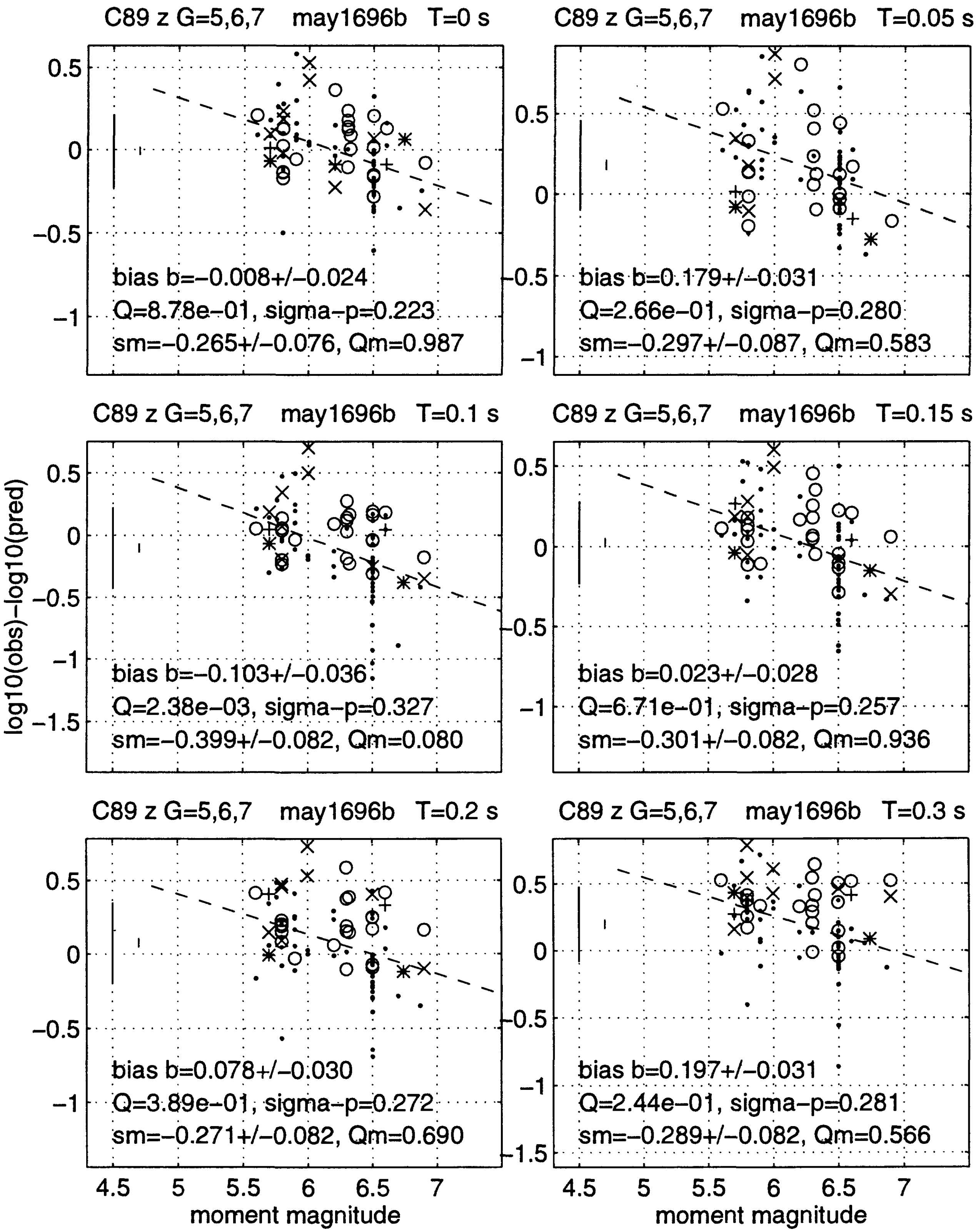

96/5/16 19:34 ymp1:[sp]may1696b4m1.eps

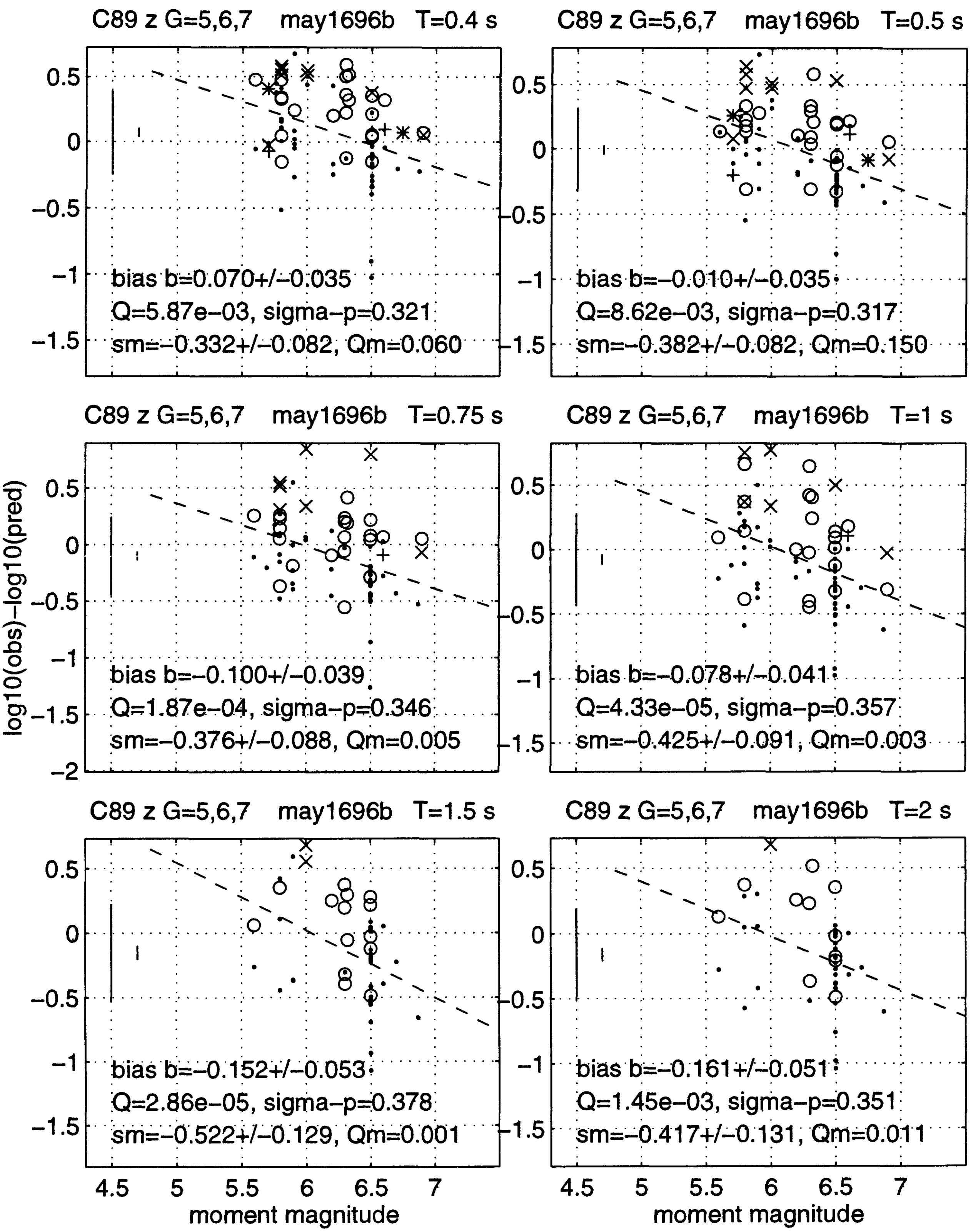

96/5/16 19:34 ymp1:[sp]may1696b4m2.eps

12h

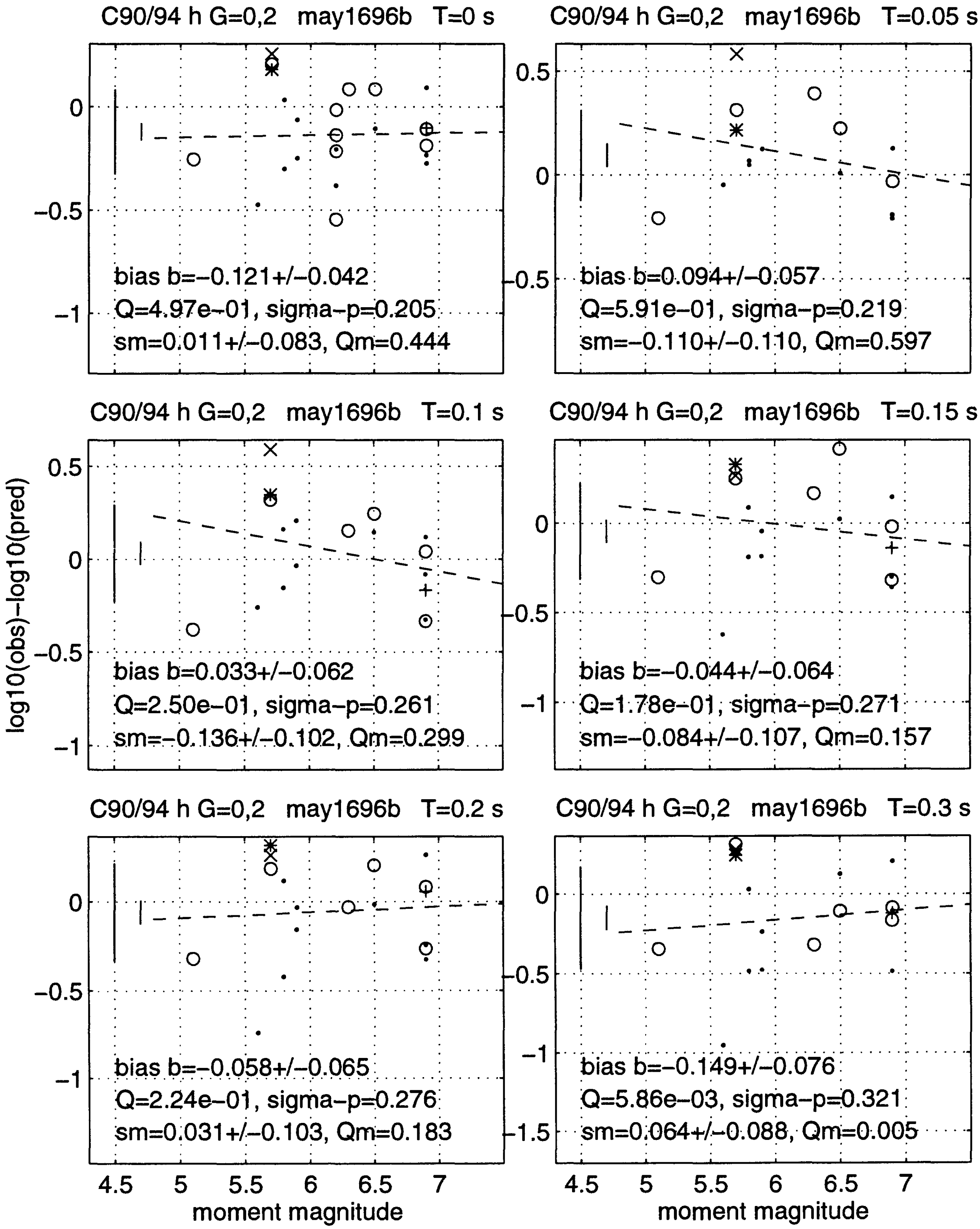

96/5/16 19:35 ymp1:[sp]may1696b5m1.eps

12i

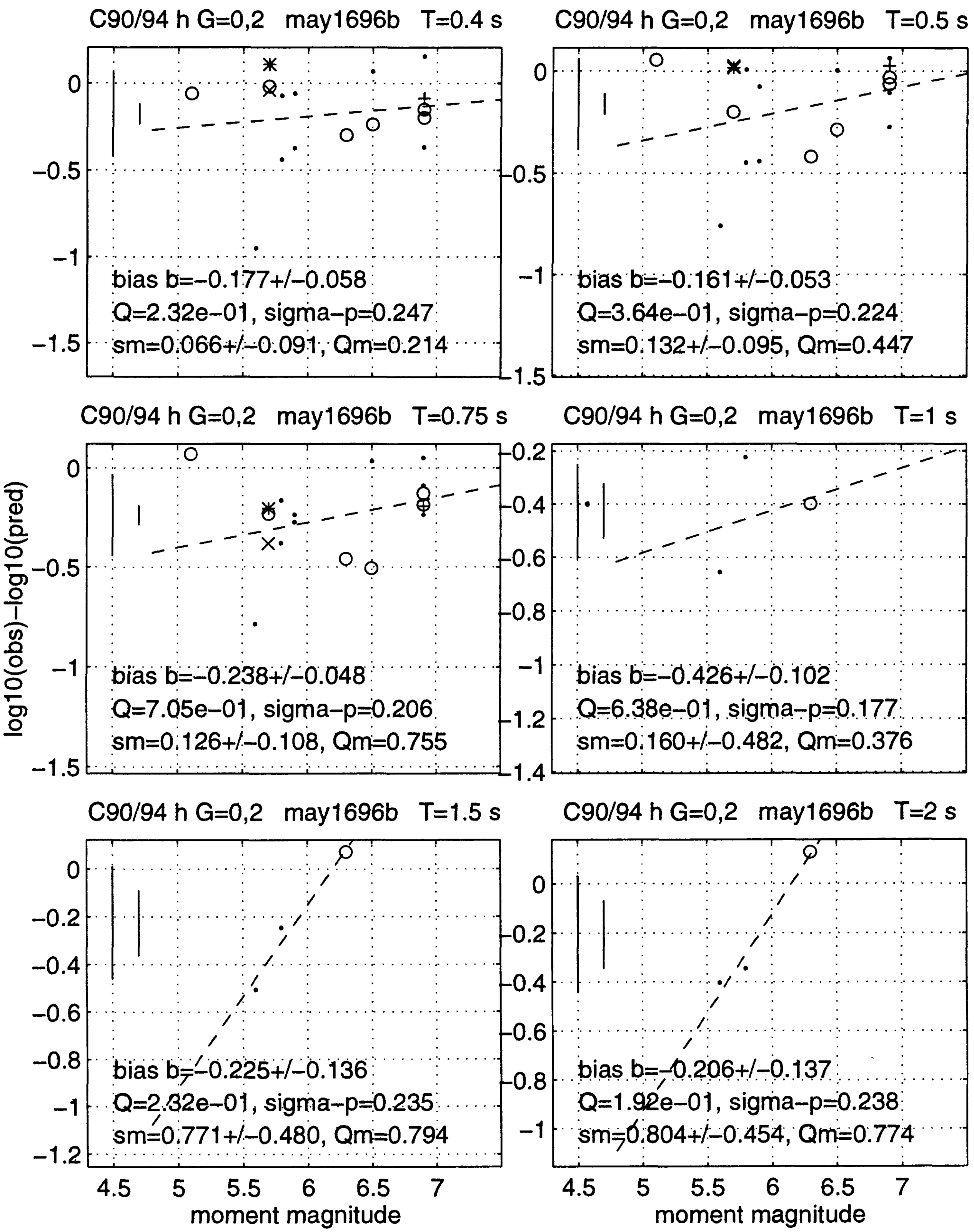

96/5/16 19:36 ymp1:[sp]may1696b5m2.eps

12j

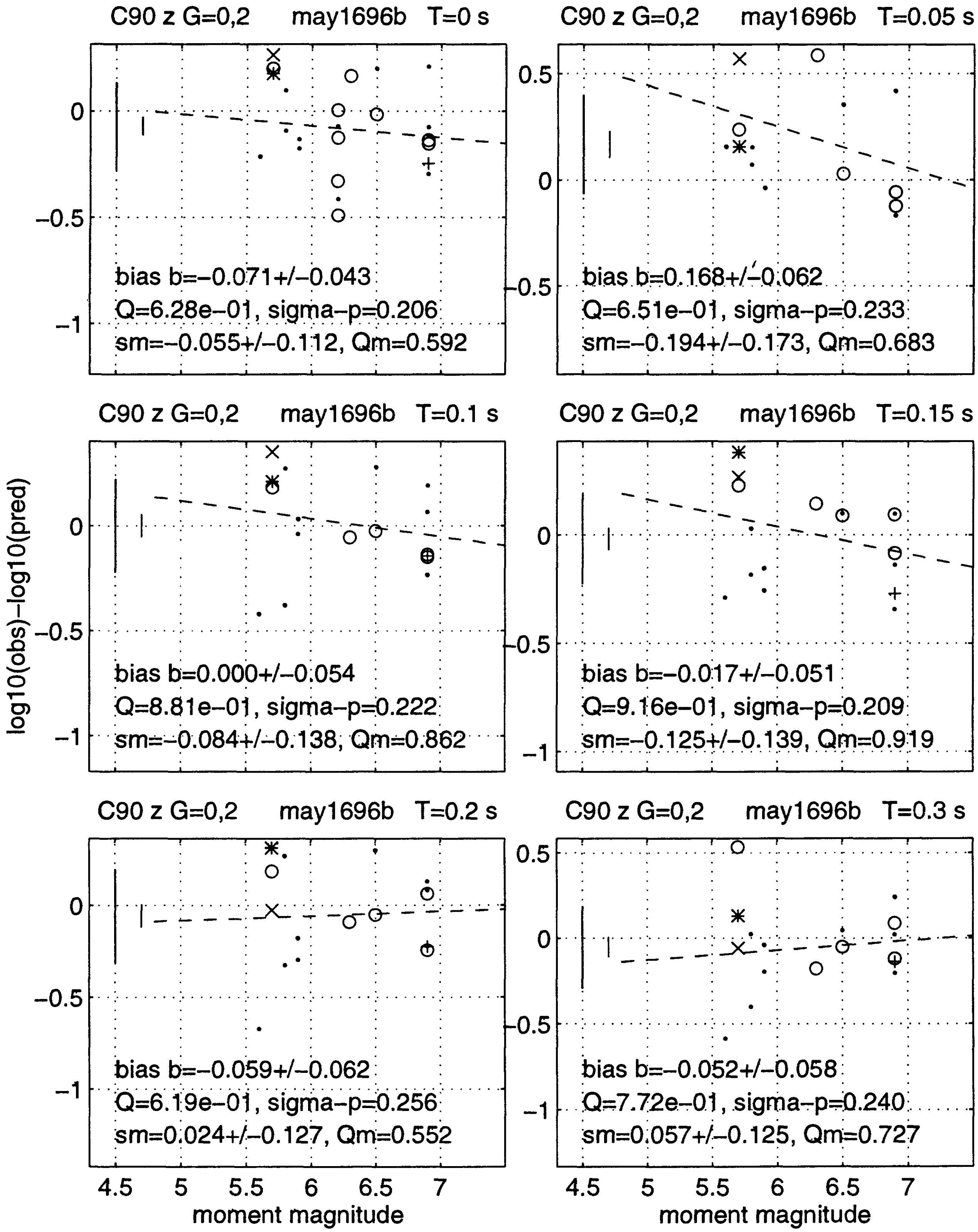

96/5/16 19:37 ymp1:[sp]may1696b6m1.eps

200

12 k

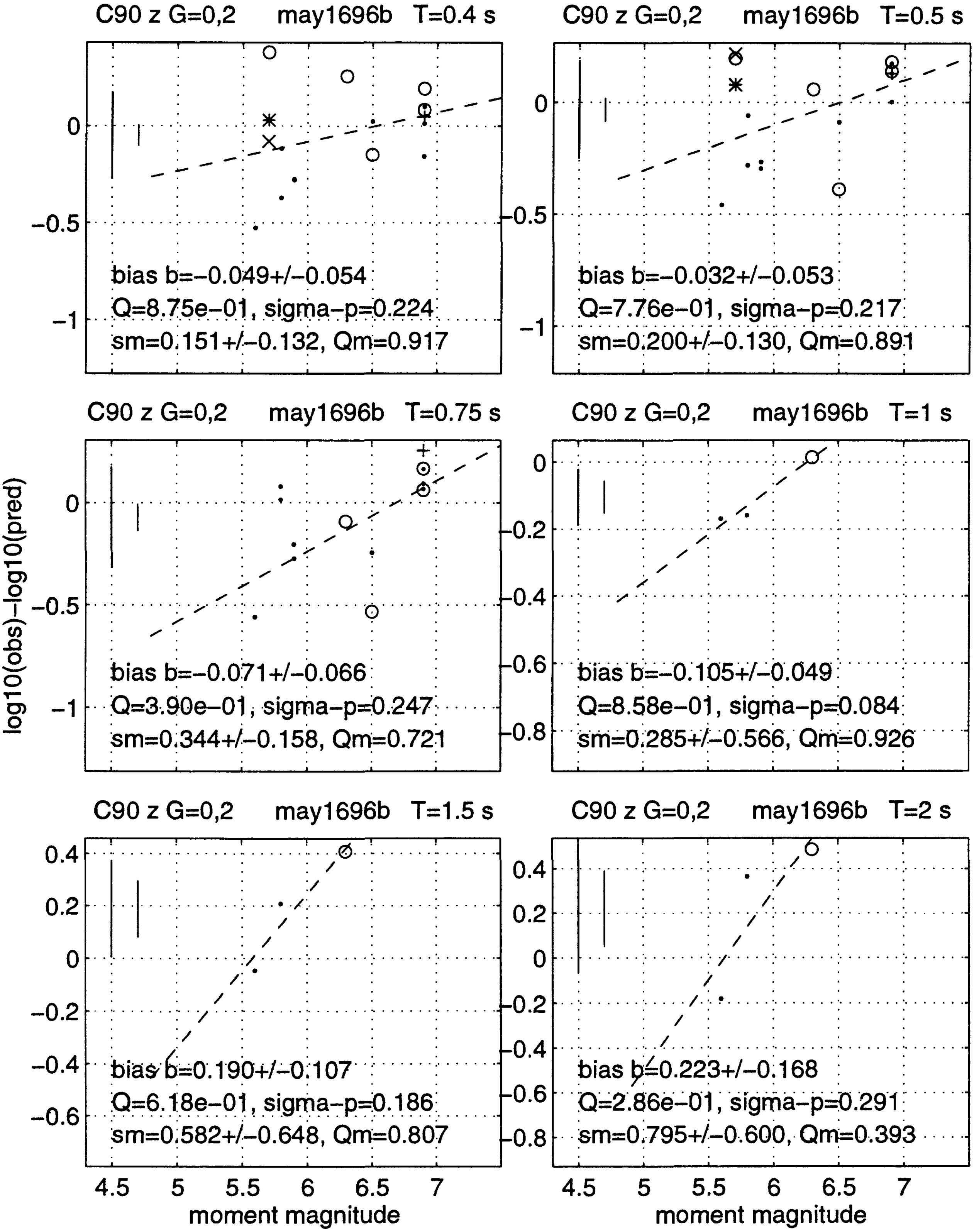

96/5/16 19:37 ymp1:[sp]may1696b6m2.eps

12 l

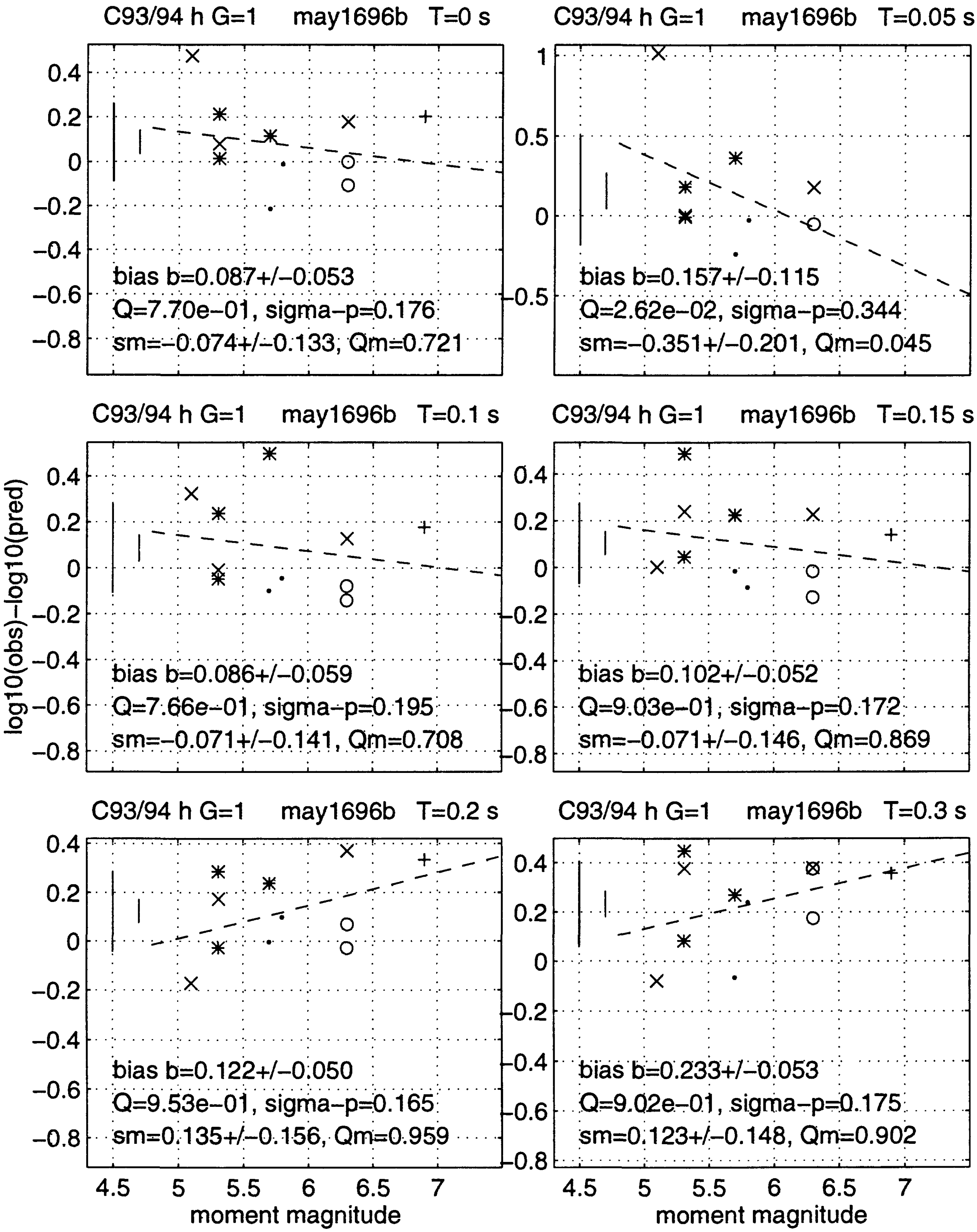

96/5/16 19:38 ymp1:[sp]may1696b7m1.eps

12m

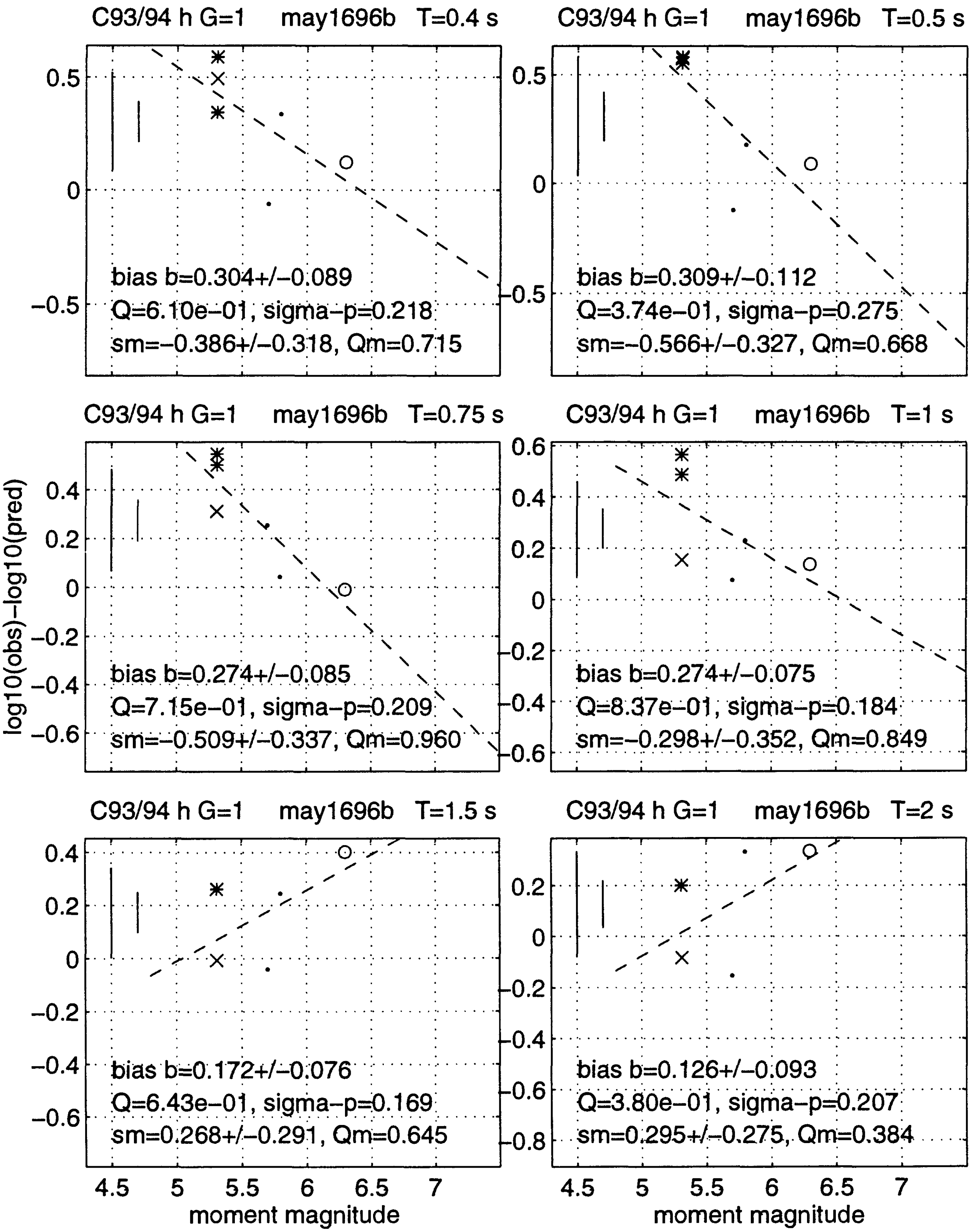

96/5/16 19:38 ymp1:[sp]may1696b7m2.eps

12n

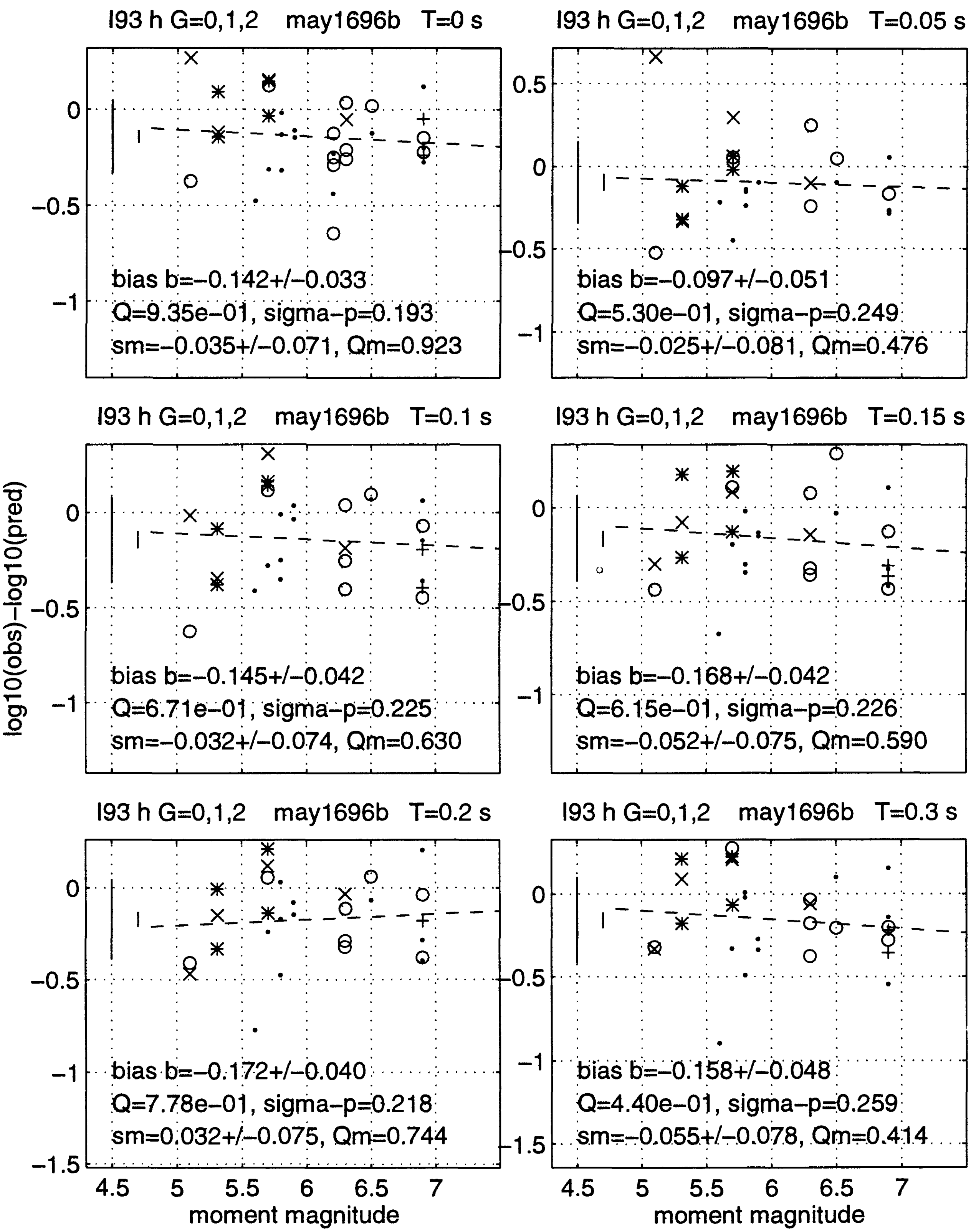

96/5/16 19:39 ymp1:[sp]may1696b8m1.eps

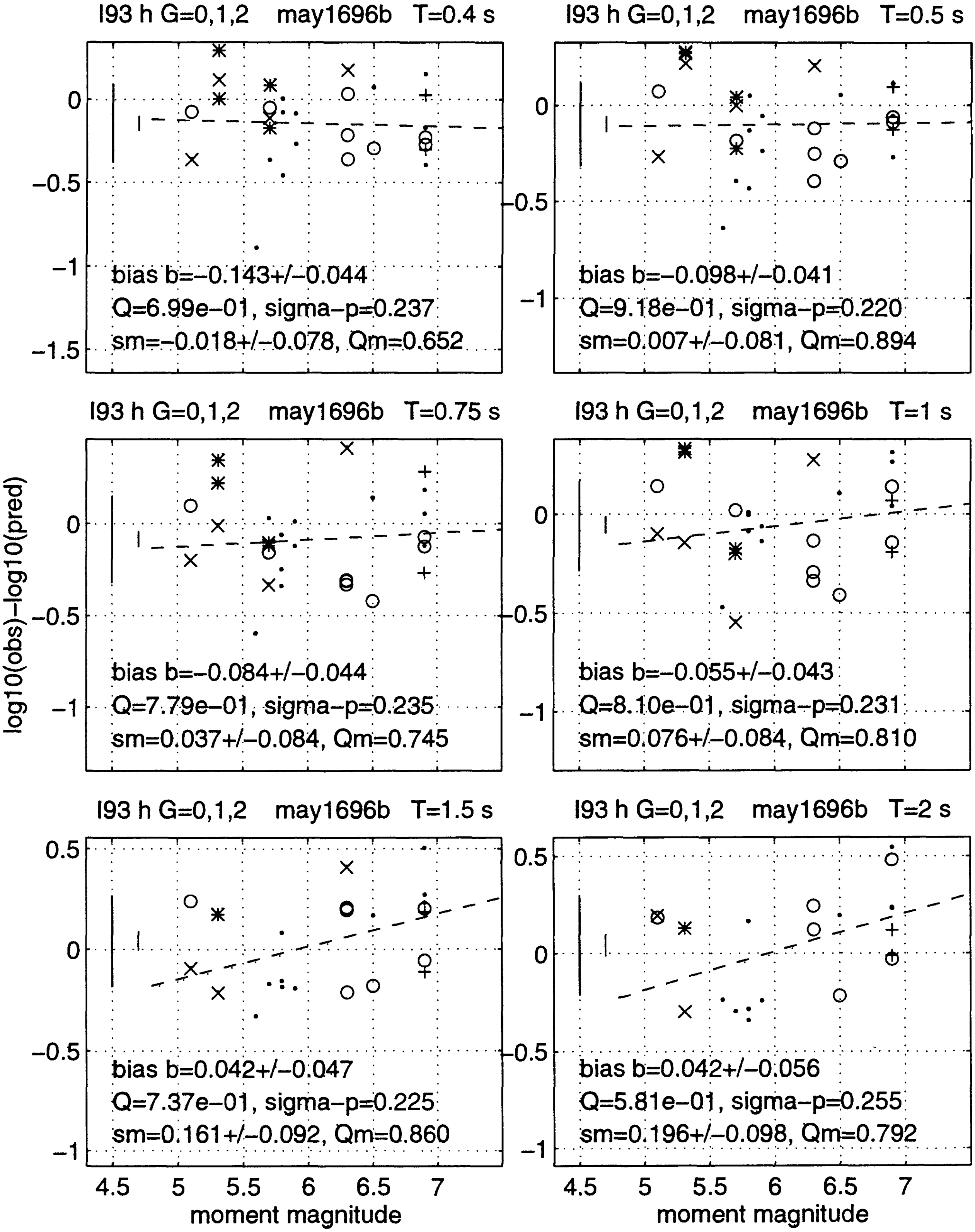

96/5/16 19:39 ymp1:[sp]may1696b8m2.eps

12 p

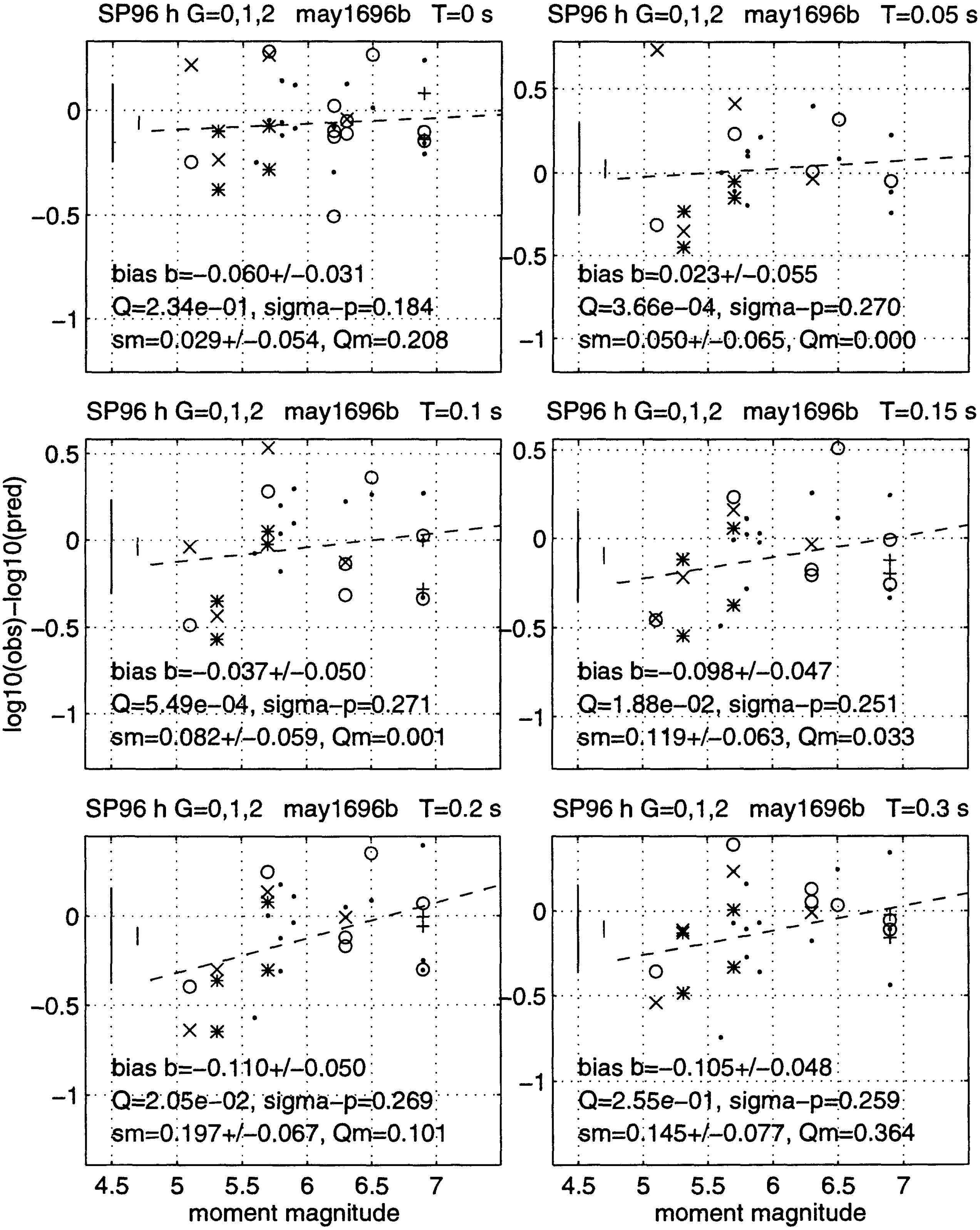

96/5/16 19:41 ymp1:[sp]may1696b9m1.eps

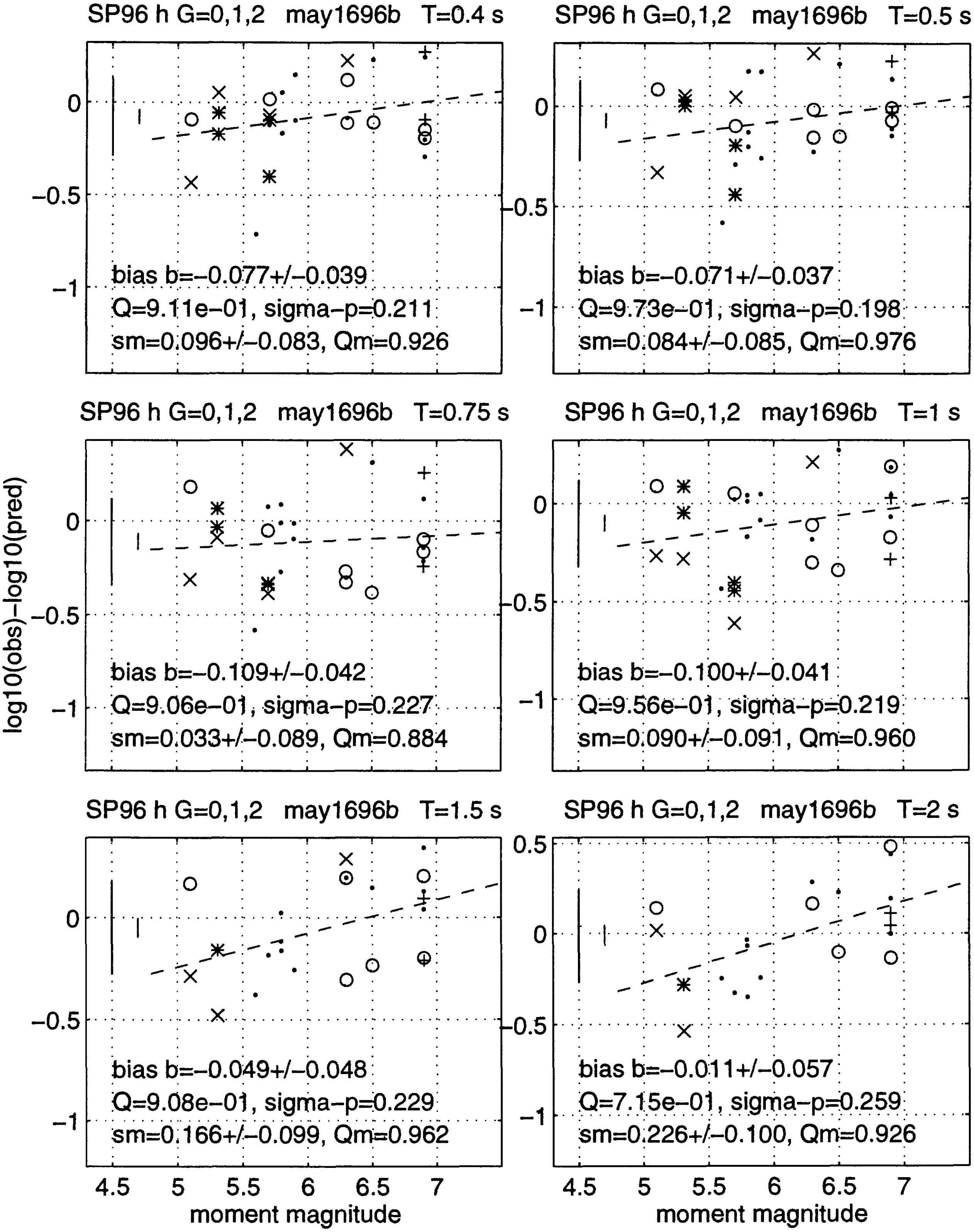

96/5/16 19:41 ymp1:[sp]may1696b9m2.eps

12 r

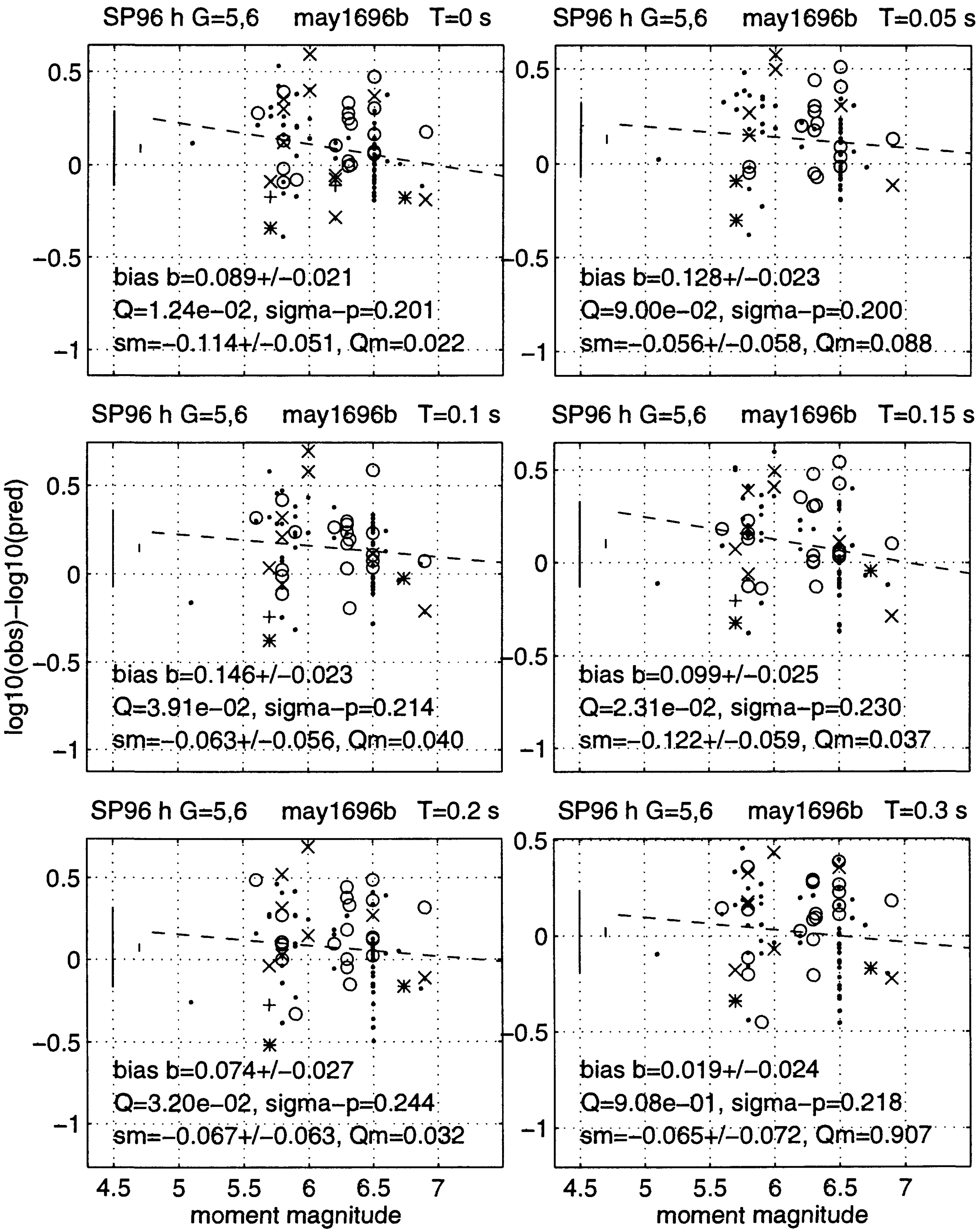

96/5/16 19:42 ymp1:[sp]may1696b10m1.ep

12 s

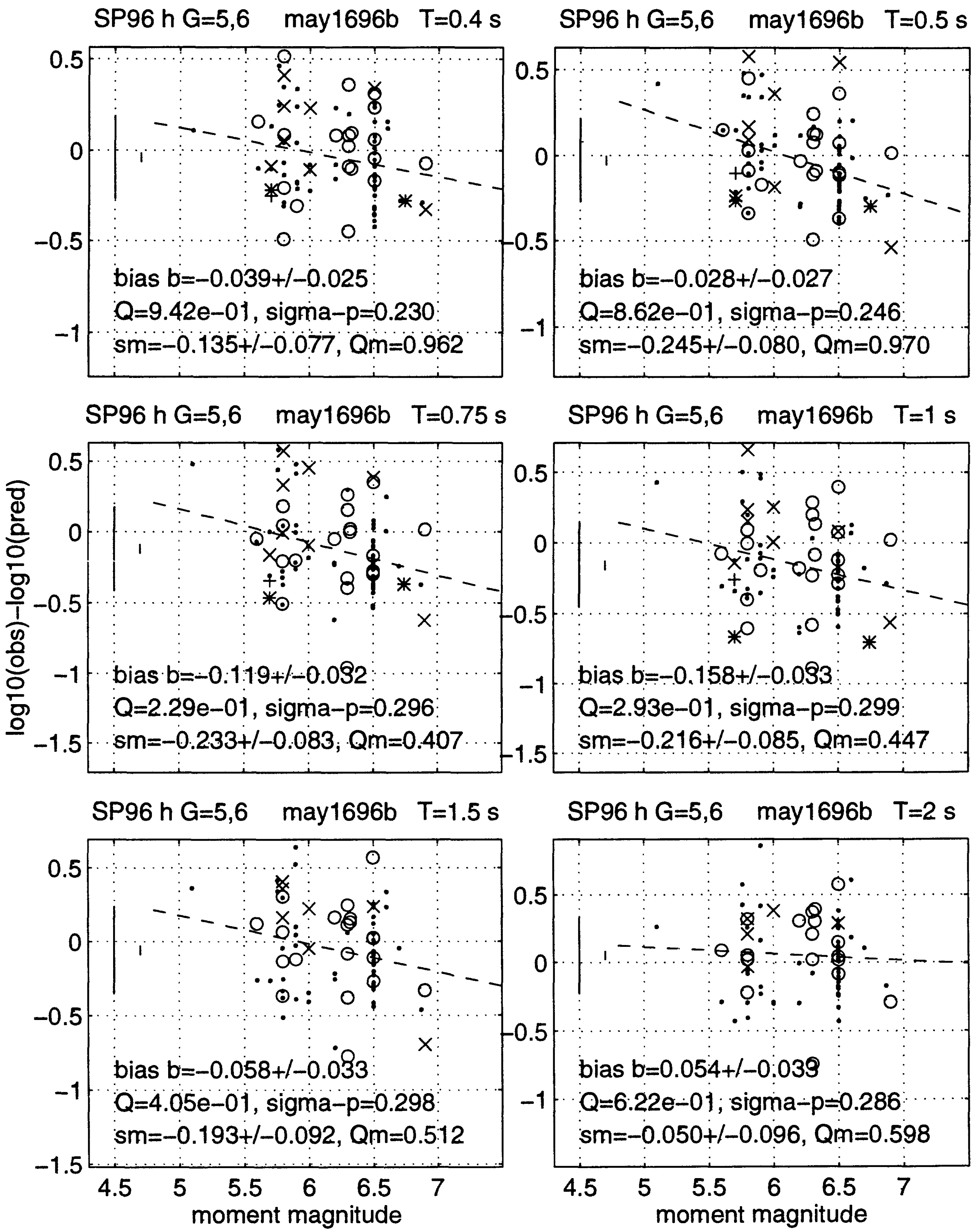

96/5/16 19:42 ymp1:[sp]may1696b10m2.ep

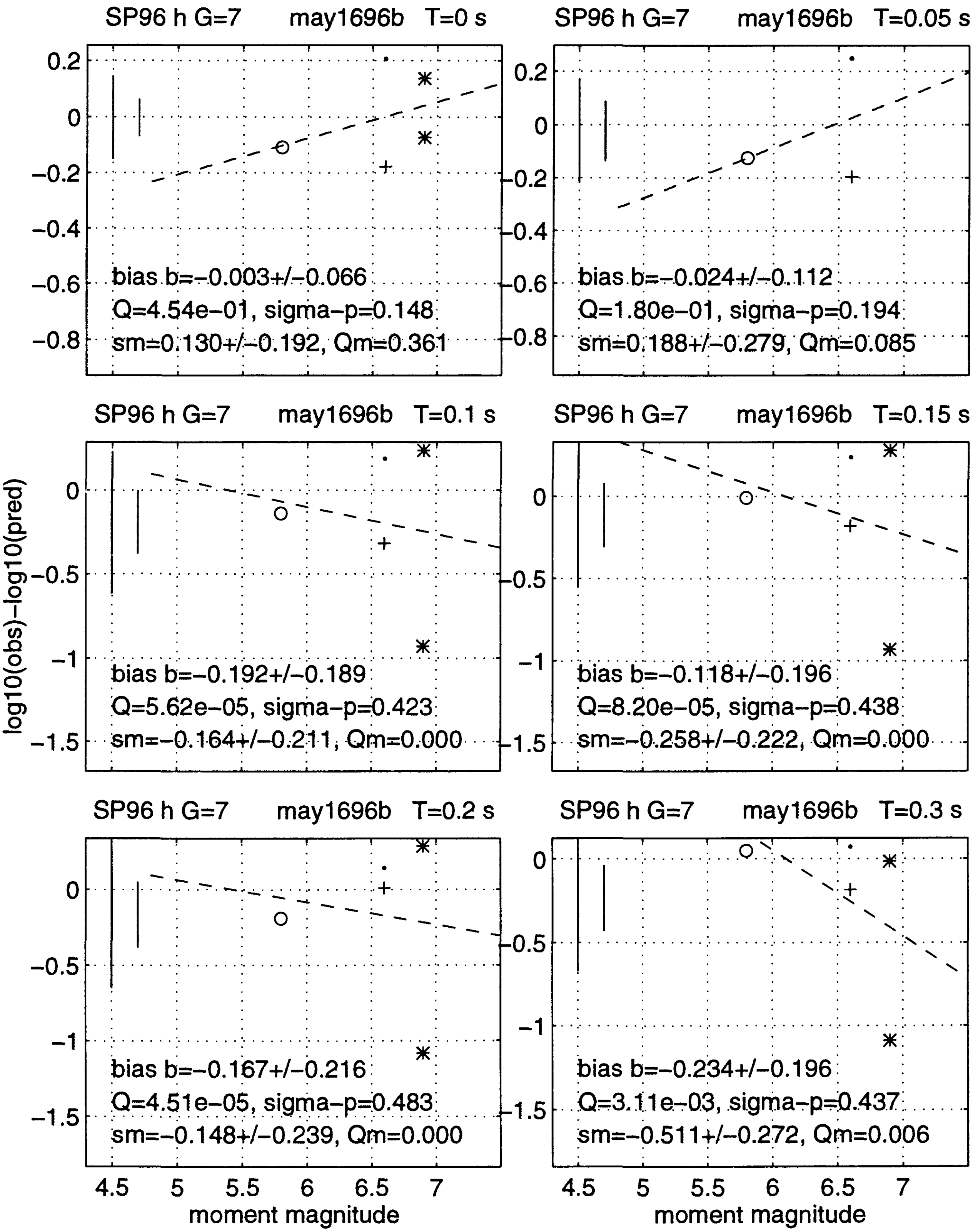

96/5/16 19:43 ymp1:[sp]may1696b11m1.ep

12 u

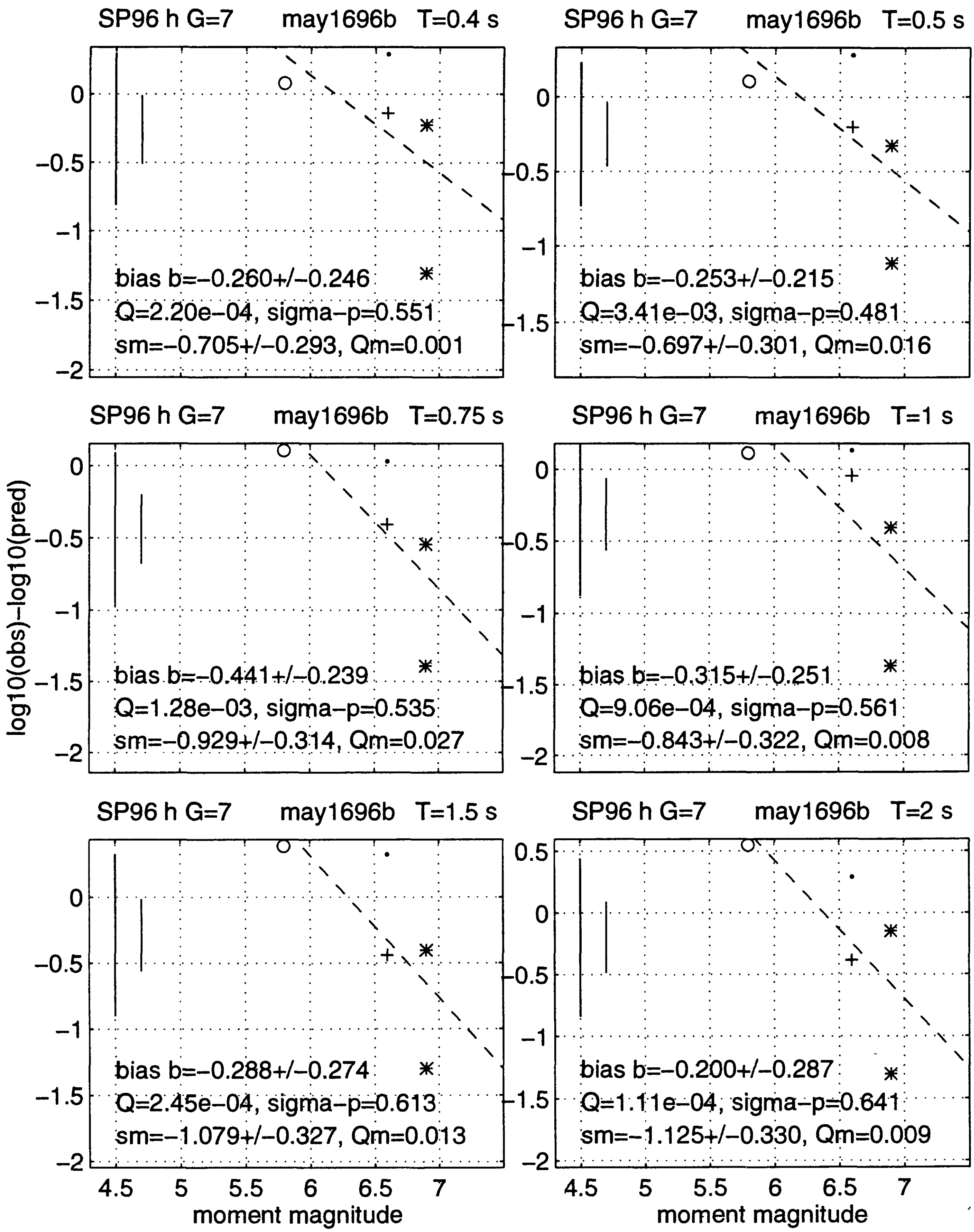

96/5/16 19:43 ymp1:[sp]may1696b11m2.ep

12v

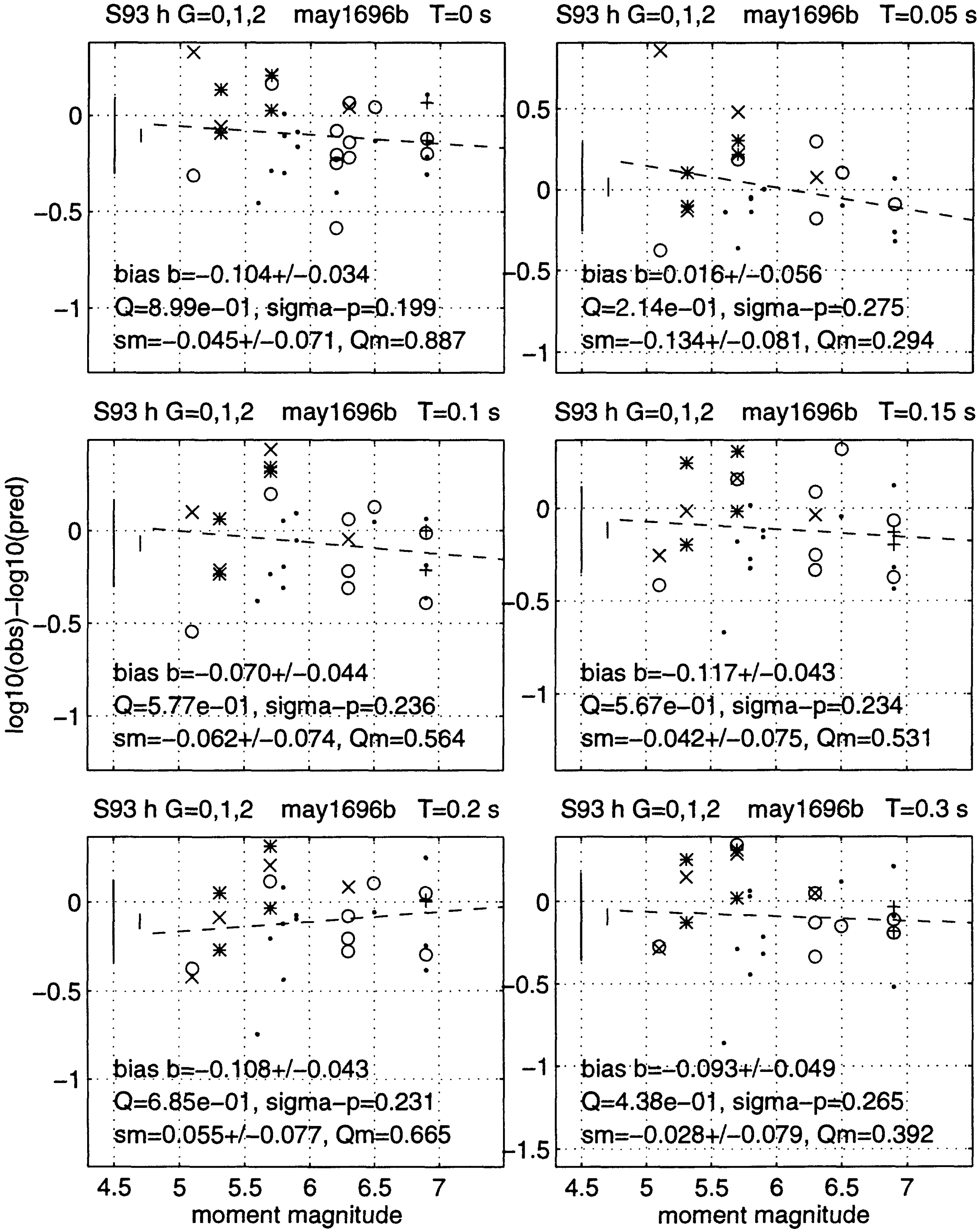

96/5/16 19:44 ymp1:[sp]may1696b12m1.ep

12 w

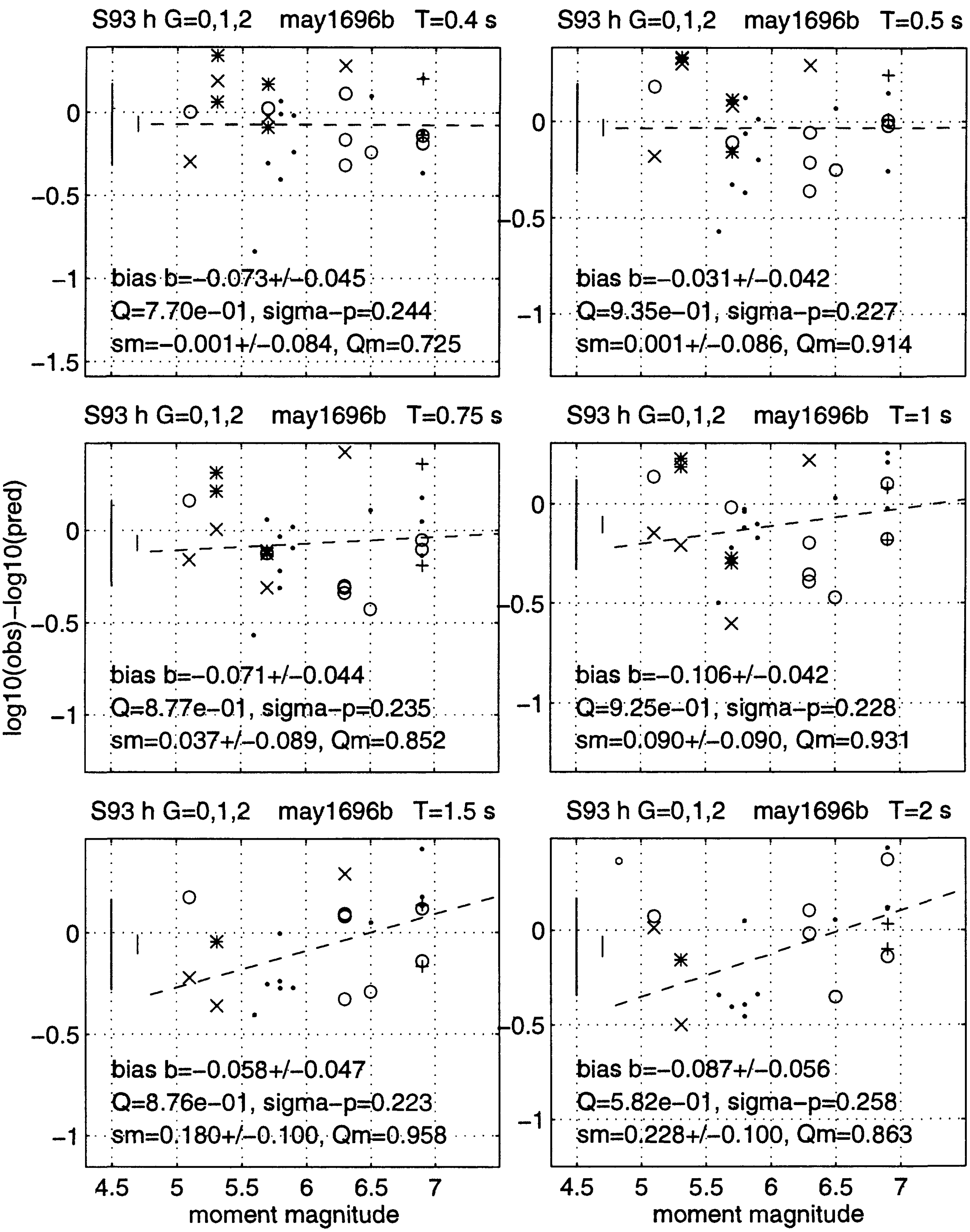

96/5/16 19:45 ymp1:[sp]may1696b12m2.ep

12 ×

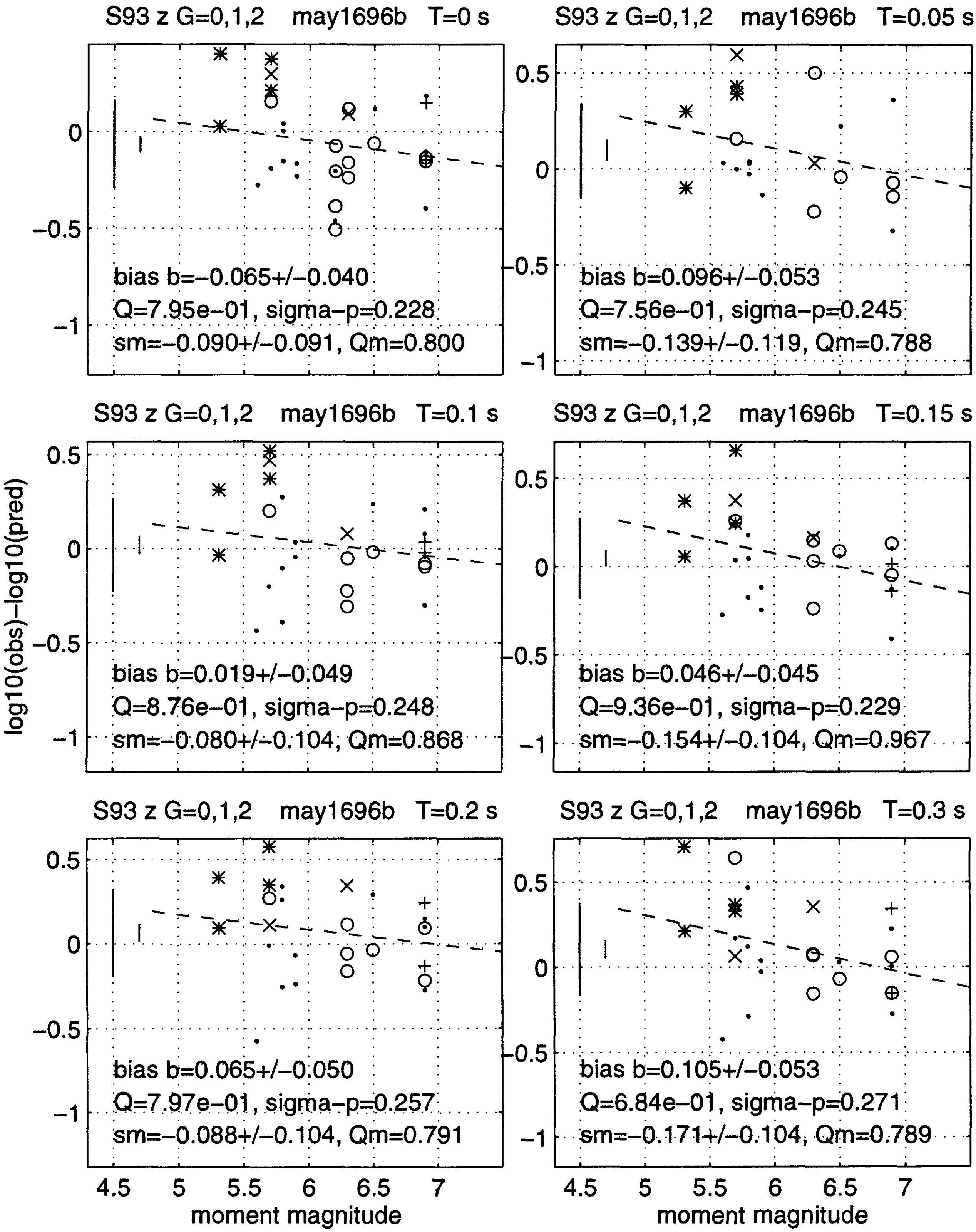

96/5/16 19:46 ymp1:[sp]may1696b13m1.ep

12Y

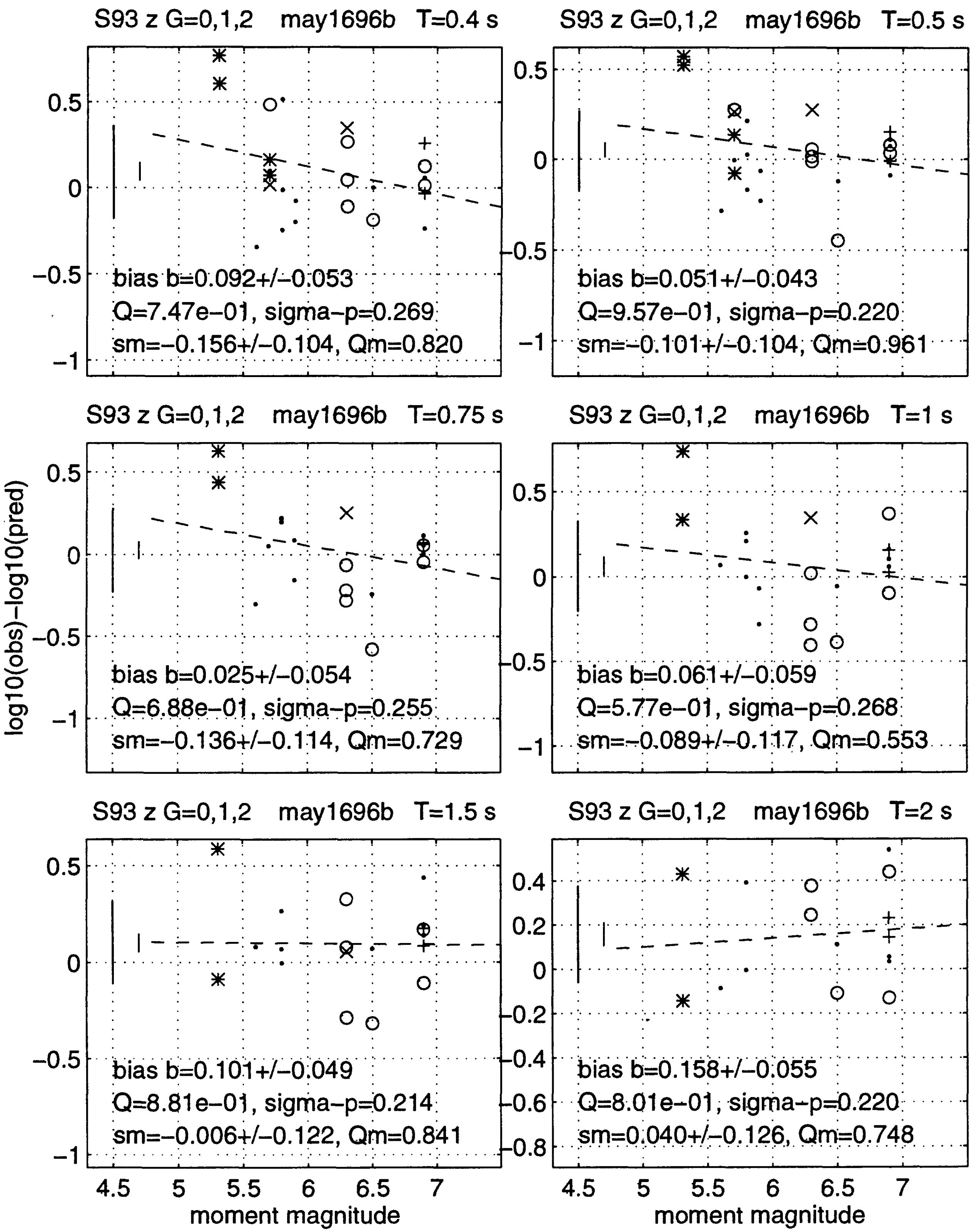

96/5/16 19:46 ymp1:[sp]may1696b13m2.ep

12z

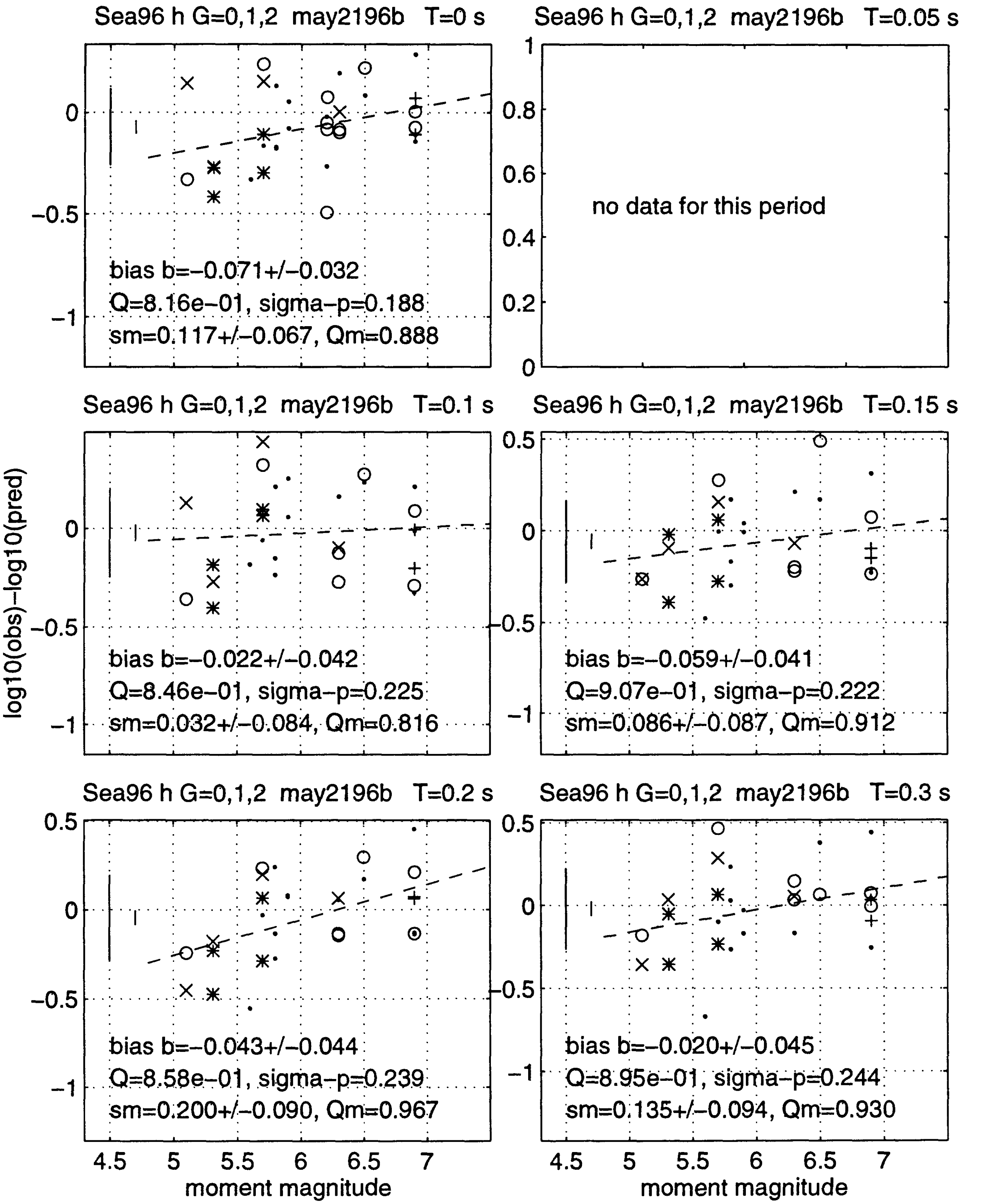

96/5/22 13:27 ymp1:[sp]may2196b22m1.ep

12 aa

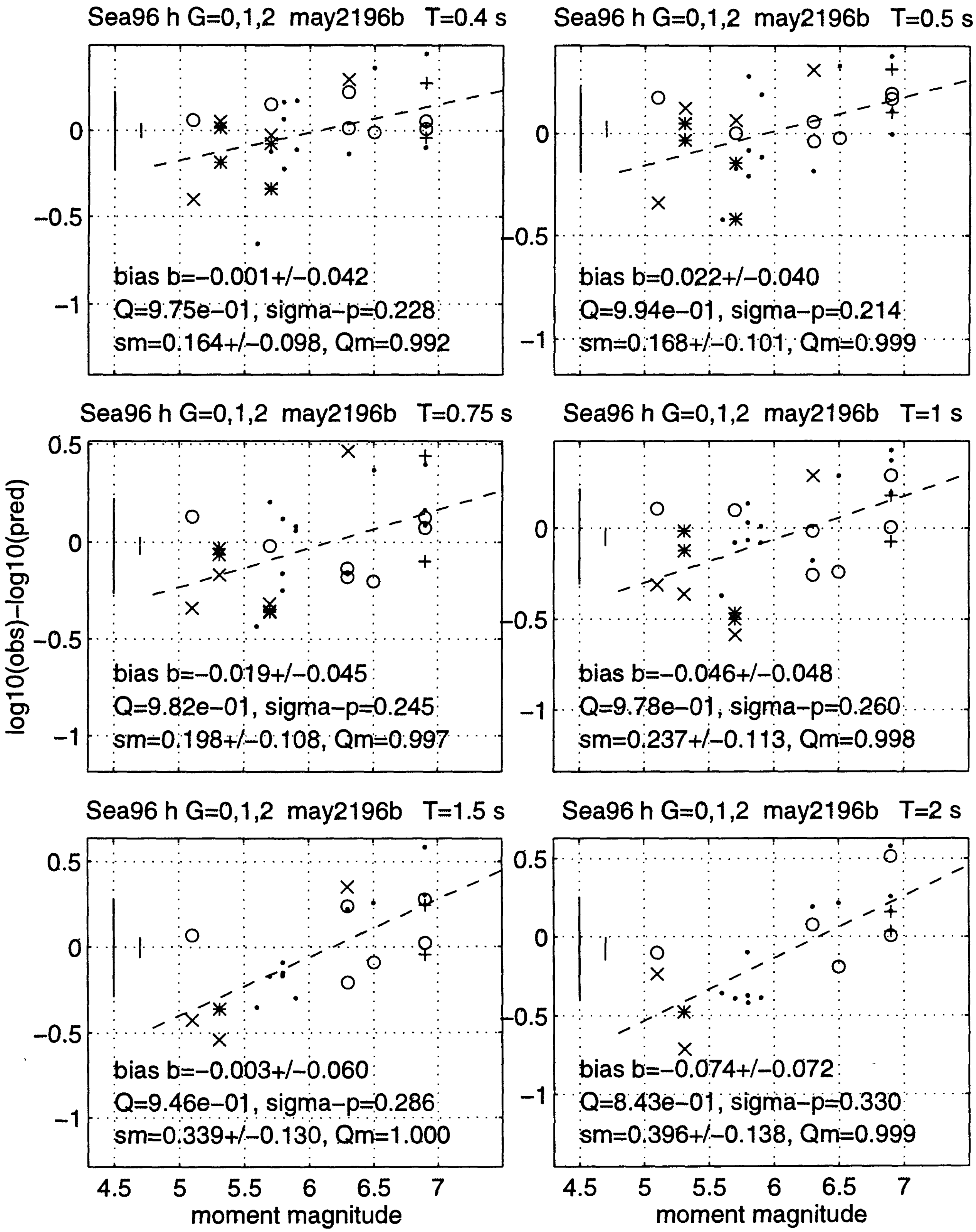

96/5/22 13:27 ymp1:[sp]may2196b22m2.ep

12ab

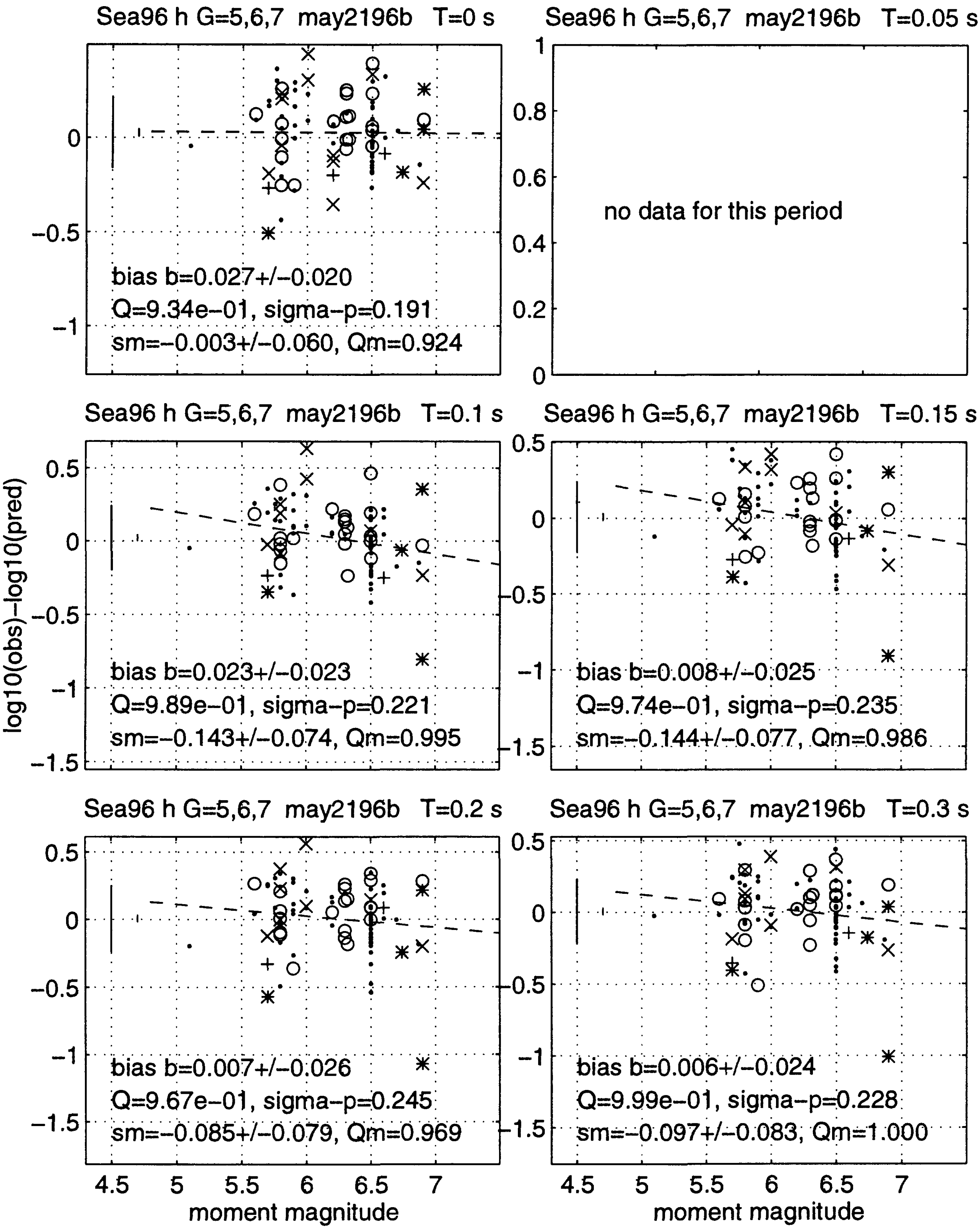

96/5/22 13:28 ymp1:[sp]may2196b23m1.ep

12 ac

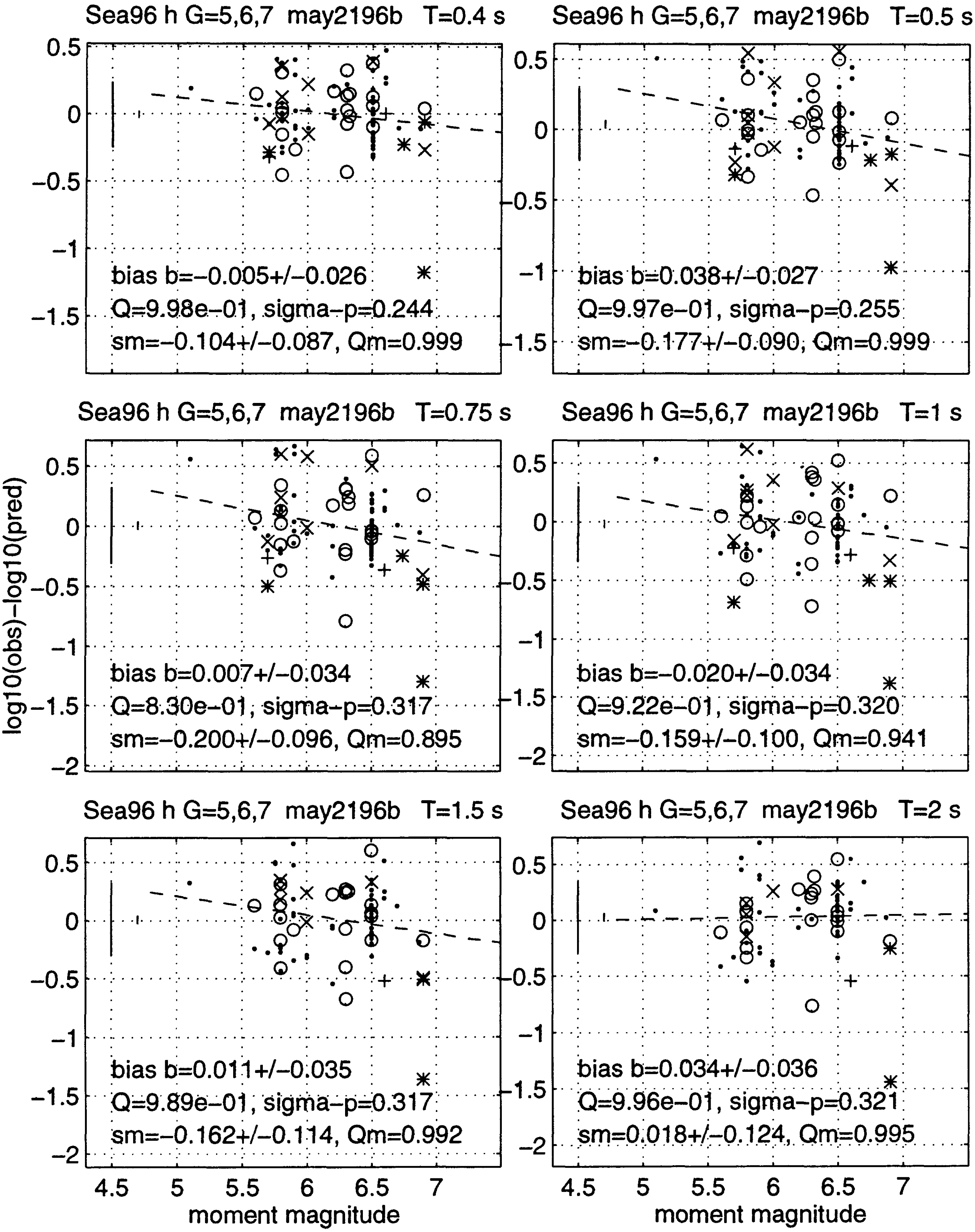

96/5/22 13:29 ymp1:[sp]may2196b23m2.ep

12 ad

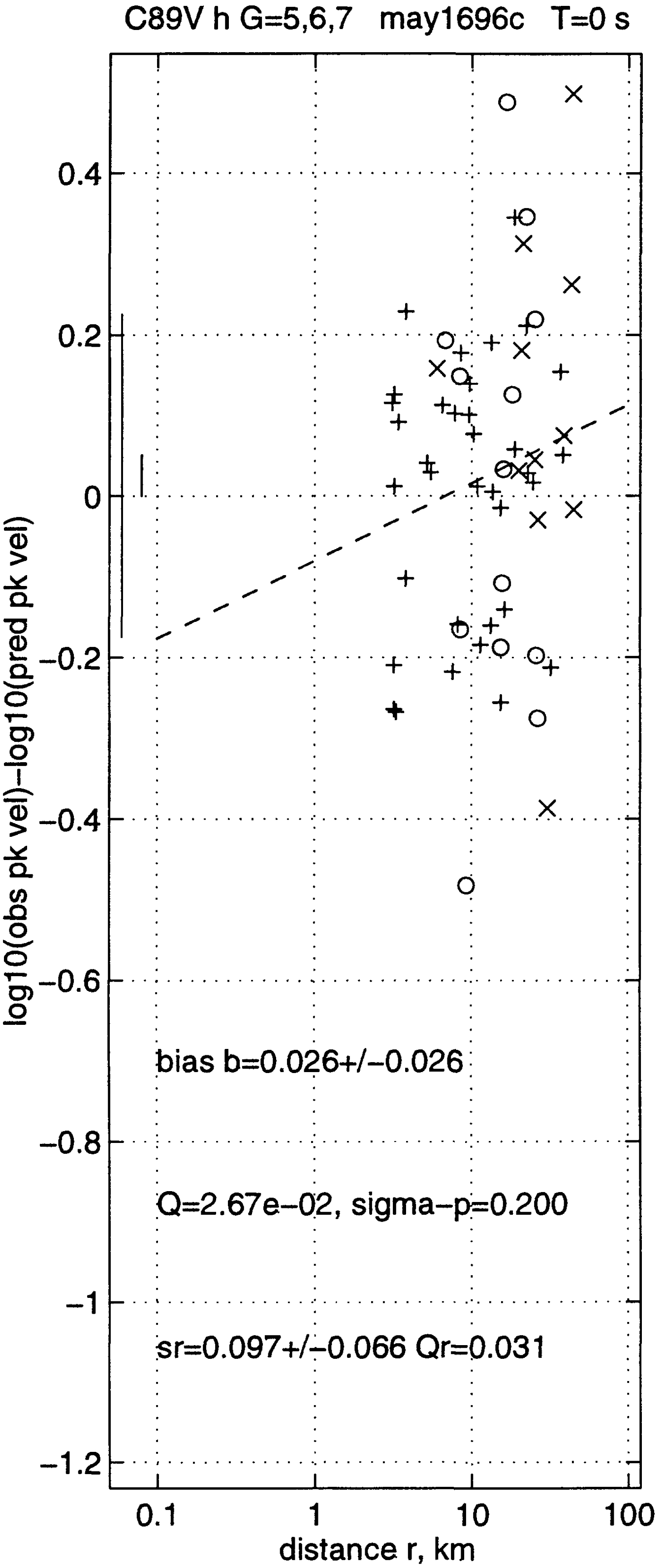
C89V h G=5,6,7 may1696c T=0 s
log10(obs pk vel)−log10(pred pk vel)
0.4
0.2
0
−0.2
−0.4
−0.6
−0.8
−1
−1.2
bias b=0.026+/−0.026
Q=2.67e−02, sigma−p=0.200
sr=0.097+/−0.066 Qr=0.031
0.1
1
10
100
distance r, km

13a

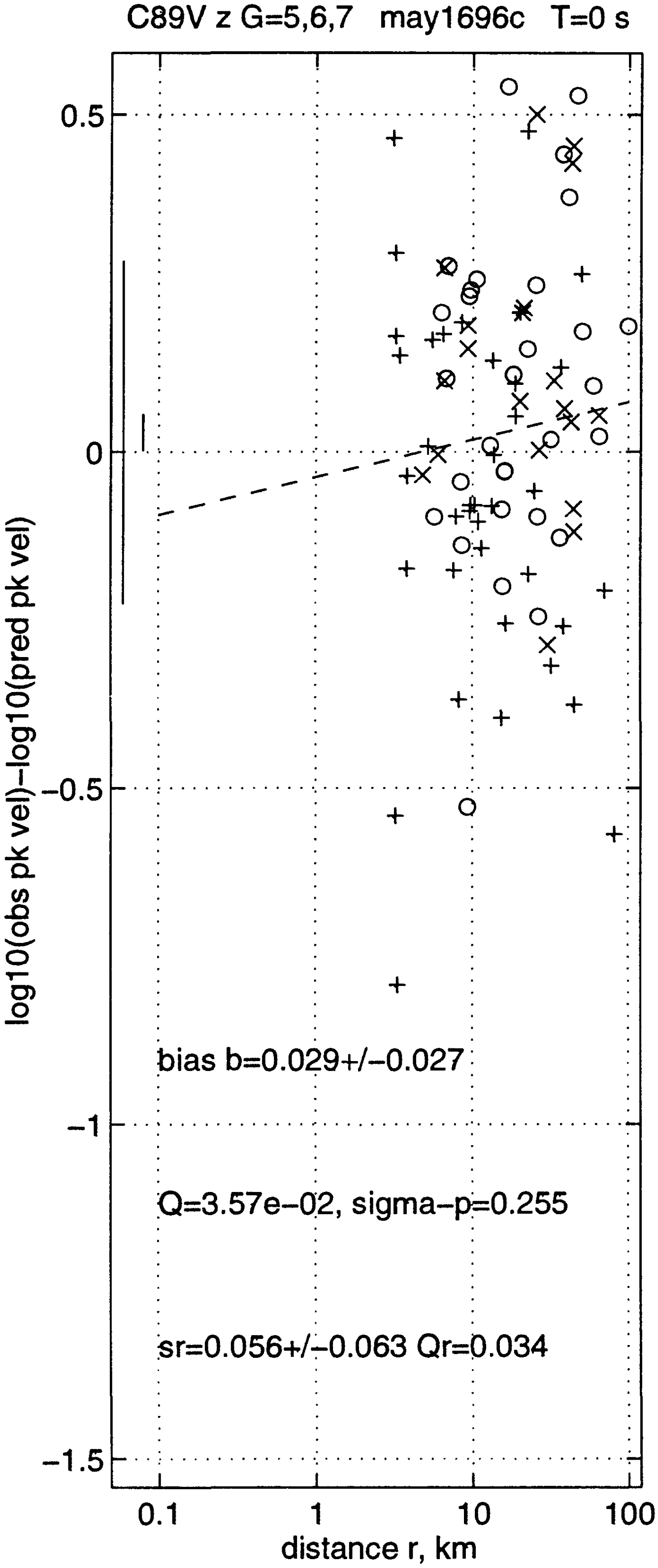
C89V z G=5,6,7 may1696c T=0 s
0.5
0
−0.5
−1
−1.5
log10(obs pk vel)−log10(pred pk vel)
bias b=0.029+/−0.027
Q=3.57e−02, sigma−p=0.255
sr=0.056+/−0.063 Qr=0.034
0.1
1
10
100
distance r, km

13b

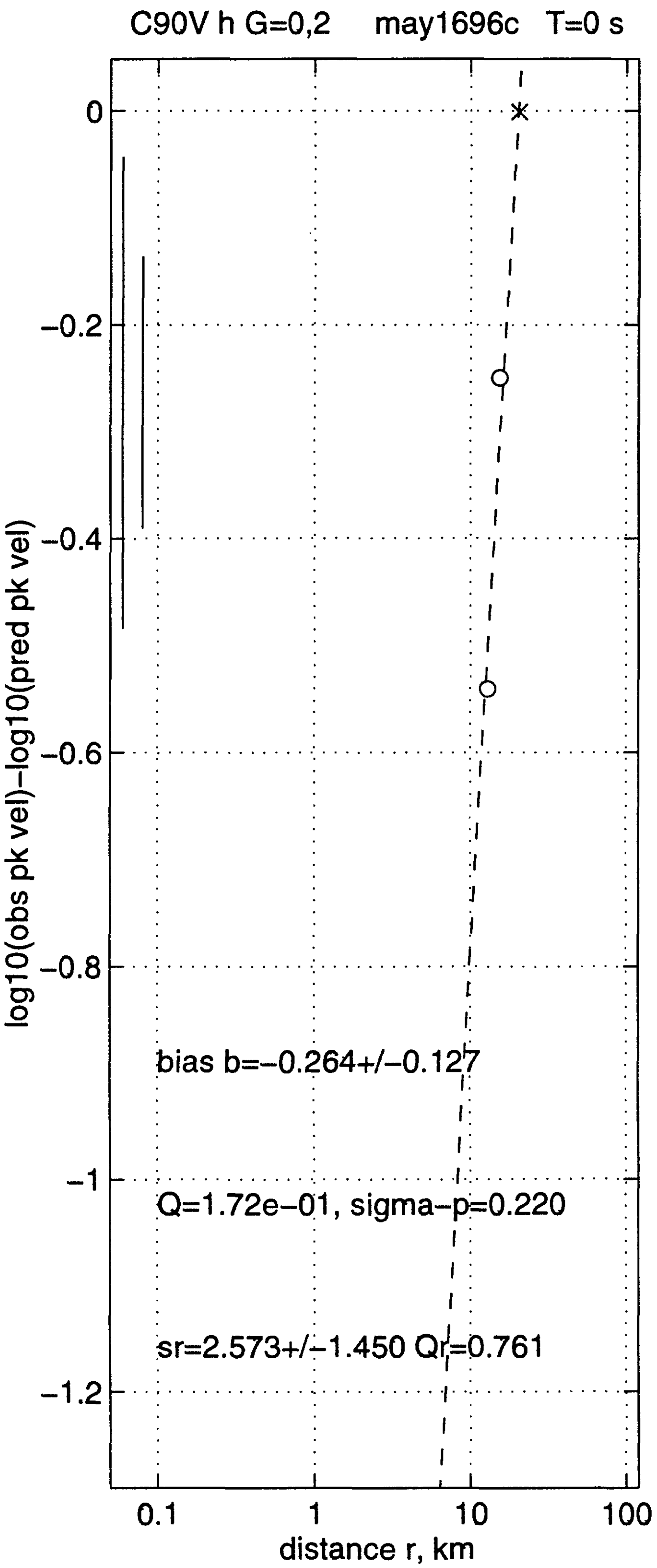
C90V h G=0,2 may1696c T=0 s
0
−0.2
−0.4
−0.6
−0.8
−1
−1.2
log10(obs pk vel)−log10(pred pk vel)
bias b=−0.264+/−0.127
Q=1.72e−01, sigma−p=0.220
sr=2.573+/−1.450 Qr=0.761
0.1
1
10
100
distance r, km

13c

C90V z G=0,2 may1696c T=0 s

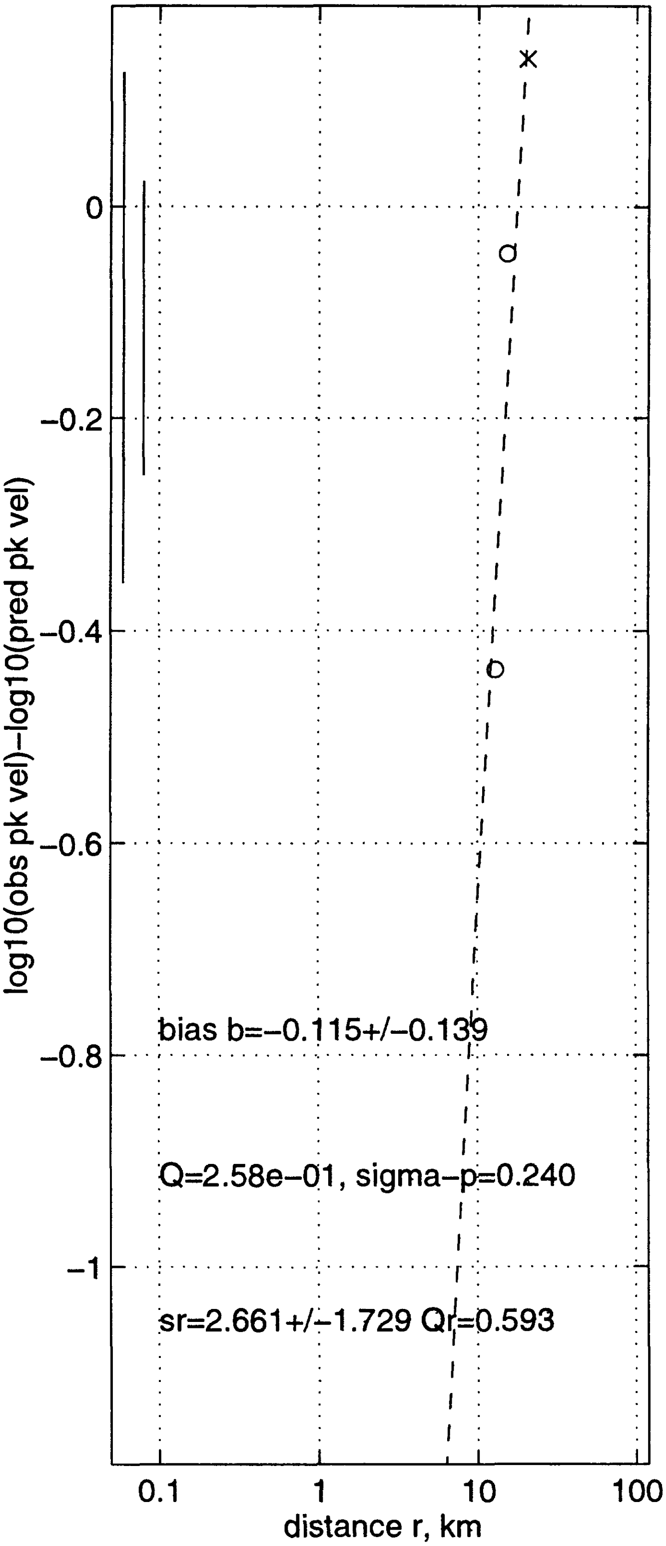

13 d

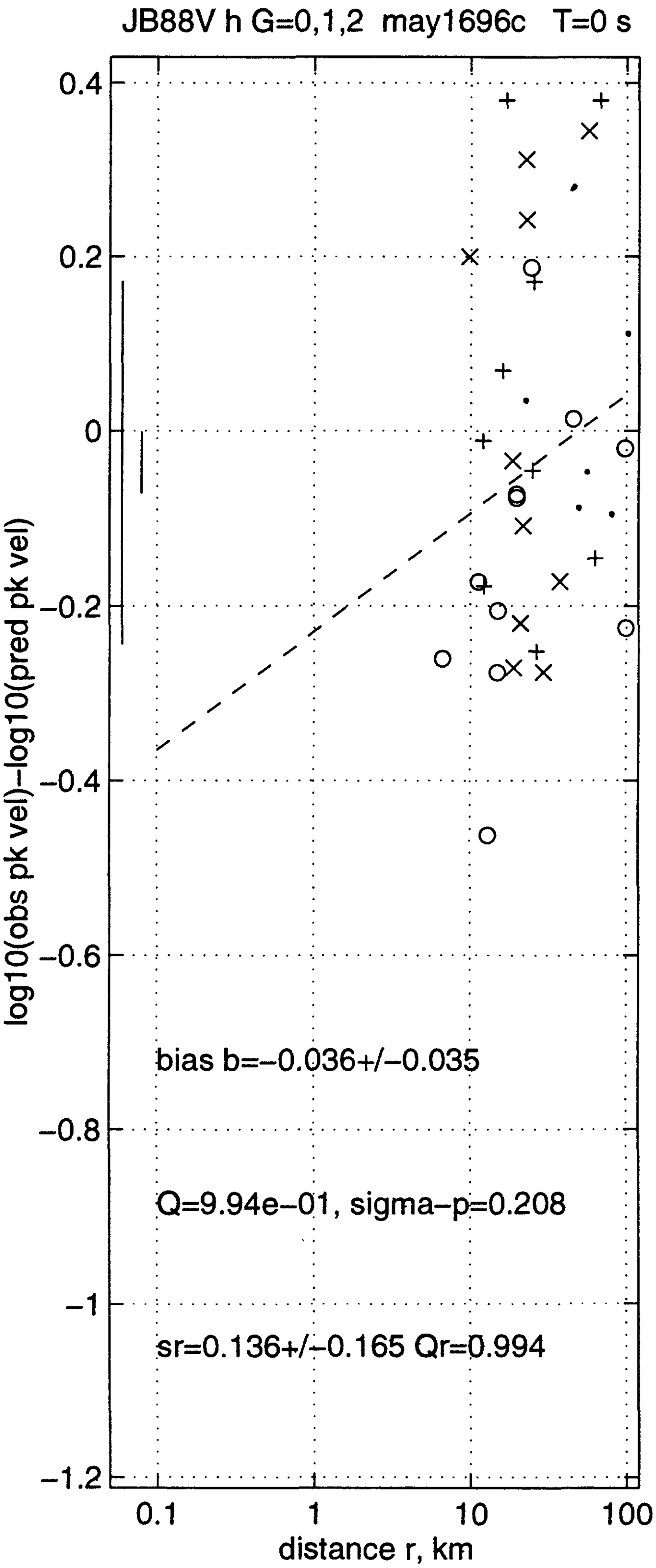
JB88V h G=0,1,2 may1696c T=0 s
0.4
0.2
0
−0.2
−0.4
−0.6
−0.8
−1
−1.2
log10(obs pk vel)−log10(pred pk vel)
bias b=−0.036+/−0.035
Q=9.94e−01, sigma−p=0.208
sr=0.136+/−0.165 Qr=0.994
0.1
1
10
100
distance r, km

13e

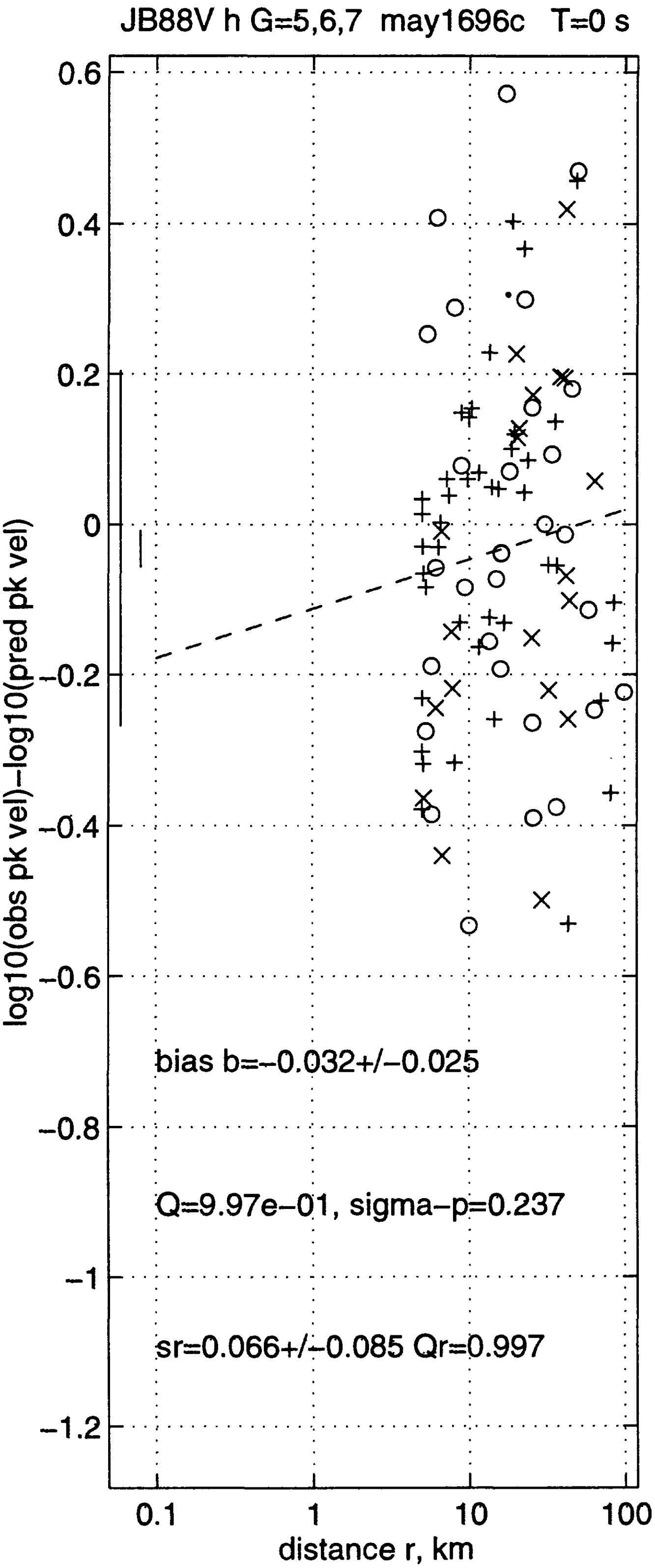
JB88V h G=5,6,7 may1696c T=0 s
0.6
0.4
0.2
0
−0.2
−0.4
−0.6
−0.8
−1
−1.2
log10(obs pk vel)−log10(pred pk vel)
bias b=−0.032+/−0.025
Q=9.97e−01, sigma−p=0.237
sr=0.066+/−0.085 Qr=0.997
0.1
1
10
100
distance r, km

13f

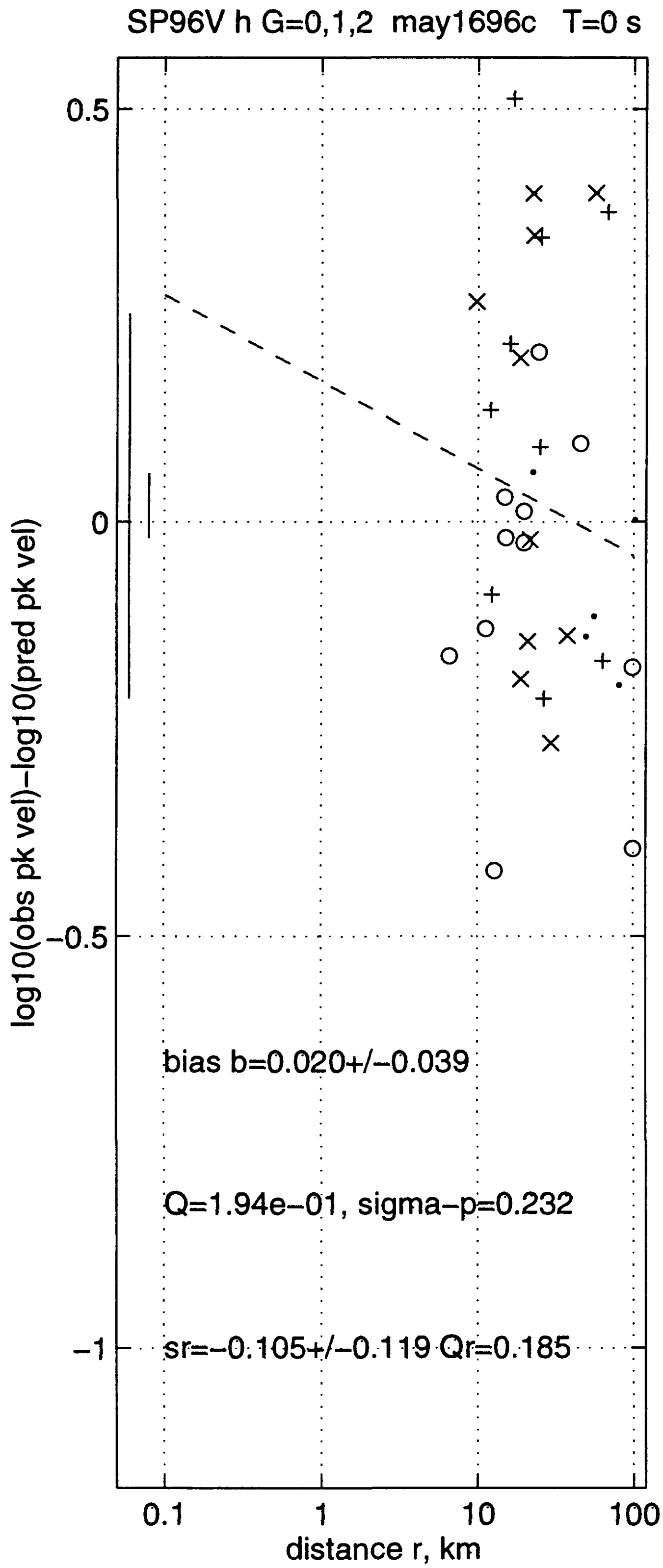

SP96V h G=0,1,2 may1696c T=0 s
0.5
0
−0.5
−1
log10(obs pk vel)−log10(pred pk vel)
bias b=0.020+/−0.039
Q=1.94e−01, sigma−p=0.232
sr=−0.105+/−0.119 Qr=0.185
0.1
1
10
100
distance r, km

13 g

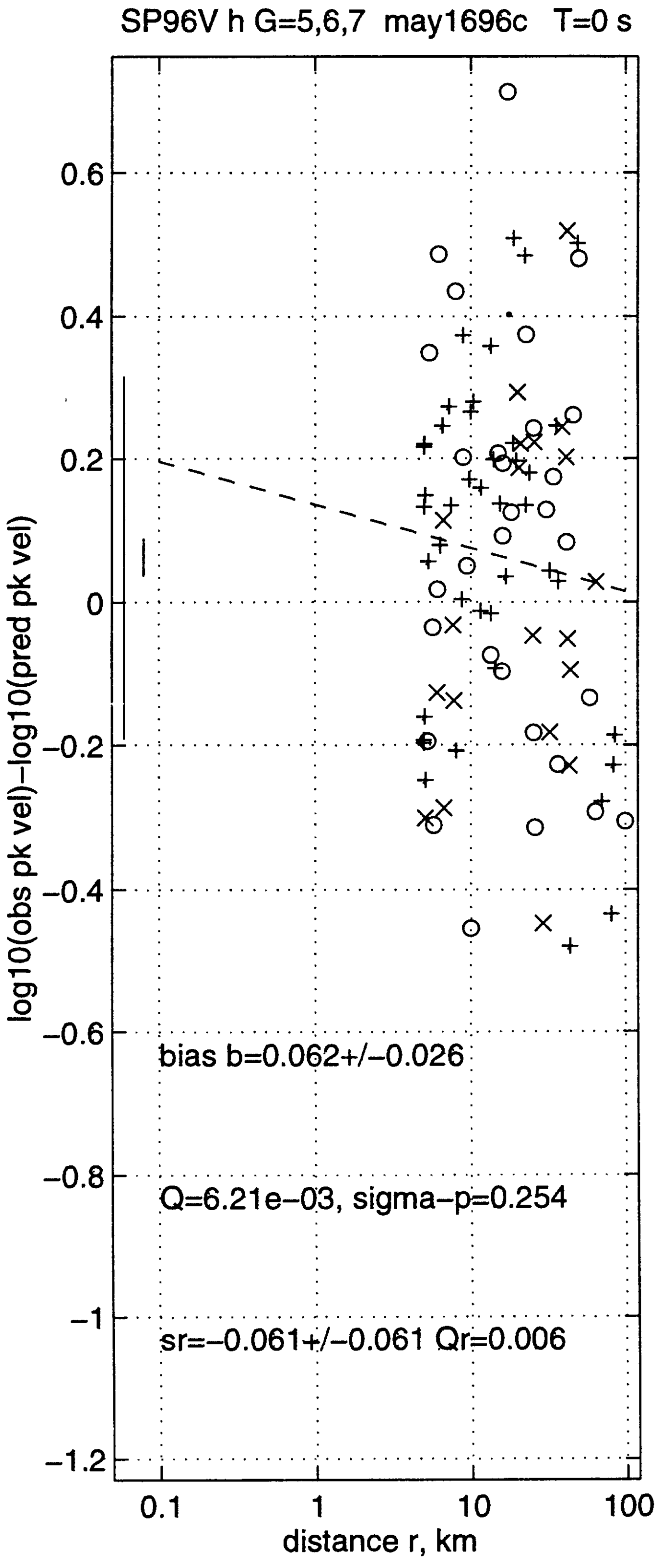
SP96V h G=5,6,7 may1696c T=0 s
log10(obs pk vel)−log10(pred pk vel)
distance r, km
bias b=0.062+/−0.026
Q=6.21e−03, sigma−p=0.254
sr=−0.061+/−0.061 Qr=0.006

13 h

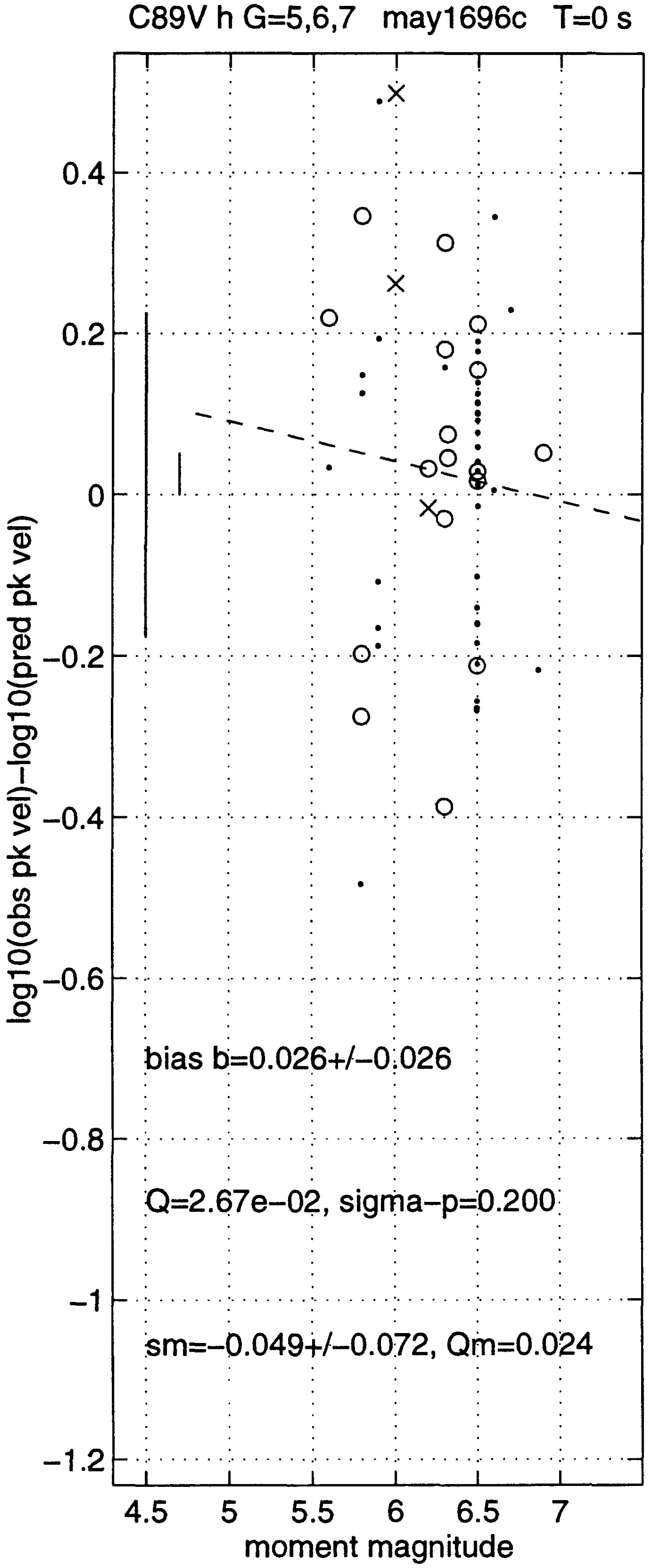
C89V h G=5,6,7 may1696c T=0 s
log10(obs pk vel)−log10(pred pk vel)
moment magnitude
bias b=0.026+/−0.026
Q=2.67e−02, sigma−p=0.200
sm=−0.049+/−0.072, Qm=0.024
0.4
0.2
0
−0.2
−0.4
−0.6
−0.8
−1
−1.2
4.5
5
5.5
6
6.5
7

14a

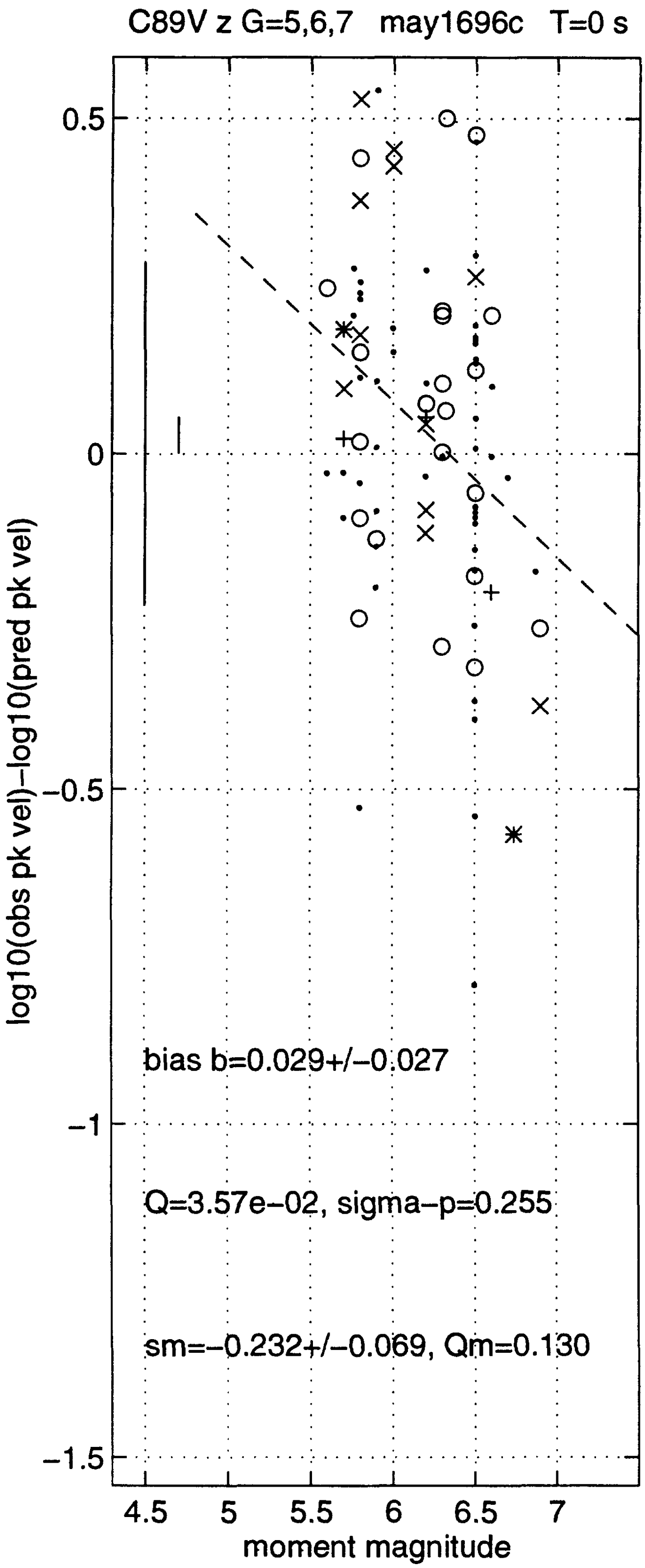

C89V z G=5,6,7 may1696c T=0 s
0.5
0
−0.5
−1
−1.5
4.5
5
5.5
6
6.5
7
log10(obs pk vel)−log10(pred pk vel)
moment magnitude
bias b=0.029+/−0.027
Q=3.57e−02, sigma−p=0.255
sm=−0.232+/−0.069, Qm=0.130

14b

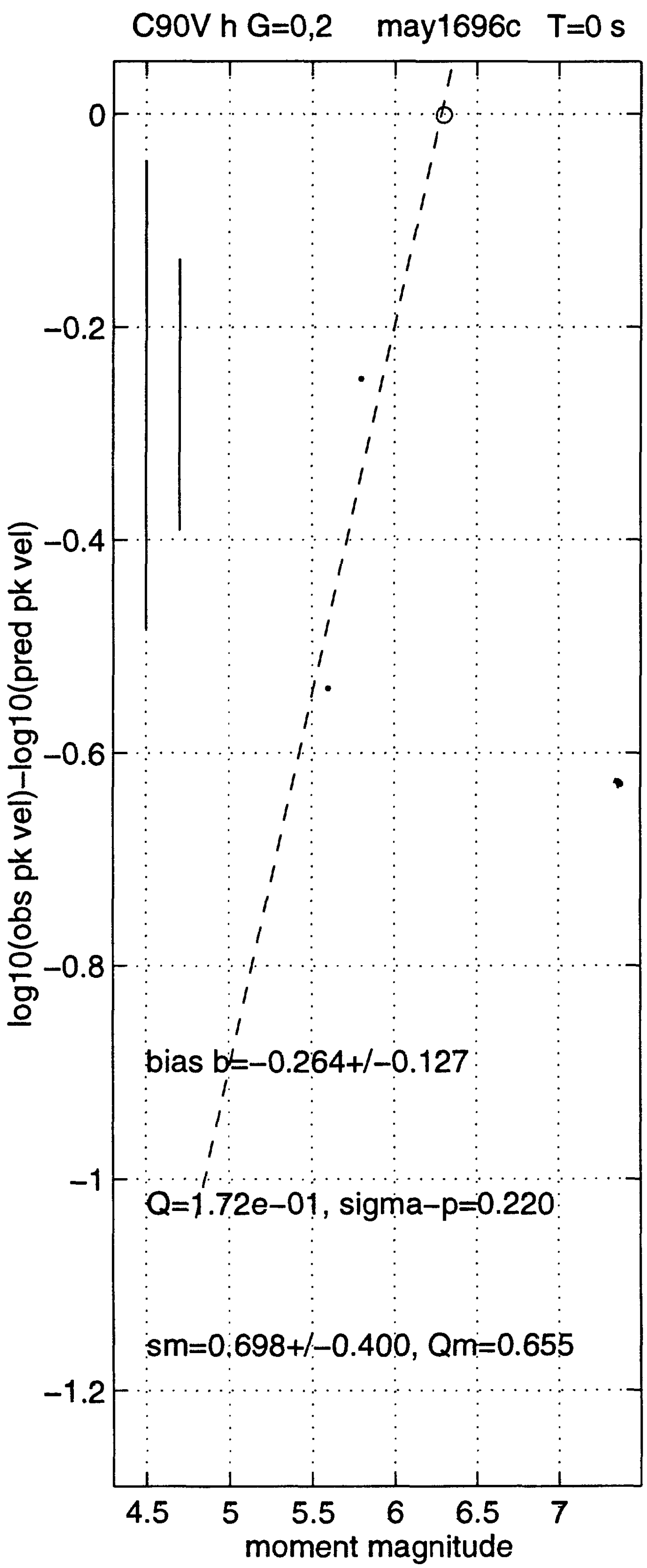

C90V h G=0,2 may1696c T=0 s
log10(obs pk vel)−log10(pred pk vel)
moment magnitude
0
−0.2
−0.4
−0.6
−0.8
−1
−1.2
4.5
5
5.5
6
6.5
7
bias b=−0.264+/−0.127
Q=1.72e−01, sigma−p=0.220
sm=0.698+/−0.400, Qm=0.655

14c

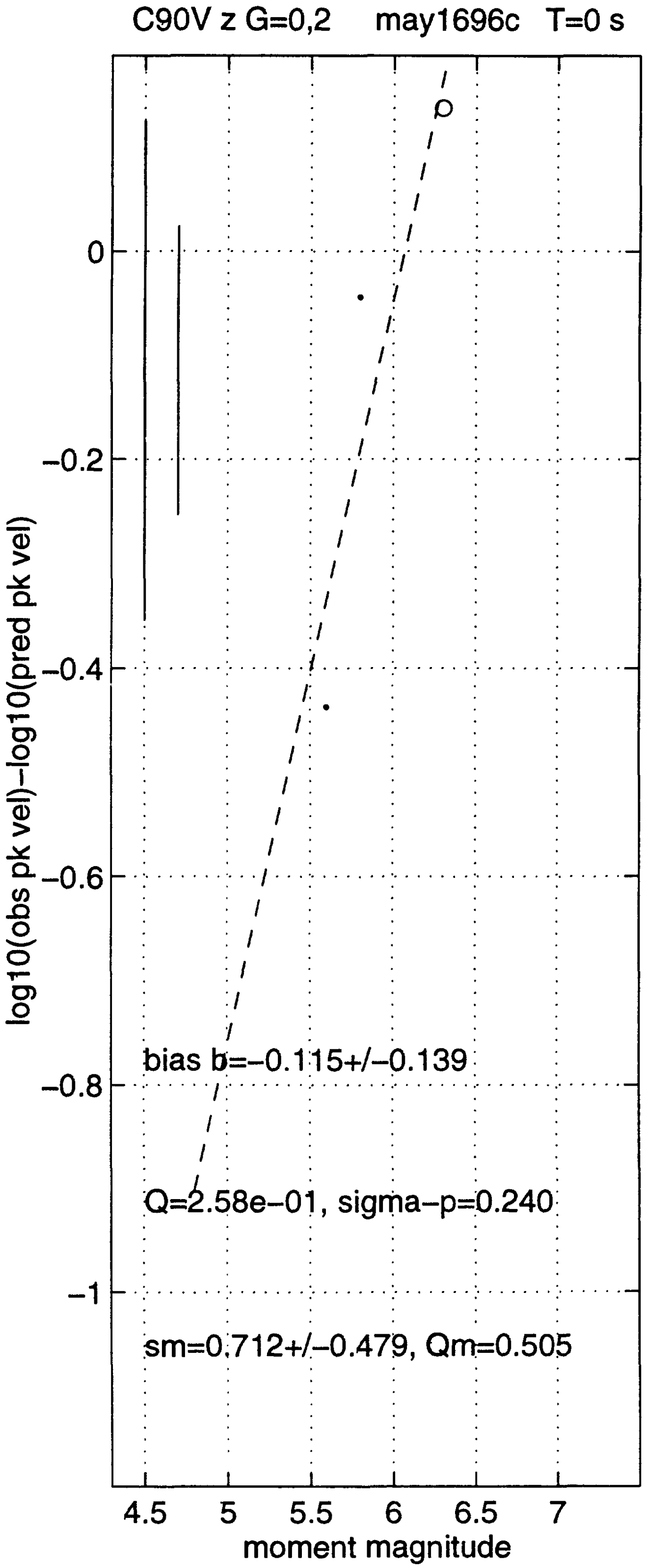
C90V z G=0,2 may1696c T=0 s
log10(obs pk vel)−log10(pred pk vel)
0
−0.2
−0.4
−0.6
−0.8
−1
bias b=−0.115+/−0.139
Q=2.58e−01, sigma−p=0.240
sm=0.712+/−0.479, Qm=0.505
4.5
5
5.5
6
6.5
7
moment magnitude

14d

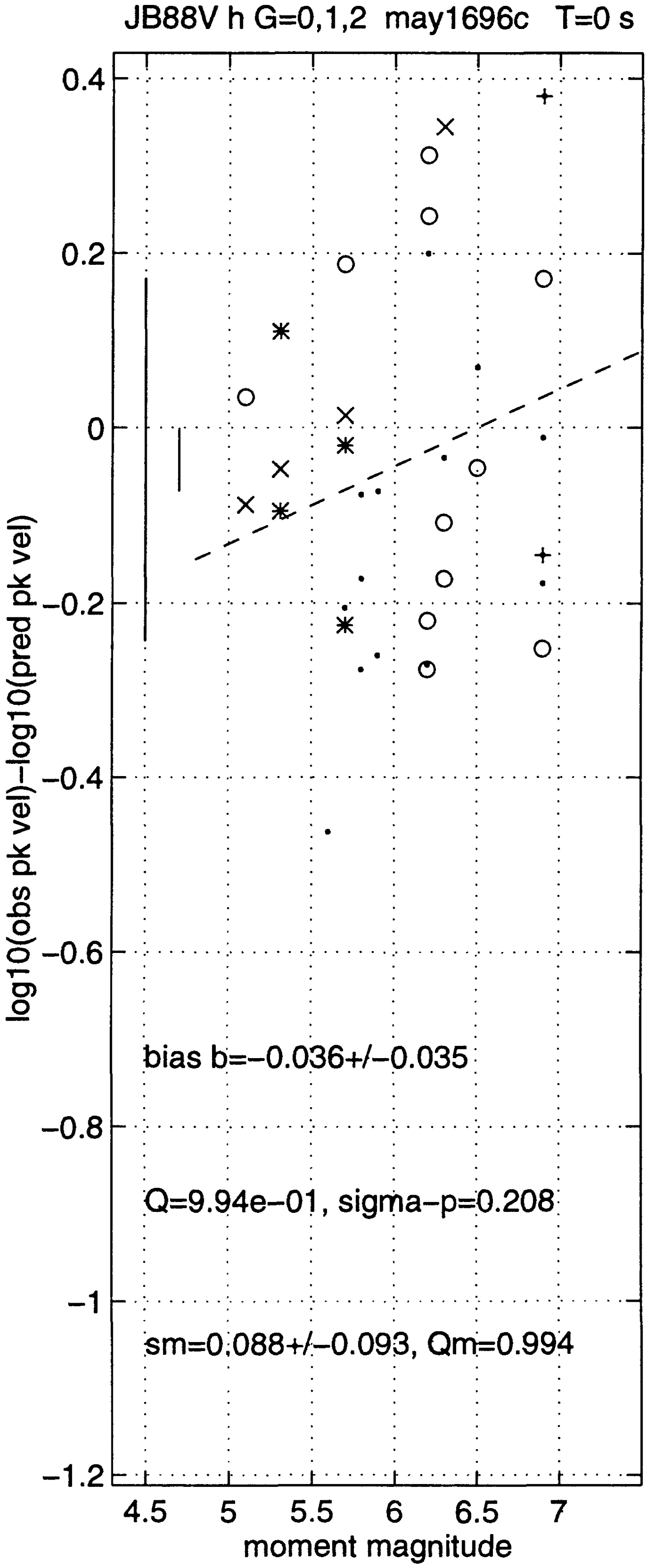
JB88V h G=0,1,2 may1696c T=0 s
0.4
0.2
0
-0.2
-0.4
-0.6
-0.8
-1
-1.2
log10(obs pk vel)-log10(pred pk vel)
bias b=-0.036+/-0.035
Q=9.94e-01, sigma-p=0.208
sm=0.088+/-0.093, Qm=0.994
4.5
5
5.5
6
6.5
7
moment magnitude

14e

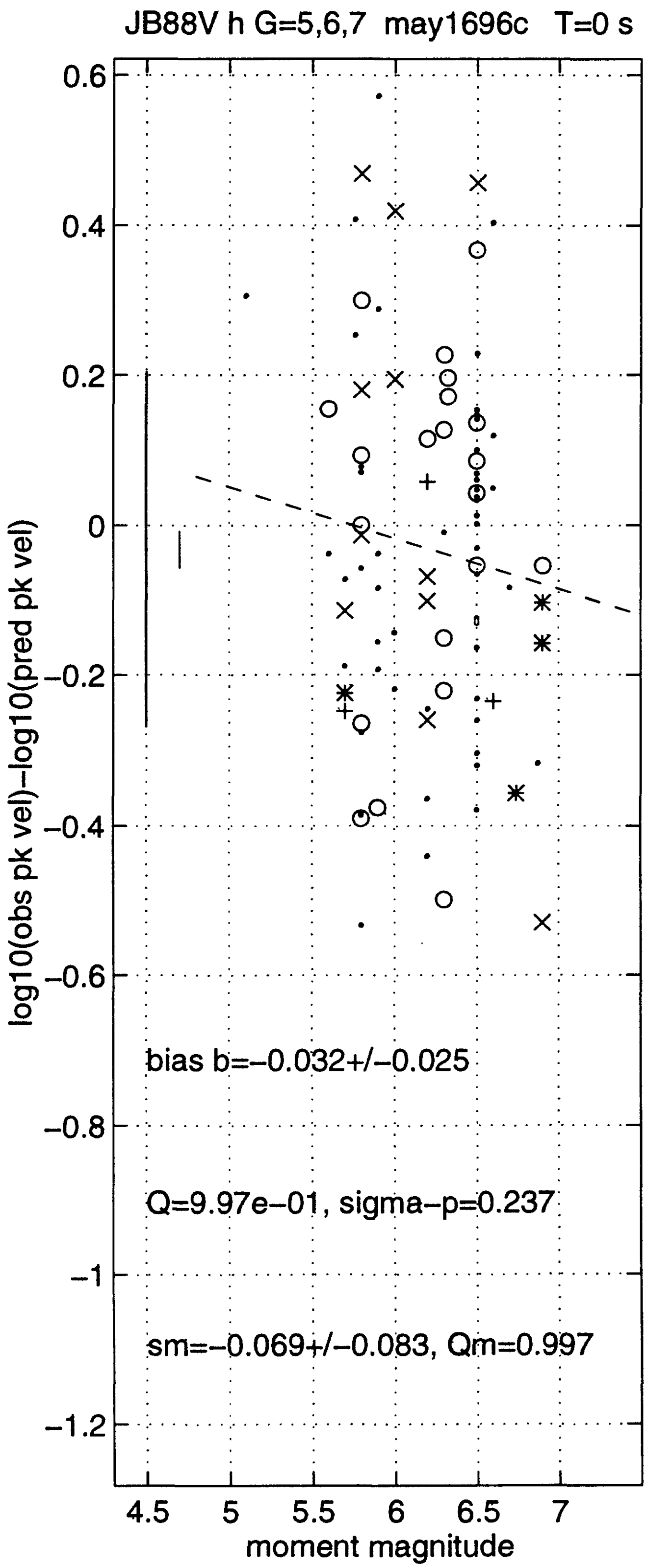

JB88V h G=5,6,7 may1696c T=0 s
0.6
0.4
0.2
0
−0.2
−0.4
−0.6
−0.8
−1
−1.2
log10(obs pk vel)−log10(pred pk vel)
bias b=−0.032+/−0.025
Q=9.97e−01, sigma−p=0.237
sm=−0.069+/−0.083, Qm=0.997
4.5
5
5.5
6
6.5
7
moment magnitude

14f

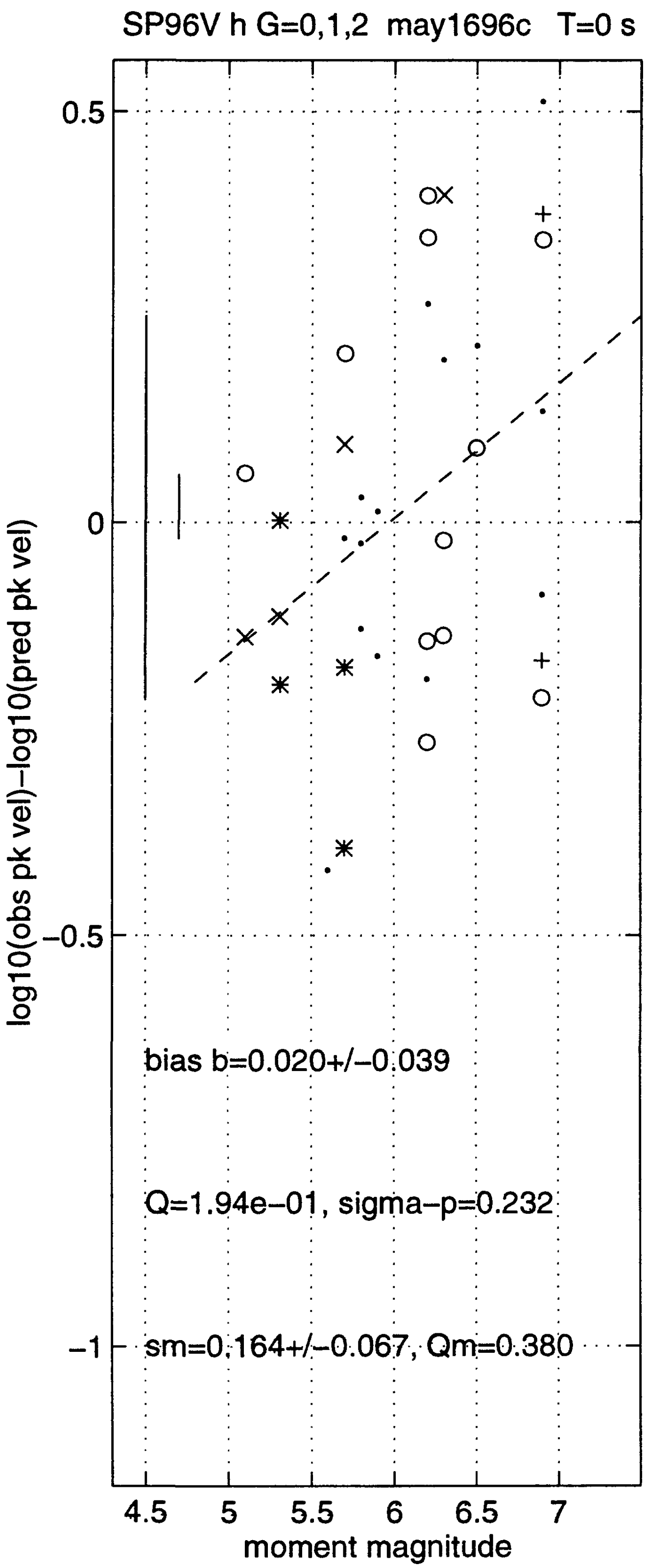
SP96V h G=0,1,2 may1696c T=0 s
0.5
0
−0.5
−1
4.5
5
5.5
6
6.5
7
moment magnitude
log10(obs pk vel)−log10(pred pk vel)
bias b=0.020+/−0.039
Q=1.94e−01, sigma−p=0.232
sm=0.164+/−0.067, Qm=0.380

14g

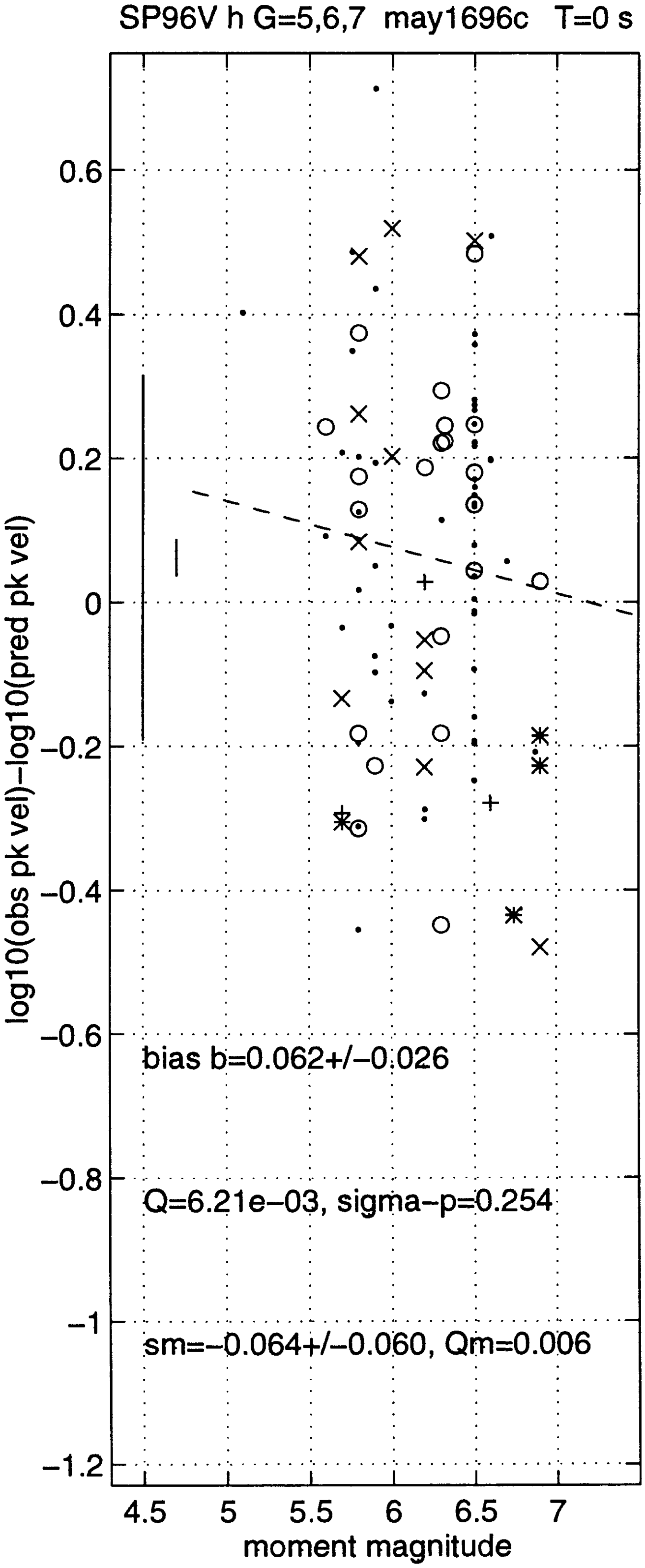

SP96V h G=5,6,7 may1696c T=0 s
log10(obs pk vel)−log10(pred pk vel)
moment magnitude
0.6
0.4
0.2
0
−0.2
−0.4
−0.6
−0.8
−1
−1.2
4.5
5
5.5
6
6.5
7
bias b=0.062+/−0.026
Q=6.21e−03, sigma−p=0.254
sm=−0.064+/−0.060, Qm=0.006

14 h

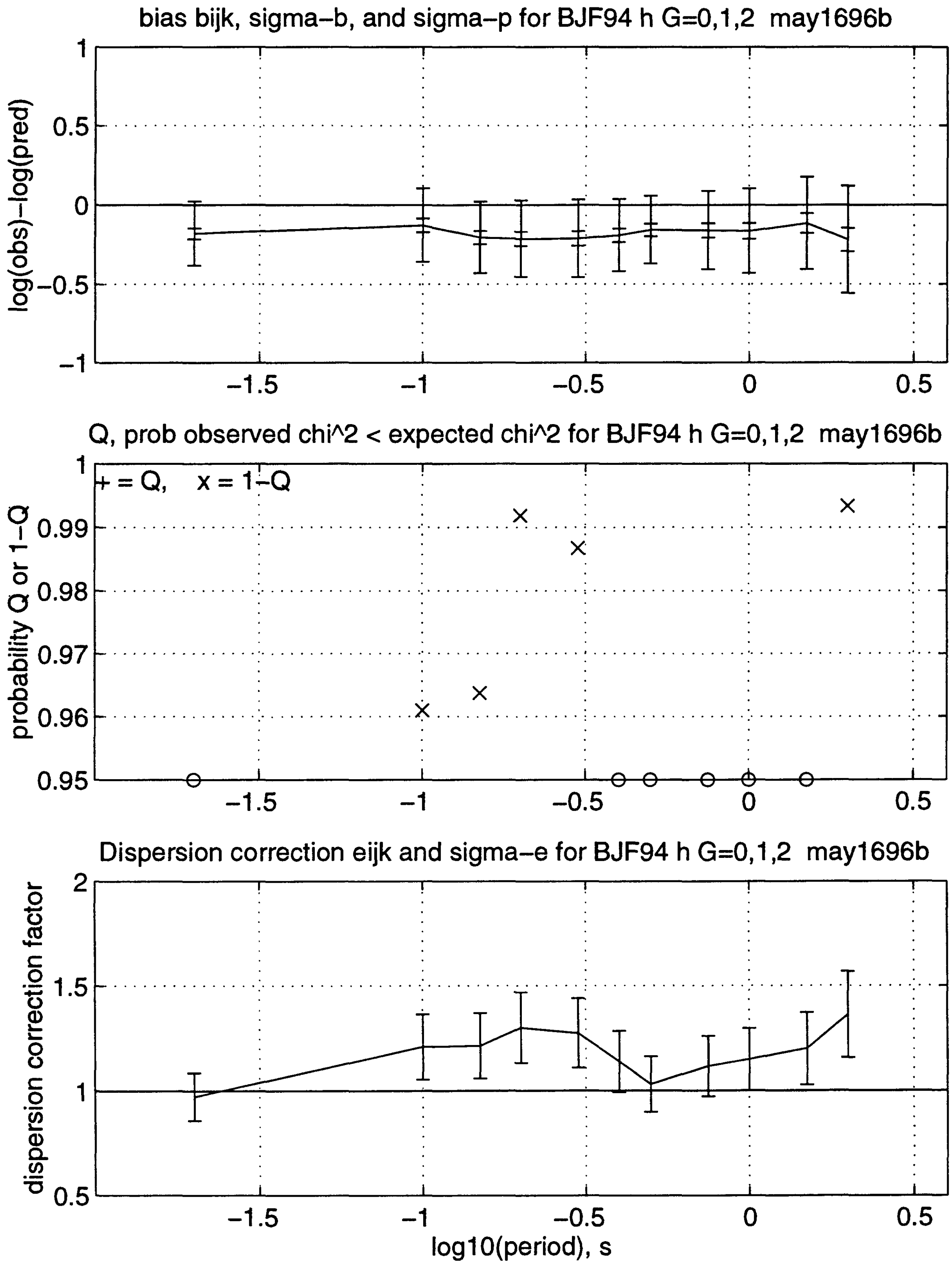

96/5/16 19:31 ymp1:[sp]may1696b1b.eps

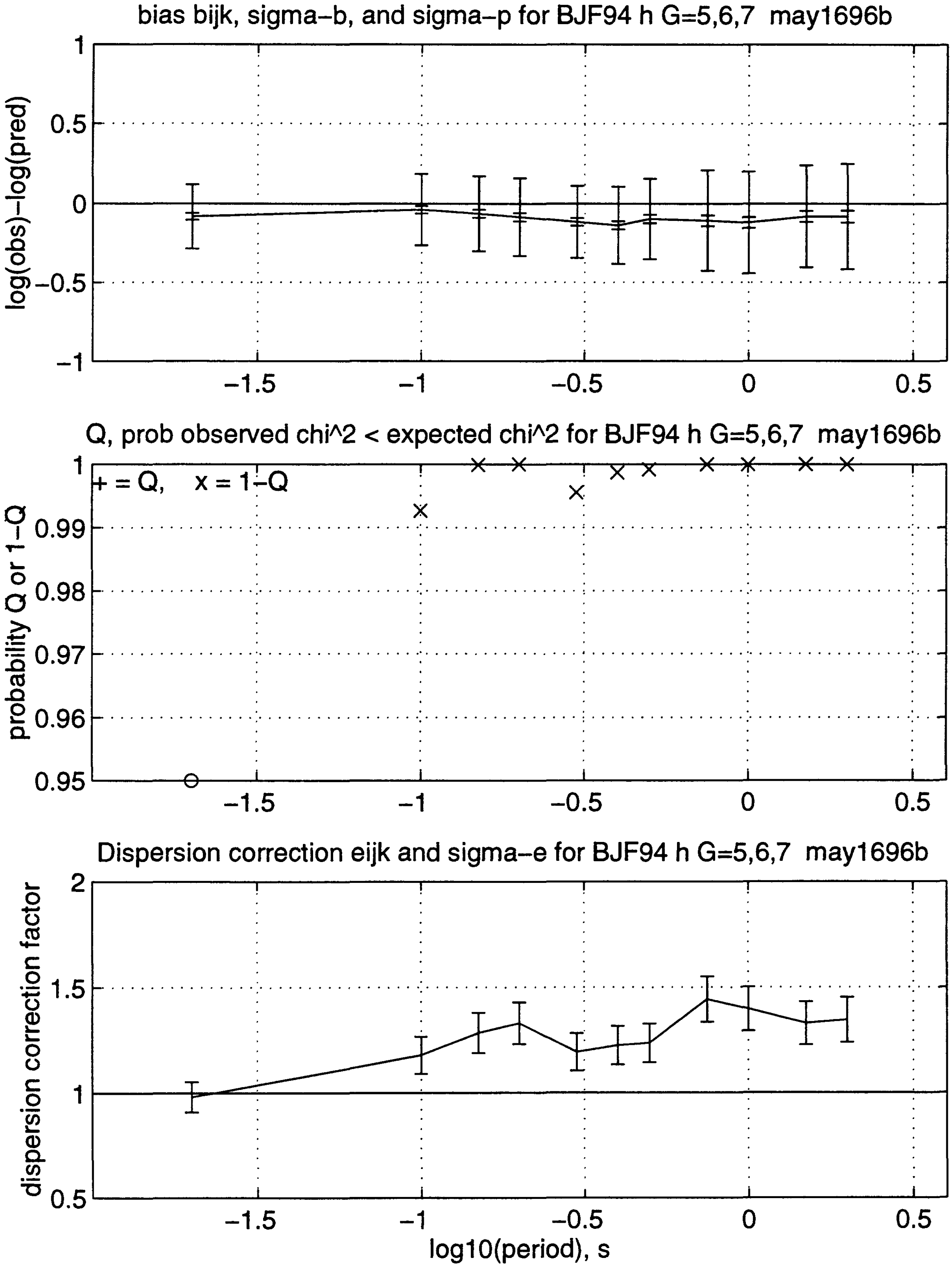

96/5/16 19:32 ymp1:[sp]may1696b2b.eps

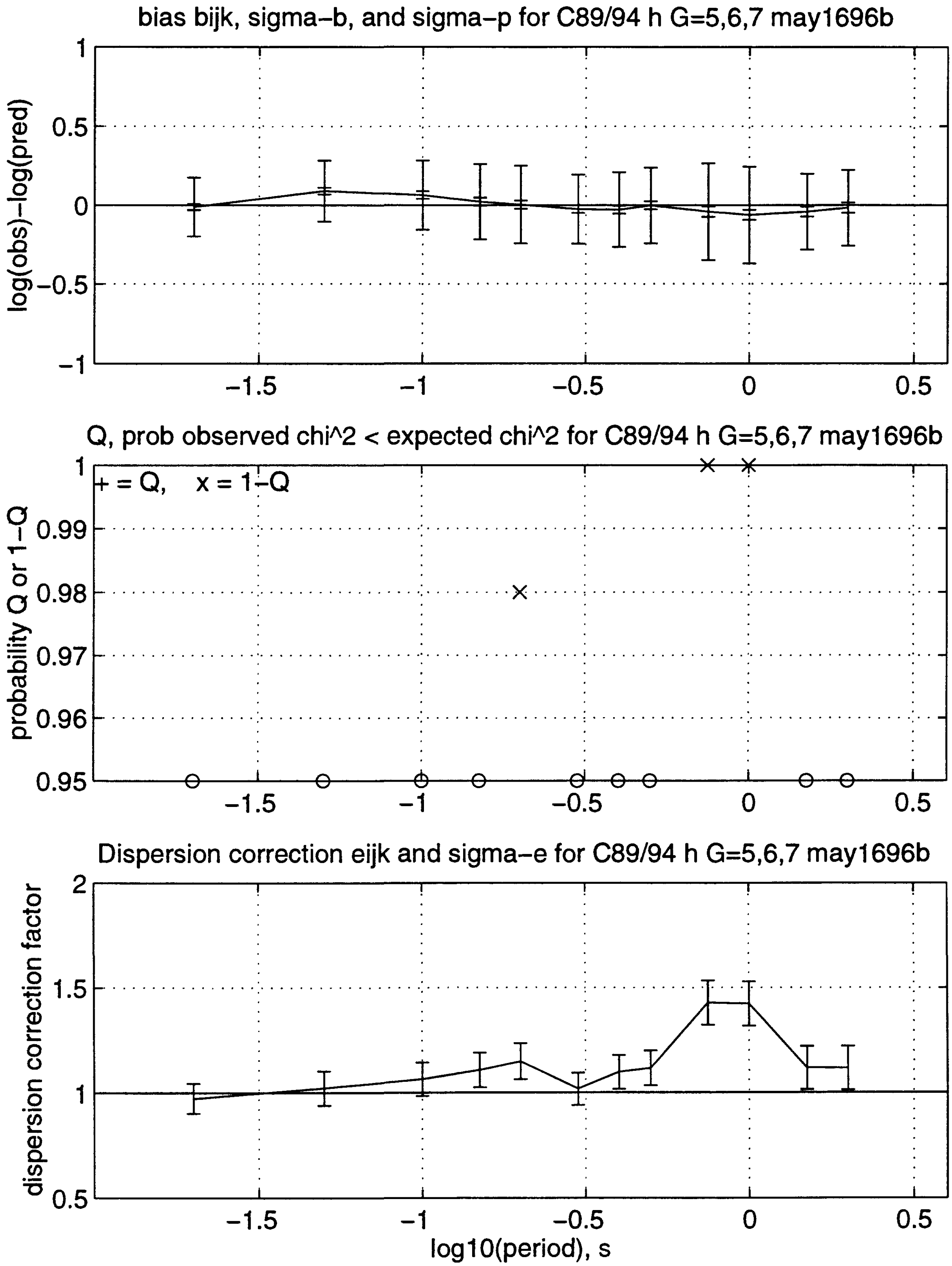

96/5/16 19:33 ymp1:[sp]may1696b3b.eps

15c

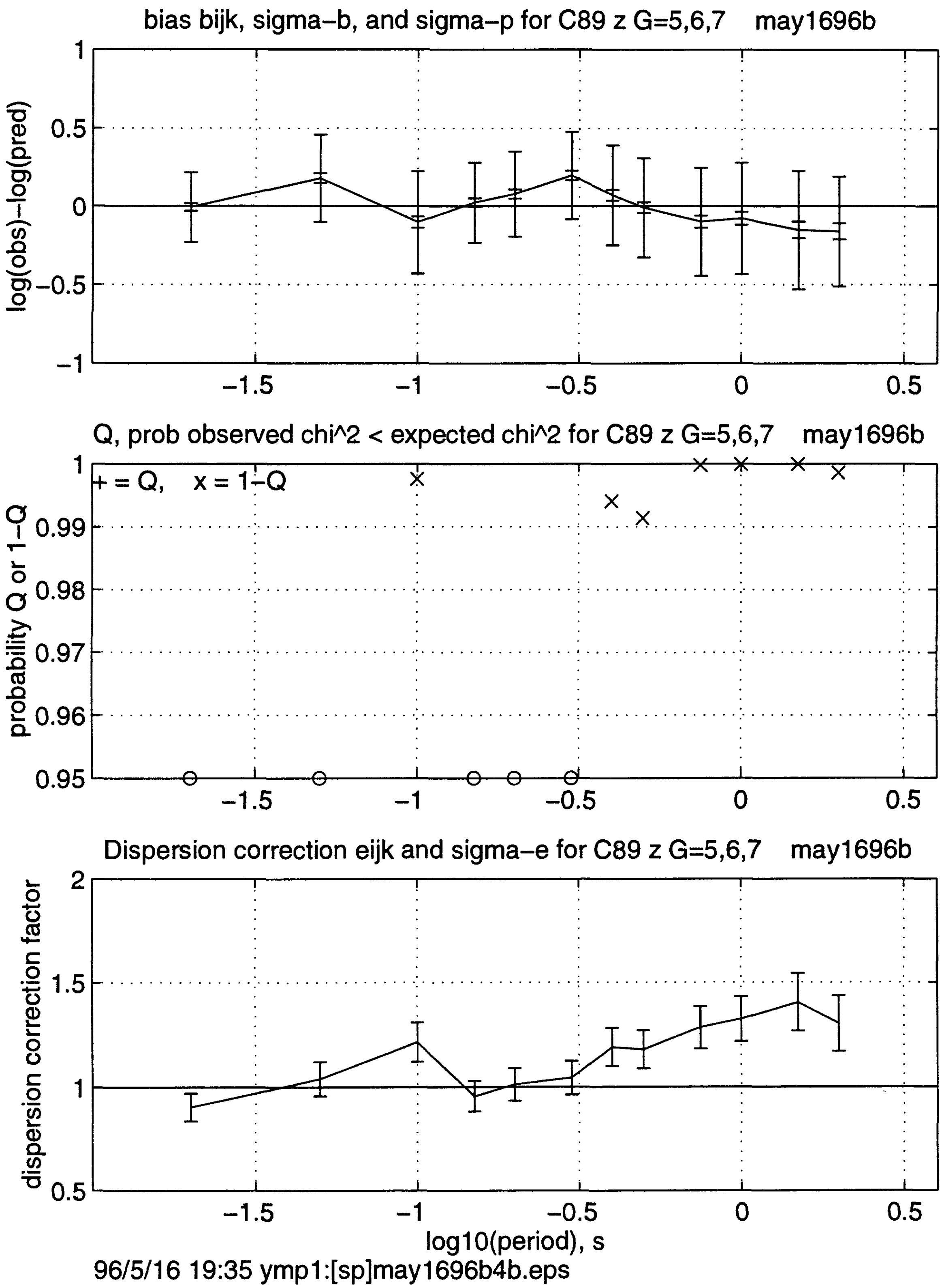

96/5/16 19:35 ymp1:[sp]may1696b4b.eps

15 d

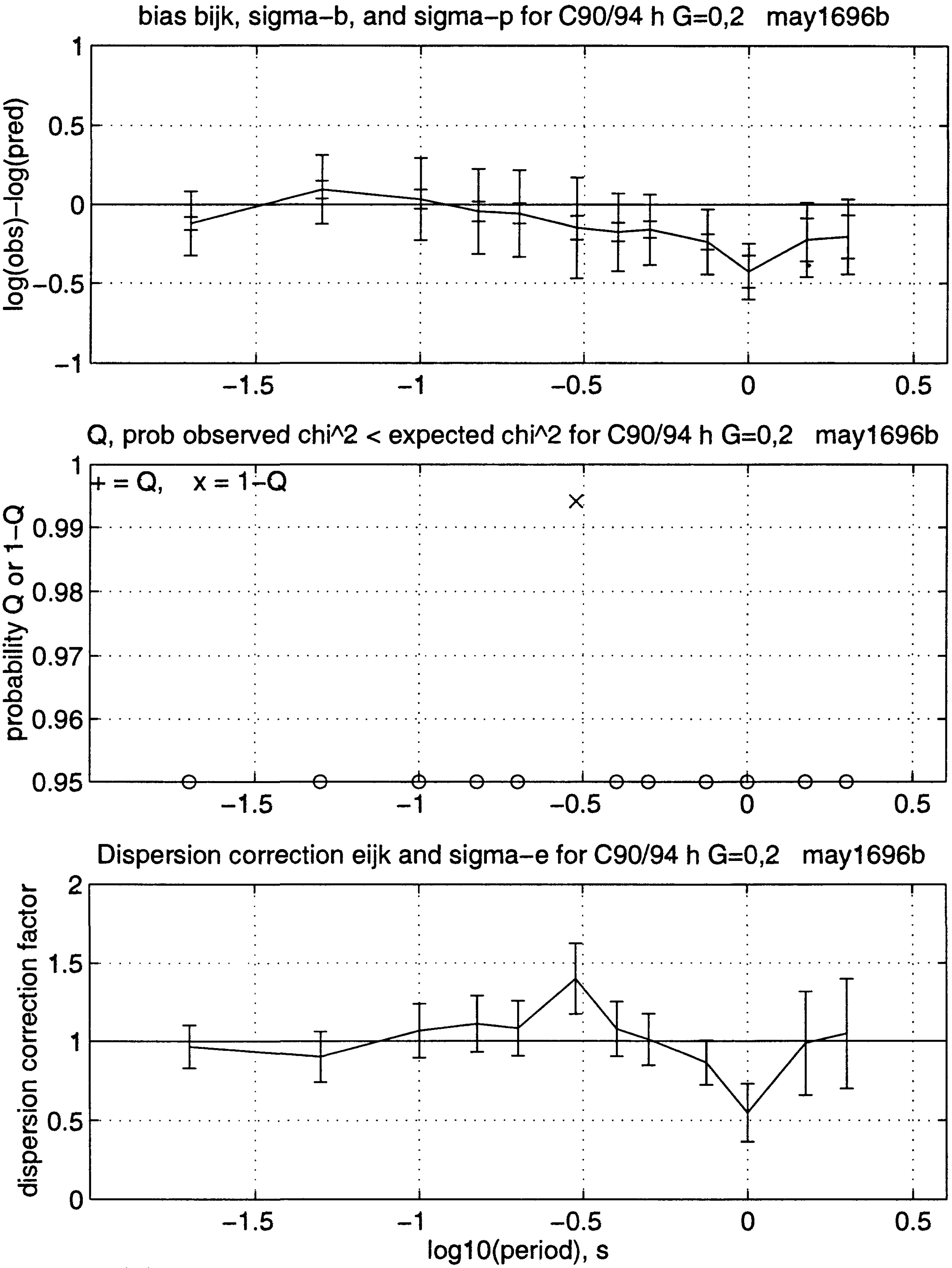

96/5/16 19:36 ymp1:[sp]may1696b5b.eps

15e

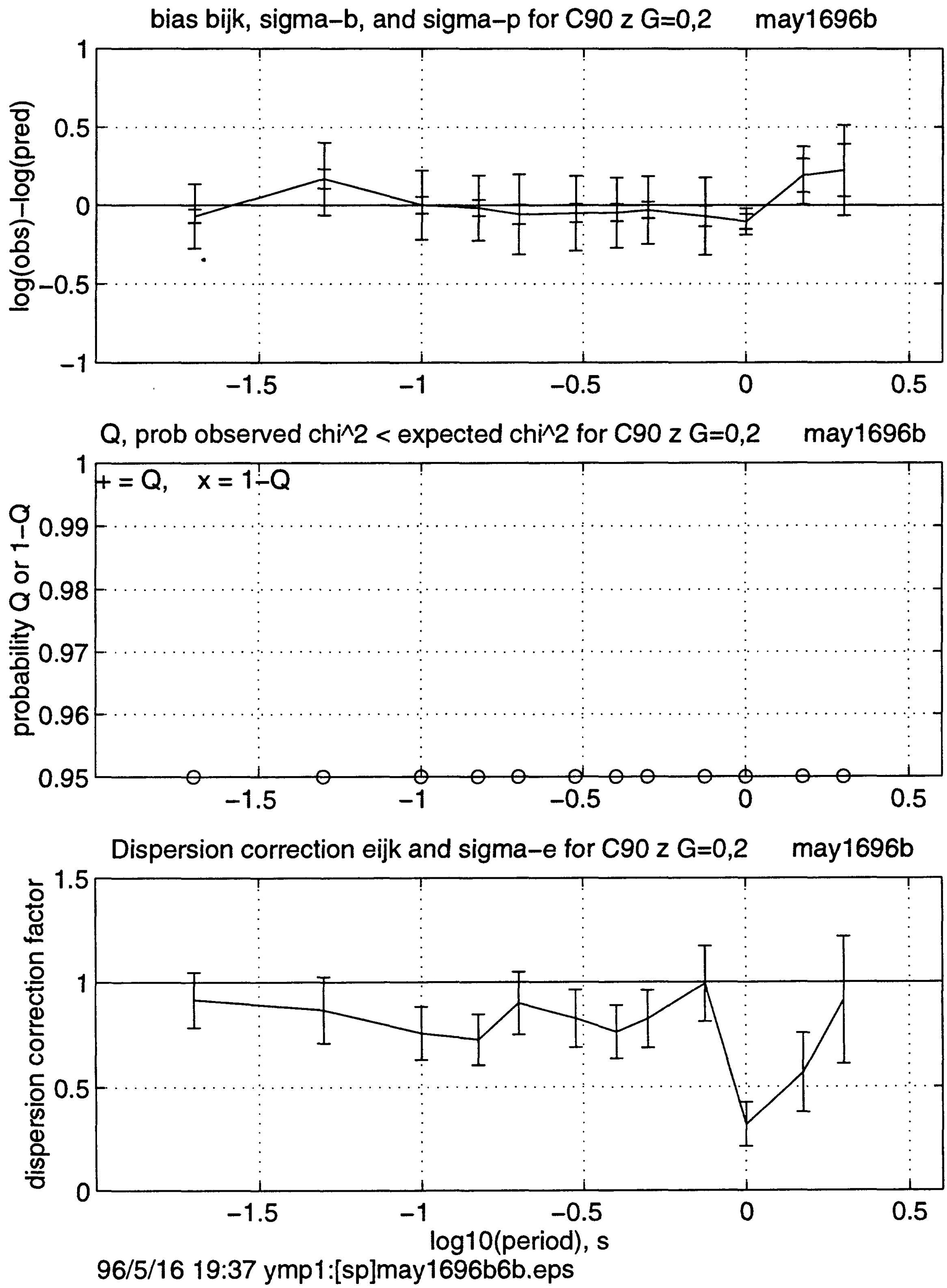
bias bijk, sigma-b, and sigma-p for C90 z G=0,2 may1696b
log(obs)-log(pred)
Q, prob observed chi^2 < expected chi^2 for C90 z G=0,2 may1696b
+ = Q, x = 1-Q
probability Q or 1-Q
Dispersion correction eijk and sigma-e for C90 z G=0,2 may1696b
dispersion correction factor
log10(period), s
96/5/16 19:37 ymp1:[sp]may1696b6b.eps

15f

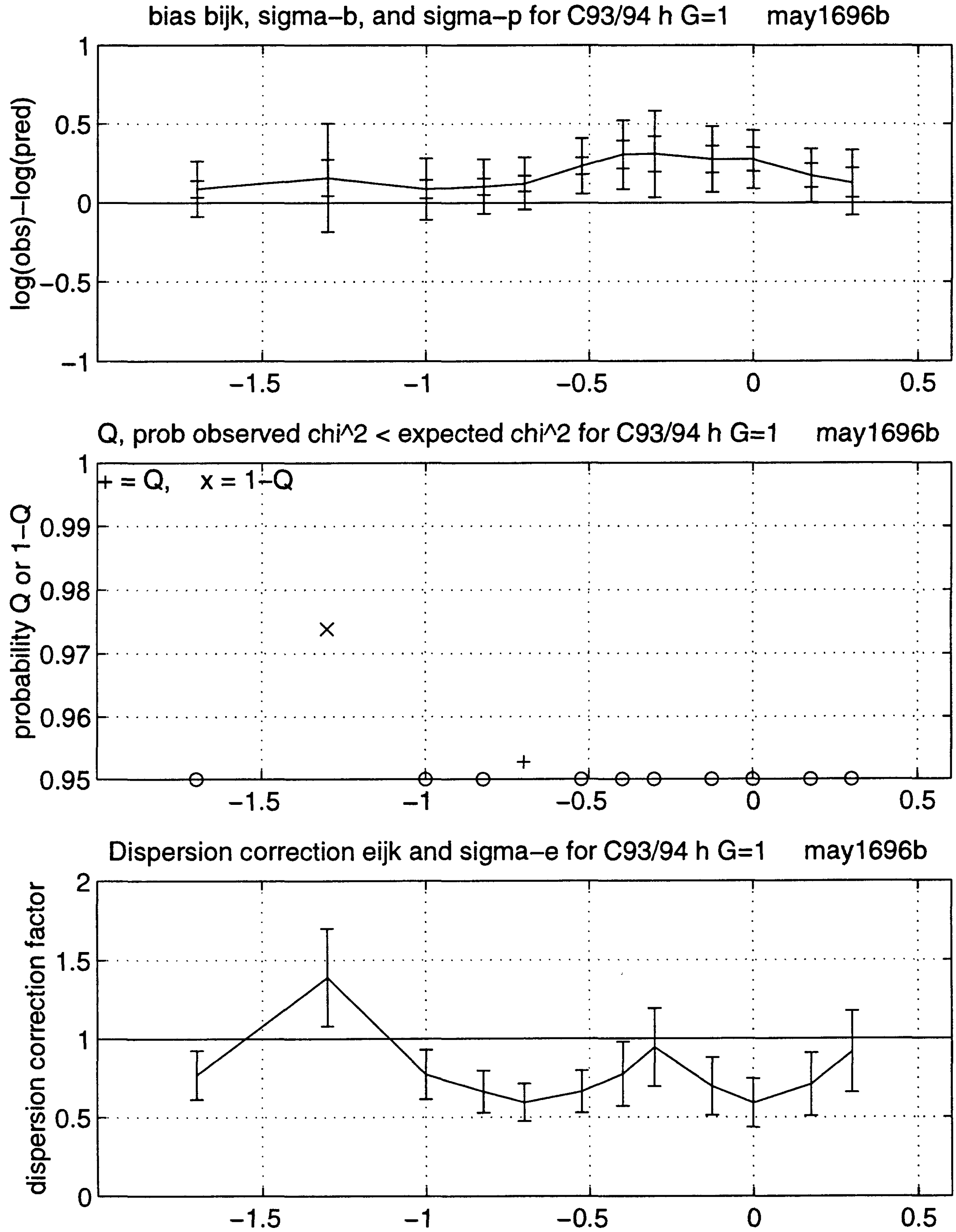

96/5/16 19:38 ymp1:[sp]may1696b7b.eps

15 g

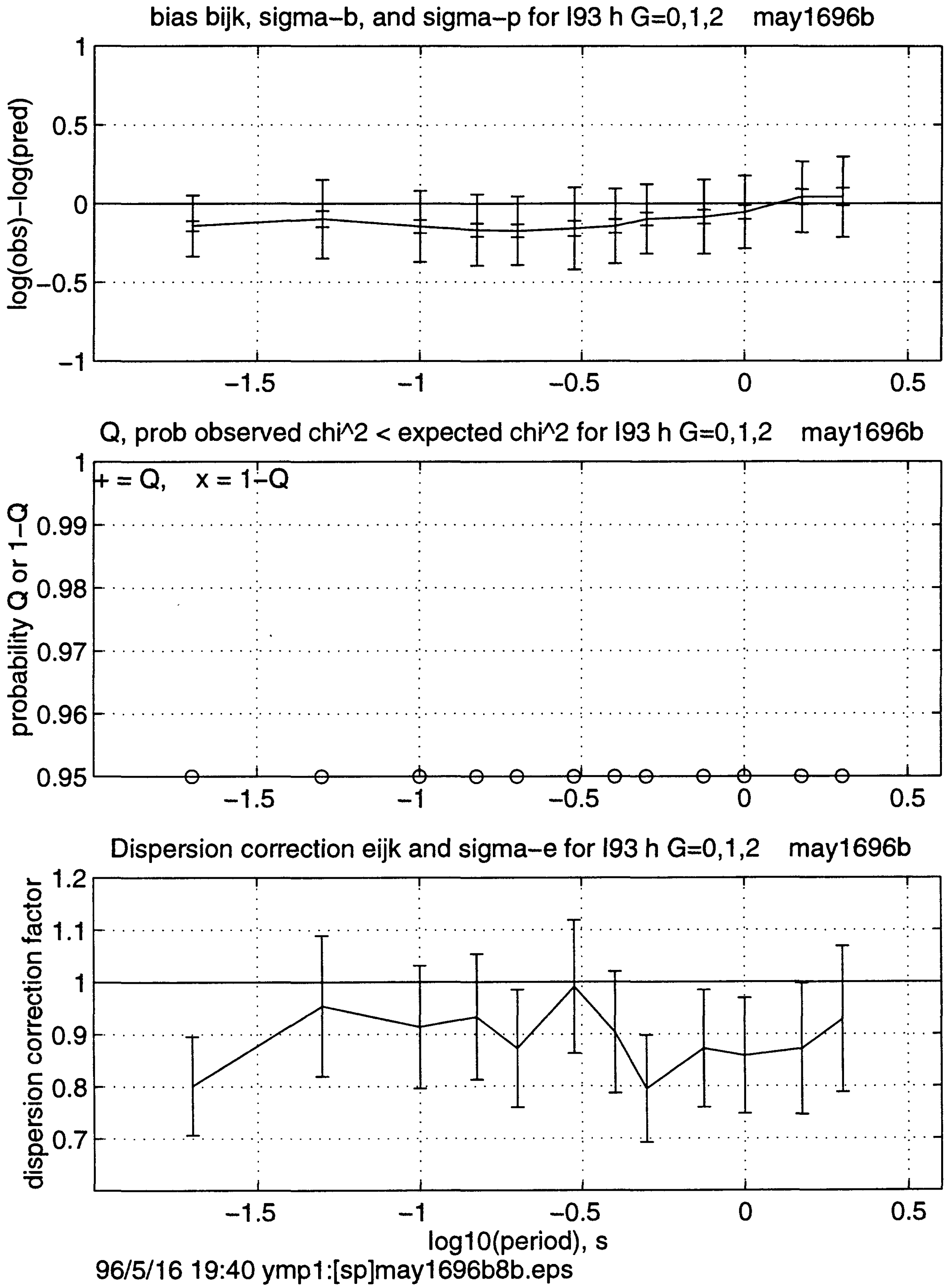
bias bijk, sigma-b, and sigma-p for I93 h G=0,1,2 may1696b
log(obs)-log(pred)
Q, prob observed chi^2 < expected chi^2 for I93 h G=0,1,2 may1696b
+ = Q, x = 1-Q
probability Q or 1-Q
Dispersion correction eijk and sigma-e for I93 h G=0,1,2 may1696b
dispersion correction factor
log10(period), s
96/5/16 19:40 ymp1:[sp]may1696b8b.eps

15 h

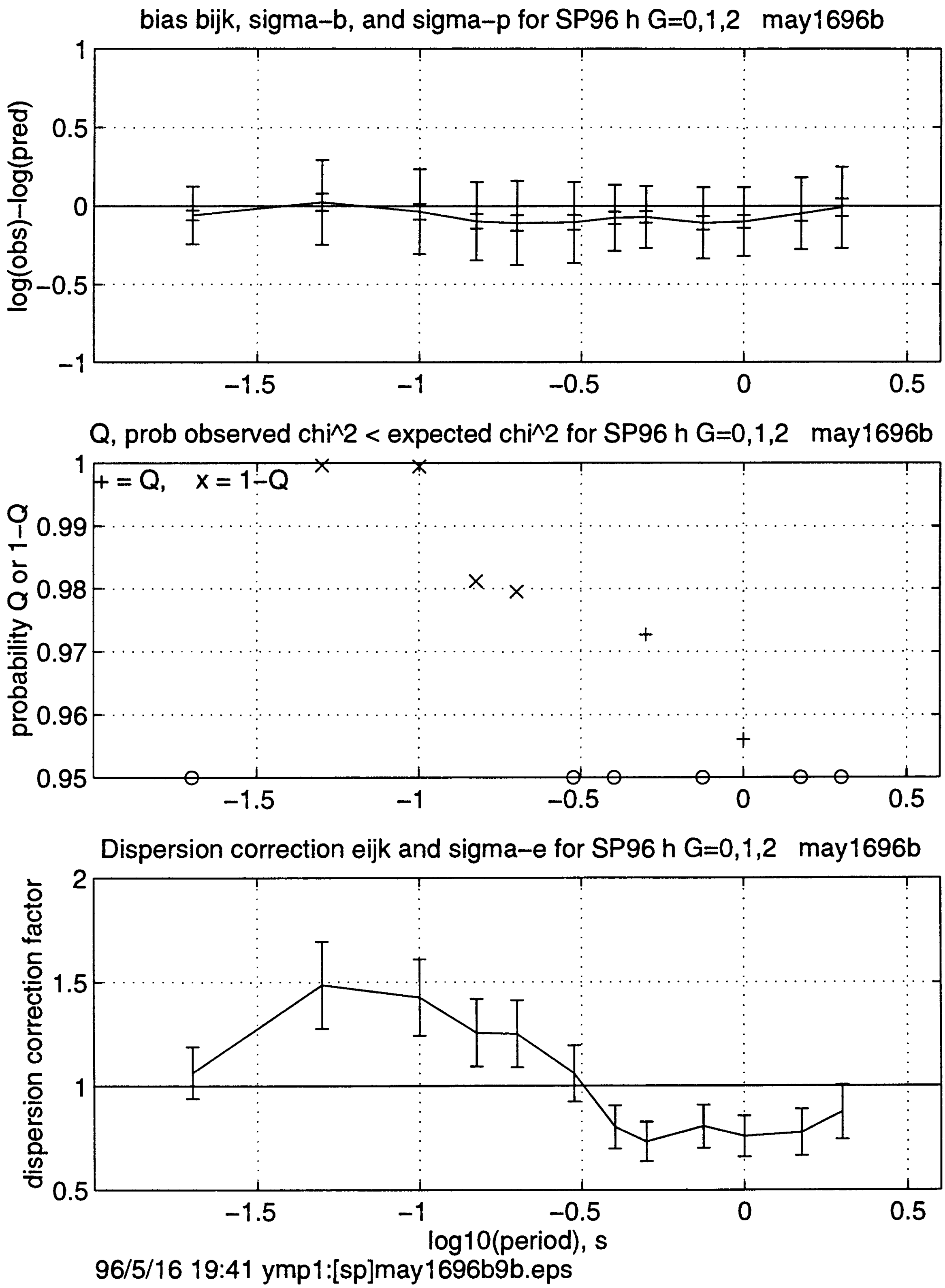
bias bijk, sigma-b, and sigma-p for SP96 h G=0,1,2 may1696b
log(obs)-log(pred)
1
0.5
0
-0.5
-1
-1.5
-1
-0.5
0
0.5
Q, prob observed chi^2 < expected chi^2 for SP96 h G=0,1,2 may1696b
+ = Q, x = 1-Q
probability Q or 1-Q
1
0.99
0.98
0.97
0.96
0.95
-1.5
-1
-0.5
0
0.5
Dispersion correction eijk and sigma-e for SP96 h G=0,1,2 may1696b
dispersion correction factor
2
1.5
1
0.5
-1.5
-1
-0.5
0
0.5
log10(period), s
96/5/16 19:41 ymp1:[sp]may1696b9b.eps

15i

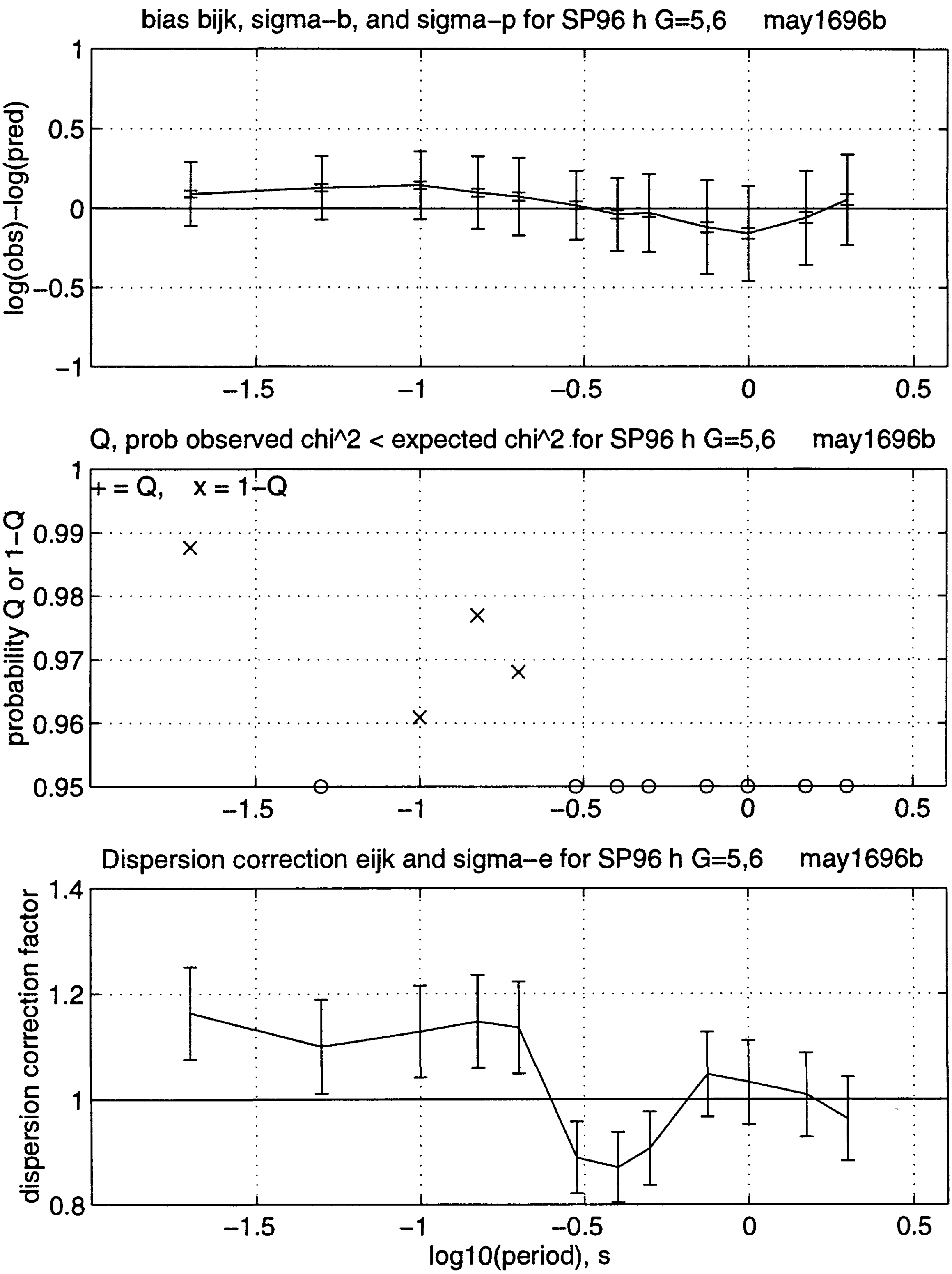

96/5/16 19:42 ymp1:[sp]may1696b10b.eps

15j

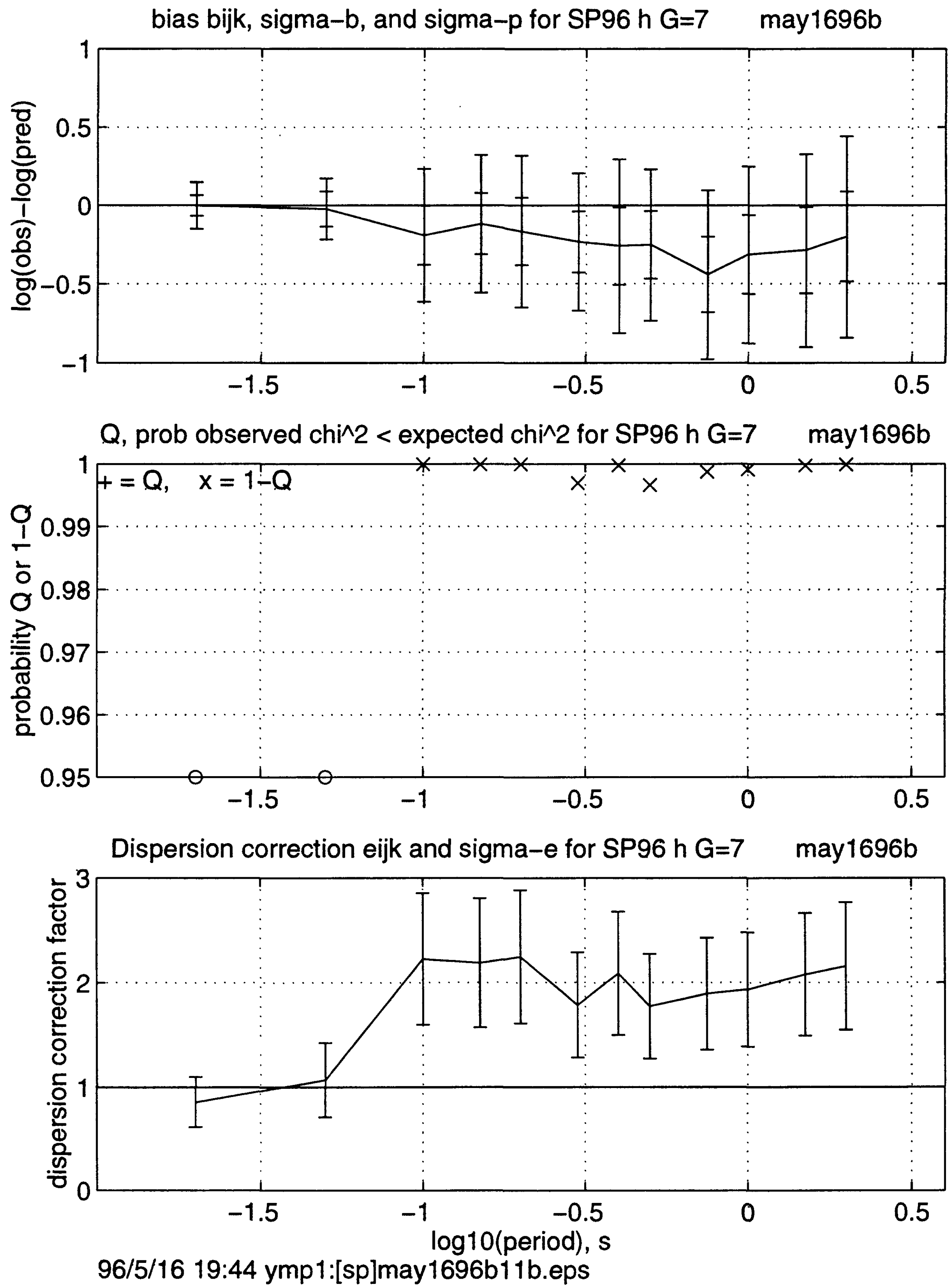
bias bijk, sigma-b, and sigma-p for SP96 h G=7 may1696b
log(obs)-log(pred)
1
0.5
0
-0.5
-1
-1.5
-1
-0.5
0
0.5
Q, prob observed chi^2 < expected chi^2 for SP96 h G=7 may1696b
+ = Q, x = 1-Q
probability Q or 1-Q
1
0.99
0.98
0.97
0.96
0.95
Dispersion correction eijk and sigma-e for SP96 h G=7 may1696b
dispersion correction factor
3
2
1
0
log10(period), s
96/5/16 19:44 ymp1:[sp]may1696b11b.eps

15k

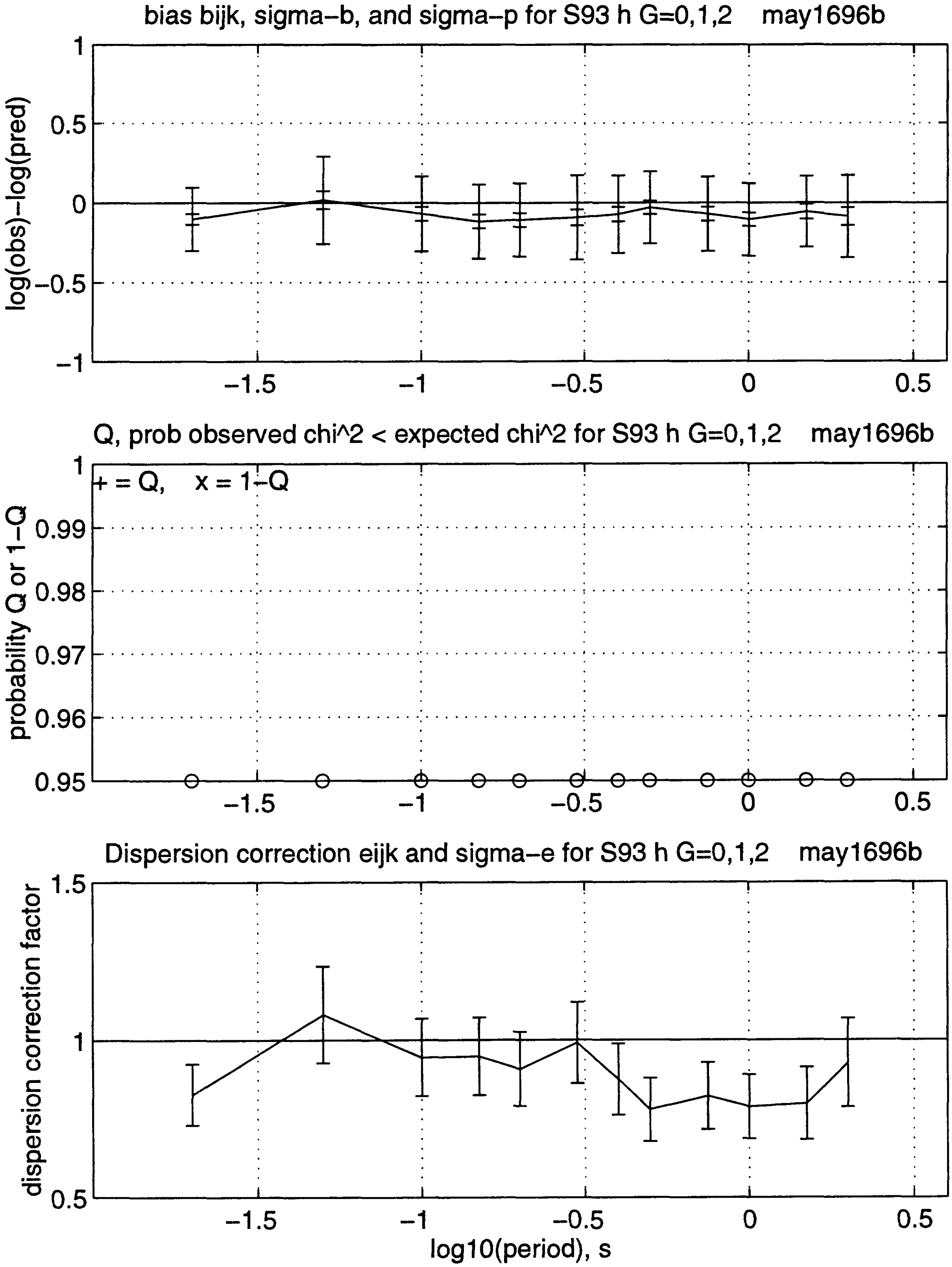

96/5/16 19:45 ymp1:[sp]may1696b12b.eps

15l

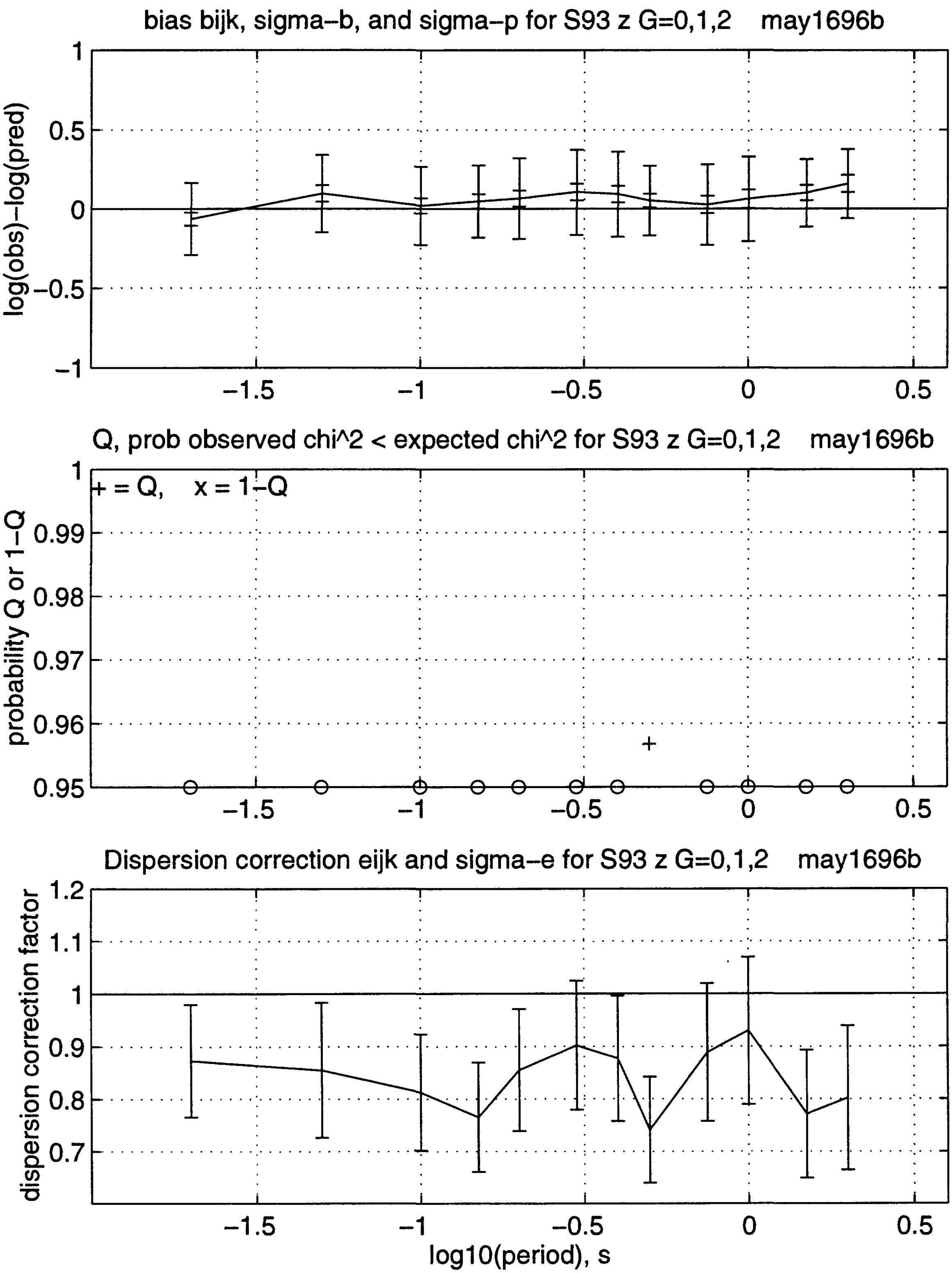

96/5/16 19:46 ymp1:[sp]may1696b13b.eps

15 m

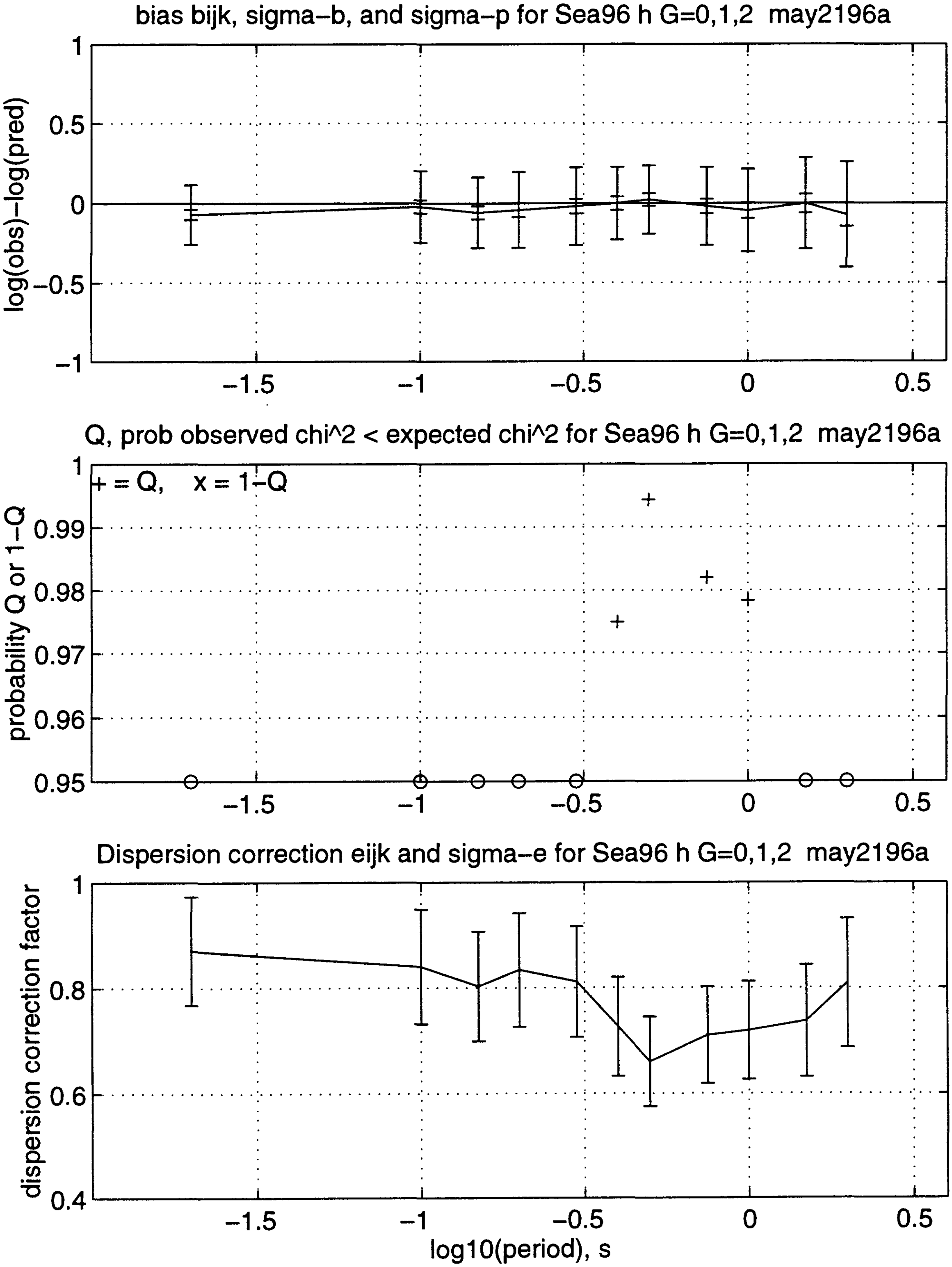

96/5/21 21:33 ymp1:[sp]may2196a22b.eps

15 n

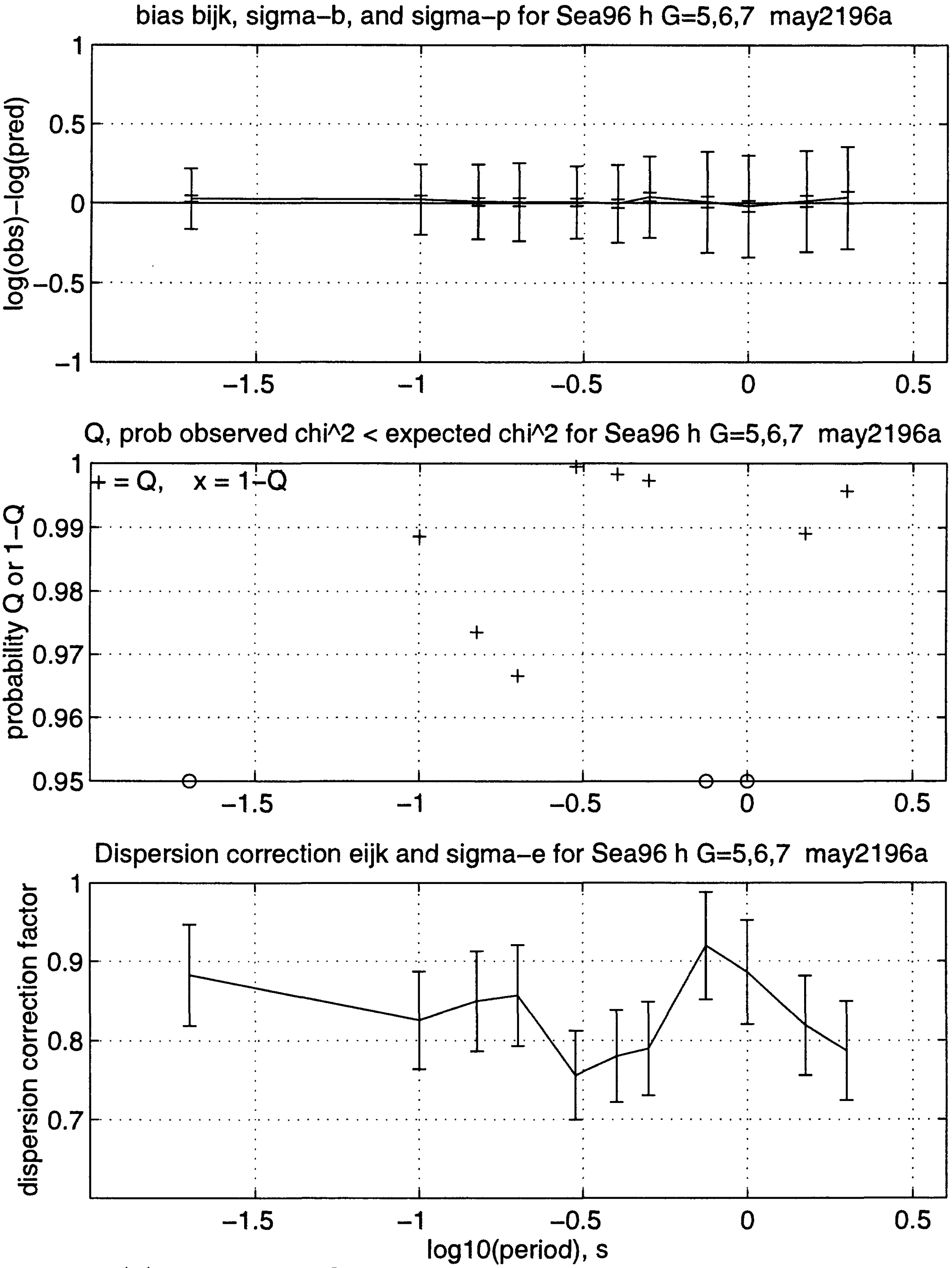

96/5/21 21:34 ymp1:[sp]may2196a23b.eps

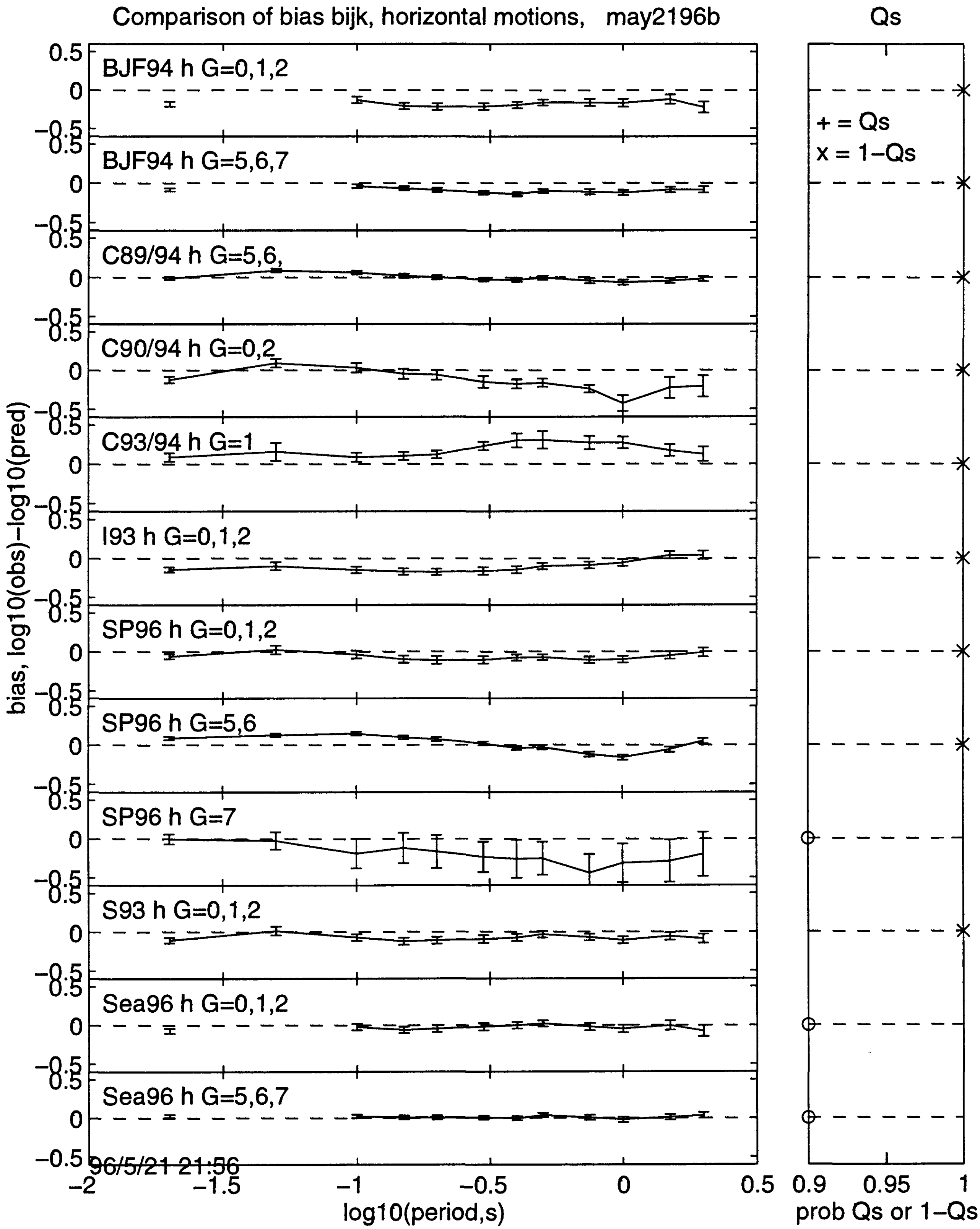
Comparison of bias bijk, horizontal motions, may2196b
Qs
BJF94 h G=0,1,2
BJF94 h G=5,6,7
C89/94 h G=5,6,
C90/94 h G=0,2
C93/94 h G=1
I93 h G=0,1,2
SP96 h G=0,1,2
SP96 h G=5,6
SP96 h G=7
S93 h G=0,1,2
Sea96 h G=0,1,2
Sea96 h G=5,6,7
+ = Qs
x = 1−Qs
bias, log10(obs)−log10(pred)
log10(period,s)
prob Qs or 1−Qs
96/5/21 21:56

16a

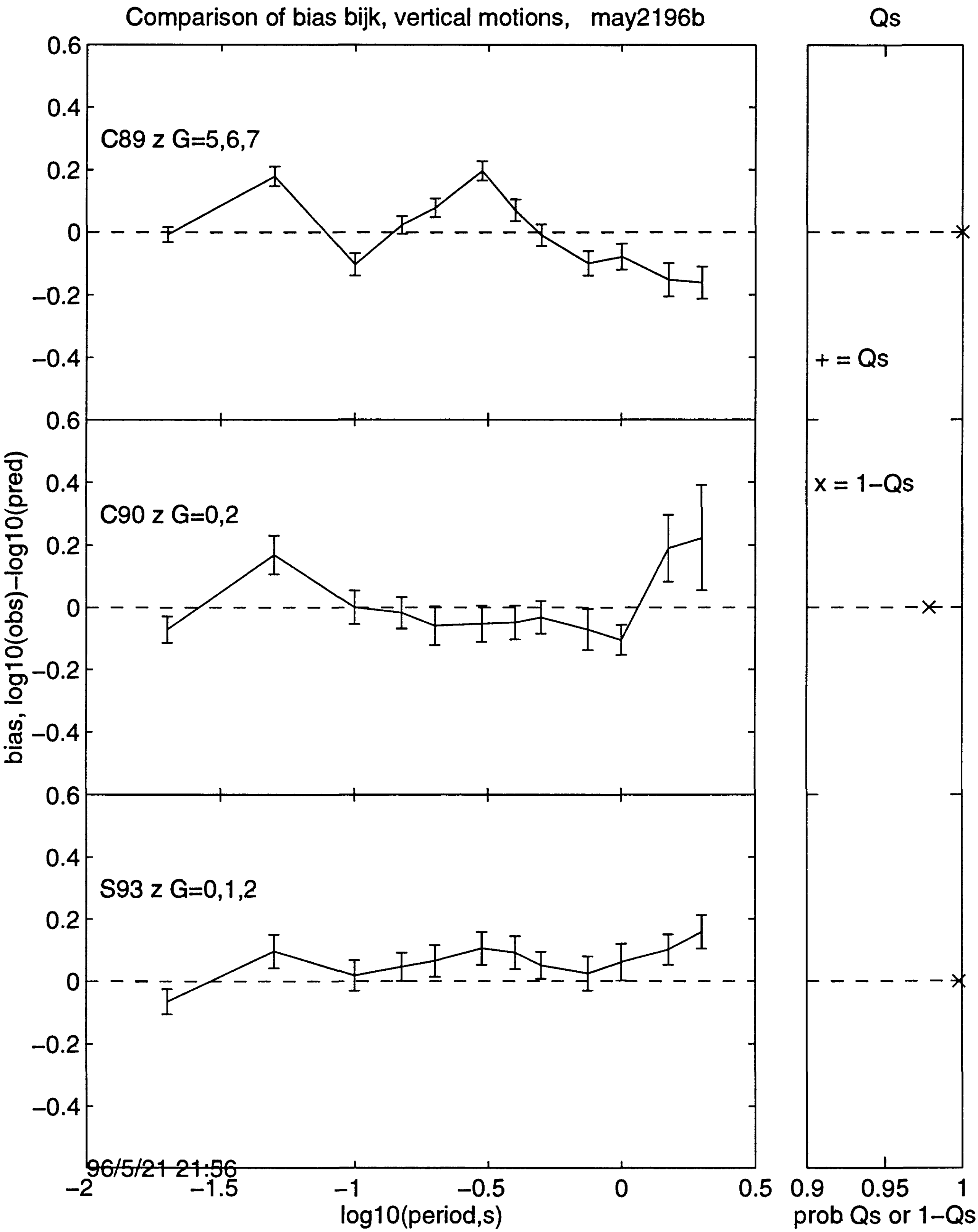
Comparison of bias bijk, vertical motions, may2196b
Qs
C89 z G=5,6,7
C90 z G=0,2
S93 z G=0,1,2
+ = Qs
x = 1−Qs
bias, log10(obs)−log10(pred)
log10(period,s)
prob Qs or 1−Qs
96/5/21 21:56
0.6
0.4
0.2
0
−0.2
−0.4
−2
−1.5
−1
−0.5
0
0.5
0.9
0.95
1

252

16 b

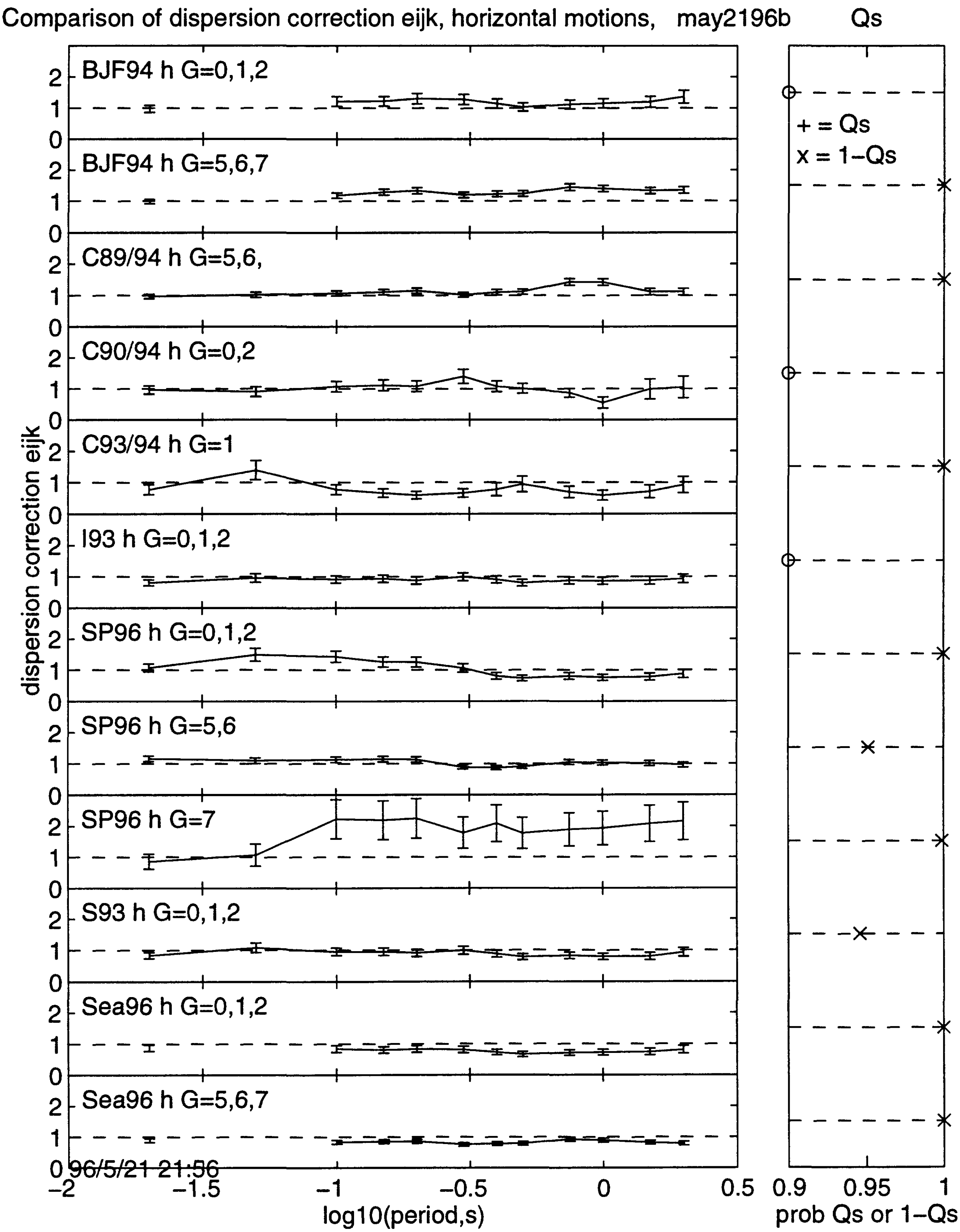
Comparison of dispersion correction eijk, horizontal motions, may2196b
Qs
BJF94 h G=0,1,2
BJF94 h G=5,6,7
C89/94 h G=5,6,
C90/94 h G=0,2
C93/94 h G=1
I93 h G=0,1,2
SP96 h G=0,1,2
SP96 h G=5,6
SP96 h G=7
S93 h G=0,1,2
Sea96 h G=0,1,2
Sea96 h G=5,6,7
dispersion correction eijk
96/5/21 21:56
log10(period,s)
+ = Qs
x = 1−Qs
prob Qs or 1−Qs

16c

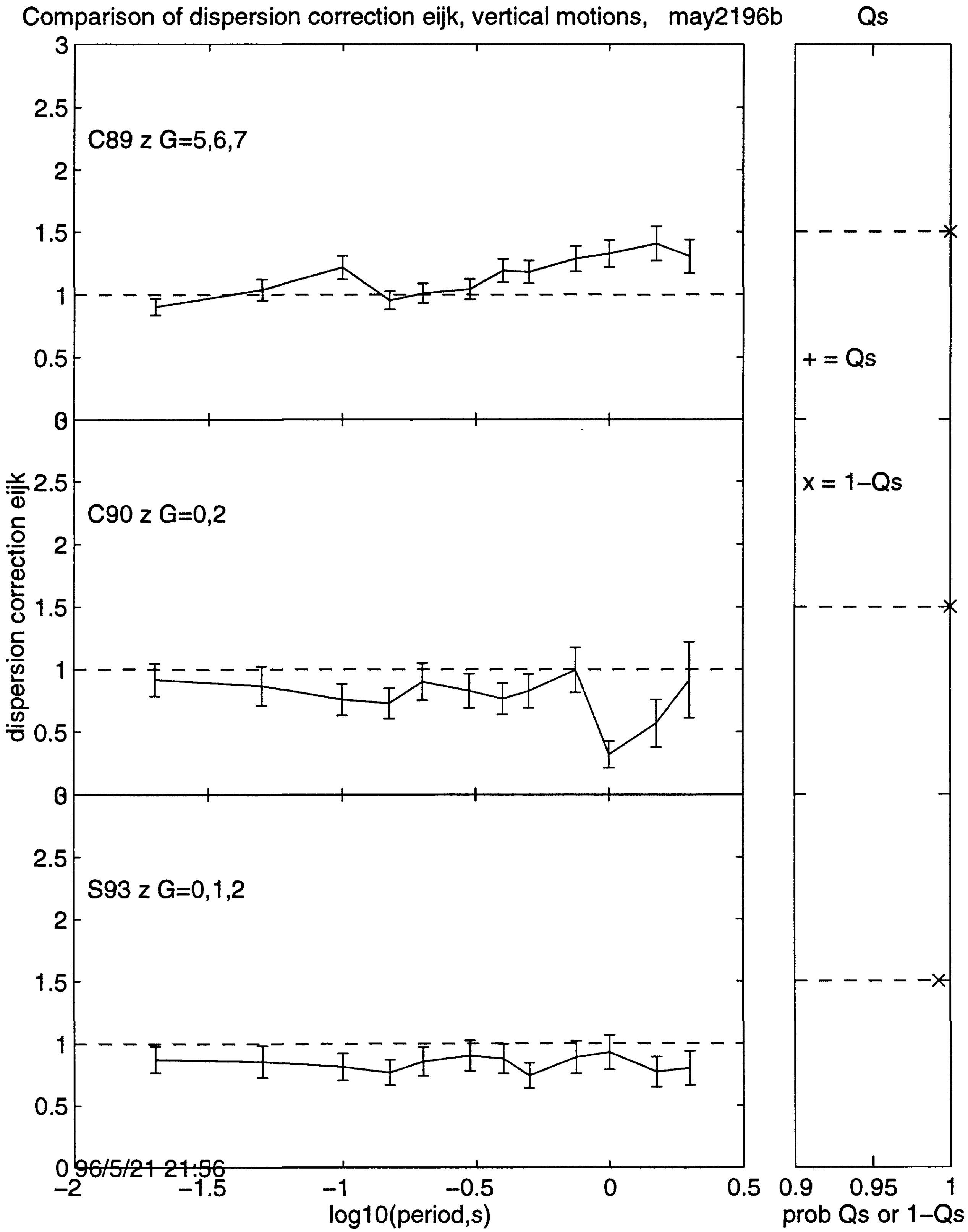
Comparison of dispersion correction eijk, vertical motions, may2196b
Qs
C89 z G=5,6,7
C90 z G=0,2
S93 z G=0,1,2
dispersion correction eijk
+ = Qs
x = 1−Qs
96/5/21 21:56
log10(period,s)
prob Qs or 1−Qs

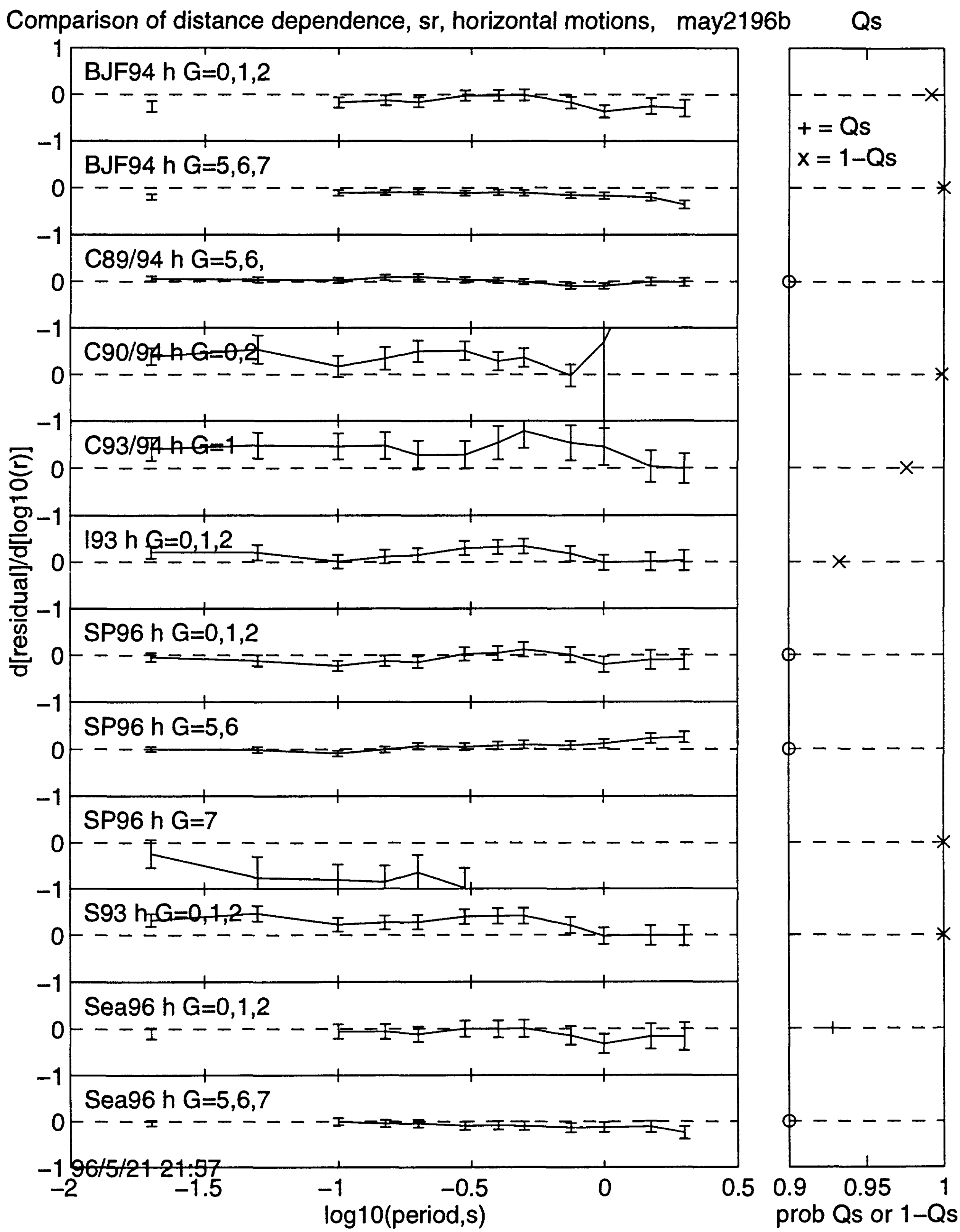

Comparison of distance dependence, sr, horizontal motions, may2196b
Qs
BJF94 h G=0,1,2
BJF94 h G=5,6,7
C89/94 h G=5,6,
C90/94 h G=0,2
C93/94 h G=1
I93 h G=0,1,2
SP96 h G=0,1,2
SP96 h G=5,6
SP96 h G=7
S93 h G=0,1,2
Sea96 h G=0,1,2
Sea96 h G=5,6,7
d[residual]/d[log10(r)]
96/5/21 21:57
log10(period,s)
+ = Qs
x = 1−Qs
prob Qs or 1−Qs

16e

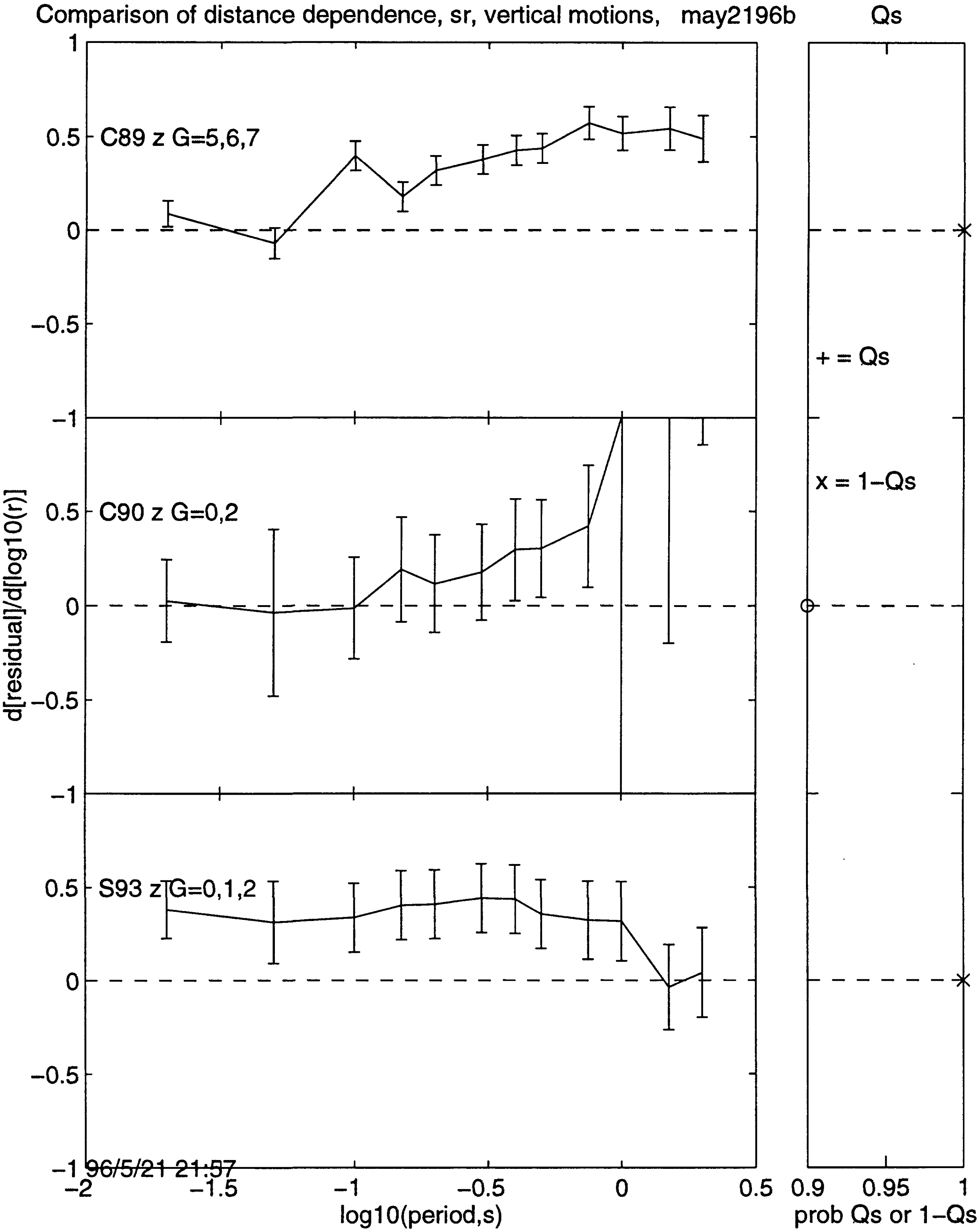

Comparison of distance dependence, sr, vertical motions, may2196b
Qs
C89 z G=5,6,7
C90 z G=0,2
S93 z G=0,1,2
d[residual]/d[log10(r)]
log10(period,s)
+ = Qs
x = 1−Qs
prob Qs or 1−Qs
96/5/21 21:57

16 f

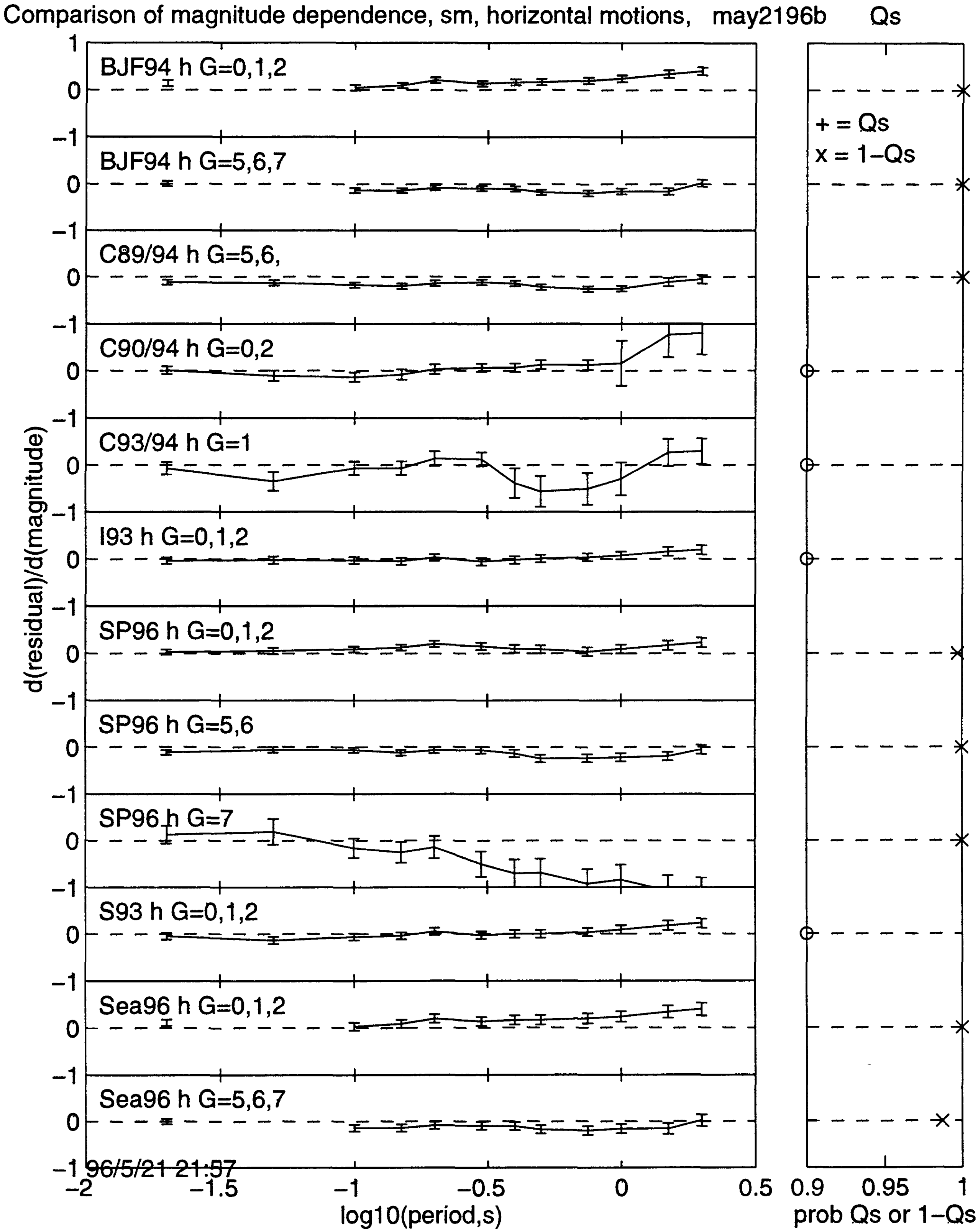
Comparison of magnitude dependence, sm, horizontal motions, may2196b Qs
BJF94 h G=0,1,2
BJF94 h G=5,6,7
C89/94 h G=5,6,
C90/94 h G=0,2
C93/94 h G=1
I93 h G=0,1,2
SP96 h G=0,1,2
SP96 h G=5,6
SP96 h G=7
S93 h G=0,1,2
Sea96 h G=0,1,2
Sea96 h G=5,6,7
96/5/21 21:57
d(residual)/d(magnitude)
log10(period,s)
+ = Qs
x = 1−Qs
prob Qs or 1−Qs

16g

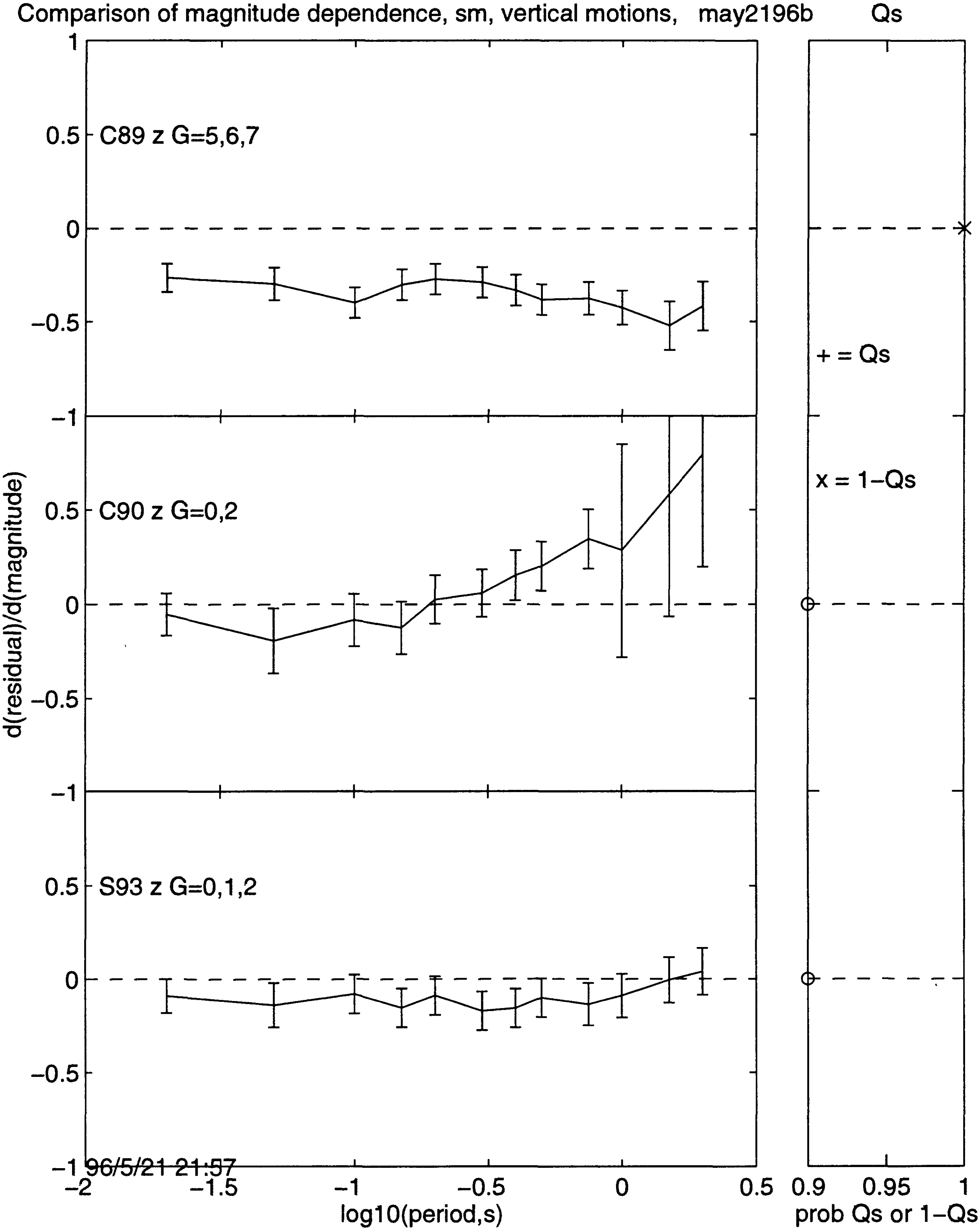
Comparison of magnitude dependence, sm, vertical motions, may2196b
Qs
C89 z G=5,6,7
C90 z G=0,2
S93 z G=0,1,2
+ = Qs
x = 1−Qs
d(residual)/d(magnitude)
log10(period,s)
prob Qs or 1−Qs
96/5/21 21:57

16 h

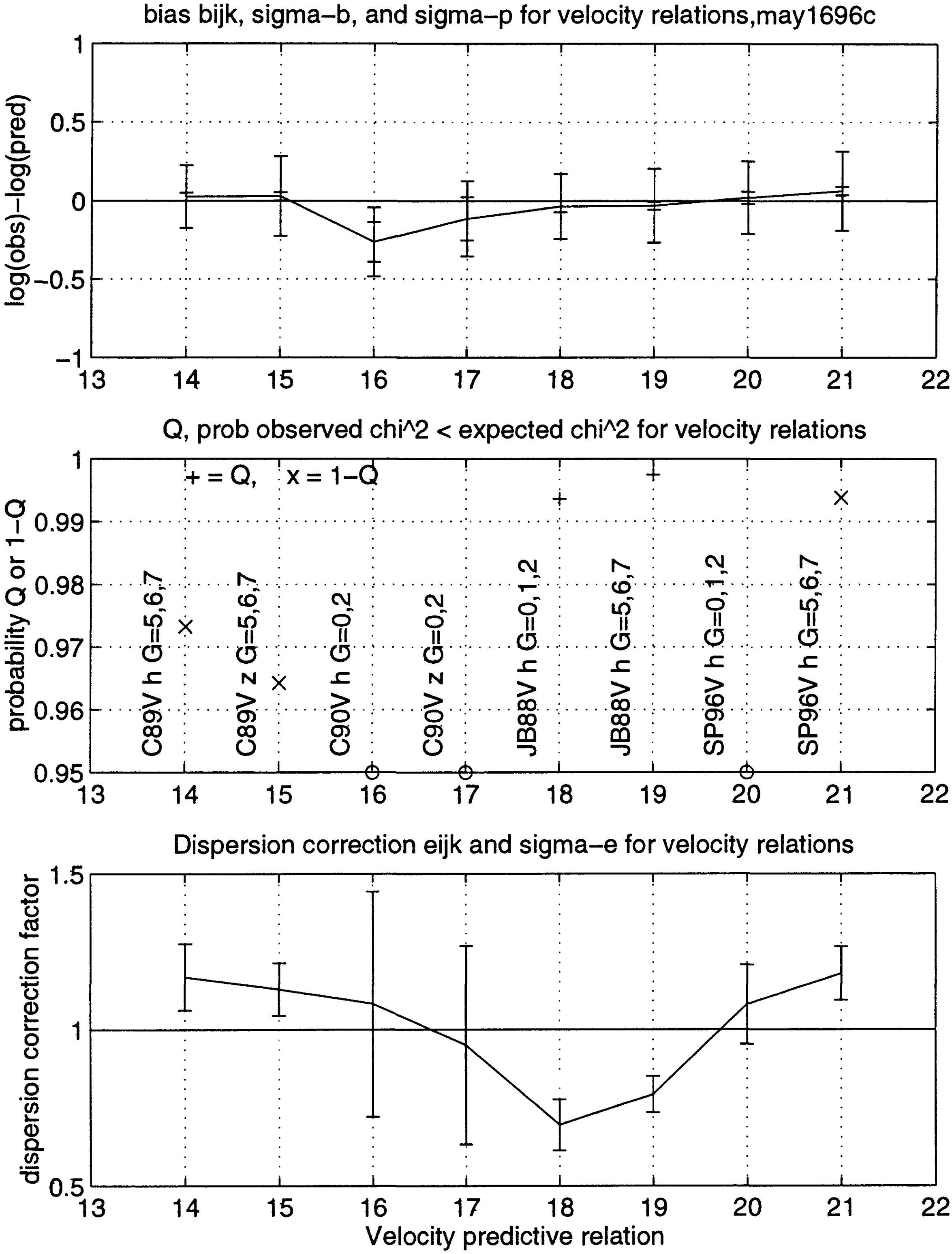

96/5/16 21:36 ymp1:[sp]may1696c23b.eps

17a

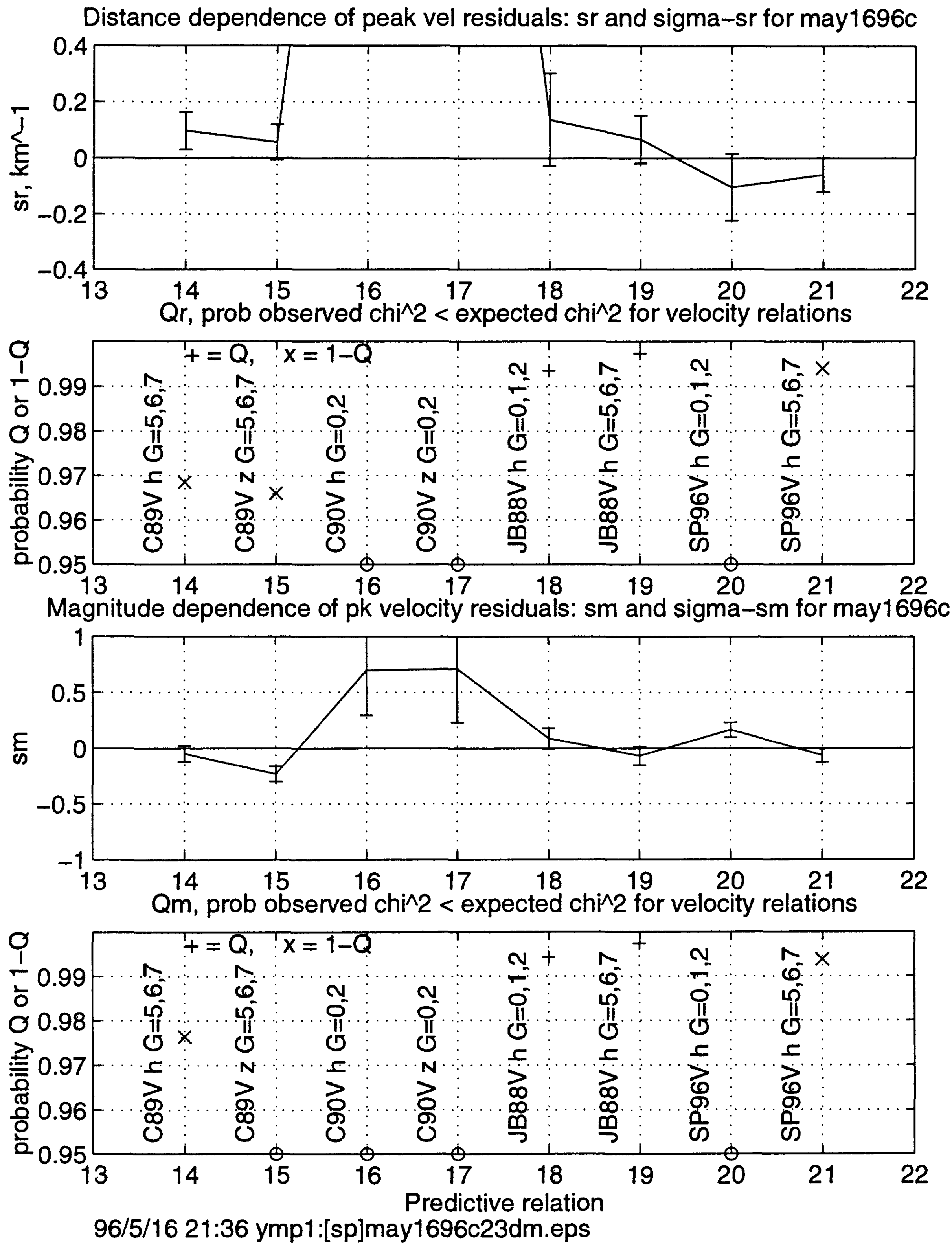
Distance dependence of peak vel residuals: sr and sigma−sr for may1696c
sr, km^−1
Qr, prob observed chi^2 < expected chi^2 for velocity relations
probability Q or 1−Q
+ = Q, x = 1−Q
C89V h G=5,6,7
C89V z G=5,6,7
C90V h G=0,2
C90V z G=0,2
JB88V h G=0,1,2
JB88V h G=5,6,7
SP96V h G=0,1,2
SP96V h G=5,6,7
Magnitude dependence of pk velocity residuals: sm and sigma−sm for may1696c
sm
Qm, prob observed chi^2 < expected chi^2 for velocity relations
Predictive relation
96/5/16 21:36 ymp1:[sp]may1696c23dm.eps

17b

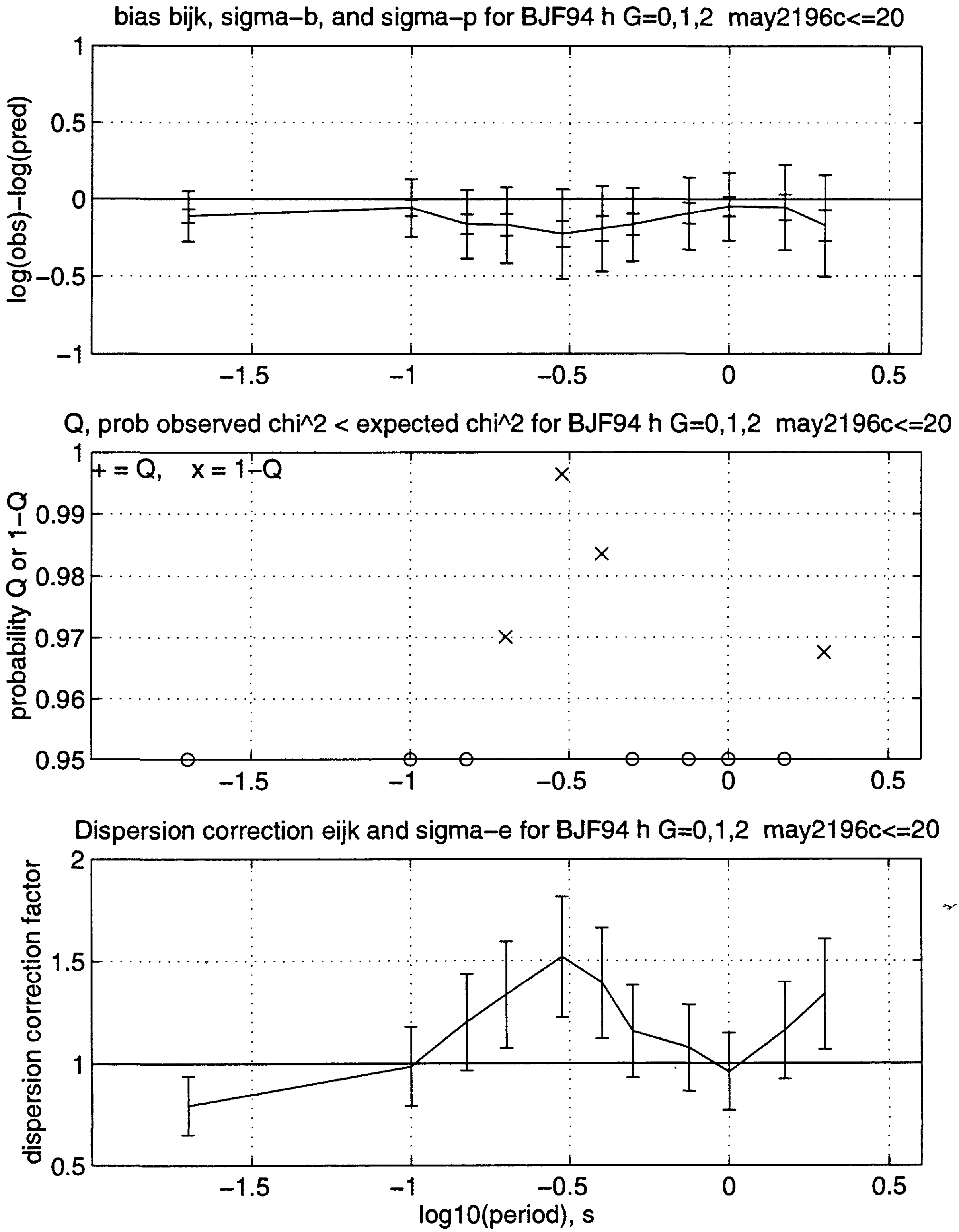

96/5/21 22:14 ymp1:[sp]may2196c<=201b.eps

18 a

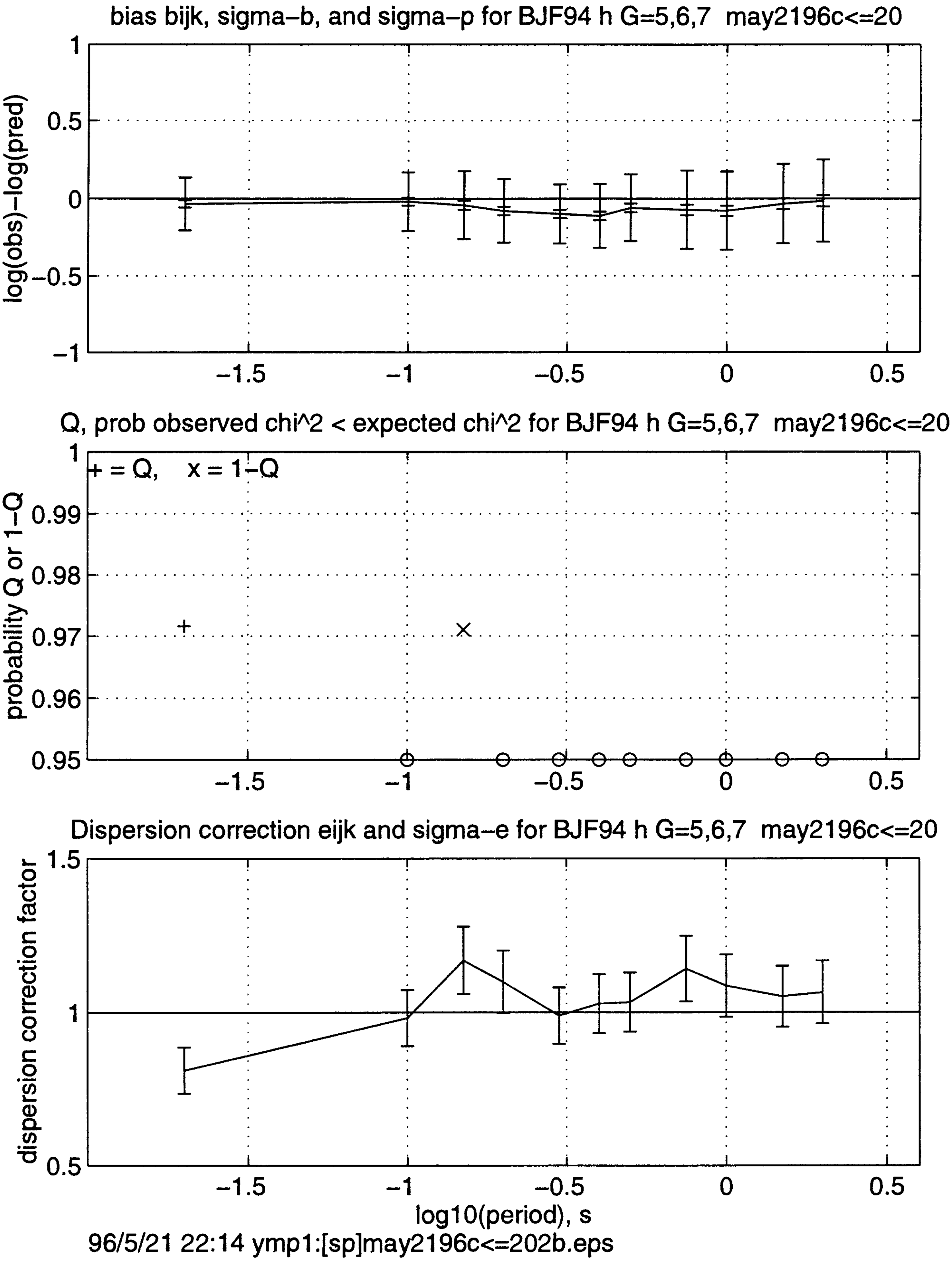
bias bijk, sigma-b, and sigma-p for BJF94 h G=5,6,7 may2196c<=20
log(obs)-log(pred)
Q, prob observed chi^2 < expected chi^2 for BJF94 h G=5,6,7 may2196c<=20
+ = Q, x = 1-Q
probability Q or 1-Q
Dispersion correction eijk and sigma-e for BJF94 h G=5,6,7 may2196c<=20
dispersion correction factor
log10(period), s
96/5/21 22:14 ymp1:[sp]may2196c<=202b.eps

18b

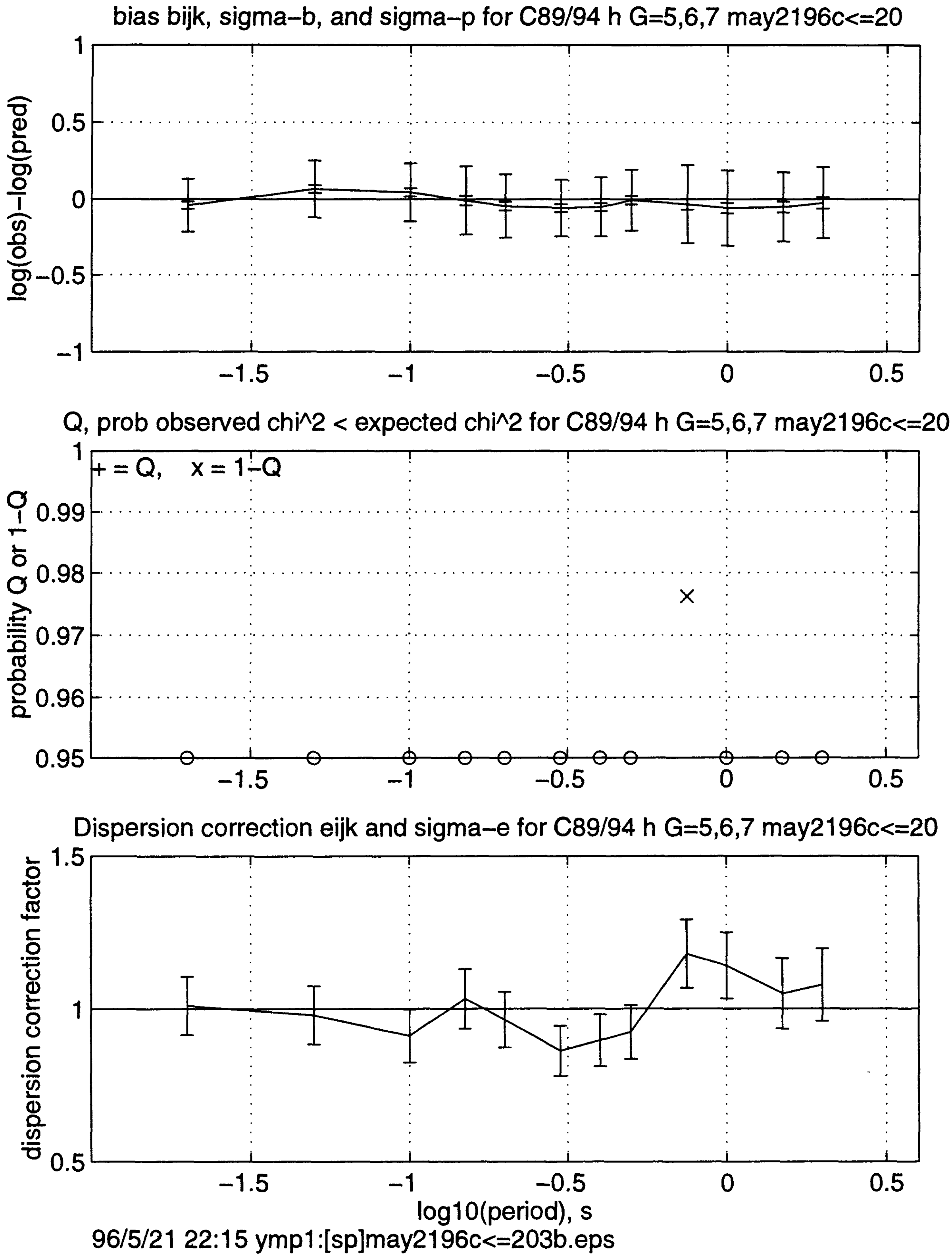
bias bijk, sigma-b, and sigma-p for C89/94 h G=5,6,7 may2196c<=20
log(obs)-log(pred)
1
0.5
0
-0.5
-1
-1.5
-1
-0.5
0
0.5
Q, prob observed chi^2 < expected chi^2 for C89/94 h G=5,6,7 may2196c<=20
+ = Q,   x = 1-Q
probability Q or 1-Q
1
0.99
0.98
0.97
0.96
0.95
-1.5
-1
-0.5
0
0.5
Dispersion correction eijk and sigma-e for C89/94 h G=5,6,7 may2196c<=20
dispersion correction factor
1.5
1
0.5
-1.5
-1
-0.5
0
0.5
log10(period), s
96/5/21 22:15 ymp1:[sp]may2196c<=203b.eps

18c

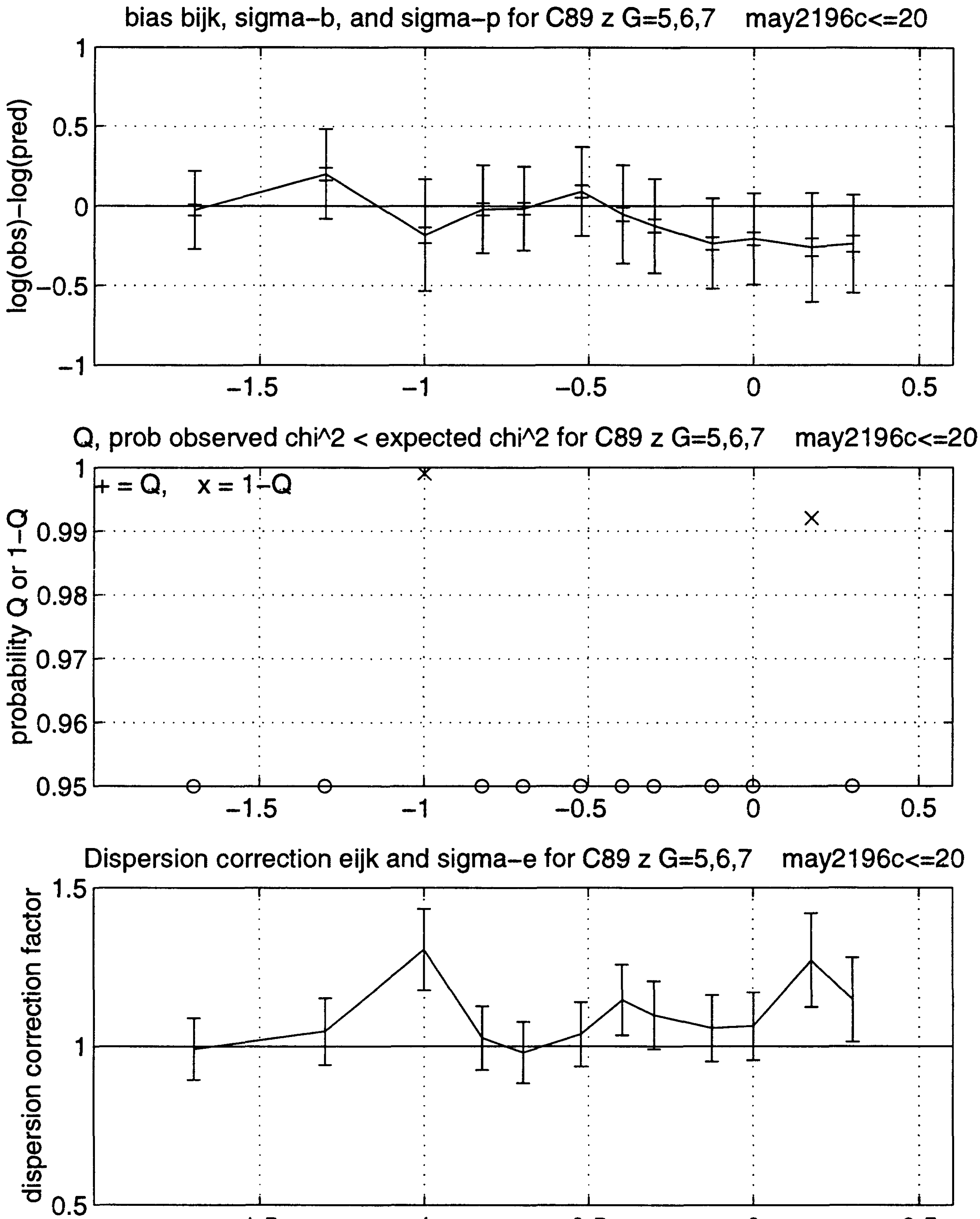

96/5/21 22:15 ymp1:[sp]may2196c<=204b.eps

18 d

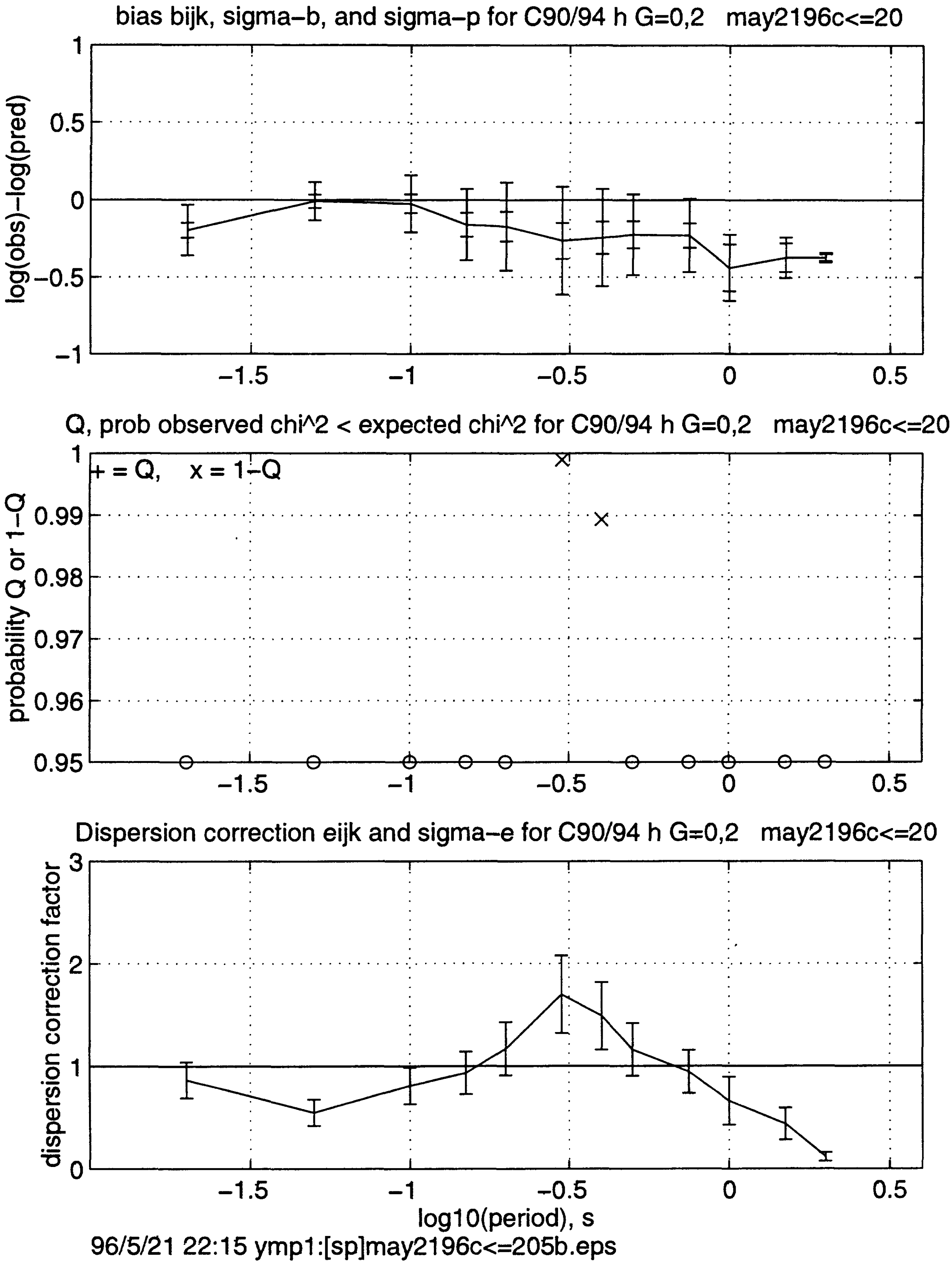
bias bijk, sigma-b, and sigma-p for C90/94 h G=0,2 may2196c<=20
log(obs)-log(pred)
Q, prob observed chi^2 < expected chi^2 for C90/94 h G=0,2 may2196c<=20
+ = Q, x = 1-Q
probability Q or 1-Q
Dispersion correction eijk and sigma-e for C90/94 h G=0,2 may2196c<=20
dispersion correction factor
log10(period), s
96/5/21 22:15 ymp1:[sp]may2196c<=205b.eps

18 e

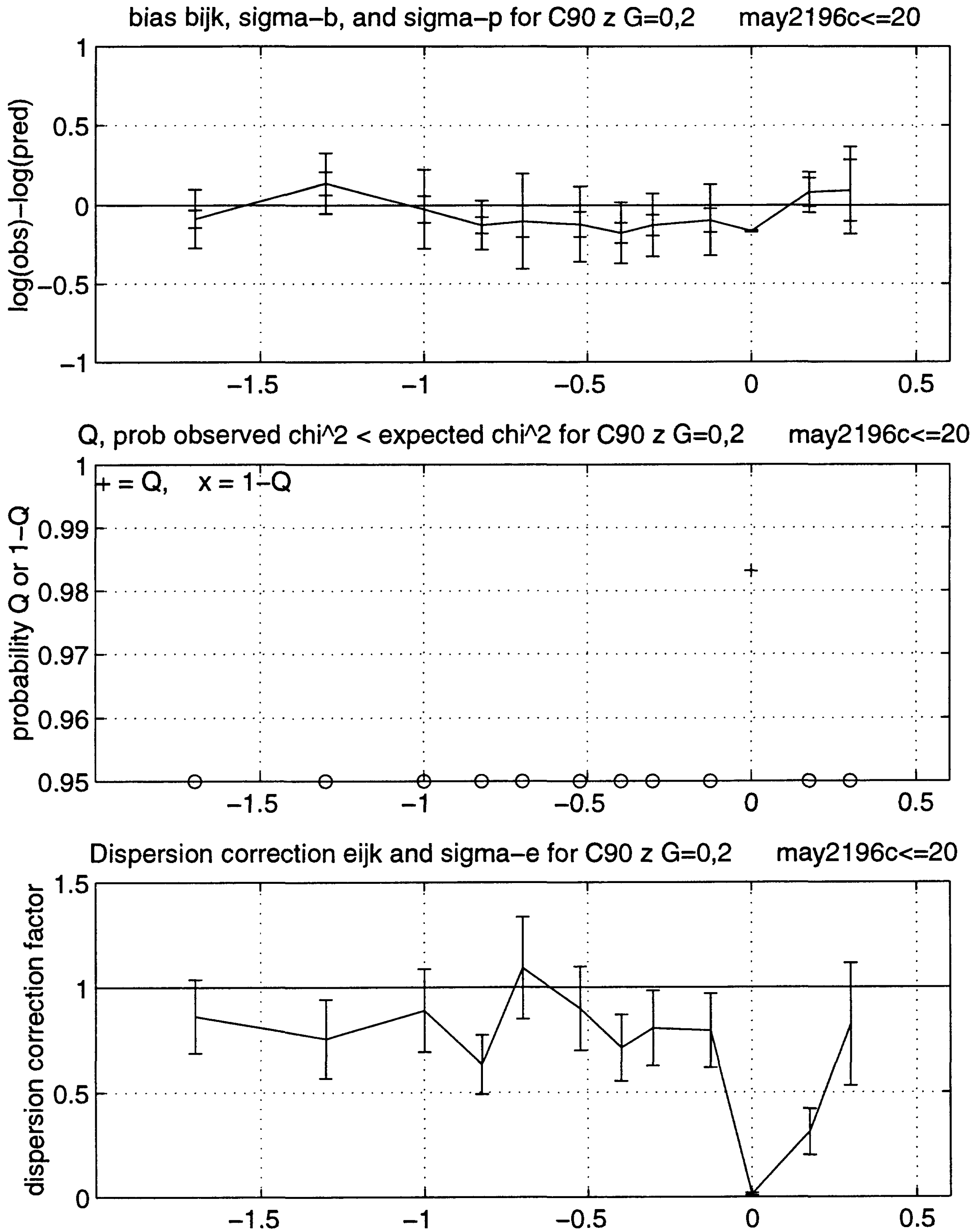

96/5/21 22:16 ymp1:[sp]may2196c<=206b.eps

18 f

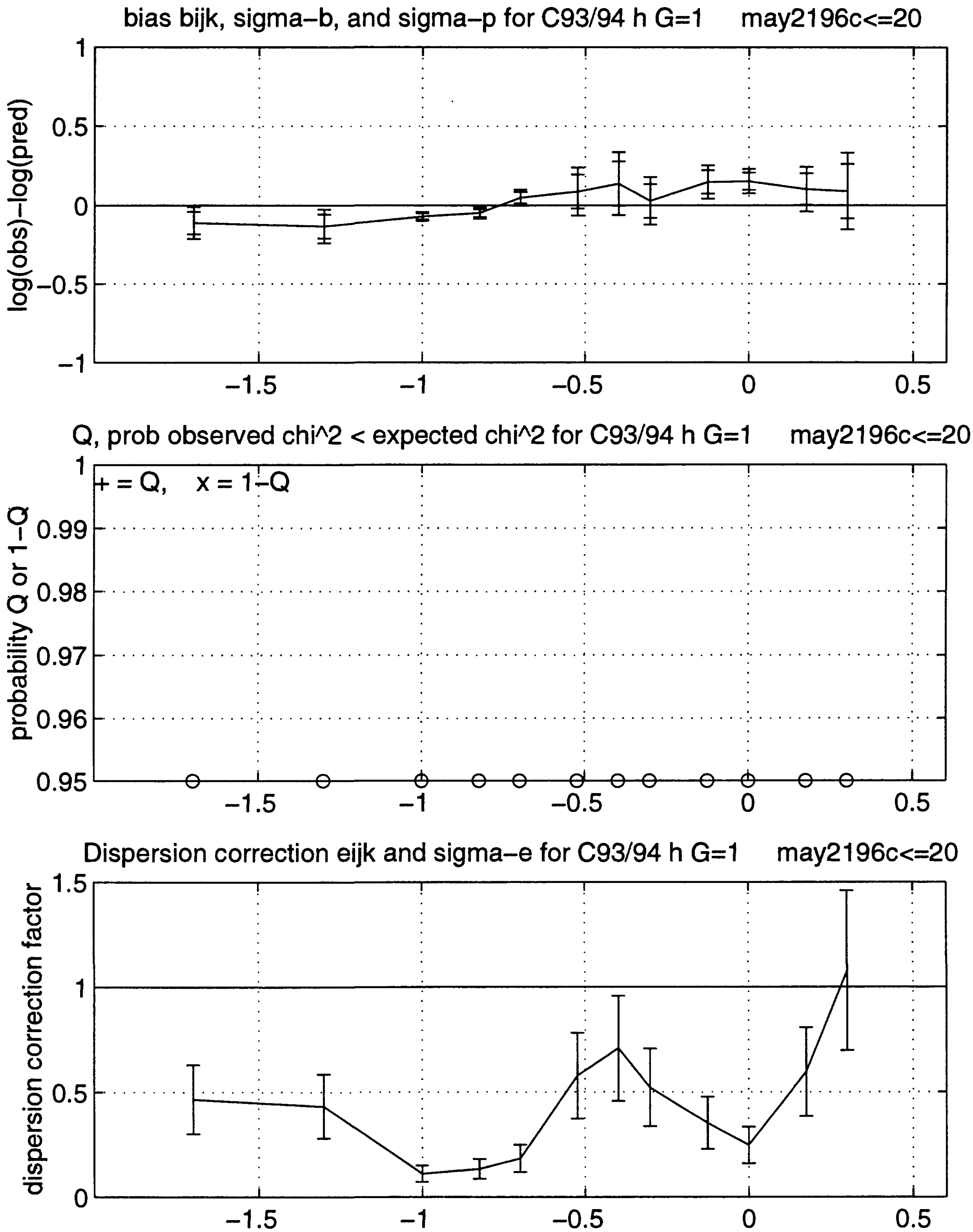

96/5/21 22:16 ymp1:[sp]may2196c<=207b.eps

18g

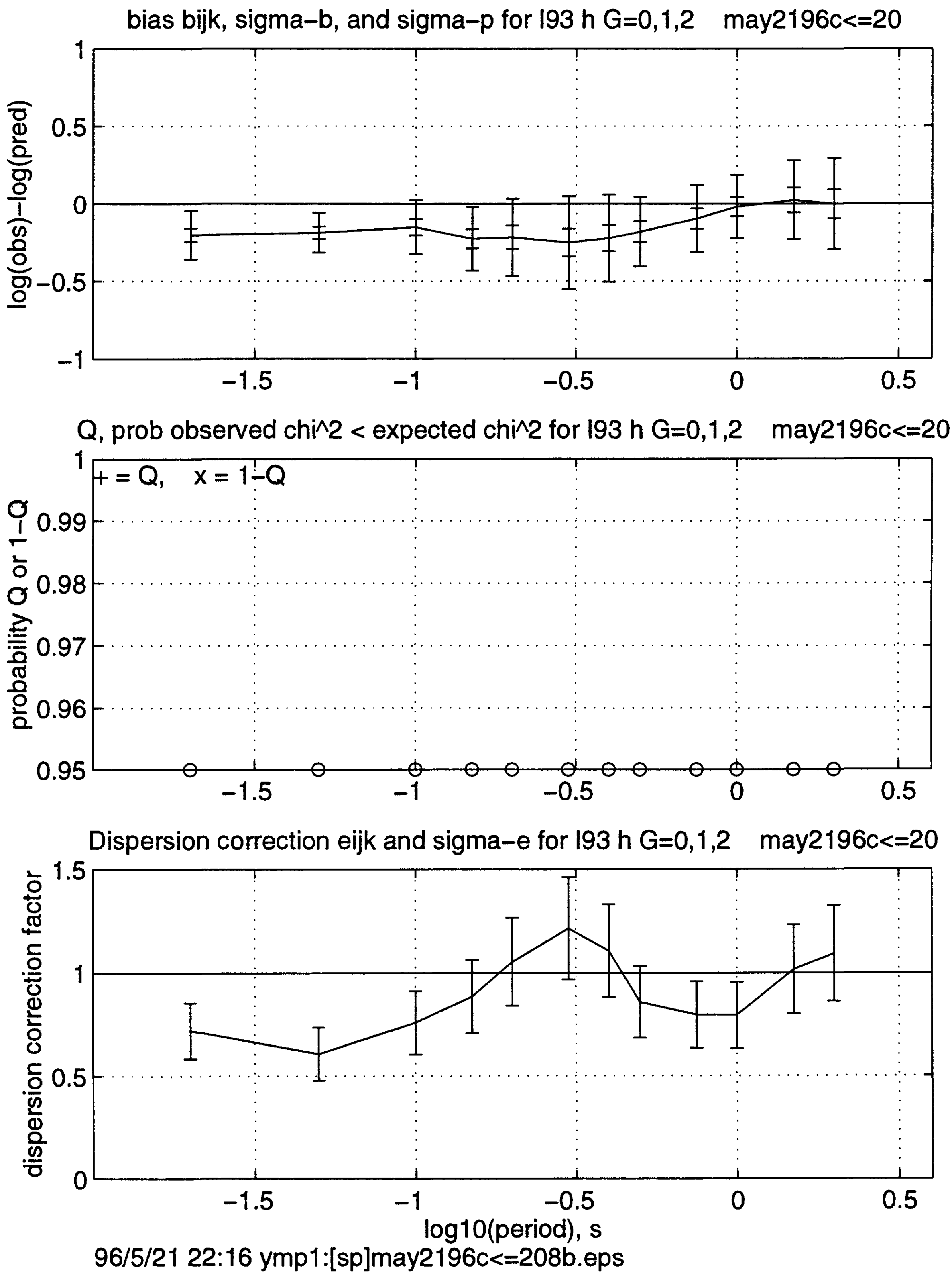

bias bijk, sigma-b, and sigma-p for I93 h G=0,1,2 may2196c<=20
log(obs)-log(pred)
1
0.5
0
-0.5
-1
-1.5
-1
-0.5
0
0.5
Q, prob observed chi^2 < expected chi^2 for I93 h G=0,1,2 may2196c<=20
+ = Q, x = 1-Q
probability Q or 1-Q
1
0.99
0.98
0.97
0.96
0.95
-1.5
-1
-0.5
0
0.5
Dispersion correction eijk and sigma-e for I93 h G=0,1,2 may2196c<=20
dispersion correction factor
1.5
1
0.5
0
-1.5
-1
-0.5
0
0.5
log10(period), s
96/5/21 22:16 ymp1:[sp]may2196c<=208b.eps

18 h

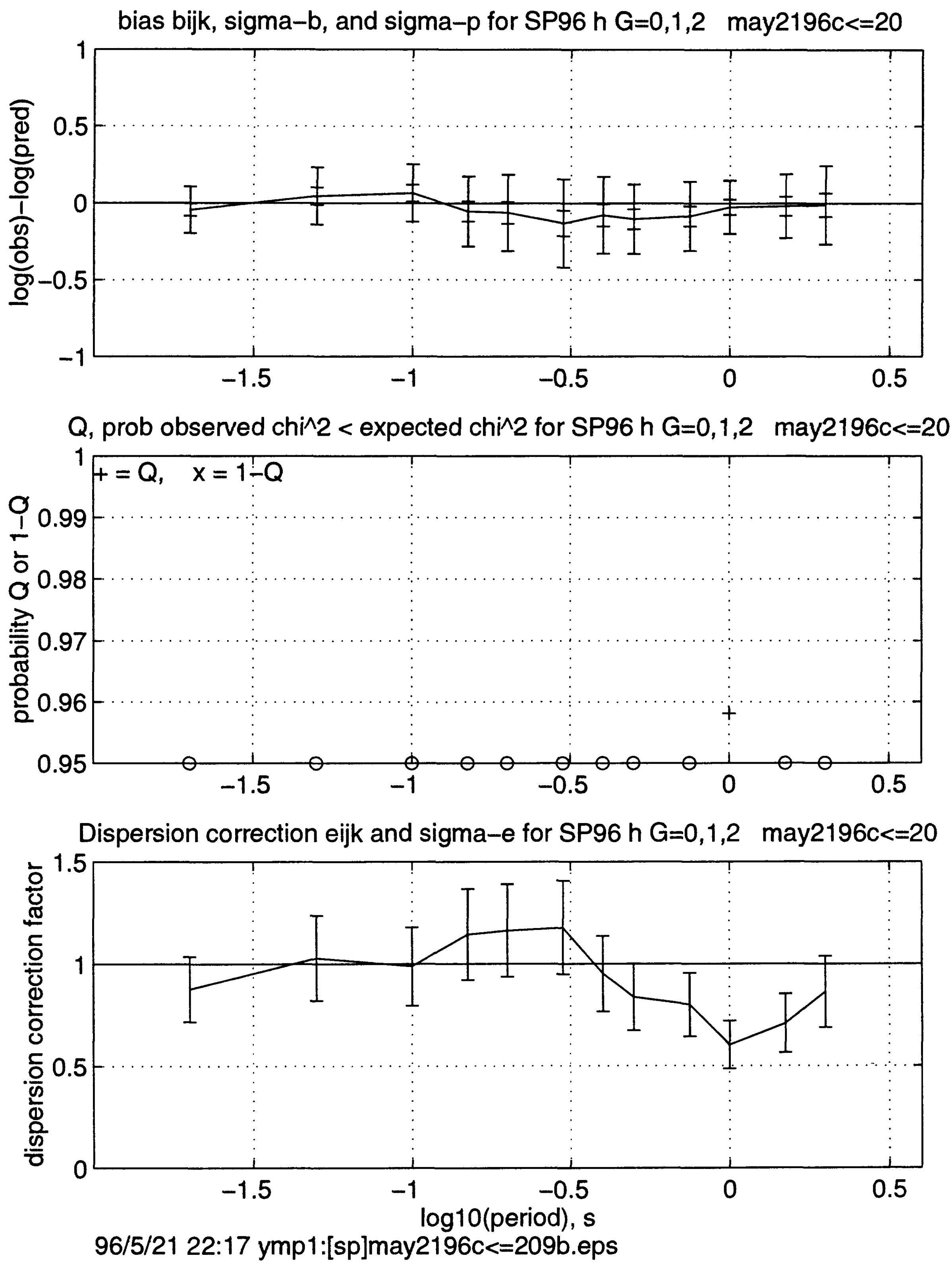
bias bijk, sigma-b, and sigma-p for SP96 h G=0,1,2 may2196c<=20
log(obs)-log(pred)
Q, prob observed chi^2 < expected chi^2 for SP96 h G=0,1,2 may2196c<=20
+ = Q, x = 1-Q
probability Q or 1-Q
Dispersion correction eijk and sigma-e for SP96 h G=0,1,2 may2196c<=20
dispersion correction factor
log10(period), s
96/5/21 22:17 ymp1:[sp]may2196c<=209b.eps

18 i

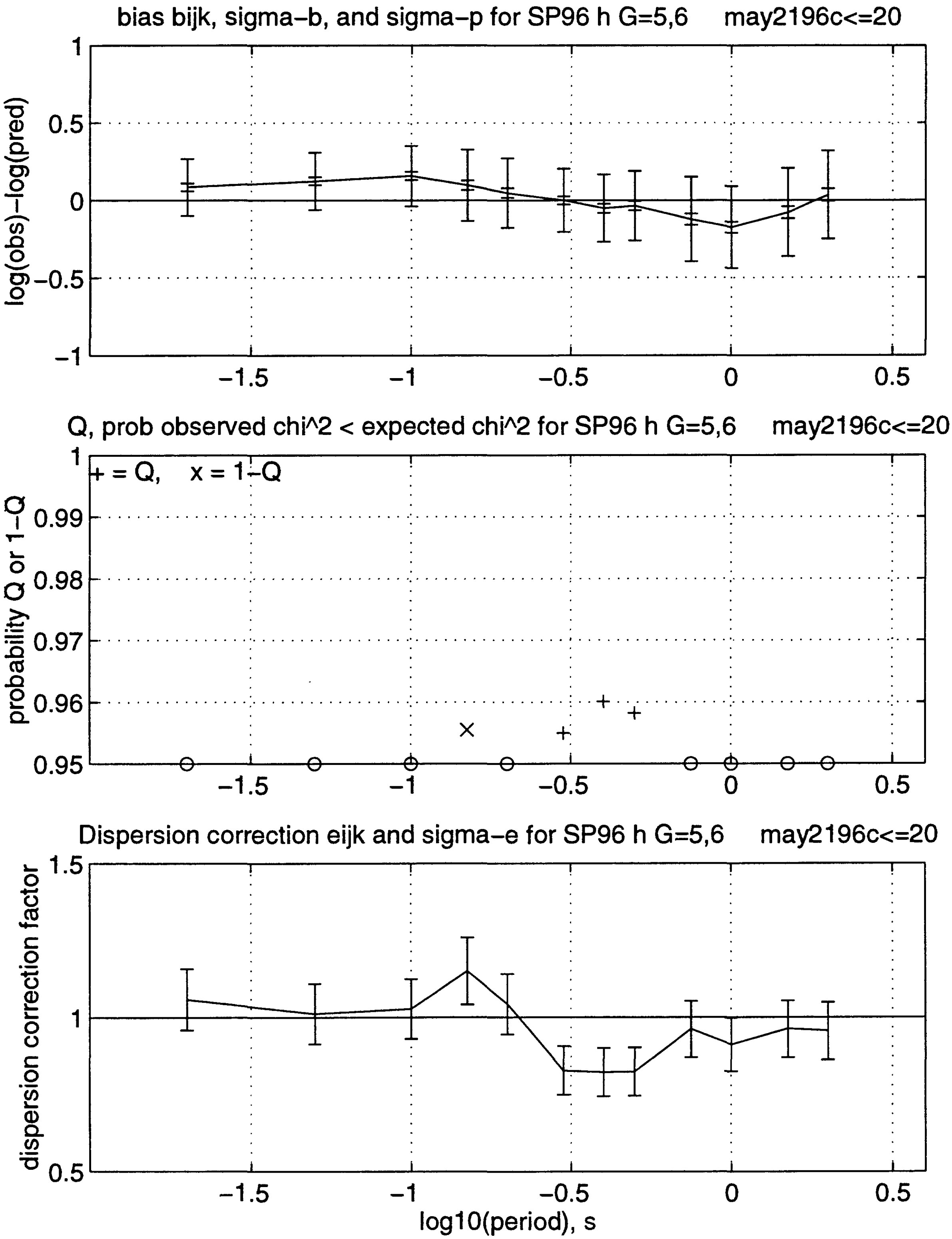

96/5/21 22:17 ymp1:[sp]may2196c<=2010b.eps

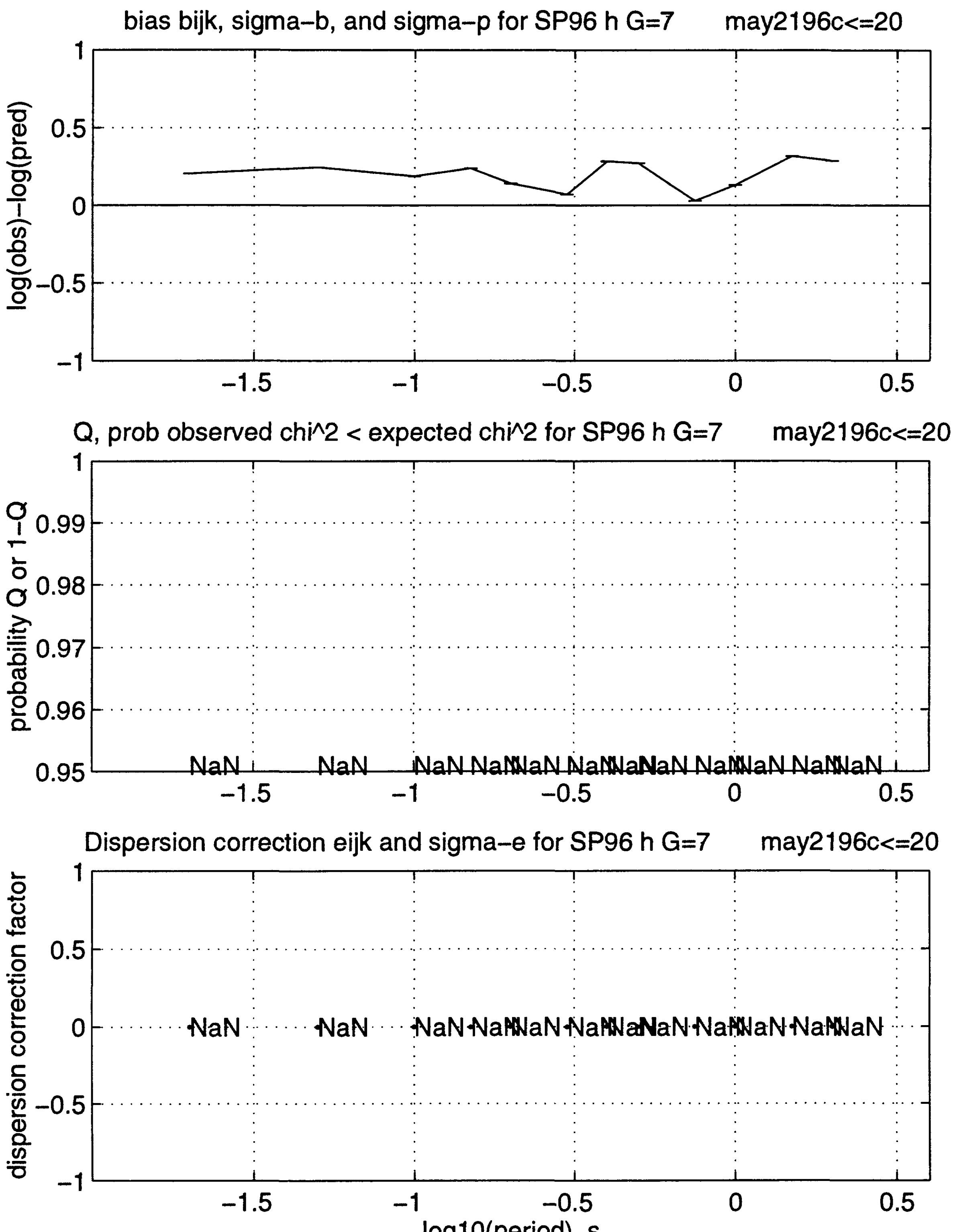

96/5/21 22:17 ymp1:[sp]may2196c<=2011b.eps

18 k

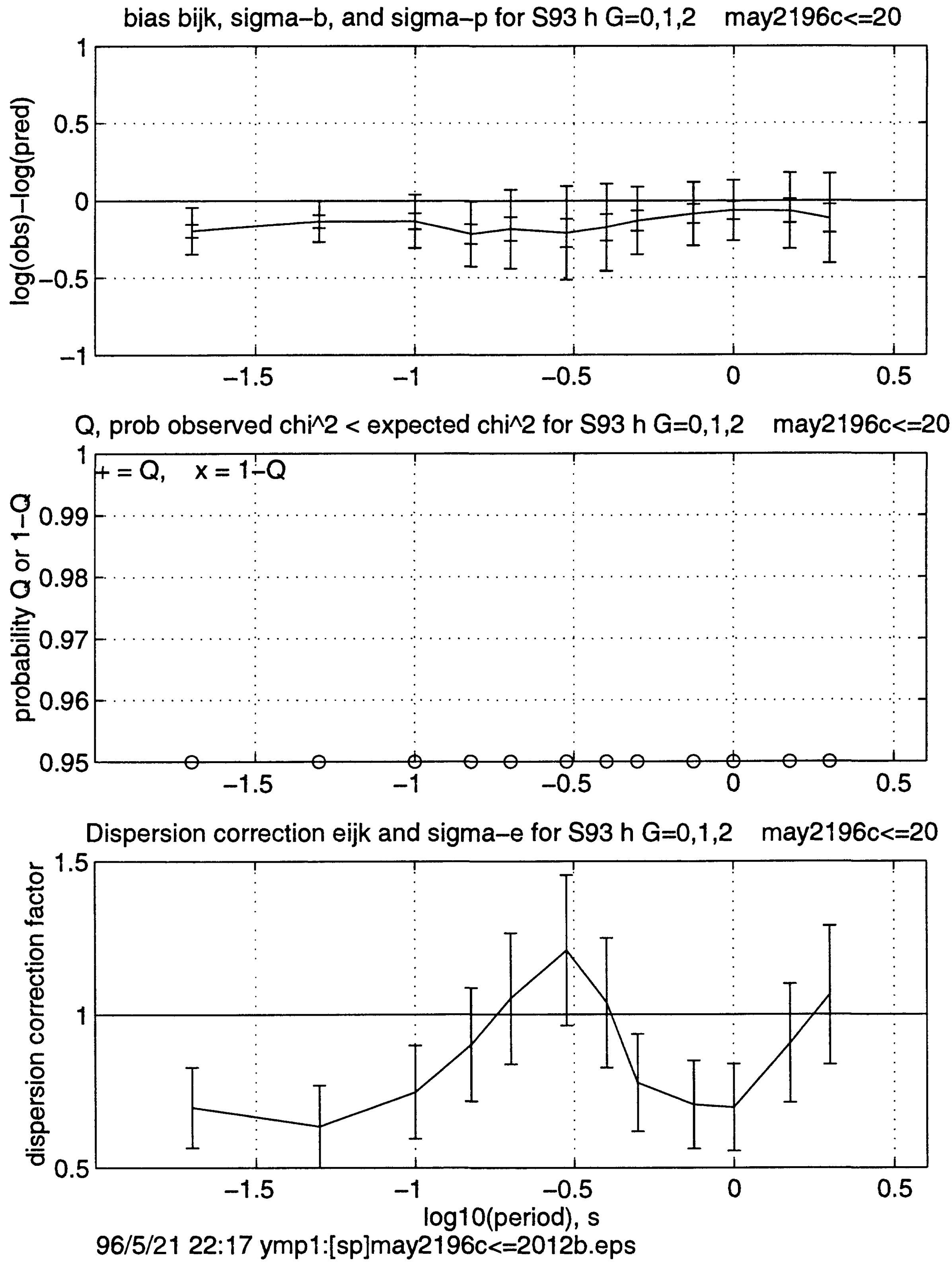
bias bijk, sigma-b, and sigma-p for S93 h G=0,1,2 may2196c<=20
log(obs)-log(pred)
Q, prob observed chi^2 < expected chi^2 for S93 h G=0,1,2 may2196c<=20
+ = Q, x = 1-Q
probability Q or 1-Q
Dispersion correction eijk and sigma-e for S93 h G=0,1,2 may2196c<=20
dispersion correction factor
log10(period), s
96/5/21 22:17 ymp1:[sp]may2196c<=2012b.eps

18 l

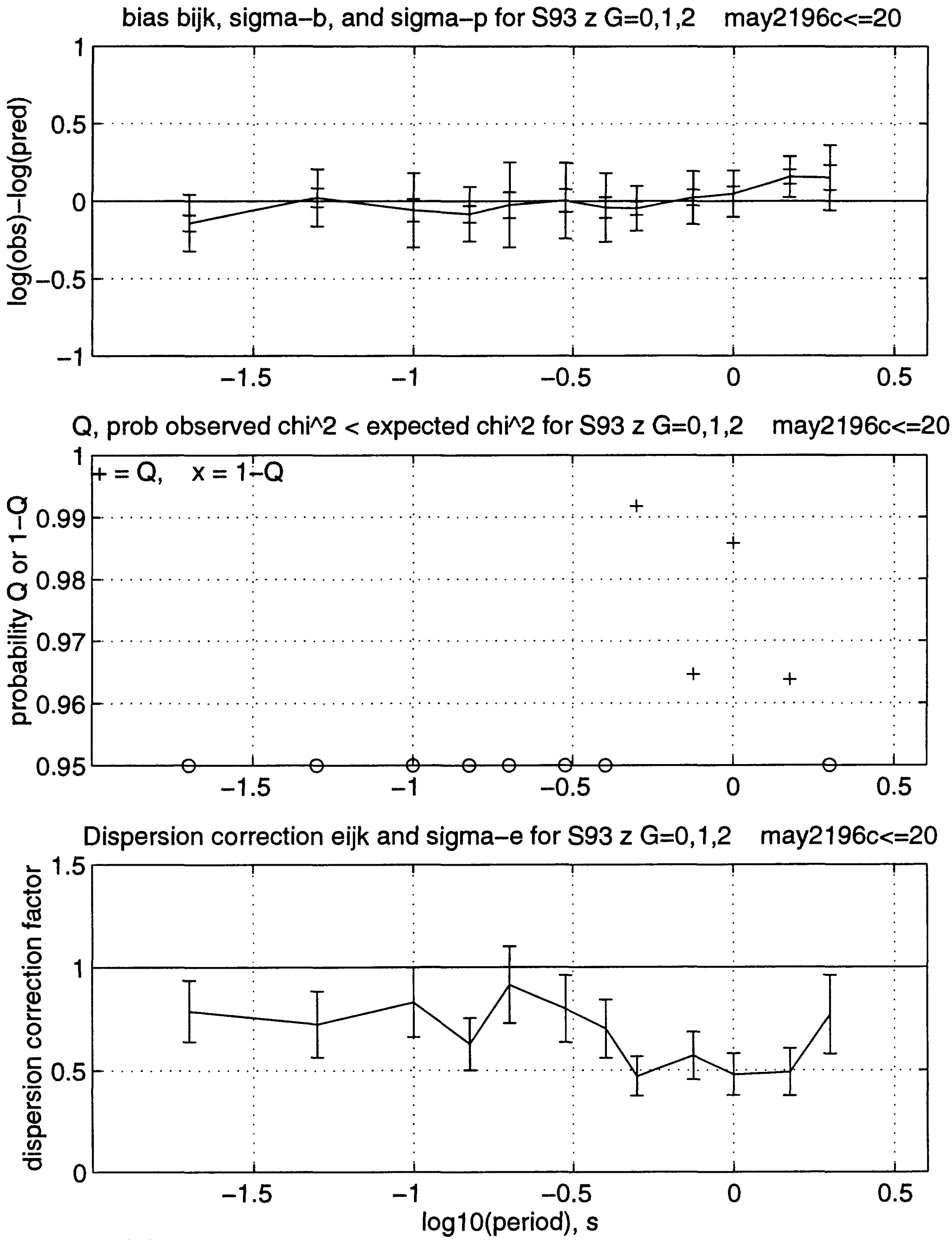

96/5/21 22:18 ymp1:[sp]may2196c<=2013b.eps

18 m

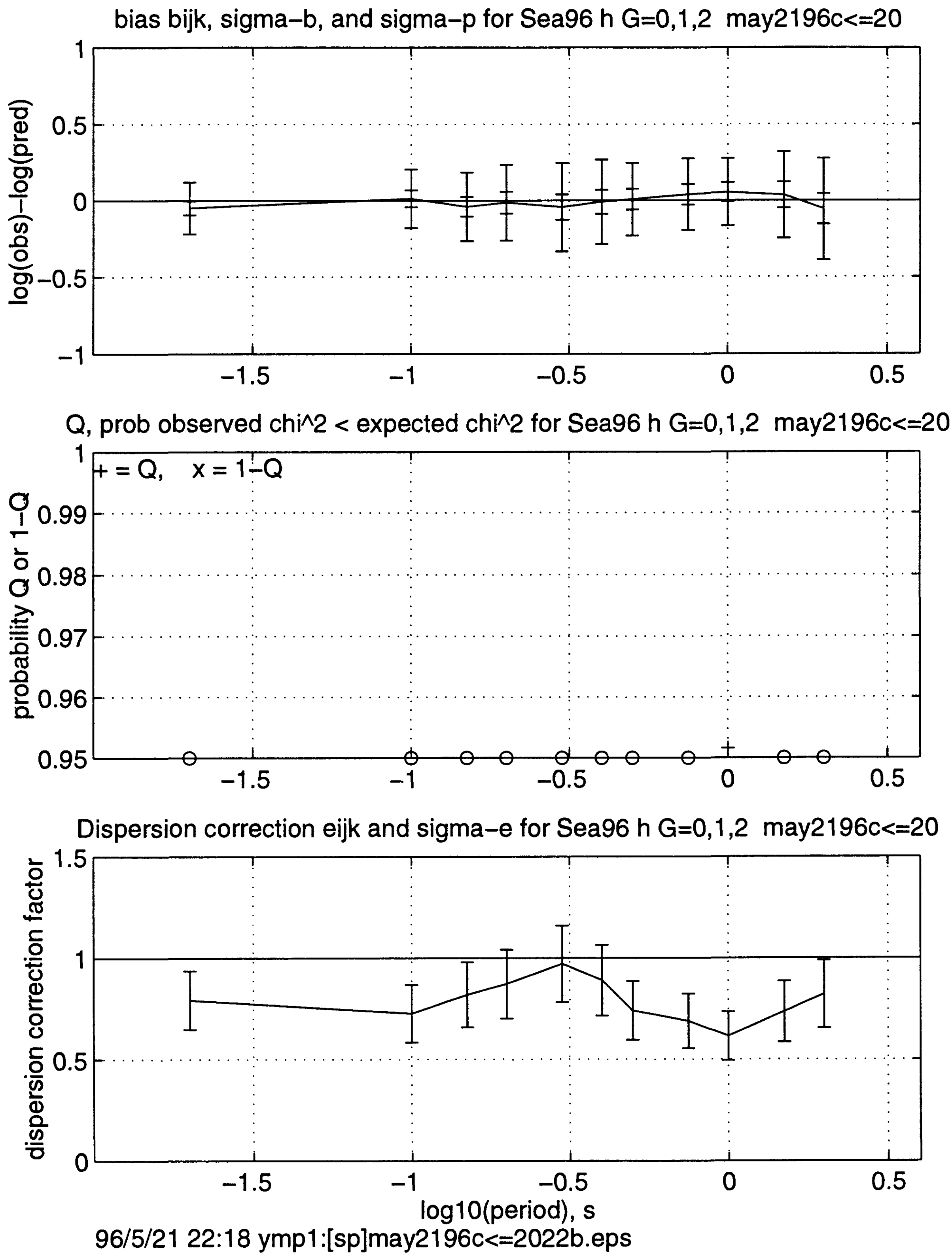
bias bijk, sigma-b, and sigma-p for Sea96 h G=0,1,2 may2196c<=20
log(obs)-log(pred)
Q, prob observed chi^2 < expected chi^2 for Sea96 h G=0,1,2 may2196c<=20
+ = Q, x = 1-Q
probability Q or 1-Q
Dispersion correction eijk and sigma-e for Sea96 h G=0,1,2 may2196c<=20
dispersion correction factor
log10(period), s
96/5/21 22:18 ymp1:[sp]may2196c<=2022b.eps

18n

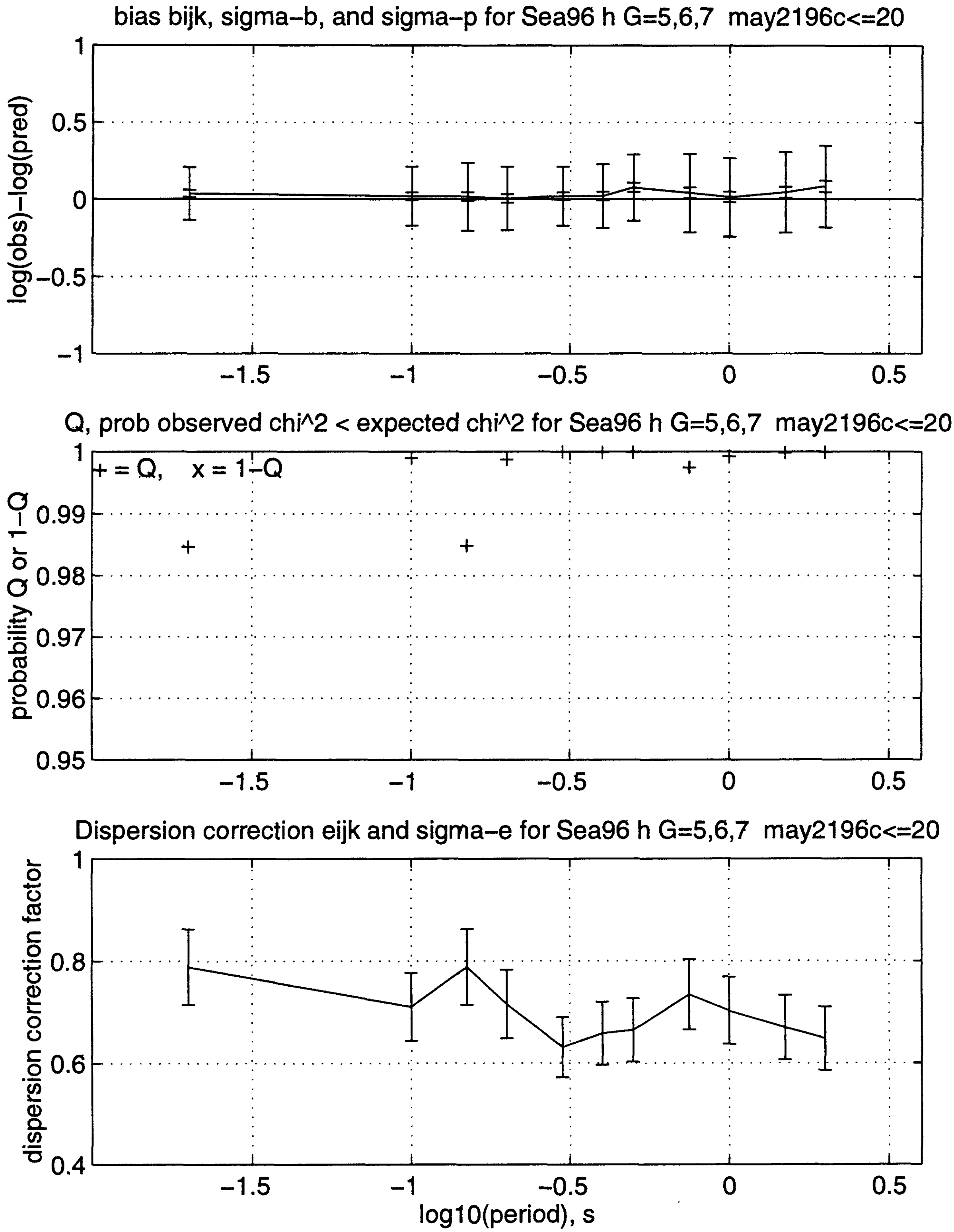

96/5/21 22:18 ymp1:[sp]may2196c<=2023b.eps

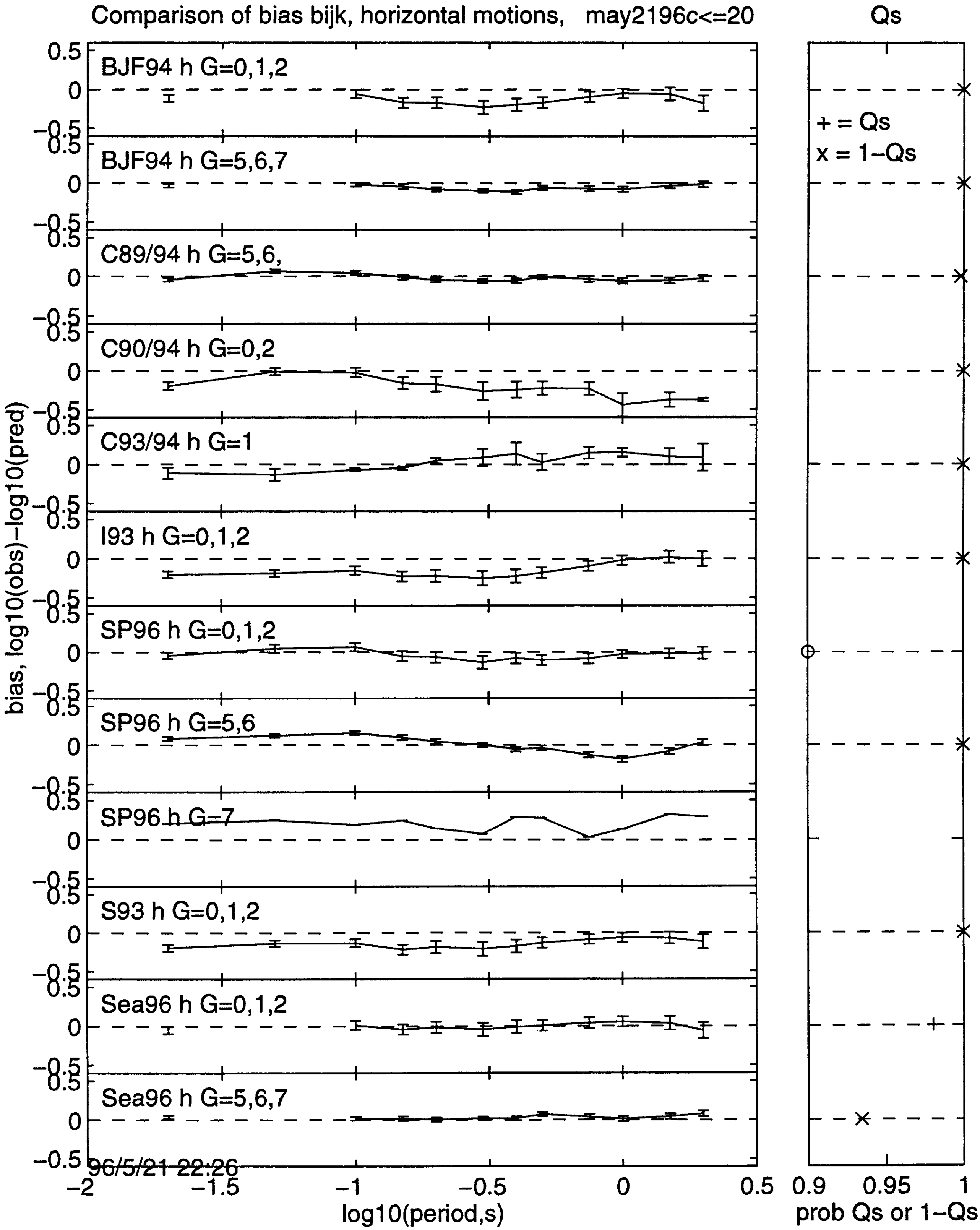

Comparison of bias bijk, horizontal motions, may2196c<=20
Qs
BJF94 h G=0,1,2
BJF94 h G=5,6,7
C89/94 h G=5,6,
C90/94 h G=0,2
C93/94 h G=1
I93 h G=0,1,2
SP96 h G=0,1,2
SP96 h G=5,6
SP96 h G=7
S93 h G=0,1,2
Sea96 h G=0,1,2
Sea96 h G=5,6,7
+ = Qs
x = 1−Qs
bias, log10(obs)−log10(pred)
log10(period,s)
prob Qs or 1−Qs
96/5/21 22:26

19a

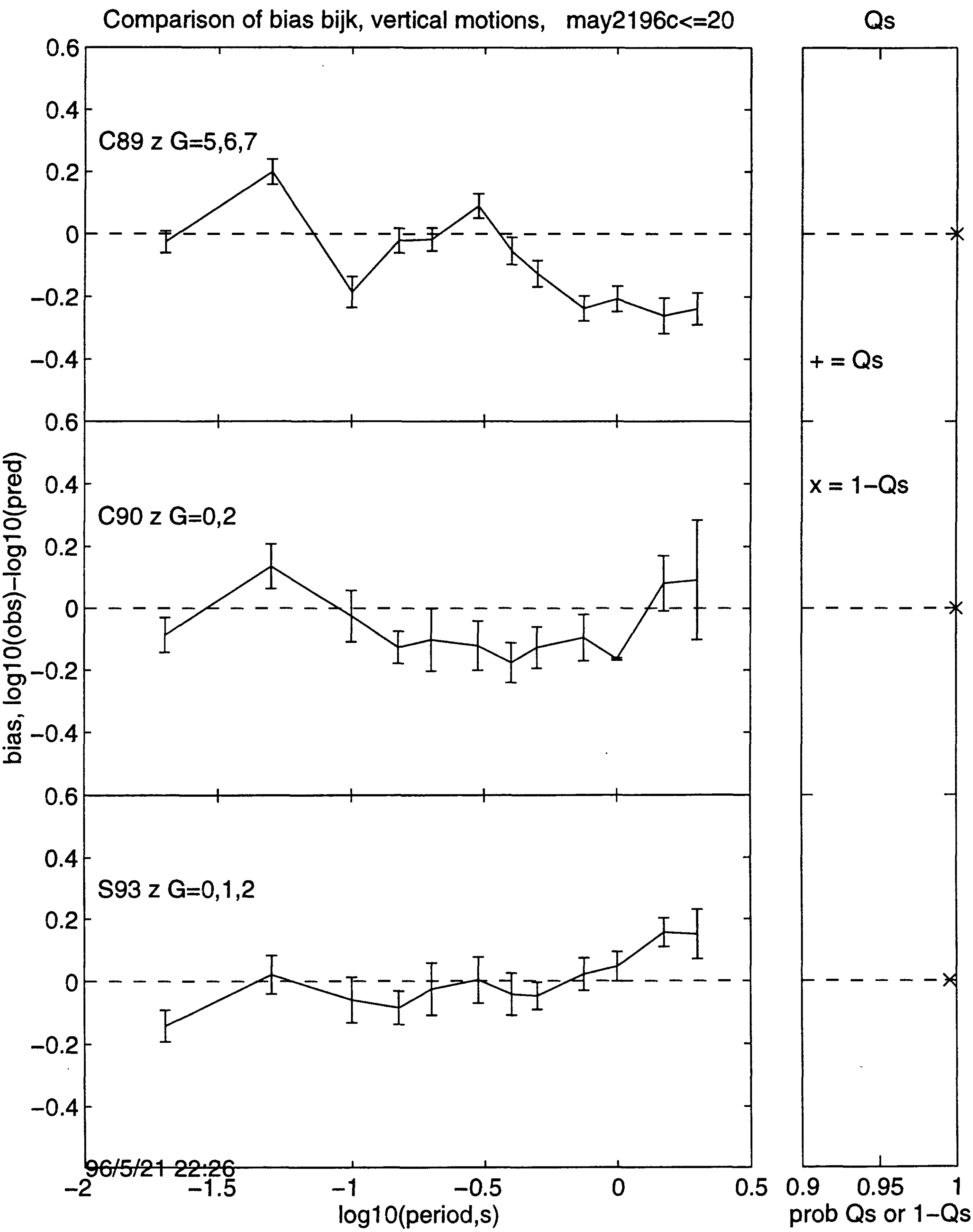

Comparison of bias bijk, vertical motions, may2196c<=20
Qs
C89 z G=5,6,7
C90 z G=0,2
S93 z G=0,1,2
+ = Qs
x = 1-Qs
bias, log10(obs)-log10(pred)
log10(period,s)
prob Qs or 1-Qs
96/5/21 22:26

19b

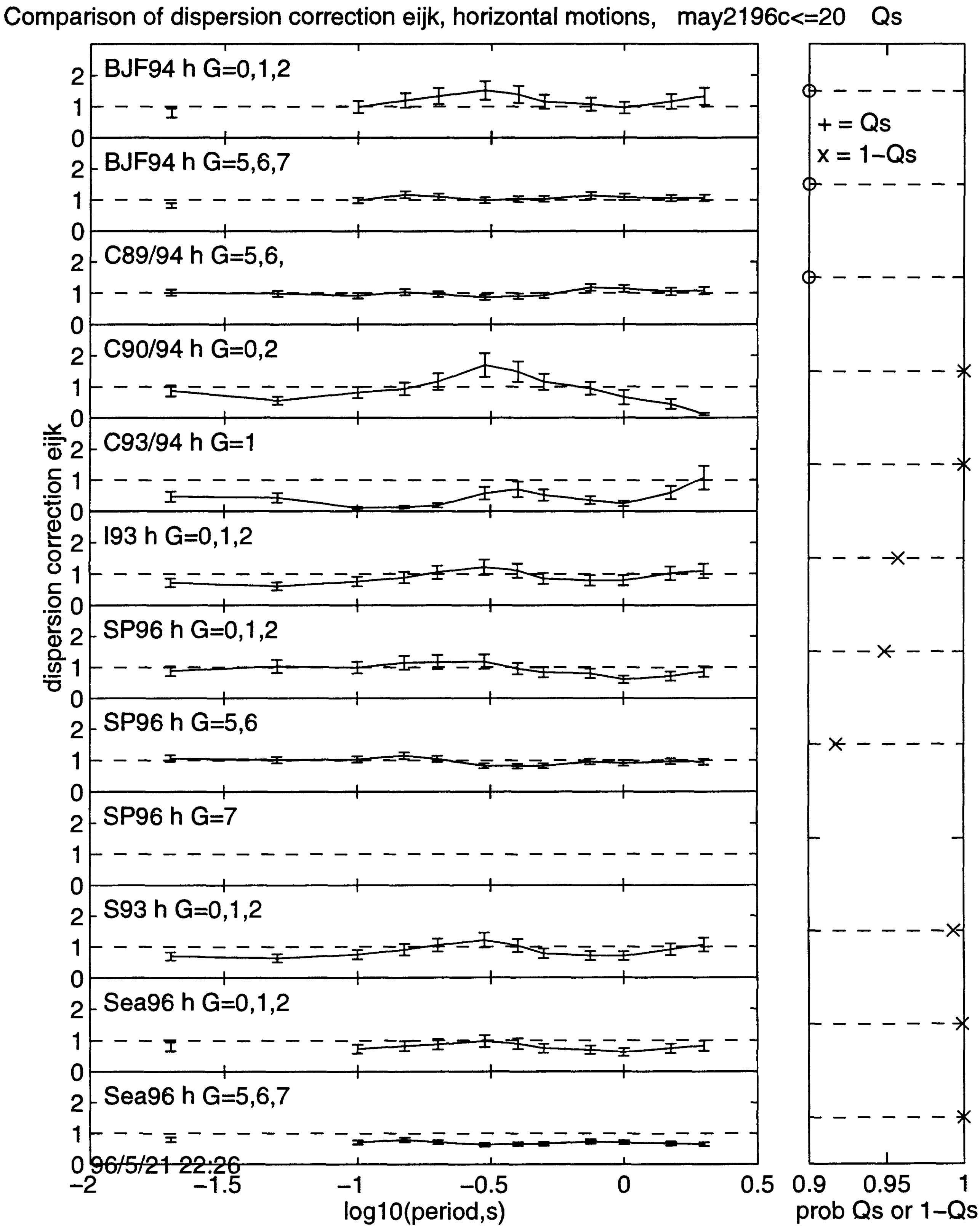

Comparison of dispersion correction eijk, horizontal motions, may2196c<=20 Qs
BJF94 h G=0,1,2
BJF94 h G=5,6,7
C89/94 h G=5,6,
C90/94 h G=0,2
C93/94 h G=1
I93 h G=0,1,2
SP96 h G=0,1,2
SP96 h G=5,6
SP96 h G=7
S93 h G=0,1,2
Sea96 h G=0,1,2
Sea96 h G=5,6,7
96/5/21 22:26
dispersion correction eijk
log10(period,s)
+ = Qs
x = 1−Qs
prob Qs or 1−Qs

19c

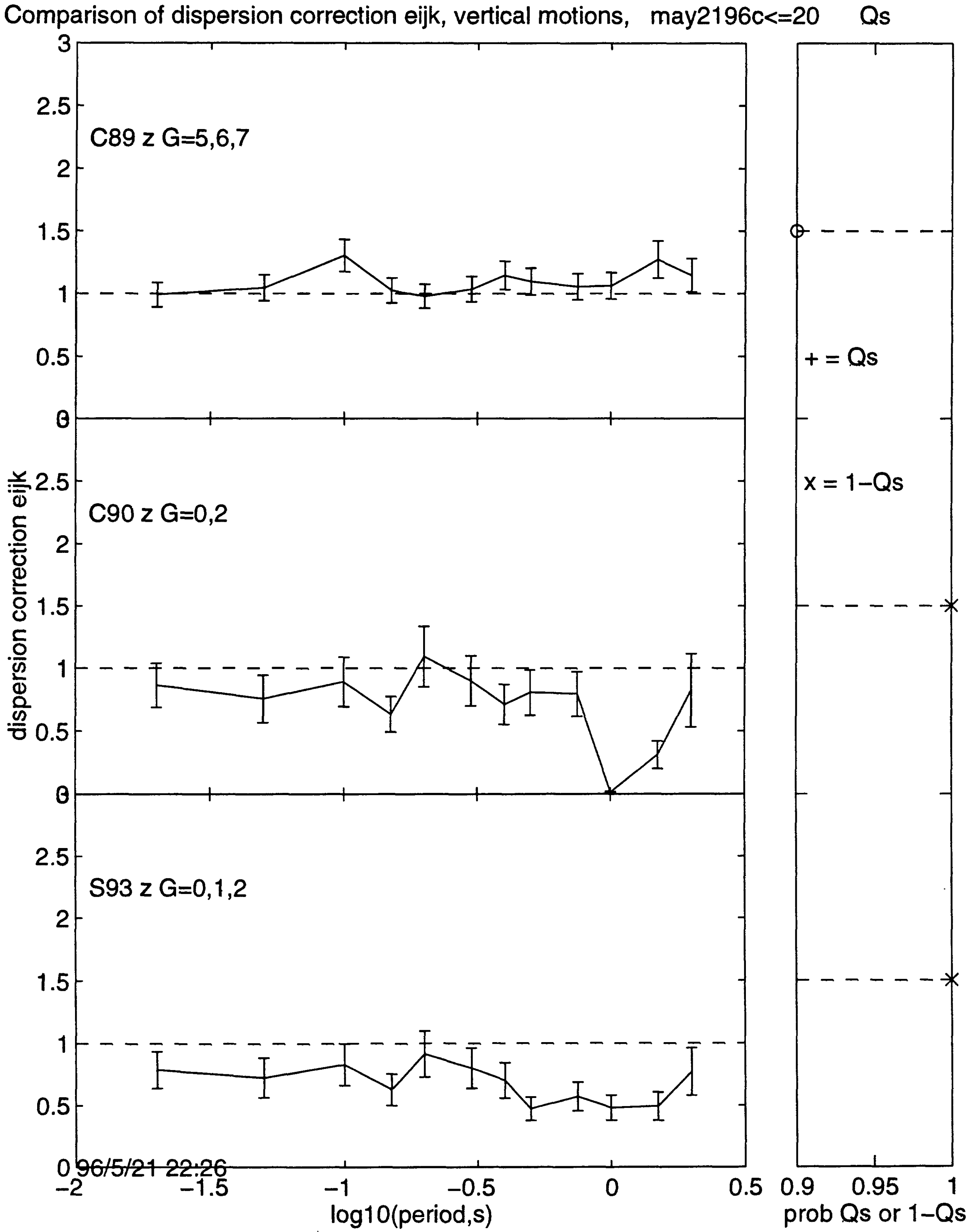

Comparison of dispersion correction eijk, vertical motions, may2196c<=20
Qs
C89 z G=5,6,7
C90 z G=0,2
S93 z G=0,1,2
dispersion correction eijk
+ = Qs
x = 1-Qs
96/5/21 22:26
log10(period,s)
prob Qs or 1-Qs

19d

Comparison of magnitude dependence, sm, horizontal motions,   may2196c<=20 Qs

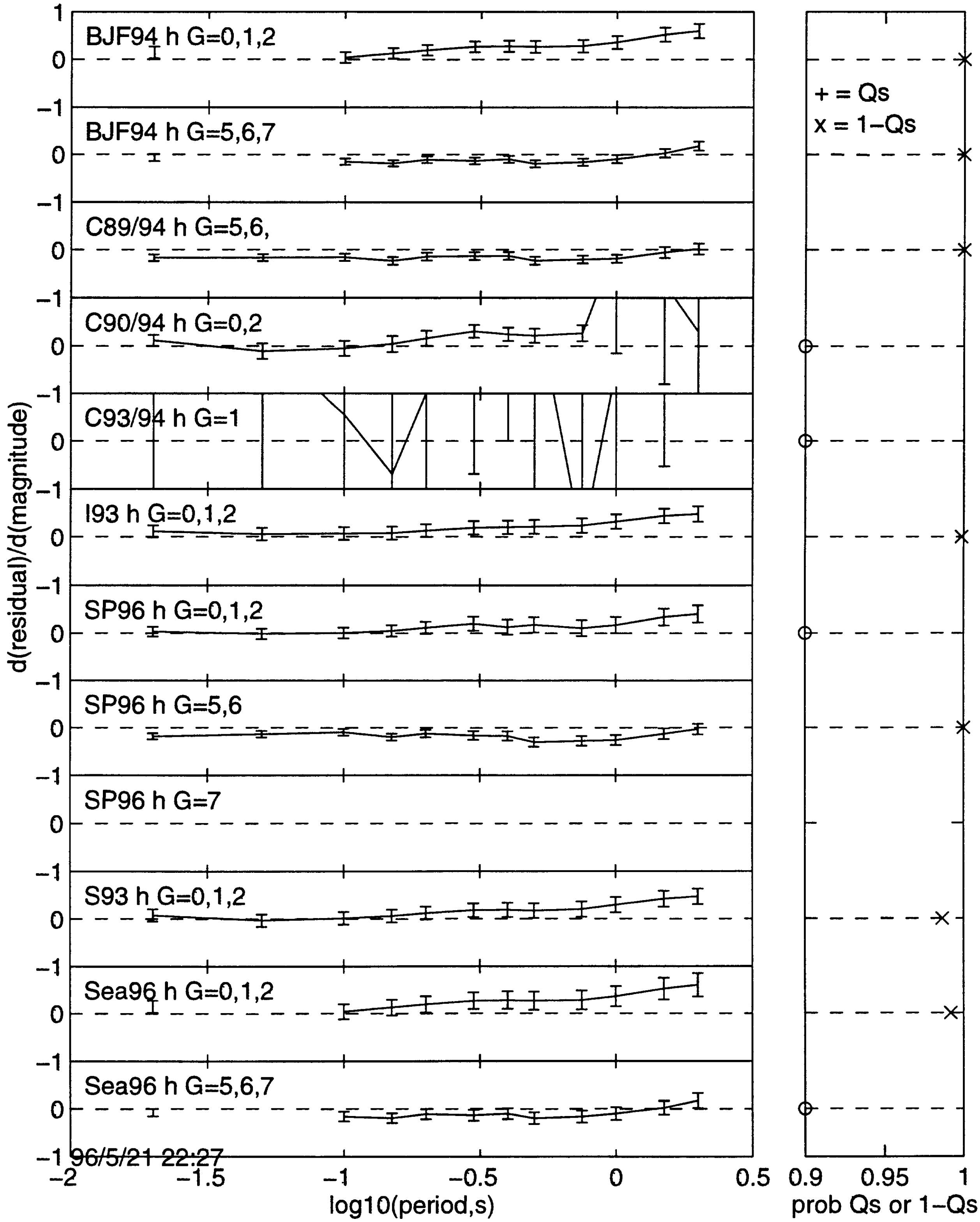

19e

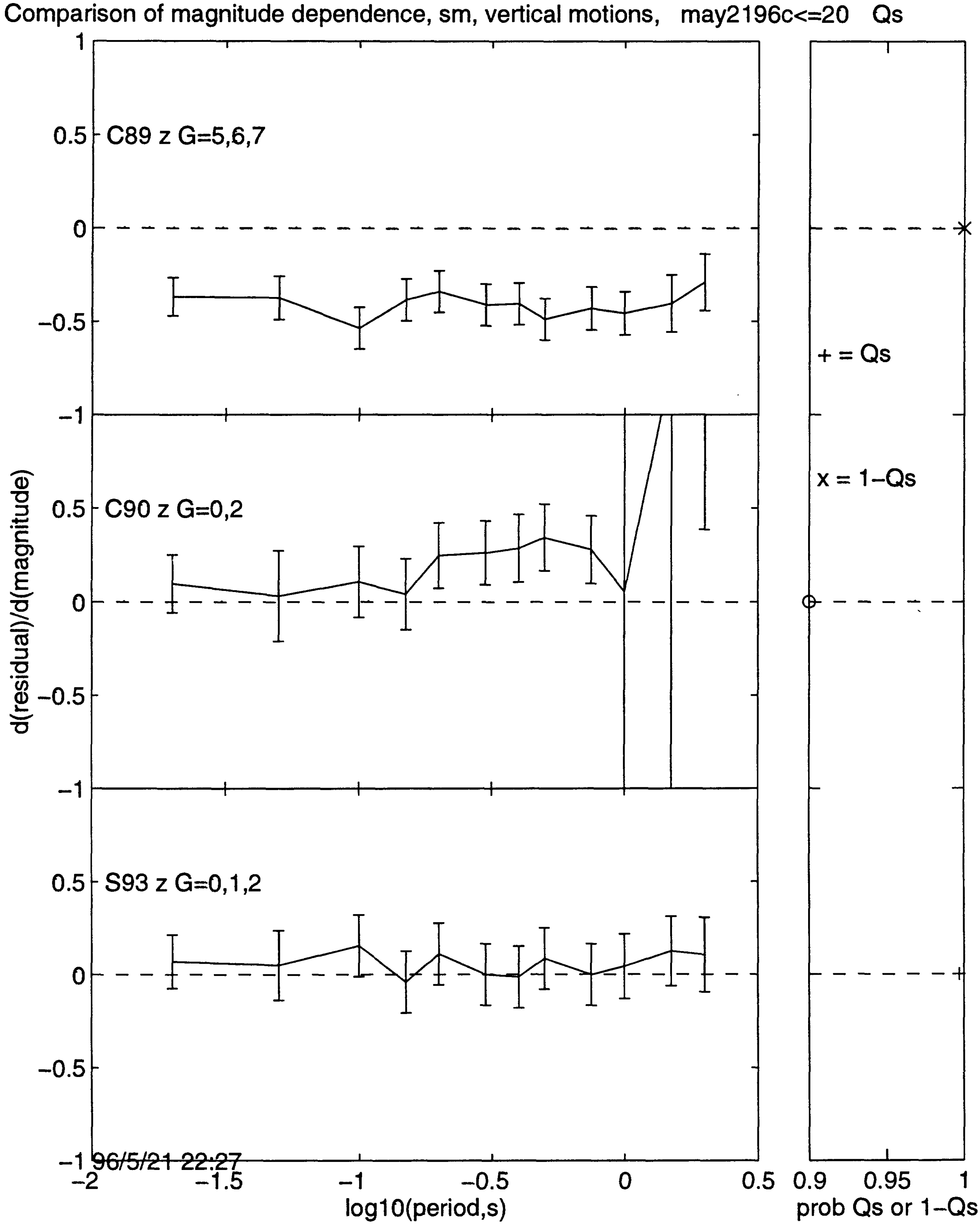
Comparison of magnitude dependence, sm, vertical motions, may2196c<=20 Qs
C89 z G=5,6,7
C90 z G=0,2
S93 z G=0,1,2
d(residual)/d(magnitude)
log10(period,s)
+ = Qs
x = 1-Qs
prob Qs or 1-Qs
96/5/21 22:27
1
0.5
0
-0.5
-1
-2
-1.5
-0.5
0.5
0.9
0.95

19f

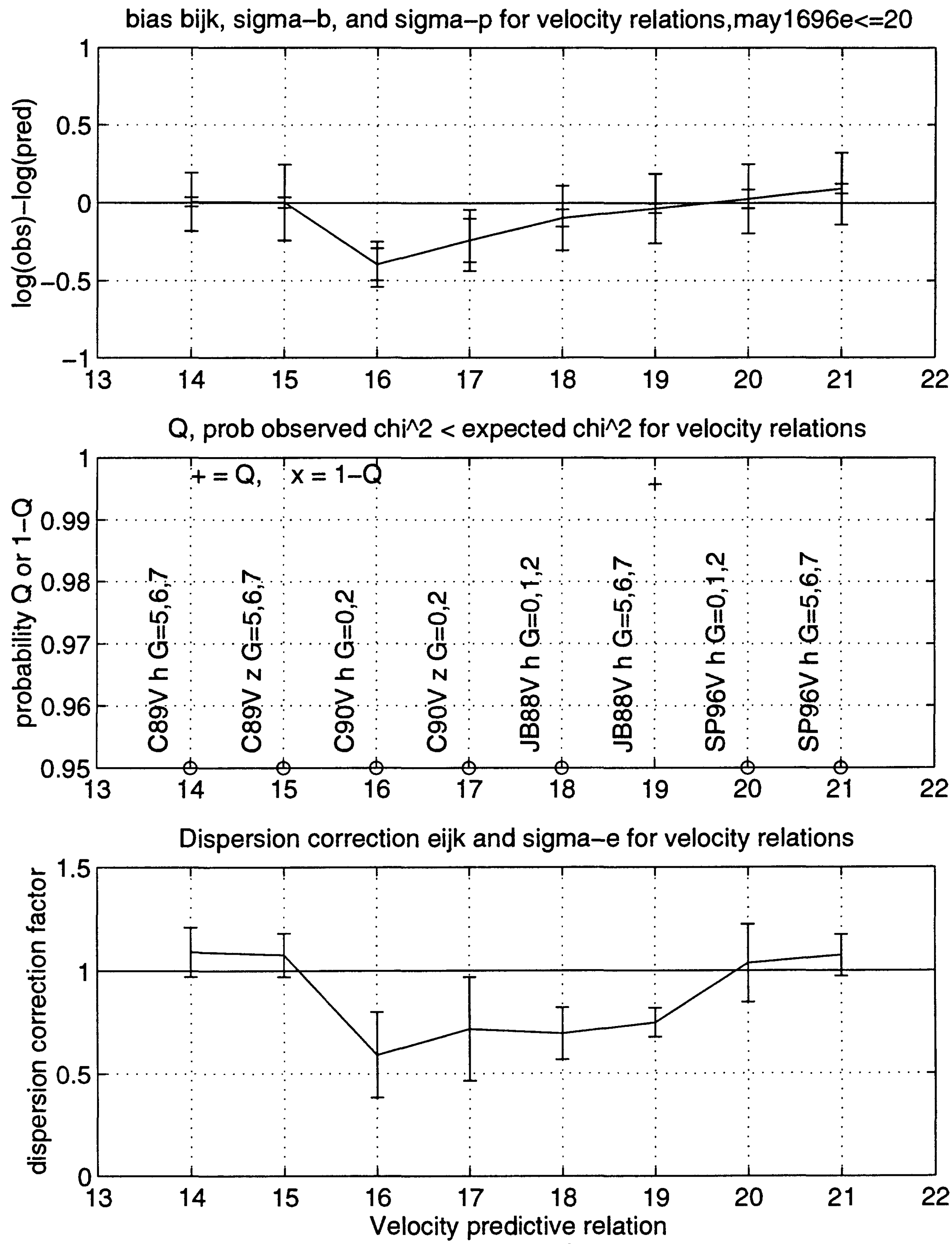

96/5/16 23:2 ymp1:[sp]may1696e<=2023b.eps

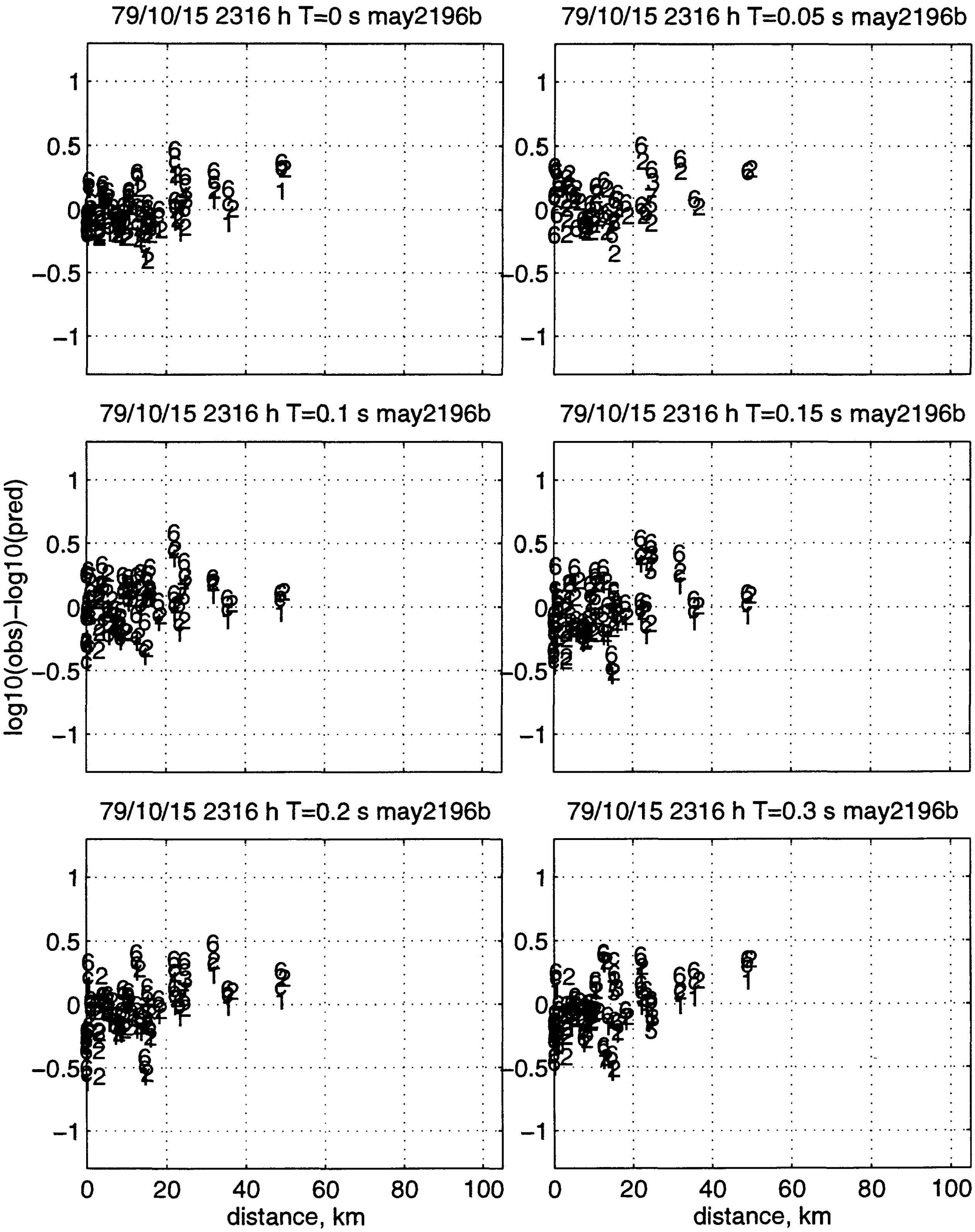
79/10/15 2316 h T=0 s may2196b
79/10/15 2316 h T=0.05 s may2196b
79/10/15 2316 h T=0.1 s may2196b
79/10/15 2316 h T=0.15 s may2196b
79/10/15 2316 h T=0.2 s may2196b
79/10/15 2316 h T=0.3 s may2196b
log10(obs)−log10(pred)
distance, km
distance, km

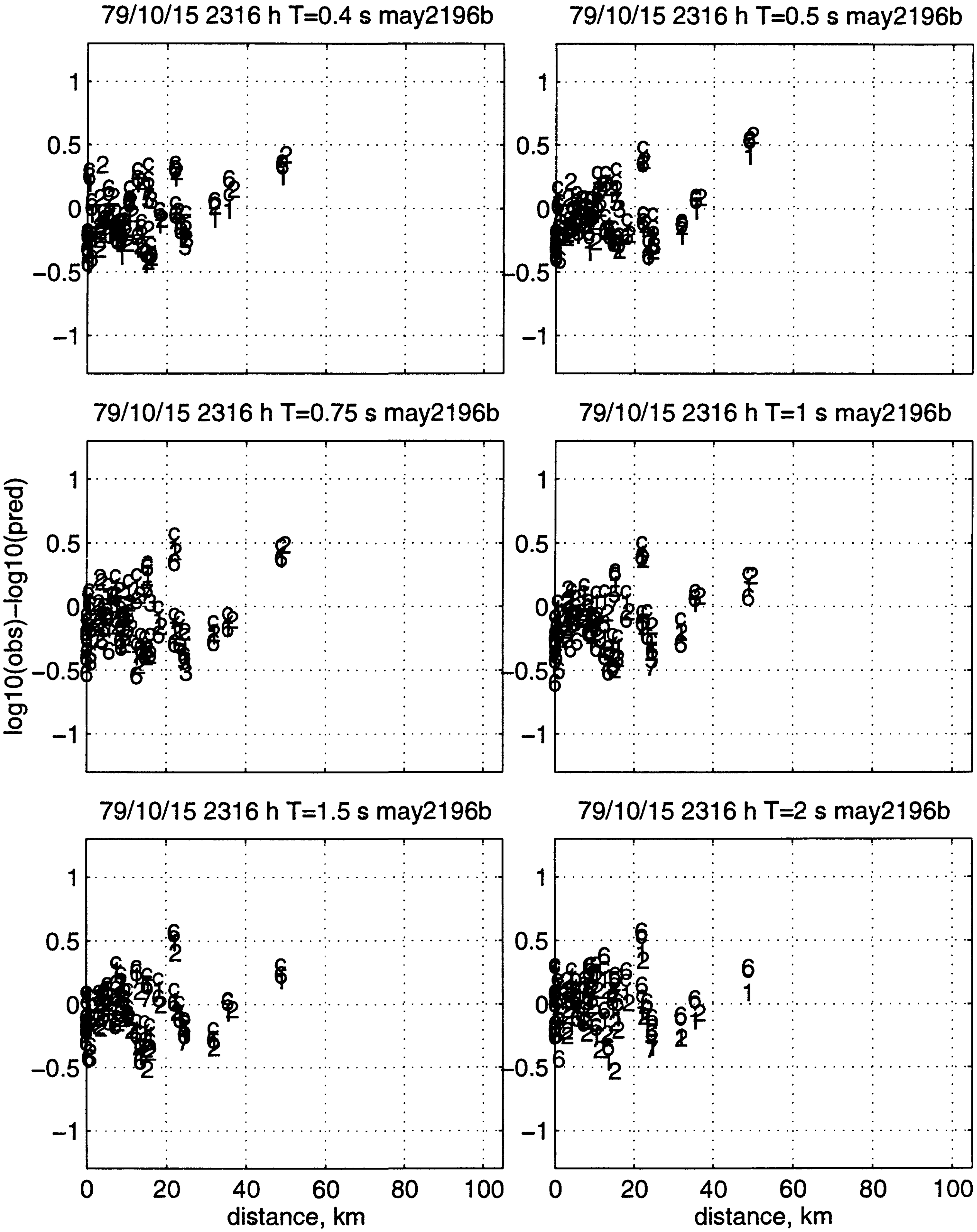
79/10/15 2316 h T=0.4 s may2196b
79/10/15 2316 h T=0.5 s may2196b
79/10/15 2316 h T=0.75 s may2196b
79/10/15 2316 h T=1 s may2196b
79/10/15 2316 h T=1.5 s may2196b
79/10/15 2316 h T=2 s may2196b
log10(obs)−log10(pred)
distance, km
distance, km

21b

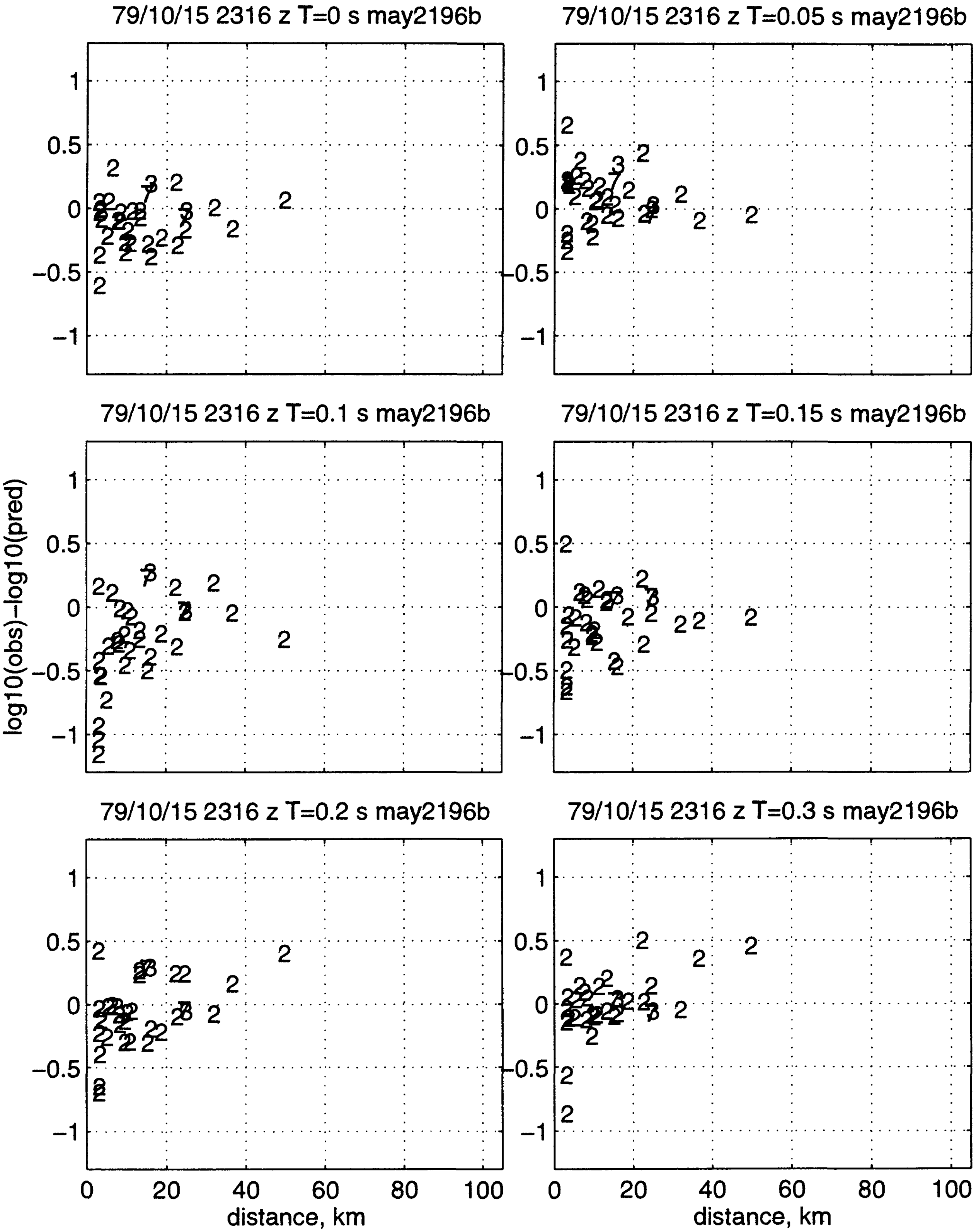

79/10/15 2316 z T=0 s may2196b
79/10/15 2316 z T=0.05 s may2196b
79/10/15 2316 z T=0.1 s may2196b
79/10/15 2316 z T=0.15 s may2196b
79/10/15 2316 z T=0.2 s may2196b
79/10/15 2316 z T=0.3 s may2196b
log10(obs)−log10(pred)
distance, km

21c

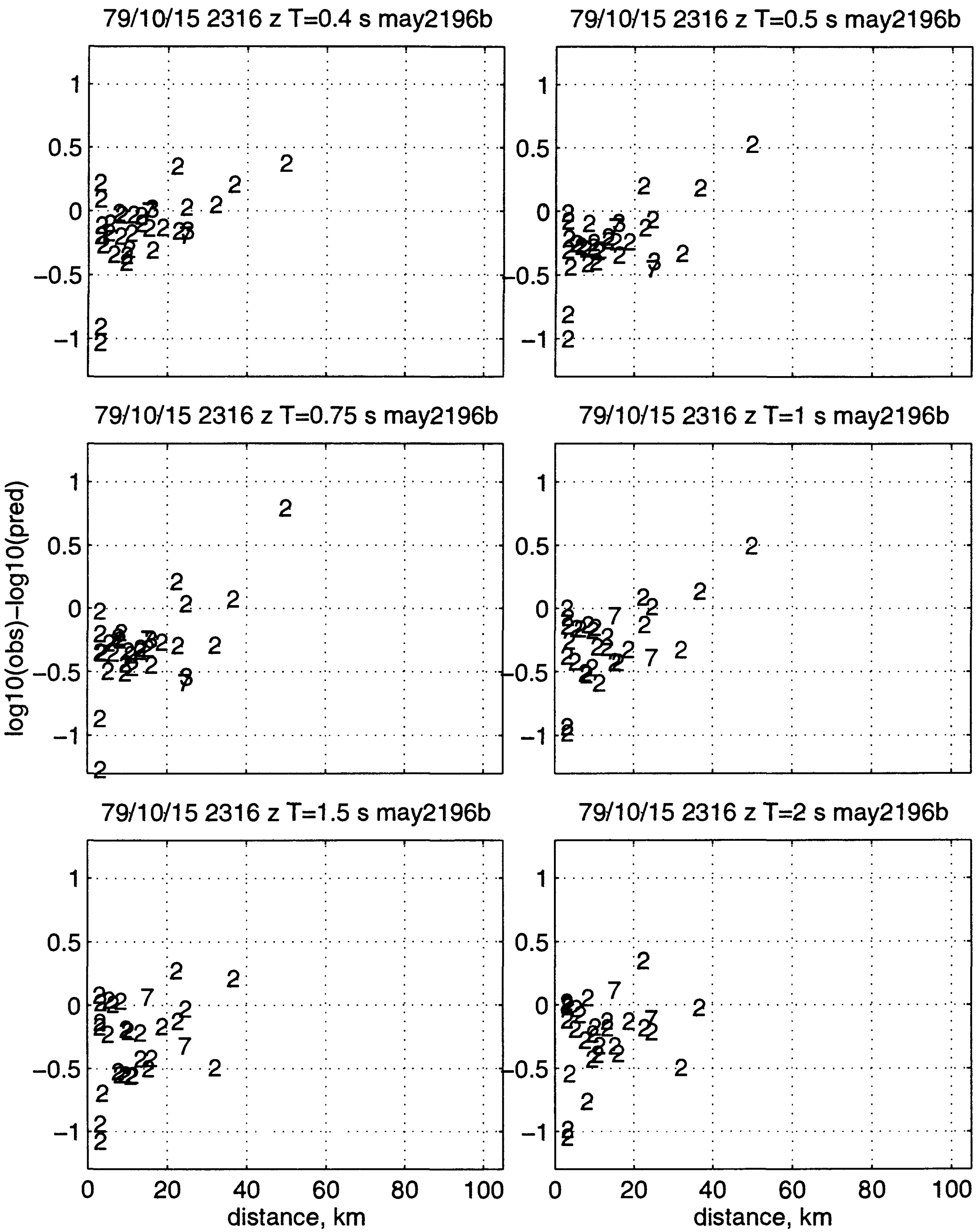
79/10/15 2316 z T=0.4 s may2196b
79/10/15 2316 z T=0.5 s may2196b
79/10/15 2316 z T=0.75 s may2196b
79/10/15 2316 z T=1 s may2196b
79/10/15 2316 z T=1.5 s may2196b
79/10/15 2316 z T=2 s may2196b
log10(obs)−log10(pred)
distance, km
distance, km

21d

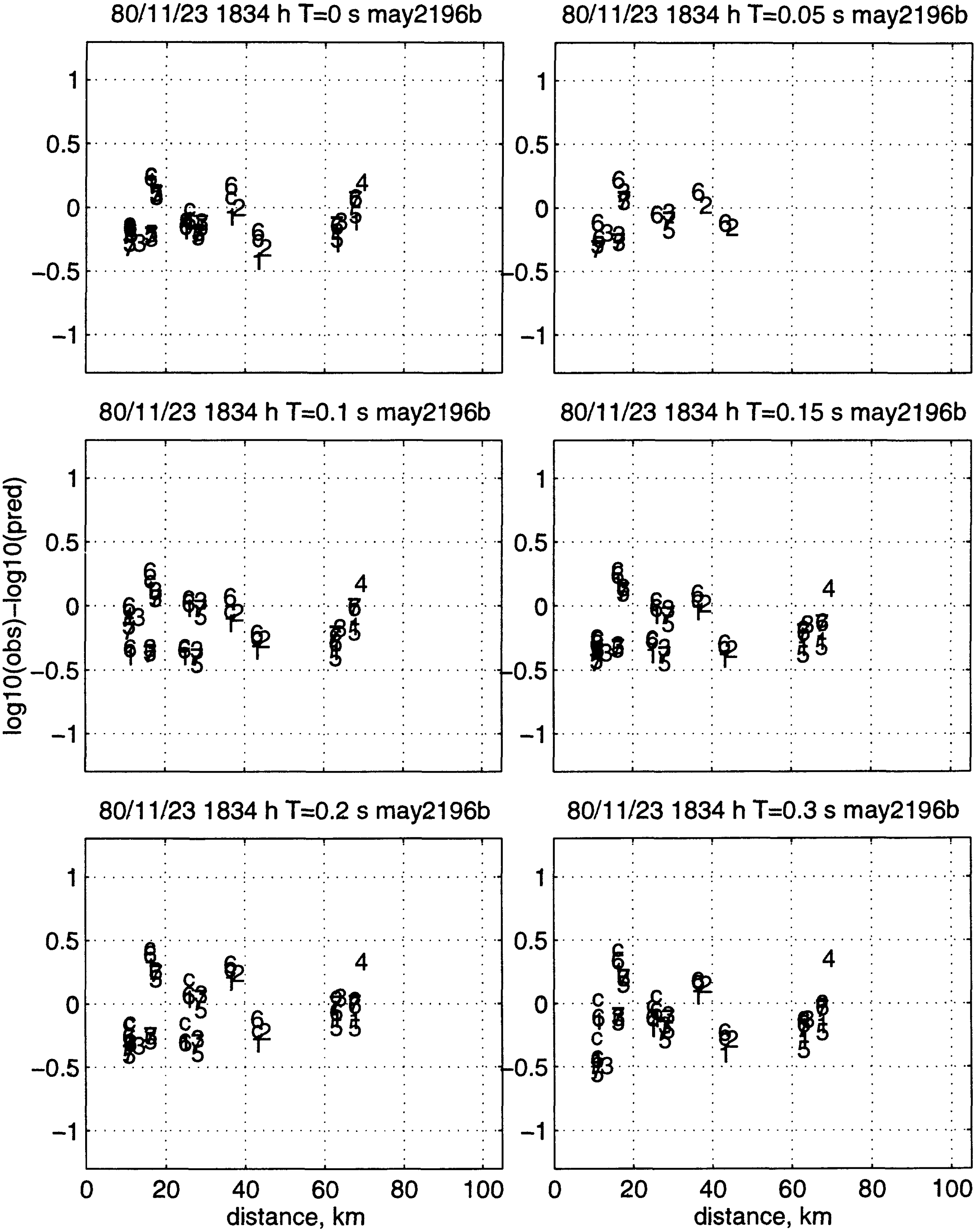
80/11/23 1834 h T=0 s may2196b
80/11/23 1834 h T=0.05 s may2196b
80/11/23 1834 h T=0.1 s may2196b
80/11/23 1834 h T=0.15 s may2196b
80/11/23 1834 h T=0.2 s may2196b
80/11/23 1834 h T=0.3 s may2196b
log10(obs)−log10(pred)
distance, km
distance, km

21e

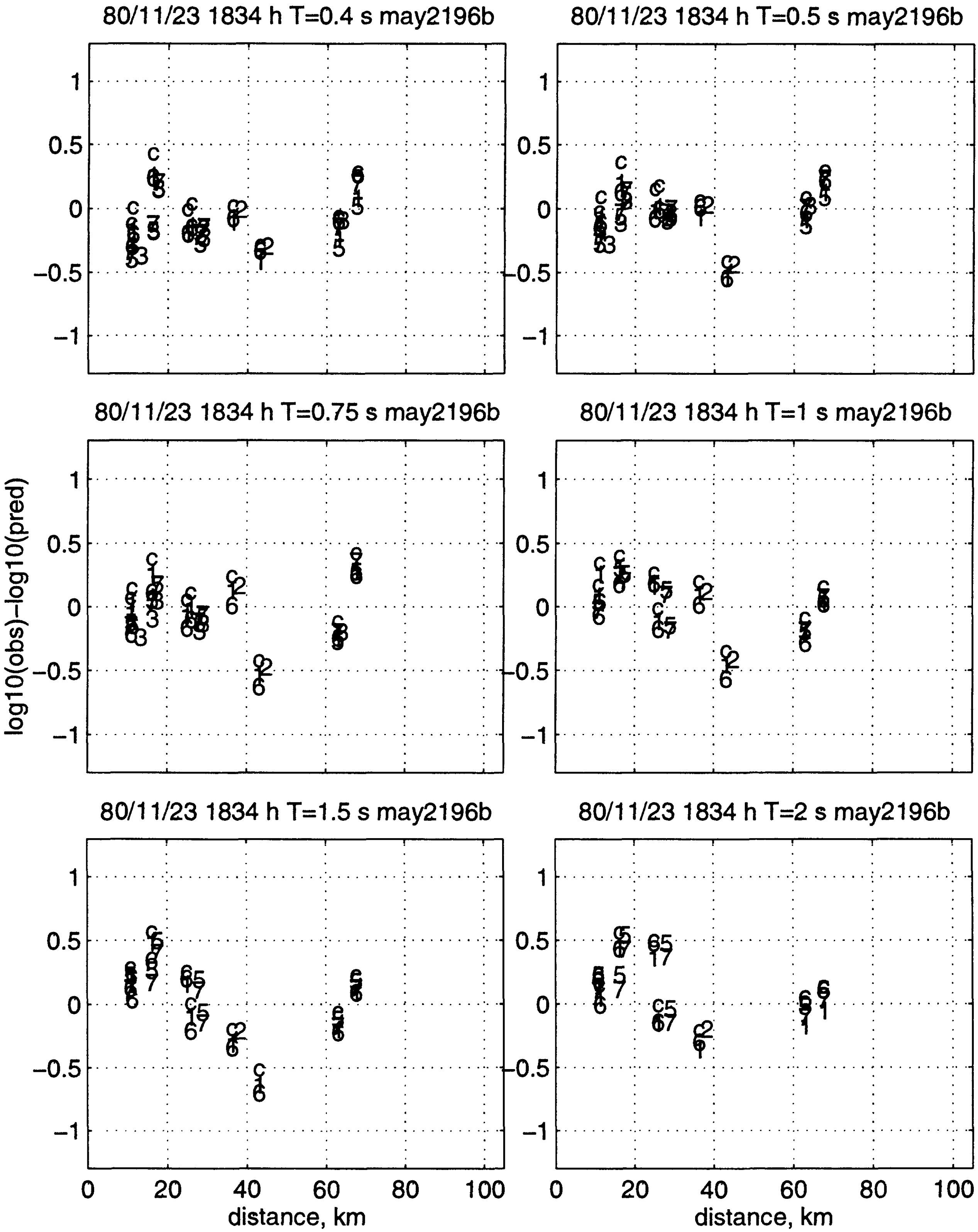
80/11/23 1834 h T=0.4 s may2196b
80/11/23 1834 h T=0.5 s may2196b
80/11/23 1834 h T=0.75 s may2196b
80/11/23 1834 h T=1 s may2196b
80/11/23 1834 h T=1.5 s may2196b
80/11/23 1834 h T=2 s may2196b
log10(obs)−log10(pred)
distance, km
distance, km

21f

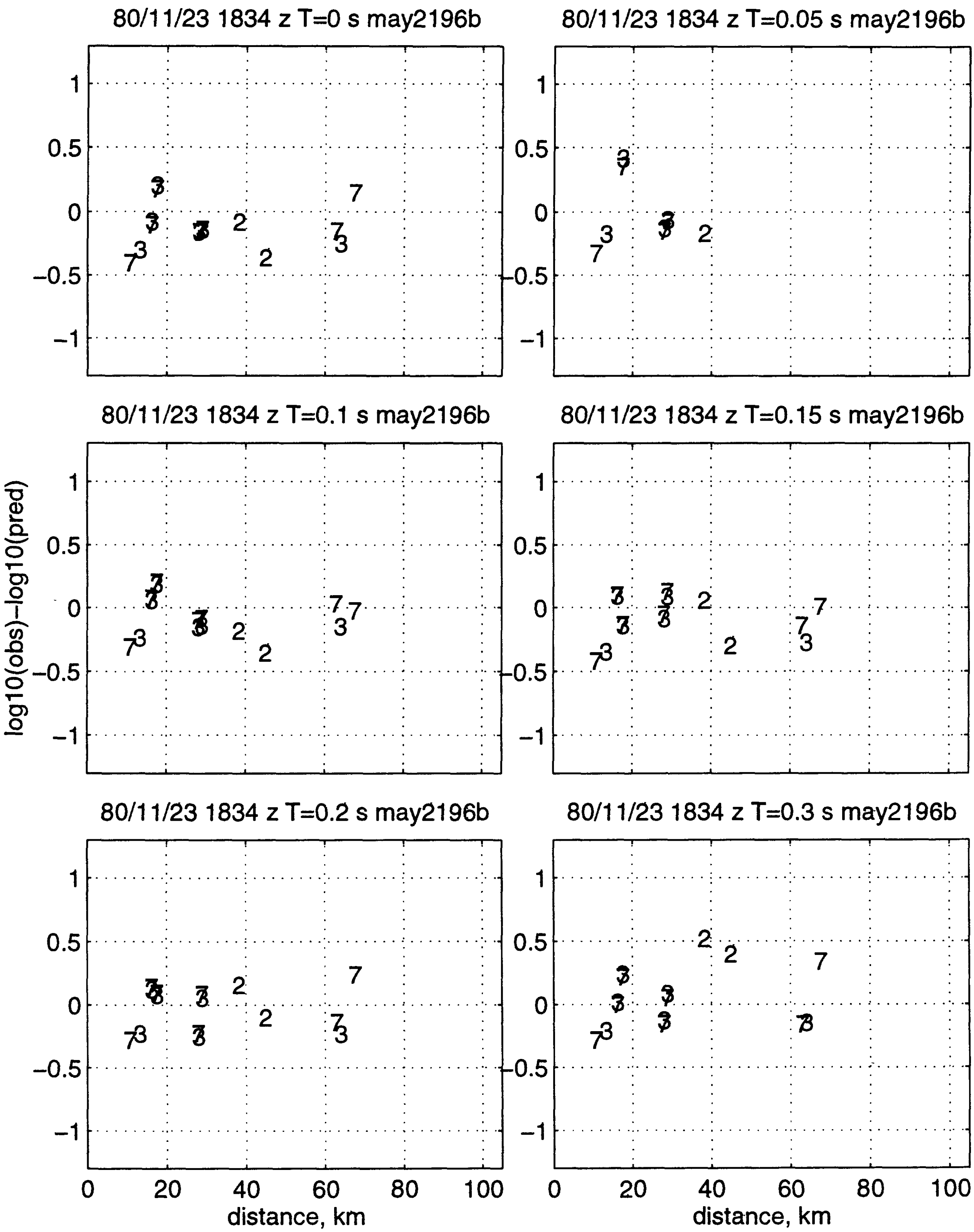
80/11/23 1834 z T=0 s may2196b
80/11/23 1834 z T=0.05 s may2196b
80/11/23 1834 z T=0.1 s may2196b
80/11/23 1834 z T=0.15 s may2196b
80/11/23 1834 z T=0.2 s may2196b
80/11/23 1834 z T=0.3 s may2196b
log10(obs)−log10(pred)
distance, km
distance, km

21g

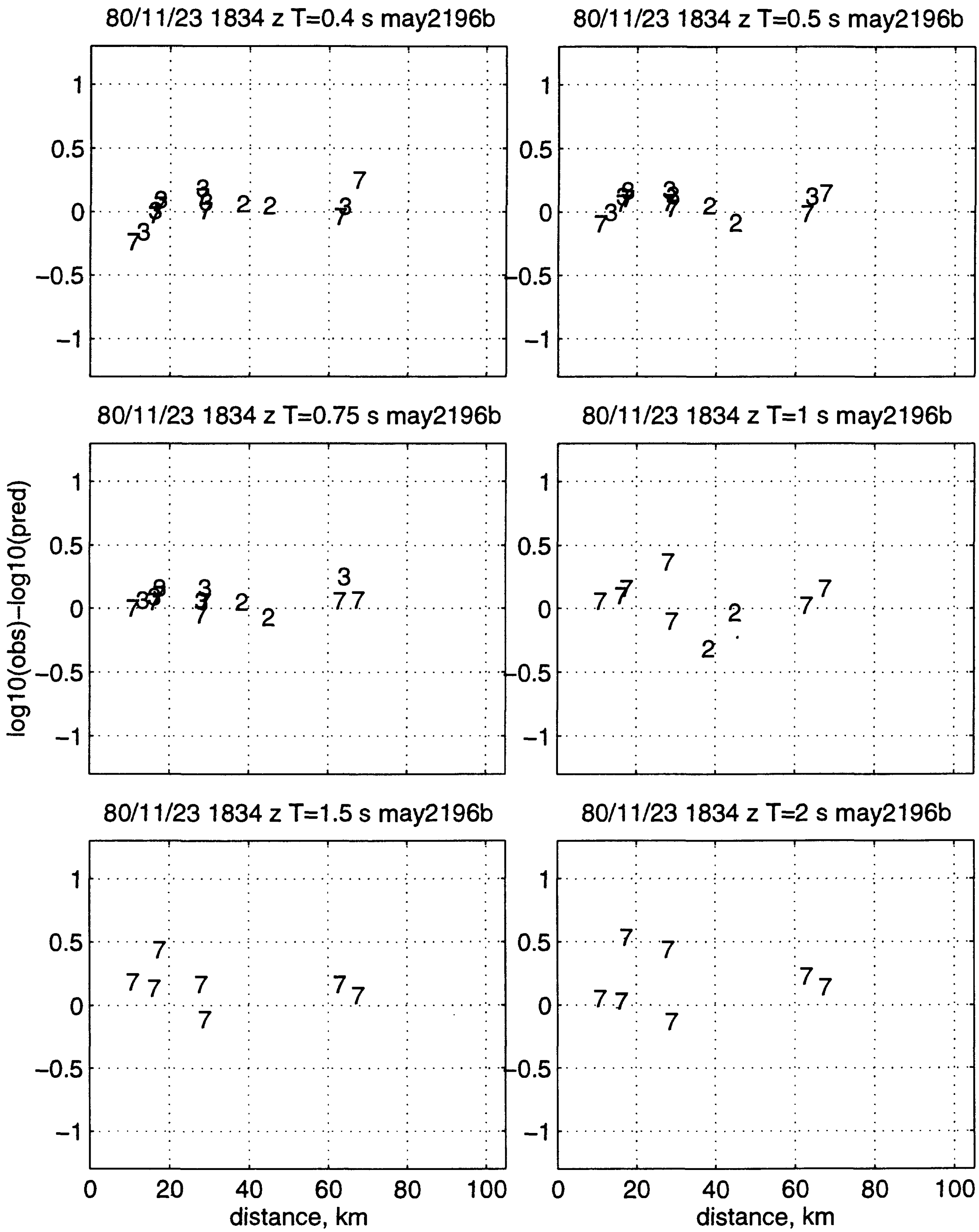
80/11/23 1834 z T=0.4 s may2196b
80/11/23 1834 z T=0.5 s may2196b
80/11/23 1834 z T=0.75 s may2196b
80/11/23 1834 z T=1 s may2196b
80/11/23 1834 z T=1.5 s may2196b
80/11/23 1834 z T=2 s may2196b
log10(obs)−log10(pred)
distance, km
distance, km

21 h

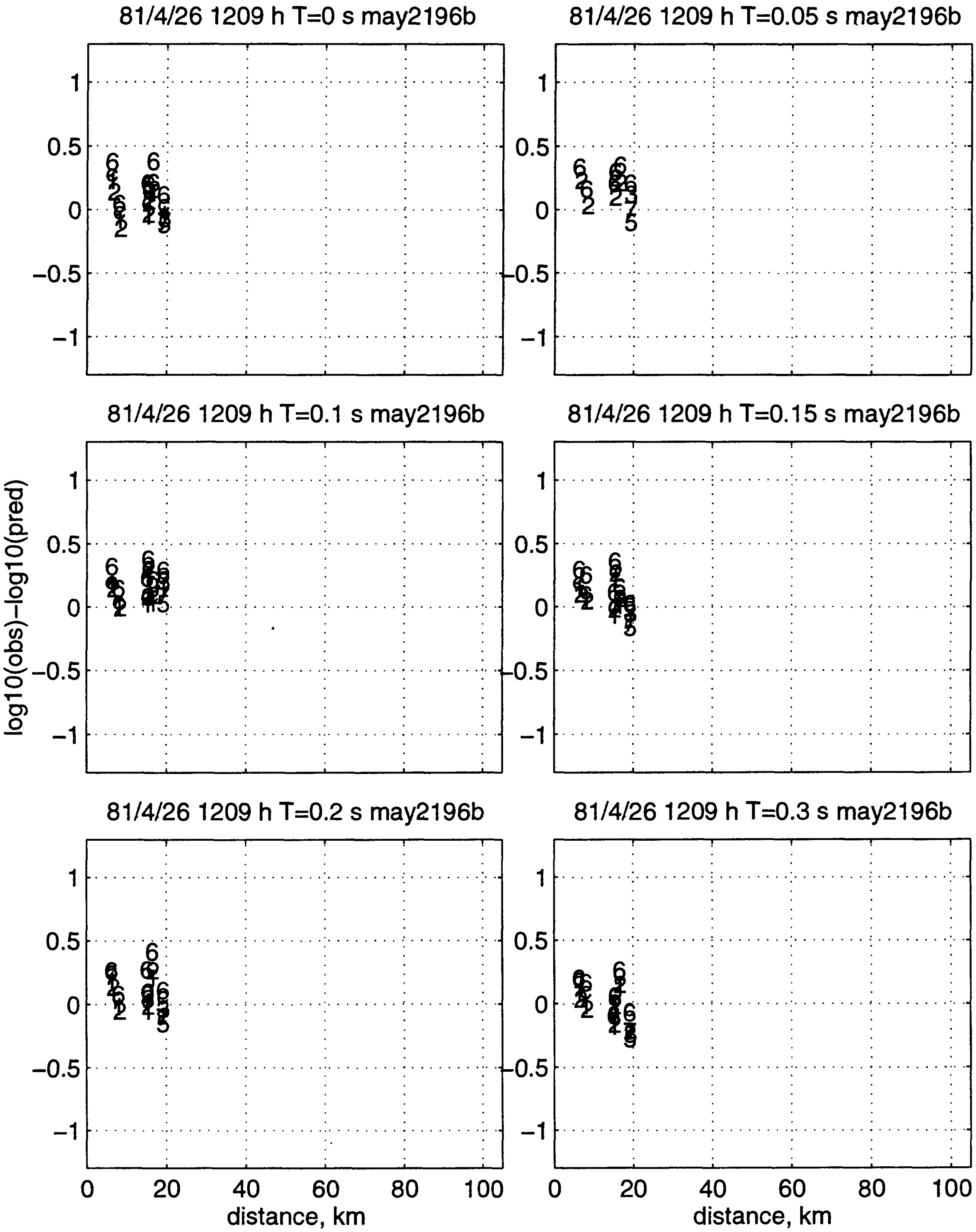
81/4/26 1209 h T=0 s may2196b
81/4/26 1209 h T=0.05 s may2196b
81/4/26 1209 h T=0.1 s may2196b
81/4/26 1209 h T=0.15 s may2196b
81/4/26 1209 h T=0.2 s may2196b
81/4/26 1209 h T=0.3 s may2196b
log10(obs)−log10(pred)
distance, km
distance, km

21i

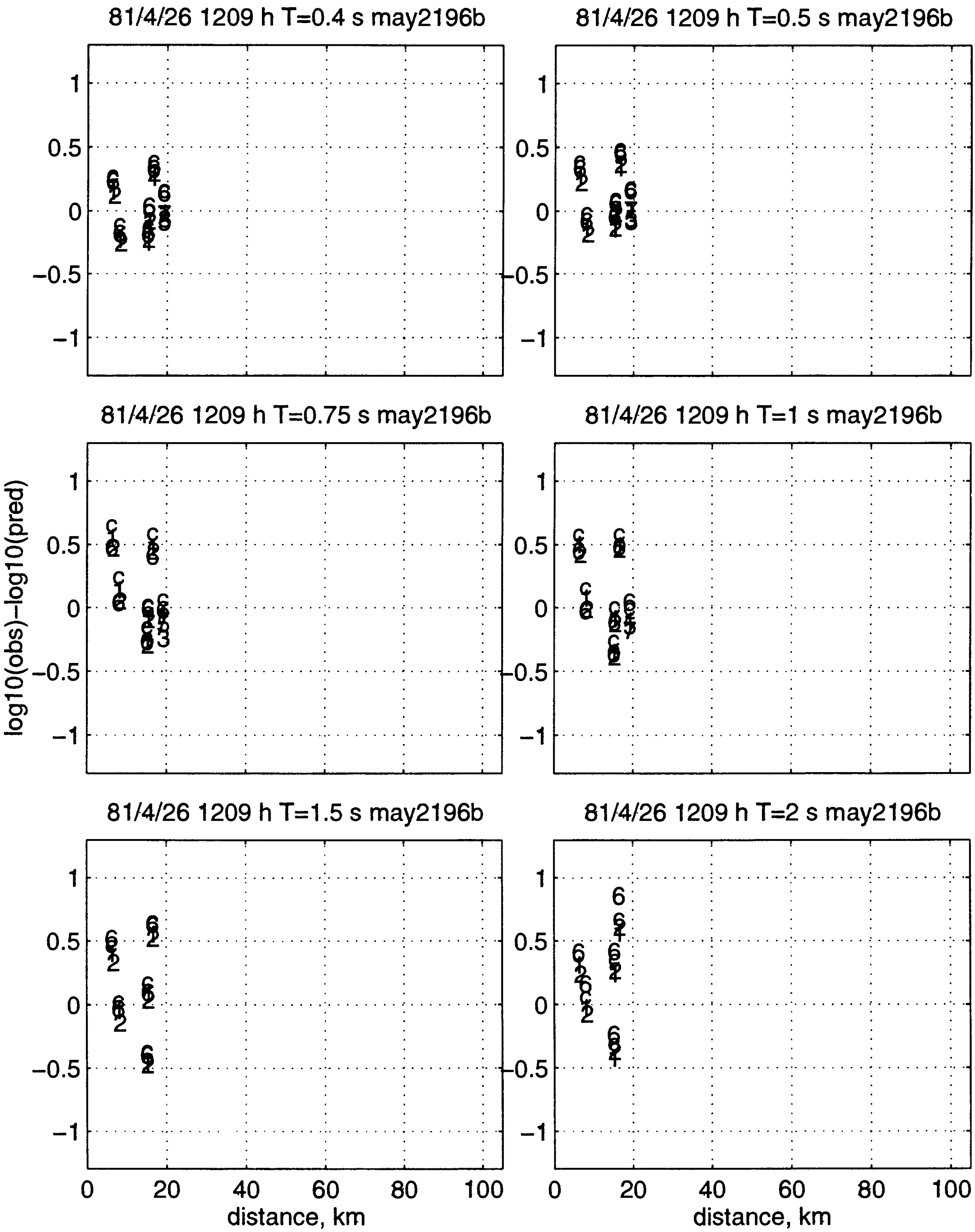
81/4/26 1209 h T=0.4 s may2196b
81/4/26 1209 h T=0.5 s may2196b
81/4/26 1209 h T=0.75 s may2196b
81/4/26 1209 h T=1 s may2196b
81/4/26 1209 h T=1.5 s may2196b
81/4/26 1209 h T=2 s may2196b
log10(obs)−log10(pred)
distance, km
distance, km

21j

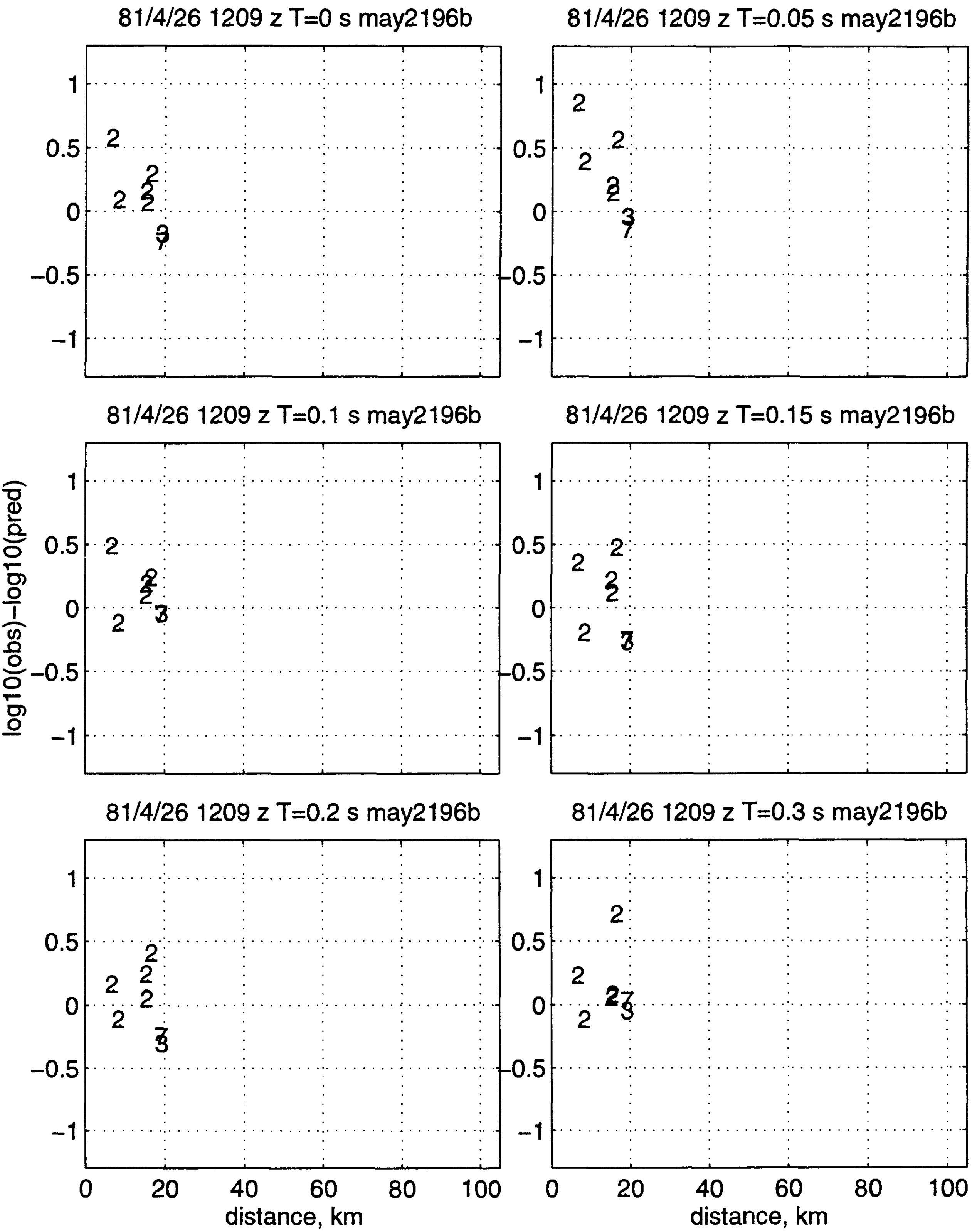
81/4/26 1209 z T=0 s may2196b
81/4/26 1209 z T=0.05 s may2196b
81/4/26 1209 z T=0.1 s may2196b
81/4/26 1209 z T=0.15 s may2196b
81/4/26 1209 z T=0.2 s may2196b
81/4/26 1209 z T=0.3 s may2196b
log10(obs)−log10(pred)
distance, km
distance, km

21k

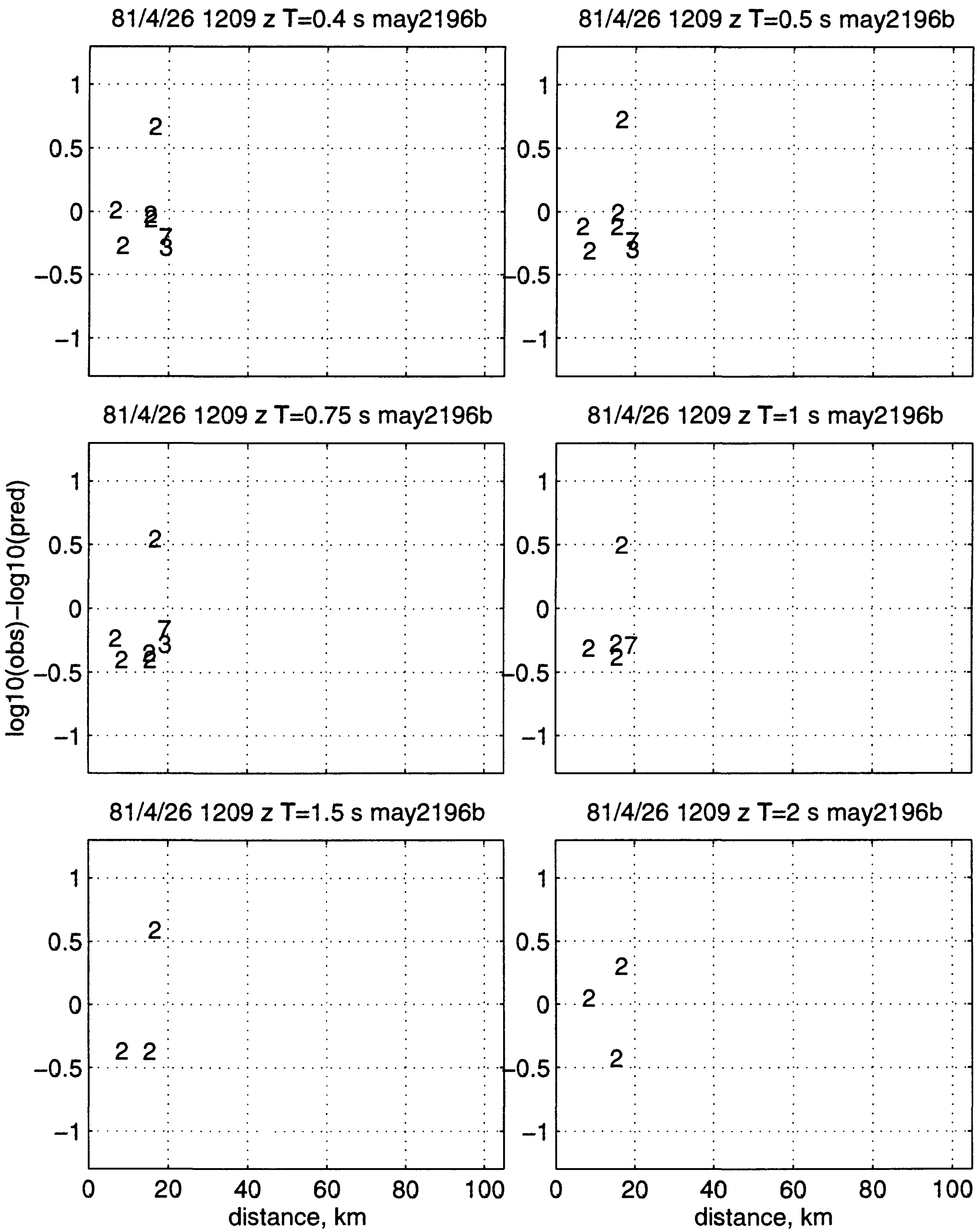
81/4/26 1209 z T=0.4 s may2196b
81/4/26 1209 z T=0.5 s may2196b
81/4/26 1209 z T=0.75 s may2196b
81/4/26 1209 z T=1 s may2196b
81/4/26 1209 z T=1.5 s may2196b
81/4/26 1209 z T=2 s may2196b
log10(obs)−log10(pred)
distance, km
distance, km

21 l

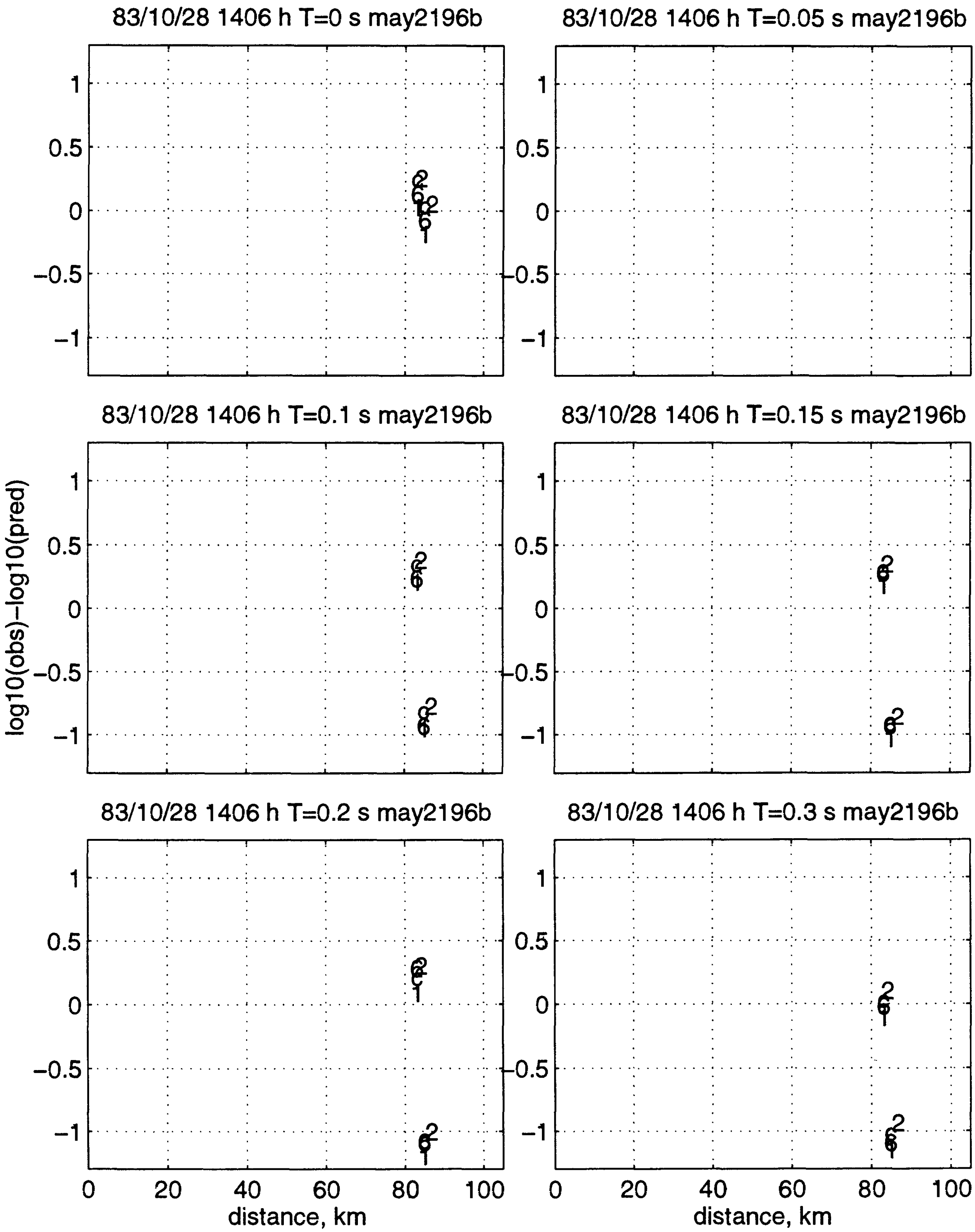
83/10/28 1406 h T=0 s may2196b
83/10/28 1406 h T=0.05 s may2196b
83/10/28 1406 h T=0.1 s may2196b
83/10/28 1406 h T=0.15 s may2196b
83/10/28 1406 h T=0.2 s may2196b
83/10/28 1406 h T=0.3 s may2196b
log10(obs)−log10(pred)
distance, km
distance, km

21m

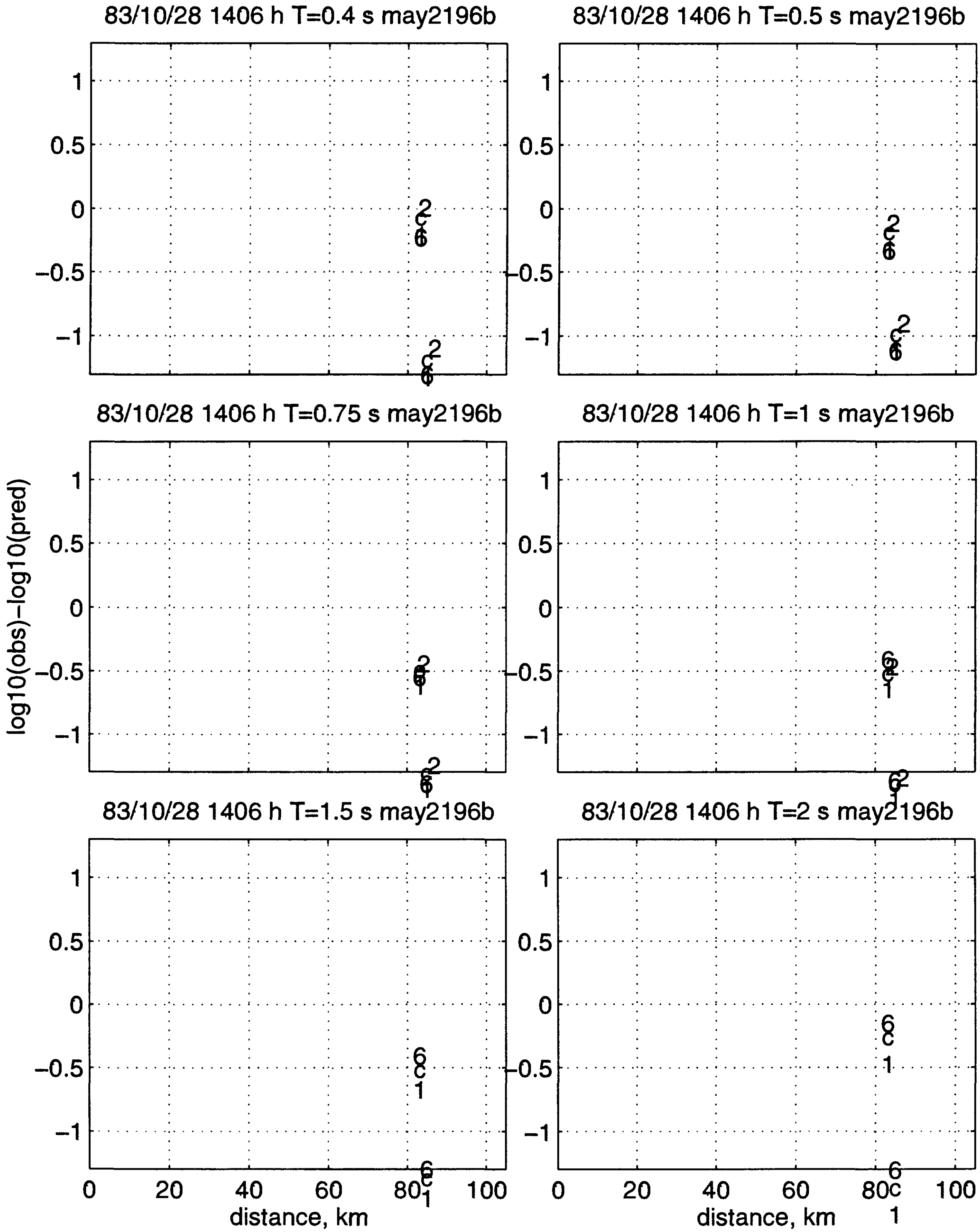
83/10/28 1406 h T=0.4 s may2196b
83/10/28 1406 h T=0.5 s may2196b
83/10/28 1406 h T=0.75 s may2196b
83/10/28 1406 h T=1 s may2196b
83/10/28 1406 h T=1.5 s may2196b
83/10/28 1406 h T=2 s may2196b
log10(obs)−log10(pred)
distance, km
distance, km

21n

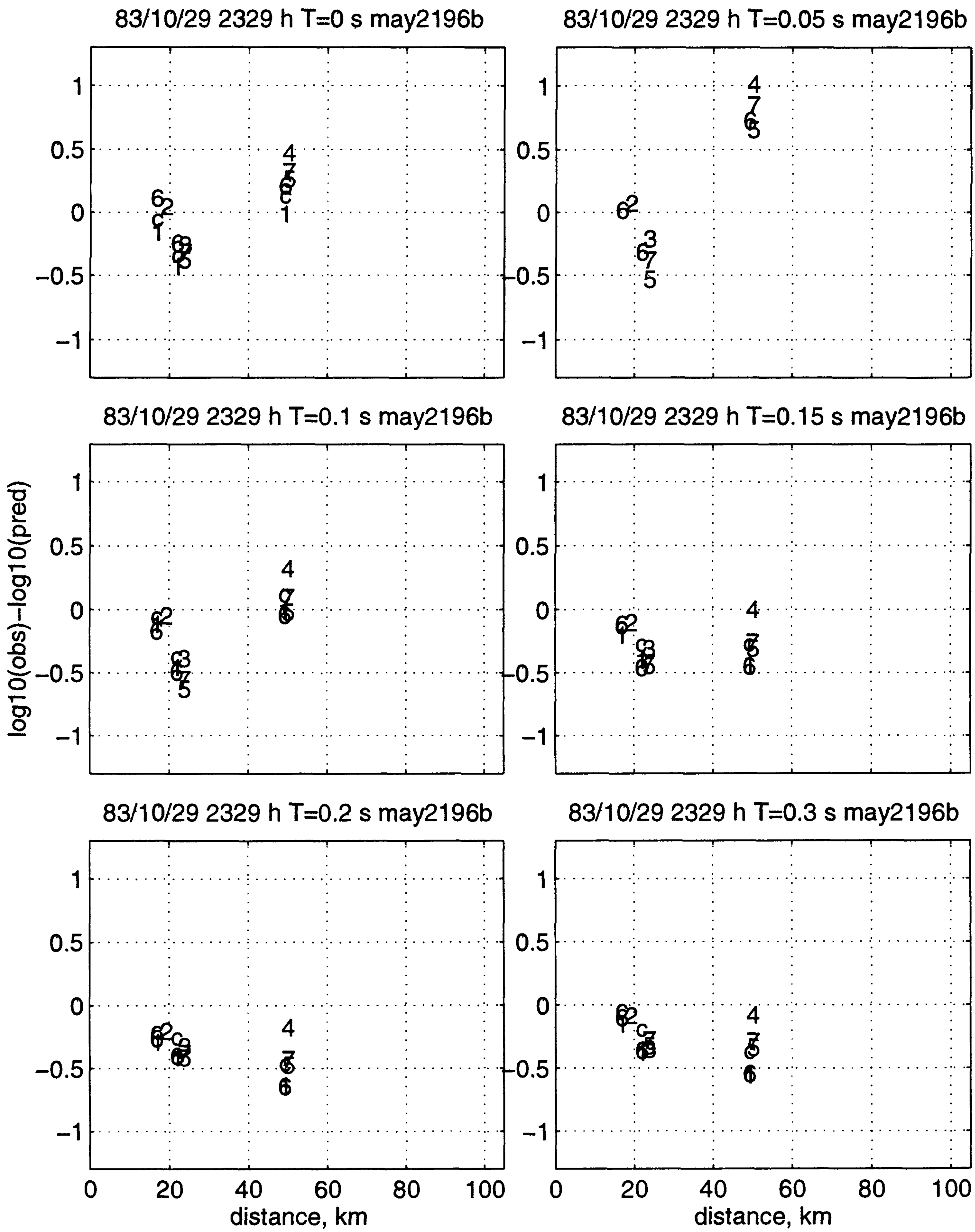
83/10/29 2329 h T=0 s may2196b
83/10/29 2329 h T=0.05 s may2196b
83/10/29 2329 h T=0.1 s may2196b
83/10/29 2329 h T=0.15 s may2196b
83/10/29 2329 h T=0.2 s may2196b
83/10/29 2329 h T=0.3 s may2196b
log10(obs)−log10(pred)
1
0.5
0
−0.5
−1
0
20
40
60
80
100
distance, km

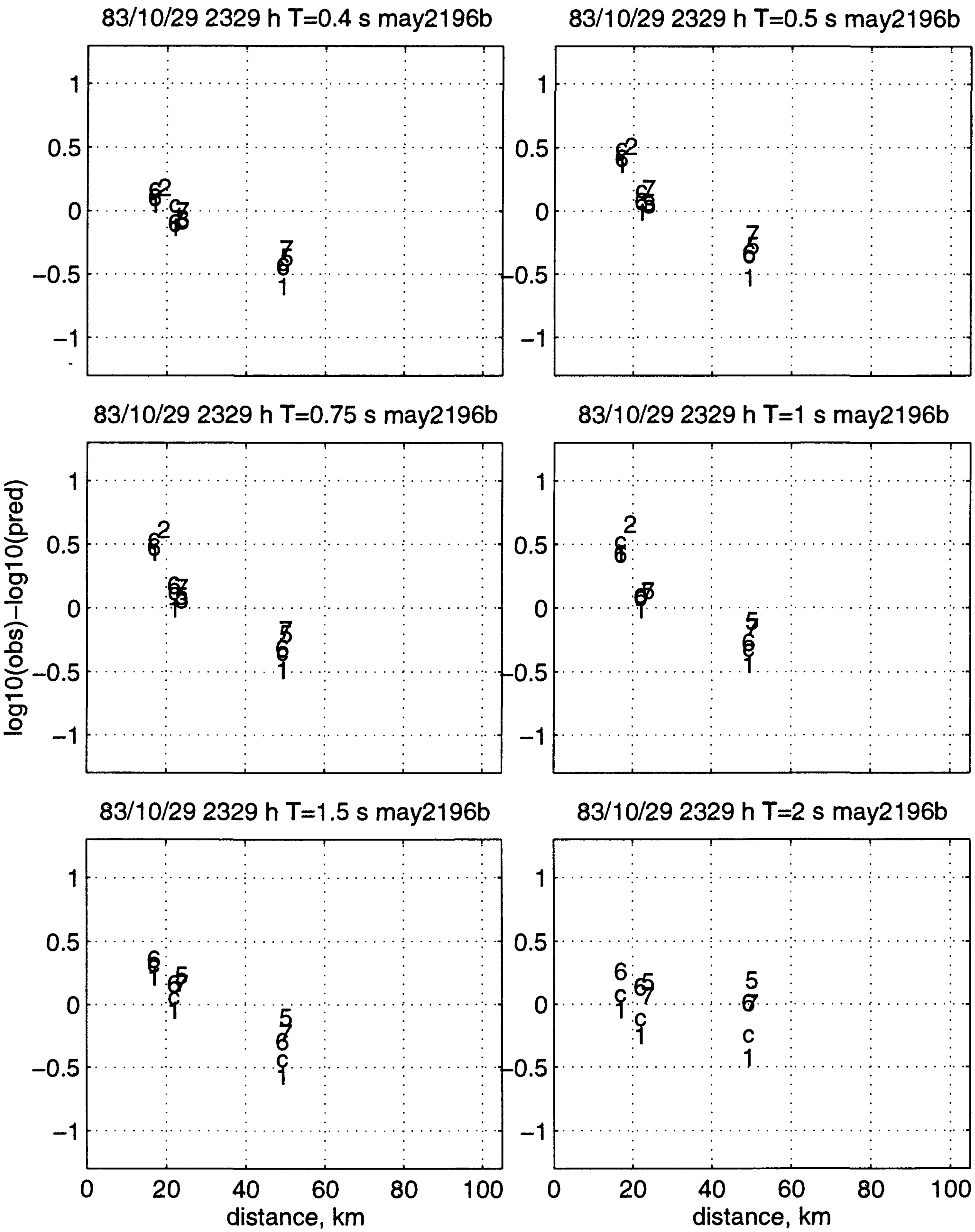

83/10/29 2329 h T=0.4 s may2196b
83/10/29 2329 h T=0.5 s may2196b
83/10/29 2329 h T=0.75 s may2196b
83/10/29 2329 h T=1 s may2196b
83/10/29 2329 h T=1.5 s may2196b
83/10/29 2329 h T=2 s may2196b
log10(obs)−log10(pred)
distance, km

21p

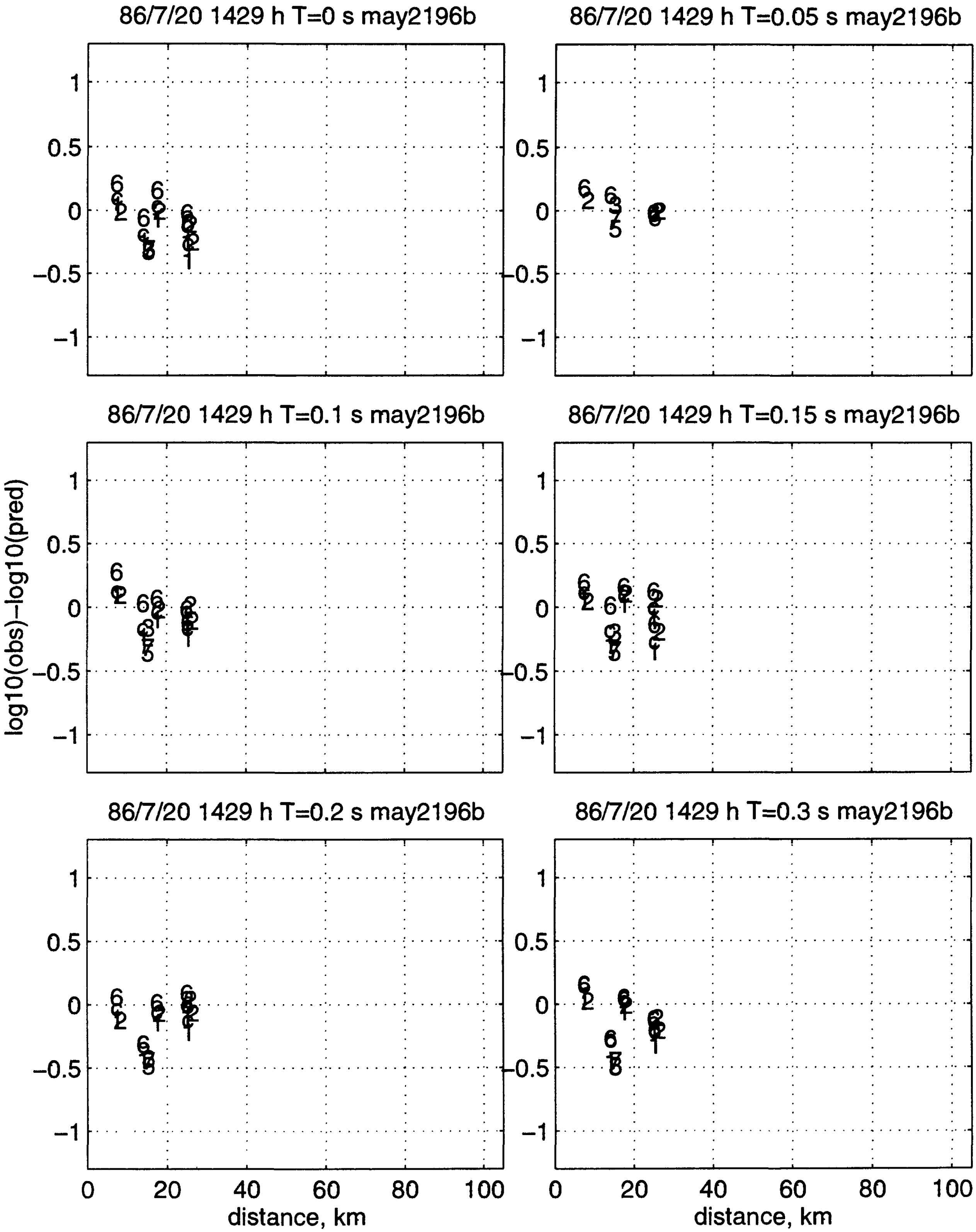
86/7/20 1429 h T=0 s may2196b
86/7/20 1429 h T=0.05 s may2196b
86/7/20 1429 h T=0.1 s may2196b
86/7/20 1429 h T=0.15 s may2196b
86/7/20 1429 h T=0.2 s may2196b
86/7/20 1429 h T=0.3 s may2196b
log10(obs)−log10(pred)
distance, km
distance, km

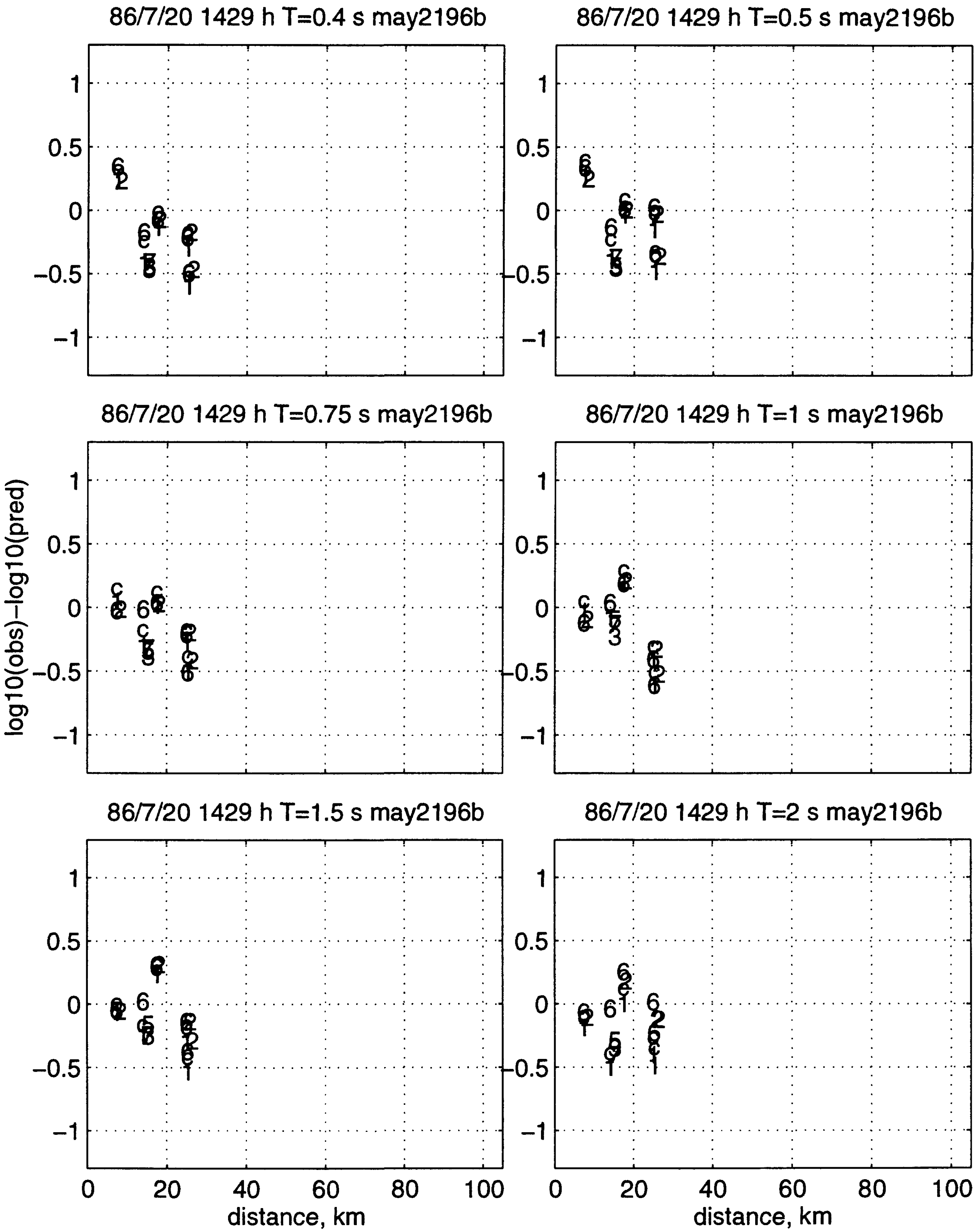
86/7/20 1429 h T=0.4 s may2196b
86/7/20 1429 h T=0.5 s may2196b
86/7/20 1429 h T=0.75 s may2196b
86/7/20 1429 h T=1 s may2196b
86/7/20 1429 h T=1.5 s may2196b
86/7/20 1429 h T=2 s may2196b
log10(obs)−log10(pred)
distance, km
distance, km

21r

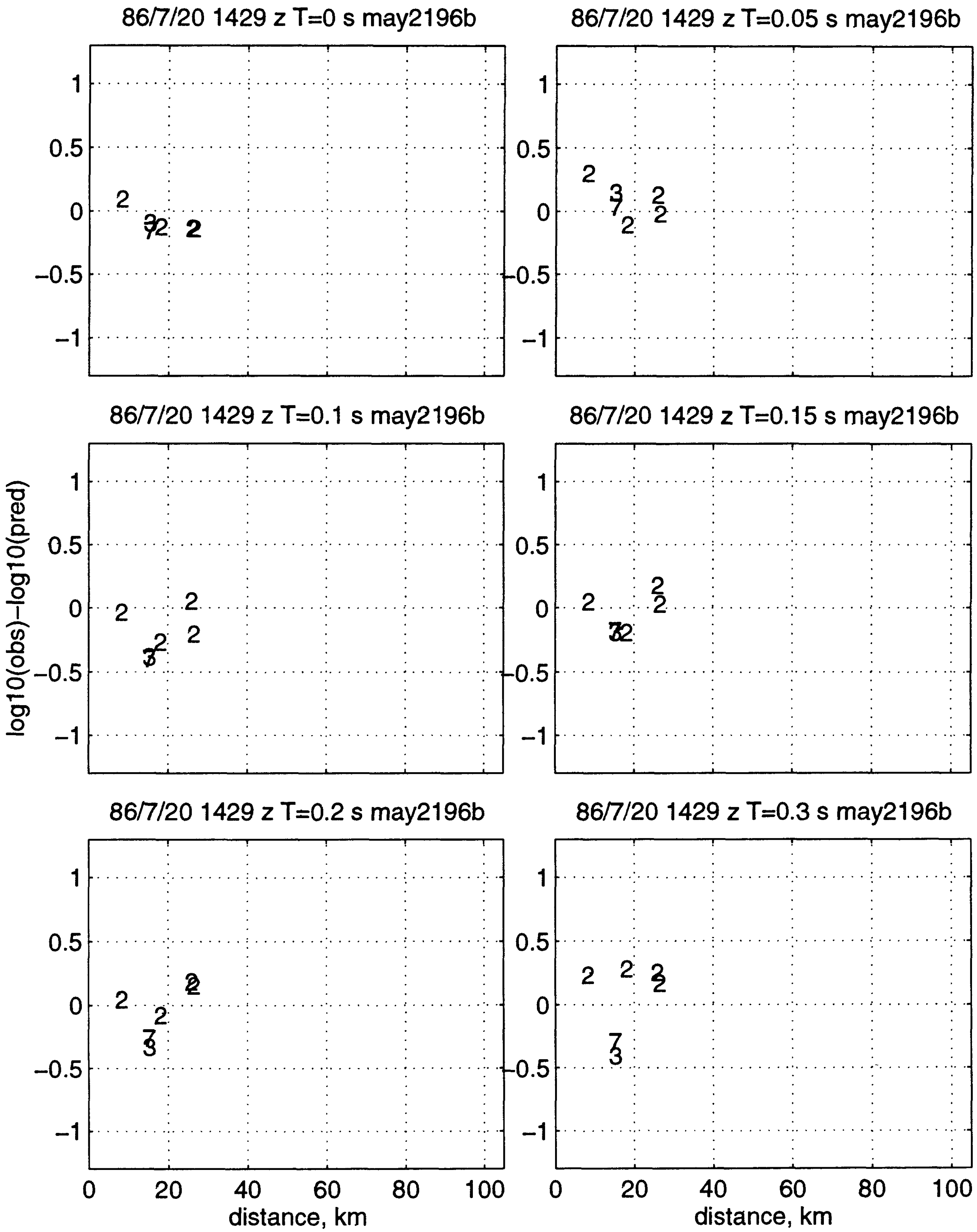

86/7/20 1429 z T=0 s may2196b
86/7/20 1429 z T=0.05 s may2196b
86/7/20 1429 z T=0.1 s may2196b
86/7/20 1429 z T=0.15 s may2196b
86/7/20 1429 z T=0.2 s may2196b
86/7/20 1429 z T=0.3 s may2196b
log10(obs)−log10(pred)
distance, km

215

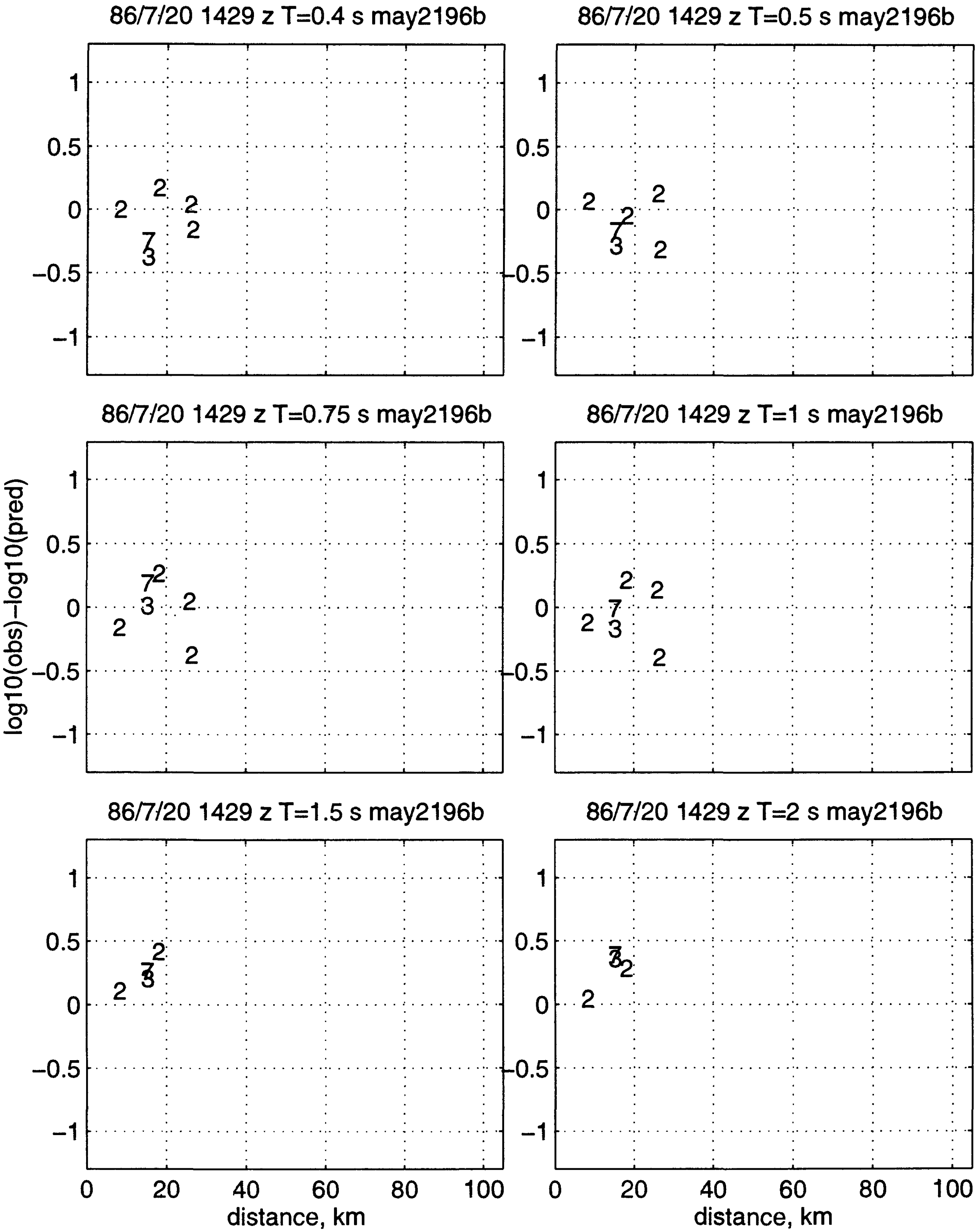

86/7/20 1429 z T=0.4 s may2196b
86/7/20 1429 z T=0.5 s may2196b
86/7/20 1429 z T=0.75 s may2196b
86/7/20 1429 z T=1 s may2196b
86/7/20 1429 z T=1.5 s may2196b
86/7/20 1429 z T=2 s may2196b
log10(obs)−log10(pred)
distance, km

21t

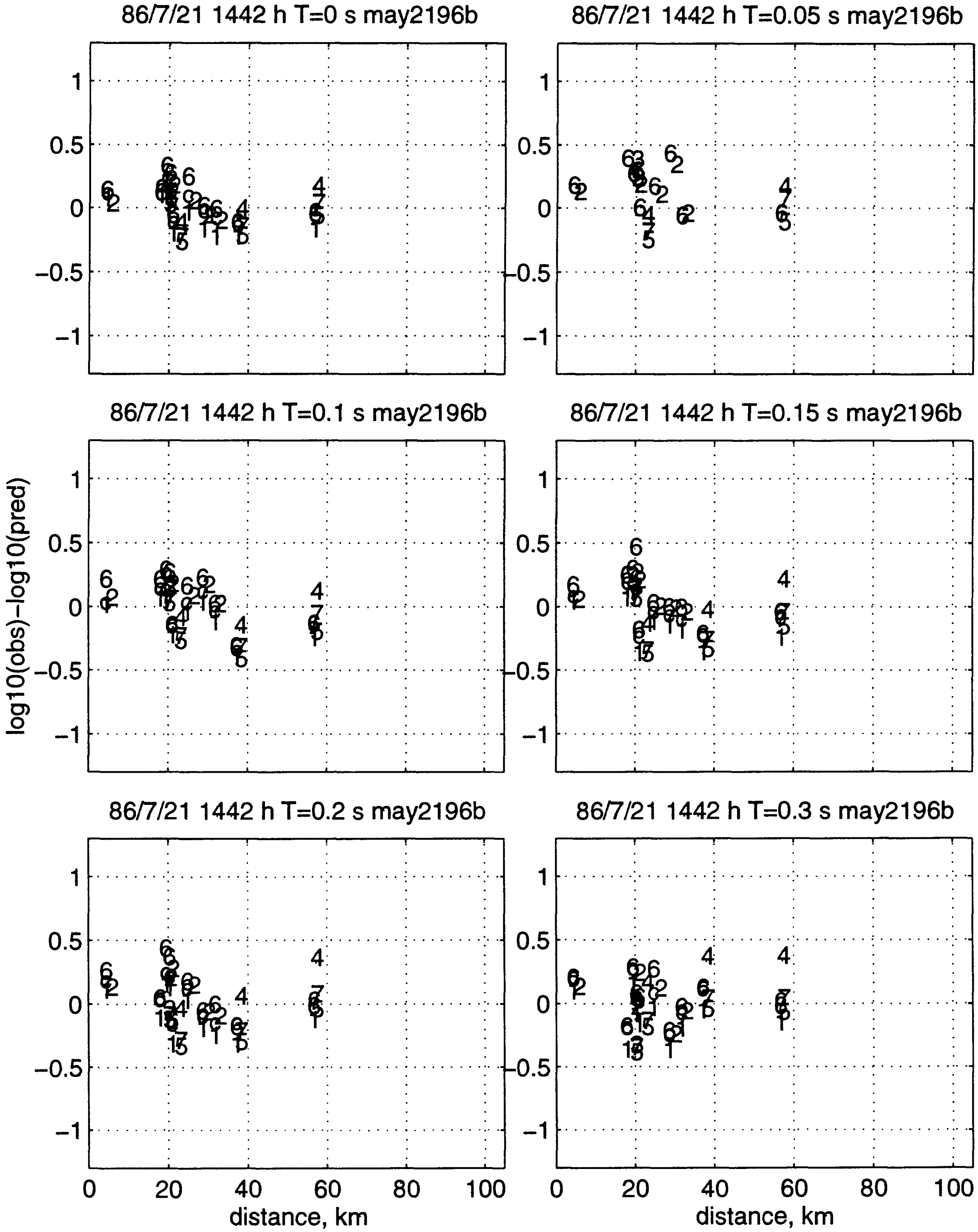
86/7/21 1442 h T=0 s may2196b
86/7/21 1442 h T=0.05 s may2196b
86/7/21 1442 h T=0.1 s may2196b
86/7/21 1442 h T=0.15 s may2196b
86/7/21 1442 h T=0.2 s may2196b
86/7/21 1442 h T=0.3 s may2196b
log10(obs)−log10(pred)
distance, km
distance, km

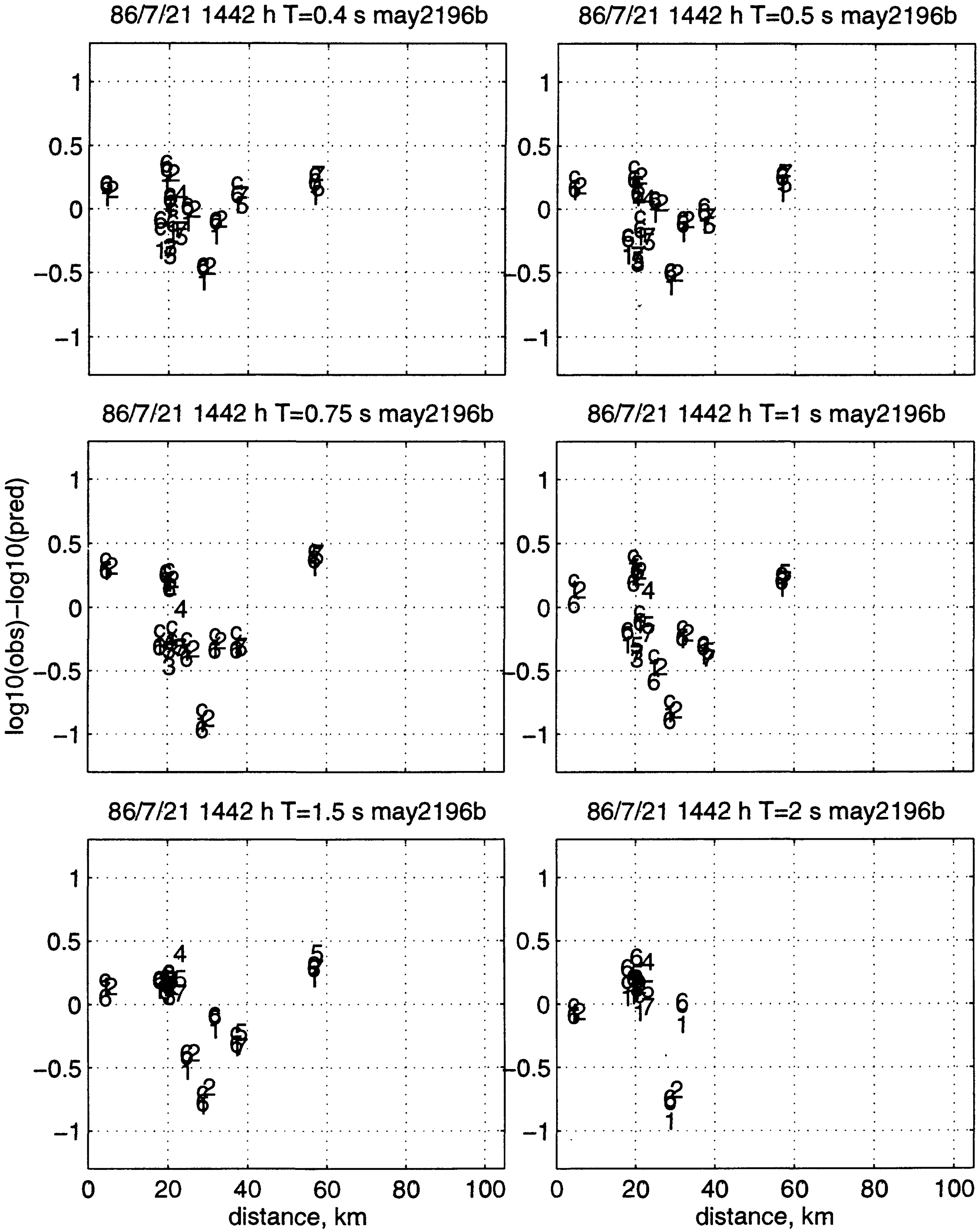
86/7/21 1442 h T=0.4 s may2196b
86/7/21 1442 h T=0.5 s may2196b
86/7/21 1442 h T=0.75 s may2196b
86/7/21 1442 h T=1 s may2196b
86/7/21 1442 h T=1.5 s may2196b
86/7/21 1442 h T=2 s may2196b
log10(obs)−log10(pred)
distance, km
distance, km
1
0.5
0
−0.5
−1
0
20
40
60
80
100

21V

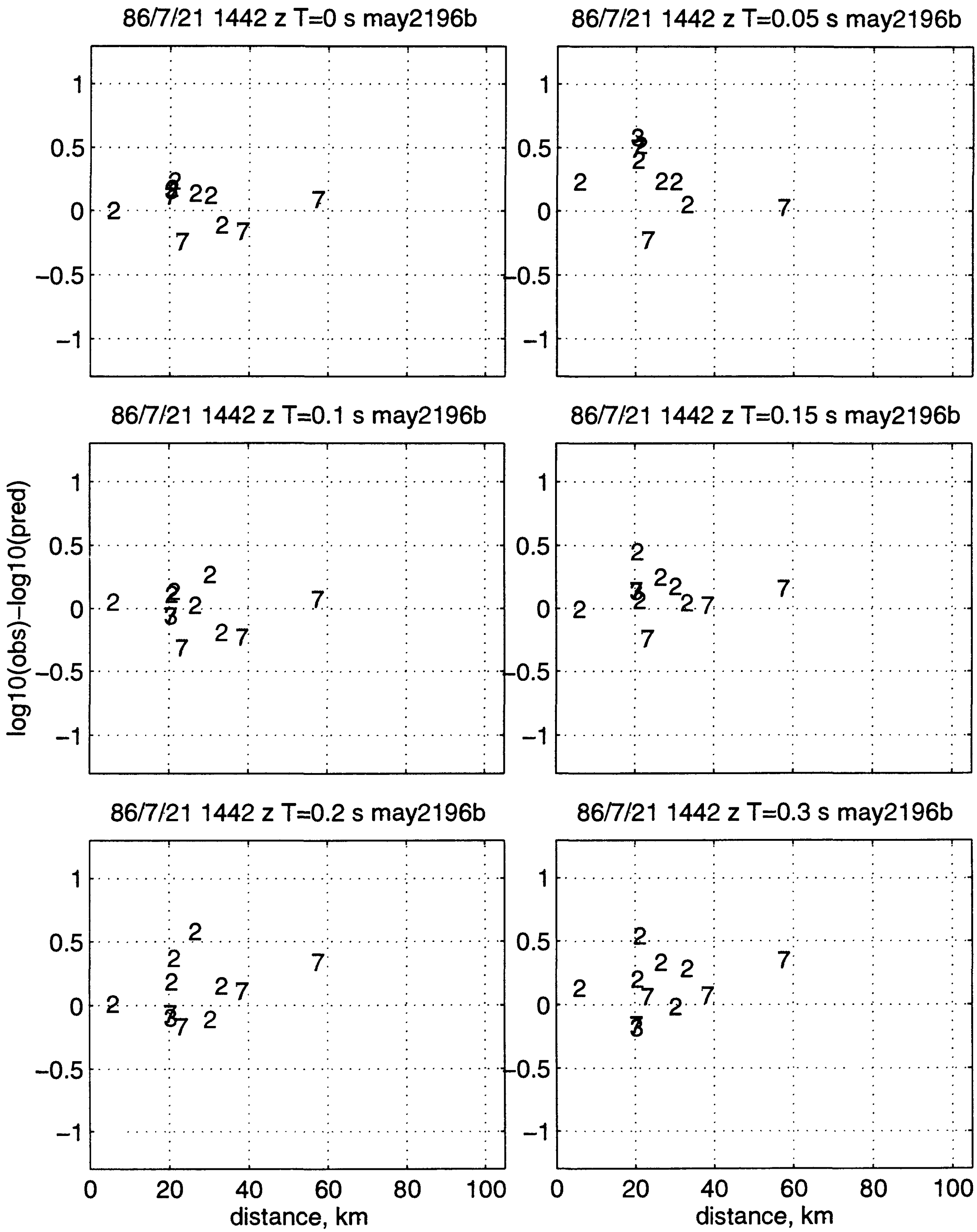
86/7/21 1442 z T=0 s may2196b
86/7/21 1442 z T=0.05 s may2196b
86/7/21 1442 z T=0.1 s may2196b
86/7/21 1442 z T=0.15 s may2196b
86/7/21 1442 z T=0.2 s may2196b
86/7/21 1442 z T=0.3 s may2196b
log10(obs)−log10(pred)
distance, km
distance, km

21w

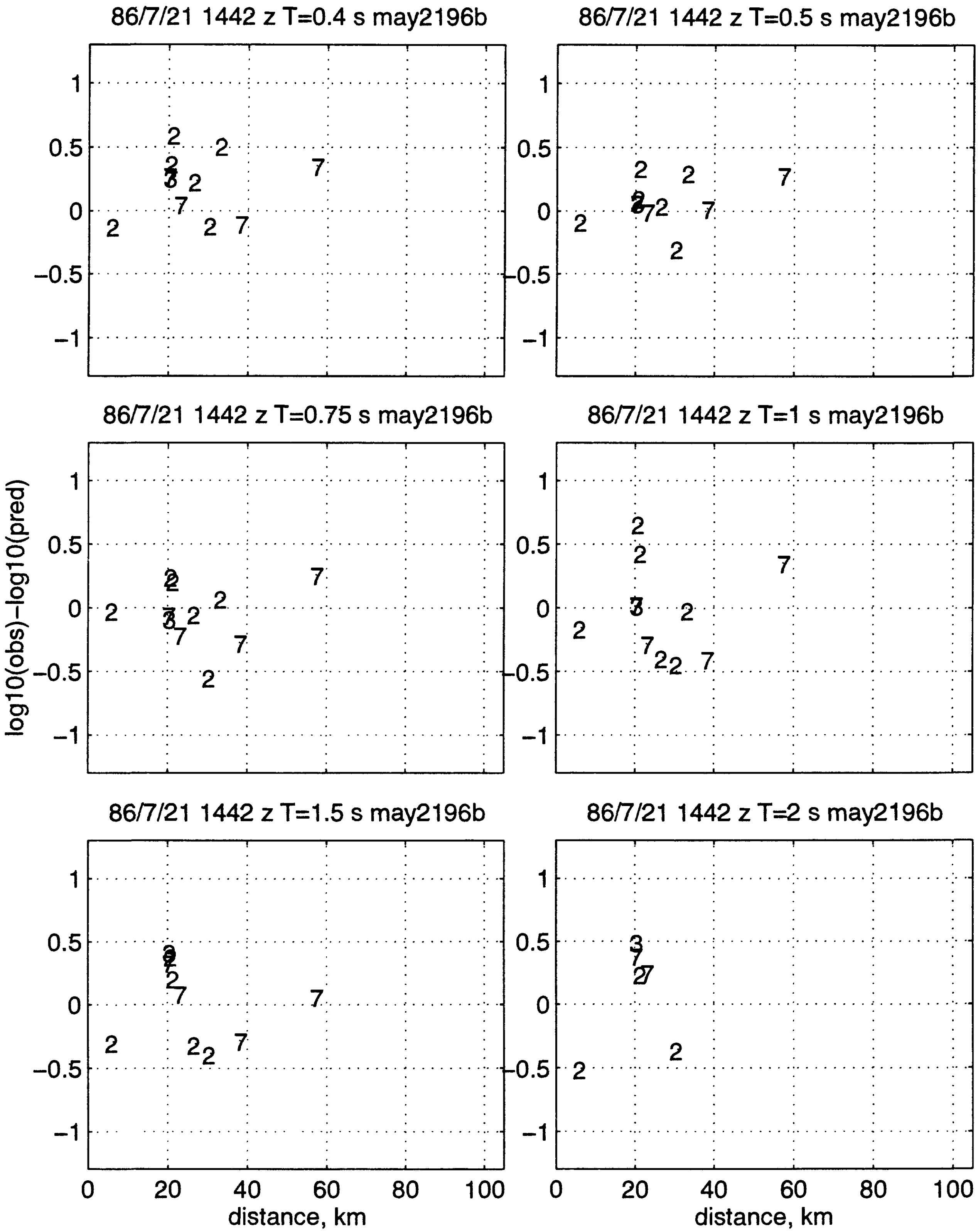
86/7/21 1442 z T=0.4 s may2196b
86/7/21 1442 z T=0.5 s may2196b
86/7/21 1442 z T=0.75 s may2196b
86/7/21 1442 z T=1 s may2196b
86/7/21 1442 z T=1.5 s may2196b
86/7/21 1442 z T=2 s may2196b
log10(obs)−log10(pred)
distance, km
distance, km

21x

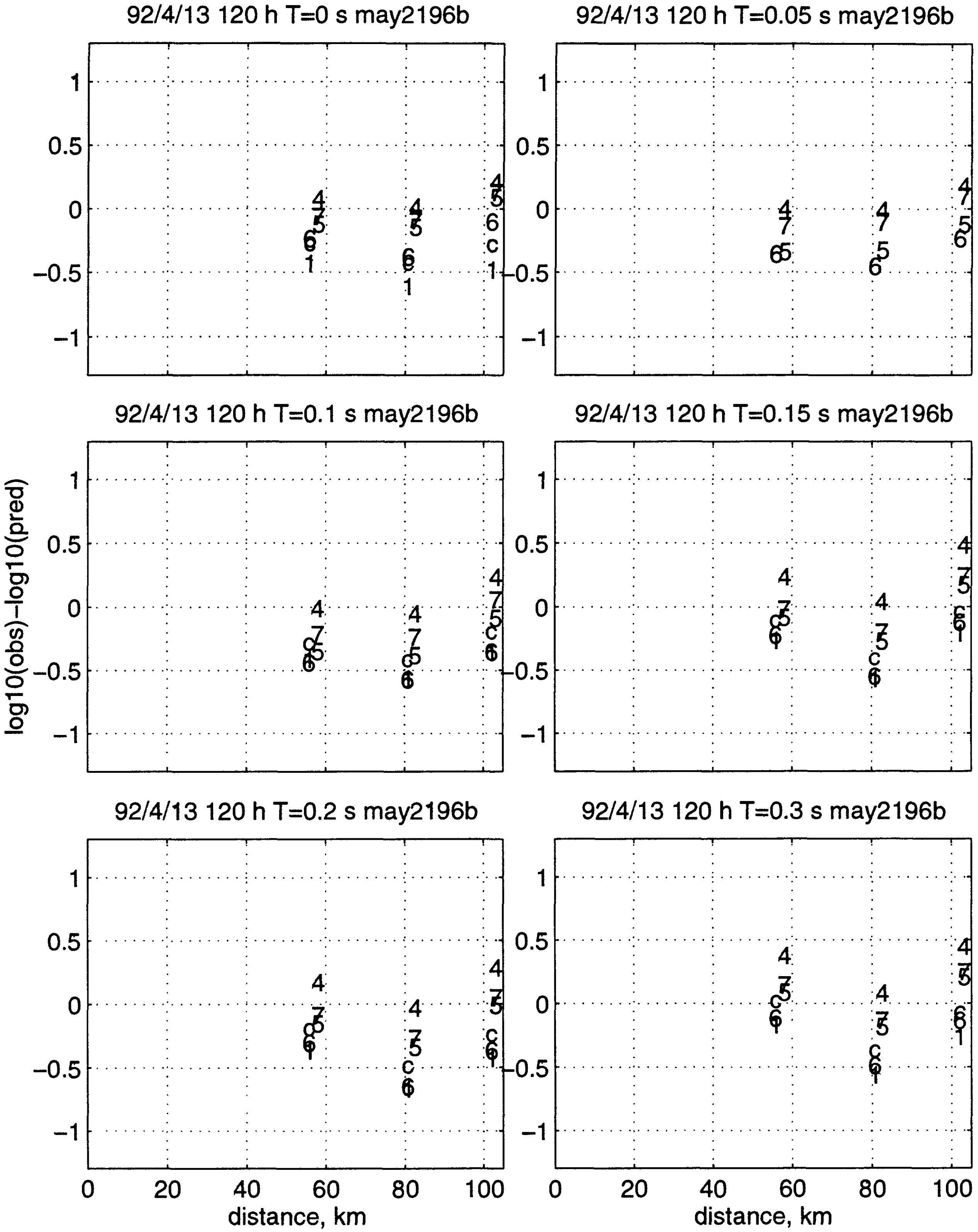

92/4/13 120 h T=0 s may2196b
92/4/13 120 h T=0.05 s may2196b
92/4/13 120 h T=0.1 s may2196b
92/4/13 120 h T=0.15 s may2196b
92/4/13 120 h T=0.2 s may2196b
92/4/13 120 h T=0.3 s may2196b
log10(obs)−log10(pred)
distance, km
distance, km

21Y

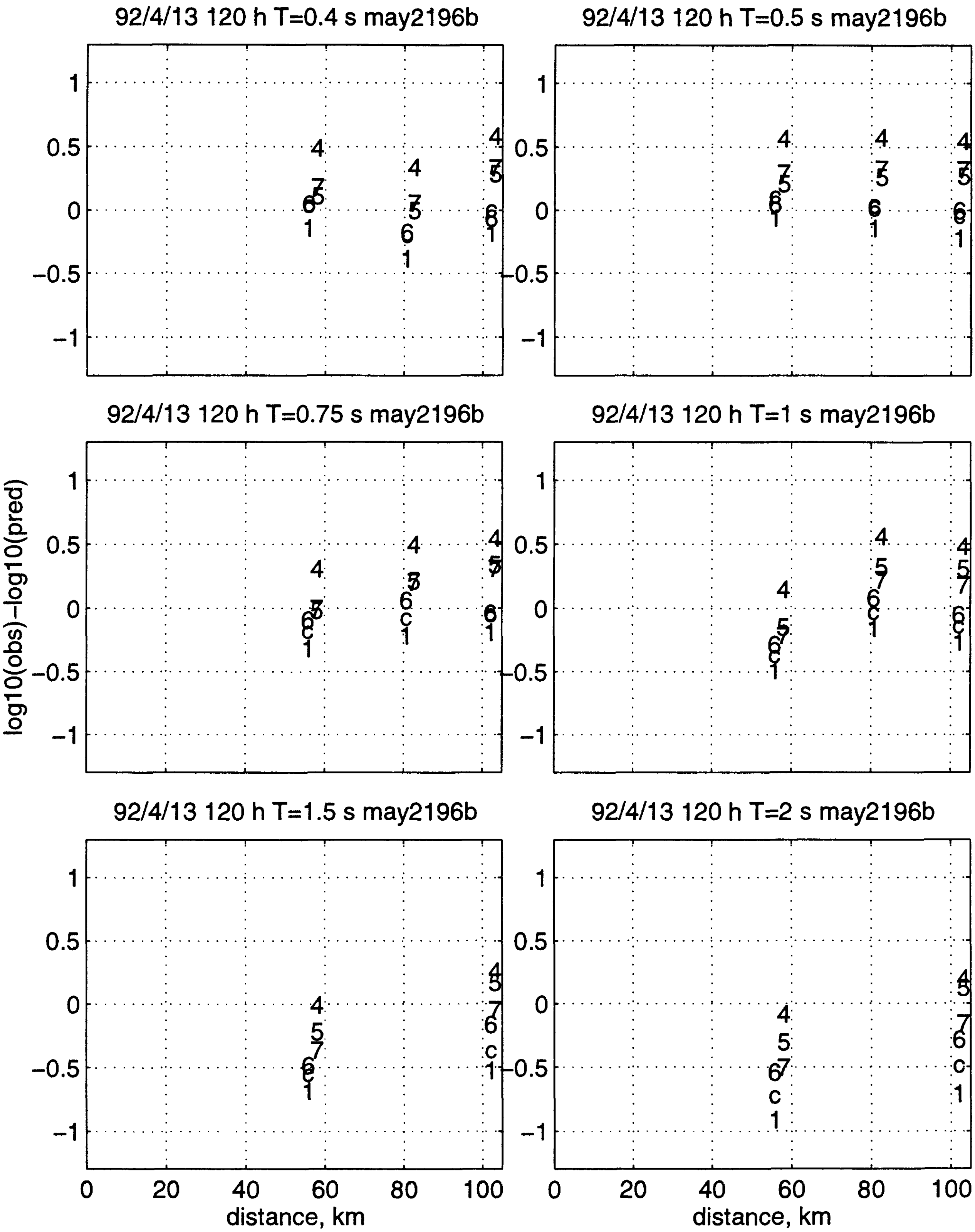
92/4/13 120 h T=0.4 s may2196b
92/4/13 120 h T=0.5 s may2196b
92/4/13 120 h T=0.75 s may2196b
92/4/13 120 h T=1 s may2196b
92/4/13 120 h T=1.5 s may2196b
92/4/13 120 h T=2 s may2196b
log10(obs)−log10(pred)
distance, km
distance, km

21 ?

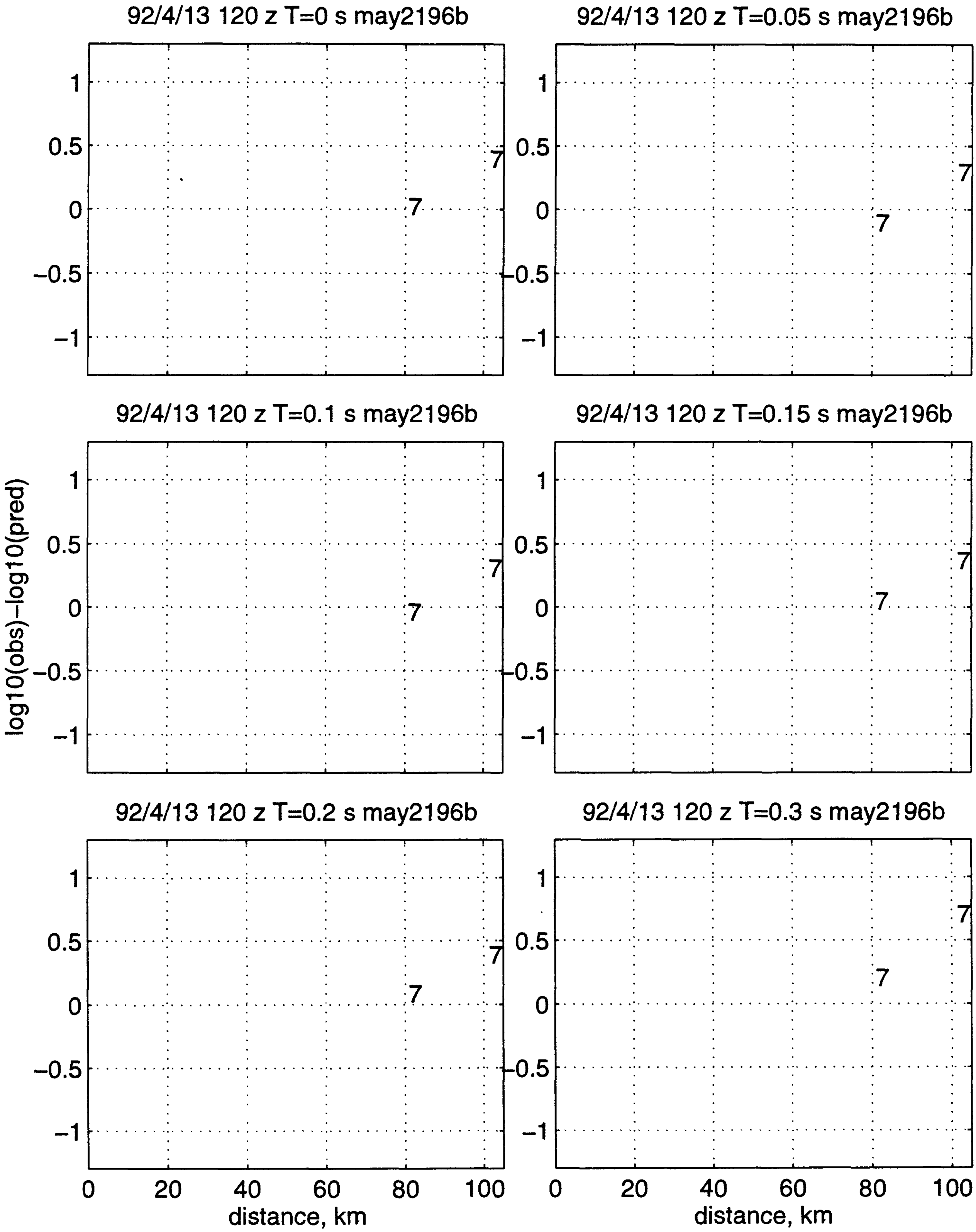
92/4/13 120 z T=0 s may2196b
92/4/13 120 z T=0.05 s may2196b
92/4/13 120 z T=0.1 s may2196b
92/4/13 120 z T=0.15 s may2196b
92/4/13 120 z T=0.2 s may2196b
92/4/13 120 z T=0.3 s may2196b
log10(obs)−log10(pred)
distance, km
distance, km
1
0.5
0
−0.5
−1
0
20
40
60
80
100
7

21aa

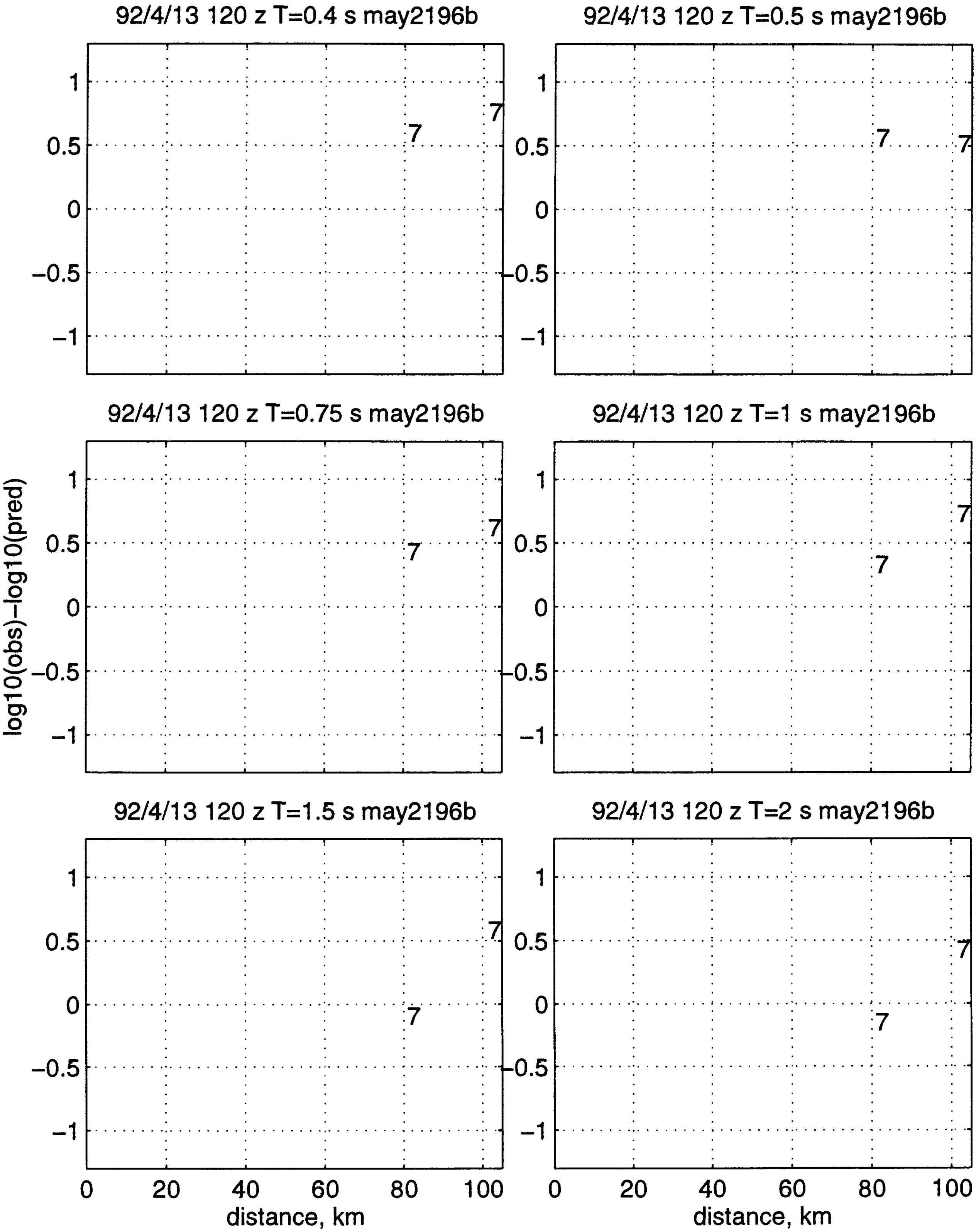
92/4/13 120 z T=0.4 s may2196b
92/4/13 120 z T=0.5 s may2196b
92/4/13 120 z T=0.75 s may2196b
92/4/13 120 z T=1 s may2196b
92/4/13 120 z T=1.5 s may2196b
92/4/13 120 z T=2 s may2196b
log10(obs)−log10(pred)
distance, km
distance, km

21 ab

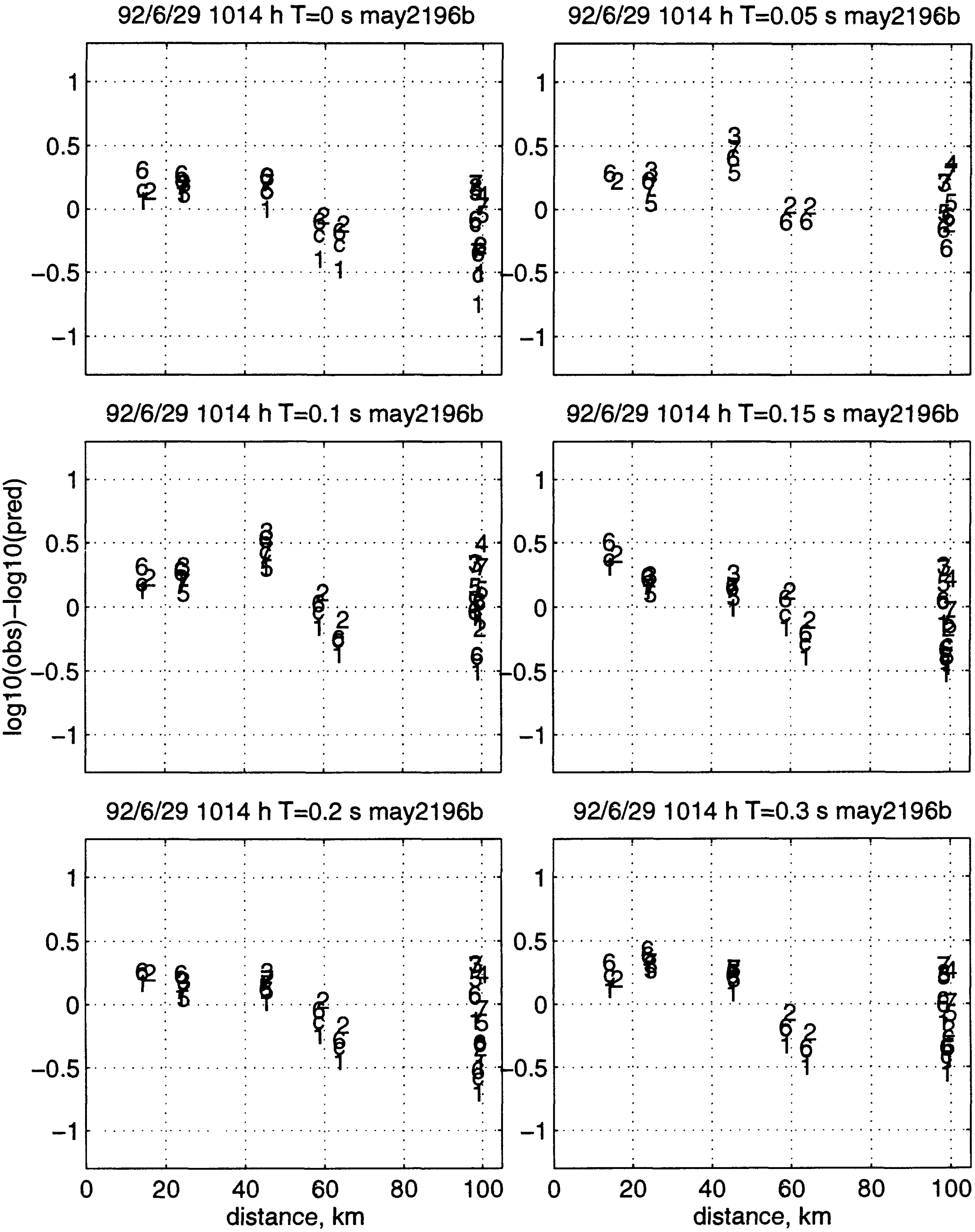
92/6/29 1014 h T=0 s may2196b
92/6/29 1014 h T=0.05 s may2196b
92/6/29 1014 h T=0.1 s may2196b
92/6/29 1014 h T=0.15 s may2196b
92/6/29 1014 h T=0.2 s may2196b
92/6/29 1014 h T=0.3 s may2196b
log10(obs)−log10(pred)
distance, km
distance, km

21 ac

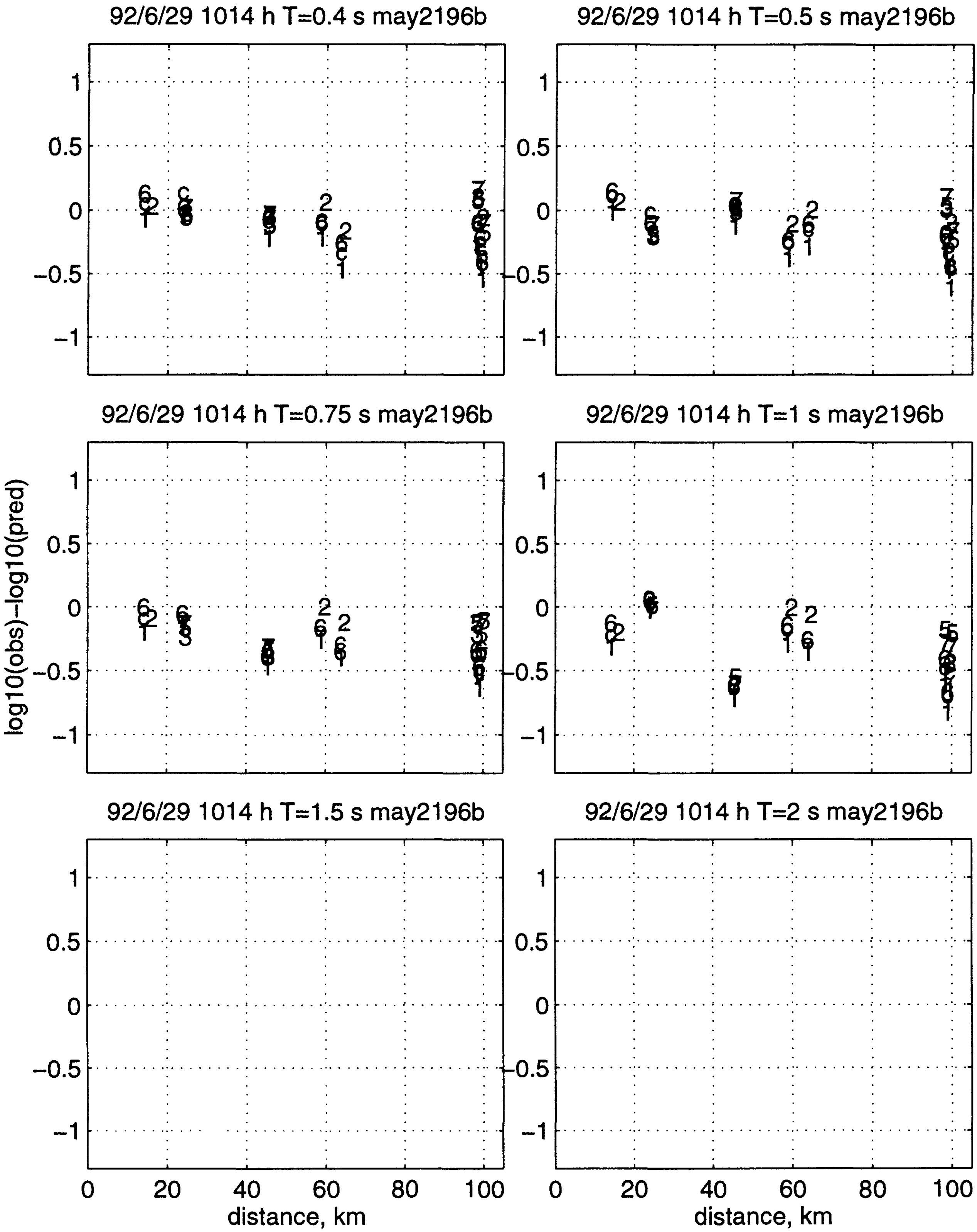
92/6/29 1014 h T=0.4 s may2196b
92/6/29 1014 h T=0.5 s may2196b
92/6/29 1014 h T=0.75 s may2196b
92/6/29 1014 h T=1 s may2196b
92/6/29 1014 h T=1.5 s may2196b
92/6/29 1014 h T=2 s may2196b
log10(obs)−log10(pred)
distance, km
distance, km

21 ad

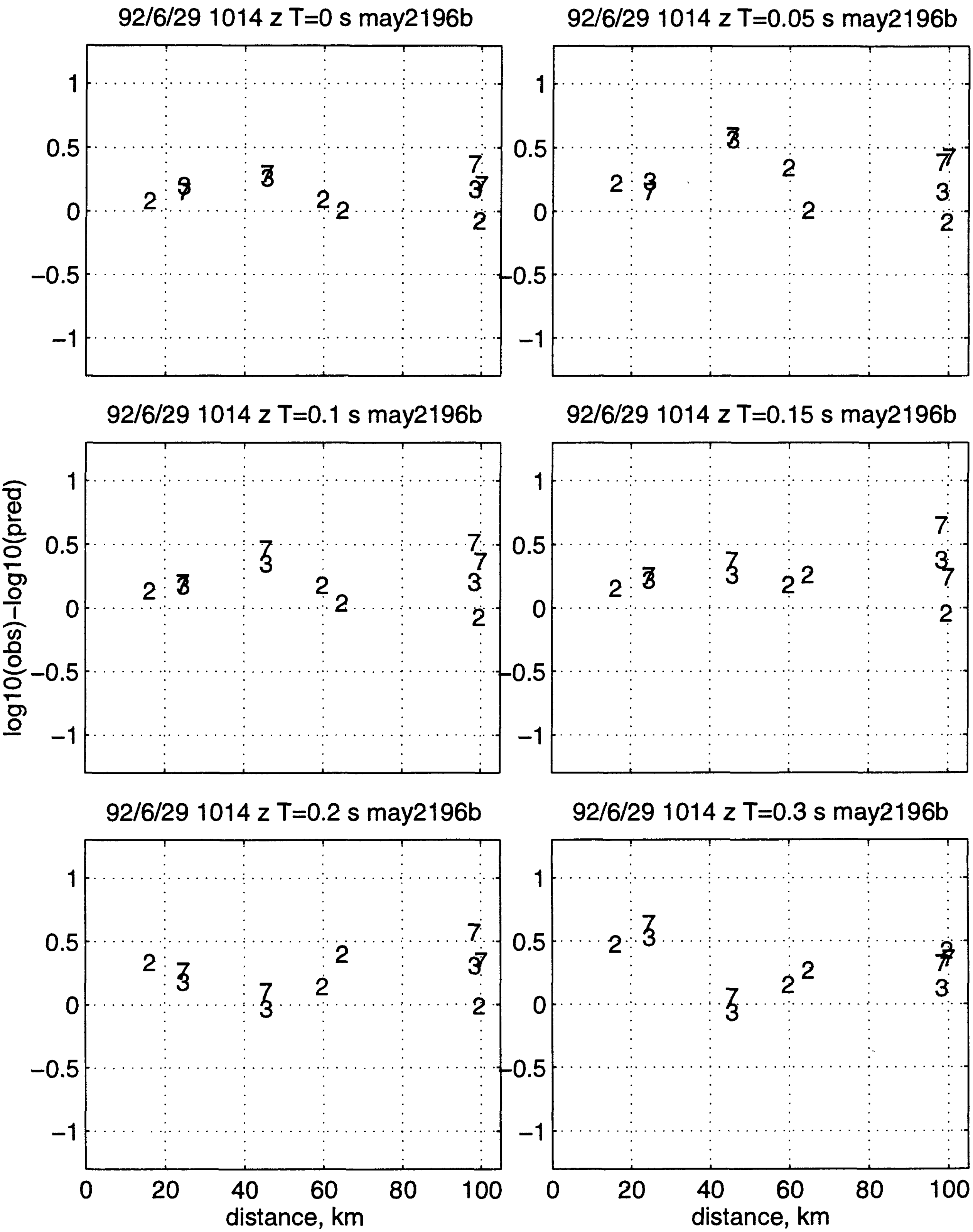
92/6/29 1014 z T=0 s may2196b
92/6/29 1014 z T=0.05 s may2196b
92/6/29 1014 z T=0.1 s may2196b
92/6/29 1014 z T=0.15 s may2196b
92/6/29 1014 z T=0.2 s may2196b
92/6/29 1014 z T=0.3 s may2196b
log10(obs)−log10(pred)
distance, km
distance, km

21ae

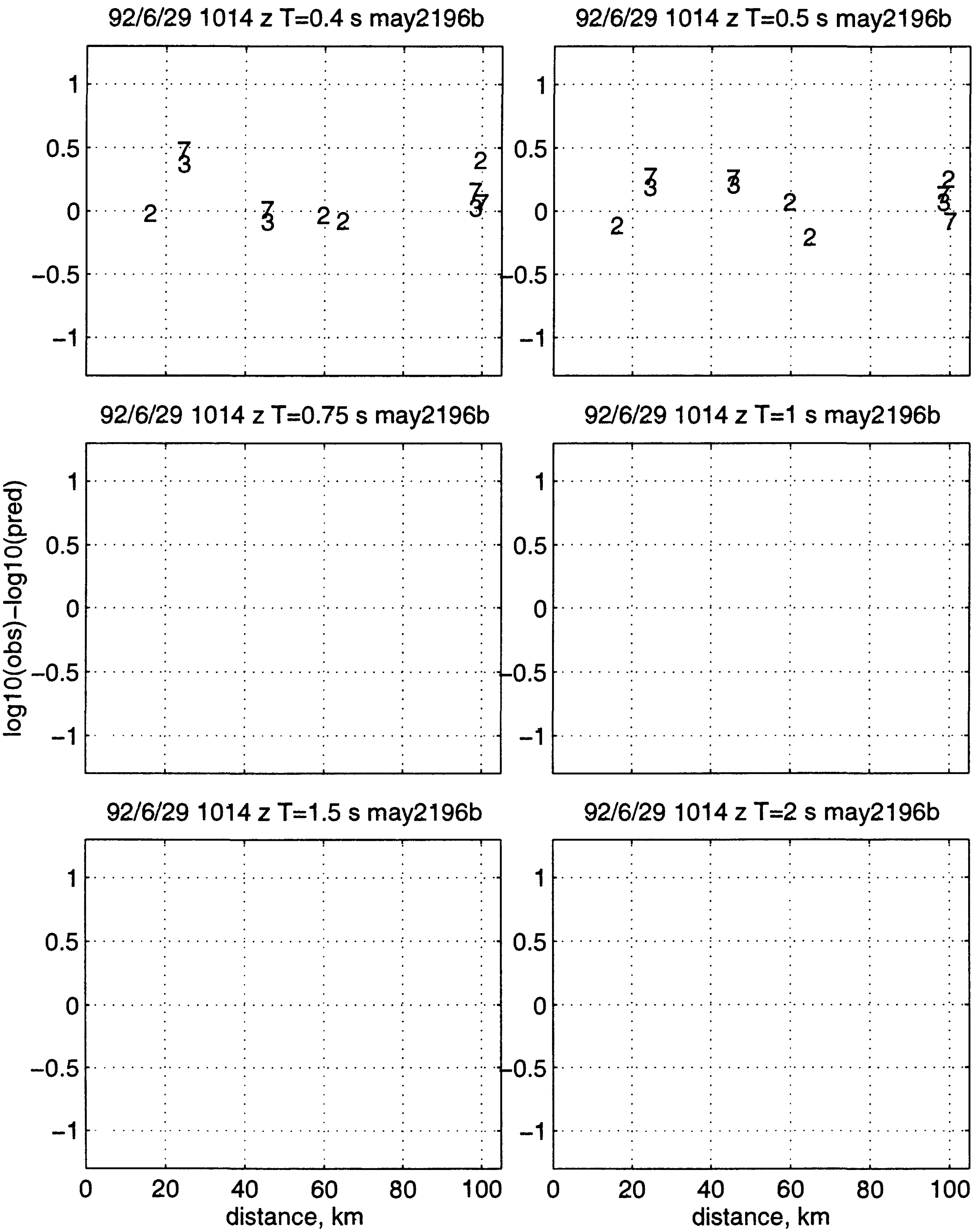
92/6/29 1014 z T=0.4 s may2196b
92/6/29 1014 z T=0.5 s may2196b
92/6/29 1014 z T=0.75 s may2196b
92/6/29 1014 z T=1 s may2196b
92/6/29 1014 z T=1.5 s may2196b
92/6/29 1014 z T=2 s may2196b
log10(obs)−log10(pred)
distance, km
distance, km

21af

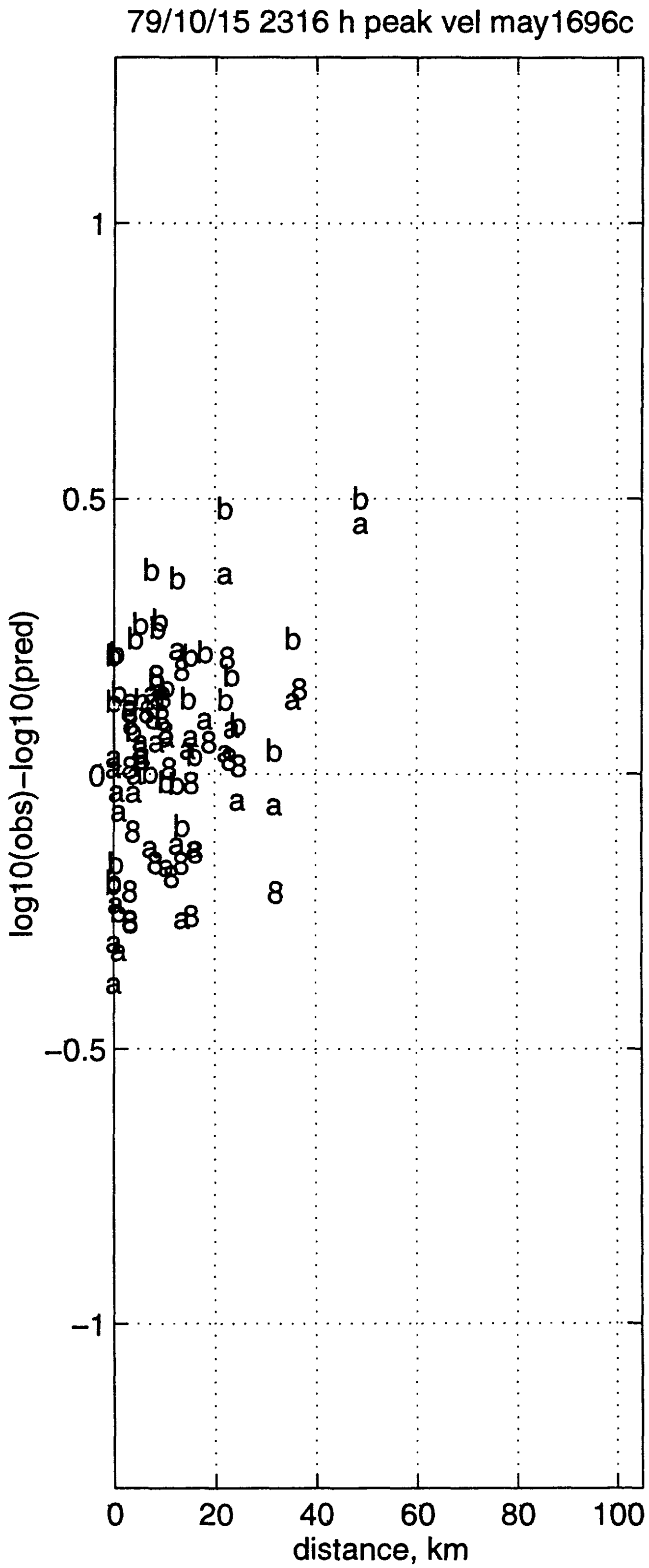
79/10/15 2316 h peak vel may1696c
log10(obs)−log10(pred)
distance, km
1
0.5
0
−0.5
−1
0
20
40
60
80
100

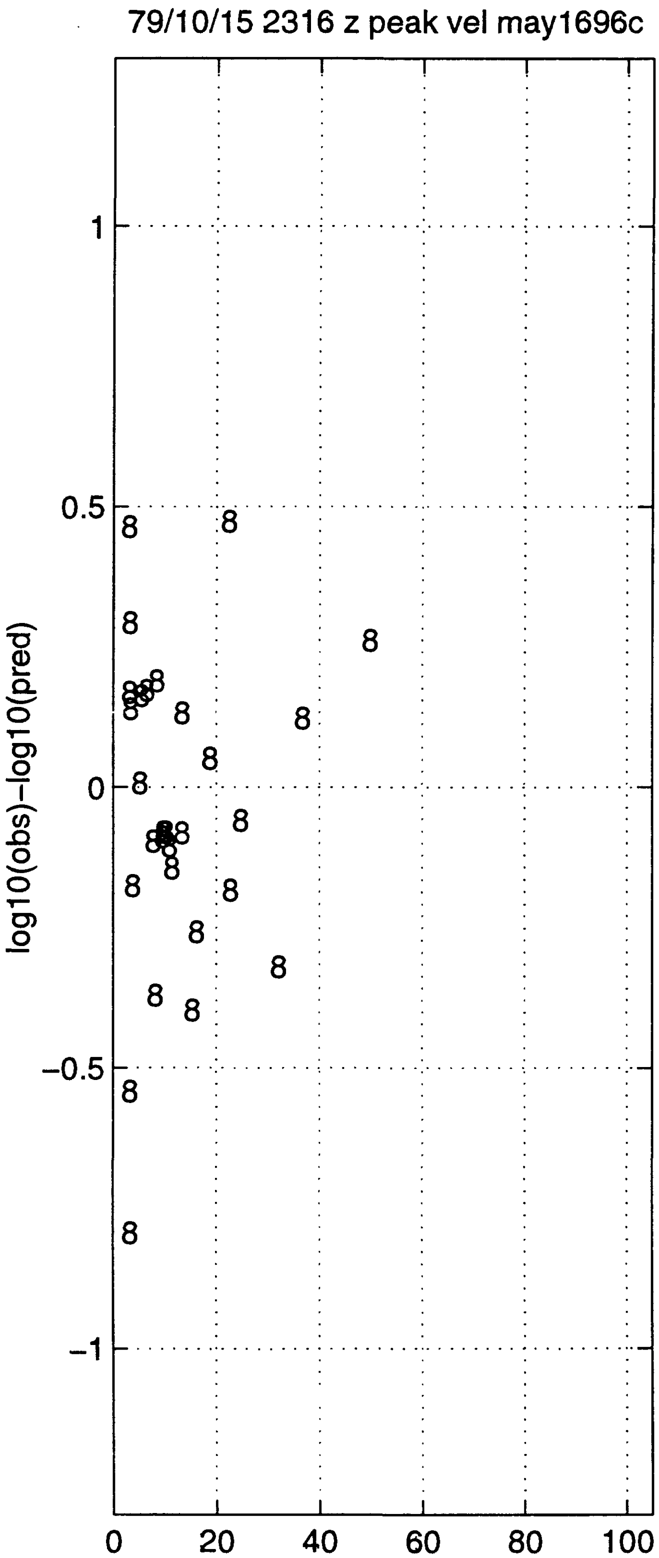

79/10/15 2316 z peak vel may1696c
log10(obs)−log10(pred)
1
0.5
0
−0.5
−1
0
20
40
60
80
100
distance, km

22 b

80/11/23 1834 h peak vel may1696c

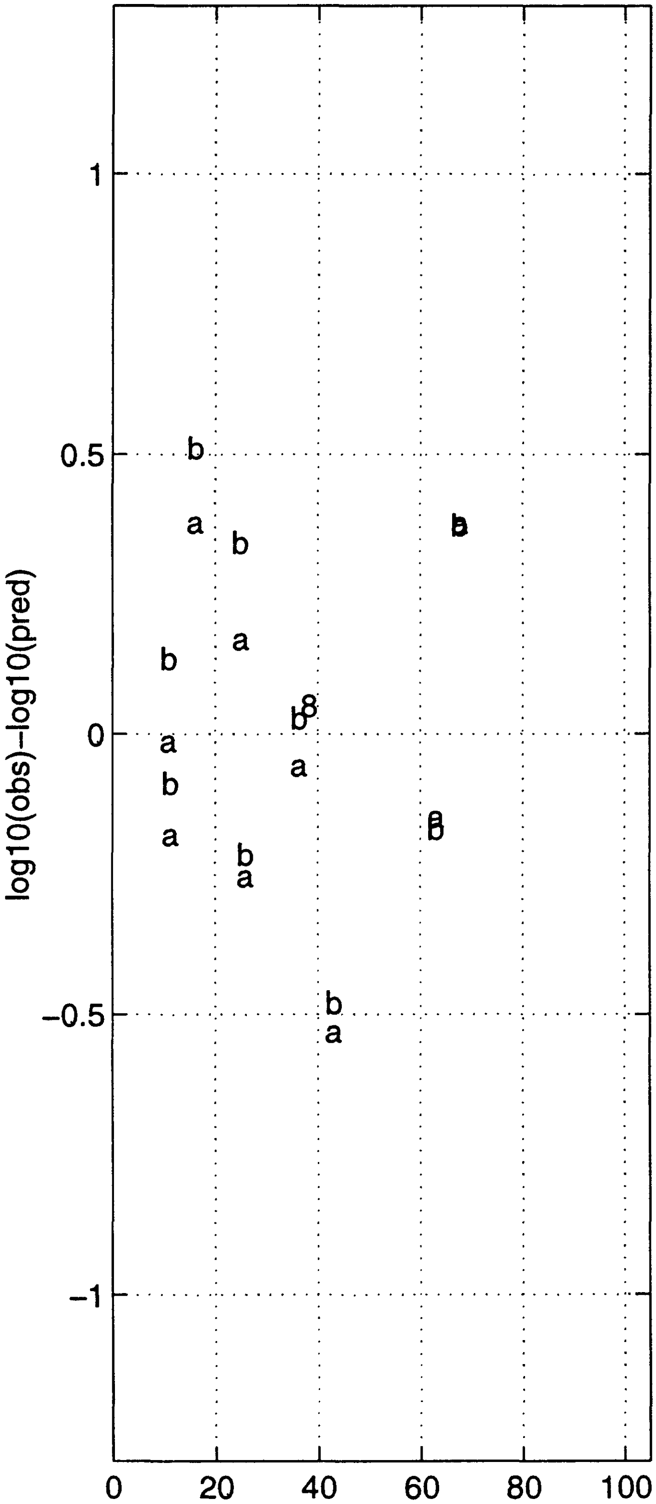

22c

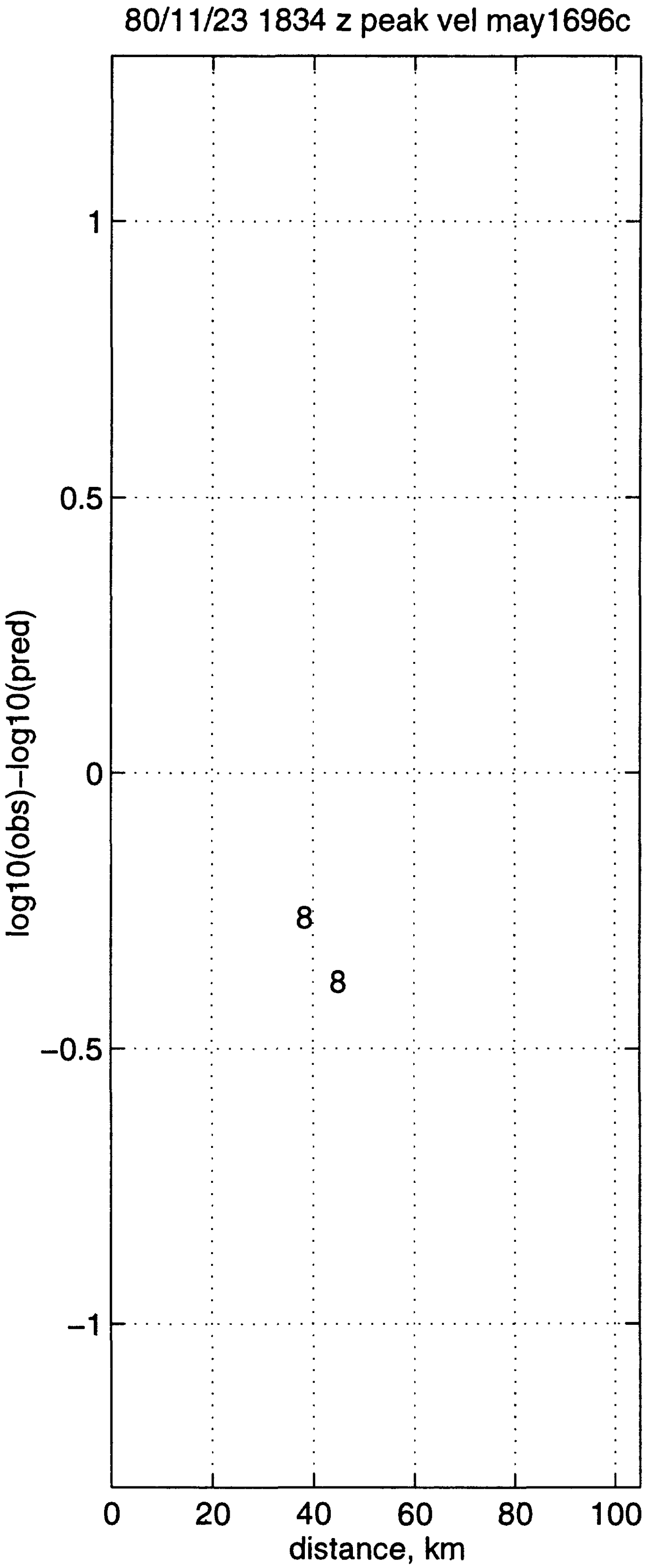
80/11/23 1834 z peak vel may1696c
log10(obs)−log10(pred)
1
0.5
0
−0.5
−1
8
8
0
20
40
60
80
100
distance, km

22 d

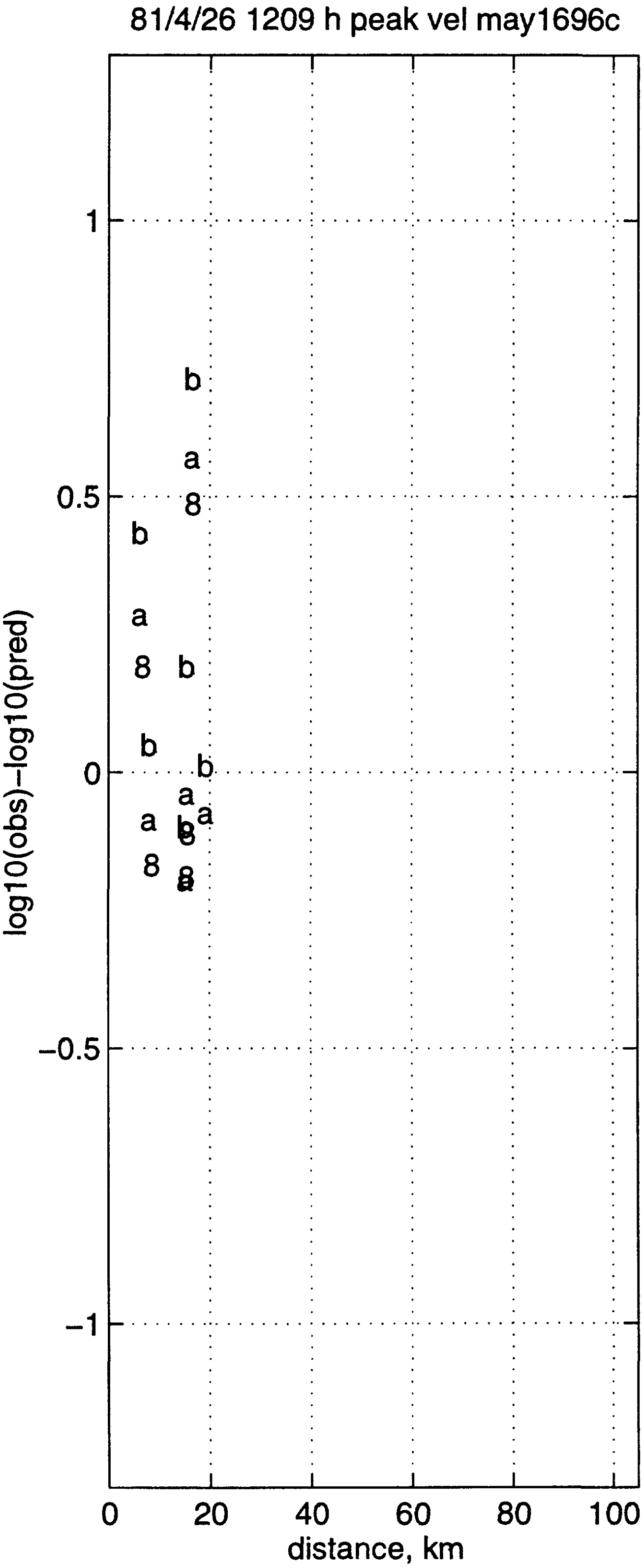

81/4/26 1209 h peak vel may1696c
log10(obs)−log10(pred)
distance, km

22e

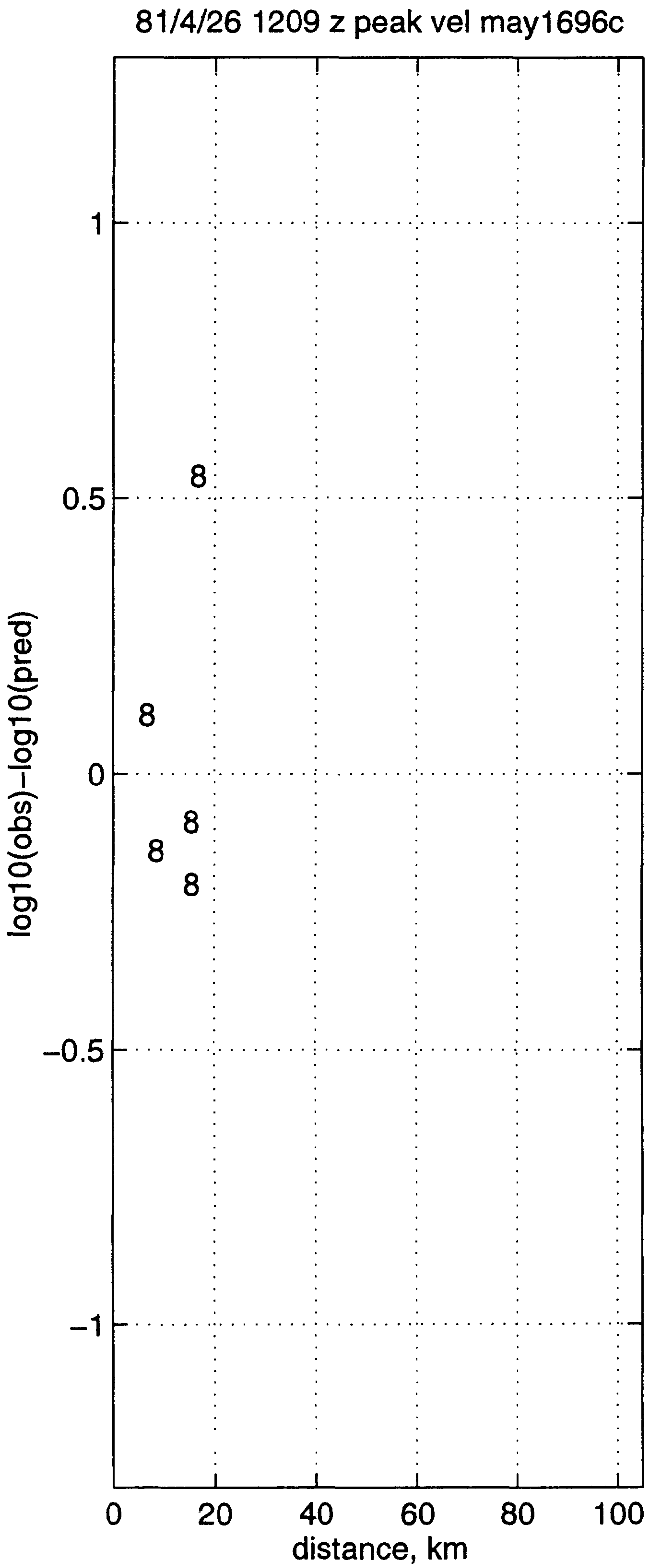
81/4/26 1209 z peak vel may1696c
log10(obs)−log10(pred)
distance, km
1
0.5
0
−0.5
−1
0
20
40
60
80
100
8
8
8
8
8

22f

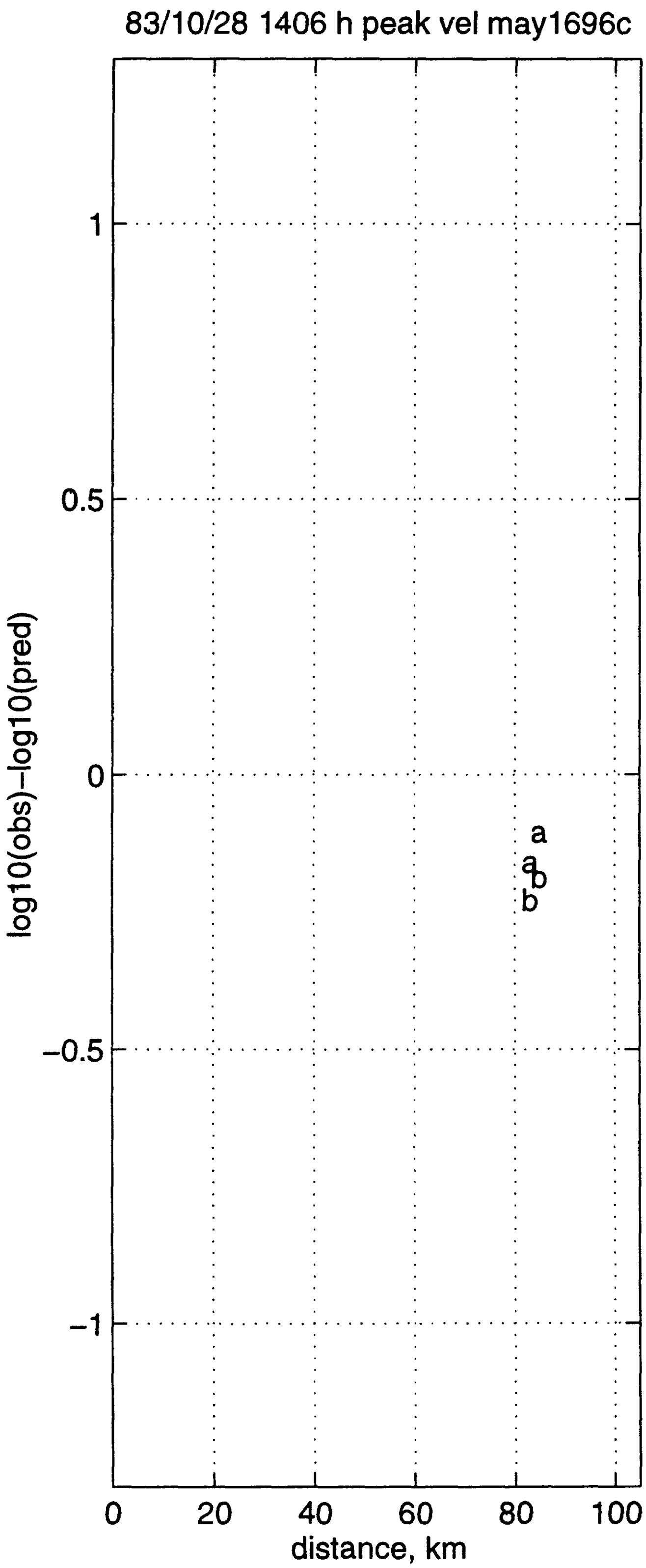
83/10/28 1406 h peak vel may1696c
log10(obs)−log10(pred)
distance, km
1
0.5
0
−0.5
−1
0
20
40
60
80
100
a
a
b
b

22g

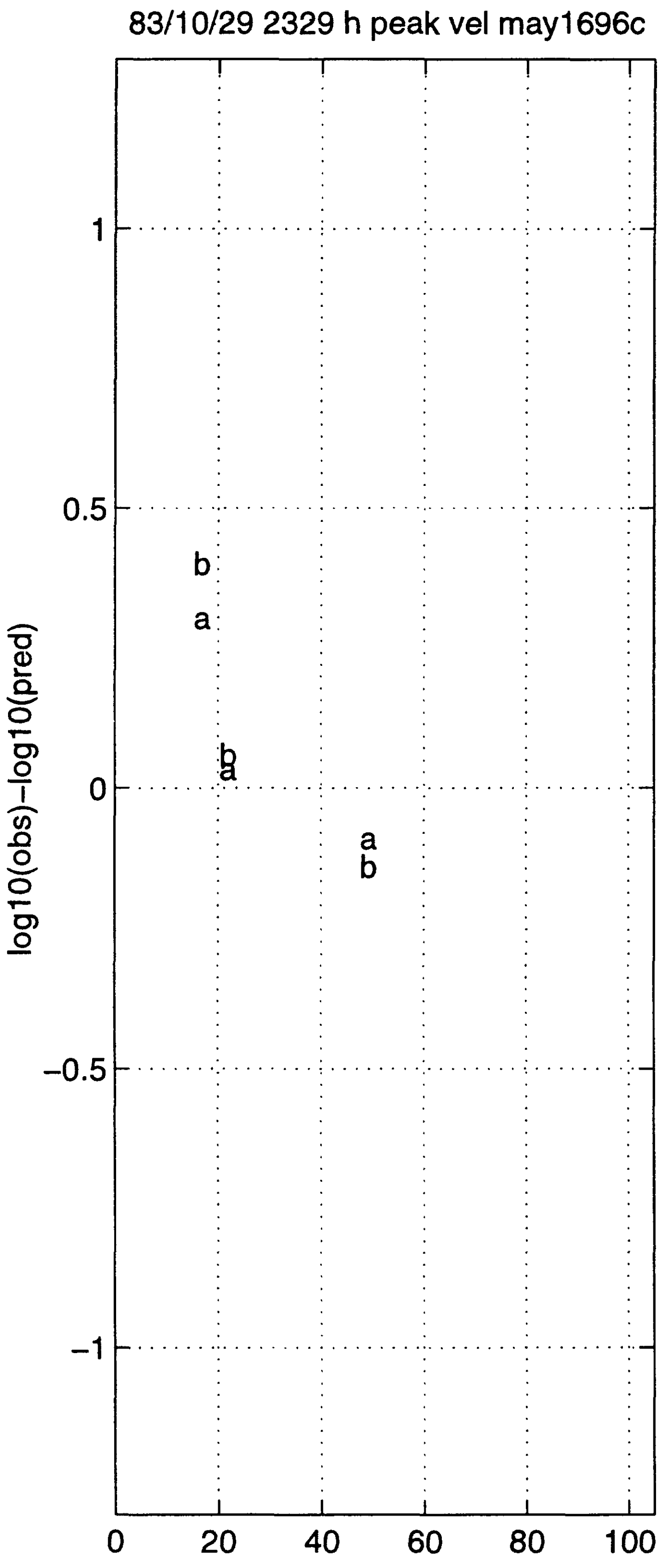
83/10/29 2329 h peak vel may1696c
log10(obs)−log10(pred)
1
0.5
0
−0.5
−1
b
a
b
a
a
b
0
20
40
60
80
100
distance, km

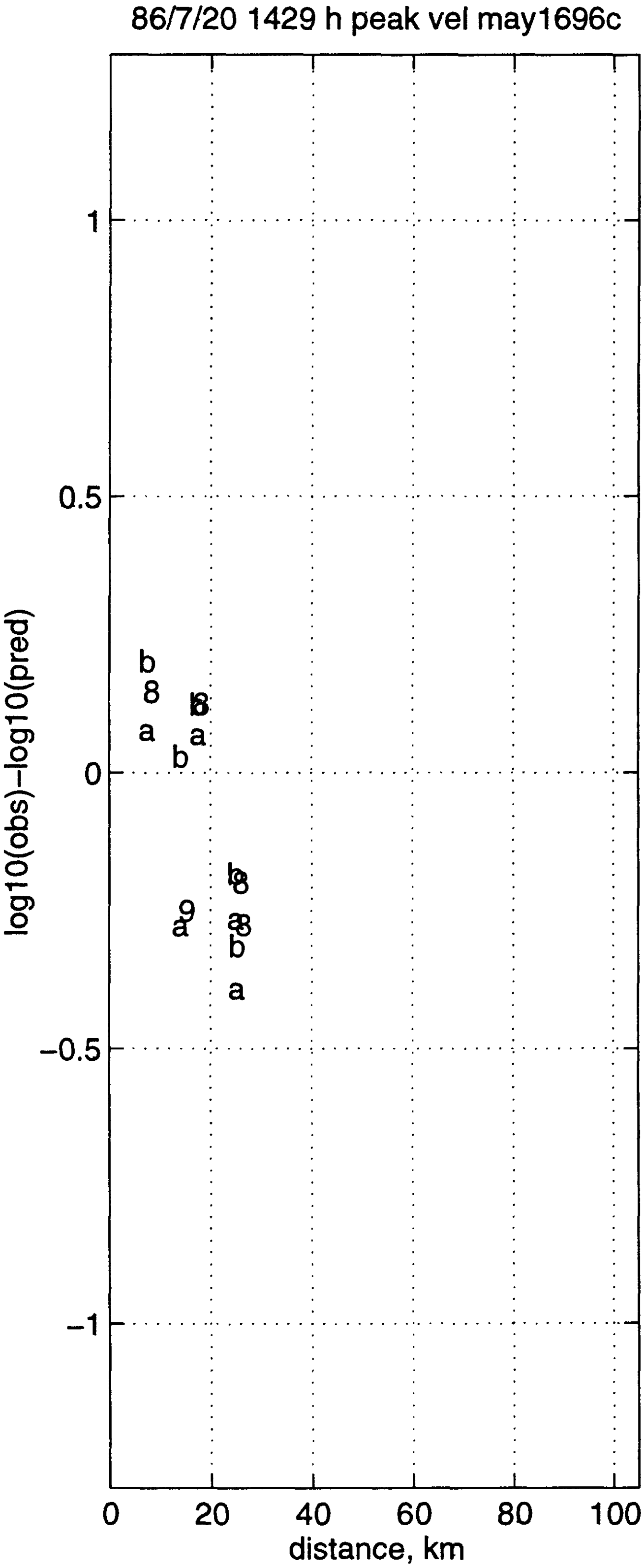
86/7/20 1429 h peak vel may1696c
log10(obs)−log10(pred)
distance, km
1
0.5
0
−0.5
−1
0
20
40
60
80
100

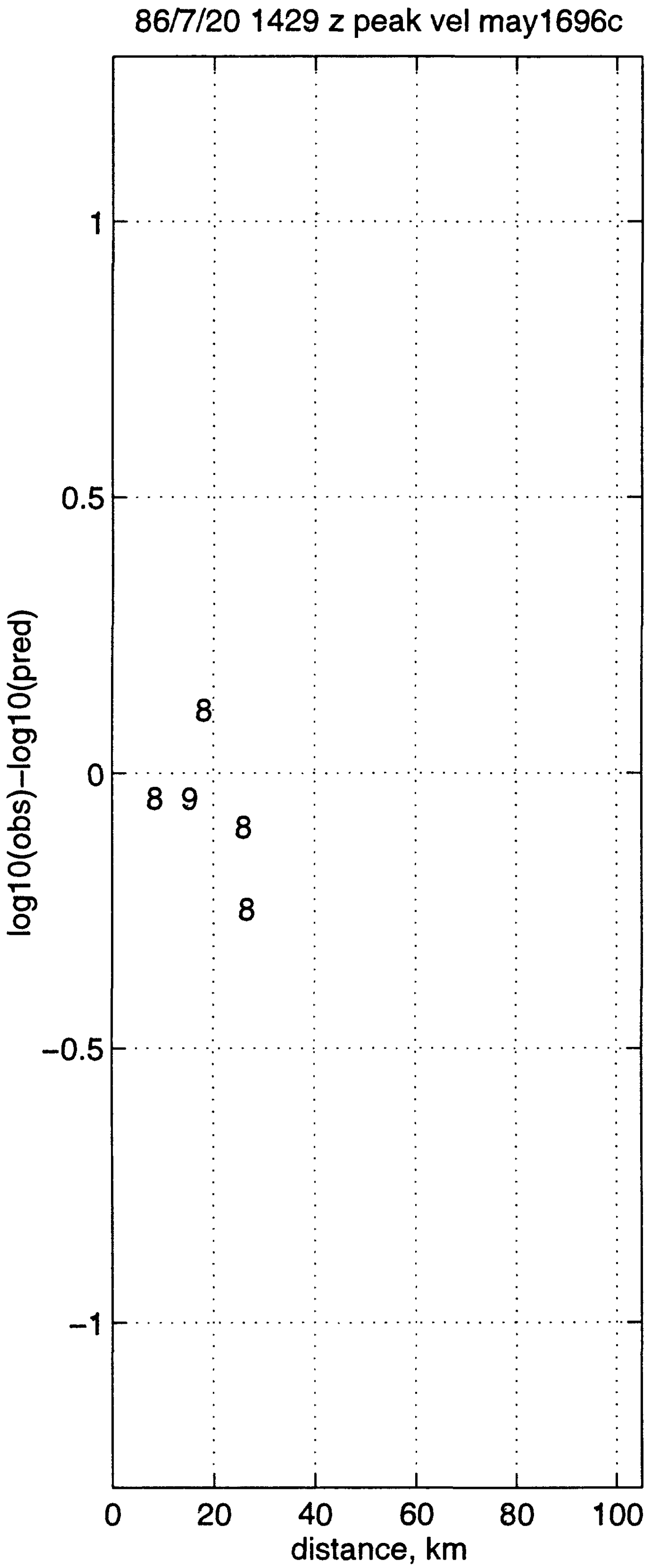
86/7/20 1429 z peak vel may1696c
log10(obs)−log10(pred)
distance, km
1
0.5
0
−0.5
−1
0
20
40
60
80
100
8
8
9
8
8

22j

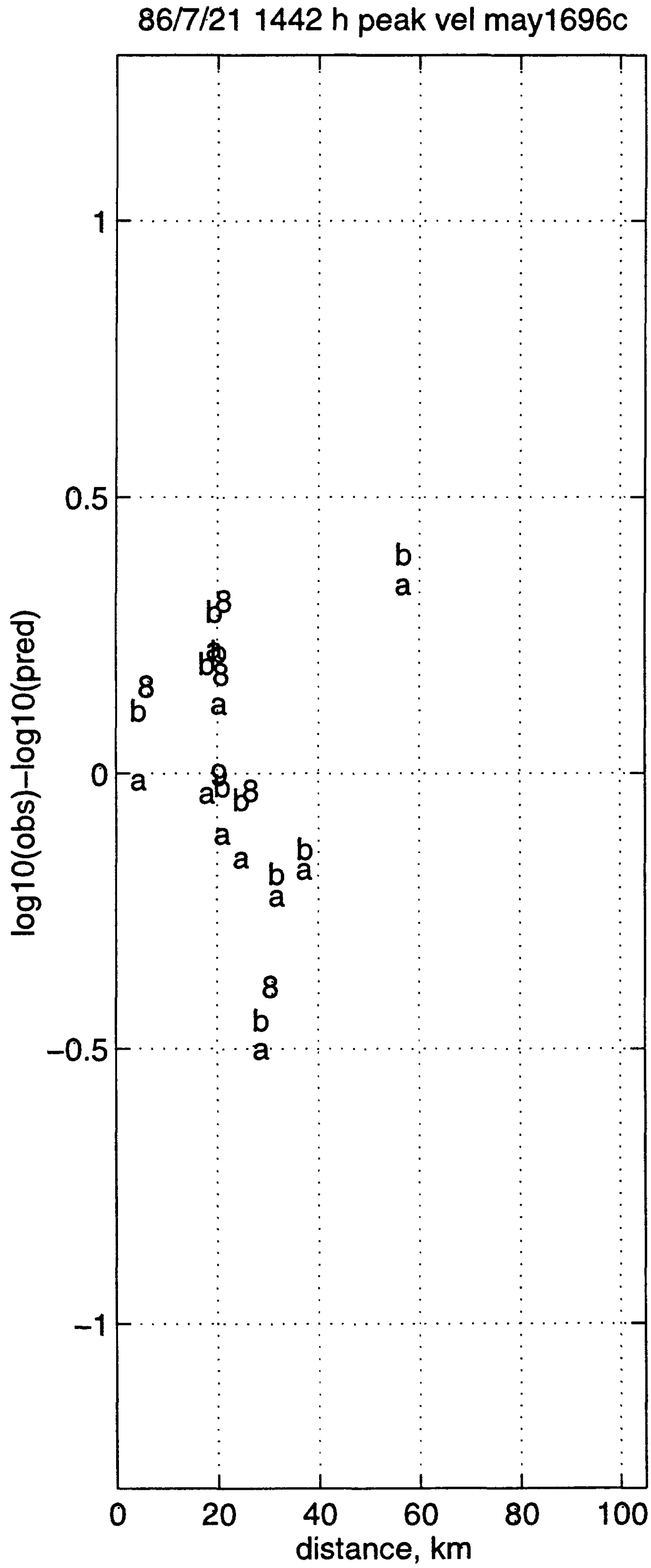

86/7/21 1442 h peak vel may1696c
log10(obs)−log10(pred)
distance, km
1
0.5
0
−0.5
−1
0
20
40
60
80
100

22k

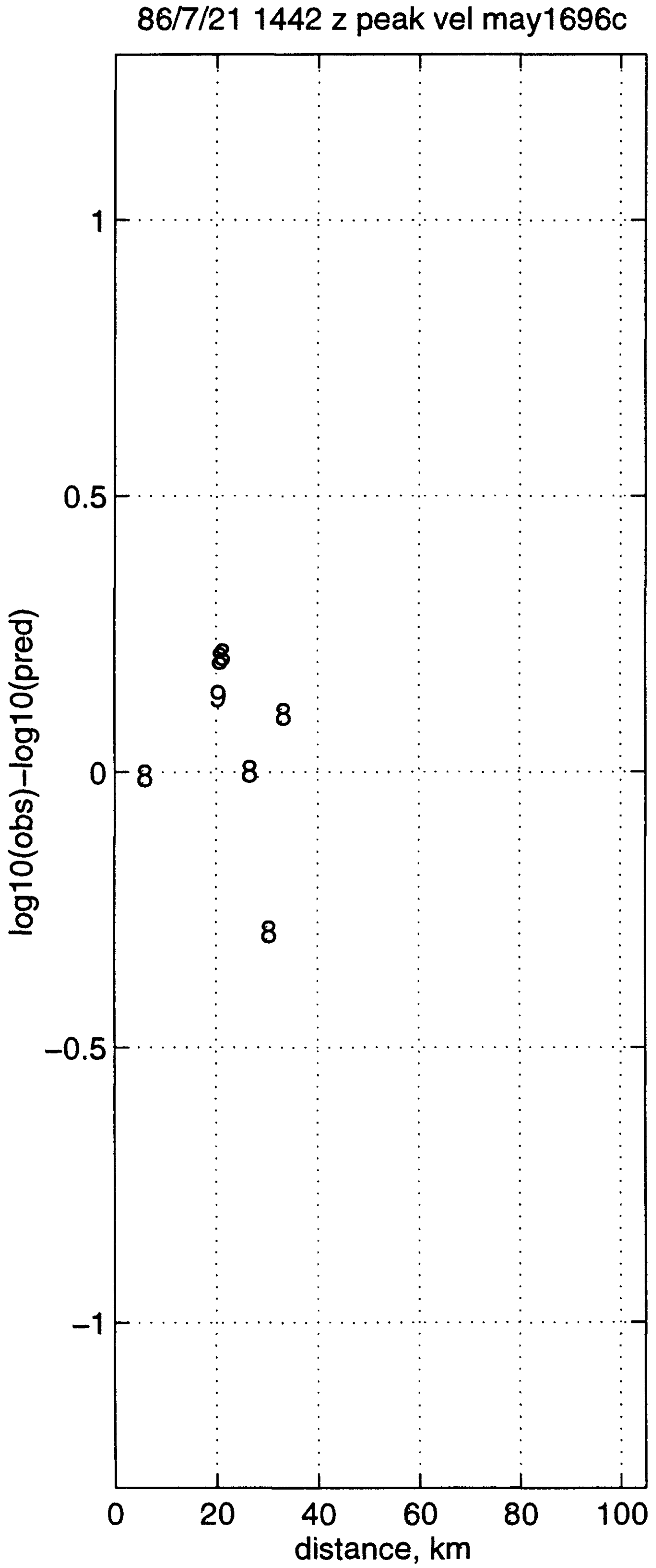
86/7/21 1442 z peak vel may1696c
log10(obs)−log10(pred)
distance, km
1
0.5
0
−0.5
−1
0
20
40
60
80
100
8
9
8
8
8
8

326

22 l

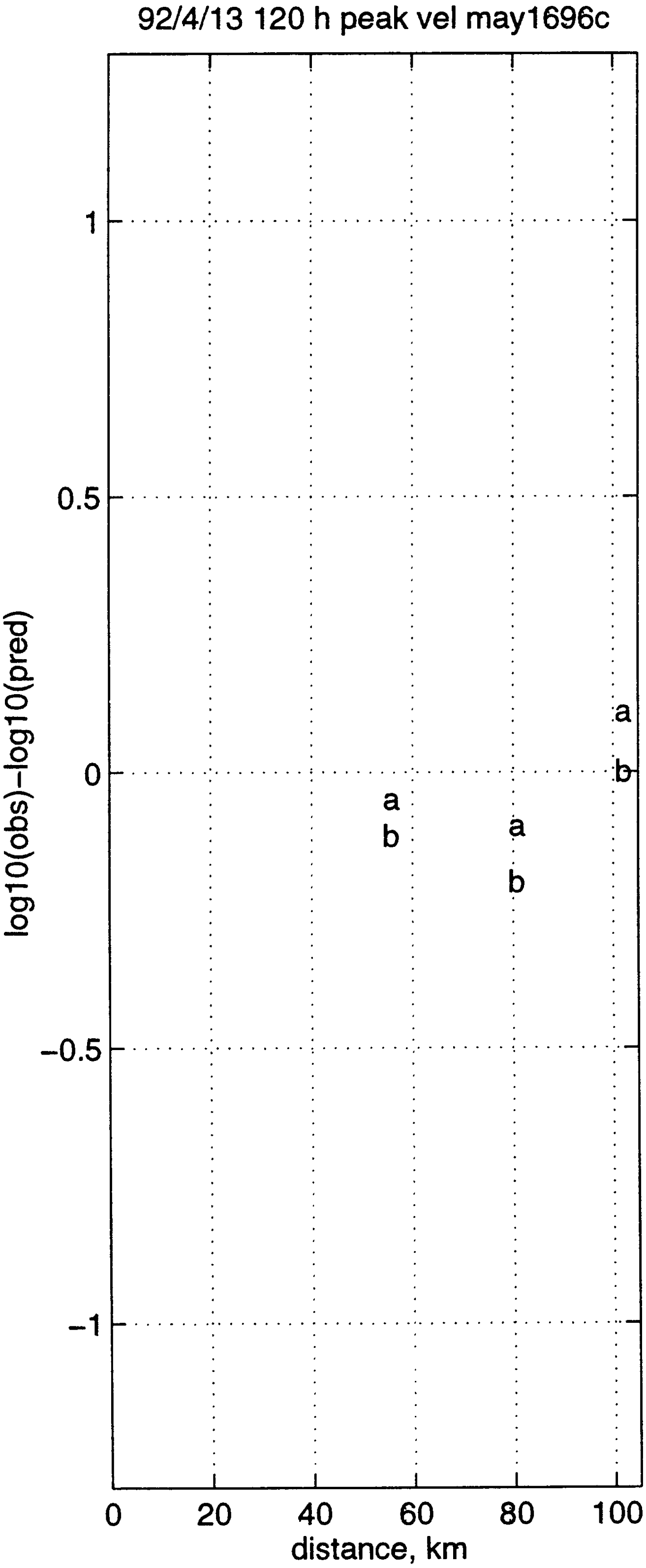
92/4/13 120 h peak vel may1696c
log10(obs)−log10(pred)
1
0.5
0
−0.5
−1
0
20
40
60
80
100
distance, km
a
b
a
b
a
b

22 m

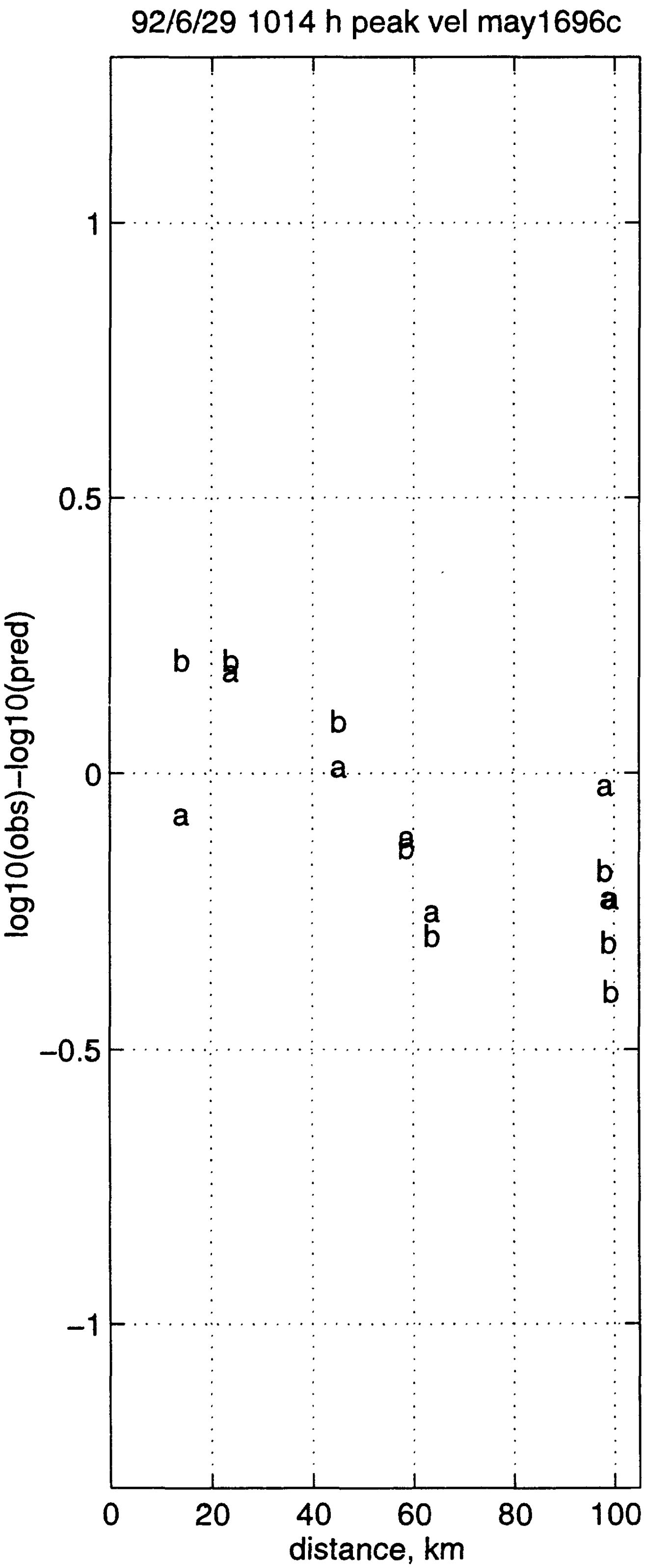
92/6/29 1014 h peak vel may1696c
log10(obs)−log10(pred)
distance, km
1
0.5
0
−0.5
−1
0
20
40
60
80
100
a
b

22n

92/6/29 1014 z peak vel may1696c

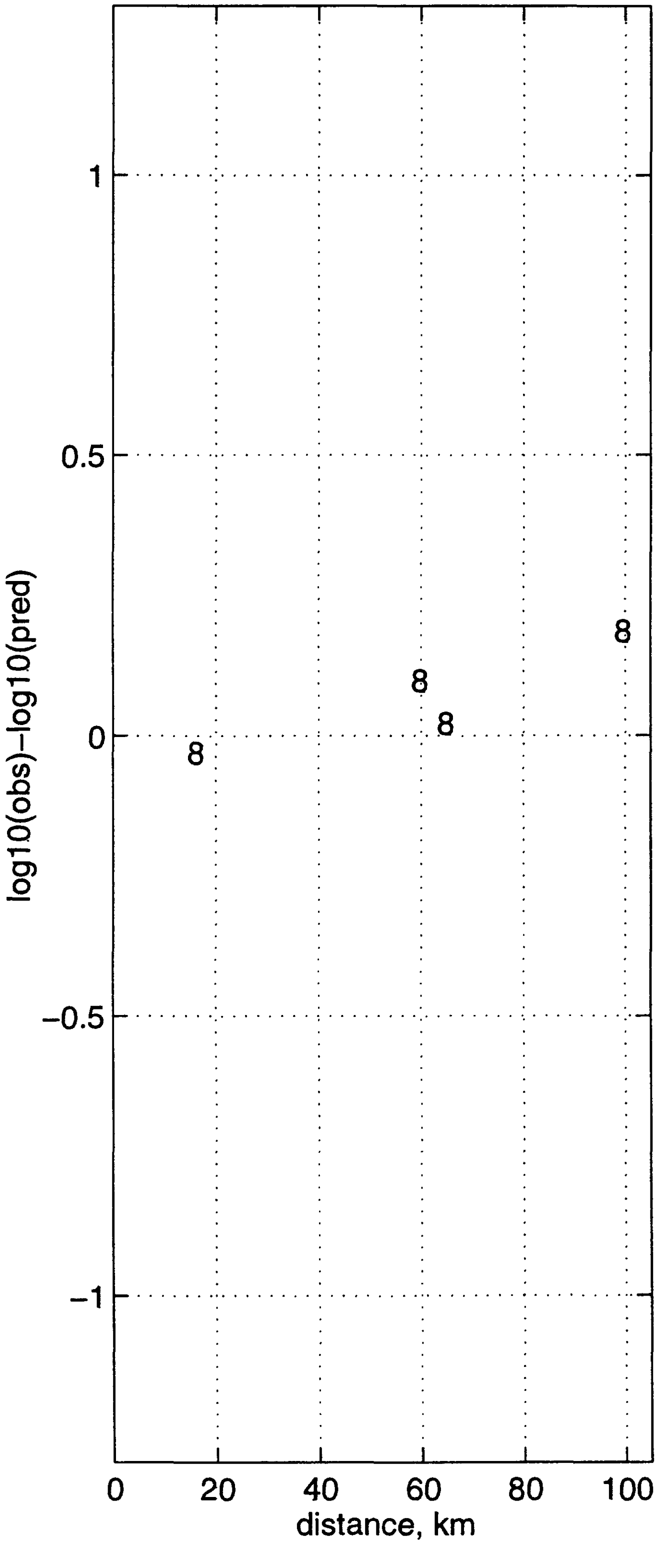

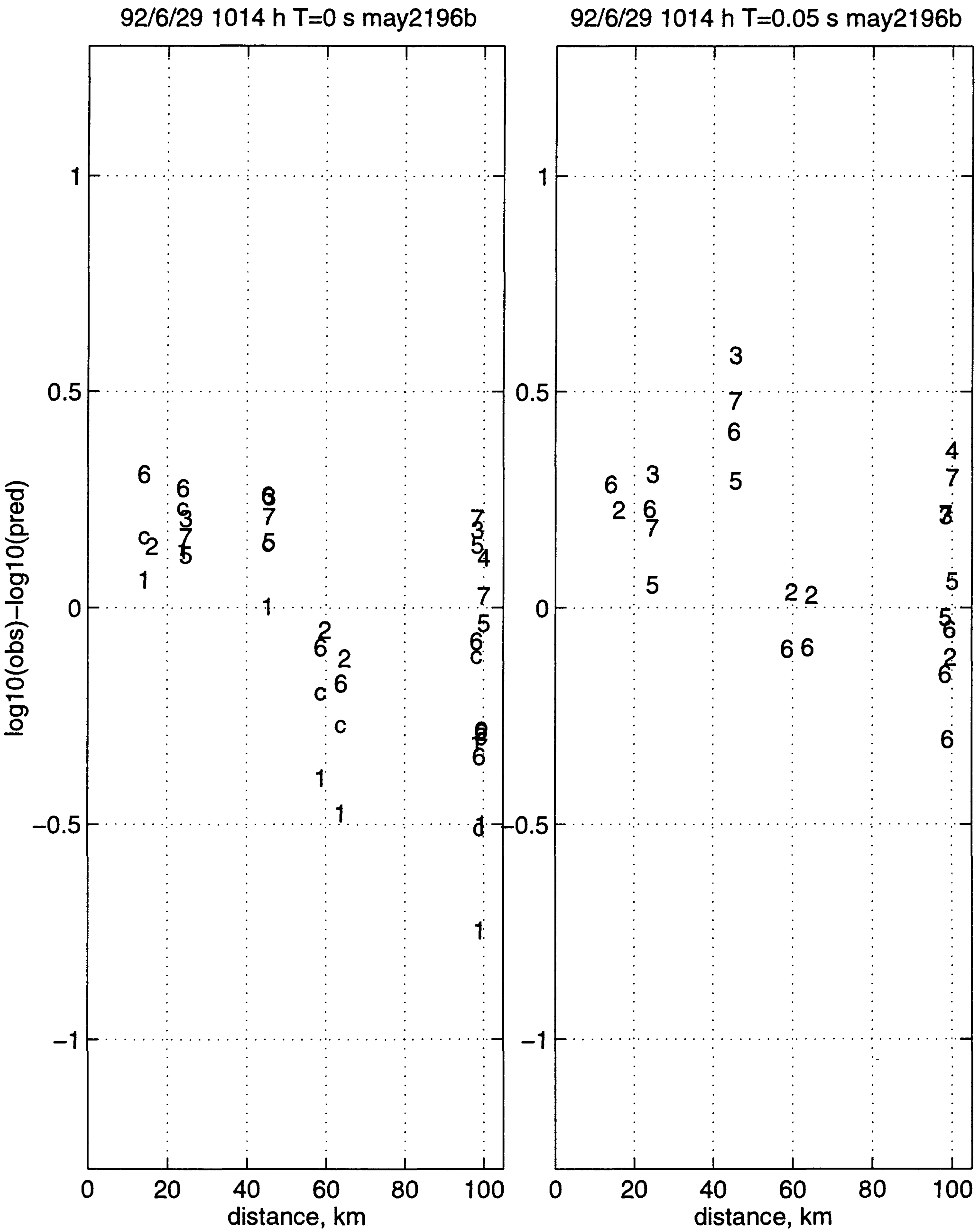
92/6/29 1014 h T=0 s may2196b
92/6/29 1014 h T=0.05 s may2196b
log10(obs)−log10(pred)
distance, km
distance, km

330

23a

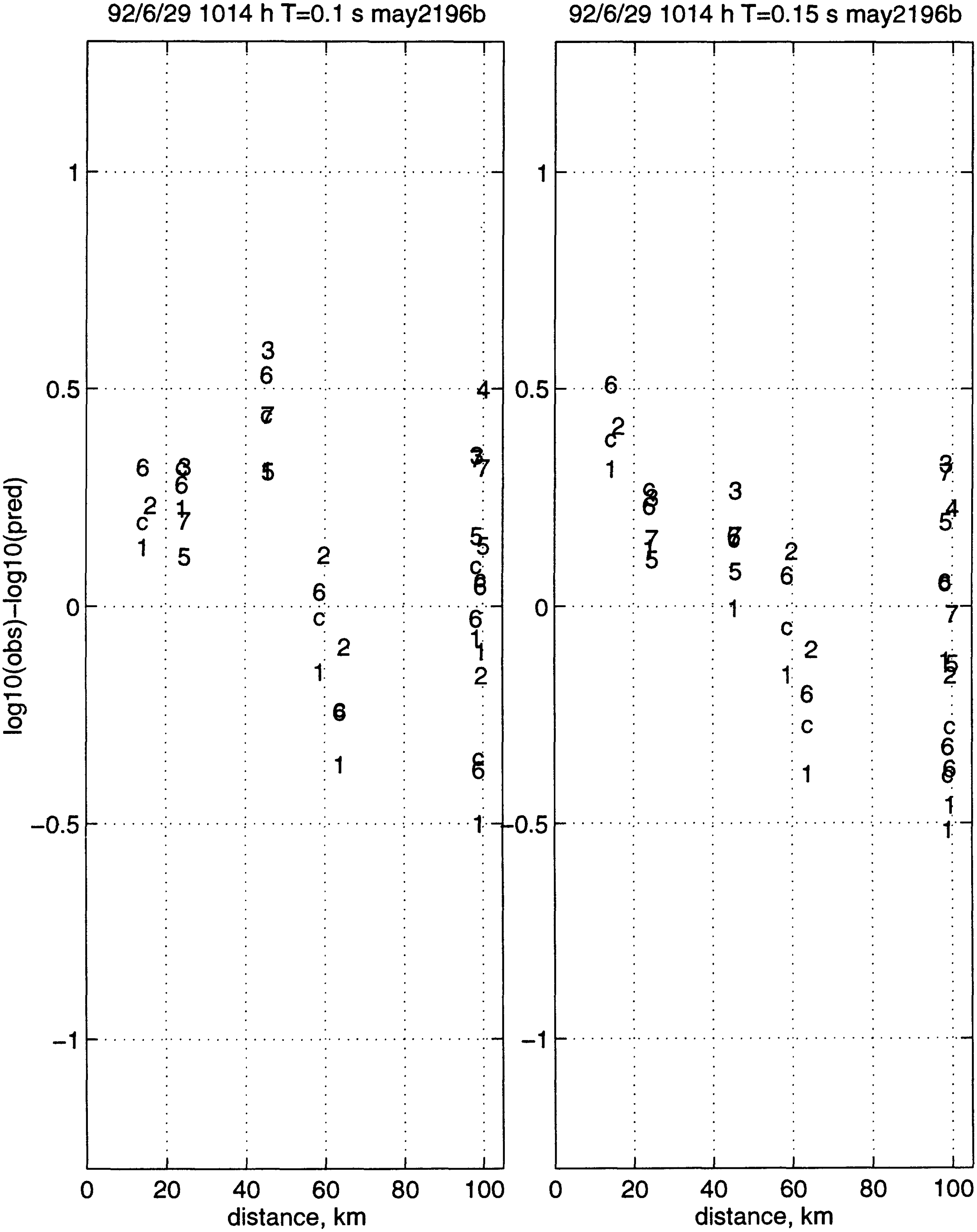
92/6/29 1014 h T=0.1 s may2196b
92/6/29 1014 h T=0.15 s may2196b
log10(obs)−log10(pred)
distance, km
distance, km

23b

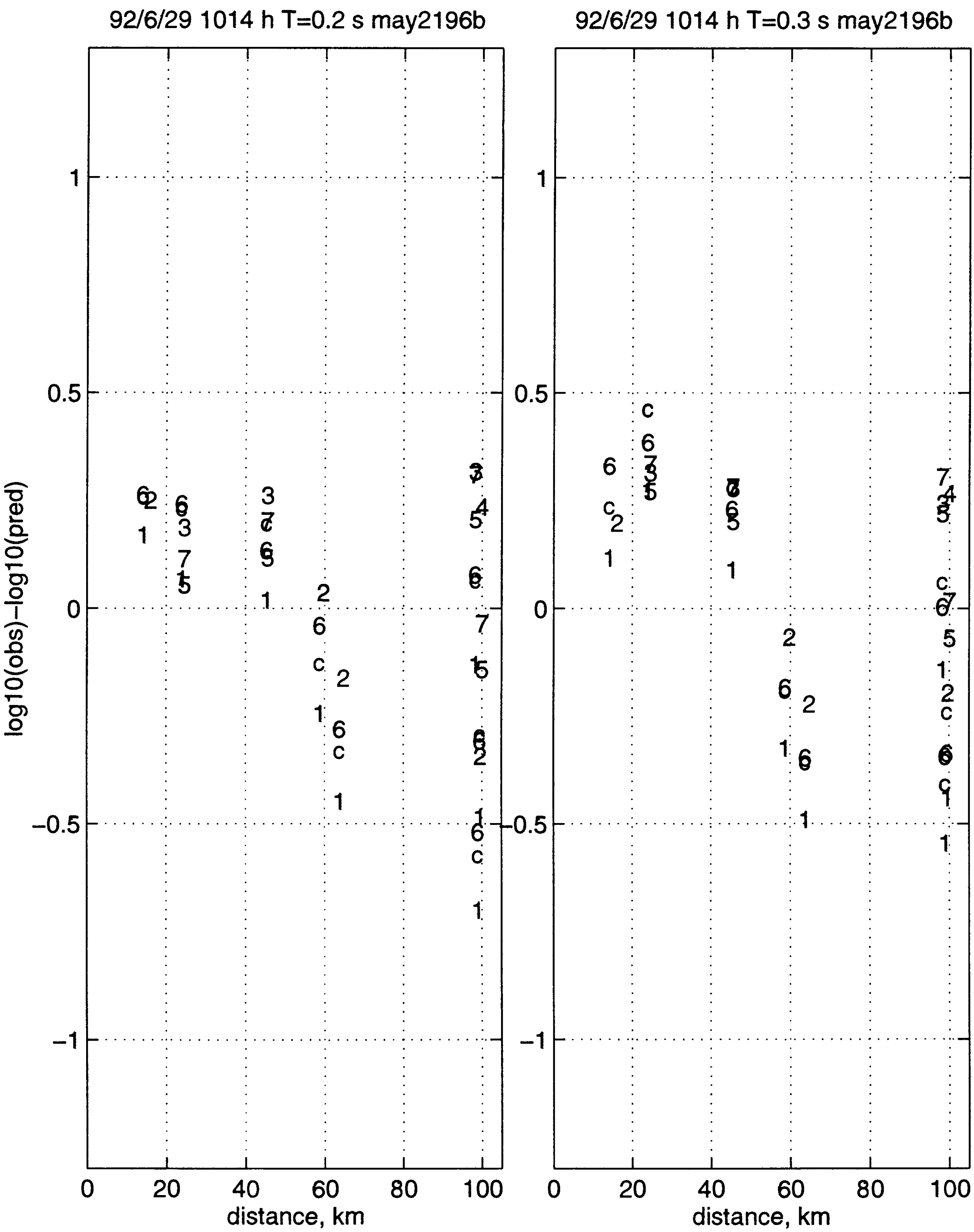

92/6/29 1014 h T=0.2 s may2196b
92/6/29 1014 h T=0.3 s may2196b
log10(obs)−log10(pred)
distance, km
distance, km

23c

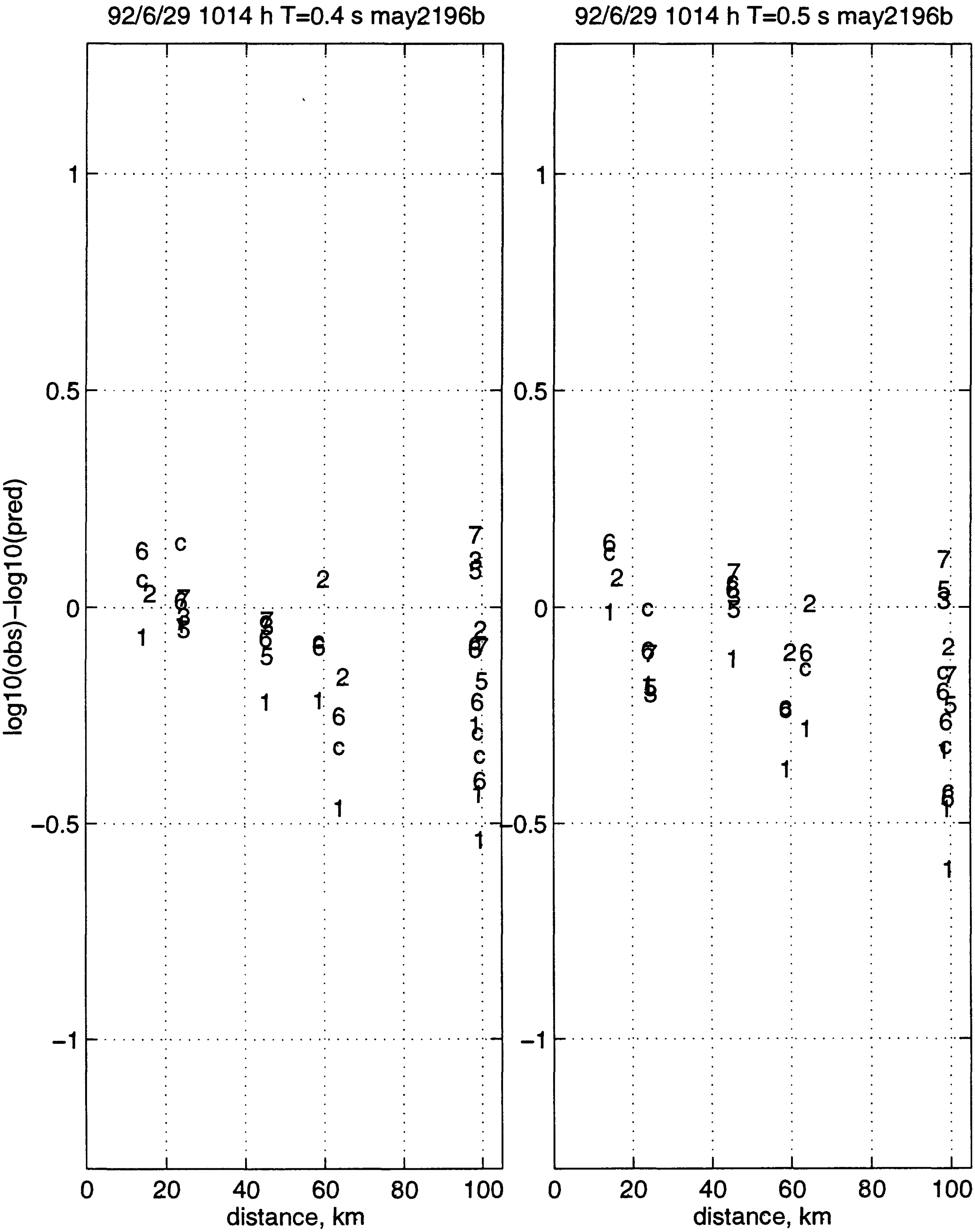
92/6/29 1014 h T=0.4 s may2196b
92/6/29 1014 h T=0.5 s may2196b
log10(obs)−log10(pred)
distance, km
distance, km

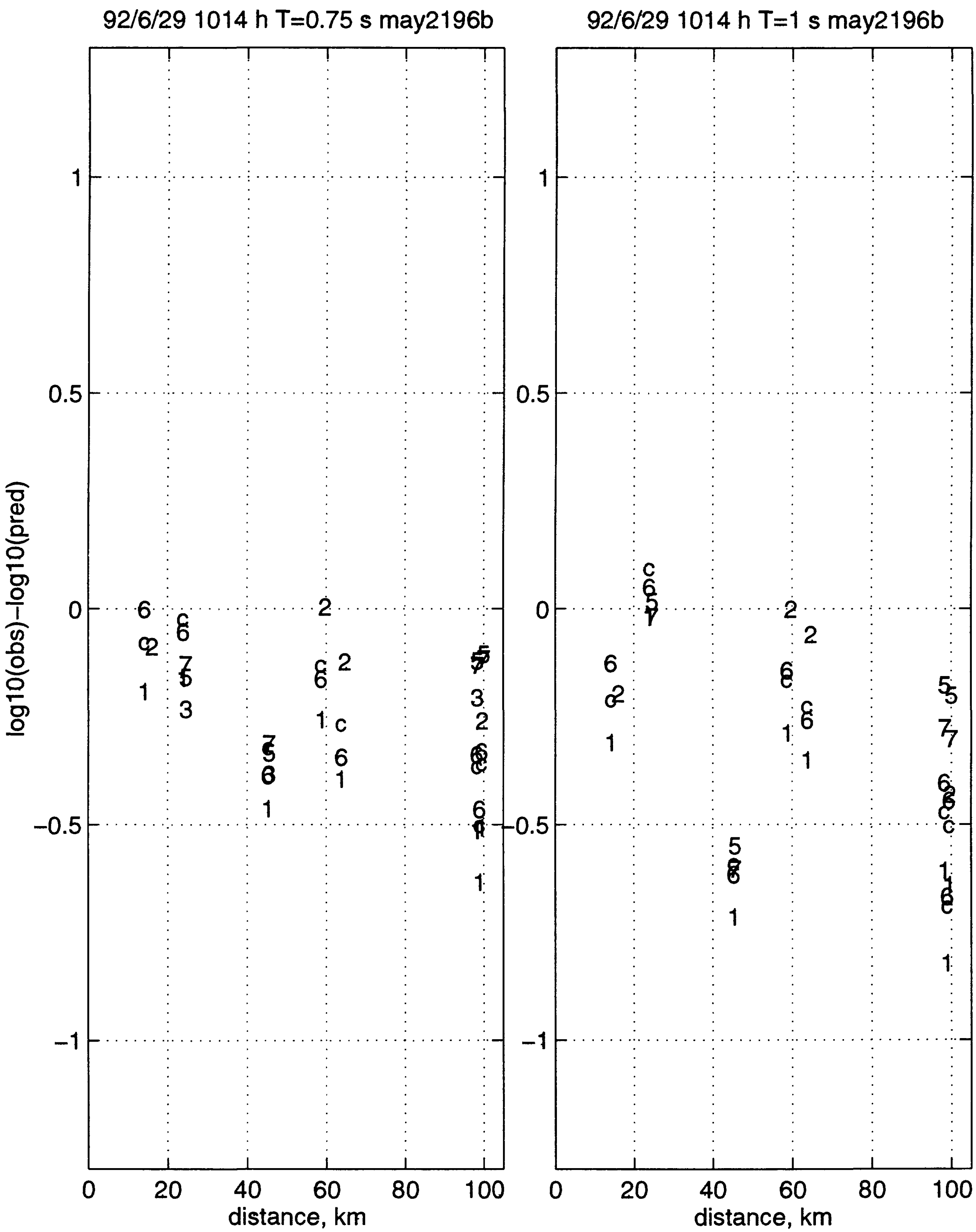
92/6/29 1014 h T=0.75 s may2196b
92/6/29 1014 h T=1 s may2196b
log10(obs)−log10(pred)
distance, km
distance, km

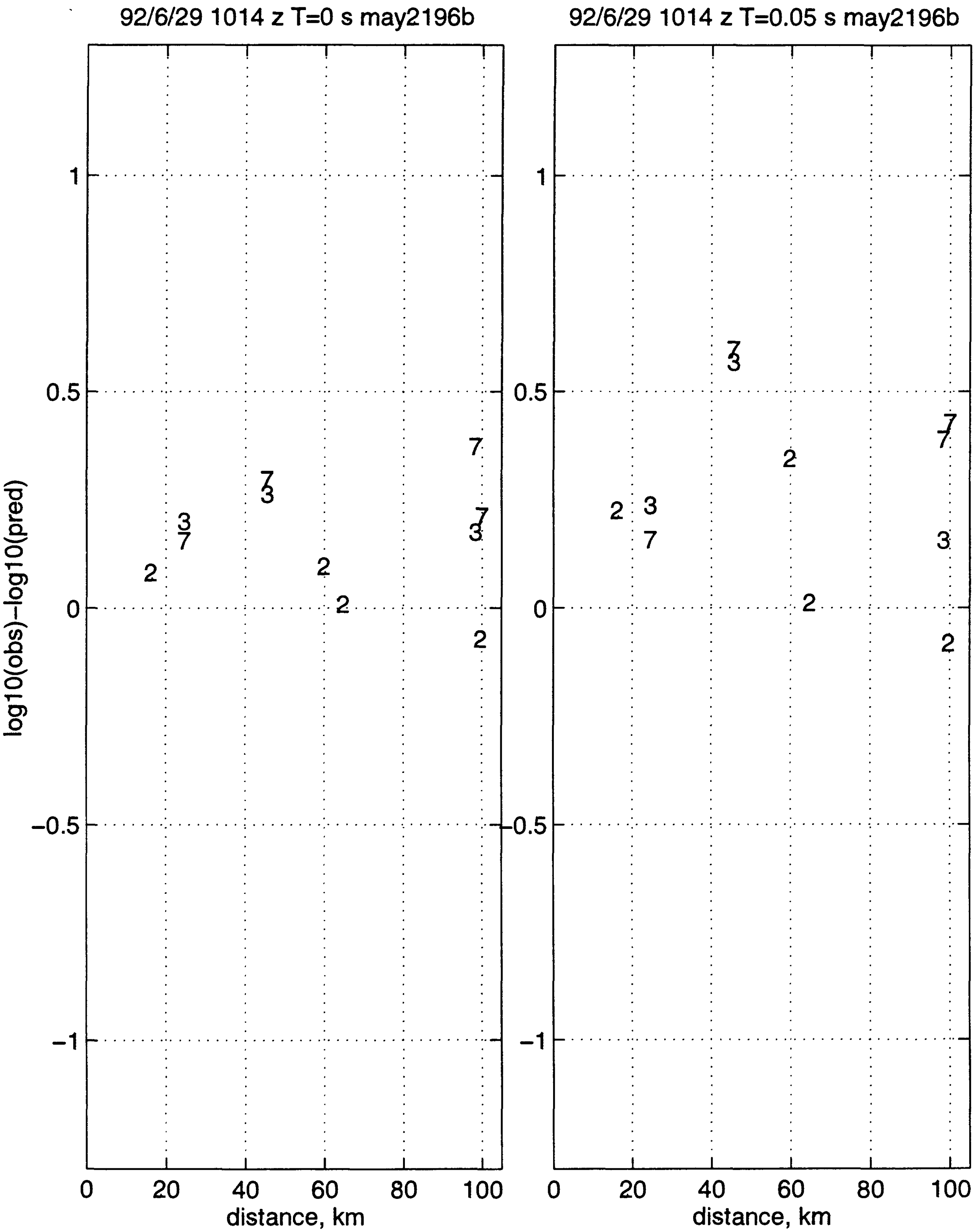
92/6/29 1014 z T=0 s may2196b
92/6/29 1014 z T=0.05 s may2196b
log10(obs)−log10(pred)
distance, km
distance, km

23f

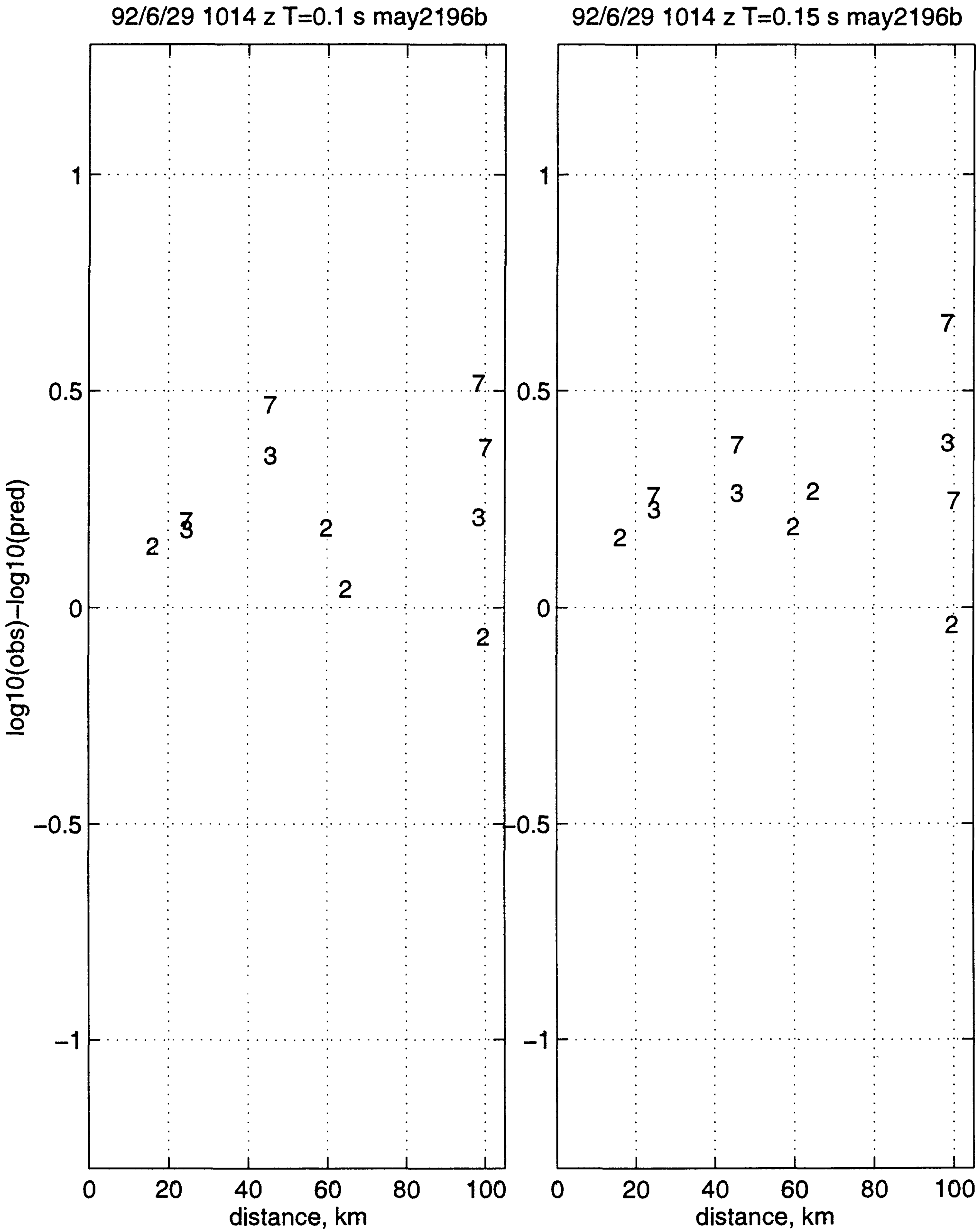
92/6/29 1014 z T=0.1 s may2196b
92/6/29 1014 z T=0.15 s may2196b
log10(obs)−log10(pred)
distance, km
distance, km

23g

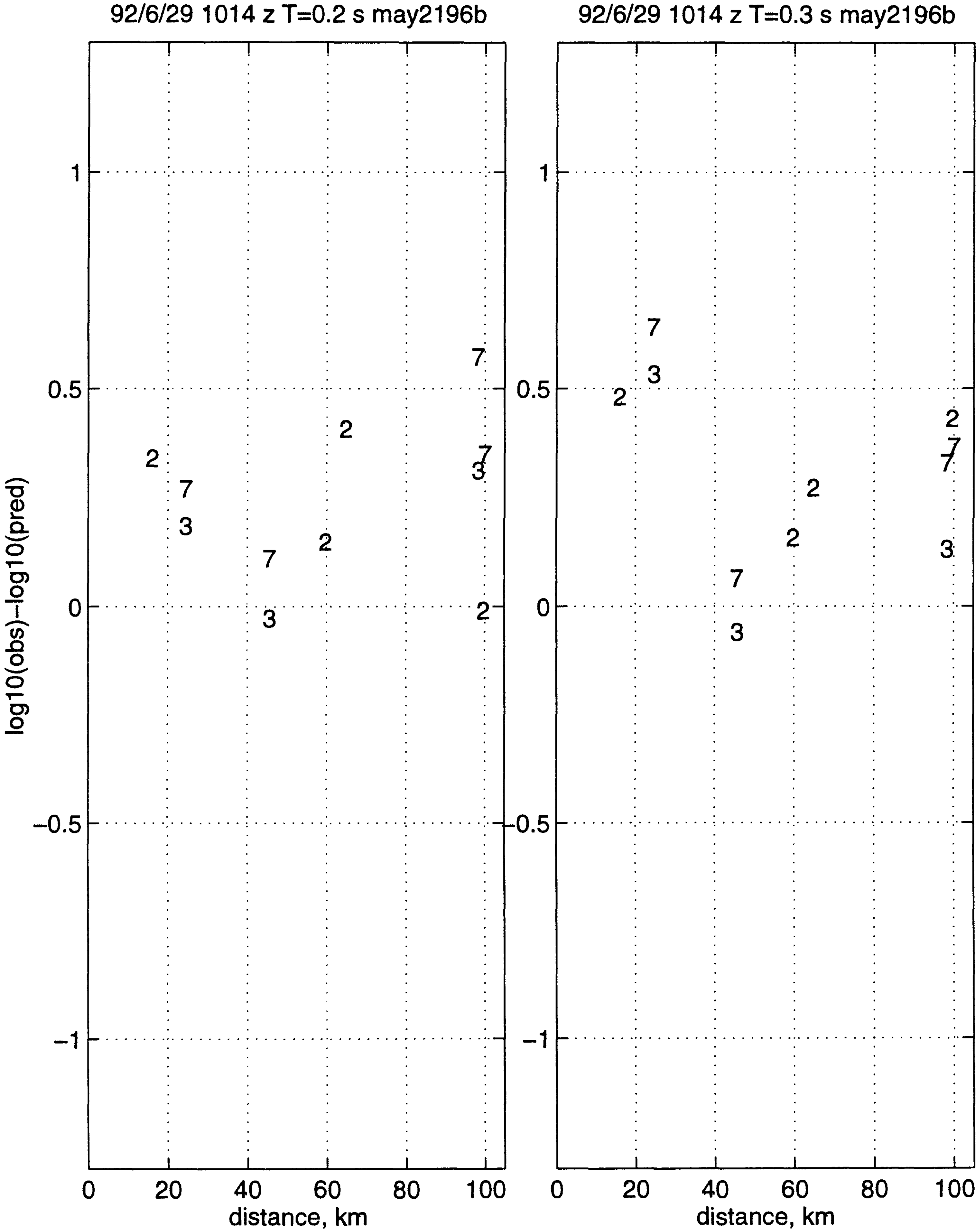
92/6/29 1014 z T=0.2 s may2196b
92/6/29 1014 z T=0.3 s may2196b
log10(obs)−log10(pred)
distance, km
distance, km

23h

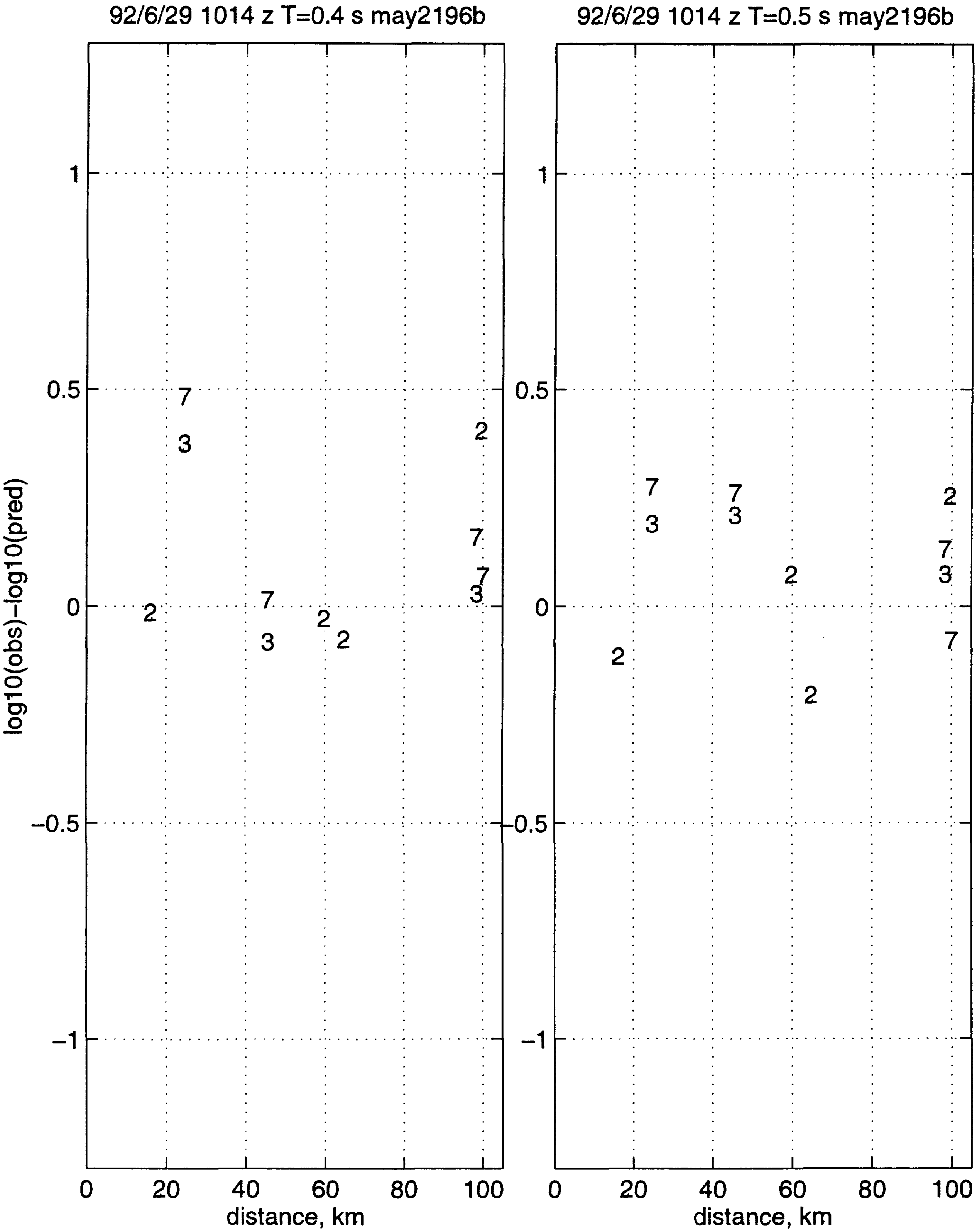
92/6/29 1014 z T=0.4 s may2196b
92/6/29 1014 z T=0.5 s may2196b
log10(obs)−log10(pred)
distance, km
distance, km
1
0.5
0
−0.5
−1
0
20
40
60
80
100

23i

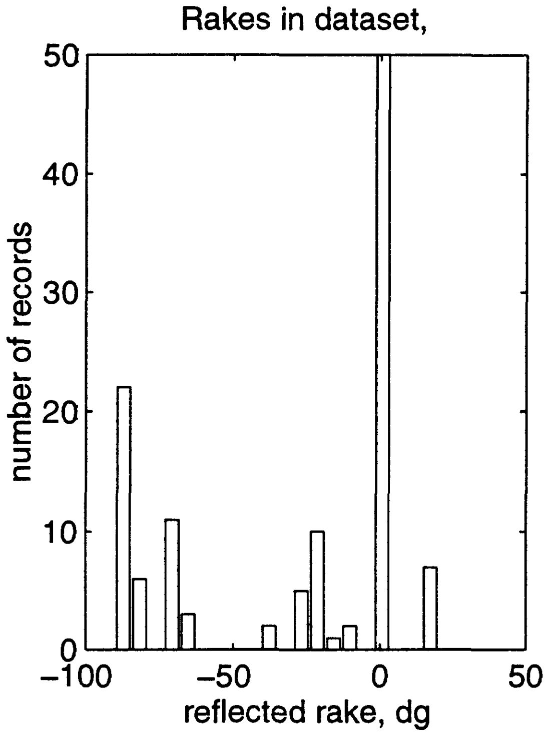

may2196b w/o TAN

mean normal residual = −0.01254

no. of normal residuals = 343

mean str−sl residual = 0.03015

no. of str−sl residuals = 837

Students t value =−2.77

Probability means differ = 0.9943

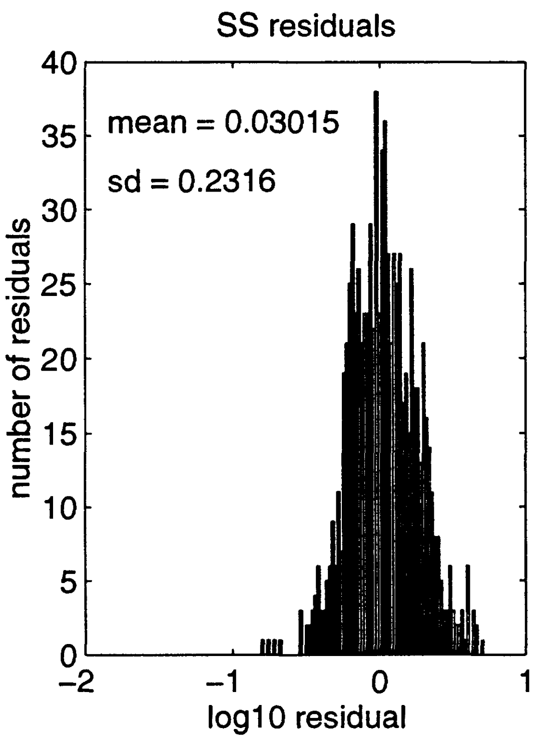

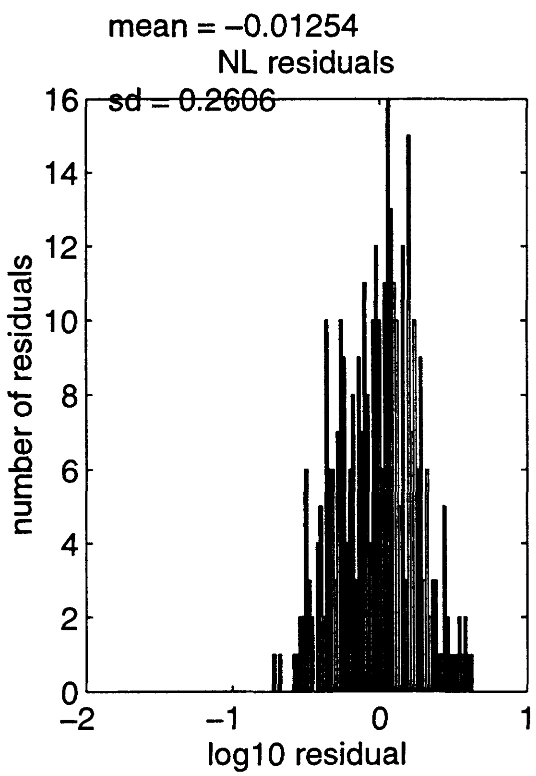

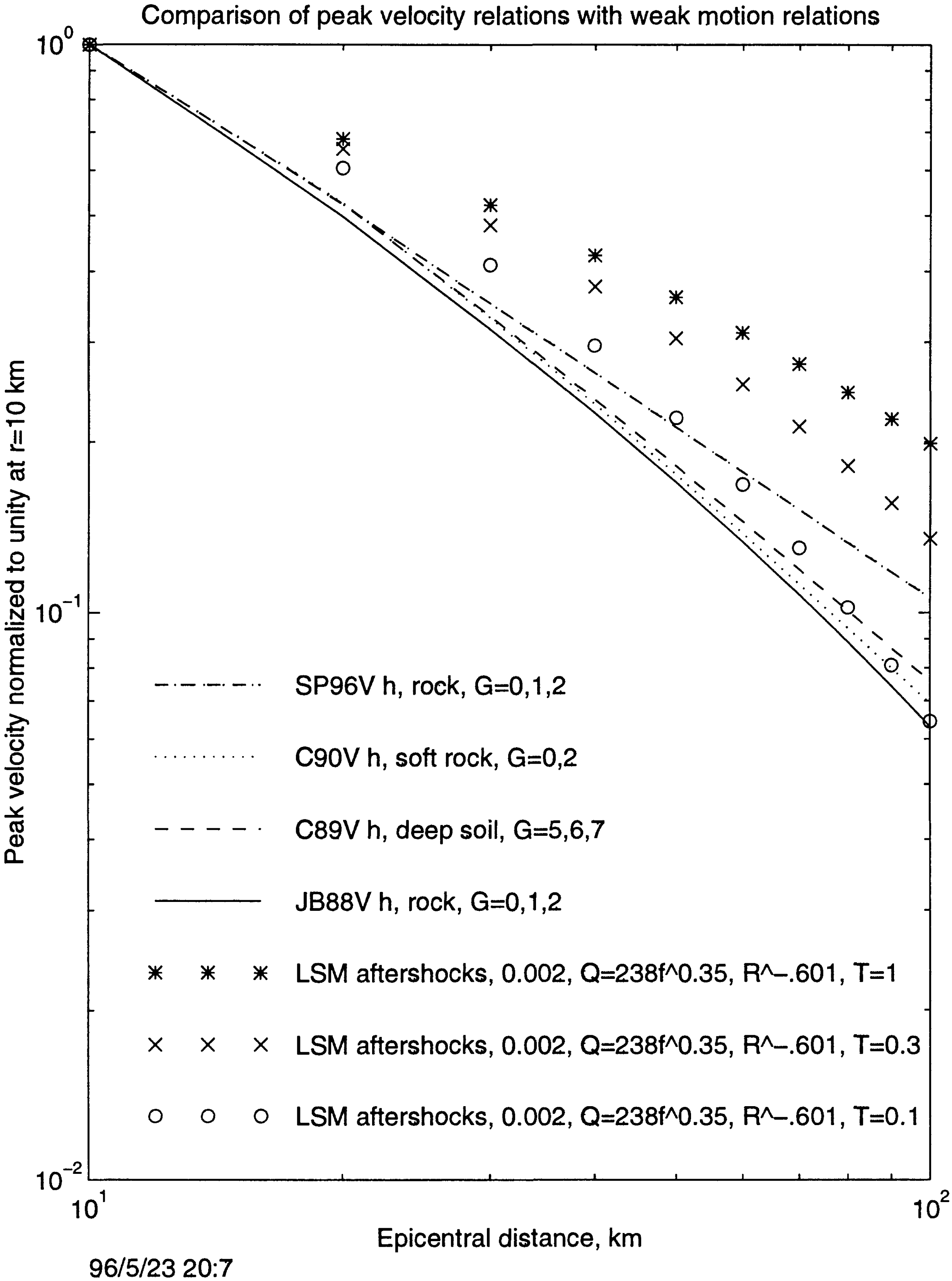

Comparison of peak velocity relations with weak motion relations
10^0
10^{-1}
10^{-2}
10^1
10^2
Peak velocity normalized to unity at r=10 km
Epicentral distance, km
SP96V h, rock, G=0,1,2
C90V h, soft rock, G=0,2
C89V h, deep soil, G=5,6,7
JB88V h, rock, G=0,1,2
LSM aftershocks, 0.002, Q=238f^0.35, R^–.601, T=1
LSM aftershocks, 0.002, Q=238f^0.35, R^–.601, T=0.3
LSM aftershocks, 0.002, Q=238f^0.35, R^–.601, T=0.1
96/5/23 20:7

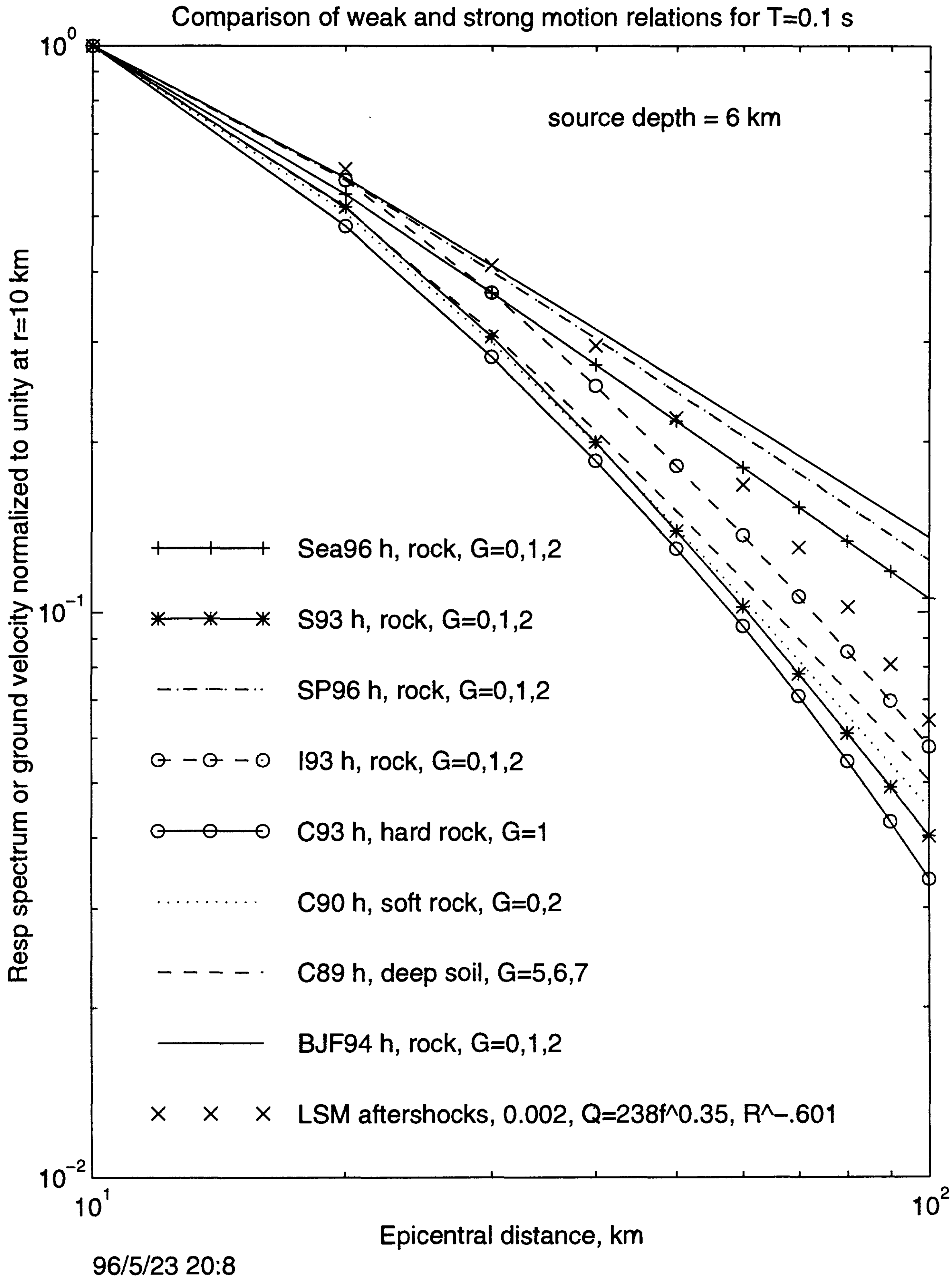

Comparison of weak and strong motion relations for T=0.1 s
source depth = 6 km
Sea96 h, rock, G=0,1,2
S93 h, rock, G=0,1,2
SP96 h, rock, G=0,1,2
I93 h, rock, G=0,1,2
C93 h, hard rock, G=1
C90 h, soft rock, G=0,2
C89 h, deep soil, G=5,6,7
BJF94 h, rock, G=0,1,2
LSM aftershocks, 0.002, Q=238f^0.35, R^-.601
Resp spectrum or ground velocity normalized to unity at r=10 km
Epicentral distance, km
96/5/23 20:8

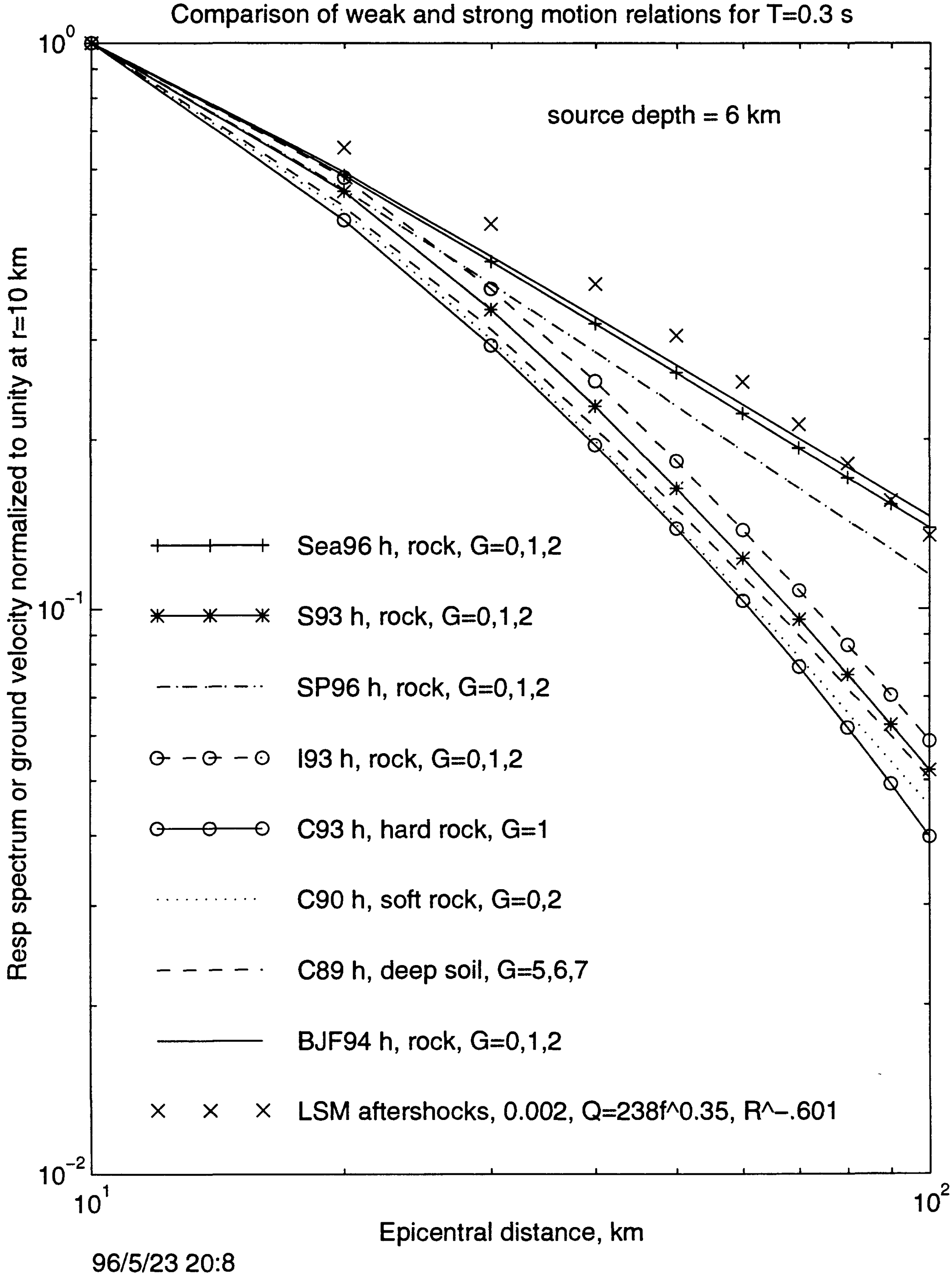
Comparison of weak and strong motion relations for T=0.3 s
source depth = 6 km
Sea96 h, rock, G=0,1,2
S93 h, rock, G=0,1,2
SP96 h, rock, G=0,1,2
I93 h, rock, G=0,1,2
C93 h, hard rock, G=1
C90 h, soft rock, G=0,2
C89 h, deep soil, G=5,6,7
BJF94 h, rock, G=0,1,2
LSM aftershocks, 0.002, Q=238f^0.35, R^-.601
Resp spectrum or ground velocity normalized to unity at r=10 km
Epicentral distance, km
10^0
10^{-1}
10^{-2}
10^1
10^2
96/5/23 20:8

266

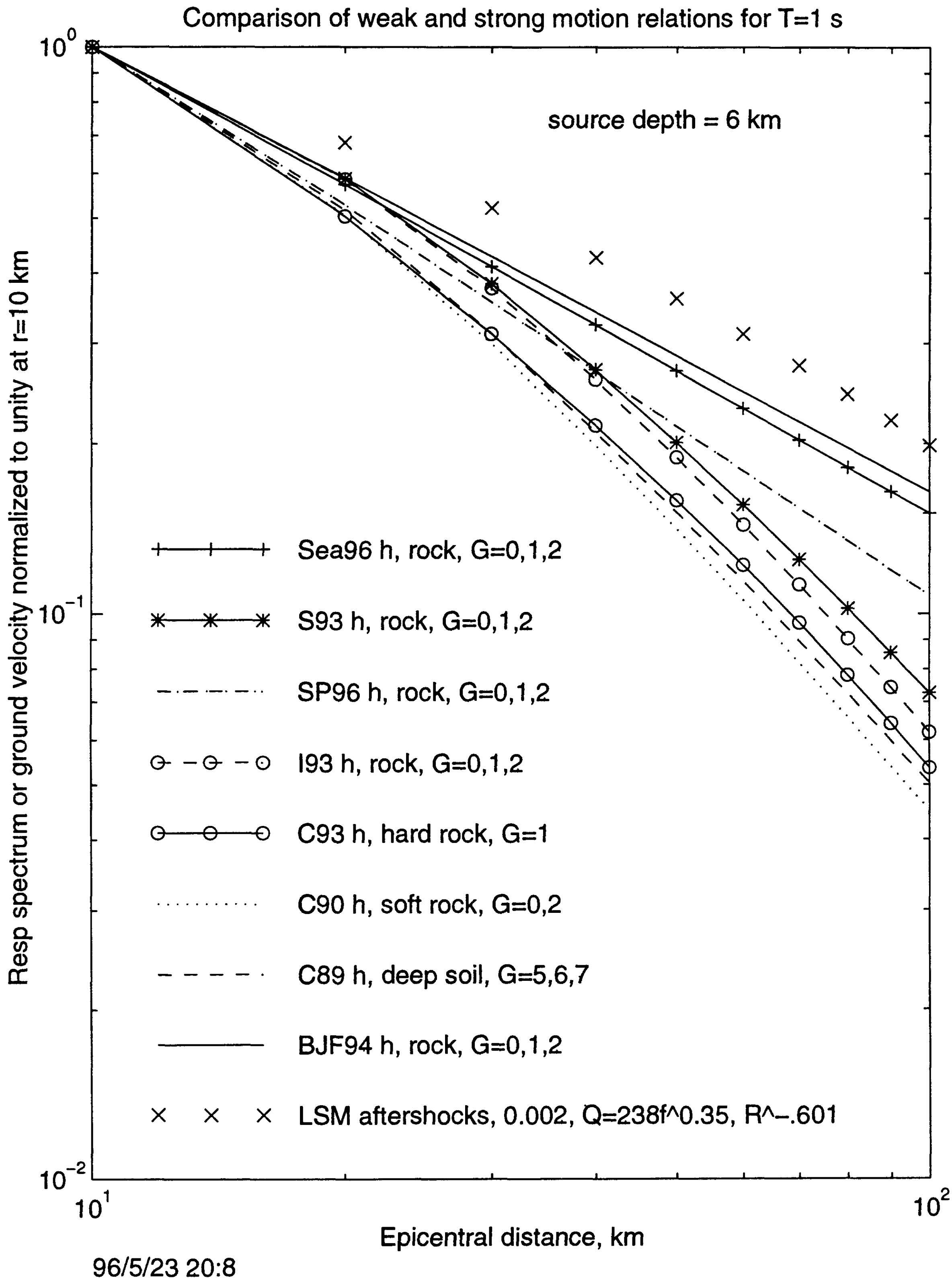
Comparison of weak and strong motion relations for T=1 s
source depth = 6 km
Sea96 h, rock, G=0,1,2
S93 h, rock, G=0,1,2
SP96 h, rock, G=0,1,2
I93 h, rock, G=0,1,2
C93 h, hard rock, G=1
C90 h, soft rock, G=0,2
C89 h, deep soil, G=5,6,7
BJF94 h, rock, G=0,1,2
LSM aftershocks, 0.002, Q=238f^0.35, R^-.601
Resp spectrum or ground velocity normalized to unity at r=10 km
Epicentral distance, km
96/5/23 20:8

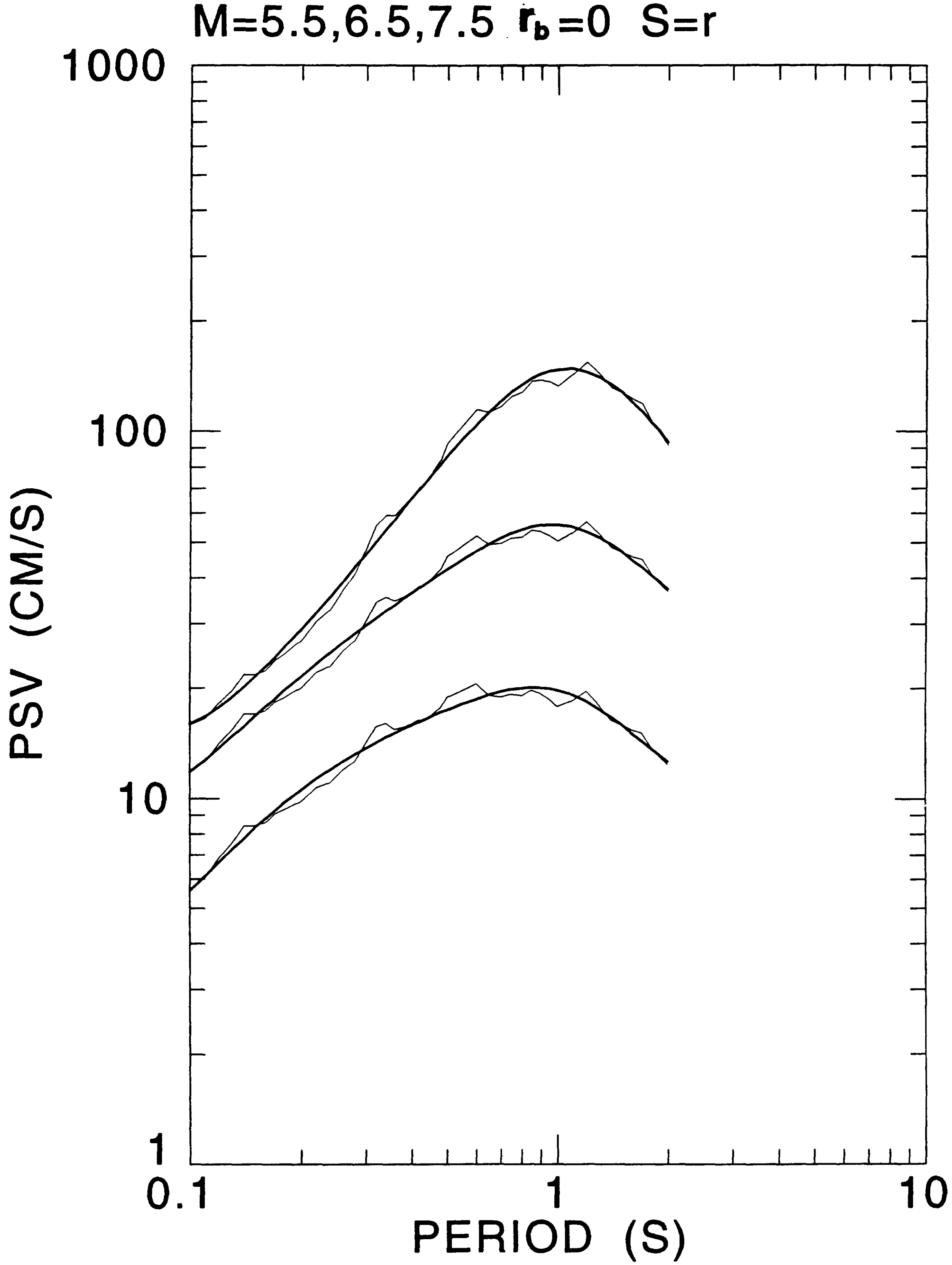

B1

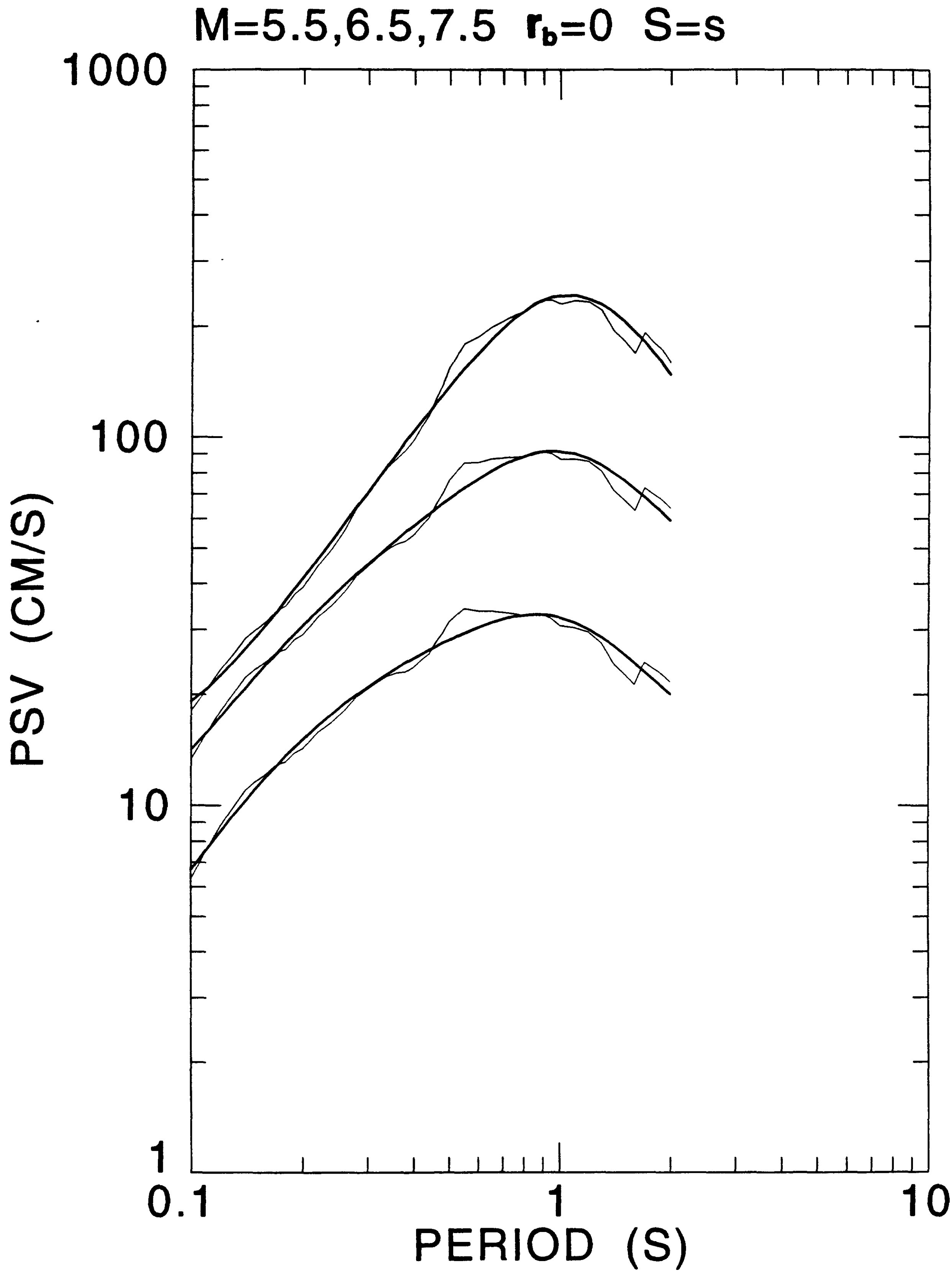

B2

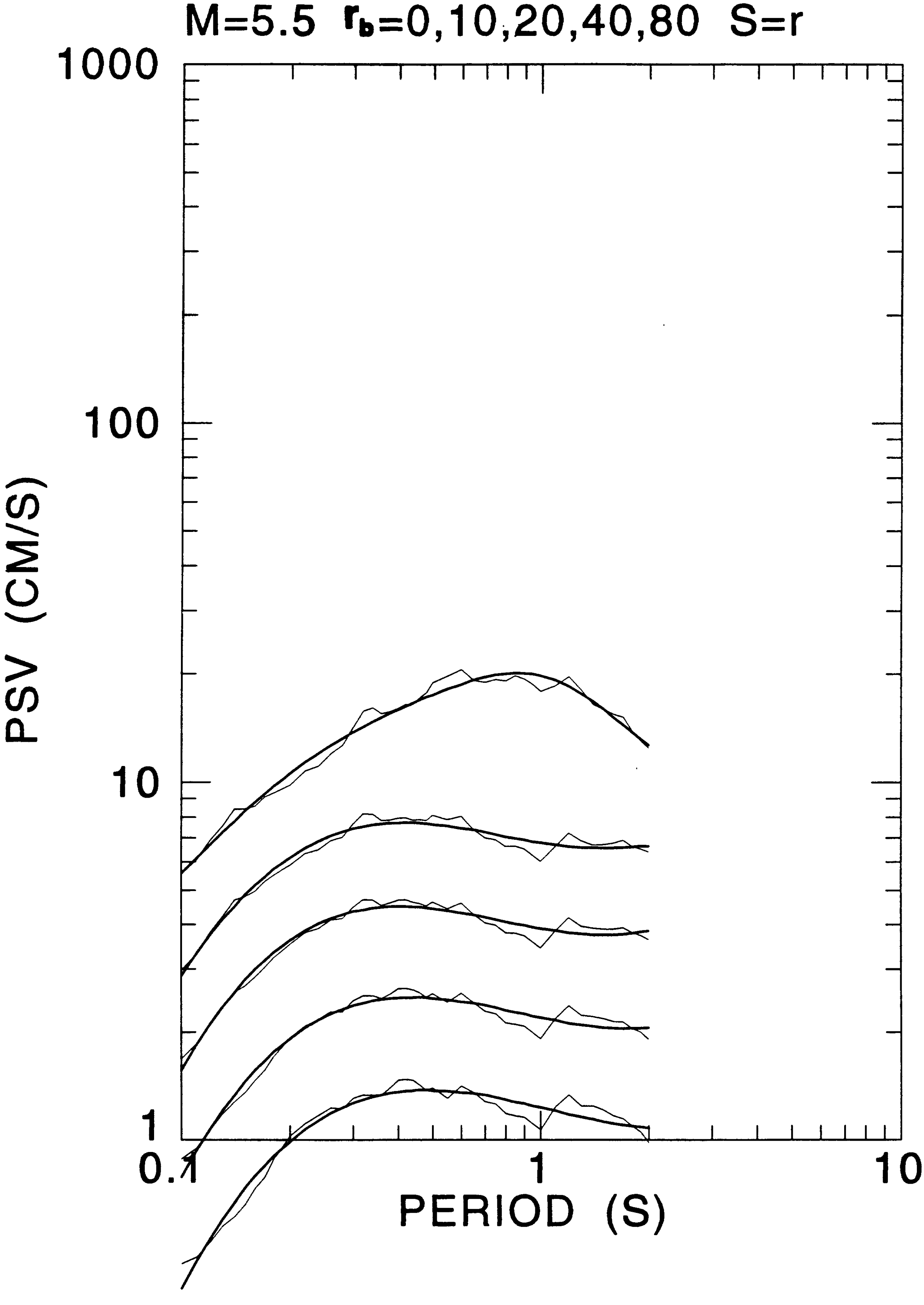

B3

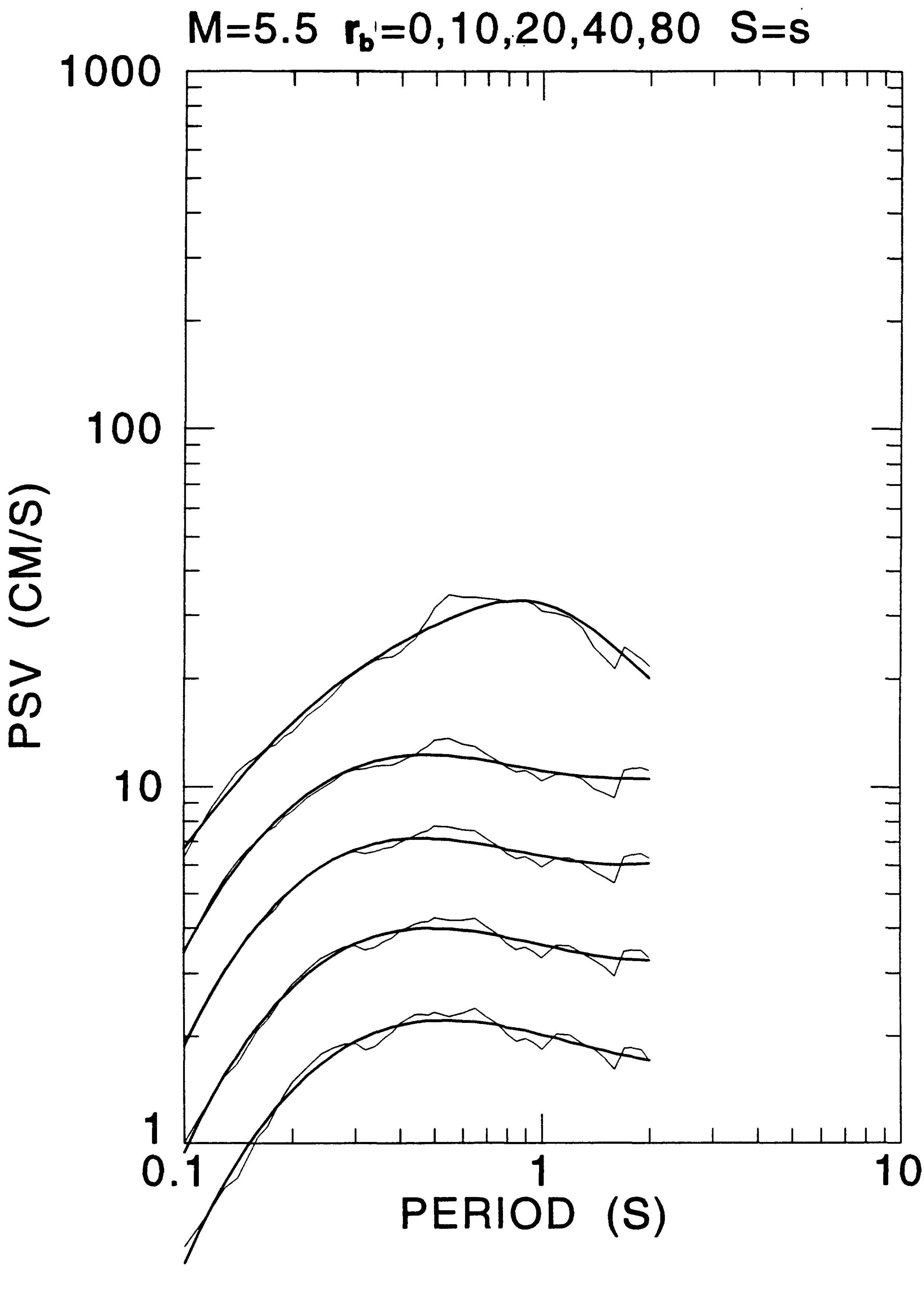

B4

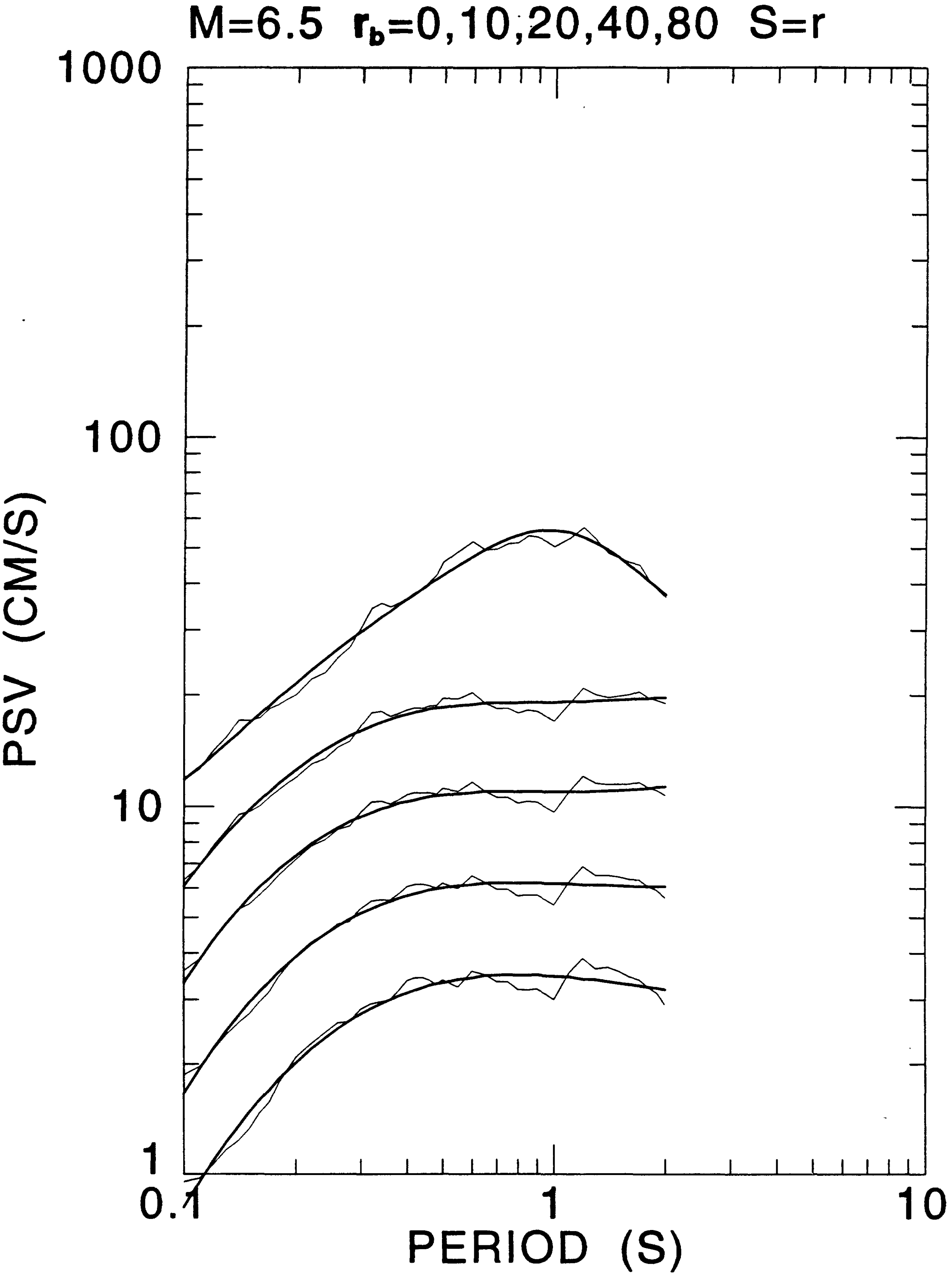

B5

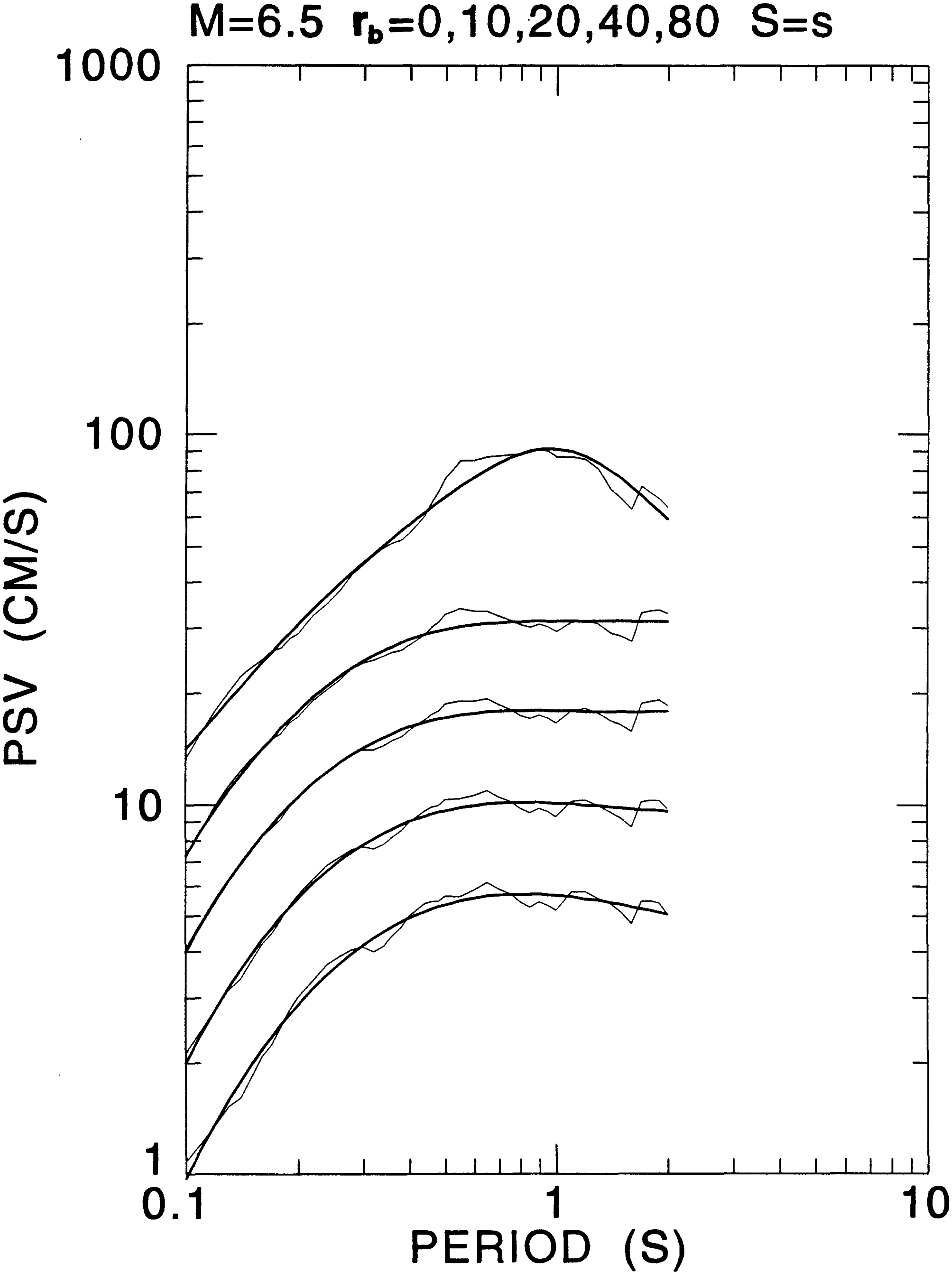

B 6

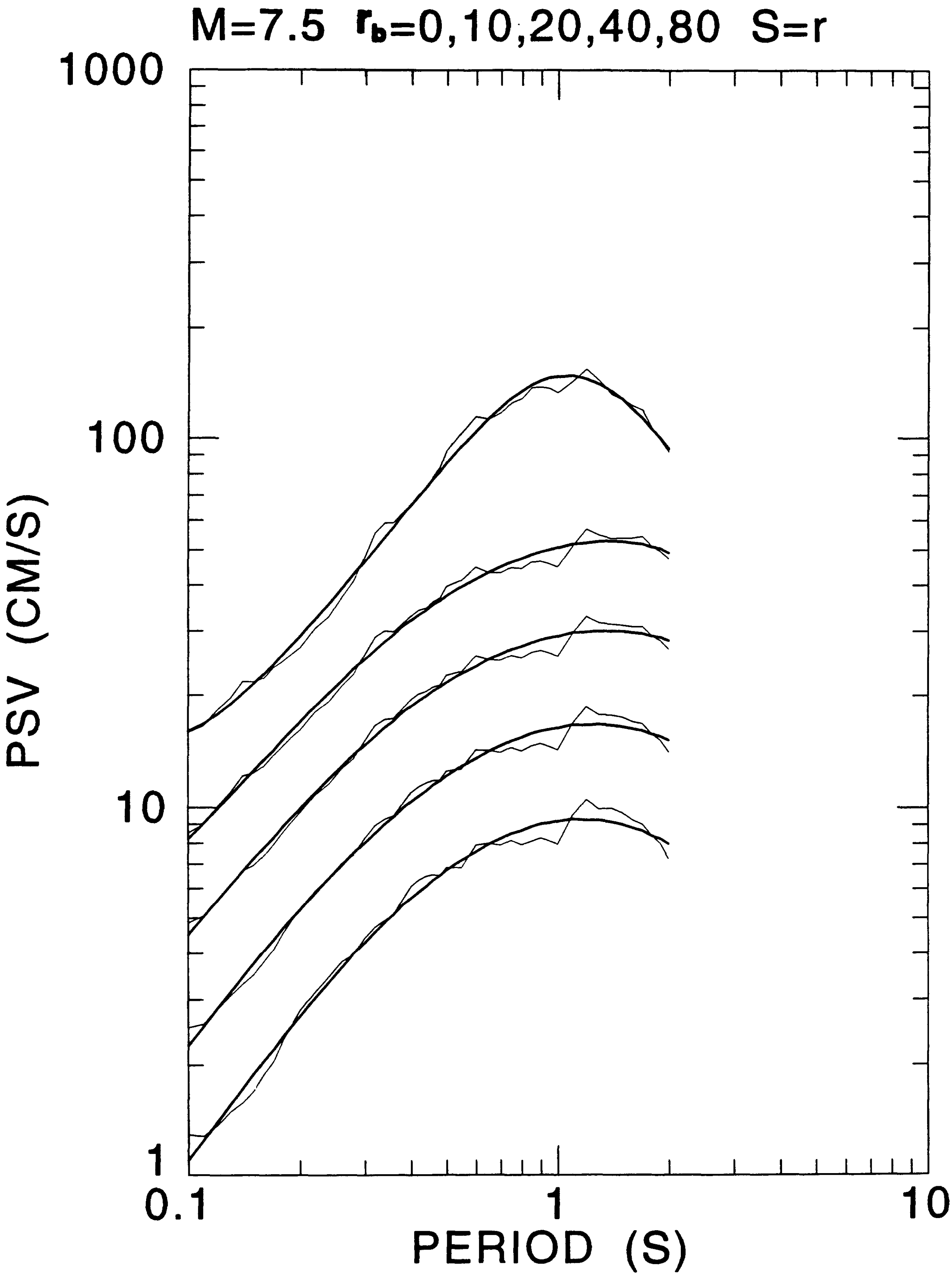

B7

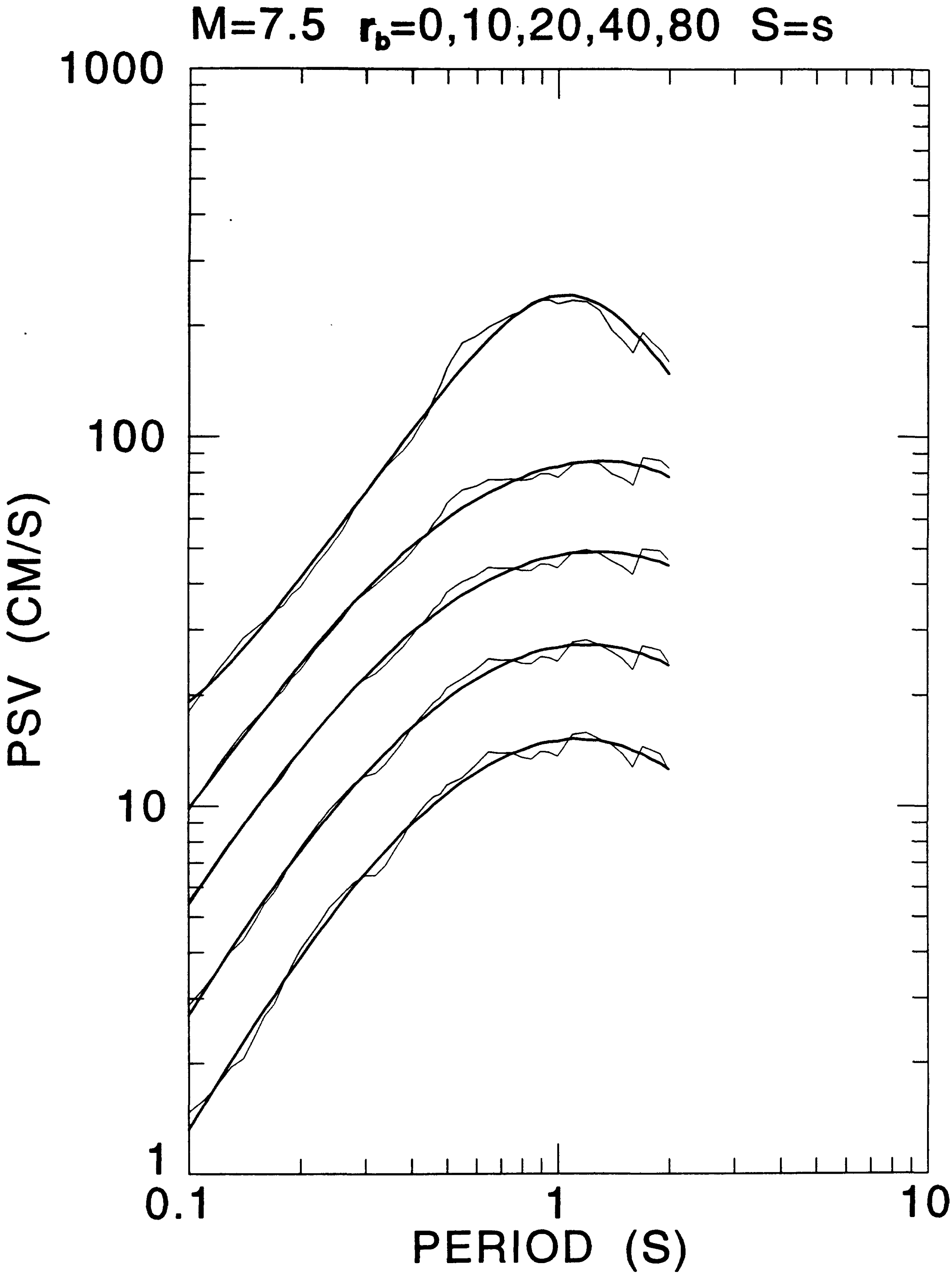

B8

351 (last page)